

International Baltic Earth Secretariat Publication No. 18, June 2020

3rd Baltic Earth Conference

Earth system changes and Baltic Sea coasts

To be held in Jastarnia, Hel Peninsula, Poland, 1 to 5 June 2020

Held online, 2-3 June 2020

Conference Proceedings

Edited by
Silke Köppen and
Marcus Reckermann

baltic.earth

Leibniz-Institut für Ostseeforschung Warnemünde

Helmholtz-Zentrum Geesthacht
Centre for Materials and Coastal Research

Impressum

International Baltic Earth Secretariat Publications
ISSN 2198-4247

International Baltic Earth Secretariat
Helmholtz-Zentrum Geesthacht GmbH
Max-Planck-Str. 1
D-21502 Geesthacht, Germany

www.baltic.earth
balticearth@hzg.de

Front page photo: Aerial view of Hel peninsula, Poland
(Piotr Mądry, with kind permission of Gmina Jastarnia)

Conference Organizers and Sponsors

Institute of Oceanology, IO-PAN
Poland

Helmholtz-Zentrum Geesthacht
Germany

Leibniz Institute for Baltic Sea Research Warnemünde
Germany

Conference Committee

Juris Aigars, Latvia
Franz Berger, Germany
Inga Dailidienė, Lithuania
Irina Danilovich, Belarus
Matthias Gröger, Sweden
Jari Haapala, Finland
Karol Kulinski, Poland (vice-chair)
Andreas Lehmann, Germany
Urmas Lips, Estonia
H. E. Markus Meier, Germany (chair)
Kai Myrberg, Finland
Anders Omstedt, Sweden
Piia Post, Estonia
Marcus Reckermann, Germany
Gregor Rehder, Germany
Anna Rutgersson, Sweden
Tarmo Soomere, Estonia
Martin Stendel, Denmark
Ralf Weisse, Germany
Marcin Weslawski, Poland
Sergey Zhuravlev, Russia

Organisation Committee

Karol Kulinski, Poland
Beata Szymczycha, Poland
Silke Köppen, Germany
H. E. Markus Meier, Germany
Marcus Reckermann, Germany

Acknowledgments

We sincerely thank the Polish Institute of Oceanology (IO-PAN) in Sopot, our local partner institution, for co-organizing this conference, in particular Jan Marcin Weslawski, Karol Kulinski and Beata Szymczycha for a dedicated and efficient collaboration in preparing the conference. Thank you to Silke Köppen of the International Baltic Earth Secretariat at Helmholtz-Zentrum Geesthacht for putting together this abstract volume and the programme booklet, next to taking care of the hundreds of other things necessary to make this concerence a success. Unfortunately, the conference cannot be held as planned, but we will be Poland in 2022, at the Hotel Dom Zdrojowy, Jastarnia, Hel peninsula, Poland, for the 4th Baltic Earth Conference.

Preface

This proceedings volume contains all accepted abstracts for the 3rd Baltic Earth Conference, which was planned to take place in Jastarnia on the Hel peninsula, at the Polish coast. Unfortunately, due to the SARS-CoV-2 pandemic, we had to cancel the physical conference.

Instead, we will have an online conference on 2 and 3 June 2020. Although only a subset of oral and poster presentations submitted to this abstract volume will be available online, we stick to the tradition to present all accepted abstracts in this volume.

The conference covers the topics of Baltic Earth, and in particular highlights the Baltic Earth Grand Challenges, as defined by the Baltic Earth Science Plan, and the topics treated by the BEAR (Baltic Earth Assessment Reports). The grand topic of the conference „Earth system changes and Baltic Sea coasts" refers to the manifold aspects of the changing Earth system of the Baltic Sea region, in the atmosphere, on land and in the sea. Climate change and the associated sea level rise, but also other human activities exert a particular pressure on the coasts of the southern Baltic Sea, of which the Hel peninsula and the Polish coasts in general are so typical. Land-sea interactions and human uses shape and modify the coasts all over the Baltic Sea.

The sessions reflect the Baltic Earth Grand Challenges and BEAR topics:

- Salinity dynamics
- Land-sea-atmosphere biogeochemical linkages
- Natural hazards and high impact events
- Sea level dynamics, coastal morphology and erosion
- Regional variability of water and energy exchanges
- Multiple drivers for regional Earth system changes
- Regional climate system modelling
- Climate change and its impacts
- New climate observation systems

We have received 110 abstracts from all over the Baltic Sea region. As usual, oral and poster abstracts will be treated equally in these proceedings; they are all sorted alphabetically within topics.

We trust that the online conference will be successful. It certainly cannot substitute a real conference where scientists come together. We hope it will be an exception, and we would like to invite you already now to the 4th Baltic Earth Conference, which will take place where the 3rd was planned: in Jastarnia on the Hel peninsula, at the Polish coast, 30 May – 3 June 2022! Please mark these dates in your calendar!

Markus Meier and Marcus Reckermann
On behalf of the Conference Committee and the Baltic Earth Science Steering Group

Contents

Contributions are sorted alphabetically within topics.

Keynotes and special talks

Dumped munitions as a pressure factor for the Baltic Ecosystem
Jacek Bełdowski, T. Lang, M. Reuter, P. Vanninen, M. Brenner, S. Popiel, M. Szala, J. Fabisiak, A. Tengberg, G. Garnaga-Budre, M. Bełdowska 1

Multiple drivers of change in coastal water quality and ecosystem status: From participatory mental mapping to systems modelling
Georgia Destouni, G. Vigouroux, S. Seifollahi-Aghmiuni, Z. Kalantari 3

Declining oxygen in the global ocean and coastal waters
Marilaure Grégoire and the IOC-Unesco Global Ocean Oxygen Network (GO2NE) group 5

Changes in flood risk at a range of scales - Globe, Europe, Baltic Sea Basin
Zbigniew W. Kundzewicz 6

A Philosophical View of the Ocean and Humanity
Anders Omstedt 8

Connecting Science, society and policy: experience of a small country
Tarmo Soomere 10

Chemical contamination of the Baltic Sea – status and future perspectives
Emma Undeman 11

The coastal processes and management in the southern Baltic Sea
Grzegorz Uścinowicz 12

Social perception of the Baltic Sea in Poland
Marcin Weslawski 13

Topic 1:
Salinity dynamics in the Baltic Sea

Baltic+ Salinity Dynamics: Towards a new view on the Baltic Sea surface salinity
Pekka Alenius, L. Tuomi, P. Roiha, V. González-Gambau, E. Olmedo, C. González-Haro, A. Turiel, J. Martínez, C. Gabarró, M. Arias, R. Catany, D. Fernández, R. Sabia 15

An introduction to the SuFMix Project: "Turbulent mixing in the Slupsk Furrow"
Anna Bulczak, D. Rak, J. Jakacki, W. Walczowski 17

Salinity dynamics of the Baltic Sea
Andreas Lehmann, K. Myrberg, P. Post..... 19

High-resolution view on downwelling by underwater glider in the Eastern Baltic Proper
Taavi Liblik, K. Salm, U. Lips..... 22

Investigating periodic interdecadal salinity changes in the Baltic Sea and their drivers
Hagen Radtke 21

The role of dissolved oxygen and salinity on the reproductive conditions of the cod in the Southern Baltic Sea
Daniel Rak, A. Bulczak, W. Walczowski, A. Przyborska 23

Long-term variability of the near-bottom oxygen, temperature and salinity in the Southern Baltic
Beata Schmidt, A. Bulczak 25

Assessment of the effect of the Slupsk Sill on transformation of the Baltic inflow water based on microstructure measurements
Viktar Zhurbas, V. Paka, M. Golenko, A. Korzh, A. Kondrashov..... 27

Rotation of floating particles in submesoscale cyclonic and anticyclonic eddies: a model study for the southeastern Baltic Sea
Viktar Zhurbas, G. Väli, N. Kuzmina..... 28

Topic 2:
Land-Sea biogeochemical linkages

Modern trophic state indexes of Baltic waters derived from structural signatures of biofilm colonies covering submerged solid substrata
Katarzyna Boniewicz-Szmyt, M. Grzegorczyk, SJ. Pogorzelski, P. Rochowski 31

Benthic fauna influence on the marine silicon cycle in the coastal zones of the southern Baltic Sea
Zusanna Borawska, B. Szymczycha, K. Koziorowska-Makuch, MJ. Silberberger, M. Szczepanek, M. Kędra..... 33

Short-term vs. long-term effects of rewetting coastal peatlands - are they fueling eutrophication and climate change with regard to nitrogen?
Anne Breznikar, JW. Dippner, M. Voss 35

Bioecological evaluation of the quality of the surface runoff from urban territories (case study of the city of Brest)
Ina Bulskaya, A. Volchak, A. Kolbas 37

Microbial Life and Phosphorus Cycling Along Salinity and Redox Gradients
Simeon Choo, S. Langer, H. Schulz-Vogt 38

High-resolution ecosystem model of the Puck Bay (southern Baltic Sea)
Dawid Dybowski, M. Janecki, A. Nowicki, L. Dzierzbicka-Głowacka, J. Jakacki 40

Interactive calculators as tools to assist farmers in estimating agricultural holding's balance and nitrogen leaching from field
Dawid Dybowski, L. Dzierzbicka-Głowacka, S. Pietrzak, D. Juszkowska 41

Assessing the impact of agriculture on the waters of the Puck Bay within the WaterPUCK project
Dawid Dybowski, L. Dzierzbicka-Głowacka, B. Szymczycha, E. Wojciechowska, A. Szymkiewicz, P. Zima, G. Pazikowska-Sapota, S. Pietrzak, M. Janecki, A. Nowicki, T. Puszkarczuk 42

Seasonality of the total alkalinity in the Gulf of Gdansk, southern Baltic Sea
Karol Kuliński, A. Winogradow, B. Szymczycha, M. Stokowski 44

Bioavailability and remineralization of sediment-derived dissolved organic carbon from the Baltic Sea depositional area
Monika Lengier, B. Szymczycha, K. Kuliński 45

Nitrogen Fixation in a coastal peatland and adjacent sediments
Tina Liesirova, T. Aarenstrup Launbjerg, L. Riemann, M. Voss 47

Photosynthesis, respiration and growth responses of Baltic Sea benthic diatoms in relation to sea-land exchange processes
Lara Prelle, A. Graiff, S. Gründling-Pfaff, V. Sommer, K. Kuriyama, U. Karsten 49

Predicting submarine groundwater discharge from coastal peatlands of northeast Germany using HYDRUS-2D
Erwin Don Racasa, B. Lennartz, M. Janssen 50

The CO_2 system variability in the vicinity of the Vistula River mouth
Marcin Stokowski, A. Winogradow, B. Szymczycha, K. Kuliński 52

Submarine groundwater discharge influence on marine CO_2 system
Beata Szymczycha, A. Winogradow, K. Kuliński 54

Estimation of phosphate ion in the waters of the rivers of the Baltic catchment (on the example of the Western Bug River)
Alexander A. Volchak, M. Taratsenkava..... 56

The impact of submarine groundwater discharge on element fluxes into a temperate shallow coastal bay
Catia M. E von Ahn, M. Böttcher, P. Feldens, A-K. Jenner, I. Schmiedinger, J. Scholten. 58

The spatiotemporal variation of Sea Surface pCO_2 in the Baltic Sea from 2002 to 2011 using Remote Sensing
Shuping Zhang, A. Rutgersson, P. Philipson 60

Topic 3:
Natural hazards and extreme events

Long-term statistics of atmospheric conditions over the Baltic Sea and meteorological features related to wind wave extremes in the Gulf of Gdańsk
Witold Cieślikiewicz, A. Cupiał..... 61

Convective Snow Bands over the Baltic Sea in an Ensemble of Regional Climate Scenarios
Christian Dieterich, M. Gröger, K. Klehmet, P. Berg, J. Jeworrek, K. Jylhä, E. Kjellström, HEM. Meier, T. Olsson, L. Wu, A. Rutgersson 63

Estimation of economic effect of the use of hydrometeorological information during exploitation of highways of Belarus
Y.A. Hledko 65

From Climate Variability to Heavy Precipitation: Learning Transfer Functions from Data
Michał Kałczyński, K. Krawiec, Z. Kundzewicz 67

Impacts of river discharge and ice phenomena on the extent of storm surges in the Odra River mouth area (the southern Baltic Sea)
Halina Kowalewska-Kalkowska 68

Coastal flooding: Joint probability of extreme water levels and waves along the Baltic Sea coast
Nadia Kudryavtseva, A. Räämet, T. Soomere..... 70

Agrothermal changes in 1961–2018 in Lithuania
Viktorija Mačiulytė, G. Stankūnavičius..... 72

Differences in stationary and non-stationary analysis of water level extremes in Latvian waters, Baltic Sea, during 1961-2018
Rain Männikus, N. Kudryavtseva, T. Soomere 74

Study of the influence of zonal and azonal factors on the maximum floods runoff in the Vistula basin (within Ukraine)
Maksym Martyniuk, V. Ovcharuk 76

Predicting extreme dry spell risk based on probability distribution in coastal region of Tunisia
Majid Mathlouthi, F. Lebdi 78

The assessment of natural hazards as a part of integrated coastal zone management: the case of Haapsalu Bay, Estonia
Valeriya Ovcharuk, M. Moniushko, S. Das 80

Maximal rivers runoff during floods different origin on the coastal zone of Northwestern part of the Black Sea
Valeriya Ovcharuk, M. Moniushko, E. Gopchenko, N. Kichuk 82

Radar-derived convective storms' climatology over Estonia during the warm season
Piia Post, T. Voormansik, T. Müürsepp 83

Definition of droughts and their recurrence in Lithuania
Egidijus Rimkus, E. Stonevičius, D. Valiukas, V. Mačiulytė 85

Projected distribution of the drought in Ukraine until 2050 under RCP4.5 and RCP6.0 climate scenarios
Inna Semenova, A. Polevoy 87

Topic 4:
Sea level dynamics in the Baltic Sea

Geophysical and geochemical characteristics of four different pockmark sites located in the Gdańsk Basin
Aleksandra Brodecka-Goluch, J. Idczak, N. Gorska, J. Bolałek 89

Short-term volumetric changes of the southern Baltic dune coast caused by various hydrodynamic conditions (case study Dziwnow Spit)
Natalia Bugajny, K. Furmańczyk 91

Land subsidence monitoring due to groundwater changes using InSAR observations - Initial results: the Swedish Islands of Gotland and Öland in the Baltic Sea
Mehdi Darvishi, F. Jaramillo 93

Morphodynamic of the southern Baltic coast – natural processes & anthropogenic impact
Joanna Dudzińska-Nowak 95

A first look to Lagrangian Coherent Structures in the Gulf of Finland as a mean to identify hotspots of surface particle aggregation
Andrea Giudici, K. Suara, T. Soomere, R. Brown 97

Sandbar switching as a factor controlling coastal erosion during storm events, Curonian Spit, Lithuania
Rasa Janušaitė, D. Jarmalavičius, D. Pupienis, G. Žilinskas, V. Karaliūnas..... 99

Mean sea level changes in the southwestern Baltic Sea over the last 190 years
Jessica Kelln, S. Dangendorf, U. Gräwe, H. Steffen, J. Patzke, J. Jensen 101

High water level variability in the North Sea and Baltic Sea and objective weather types
Jens Möller, P. Löwe..... 102

The impact of dredging works performed during construction of an offshore Wind Farm upon the adjacent areas of the Baltic Sea
Anna Przyborska, J. Jakacki 103

ESA Baltic+ SEAL: Using the Baltic Sea as a test-bed for developing advanced, regionalised sea-level products
Laura Rautiainen, L. Tuomi, J. Särkkä, M. Johansson, FL. Müller, M. Passaro, A. Abulaitijiang, OB. Andersen, D. Dettmering, JL. Høyer, J. Oelsmann, IM. Ringgaard, E. Rinne, R. Scarrott, C. Schwatke, F. Seitz, K. Skovgaard Madsen, A. Ambrozio, M. Restano, J. Benveniste 105

Overview of Remote Sensing Methods for Run Up Tracing After High Energy Events on Sandy Beaches, Baltic Sea Coast, Lithuania
Kristina Viršilaitė, D. Pupienis..... 107

Applicability assessment of multi-date medium resolution satellite remote sensing data for detection and interpretation of coastline fluctuations: case study Russian part of the eastern Gulf of Finland
Eugenia Volynets, A. Volynetc, E. Panidi..... 109

Characteristics of seasonal changes of the Baltic Sea extreme water levels
Tomasz Wolski, B. Wiśniewski..... 111

Coastal foredunes along the southern Baltic Sea – their current development and future scenarios inferred from numerical modelling
Wenyan Zhang, J. Dudzinska-Nowak 113

Topic 5:
Regional variability of water and energy exchanges

The peculiarities of the moistening regime in the accordance to the climate change at the eastern part of the Baltic Sea Basin with a focus on Belarus
Irina Danilovich..... 115

Complementing ERA5 and E-OBS20 with high-resolution river discharge over Europe
Stefan Hagemann, T. Stacke..... 117

Linking weather types to tense dewatering situations of the Kiel Canal
Corinna Jensen, J. Möller, P. Löwe, N. Schade 119

Assessment of the impact of the Grodno hydroelectric power station on the hydrological regime of the Neman River (within the borders of Belarus)
Alena Kvach, M. Asadchaya, L. Zhuravovich 121

Mid-winter stratification formation in the Gulf of Finland
Taavi Liblik, G. Väli, M.-J. Lilover, J. Laanemets, V. Kikas, I. Lips 123

Intermediate plumes of low oxygen in the southeastern Baltic Sea
Vadim Paka, M. Golenko, V. Zhurbas, A. Korzh, A. Kondrashov 124

Impact of climate change on the water management of the Kiel Canal – A case study
Nils H. Schade, A-D. Ebner von Eschenbach, J. Moeller, V. Neemann 125

Changes in the hydrological seasons of Estonian rivers during the period 1928-2017
Mait Sepp 127

Changes in wind parameters in Estonia during the period 1966-2016
Mait Sepp, A. Kull, P. Post 128

Evaluation of changes in the River Viliya annual runoff under the fluctuation climate conditions
Alexander A. Volchak, S. Parfomuk, S. Sidak 130

Small-scale spatial variability of hydro-physical properties of differently degraded peat
Miaorun Wang, H. Liu, B. Lennartz 132

Features of the formation of hanging dam and ice jam on the rivers of Belarus in a changing climate
Ludmilla Zhuravovich, A. Kvach, M. Asadchaya 133

Topic 6:
Multiple drivers of regional Earth system changes

Decision support tools for the management of eastern Baltic Sea coasts
Mojtaba Barzehkar, K. Parnell, T. Soomere 135

Environmental window of summer blooms in the eastern Baltic Sea
Oscar Beltran-Perez, J. Waniek 137

First results of model sensitivity studies on the influence of global changes to the Baltic Seas
Birte-Marie Ehlers, F. Janssen, J. Abalichin 139

Assessment of the state of pollution of the Ukrainian part of the Black Sea
Maryna Moniushko, V. Ovcharuk 140

Comparison of different data sets for mapping of hypoxic and euxinic regions in the Baltic Sea deep waters
Michael Naumann, S. Feistel 142

The application of coastal geomorphic process concepts to eastern Baltic Sea conditions in a changing climate
Kevin E. Parnell, T. Soomere 143

Accuracy assessment of ESA CCI LC over Eastern Europe and the Baltic States from a climate modelling perspective – identification of spatial inaccuracy patterns and misclassification issues using a fuzzy comparison method
Vanessa Reinhart, P. Hoffmann, B. Bechtel, D. Rechid, J. Boehner 145

Modeling the distribution of microplastics coming with river runoff in the eastern part of the Gulf of Finland
Vladimir A. Ryabchenko, S. D. Martyanov, A. V. Isaev, G. Martin 147

Coastal dunes ecosystems change according to normalized difference vegetation index (the case study of Curonian Lagoon)
Rasa Šimanauskienė, R. Linkevičienė, J. Taminskas, R. Povilanskas 149

EI-GEO Environmental Impact of Geosynthetics in Aquatic Systems
Franz-Georg Simon, H. Barqawi, B. Chubarenko, E. Esiukova, I. Putna-Nimane, I. Barda, E. Strode, I. Purina 151

Atmospheric transport and seasonal variability of trace elements and polycyclic aromatic hydrocarbons in fine-aerosol fraction at the coastal site in Gdynia, Poland
Patrycja Siudek, I. Waszak 153

Inlet polynyas of coastal lagoons of the Baltic sea and other reservoirs of the temperate climate of the northern hemisphere
Ekaterina Zhelezova 155

Topic 7:
Regional climate system modeling

NEMO (Nucleus for European Modeling of the Ocean) regional configuration for the Baltic Sea domain – validation of the water exchange through the Danish Straits.
Jan Andrzejewski, J. Jakacki 157

Moving climate zones and climate change impact on anomalous weather phenomena in the Euro-Cordex / Baltic Sea region
Matthias Gröger, C. Dieterich, H.E.M. Meier 159

Applying the new regional coupled system model GCOAST-AHOI over Europe
Ha Ho-Hagemann, S. Hagemann, S. Grayek, R. Petrik, B. Rockel, J. Staneva, F. Feser, C. Schrum 161

Simulated climate in the Baltic Sea region in a standalone atmospheric RCM and in an atmosphere-ocean model: evaluation and future climate change
Erik Kjellström, C. Dieterich, G. Nikulin, M. Wu, O.B. Christensen, M. Gröger, H.E.M. Meier 163

Convection permitting regional climate modelling in northern Europe – first results on the summertime precipitation climate from NorCP
Erik Kjellström, D. Belušić, P. Lind, D. Lindstedt, E. Toivonen, R. A. Pedersen, O.B. Christensen, O. Landgren, A. Dobler 165

Uncertainties of Baltic Sea future projections under different shared socioeconomic pathways
H. E. Markus Meier, C. Dieterich, M. Gröger 167

Objective analysis of climatological fronts in the Atlantic-European sector
Katsiaryna Sumak, I. Semenova 169

Does internally generated hydrodynamic noise matter in the Baltic Sea?
Hans von Storch, A. Omstedt, J. Elken 170

Topic 8:
Climate Change and its impacts

Research of climate change in South-Eastern Baltic sea coastal areas
Inga Dailidienė, I. Razbadauskaitė-Venskė, R. Dailidė, L. Davilienė 173

Reanalysis based assessment of tropospheric thickness trends in Baltic Sea region
Alina Lerner, A. Männik 175

Changes in haptophyte community structures and the climate in the Arkona Basin (Baltic Sea) over the last 11 kyr recorded by long-chain alkenone distributions and proxies
Barbara W. Massalska, G. M. Weiss, R. Hennekam, G-J. Reichart, J. S. Sinninghe Damsté, S. Schouten, M.T.J. van der Meer 177

Changes in precipitation in the cold period in Belarus under conditions of modern climate warming
Viktor Melnik, I. Buyakov 179

Estimating the wave statistics bias in the partially ice-covered regions of the Baltic Sea
Fatemeh Najafzadeh, N. Kudryavtseva, A. Giudici, T. Soomere 181

Trend and 7-9-year oscillation of near surface air temperature over Mecklenburg-Vorpommern (Germany) induced by global warming and oceanic processes
Dieter H. W. Peters, C. Zülicke 183

Climate changes in the Baltic sea region as inferred from large RCM ensemble projection
Anastasia Pikaleva, I. Shkolnik, S. Efimov 184

The overturning circulation of the Baltic Sea and its sensitivity to long-term atmospheric and hydrological changes
Manja Placke, H.E.M. Meier, T. Neumann 185

Wave scenarios for the Gulf of Bothnia
Jari Särkkä, L. Tuomi, S. Siiriä, A. Höglund 187

The future of the Gulf of Bothnia: NEMO-SCOBI SmartSea scenarios from the present until 2060
Simo-Matti Siiriä, S. Fredrikson, A. Oikkonen, J. Hieronymus, A. Höglund, P. Roiha, J. Särkkä, L. Arneborg, L. Tuomi 188

Trends in total heat content in a very long climate change simulation
Martin Stendel 189

Surveying opinions among environmental students on climate science and Baltic Sea issues
Hans von Storch 190

Intraannual and longterm variability of wind in Poland in the period 1966-2018
Joanna Wibig 192

Long-term observations of nitrous oxide and methane at the Boknis Eck Time-Series Station in the Eckernförde Bay (southwestern Baltic Sea)
Ma Xiao, S. Lennartz, H. Bange 194

Topic 9:
New climate observation systems

Monitoring lake ice extent using optical satellite data
Kirsikka Heinilä, O. Mattila, S. Metsämäki, S. Väkevä, K. Luojus, G. Schwaizer, S. Koponen 197

Using InSAR observations to understand changes to coastal and inland water resources in the Baltic basin
Fernando Jaramillo, S. Aminjafari, M. Nia, M. Darvishi, J. García 199

The Sea Baltic Poland: citizen observations of surface water properties
Tomasz Kijewski, A. Palacz, B. Szymczycha, E. Borkowska, T. Zieliński 200

Utilization of Earth Observation to support biogeochemical modeling
Sampsa Koponen, T. Neumann, D. Müller, C. Brockmann, C. Mazeran, P. Philipson, K. Kallio, J. Attila, S. Väkevä 201

eCUDO.pl - Oceanographic Data and Information System for Polish Baltic data resources
Mirosława Ostrowska, M. Wójcik, U. Pączek, L. Szymanek, M. Wichorowski 203

SatBałtyk System - modern tool for tracking changes in the Baltic Sea environment
Mirosława Ostrowska, M. Darecki, A. Krężel, D. Ficek, K. Furmańczyk, T. Zapadka, M. Kowalewski, M. Konik 204

Development of the Argo measurement system for responding challenges in the northern Baltic Sea
Petra Roiha, S. Siiriä, L. Tuomi, P. Alenius, T. Purokoski 206

ARGO floats – the modern tool for the Southern Baltic monitoring
Waldemar Walczowski, M. Merchel, D. Rak, P. Wieczorek 208

Keynotes and special talks

Dumped munitions as a pressure factor for the Baltic Ecosystem

Jacek Bełdowski[1], Thomas Lang[2], Matthias Reuter[3], Paula Vanninen[4], Matthias Brenner[5], Stanisław Popiel[6], Mateusz Szala[6], Jacek Fabisiak[7], Andreas Tengberg[8], Galina Garnaga-Budre[9], Magdalena Bełdowska[10]

1. Institute of Oceanology Polish Academy of Sciences, Sopot, Poland
2. Thuenen Institute for Fisheries Ecology, Bremerhaven, Germany
3. Technical University of Claustahl, Germany
4. Alfred Wegener Institute for Polar Research, Bremerhaven, Germany
5. VERIFIN, Helsinki, Finland
6. Military University of Technology, Warsaw, Poland
7. Polish Naval Academy, Gdynia, Poland
8. Chalmers University of Technology, Gothenburg, Sweden
9. Lithuanian Environemntal Protection Agency, Klaipeda, Lithuania
10. University of Gdańsk, Poland

1. Introduction

Chemical and conventional ammunition dumped in the Baltic Sea and the Skagerrak contain a wide range of hazardous substances(Tobias Knobloch et al., 2013). Considering the growing use of the seabed for economic purposes (offshore wind farms, pipelines etc.), the likelihood of disturbing dumped containers with chemical warfare agents, causing direct emissions to the surrounding environment and risk of human and wildlife exposure, is increasing. In addition, the containers are deteriorating due to e.g. corrosion. For all these reasons there is an ongoing discussion on how to assess and manage the environmental risk of dumped ammunition, especially in areas where their location is likely to cause a conflict with maritime activities.

2. Materials and Methods

Project DAIMON has performed several studies in both conventional and chemical munition dumpsites. This studies included different risk factors, such as density of munitions on seabed, their corrosion status and pollution of nearby sediments. New approaches for analysis of both CWAs and toxic explosive related chemicals on a one method using sophisticated high resolution mass spectrometry have been tested and applied in pilot studies, Further experiments were carried out to confirm the structure of newly discovered CWAs using liquid chromatography-high resolution tandem mass spectrometry and NMR(Soderstrom et al., 2018).
Studies were performed in three chemical munition dumpsites (Gotland Deep, Bornholm Deep and Gdansk Deep) (Figure 1) and at conventional munition dumpsite in Kolberger Heide, close to Kiel Harbor on German Coast.

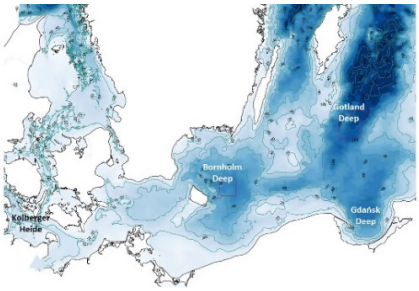


Figure 1. Study areas – chemical munition dumpsites at Bornholm, Gotland and Gdansk Deeps, and conventional munition dumpsite at Kolberger Heide

3. Chemical Warfare Agents

Even though a few indications of active agents at ppt (ng agent per g-1 sediment) levels were noted for mustard gas, the main indications for leakage of hazardous chemicals is based on oxidation/degradation products in the ppb range (µg agent per g^{-1} sediment). Analysis are still on the way, but results will be given in final presentation. Comparison of the distance between contaminated and non-contaminated samples leads to the conclusion that the pollution of sediments with CWA is local and strongly depends on the type of seabed, the condition of the munitions and the prevailing bottom currents The Gotland deep dumping activities were characterized by item by item dumping in a relative large area which reflects that only 21% of the samples were positive for dumped material. This while the Bornholm dumping activities was performed in a relative small area including scuttling of ships packed with chemical munition as well item by item dumping contained 86% of the samples remains of chemical warfare agents. Target chemicals were found in all studied areas. These results indicates that CW also could be dumped in the transport route between harbours and areas designated as the official dumping sites at Gotland and Bornholm deep. However identifications in the non-official dumping sites in Slupsk Furrow and Gdansk deep was were made only by one of three laboratories and requires final confirmation from alternative source.

4. Munition Primers

Obtained results show that dumped conventional munitions act as mercury sources to the bottom sediments. The compound responsible is mercury fulminate. Sedimentary mercury present in those sites is most likely associated with the fulminate used in munition primers, although only in two, out of eight, sediment samples the presence of mercury fulminate was identified by fingerprinting – in remaining samples it was masked by environmental transformation of mercury, which may indicate that the leakage of fulminate has occurred some time ago. The range of contamination in terms of distance from the source is estimated to be below 100 m, with power curve approximating best of concentration signal vs distance (Figure 2). However, methyl mercury concentrations in the dumpsite area are elevated indicating that overall impact of many munition objects may by far exceed the effects of ionic mercury as, toxic methyl mercury, able to enter the food chain may be

present in higher concentration all across the dumpsite.In the Bornholm Deep, mercury signal associated with dumped munitions is significantly weaker than in the Kolberger Heide , most likely because chemical munitions were mostly dumped without primers there, Elevated mercury in this site may originate from warfare agents impurities, rather than actual mercury fulminate.

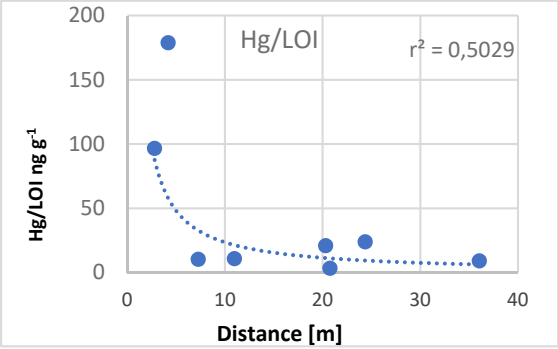


Figure 2. Mercury concentration in sediments close to dumped conventional munitions - concentration vs distance

5. Explosives

In this study we have analyzed two types of samples: sediments and explosives lumps. Limit of quantification of all analyzed compounds were between 0.5-10 µg/kg and limit of detection were between 0.16-3.3 µg/kg. We have analyzed 48 samples, from those samples up to 35 were contaminated with explosives and their degradation products. It should be notice that 29 sediment samples contained real TNT in concentration between 6.5 to 84.1 µg/kg. The main degradation products present in samples were as follow: 4-nitrotoluene; 1,3-dinitrobenzene; 1,3,5-trinitrobenzene; 2,4-dinitrotoluene and 2,6-dinitrotoluene. All samples in which explosives were detected also contained CWA's degradation products from both groups sulphur- and arsenic compounds. In case of lump, chemical analysis allow us for identification of three major compounds: TNT, RDX and aluminium powder. Based on the obtained results the composition of this material was: TNT (41%), RDX (53%), aluminium powder (5%), and degradation products (below 1%). The resulting composition indicates that the analysed material can be classified to the "torpex" family. This composition has been widely used during the World War II, for example in aerial bombs and torpedoes. Regarding the state of explosives, we can conclude that explosives lumps are in very good condition and they still might detonate after being initiated. Therefore, apart from environmental risk they may represent human hazard when lifted up.

6. Conclusions

Pollution of sediments with degradation products of chemical warfare agents, explosives, and mercury coming from munition primers is observed within all studied dumpsites. The magnitude of associated concentrations are low, but spreading to larger area (up to 100m radius) was observed. Taking into account large number of munitions in the Baltic Sea bottom, such local sources may have a real impact on the environment.

7. Acknowledgements

The research work was co-funded by the European Union (European Regional Development Fund) under the Interreg Baltic Sea Region Programme 2014-2020, project #X005 DAIMON 2. The research work was conducted as a part of an international project co-financed from the funds of the Polish Ministry of Science and Higher Education programme entitled "International Co-financed Projects" in the years 2019-2021; agreement no. 5051/INTERREG BSR/2019/2.

References

Soderstrom, M., Ostin, A., Qvarnstrom, J., Magnusson, R., Rattfelt-Nyholm, J., Vaher, M., Joul, P., Lees, H., Kaljurand, M., Szubska, M., Vanninen, P., Beldowski, J., 2018. Chemical Analysis of Dumped Chemical Warfare Agents During the MODUM Project. Towards the Monitoring of Dumped Munitions Threat (Modum): A Study of Chemical Munitions Dumpsites in the Baltic Sea, 71-103.

Tobias Knobloch, Jacek Bełdowski, Claus Böttcher, Martin Söderström, Niels-Peter Rühl, Sternheim, J., 2013. Chemical Munitions Dumped in the Baltic Sea. Report of the ad hoc Expert Group to Update and Review the Existing Information on Dumped Chemical Munitions in the Baltic Sea (HELCOM MUNI) Baltic Sea Environmental Proceedings. HELCOM, p. 129.

Multiple drivers of change in coastal water quality and ecosystem status: From participatory mental mapping to systems modelling

Georgia Destouni, Guillaume Vigouroux, Samaneh Seifollahi-Aghmiuni and Zahra Kalantari

Department of Physical Geography, Stockholm University, Stockholm, Sweden (georgia.destouni@natgeo.su.se)

1. Introduction

With an overarching land-sea interaction perspective on coastal systems, this paper highlights the solution-focused study of a Baltic coastal case within the EU Horizon 2020 project COASTAL: Collaborative land-sea interaction platform (https://h2020-coastal.eu). The Baltic case includes the Swedish Water Management District and coastal parts of the Northern Baltic Proper marine basin (Figure 1). For this coastal region of relatively rapid population and economic growth, solutions are sought for sustainable synergistic cross-sectoral measures towards improved coastal water quality and ecosystem status under ongoing and forthcoming climate and other regional change pressures.

In this work, the complexities of land-sea interactions and transition pathways towards coastal improvements are approached and investigated by four complementary methods: mechanistic physical-system simulations (Vigouroux et al., 2019), along with participatory-qualitative (Tiller et al., 2016), stakeholder-validated semi-quantitative (Kosko, 1986), and related fully quantitative cross-sector/system stock-flow modelling (Sterman, 2000). The paper highlights the application of these methods for analysis of sustainable improvement scenarios and transition pathways in the Baltic coastal case (Figure 1) with its multiple change drivers.

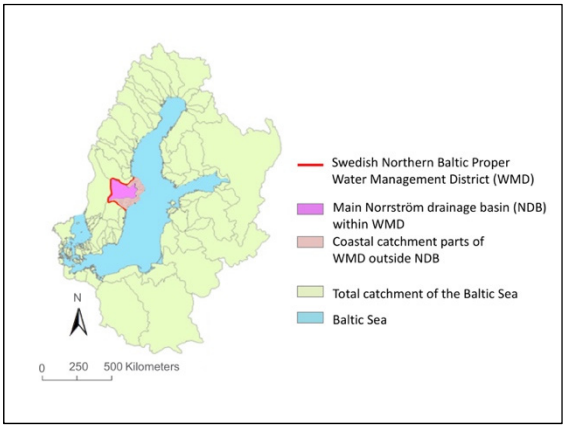


Figure 1. Location and extent of the Swedish Northern Baltic Proper Water Management District (WMD) and the main Norrström Drainage Basin (NDB) and other coastal catchment parts within it.

2. Methods

The methods used for the Baltic coastal case study include: A) Mechanistic coastal-system simulations of water quality and ecosystem status responses to various climate and land-sea nutrient management scenarios, using the modelling approach of Vigouroux et al. (2019). B) Participatory co-creation of Causal Loop Diagrams (CLDs; for the method, see e.g. Tiller et al. (2016)), used as qualitative mental maps of the perceptions of main land-sea change drivers and interactions by multiple stakeholders, representing different land-coast-sea sectors and perspectives. C) CLD unification and further development to a Fuzzy Cognitive Map (FCM; for the method, see e.g. Kosko (1986)) that, after stakeholder validation, is used for formulation and semi-quantitative analysis of land-sea interaction and change scenarios. D) Stock-flow Systems Dynamics (SD) modelling (for the method, see e.g. Sterman (2000)) of key quantifiable parts of the FCM, used for fully quantitative scenario analysis, based on and further developing previous model results for equilibrium interactions in the specific Baltic case (Baresel and Destouni, 2005).

The modelling approach of Vigouroux et al. (2019) has been used for the mechanistic simulations of coastal water quality and ecosystem status (Method A) with focus on the Himmerfjärden Bay as part of the Baltic case study (Figure 2).

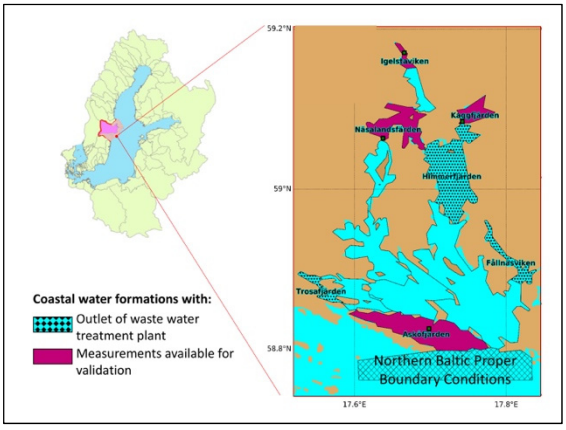


Figure 2. The Himmerfjärden Bay location and spatial configuration in relation to the Swedish Water Management District on land (Figure 1) and the coastal boundary to the marine basin of Northern Baltic Proper.

From available hydro-climatic data, three different climate scenarios have been formulated and used to drive the Himmerfjärden Bay simulations, representing observed near-past conditions of: dry-cold, dry-warm, and wet-warm years. Moreover, five nutrient and eutrophication management scenarios have been simulated for each representative hydro-climatic year scenario. The management scenarios include: (0) The base case of current conditions with no additional management measures; (1) Reduced nitrogen and phosphorus (P) loads from land by 50% (achieved by inland measures for both point and diffuse sources); (2) Aerobic coast conditions with no internal P loading (achieved by local coastal measures, e.g., of artificial oxygenation or chemical binding); (3) Good ecological status at the sea boundary (achieved by measures in other coastal areas and the sea); (4) Combined land and sea measures (1) and (3).

For the linked methodological chain of CLD, FCM and SD model development (Methods B-D), relevant stakeholders from land, coast, and sea sectors have been

engaged in six thematic sector workshops. In these, a CLD has been co-created by the stakeholders in each sector workshop, representing their perceptions of the key cross-sector and land-sea interactions for coastal water quality and ecosystem status in the studied Baltic case (Figure 1). In a follow-up, multi-sector workshop, stakeholders from the previous sector workshops have also jointly checked, adjusted, and validated the FCM development and unification from the different sector CLDs done by the study authors. The latter have further identified main quantifiable parts (based on available data and mechanistic models/results) of the FCM for consideration in the fully quantitative SD modelling and scenario analysis towards identification of possible synergistic measures for achieving the required improvements in coastal water quality and ecosystem status.

3. Result exemplification and discussion

Figure 3 shows results for Chlorophyll a (Chl a) from the mechanistic physical-system simulations of coastal change scenarios for the Himmerfjärden Bay (Figure 2). The results are shown in terms of the proportion of coastal area reaching good component status (in terms of the EU Water Framework Directive) with regard to the Chl a component under the different hydro-climatic and management scenarios. Overall, the mechanistic simulation results show that both land-based and sea-based measures can improve the coastal conditions, to different degrees for different water quality and ecosystem status components. Furthermore, the prevailing hydro-climate can considerably affect the efficiency of management measures.

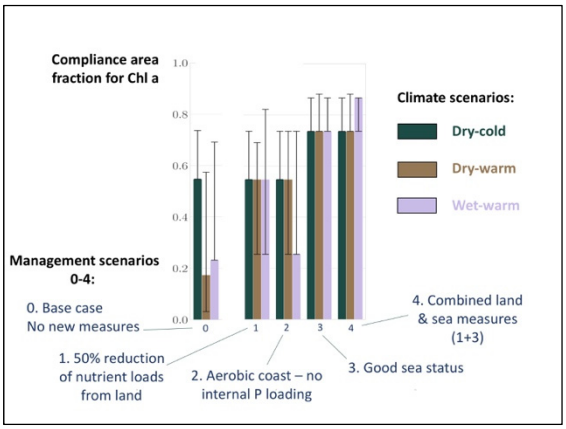


Figure 3. Proportion of coastal area reaching good component status for Chlorophyll a (Chl a) under different simulated hydro-climatic and management (0-4) scenarios. Whiskers indicate the status classification uncertainty for ±10% status variation around average status class.

Figure 4 further shows a conceptual interaction model, developed through the methodological CLD, FCM and SD chain, in terms of main flows of total nitrogen through and among key sectors and systems for coastal water quality and ecosystem status in the studied Baltic case. The nitrogen flows are quantifiable for this case based on previous interaction modelling and results for equilibrium conditions by Baresel and Destouni (2015). In the present, still ongoing study, these equilibrium conditions represent an initial system state that is perturbed in scenarios of different climate, policy, socio-economic change drivers. These drivers act on and through the different sector and natural subsystem components (stocks) and associated nitrogen flows in the SD model (Figure 4, with analogous interaction conceptualizations developed, used and coupled also for water and phosphorus). Such scenario analysis can trace the propagation of change impacts, feedbacks, and management implications through the whole multi-sector system. It also links to the mechanistic physical-system modelling (Figure 3) by its aim to identify synergistic cross-sectoral measures that can yield the measure effects required for achieving the coastal water quality and ecosystem status improvements quantified as possible in that modelling.

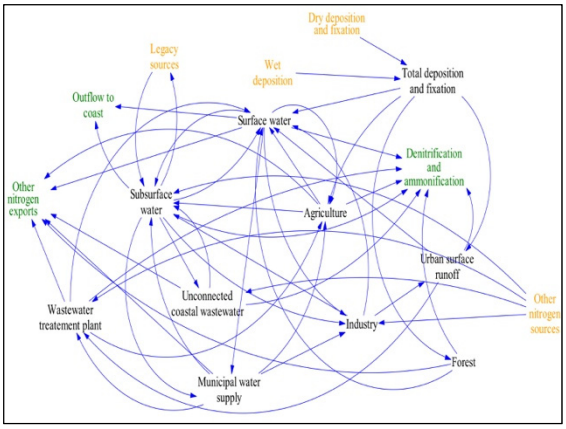


Figure 4. Conceptual model of stakeholder-identified key cross-sectoral nitrogen flow interactions and feedbacks for coastal water quality and ecosystem status.

References

Baresel C., Destouni G. (2005) Novel quantification of coupled natural and cross-sectoral water and nutrient/pollutant flows for environmental management, Environmental Science & Technology, 39, 16, pp. 6182 – 6190

Kosko B. (1986) Fuzzy cognitive maps, Int. J. Man-Mach. Stud., 24, 1, pp. 65-75

Sterman J.D. (2000) Business Dynamics: Systems Thinking and Modeling for a Complex World, Irwin/McGraw-Hill, pp. 982

Tiller R.G., De Kok J.-L., Vermeiren K., Richards R., Van Ardelan M., Bailey J. (2016) Stakeholder perceptions of links between environmental changes to their socio-ecological system and their adaptive capacity in the region of Troms, Norway, Front. Mar. Sci., 3, Art. 267

Vigouroux G., Destouni G., Jönsson A., Cvetkovic V. (2019) A scalable dynamic characterisation approach for water quality management in semi-enclosed seas and archipelagos, Marine Pollution Bulletin, 139, pp. 311–327

Declining oxygen in the global ocean and coastal waters

Marilaure Grégoire and the IOC-Unesco Global Ocean Oxygen Network (GO2NE) group

MAST research group (Modelling for Aquatic Systems) Freshwater and OCeanic science Unit of reSearch (FOCUS), Department of Astrophysics, Geophysics and Oceanography (AGO), University of Liège, Belgium, (mgregoire@uliege.be)

Since about 1960, ocean deoxygenation is occurring in the coastal and global ocean and is expected to worsen in a warming world with consequences on living organisms and on regional and global budgets of essential elements.

Better understanding of the deoxygenation process can be achieved by access to accurate observations and to furthering the reliability and coupling capabilities of physical, biogeochemical, plankton and benthic foodweb, and upper trophic level models. Rapid advancement is being made in each of the modeling types, as well as in how best to couple them, in order to generate “climate to fish” models (e.g. Rose et al. 2010) that include oxygen effects. A regular monitoring of the state of the ocean with respect to oxygen based on observations and modelling offers new knowledge on the fundamental processes like global circulation, photosynthesis, respiration and interactions with the atmosphere. Oxygen maps (climatologies) are regularly produced for the global ocean based essentially on ship based data (e.g. Stramma et al., 2008, Schmidtko et al., 2017). Once quality checked, the oxygen time series delivered by Argo floats have the potential to enhance these climatologies by providing a high frequency signal. The lack of openly available oxygen data from the coastal ocean in a centralized database prevents a similar global mapping of oxygen for the coastal ocean. This would be needed in order to update the inventory of Diaz and Rosenberg (2008) and to reassess the state of deoxygenation in coastal waters.

The success of combating deoxygenation relies on our capacity to understand and anticipate its consequences in an environment affected by local, regional, and global processes. State-of-the-art models have capabilities to simulate the deoxygenation process in the global and coastal ocean, and their parameterizations and skill (validation) should continuously evolve and improve. Model development needs new observations and dedicated experiments, in particular in low oxygen and anoxic waters that are particularly challenging to measure and to model. Oxygen levels act as a “switch” for nutrient cycling and availability. The detailed nature of these thresholds and their ecological and biogeochemical implications are still a matter of intense scientific investigation.

In this presentation, we will address the deoxygenation issue in the coastal and world ocean with specific examples taken from the Black Sea.

Changes in flood risk at a range of scales - Globe, Europe, Baltic Sea Basin

Zbigniew W. Kundzewicz
Institute for Agricultural and Forest Environment, Polish Academy of Sciences, Poznań, Poland
(kundzewicz@yahoo.com)

1. Introduction

Despite all the gigantic investments on flood defenses, flooding remains a serious problem at any spatial scale – of the Globe, the European continent, and the Baltic Sea Basin. Damages caused by floods continue to increase, so that flood risk reduction has become a widely recognized priority. Floods constitute a burden, not only because of the high economic and social damage but also because of the costs of safety measures and structural flood defenses in particular. The main reasons for the increasing flood risk are: presence of settlements and the growing value of assets in flood-prone areas; climate change as well as land-use and land-cover change.

The term "risk" is being used in different ways in different situations, where an object of value is at stake and where the outcome is uncertain. Typically, risk is assumed to be a function of hazard, exposure and vulnerability. Hazard can be interpreted as the potential occurrence of a physical event, such as flood, that may cause adverse impacts. Exposure is the presence of people and assets in places and settings that could be adversely affected. Vulnerability is the propensity or predisposition to be adversely affected.

The present contribution discusses changes in components of flood risk at a range of spatial scales – from global to continental (Europe) to regional / sub-continental (Baltic Sea Basin).

2. Drivers of flood risk change

The flood risk depends on many climatic and non-climatic drivers, natural and anthropogenic. Principal climatic drivers are: precipitation (total, phase, seasonality and intensity), temperature, and snow melt. Among causes that intensify the adverse consequences of floods are: development of areas near watercourses and accumulation of wealth and sensitive objects in such areas, modifications of the landscape (river training works, urbanization, loss of flood plains and wetlands, deforestation, changes in agricultural land use, increase in soil compaction and impervious surfaces, etc.), as well as a lack of risk awareness (partially on account of the excessive trust in structural flood control measures). Urbanization and sealing of ground surface significantly increase surface water runoff and decrease water storage in the drainage basin. However, widespread "resistance" efforts are undertaken to counterbalance the growing "load".

3. Observations

High material losses generated by floods have been recorded recently many times, in both less developed and industrialized countries. Moreover, destructive floods continue to kill people, especially in developing world and bring human suffering wherever they hit (Kundzewicz, 2019b). In some countries, recurrent flooding of cropland has taken a heavy toll in terms of lost agricultural production, food shortages, interrupted food supplies, and undernutrition (Kron et al., 2019). In this contribution, observed changes in flood hazard, related to flood magnitude, frequency, timing, damage as well as changes in flood generation mechanism will be discussed, as also changes to exposure and vulnerability.

The nature of disastrous floods seems to have changed recently, with increasing frequency and amplitude of heavy precipitation and flash and urban floods, as well as riverine and coastal flooding. There is more room for water vapor in the warmer atmosphere, hence potential for intense precipitation and floods has been increasing. Indeed, higher and more intense precipitation has already been observed in many (but not all) areas of the globe.

However, the climate track in flood hazard is indeed complex and not ubiquitous. It may depend on the flood generation mechanism.

Owing to the growing anthropopressure, activities like urbanization, construction of roads, deforestation, agricultural land expansion, and reclamation of wetlands and lakes have been progressing, worldwide. This has reduced the available water storage capacity in river basins, increased the value of the runoff coefficient, and aggravated flood hazard and flood risk. Flood loss potential has ubiquitously increased – there is simply more to lose.

The present contribution reviews major tendencies in flood risk and flood hazard at a range of scales, drawing from studies in trend detection in global and pan-European data (Kundzewicz et al., 2005; Madsen et al., 2014; Mangini et al., 2018; Blöschl et al., 2017) as well as indicating sub-national risks, e.g. related to flash urban floods in Northern Poland.

However, there has been no persuading and conclusive and general finding as to how climate change affects flood behavior, in light of data observed so far, except for some indications of regional changes in timing of floods in some areas, with increasing late autumn and winter floods (caused by rain) and fewer ice-jam-related floods in the warming climate. The natural variability in observation records is overwhelming.

In addition to climate change component, there is an important driver contributing to non-stationarity of flood hazard and risk. It is the climate variability link, related to quasi-periodic oscillation in the atmosphere-ocean system. It was found to considerably influence the probability of occurrence of destructive water abundance in many regions (Kundzewicz et al., 2019a).

However, in general, it is difficult to disentangle the climatic change component in maximum river flow or flood damage records from strong natural variability and anthropogenic, non-climatic changes.

Economic losses from floods have greatly increased, principally driven by the expanding exposure of assets at risk. However, it is rarely possible to attribute rain-generated peak streamflow trends to anthropogenic

climate change over the past several decades (Kundzewicz et al., 2014).

Nevertheless, Kundzewicz et al. (2018b) showed that the number of large floods has been increasing in Europe.

4. Projections

Many existing studies of flood hazard projections demonstrate the likely increases in both frequency and magnitude of flood events in many, but not all regions, in the future, due to a combination of anthropogenic and climatic factors. Yet, there are multiple factors driving flood hazard and flood risk and there is a considerable uncertainty in our assessments, in particular regarding projections for the future.

The tendency of heavier precipitation, consistent with Clausius-Clapeyron equation, is expected to strengthen in the warmer world, directly impacting flood risk. However, there is a large difference between flood hazard projections obtained by using different scenarios and different climate and hydrological models (Kundzewicz et al., 2017). Therefore, common-sense changes to flood-related design rules, aimed at flood risk reduction, have been introduced in some countries of Europe, based more on precautionary principle rather than on robust science. The design flood was adjusted upward in light of projections for the warmer climate.

Undoubtedly, in the warming world, there is a growing risk of coastal flooding associated with storm surge under sea level rise, also in the Hel Peninsula in Poland, where the present conference is held.

However, it is a robust statement that, in general, today's climate models are still not good enough at producing reliable local climate extremes due to, inter alia, inadequate (coarse) resolution. There is hope that, with improving resolution, models will be able to grasp details of extreme events in a more accurate and trustworthy way. It is necessary to continue examination of the updated records of flood-related indices, trying to search for changes that influence flood hazard and flood risk in river basins.

In this contribution, projected changes in intense precipitation and high river discharge are reviewed and discussed at a range of spatial scales.

5. Flood risk reduction

Risk reduction, in the spirit of the Floods Directive of the European Union, requires dedicated efforts to decrease each one of the three components of risk: hazard, exposure and vulnerability. Increases in hazard (natural and anthropogenic) can be difficult and costly to reduce. However, changes in exposure and vulnerability are predominantly anthropogenously-based as people either move into harm's way and increase the damage potential or see potential harm move closer to them as a result of technological measures (Kron et al., 2019).

Some deleterious impacts of floods are preventable or at least can be reduced because of the opportunity of primary prevention through existing, and – in many places – affordable, technologies such as early warning systems, some flood defenses, and risk transfer options. Also awareness raising and education can be effective in protecting people from adverse impact of floods.

There are multiple flood-risk–management strategies. Unfortunately, we neither manage keeping destructive waters away from people (defense strategy) at all times nor keeping people away from destructive waters (prevention strategy). It is, therefore, necessary to embark on a diversified portfolio of approaches. Flood mitigation focuses on decreasing the consequences of floods through measures within the vulnerable area. Flood preparation embraces flood forecasting and warning systems, disaster management, and evacuation plans. Fast recovery after a flood event is enhanced by prompt reconstruction plans (providing a window of opportunity for flood proofing the new buildings or relocating inhabitants from unsafe to safer areas) as well as compensation or insurance systems (Kundzewicz et al., 2018a).

According to Willner et al. (2018), considerable adaptation efforts will be required in most of the world in order to preserve future high-end river flood risk at present levels.

References

Blöschl, G. et al. (2017) Changing climate shifts timing of European floods. *Science* 357, 588–590,

Kron, W. et al. (2019) Reduction of flood risk in Europe - Reflections from a reinsurance perspective. *J. Hydrol.* 576: 197-209.

Kundzewicz, Z. W. et al. (2005) Trend detection in river flow series: 1. Annual maximum flow. *Hydrol. Sci. J.* 50(5), 797–810.

Kundzewicz, Z.W. et al. (2014) Flood risk and climate change: global and regional perspectives. *Hydrol. Sci. J.* 59(1), 1-28.

Kundzewicz, Z.W. et al. (2017) Differences in flood hazard projections in Europe - their causes and consequences for decision making. *Hydrol. Sci. J.* 62(1), 1-14.

Kundzewicz, Z. W. et al. (2018a) Flood risk reduction: structural measures and diverse strategies. *Proceedings of the National Academy of Science of USA (PNAS)* 115(49), 12321–12325.

Kundzewicz, Z.W., Pińskwar, I., Brakenridge, G.R. (2018b) Changes in river flood hazard in Europe: a review. *Hydrology Research* 49(2), 294-302.

Kundzewicz, Z.W.; Szwed, M.; Pinskwar, I. (2019a) Climate variability and floods-A global review. *Water* 11(7), 1399.

Kundzewicz, Z.W. et al. (2019b) Flood risk in a range of spatial perspectives - from global to local scales. *Natural Hazards and Earth System Sciences* 19(7): 1319-1328.

Madsen, H et al. (2014) Review of trend analysis and climate change projections of extreme precipitation and floods in Europe, *J. Hydrol.* 519, 3634–3650.

Mangini, W. et al. (2018) Detection of trends in magnitude and frequency of flood peaks across Europe. *Hydrol. Sci. J.* 63(4), 493-512.

Willner, S.N. et al. (2018) Adaptation required to preserve future high-end river flood risk at present levels. *Sci. Adv*. 4 (1).

A Philosophical View of the Ocean and Humanity

Anders Omstedt

Department of Marine Sciences, University of Gothenburg, Sweden (anders.omstedt@marine.gu.se)

1. Introduction

The ocean and its coastal seas are increasingly threatened by relentless anthropogenic pressures. Natural scientists are struggling to address these threats, and doing so requires a broad understanding of various natural science disciplines, such as oceanography, meteorology, hydrology, geology, geography, chemistry, and biology, but also of human behavior from disciplines such as literature, psychology, history, philosophy, law, sociology, political science, and economics. What is certain is that human society must change its behavior with the goal of achieving sustainable interaction with the ocean.

The ocean's services to humankind are enormous and fundamental, and their value is inestimable. A change in human behavior towards the ocean should be based on something other than simplistic and reductive economic costing. The change needs to be based on a fundamental shift in our understanding of ocean and human values and how we interact with one another and with our environment.



Photograph 1 and 2. What is our relationship to the ocean? (Photo: Hillevi Nagel).

The presentation illustrates a recent book (Omstedt, 2020) about the ocean and about the future. It is written in two modes, a concerned analytical scientific mode and an intuitive artistic mode in which the ocean is given a voice. The disconnection in the relationship between human dependency on and treatments of the ocean is examined in a dialogue between these two modes. The book illustrates how science and the arts can be connected to increase our awareness of the state of the ocean and support behavioral change.

2. Science a knowledge source for solving problems

Scientists are trained in critical, analytical thinking and strive to deepen their understanding by exploring their fields in ever greater detail, at the same time as society has become increasingly specialized. The scientific method is strong, and it has made great progress in recent centuries. However, the management of the ocean and its coastal seas is failing, and these areas face increasing threats from intense anthropogenic pressures. Society expects more from the scientific community, and trans-disciplinary programs have accordingly been initiated to address global grand challenges. Large efforts have been made to formulate and take steps towards a sustainable global pathway e.g. through the United Nations 2030 goals. The United Nations has also declared 2021-2030 as the decade of ocean science for sustainable development.

3. The arts a knowledge source for humanity

Humans are connected to one another through their emotional life, which is often expressed in the arts. The arts involve many aspects of creativity and entail thinking in a way different from analytical thinking and using a different logic but addresses often similar aspects such as human conditions and relation to the environment. While the arts touch on individual experience, they derive much of their power from what humans have in common with one another and with nature. The arts are free from scientific restrictions and can give free voice to our emotional life.

Our relation to nature has been illustrated in many poems and novels. Samuel Taylor Coleridge's 1798 poem, *The Rime of the Ancient Mariner*, treats how the senseless killing of an albatross brought punishment in the form of isolation and death in life and can today be looked on as a future scenarios what can happen when we misuse the ocean and fill it with plastics: Dying sea birds filled with plastics garbage can help us to understand our dysfunctional state of mind that lack the inspiration or spirit needed to serve the ocean. Perhaps marine problems are mental problems, and humans need to better understand their role on Earth before they can live in balance with nature?

The epic poem from Finland, The Kalevala, originated in oral tradition but has since been transcribed. The first chapter describes how everything began and how the great singer Väinämöinen was born. In the beginning, Ilmatar, the goddess of the air and nature, decided to enter the water, where she became pregnant by the sea. After many years and many complications, she gave birth to Väinämöinen, the bold bard about whom The Kalevala tells many stories. The Kalevala originated in oral epic poetry collected in Karelia, eastern Finland and north-western Russia, by Lönnrot in the 19th century. It forms one of the most important works in Finnish literature and provided strong inspiration. Maybe storytelling is as important for mental health as planktons are for the ocean?

How scientific truth comes into conflict with society is illustrated in Henrik Ibsen's 1882 play An Enemy of the People. The conflict starts with Dr. Stockmann investigating the water in the city spa and ends with destruction. Ibsen's drama about a whistleblower is still

relevant today when scientists or other experts try to communicate new results that come into conflict with society's beliefs or economic and social interests. The drama demonstrates how new knowledge can become dangerous for the society.

In The Old Man and the Sea by Ernest Hemingway, the shift from sustainable to unsustainable fishing was already imagined in 1952, illustrating an attitude change towards the ocean going into an era of destructive overfishing.

In 1962, Rachel Carson published her famous book Silent Spring about the increasing danger of using pesticides such as DDT to fight insects. The book was dedicated to Albert Schweitzer who had written: 'Man has lost the capacity to foresee and to forestall. He will end by destroying the earth'. Few books have made such an impact on the general public's awareness of environmental degradation. But still new and damaging chemicals awash our seas.

4. Connecting science and the arts

By the end of this century it is estimated that the human population will have grown to over 10 billion people, and by 2050 almost 70% are expected to be living in urban areas and megacities increasingly alienated from the marine environment with its pervasive plastic contamination. Today's young generation will need to respond too many of today's alarming warning signs. Perhaps the most important question to be addressed is how humans can direct marine development onto a sustainable path while preserving their humanity.

With a growing global population and increasing urbanization, there will be increased competition for resources and space. This may lead to alienation and increased marine destruction. In climate change scenarios, one speaks of a future of increased fragmentation. A green global world that is able to address rather than surrender to future challenges will require new and different values. Antidotes to narrow thinking, fragmented vision, alienation, despair, and fear involve the integration of curiosity, courage, listening, hope, and simplicity in daily life.



Photograph 3. How can science and the arts meet?
(Photo: Sabine Billerbeck).

5. Summary or orchestration

The communication strategy of simply sharing more and more facts related to the ocean and coastal seas is not enough to ensure marine improvements. Something else is needed that can add emotional resonance. The humanities and art forms such as the visual arts, dance, theatre, literature, storytelling and film are modes of expression and communication that can imbue science with emotion and promote changes in attitudes. Presenting marine science without connecting it to human or societal values could even increase our alienation from the sea.

The ocean and humans utter many tones but melody is often missing. Beauty and vulnerability are fundamental to both the ocean and humans, but humans seem resistant to the inspiration they need. Social and emotional fragmentation and business-as-usual will destroy the planet. Rethinking and listening are needed. Stand up for curiosity and stand up for health. Be proud of the UN 2030 Agenda and go for it! Harmony is the utmost gift that will create an inspiring symphony that serves us, and the ocean.



Photograph 4. Ocean we need for a future we want
(Photo: Hillevi Nagel).

References

Omstedt, A. (2020). A Philosophic View of the Ocean and Humanity. Springer Nature, ISBN 978-3-030-36679-7, in press.

Connecting science, society and policy: experience of a small country

Tarmo Soomere

President of Estonian Academy of Sciences, Tallinn, Estonia (tarmo.soomere@akadeemia.ee)
Professor of Coastal Engineering, Head of Wave Engineering Laboratory, Department of Cybernetics, School of Science, Tallinn University of Technology, Tallinn, Estonia (soomere@cs.ioc.ee)

One of the reasons behind the recent skidding of society to a post-truth world is that both the pattern of knowledge production and the pattern of using this knowledge have been radically altered. A strong chain, localized in space and configured in time, once connected a scientist in a laboratory with an inventor in an adjacent room, then involved an engineer in a neighboring house, and ended up at a factory next street. The scientist was paid from the profit of the factory.

The production of knowledge is today disconnected from its use in both space and time. Many excellent scientists contribute to the global knowledge pool. Numerous inventors, engineers and entrepreneurs fish, in parallel, for ideas in this pool. The successful catches are converted into new “cool” items. The subsequent production and sales generate public tax money, from which a large part of science is funded.

It is natural that society reacts to these rapid alterations. The described disconnection creates a chance for “alternative facts” to spread and space for reprehensible brokers to survive. There are ways to change this situation and to build reasonable science-society and science-policy interfaces. The starting point is the understanding in the academic landscape that it is the duty of scientists to explain to society the core of the changes, to communicate in a comprehensible manner the meaning of uncertainties (that are particularly large in environmental issues) and the intrinsic nature of continuous improvement of scientific knowledge. These efforts are only successful if the responsible people set an example of knowledgeable use of the message of science.

I shall present a selection of efforts to channel the output of research to policy-making in Estonia and on the European level based on examples of communication of marine science. We make use of favorable features of the small country and unique solutions that rely on high connectivity of society. Science-policy interface functions at various levels: institutional, formal ad hoc activities and even more effectively via personal contacts of scientists with policy-makers and governmental officers. To ensure that the message from academia remains undistorted until the decision-making level, efforts are made towards bringing together leading scientists and policy-makers.

Chemical contamination of the Baltic Sea – status and future perspectives

Emma Undeman

Stockholm University Baltic Sea Centre, Stockholm, Sweden (emma.undeman@su.se)

1. Chemical use in a changing world

Chemicals emitted partly or exclusively as a result of human activities are present as contaminants in the Baltic Sea. Historically, well-known pollutants such as PCBs and DDT have severely impacted wild-life populations in the Baltic Sea. Implementation of strict regulations for a range of pollutants and technical development to treat and prevent waste streams during the last decades of the 20th century have resulted in a recovery of the threatened populations.

At the same time, the world has changed. We are nowadays aware of many risks associated with the use of chemicals, and have developed legislations and methodologies for risk assessment. Yet, we now use a larger number of chemicals, in a broader range of applications, and in increasing volumes.

Because of the opposite trends for legacy pollutants and emerging chemical threats, no one can answer the seemingly simple question: is the chemical pollution of the Baltic Sea increasing or decreasing?

And because of lacking information regarding use and emissions of most chemicals on the market and those that are unintentionally formed/released (and their degradation products), combined with limitations of currently employed analytical methods, the current mixture of anthropogenic contaminants in the sea is not well characterized.

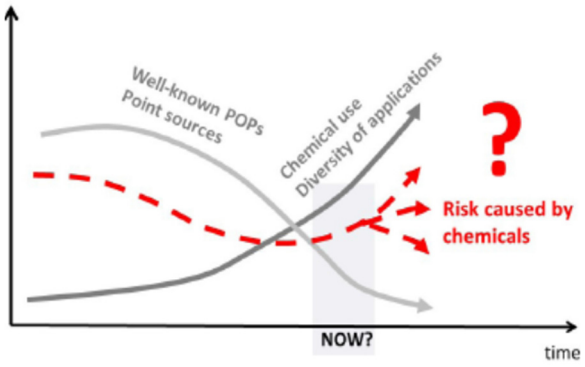


Figure 1. Emissions of well-known pollutants have decreased over time, whereas modern chemical use and diversity of applications increase, and with that the potential risk. Sobek and Undeman (2019)

2. Challenges for the management of chemicals in the Baltic Sea

In this presentation, I give an overview of how the status with respect to chemical pollution of the Baltic Sea is currently evaluated and discuss some of the challenges that chemicals management face: the difficult task of identifying chemicals to prioritize, the slow pace of chemicals risk assessment, our limited capacity to monitor chemicals in the field, and the difficulty of considering combined effects of all chemicals comprising the mixture in the sea on all plausible end points.

Research is ongoing to meet these challenges, and a modernization of how society manages chemicals to be able to balance the benefits of the chemicals we use and the risk that they will have adverse environmental effects is warranted.

Several science-based approaches have been suggested that could improve chemicals management, e.g. to give persistence of a chemical in the environment stronger emphasis in risk assessments as potential effects of stable compounds are, as history has taught us, not easily reversed. Novel analytical methods have been developed that can be used to screen for a large number of chemicals in environmental samples at the same time, and help identify chemicals that accumulate in the Baltic Sea. Exposure modelling exercises have concluded that better information regarding production volumes and use of the thousands of chemicals on the market is needed to improve predictions and ranking of chemicals based on environmental concentrations.

3. Future changes of environmental conditions in the Baltic Sea influences transport and fate of anthropogenic chemicals

Another challenge for chemicals management is that future changes in environmental conditions, such as climate and biogeochemical processes, also may influence chemical transport and fate, and hence the risk of chemical concentrations exceeding effect thresholds in the field. In particular, hydrophobic organic contaminants have a tendency to partition from air and water into organic phases, making such environmental matrices important transfer vectors and sinks for these chemicals. The transport and fate of hydrophobic organic contaminants in the environment is hence closely linked to the cycling of organic carbon (Nizzetto et al. 2010).

I here give examples of how future development of climate change and carbon cycling in the Baltic Sea and its catchment may influence processes such as river transport, air-water exchange, downward transport via sedimentation and degradation in the water column.

References

Sobek, A., Undeman, E. (2019). Tunnel vision in current chemicals management cannot deal with the unknown risk of synthetic chemicals in aquatic systems. Acta Limnologica Brasiliensia, 31, e106.

Nizzetto, L., Macleod, M., Borgå, K., Cabrerizo, A., Dachs, J., et al. (2010). Past, present, and future controls on levels of persistent organic pollutants in the global environment. Environ. Sci. Technol., 44, 17, 6526-6531

The coastal processes and management in the southern Baltic Sea

Grzegorz Uścinowicz

Polish Geological Institute - National Research Institute, Marine Geolog Branch, Kościerska 5 st., 80328, Gdańsk, Poland e-mal: grzegorz.uscinowicz@pgi.gov.pl

The South Baltic is characterized by three basic types of the coast, within which a set of common processes forming their shape as well as a range of individual ones can be identified for each type.

The most spectacular changes can be observed within the cliff coasts. They manifest themselves through raising strong emotions mass wasting processes of various forms: from simple earth slumps, topples and debris flows through slightly more complex landslides formed within homogeneous sediments, to complex landslides threatening the infrastructure.

The barrier coasts for a change, commonly associated with wide beaches, are susceptible to the influence of storm surges causing erosion of the dunes and in extreme form even breaking the barrier and in results flooding of hinterland low-lying areas.

In opposition to the above, somehow remain alluvial coasts (wetlands), which due to their marginal occurrence in the South Baltic landscape are often overlooked in discussions about the coast although forms an important ecosystems around the lagoons.

The above short remarks about changes in the coastline of the Baltic Sea are based on observations that almost anyone can make - independently of experience and correctness of assessment of causes and effects. At the same time, in the "universal consciousness" there is almost no understanding that the marine coastal zone is a very complex system.

In such geosystem, seemingly clear processes that can be observed with the naked eye are often ambiguous, resulting from unobvious phenomena and carrying unexpected, often distant in time effects.

There are more and more facts that the coastal zone of the sea is much more complicated that we thought before.

Simultaneously, coastal areas have always been important for economic and social reasons. They are subject to pressure from settlements, touristic industry and other branches of economy and as such are an important part of socio-economic development. Therefore, the study of natural processes related to the geological conditions of the coast is becoming a growing challenge in the development and management of the coastal zone. Especially in the face of growing requirements related to climate change, which force us to adapt and mitigate instead of a hard confrontation with the forces of nature.

Social perception of the Baltic Sea in Poland

Marcin Weslawski

Institute of Oceanology of Polish Academy of Sciences, Sopot, Poland; (weslaw@iopan.gda.pl)

Deep environmental crisis of the coastal Baltic waters that resulted in massive habitat degradation, coastal fishery crisis and ban for water sports happened in 1975-1990.

Since that time, and after the EU membership the environmental situation improved with massive waste water treatment, new investments and modernization of agriculture and industry. Recent years brought new stress to the Baltic - diminished North Sea exchange, rapid warming and spread of the anoxic zones as well as the new crisis in the cod fishery.

The Polish general public was traditionally not very much concerned about the Baltic state, yet in recent years the environment - together with the political pressure of the fishery become an important part of the public debate.

Opposing stakeholders are fishermen who want to declare Baltic an ecological catastrophic region, while tourist operators are opposing this narrative. Both sides seek support among politics and scientists to support their oppinions.

Scientists, trying to stay "value free" and objective are having difficult time as those who use the taxpayers money and shall report their view.

Topic 1

Salinity dynamics in the Baltic Sea

Baltic+ Salinity Dynamics: Towards a new view on the Baltic Sea surface salinity

Pekka Alenius[1], Laura Tuomi[1], Petra Roiha[1], Verónica González-Gambau[2], Estrella Olmedo[2], Cristina González-Haro[2], Antonio Turiel[2], Justino Martínez[2], Carolina Gabarró[2], Manuel Arias[3], Rafael Catany[3], Diego Fernández[4] and Roberto Sabia[4]

[1] Finnish Meteorological Institute, Helsinki, Finland (pekka.alenius@fmi.fi)
[2] Barcelona Expert Center & Institute of Marine Sciences, CSIC, Barcelona, Spain
[3] ARGANS Ltd, Plymouth, United Kingdom
[4] European Space Agency, Frascati, Italy

1. Background

The Baltic Sea is a semi-enclosed, seasonally variable brackish water sea that is very vulnerable to environmental changes. Ecosystem health of the sea is of concern to the Baltic Sea countries where a population of about 85 million persons affect the sea.

Baltic Sea conditions have been studied and monitored for over 100 years with regular, though spatially and temporally rather sparse, ship observations since 1898. Remote sensing has been used for decades to follow the ice conditions, surface temperature and algal blooms and to get an instantaneous view of the whole sea at once. However, salinity conditions that are important for the horizontal and vertical gradients and the dynamics in the Baltic Sea have remained outside of such a quick overall synoptic view so far.

2. Surface salinity in the Baltic Sea

Salinity field of the Baltic Sea depends on the water exchange between the Baltic Sea and the North Sea and freshwater input from rivers and precipitation. The water balance is positive. Salinity dynamics are strongly driven by the occasional major saline inflows, which are not seen at the sea surface by current state of art observations. The surface salinity distribution depends much more on the freshwater input. There are small SSS gradients between the sub-basins (Fig. 1). The largest horizontal salinity gradients are in the entrance of the Baltic Sea where they are too strong to be shown in the same figure with the internal gradients.

The deep-water salinity conditions have been studied a lot because they are strongly related to the main oceanographic dynamics and to the strong vertical stratification that causes environmental problems in the Baltic Sea proper deep-water. However, the surface salinity field is also of interest because it is linked e.g. to the marine ecosystem's freshwater tolerance. Surface properties of the water column are also connected to wind induced processes such as upwellings, movement of fronts and vertical mixing which alter water properties at least down to the halocline.

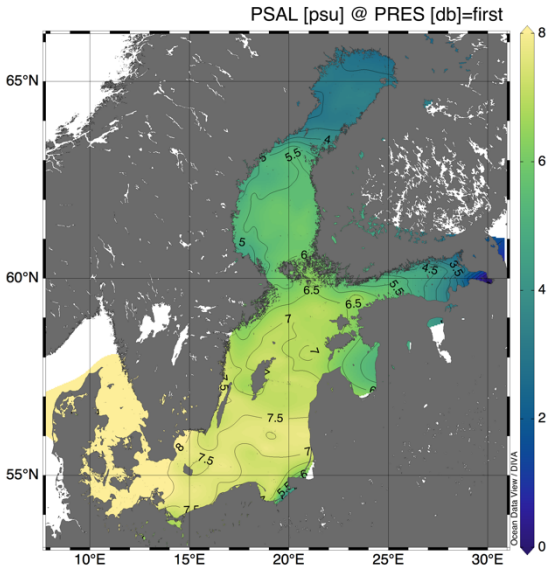


Figure 1. Rough estimate of the surface salinity distribution of the Baltic Sea obtained from HELCOM (www.helcom.fi) monitoring data (https://ocean.ices.dk/helcom/).

3. New way to observe the surface salinity

Satellite data has been routinely used to monitor the Baltic Sea surface, like ice conditions, temperature and algae blooms for decades. That data describes rather well the dynamics of the sea surface layer, but comparable synoptic salinity information with large spatial coverage is needed, too.

However, the Baltic Sea is one of the most challenging regions for the retrieval of surface salinity from L-band satellite measurements. Nowadays, available EO-based SSS products are quite limited over this region both in terms of spatio-temporal coverage and quality. This is mainly due to several technical limitations that strongly affect the L-band satellite brightness temperature (TB) measurements particularly over semi-enclosed seas, such as the high contamination by Radio-Frequency Interference (RFI) sources and the contamination close to land and ice edges. Besides, the sensitivity of TB to SSS changes is very low in cold waters and much larger errors are expected compared to temperate oceans. Moreover, salinity and temperature values are very low in this basin, which implies that dielectric constant models are not fully tested in such conditions.

During the last decade surface salinity remote sensing has developed a lot in the World Ocean and that has

encouraged to examine its use in the more challenging low-salinity marginal seas.

Within the ESA-funded project Baltic+ Salinity Dynamics lead by ARGANS Ltd (UK), Barcelona Expert Centre (BEC/ICM-CSIC, Spain) is developing innovative dedicated SSS product over the Baltic Sea from the measurements of the Earth Explorer SMOS (Soil Moisture and Ocean Salinity) satellite. Finnish Meteorological Institute participates in the validation of the product and giving expert knowledge about the salinity measurements and dynamics in the Baltic Sea.

During the first year of the project, 2019, BEC developed the algorithms that have allowed to generate the first regional SMOS SSS product (a 3-year time-series), which is currently under validation against in-situ measurements. Figure 2 shows two examples of SSS maps from April and July 2013, respectively. Generally, the observed SSS patterns are coherent with circulation inferred from altimetric maps, but there are still areas or regions where the product seem to be badly distorted and further work is needed to cope that.

Feedback from the users is most welcome (see link to Baltic+ website below) both to identify the limitations and to identify the possible use cases of the product. In any case additional technical developments will be addressed in a second version of the product. In 2020 our emphasis will be in assessing the performance of the system and in investigating the added value of the product to the scientific challenges that are related to salinity. This regional dedicated SSS satellite retrieval might bring new insights on annual trends of the SSS and on long-term salinity changes.

We hope that the product will also be useful as a reference for numerical model validation and for data assimilation. The potential scientific impact of this satellite SSS product in advancing on-going regional research initiatives like the Baltic Earth Working Group on Salinity dynamics will be discussed.

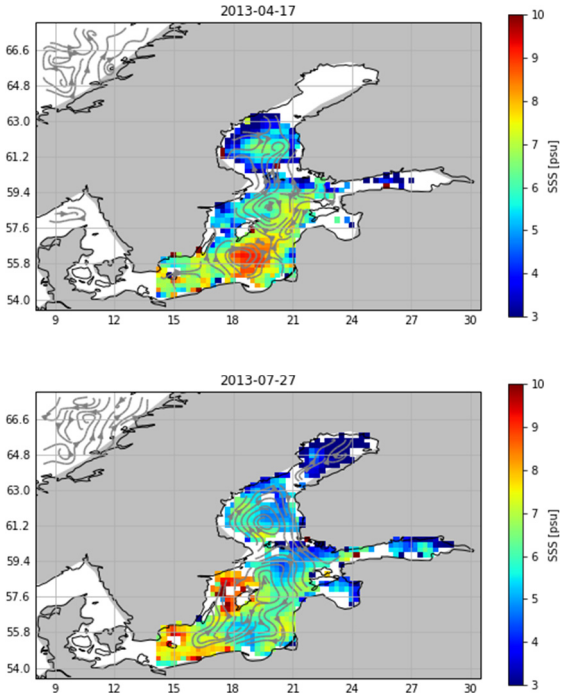


Figure 2. Color: Baltic+ SSS v1 product (9-days, 0.25 deg) in April 2013 (top) and July 2013 (bottom). Streamlines: Geostrophic velocity from CMEMS. The spatial coverage in some gulfs and straits is limited, mainly during the cold season. We are working to improve the coverage of SSS maps in a second version of the SSS product.

For further information on Baltic+ Salinity Dynamics see: https://balticsalinity.argans.co.uk/

An introduction to the SuFMix Project: “Turbulent mixing in the Slupsk Furrow”.

Anna I Bulczak, Daniel Rak, Jaromir Jakacki and Waldemar Walczowski

Institute of Oceanology, Polish Academy of sciences, Sopot, Poland (abulczak@iopan.pl)

1. Introduction and motivation for the project

Turbulent mixing in the ocean is essential for the regulation of the transport of heat, freshwater, biogeochemical tracers and therefore has strong implications for the Earth’s climate. Here we present an overview of the SuFMIX (Turbulent mixing in the Slupsk Furrow) project that has started in February 2020 and will last for the next three years. The aim of the project is to identify, describe and analyse the main mechanisms responsible for the vertical transport and mixing of waters in the Slupsk Furrow, in the area located in the southern Baltic Sea in the Polish Economic Zone (Fig. 1). This region, connecting western and eastern parts of the Baltic, is located on the main pathway of the inflow waters from the North Sea, which provide salt and oxygen to the deep waters, and therefore is of key importance for the Baltic circulation and ecosystem. The main emphasis of the project is to determine the contributions of the dynamic factors such as: internal waves, mesoscale eddies and surface waves, in the processes of vertical mixing in the Slupsk Furrow.

The key project’s research hypothesis states that internal waves and mesoscale eddies are significant driving mechanisms responsible for the salt exchange across the halocline in the tideless Baltic Sea. Internal waves force the vertical mixing of salt, heat and water masses at the scale of the entire basin (Thorpe, 2005). Mesoscale eddies are responsible for the transfer of energy and momentum through horizontal and vertical movement of waters and mixing. We argue that these phenomena are of great importance in the Slupsk Furrow where strong mixing and interaction with the bottom topography is expected to occur. Mesoscale eddies were often observed by the Institute of Oceanology Polish Academy of Sciences (IOPAS) at the Slupsk Sill and Slupsk Furrow (Piechura and Beszczyńska-Moeller, 2003; Rak and Wieczorek, 2012; Bulczak et al., 2016). Interaction with the sloping topography can cause an eastward movement of eddies and their gradual decay. This process can be a major source of mixing at the halocline and its role is underestimated (Reissmann et al., 2009). We hypothesize that internal waves may also contribute to the transport of dense waters above the Slupsk Sill and their mixing with the fresher ambient waters. These phenomena were often observed in the Baltic Sea but their contribution to the mixing is not known (Reissmann et al., 2009).

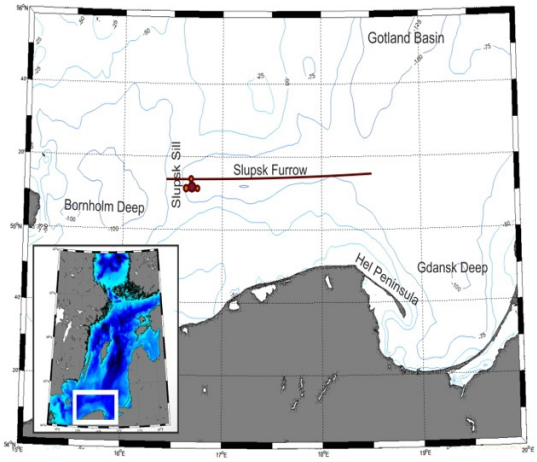


Figure 1. Left: Region of investigation. IO PAS R/v Oceania cruise track is shown in red. The locations of moorings are shown as red dots. The large meteorological-oceanographic buoy currently operating in the Slupsk Furrow is located in the centre, and the three moorings that will be deployed during the proposed project are placed around it forming a triangle.

2. Significance of the project

In the Baltic Sea very few studies analysed the effect of internal-waves mixing on turbulence and mixing in bottom boundary layer (BBL) (Reissmann et al. 2009). Turbulent mixing in the BBL, especially on the sloping topography, is expected to be one of the primary vertical transport mechanisms in stratified seas (Thorpe 2005) and therefore in the Baltic Sea. The long-term mooring observations suggest that other dynamical processes, such as narrow currents and mesoscale eddies, contribute to the deep water mixing (Reissmann et al. 2009). However, these processes are not yet fully understood. The greatest energy dissipation rates occur in the surface and bottom boundary layers and at the depth corresponding to the maximum location of the vertical density gradient (Bogucki and Garrett, 1993) and internal waves could significantly strengthen mixing there (van der Lee and Umlauf, 2011). However, our knowledge about this process is very limited due to unavailability of mixing measurements in the Polish Economic Zone.

3. The project concept

The project will consist of a combination of various components and methods: *in situ* measurements campaign (WP2), the process studies that analyse and interpret collected oceanographic data (WP3) and numerical modelling and analysis of modelled results (WP4) (Fig. 2). Reissmann et al. (2009) emphasized the ecological impact of deep water mixing and pointed out that there is not enough data to understand mixing caused by internal waves. Therefore, the most important part of the project will be devoted to gather data necessary to understand internal waves and explaining how they

contribute to the observed mixing and how this mixing affects deep water ventilation. Furthermore, an important part of the project consists of the formulation of the numerical methods for internal waves in the shallow waters of the Southern Baltic, in order to advance our understanding of internal wave generation, dynamics and mixing.

Various approaches to the problem will be applied. The experimental work will use a variety of *in situ* measurements dedicated to measure mixing strength, internal waves amplitudes and propagation, their contribution to the observed mixing intensity and the associated effects on the near-bottom ventilation. Underwater mooring arrays will be deployed in the Slupsk Furrow in a close proximity to the currently operating IO PAS meteorological buoy (Fig 1).

4. Preliminary results

CTD data from the Slupsk Furrow collected by IOPAS clearly indicated the existence and intensification of the mesoscale eddies (Zurbas et al., 2012). In February and November 2019 during IO PAS cruise in the Southern Baltic, an initial measurements of micro-scale turbulence were performed along the Southern Baltic. Profiles of the eddy kinetic energy dissipation rate reported different intensity of mixing across the southern Baltic (10^{-4}-10^{-9} W/kg). In the Slupsk Furrow an enhanced shear produced turbulence below the pycnocline (60-90 m) (Fig 2). In the Slupsk Sill the maximum mixing occurred close to the sea surface, decreased to the minimum at around 40 m, which was still above the pycnocline, and increased again in the narrow band of the upper pycnocline. To sum up, our recent measurements of the micro-scale mixing demonstrate that an enhanced mixing is associated with the pycnocline region, bottom and surface boundary layers. During the conference more results from the project will be shown that compare dissipation rates calculated from the measurements of two different instruments: 1MHz ADCP and VMP-250 microstructure profiling probe.

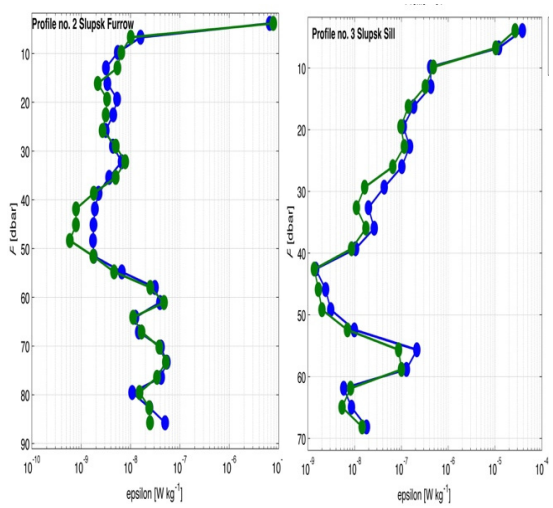


Fig 2. Profiles of the eddy kinetic energy dissipation rates [W/kg] in the Slupsk Sill and Slupsk Furrow, calculated from the microstructure shear profiles collected in February 2019 during r/v Oceania IO PAS research cruise.

References

Bogucki, D., & Garrett, C. (1993). A simple model for the shear-induced decay of an internal solitary wave. Journal of physical oceanography, 23(8), 1767-1776.

Bulczak A.I, Rak D., Schmidt B., Beldowski J. (2016) Observations of near-bottom currents in the Bornholm Basin, Slupsk Furrow and the Gdansk Deep. Deep Sea Research 2.

Carstensen, J., Andersen, J.H., Gustafsson, B.G., Conley, D.J., (2014). Deoxygenation of the Baltic Sea during the last century, Proc. Natl.Acad. Sci. U. S. A., 111(15), 5628–5633, doi:10.1073/pnas.1323156111

Holtermann, P. Prien,M. Naumann, V. Mohrholz, and L. Umlauf (2017), Deepwater dynamics and mixing processes during a major inflow event in the central Baltic Sea,J. Geophys. Res. Oceans, 122, 6648–6667.

Kõuts, T., Omstedt, A.,(1993) Deep water exchange in the Baltic proper. Tellus, 45A, 311-324.

Lappe, C., and L. Umlauf (2016), Efficient boundary mixing due to near-inertial waves in a nontidal basin: Observations from the Baltic Sea, J.Geophys. Res. Oceans, 121, 8287–8304.

Lumley, J., and E. Terray, (1983) Kinematics of turbulence convected by a random wave field. J. Phys. Oceanogr.,13, 2000–2002.

Meier, H. E. M., and F. Kauker (2003), Modeling decadal variability of the Baltic Sea: 2. Role of freshwater inflow and large-scale atmospheric circulation for salinity, J. Geophys. Res., 108(C11), 3368.

Meier, H.E.M., Feistel, R., Piechura, J., Arneborg, L., Burchard, H., Fiekas, V., Golenko, N., Kuzmina, N., Mohrholz, V., Nohr, C., Paka, V. T., et, al.(2006) Ventilation of the Baltic Sea deep water: A brief review of present knowledge from observations and models. Oceanologia 48, 133-164.

Mohrholz, V., Naumann, M.,Nausch, G., Krüger, S., Gräwe, U., (2015) Fresh oxygen for the Baltic Sea — An exceptional saline inflow after a decade of stagnation, J. Mar. Syst., 48, 152–166.

Neumann, T., Radtke H., Seifert T., (2017) On the importance of Major Baltic Inflows for oxygenation of the central Baltic Sea, J. Geophys. Res. Oceans, 122.

Piechura, J., Walczowski, W., Beszczyńska-Mőller A., (1997) On the structure and dynamics of the water in the Słupsk Furrow. Oceanologia 39(1),35–54.

Piechura, J. A., Beszczyńska-Moeller, (2003). Inflow waters in the deep regions of the southern Baltic Sea – transport and transformations, Oceanology, 45(4), pp 593-621.

Rak D. and Wieczorek P., (2012), Variability of temperature and salinity over the last decade in selected regions of the southern Baltic Sea, Oceanologia, no. 54(3), pp. 339-354.

Reissmann J., Burchard H., Feistel R., et al. (2009) State-of-the-art review on vertical mixing in the Baltic Sea and consequences for eutrophication, Progr. Oceanogr., 82, 47-80.

Schmidt B, Wodzinowski T., Bulczak A.I. (in review) Long-term variability of the near-bottom oxygen, temperature and salinity in the southern Baltic. Journal of Marine Systems.

Thorpe, S. A., (1977) Turbulence and mixing in a Scottish loch. *Philos. Trans. Roy. Soc.*, 286, 125–181.

Thorpe S.A. (2005) The turbulent Ocean. Cambridge University Press, New York.

Van der Lee E.M. and Umlauf L. (2011) Internal-wave mixing in the Baltic Sea: Near-inertial waves in the absence of tides. J. Geophys. Res. 116, C10016.

Wiles, P., T. Rippeth, H. J. Simpson, and P. Hendricks, (2006) A novel technique for measuring the rate of turbulent dissipation in the marine environment. Geophys. Res. Lett., 33.

Salinity dynamics of the Baltic Sea

Andreas Lehmann[1], Kai Myrberg[2] and Piia Post[3]

[1] GEOMAR, Hellmholtz Centre for Ocean Research Kiel Germany (alehmann@geomar.de)
[2] SYKE Finnish Environmental Institute/Marine Research Centre, Helsinki, Finland
[3]University of Tartu, Institute of Physics, Tartu, Estonia

1. Introduction

The salinity in the Baltic Sea is not a mere oceanographic topic but consists of the complete water and energy cycle which have Baltic-specific features. Salinity, and especially its low basic value and large variations in the Baltic Sea, is also an elementary factor controlling the ecosystem behavior of the Baltic Sea. The salinity dynamics is controlled by a number of factors: net precipitation, river runoff, surface outflow of Baltic fresh waters and the compensating deep inflow of higher saline waters from the Kattegat. In addition, the salinity dynamics is dictated by the irregular barotropic exchange flows such as MBIs (Major Baltic Inflows, Matthäus and Franck, 1990) and LVC (Large volume changes, Lehmann et al. 2017).

Furthermore, due to forecasted increase in precipitation during coming decades, scenario studies indicate even a decrease in salinity of about 0.6 g/kg in the ensemble mean until the end of the century (Saraiva et al., 2019). Since the Baltic Sea ecosystem has adapted to the present salinity regime, expected changes would exert a considerable stress on marine fauna and flora with associated negative social-economic consequences for the Baltic Sea countries.

Even if the Baltic Sea physics has been investigated for a long time, our present understanding of salinity changes is still very limited. Not surprisingly, future projections of the salinity evolution are rather uncertain. More detailed investigations on regional precipitation patterns and their relations to river runoff, atmospheric variability, wind forcing, the exchange between the sub-basins and turbulent mixing processes, are still needed. Furthermore, there is also a need for new climate projections simulations with improved atmospheric and oceanographic coupled model systems (Meier et al., 2019). Suggested general key research areas are the interrelation between decadal/climate variability and salinity, baroclinic and barotropic water mass exchanges. Do we understand the dynamics of the present-day salinity distribution, and can we predict MBIs/LVCs?

In addition, detailed studies on the regional salinity distribution/variability and associated circulation patterns, including salinity fluxes between the coastal areas and the open sea and within the sub-basins, are still needed to study. Since BACCII, which was published in 2015, collecting mostly research results until 2012, new research has been carried out on the salinity dynamics of the Baltic Sea stimulated e.g. through the Baltic Earth network. Especially, after recent MBIs in December 2014, 2015 and 2016 a number of new studies emerged on that. The research focused on key topics such as: the interrelation between decadal climate variability and salinity, the water mass exchange and MBIs and the associated atmospheric conditions, salinity variability and fluxes on different scales (detection and attribution to climate change), changes in the salt budget, and associated changes in the circulation of the Baltic Sea. Using long term data series of sea level, river discharge, and salinity from the Belt Sea and the Sound a continuous series of barotropic inflows has been reconstructed for the period from 1887 till present by Mohrholz, (2018).

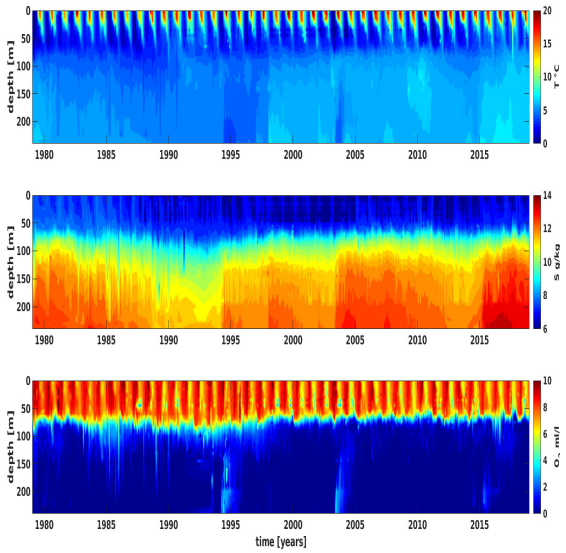


Figure 1. SD 28, eastern Gotland basin, area averaged monthly T-, S-, O_2-profiles. ICES data set on Ocean Hydrography (2009) .

2. Conclusions

Long-term salinity dynamics is controlled by river runoff and net precipitation and the governing east-west wind conditions. However, the recent decrease of surface salinity (Fig. 1) could not be explained by an increase in annual runoff (Liblik & Lips 2019). The mid-term and short term (monthly/annual/decadal) salinity dynamics is much more complex with strong salinity variability also affecting temperature and oxygen. Over recent decades negative salinity trends of about 0.1-0.2 g/kg/decade appear at the surface, 0.4-0.6 °C/decade for temperature and 0.1-0.2 ml/l/decade for oxygen (Fig. 2). The temperature trend is about the same as the air temperature trend. The trend in oxygen is strongly related to the increasing temperatures (changing solubility and oxygen depletion rates) with maximum negative trends up to 1 ml/l/decade in the area of the halocline (Bornholm and Gotland Basin). For the negative trend of surface salinity it is assumed that runoff and net precipitation play a role. However, in deeper parts the salinity trend (0.2-0.5 g/kg/decade) is reversed, although the frequency of barotropic and major saltwater inflows did not increase.

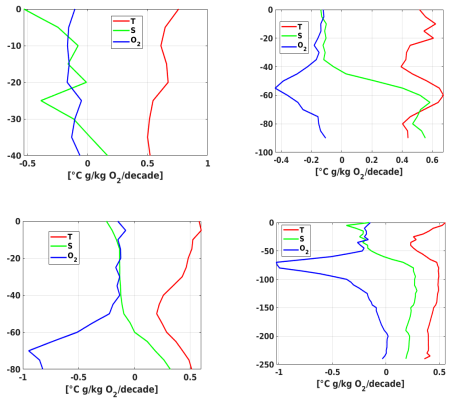


Figure 2 Trend profiles of temperature, salinity and oxygen for different areas of the Baltic Sea (1979-2018), Arkona Basin (upper left), Bornholm Basin (upper right), Gdansk Basin (lower left) and eastern Gotland Basin (lower right), data based on ICES data set on Ocean Hydrography.

The environmental interaction between fish larvae and salinity dynamics has also been under investigation. Recently observed summer inflows of saline water masses from the North Sea and Kattegat area into the central Baltic Sea might resulted in a higher connectivity between the nursery areas of pelagic fish species west of their major spawning grounds and the spawning stocks, e.g. for Baltic cod and flounder. Backward migration to the major spawning areas when the fish reach maturity could be expected and would properly help to increase the recruitment of these species. Unfortunately, detailed information about this process are presently not available.

References

BACC II Author Team (2015) Second assessment of climate change for the Baltic Sea Basin. Regional Climate Studies. Springer. https://doi.org/10.1007/978-3-319-16006-1.

Lehmann, A., Höflich, K., Post, P. and Myrberg, K. (2017). Pathways of deep cyclones associated with large volume changes (LVCs) and major Baltic inflows (MBIs). Journal of Marine Systems 167, 11–18.

Liblik, T., and Lips, U. (2019). Stratification has strengthened in the Baltic Sea – an analysis of 35 years of observational data. Front. Earth Sci. Under revi.

Matthäus, W. and Franck, H. (1990) The water volume penetrating into the Baltic Sea in connection with major Baltic inflows. Gerlands Beiträge zur Geophysik 99, 377–386, Lepizig.

Meier, H. E. M., M. Edman, K. Eilola, M. Placke, T. Neumann, H. Andersson, S.-E. Brunnabend, C. Dieterich, C. Frauen, R. Friedland, M. Gröger, B. G. Gustafsson, E. Gustafsson, A. Isaev, M. Kniebusch, I. Kuznetsov, B. Müller-Karulis, M. Naumann, A. Omstedt, V. Ryabchenko, S. Saraiva, and O. P. Savchuk (2019) Assessment of uncertainties in scenario simulations of biogeochemical cycles in the Baltic Sea. Frontiers in Marine Science, 6:46, https://doi.org/10.3389/fmars.2019.00046

Mohrholz, V. (2018). Major Baltic Inflow Statistics – Revised. Frontiers in Marine Science 5, 384. https://doi.org/10.3389/fmars.2018.00384.

Saraiva S., H. E. M. Meier, Helén Andersson, Anders Höglund, Christian Dieterich, Robinson Hordoir, and Kari Eilola (2019) Baltic Sea ecosystem response to various nutrient load scenarios in present and future climates. Climate Dynamics, 52: 3369, https://doi.org/10.1007/s00382-018-4330-0

High-resolution view on downwelling by underwater glider in the Eastern Baltic Proper

Taavi Liblik, Kai Salm, Urmas Lips

Tallinn University of Technology, Estonia, Tallinn (taavi.liblik@taltech.ee)

1. Background

As the Baltic Sea is land-locked basin, wind from any direction causes an upwelling at some coastal section. Moreover, simultaneously with upwelling downwelling at opposite coast should occur. Due to its immediate effects, e.g. lowered sea surface temperature or upward nutrient flux, upwelling process has been rigorously studied in the Baltic Sea in recent decades. Probably one reason for latter is also relatively easy detection of an upwelling by remote sensing. Contrary, downwelling process got much less attention by research.

Recent observations in the Gulf of Finland have displayed importance of the downwelling process in the Baltic Sea. Southwesterly winds cause eastward transport and accumulation of the upper layer water in the gulf. As a result, upper mixed layer depth increases in the whole gulf (Liblik and Lips, 2017) and sub-halocline layer flows out from the gulf to compensate the inflow in the upper layer (Liblik et al., 2013). In the case of southwesterly wind prevailing, upper mixed layer thickness can be >40 m at the southern coast of the gulf while in the northern side upwelling occurs in summer (Liblik and Lips, 2017). The downwelling process in the Baltic Proper is not well understood. There has been episodic surveys across the Baltic Proper (e.g. Lass et al., 2010), but common understanding of the pycnocline inclinations is lacking.

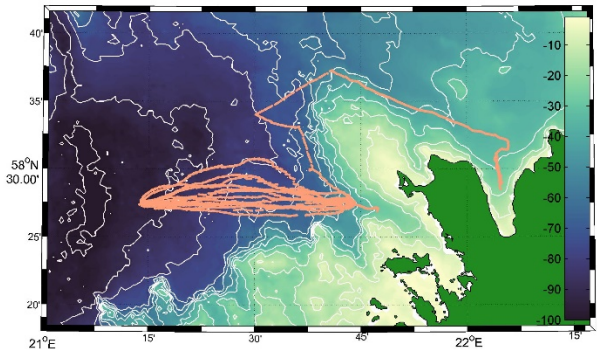


Figure 1. Glider survey in the Baltic Proper near NW coast of Saaremaa Island. Background color contours and white lines (with step of 10 m) represent the sea depth.

2. Data and results

Taking the wind statistics (Soomere and Keevallik, 2001) and geomorphology, eastern coast of the Baltic Proper should be one of the major downwelling areas in the Baltic Sea. In order to understand the downwelling process we conducted glider measurements in the Eastern Baltic Proper near Saaremaa Island. Repeated measurements with autonomous underwater glider were carried out in the 30 km long zonal section from 24 September to 23 October 2019. Glider was deployed in the open sea near NW of Saaremaa Island and it mapped the water column structure in the section by 15 repeated visits. Glider was piloted to Tagalaht Bay for the recovery due to difficult weather conditions (see Fig. 1).

The mixed layer depth increased from 20 m in the beginning of the survey to 60 m depth by the end of survey. Temperature and salinity of the upper mixed layer changed from 16-17 °C and 6.7 g kg-1 to 13 °C and 7.0 g kg-1, respectively. Thermal convection due to heat loss to atmosphere, wind mixing and boundary mixing are responsible for this change. Deepening of the upper mixed layer was not even, but gradual during the experiment. Downwelling signal, i.e. strong inclination of the pycnocline were observed in two periods. Likewise, the relaxation of the downwelling were observed. The zonal pycnocline distributions during downwellings showed different shapes. For instance, quite even inclination of the pycnocline from 30 m depth in the western end of the section to 60 m near the eastern end of the section were observed in mid-September. Two days later mixed layer depth was ca 60 m in the eastern half of the section. Steep inclination of the pycnocline from 60 to 30 m depth were observed in the 7-8 km segment of the section. The forcing behind these changes in the water column structure and the role of downwelling events in the seasonal decay of stratification will be analysed and presented. Another glider mission is planned in the same section in March 2020.

3. Acknowledgements

We would like to thank Fred Buschmann for the help in glider deployment/recovery operations in the sea. This work was financially supported by the Estonian Research Council grant (PRG602) and by the European Regional Development Fund within National Programme for Addressing Socio-Economic Challenges through R&D (RITA).

References

Lass, H.-U., Mohrholz, V., Nausch, G. and Siegel, H.: On phosphate pumping into the surface layer of the eastern Gotland Basin by upwelling, J. Mar. Syst., 80(1), 71–89, doi:10.1016/j.jmarsys.2009.10.002, 2010.

Liblik, T. and Lips, U.: Variability of pycnoclines in a three-layer, large estuary: the Gulf of Finland, Boreal Environ. Res., 22, 27–47, 2017.

Liblik, T., Laanemets, J., Raudsepp, U., Elken, J. and Suhhova, I.: Estuarine circulation reversals and related rapid changes in winter near-bottom oxygen conditions in the Gulf of Finland, Baltic Sea, Ocean Sci., 9, 917–930, 2013.

Soomere, T. and Keevallik, S.: Anisotropy of moderate and strong winds in the Baltic Proper. [online] Available from: http://kirj.ee/public/va_te/t50-1-3.pdf (Accessed 7 February 2019), 2001.

Investigating periodic interdecadal salinity changes in the Baltic Sea and their drivers

Hagen Radtke

Leibniz Institute for Baltic Sea Research Warnemünde, Germany (hagen.radtke@io-warnemuende.de)

1. Interdecadal salinity variations and runoff

Baltic Sea salinity shows a periodic variation with about 30 years in duration and 0.3 g/kg in peak-to-peak amplitude. This oscillation has been known for decades and has been related to changes in river runoff (Malmberg and Svansson 1982) because a similar periodicity can be seen in runoff reconstructions (Meier and Kauker 2003, Gailiušis et al. 2011). Runoff variations essentially cause baroclinic circulation changes.

2. Variations in salt transport by Major Baltic Inflows

A new time series for salt import during Major Baltic Inflows was published by Mohrholz (2018) which also shows the same periodic interdecadal variation. This is intuitive from the salt budget, but the regularity is on the other hand surprising, since the occurrence of large inflow events is linked to specific weather conditions whose distribution in time contains a strong random component. Still, the link between inflows and the interdecadal salinity variations has also been discussed (Höflich 2018) and the salinity variations were shown to be related to this mostly barotropic effect.

3. Model approach

To improve our understanding, we conducted a 150-years hydrodynamic model run to investigate the role of these two possible drivers. We used the GETM hydrodynamic model at 1 nautical mile horizontal resolution (Gräwe et al. 2019), driven by the atmospheric reconstruction dataset HIRESAFF v2 (Schenk and Zorita 2012). The salinity variations showing up in long-term observations could be reproduced by the model in their period, magnitude and phase. This enables us to investigate the effect in the model world, i.e., with a complete temporal coverage uncompromised by observation gaps especially before the 1960s when observations were less complete.

4. Wavelet analysis

Wavelet decomposition and the analysis of wavelet coherence allowed us to assess with higher precision whether the phase and period match between the salinity changes and the two possible drivers. We could show that both freshwater and inflow variation had the correct periodicity and phase to possibly cause the salinity variations. The fact that the oscillations in the bottom water lead those at the surface in time advocates for the inflow variation as the actual main cause. However, it could be possible that both runoff and inflow variation are caused by the same atmospheric mechanism and are therefore impossible to disentangle by time series analysis alone.

5. Direct runoff effect

So, we built a simplified conceptual model (Figure 1), driven by the numerical model output, to see how much of the interdecadal salinity changes near the surface are caused by a direct dilution by freshwater. It turned out that only one fourth of the oscillation could be explained by this effect.

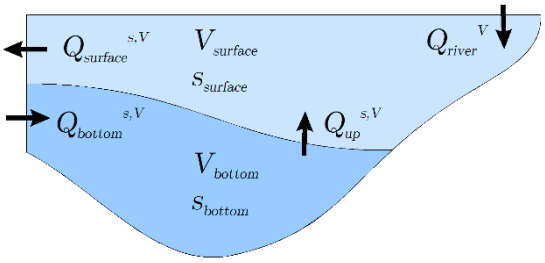


Figure 1. Conceptual model for assessing the direct dilution effect on interdecadal salinity variations in the Baltic Sea (Radtke et al. 2019)

6. Sensitivity experiments

To actually attribute the salinity variations to their driver, we conducted sensitivity experiments with either highpass-filtered wind fields or highpass-filtered runoff. Results of these experiments will be discussed in this presentation.

References

Gailiušis, B., Kriaučiūnienė, J., Jakimavičius, D., Šarauskienė, D. (2011) The variability of long–term runoff series in the Baltic Sea drainage basin, Baltica 24, 45–54.

Gräwe, U., Klingbeil, K., Kelln, J., Dangendorf, S. (2019) Decomposing mean sea level rise in a semi-enclosed basin, the Baltic Sea, Journal of Climate 32.

Höflich, K., Lehmann, A. (2018). Decadal variations in barotropic inflow characteristics and their relation with Baltic Sea salinity variability. Zenodo.

Malmberg, S.-A., Svansson, A. (1982) Variations in the physical marine environment in relation to climate, Tech. Rep. 1982/Gen:4, ICES, Copenhagen

Meier, H. E. M., Kauker, F. (2003) Modeling decadal variability of the Baltic Sea: 2. Role of freshwater inflow and large-scale atmospheric circulation for salinity, JGR-Oceans, 108, 3368

Mohrholz, V. (2018) Major Baltic Inflow Statistics – Revised. Frontiers in Marine Science 5:384.

Radtke, H., Brunnabend, S.-E., Gräwe, U., Meier, H.E.M. (2019) Explaining interdecadal salinity changes in the Baltic Sea in a 1850-2008 hindcast simulation. Climate of the Past - Discussions.

Schenk, F., Zorita, E. (2012) Reconstruction of high resolution atmospheric fields for Northern Europe using analog-upscaling, Climate of the Past, 8, 1681.

The role of dissolved oxygen and salinity on the reproductive conditions of the cod in the Southern Baltic Sea

Daniel Rak, Anna Bulczak, Waldemar Walczowski, Anna Przyborska

Institute of Oceanology, Polish Academy of Science, Sopot, Poland (rak@iopan.gda.pl)

1. Introduction

Dissolved oxygen concentration (DOC) as well as salinity are an important properties of water, affecting the structure and intensity of sea life. The DO content in the deeps of the Baltic is strongly limited. The Baltic Sea is currently one of the largest dead zones in the world (Conley et al. 2002; Diaz and Rosenberg 2008). Indeed, the extents of hypoxia and anoxia zones have been expanding in the Baltic Proper, the Gulf of Finland and the Gulf of Riga (Hansson and Andersson, 2016). The coverage of these zones increased from ca 5% between 1960 and 1995 up to ca 17% from 2000 to 2016. This has great impact on the spawning of the Baltic cods (Gadus morhua). Because of the low oxygen content at the depth where the Baltic cods (Gadus morhua) eggs sink, the cod cannot reproduce. Superimposed on this primary driver, oxygen content and temperature have a significant effect on egg/larva development and survival.

The aim of this poster was to describe the recent variability of DO in southern Baltic sea and examine its impact on the Baltic cod's spermatozoa activation and the neutral buoyancy layers.

2. Data and methods

The hydrographic data used in this poster were obtained by the Institute of Oceanology, Polish Academy of Sciences (IO PAN) and the Institute of Oceanology, P.P. Shirshov Russian Academy of Sciences (IO RAN).

IO PAN used towed CTD (Conductivity, Temperature, Depth) and Oxygen probes to acquire high-resolution transect records along the main profile in the southern Baltic (Figure 1). IO RAN used a moored Aqualog System located at 55° 12.7' N 16° 41.2' E to gather data on the eastern slope of the Słupsk Sill.

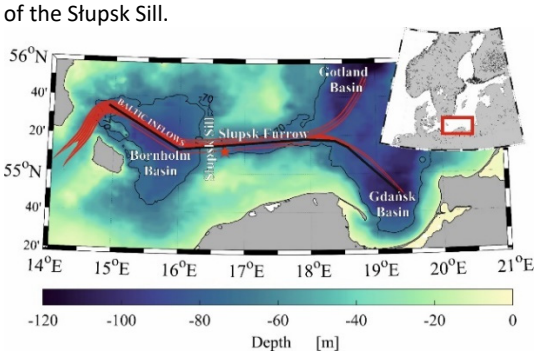


Figure 1. Location of measurements in the southern Baltic Sea. The solid black line represents the main course taken by r/v Oceania, and the star shows the position of the Aqualog.

3. Results

Dissolved oxygen and proper salinity in the marine environment are an important requirement for survival. For the Baltic cod, oxygen is necessary from the early stage of existence. In order to begin the spawning process, physical water properties need to fit cod's requirements. In the Bornholm Basin the critical value of salinity for spermatozoa activation is *S>11–12 PSU* (Nissling and Westin, 1997). The neutral egg buoyancy is maintained for the salinity about *14.5±1.2 PSU*. During the incubation process cod's egg can survive while the dissolved oxygen level is higher than *2 mg* l^{-1} (Wieland et al., 1994; Rohlf, 1999). However, below DO *5 mg* l^{-1} the declining of the cod's stock process begins (Köster et al., 2005). In the Bornholm Basin the spermatozoa activation waters are found in the 21 m thickness layer at average depth about 62 m, while in the Słupsk Furrow it is 19 m thinness layer at average depth of 71 m (Figure 2).

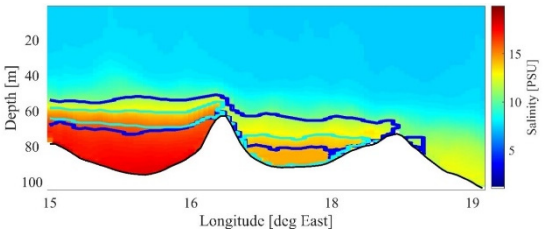


Figure 2. The cod's spermatozoa activation layer (blue lines) and neutral egg buoyancy layer along the main axis in the Southern Baltic Sea.

The differences between the lower limit of spermatozoa activation layer in the Bornholm Basin and the Słupsk Furrow results from the deep layer DO conditions. After fertilization, the egg enters the optimum depth determined by its natural buoyancy. In the Bornholm Basin the neutral buoyancy layer (65±5 m) is found within of spermatozoa activation layer. However, in the Słupsk Furrow, fertilized egg can be found at a depth from 75 to seabed, where only upper limit is in the range of spermatozoa activation. Therefore, fertilized egg can sink to reach optimum depth. Based on average values of salinity and DO there is no cod's spermatozoa activation and egg's natural buoyancy layers in the Gdańsk Deep. However, inflows from the North Sea can guarantee the existence of those layers (Figure 3).

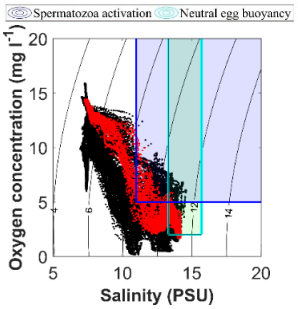


Figure 3. The OS diagrams for the Gdańsk Deep. The red dots represent the MBI, May 2015.

4. Conclusion

- In the Bornholm Basin the cod eggs may exist in the layer where they were fertilized.
- In Słupsk Furrow, the eggs can leave the fertilization layer and sink to the bottom, because natural buoyancy layer only partly covers the spermatozoa layer. After fertilizing eggs can survive in the bottom layer of the Slupsk Furrow.
- In the Gdańsk Deep, there are no conditions which can guarantee the egg surviving during stagnation period. Stronger advection can bring saline, oxygenated waters to this region, which will guarantee the existence of the spermatozoa activation and neutral buoyancy layers. After the MBI 2014, those layers were separated in the Gdańsk Deep.

References

Conley D. J., Björck S., Bonsdorff E., Carstensen J., Destouni G., Gustafsson B. G., Hietanen S., Kortekaas M., Kuosa H., Meier M., Müller-Karulis B., Nordberg K., Norkko A., Nürnberg G., Pitkänen H., Rabalais N. N., Rosenberg R., Savchuk O. P., Slomp C. P., Voss M., Wulff F., Zillén L., (2009). Controlling Eutrophication: Nitrogen and Phosphorus. Environmental Science & Technology. 43 (10), 3412-3420.

Diaz, R. J. and Rosenberg, R., (2008). Spreading dead zones and consequences for marine ecosystems. Science321(5891), 926–929. DOI: 10.1126/science.1156401.

Hansson M., Andersson L., (2016). Oxygen Survey in the Baltic Sea 2015: Extent of Anoxia and Hypoxia, 1960-2015. The major inflow in December 2014. SMHI.

Köster, F. W., Möllmann, C., Hinrichsen, H-H., Wieland, K., Tomkiewicz, J., Kraus, G., Voss, R., et al. (2005). Baltic cod recruitment—the impact of climate variability on key processes. ICES Journal of Marine Science, 62: 1408 –1425.

Mohrholz V., Naumann M., Nausch G., Krüger S., Gräwe U., (2015). Fresh oxygen for the Baltic Sea - An exceptional saline inflow after a decade of stagnation. J Marine Syst 148:152–166.

Nissling, A., and Westin, L. (1997). Salinity requirements for successful spawning of Baltic and Belt Sea cod and the potential for cod stock interactions in the Baltic Sea. Marine Ecology Progress Series, 152: 261–271.

Wieland, K., Waller, U., and Schnack, D. (1994). Development of Baltic cod eggs at different levels of temperature and oxygen content. Dana, 10: 163–177.

Rohlf, N. (1999). Verhaltensanderungen der Larven des Ostseedorsches (Gadus morhua callarias) wahrend der Dottersackphase. Berichte aus dem Institutes fur Meereskunde, 312.

Long-term variability of the near-bottom oxygen, temperature and salinity in the Southern Baltic

Beata Schmidt[1] and Anna Bulczak[2]

[1] National Marine Fisheries Research Institute, 1 Hugo Kolataja, 81-332 Gdynia, Poland (bschmidt@mir.gdynia.pl)
[2] Institute of Oceanology Polish Academy of Sciences, 55 Powstancow Warszawy, 81-712 Sopot, Poland

1. Introduction

The bottom conditions in the deep basins are a sensitive indicator of the health of the Baltic ecosystem, that ecological status, due to its location and bathymetry, is strongly influenced by natural and anthropogenic causes. The Baltic Sea is vertically stratified with the permanent halocline presents at depths between 60-80m, and the renewal of the near-bottom layers in the deep Baltic basins occurs mainly during barotropic inflows 'so called' major Baltic inflows (MBIs) (Matthäus and Franck, 1992; Fisher and Matthaus, 1996).

The main aim of this study is to describe the long-term variability of the near-bottom oxygen concentration, salinity and temperature in the three basins of the Southern Baltic: the Bornholm Basin (BB), Slupsk Furrow (SF) and the Gdansk Deep (GD) and to demonstrate the impact of the inflow events on the deep ventilation in those basins.

2. Data and Methods

The near-bottom temperature, salinity and dissolved oxygen (DO) concentrations were measured in three basins of the Southern Baltic: BB in the Bornholm Basin, SF in the Slupsk Furrow and GD in the Gdansk Deep by the National Marine Fisheries Research Institute from Gdynia, Poland during research cruises between 1946 and 2016 (Fig. 1). The ICES data (the International Council for the Exploration of the Sea, 2014) were also used to form monthly time series of the near-bottom properties. The ICES data located in vicinity (up to 4.5 km) of the NMFRI stations with similar bottom depth, were included into the analysis. The analysed time was covered with monthly temporal resolution by at least 60% in all three basins in 1946-2016.

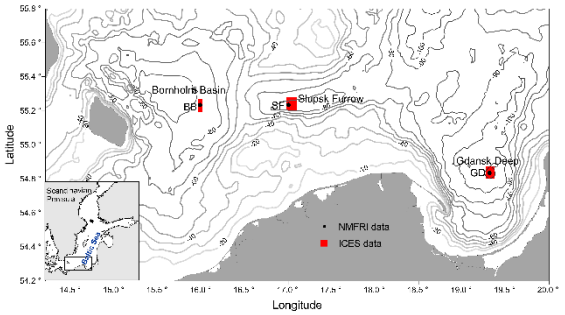


Figure 1. Locations of the three monitoring stations of the NMRFI, Poland in the Bornholm Basin, Slupsk Furrow and the Gdansk Deep, where near-bottom oxygen, salinity and temperature were measured at 1 m above the sea bed (black dots) and the areas of the ICES data (red). The contours denote bathymetry and are shown at every 10 m.

3. Results

The long-term trends in oxygen content are very similar in all basins (Fig. 2); since 1946, the near-bottom oxygen gradually decreased until 2000 reaching the long-term minimum. This coincided with the salinity and temperature minimum and was linked to the reduced frequency and volume of the barotropic inflows due to their decadal variability (Mohrholz, 2018). Since 2000 oxygen concentrations recovered slowly in all three basins and in 2016 their long-term means were close to the 1970's levels.

The long-term trends in salinity (Fig. 2B) show minima around 1989 in BB and SF and a year later in GD, however the mean salinity for years before and after stagnation period (Mohrholz, 2018) did not differ significantly. The long-term trends in temperature (Fig. 6C) also show fluctuations, most visible in the Bornholm Basin. In BB temperature reached the long-term minimum in 1993, whereas in SF and GD the minimum was reached in 1986 and 1987 respectively. In all basins the near-bottom temperature increased during the last 71 years.

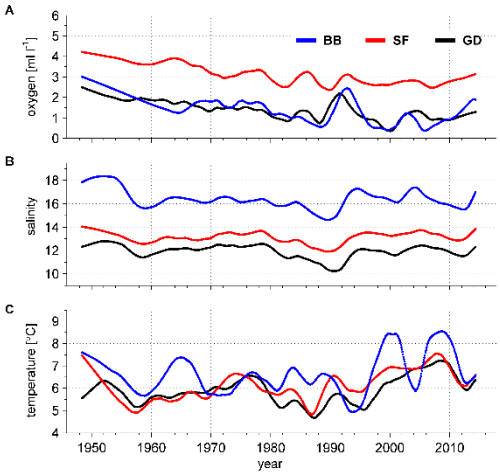


Figure 2. The long-term trends of oxygen, salinity and temperature calculated as 5-year long moving average for the Bornholm Basin, Slupsk Furrow and the Gdansk Deep.

Detailed analysis of changes in the bottom-water properties during inflow propagation showed that SF contributes to the ventilation of GD with a 1-3-month lag (Fig. 3). The results indicate that the dynamical processes present in SF directly influence bottom water properties in GD and the smaller barotropic and baroclinic inflows are very important for the bottom ventilation of the downstream basins like SF and GD.

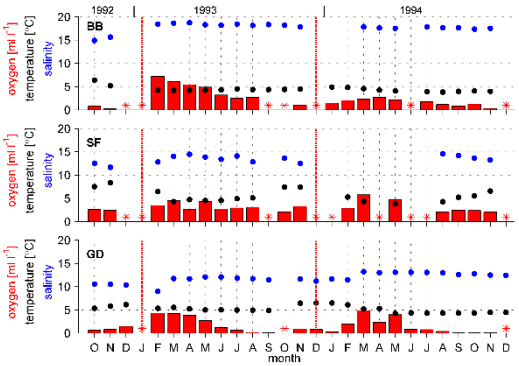


Figure 3. The near-bottom water properties after MBI event in 1993 and the weaker inflows that occur a year after recorded in the BB, SF and GD. The time of inflow events recorded in the Danish Stairs are marked by dashed red lines according to Mohrholz (2018). The stars mark the months with no oxygen data.

The mean and decadal variability of the seasonal cycle of the near-bottom properties were also analysed. It was found that the mean (1946-2016) annual cycle of the bottom oxygen content in SF and GD are sinusoidal with the highest values occurring in March and the lowest in September. The range of the oxygen mean seasonal cycle decreases easterly from 1.6 ml l^{-1} in BB through 1.3 ml l^{-1} in SF to 1.2 ml l^{-1} in GD. In BB and SF, the minimum bottom temperatures occur in the summer and the maximum in the winter. The strongest temperature variation through a year (3°C) occurs in SF and is much weaker in BB (1.5°C) and GD (1°C). The salinity is relatively constant during the year in all basins, however in BB and GD a drop in salinity is visible in the autumn. The range of the seasonal salinity variation is about 0.5 psu. The range of the mean DO seasonal cycle decreased by 0.2 ml l^{-1} in BB, 0.6 ml l^{-1} in SF and 0.4 ml l^{-1} in GD between 1946-1980 and 1995-2016.

References

Fischer H Matthäus W (1996) The importance of the Drogden Sill in the Sound for major Baltic inflows. J. Mar. Syst. 9, 137–157

Matthäus W Franck H (1992) Characteristics of major Baltic inflows—A statistical analysis. Cont. Shelf Res., 12(12), 1375–1400

Mohrholz V (2018) Major Baltic Inflow Statistics – Revised. Frontiers in Marine Science. Doi:10.3389/fmars.2018.00384

Acknowledgements:
This work was conducted as a part of statutory activities of the Department of Fisheries Oceanography and Marine Ecology of the National Marine Fisheries Research Institute (NMFRI) in Gdynia (Poland) and statutory activities of the Institute of Oceanology, Polish Academy of Sciences theme II.1.

Assessment of the effect of the Slupsk Sill on transformation of the Baltic inflow water based on microstructure measurements

Victor Zhurbas, Vadim Paka, Maria Golenko, Andrey Korzh, Alexey Kondrashov

Shirshov Institute of Oceanology, Russian Academy of Sciences, Moscow, Russia (zhurbas@ocean.ru)

Measurements performed by a loosely tethered free-falling microstructure profiler in the vicinity of the Słupsk Sill (fig. 1) revealed a high turbulence dissipation spot immediately beyond the sill to the east in the near-bottom layer filled with east-ward spreading saltwater (fig. 2). An approach is developed to quantitatively estimate the role of a topographic obstacle like the Słupsk Sill in mixing/transformation of inflow waters using data of microstructure measurements. To do this, first, based on vertical profiles of specific dissipation rate of kinetic energy of turbulence and potential density, the rate of entrainment of low salinity water from the overlying layer to the near-bottom turbulent saltwater layer is calculated. Then, assuming that in the near-bottom saltwater flow, the critical value of the Froude number is reached directly at the Sill, the flow volume rate is estimated. Finally, from the balance between advection and turbulent entrainment, the change in salinity of the eastward spreading saltwater due to intensification of mixing at the Sill can be evaluated. Using data of microstructure measurements available, the mixing hot spot at the Słupsk Sill was found to be responsible for approximately 5 percent of the inflow water salinity decrease en route from the Arkona Basin to the Gotland Deep (Zhurbas et al., 2019).

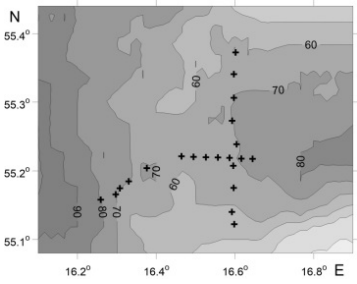


Figure 1. Close-up bathymetric map of the Słupsk Sill area. The black crosses depict the location of measurements by microstructure profiler "Baklan". The cross-sill (quasi-zonal) and along-sill (quasi-meridional) transects were performed on July 2, 2017, and July 4–5, 2017, respectively.

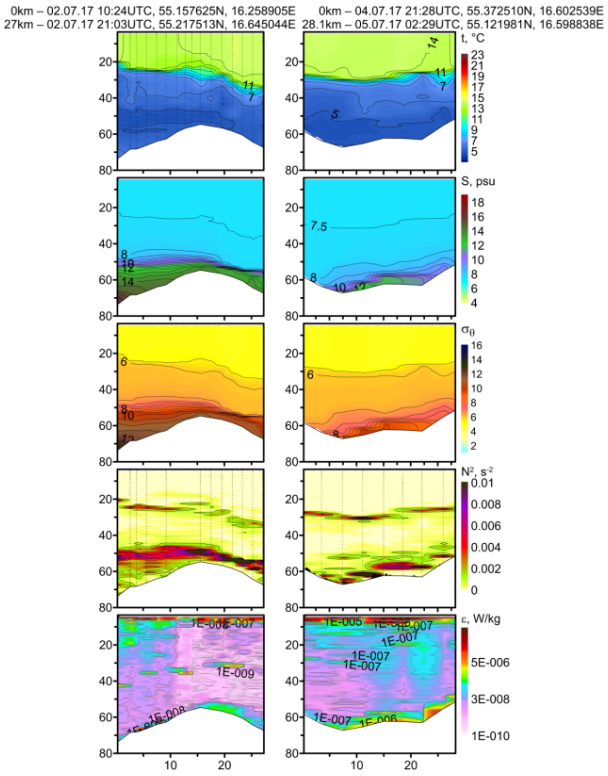


Figure 2. Temperature t, salinity S, potential density anomaly σ_θ, squared buoyancy frequency N^2 , and dissipation rate of turbulence kinetic energy ε versus distance [km] and depth [m] for the transects across (left) and along (right) the Słupsk Sill. Note that the distance axis is directed to the east for the left-hand panels and to the south for the right-hand panels.

The reported study was funded by the state assignment of IO RAS, theme N 0149-2019-0013, and RFBR according to the research projects № 18-05-80031.

References

Zhurbas V.M., Paka V.T., Golenko M.N., Korzh A.O. (2019) Transformation of eastward spreading saline water at the Słupk Sill of the Baltic Sea: an estimate based on microstructure measurements, Fundamentalnaya i Prikladnaya Gidrofizika, Vol. 12, No. 2, pp. 43–49. DOI: 10.7868/S2073667319020060

Rotation of floating particles in submesoscale cyclonic and anticyclonic eddies: a model study for the southeastern Baltic Sea

Victor Zhurbas[1], Germo Väli[2] and Natalia Kuzmina[1]

[1] Shirshov Institute of Oceanology, Russian Academy of Sciences, Moscow, Russia
[2] Department of Marine Systems, Tallinn University of Technology, Tallinn, Estonia

1. Introduction

Spiral structures that can be treated as signatures of submesoscale eddies are a common feature on synthetic aperture radar (SAR), infrared and optical satellite images of the sea surface (e.g., Munk et al., 2000; Laanemets et al., 2011; Karimova et al., 2012; Ginzburg et al., 2017). The spirals are broadly distributed in the World Ocean, 10–25 km in size and overwhelmingly cyclonic (Munk et al., 2000).

To our mind the common occurrence of spirals on satellite images of the sea surface hints that the winding of the linear features of a tracer concentration in the course of the development of horizontal shear instabilities and/or mixed layer baroclinic instabilities is not the only way to generate the spirals. Rather, one may expect, based on modeling results (Väli et al., 2018), that the spirals can also be generated by the advection of a floating tracer in a velocity field inherent to mature, relatively long-living submesoscale eddies referred to by McWilliams (2016) as submesoscale coherent vortices, and the initial tracer distribution is not necessarily characterized by the linear surface features. If it holds, then for the predominance of cyclonic spirals over anticyclonic spirals, some properties of the rotary motion of floating particles, such as angular velocity, differential rotation and helicity, should be different for cyclonic and anticyclonic eddies.

The objective of this work is to understand the dominance of observed cyclonic spirals by assessing differences between the rotary motion of floating particles around the center of submesoscale cyclonic and anticyclonic eddies using high resolution modeling of the Baltic Sea.

2. Materials and methods

2.1 Model description

The General Estuarine Transport Model (GETM) (Burchard and Bolding, 2002) was applied to simulate the meso- and submesoscale variability of temperature, salinity, currents, and overall dynamics in the southeastern Baltic Sea.

The horizontal grid of the high-resolution nested model with uniform step of 0.125 nautical miles (approximately 232 m) all over the computational domain, which covers the central Baltic Sea along with the Gulf of Finland and Gulf of Riga (Fig. 1), was applied while in the vertical direction 60 adaptive layers were used. The digital topography of the Baltic Sea with the resolution of 0.25 nautical miles (approximately 500 m) was obtained from the Baltic Sea Bathymetry Database (http://data.bshc.pro/) and interpolated bi-lineally to approximately 250 m resolution.

The model simulation run was performed from 1 April to 9 October 2015. The model domain had the western open boundary in the Arkona Basin and the northern open boundary at the entrance to the Bothnian Sea. For the open boundary conditions the one-way nesting approach was used and the results from the coarse resolution model were utilized at the boundaries. The coarse resolution model covers the entire Baltic Sea with an open boundary in the Kattegat and has the horizontal resolution of 0.5 nautical miles (926 m) over the whole model domain (Zhurbas et al., 2018).

The atmospheric forcing (the wind stress and surface heat flux components) is calculated from the wind, solar radiation, air temperature, total cloudiness and relative humidity data generated by HIRLAM (High Resolution Limited Area Model) maintained operationally by the Estonian Weather Service with the spatial resolution of 11 km and temporal resolution of 1 hour (Männik and Merilain, 2007).

More detailed overview about the model system is given by Zhurbas et al (2019).

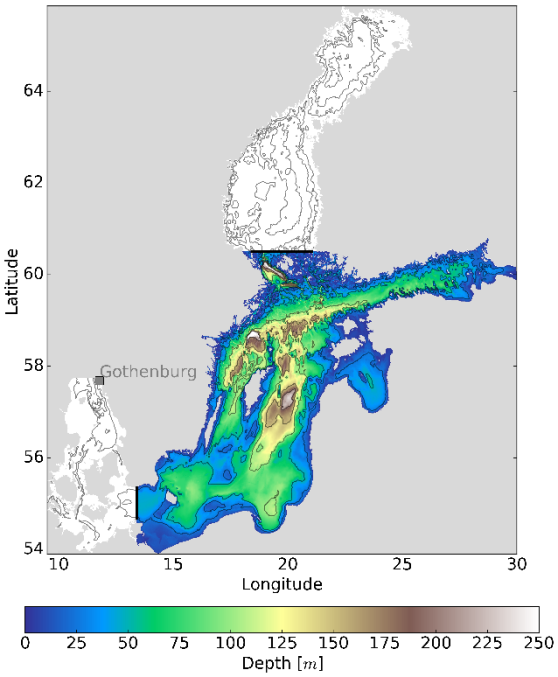


Figure 1. Map of the high-resolution model domain (filled colors) with the open boundary locations (black lines). The coarse resolution model domain (blank contours C filled colors) has an open boundary close to the Gothenburg station.

2.2 Application of particles

In order to characterize the submesoscale eddies, we estimated eddy radius R, the dependence of angular velocity of rotation ω(r) on radial distance from the eddy centre r, angular velocity in the eddy centre $\omega_0 \equiv \omega(0)$, differential rotation parameter Dif=ω(0)/ω(R) and helicity parameter $Hel = \frac{\delta r}{r} = \frac{r_2 - r_1}{0.5(r_1 + r_2)}$.

Large value of Dif and ω_0 and the negative value of Hel(r) favour the formation of spirals in the tracer field from linear features.

3. Results and discussion

Modelled snapshot of surface layer temperature, salinity and currents with submesoscale resolution in the southeastern Baltic Sea for 15 May demonstrate a quite dense packing of the sea surface with submesoscale eddies. Looking at the snapshots of the surface layer currents (panels (c) in Figs. 2), one cannot see any predominance of the number of cyclones over the number of anticyclones or vice versa. However, the surface layer temperature and salinity snapshots (panels (a) and (b), respectively), clearly demonstrate a large number of spiral structures linked with the submesoscale cyclonic eddies, while the submesoscale anticyclones, as a rule, do not manifest themselves by well-defined spirals.

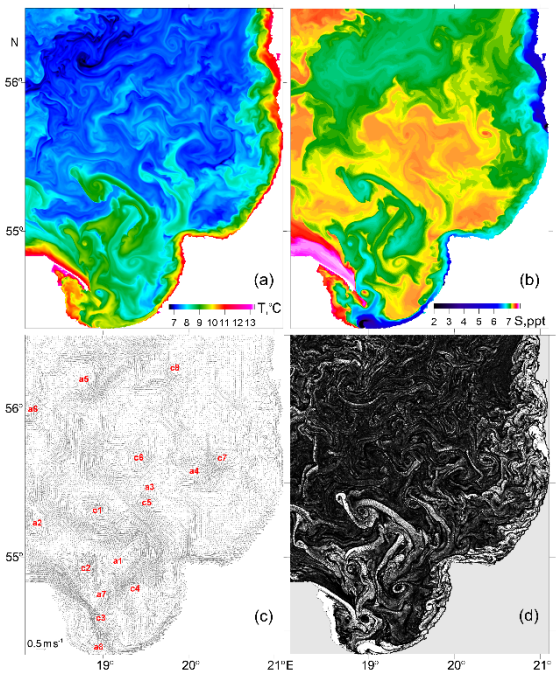


Figure 2. Modelled fields of the surface layer parameters in the southeastern Baltic Sea on 15 May 2015, 12:00: temperature (a), salinity (b), current velocity (c), and spatial distribution of uniformly released synthetic floating Lagrangian particles (d) after 1 day of advection.

The numerical experiments showed that the cyclonic spirals can be formed both from a horizontally uniform initial distribution of floating particles and from the initially lined up particle clusters during the advection time of the order of 1 day. While the formation of the predominantly cyclonic spirals in the tracer field from the linear features in the course of development of horizontal shear instabilities and the mixed-layer baroclinic instabilities is a well-known effect which was thoroughly discussed by Munk et al. (2000) and Eldevik and Dysthe (2002), a quick regrouping of the floating particles from horizontally uniform distribution to cyclonic spirals in the course of advection in the submesoscale velocity field is a surprising phenomenon which was first mentioned by Väli et al. (2018).

We addressed several rotary characteristics of submesoscale eddies which could be potentially responsible for the predominant formation of cyclonic spirals in the tracer field such as:

- normalized frequency of rotation in the eddy centre $\Omega_0=2\omega_0/f$ (the higher the frequency, the faster the spiral can be formed);
- differential rotation parameter $Dif=\omega(0)/\omega(R)$ (the spirals cannot be formed from linear features at the solid-body rotation when Dif=0);
- helicity parameter $\langle Hel\rangle$ (if $\langle Hel\rangle<0$ the particles shift towards the eddy centre which makes the spiral more visible, and, on the contrary, if $\langle Hel\rangle>0$ the particles shift away from the eddy centre which makes the spiral less visible).

To calculate Ω_0, Dif, $\langle Hel\rangle$ and eddy radius R, the pseudo-trajectories of synthetic floating particles in a frozen velocity field (i.e. the velocity field simulated by the circulation model for a given instant was kept stationary for the entire period of advection) were calculated. We obtained estimates of Ω_0, Dif, $\langle Hel\rangle$ and R for 18 cyclonic and 18 anticyclonic submesoscale eddies simulated in the southeastern Baltic Sea in May–July 2015.

The statistics of the R indicated that the submesoscale cyclonic eddies are indistinguishable by size from the submesoscale anticyclonic eddies.

In contrast to R, the difference of all three rotary characteristics (Ω_0, Dif, Hek) indicated the predominant formation of cyclonic spirals in the tracer field. On the average the submesoscale cyclonic eddies, in comparison to the anticyclonic ones, rotate three times faster, have three times larger difference of the frequency of rotation between the eddy centre and the periphery, as well as display the tendency of shifting floating particles towards the eddy centre ($\langle Hel\rangle<0$).

References

Burchard, H., and Bolding, K. (2002) GETM – a general estuarine transport model, Scientific documentation, Technical report EUR 20253 en. In: Tech. rep., European Commission. Ispra, Italy.

Ginzburg, A. I., Krek, E. V., Kostianoy, A. G., and Solovyev, D. M. (2017) Evolution of mesoscale anticyclonic vortex and vortex dipoles/multipoles on its base in the south-eastern Baltic (satellite information May-July 2015), Okeanologicheskie issledovaniya (Journal of Oceanological Research), 45(1), 10-22

Karimova, S. S., Lavrova, O. Yu., and Solov'ev, D. M. (2012) Observation of Eddy Structures in the Baltic Sea with the Use of Radiolocation and Radiometric Satellite Data, Izvestiya, Atmospheric and Oceanic Physics, 48(9), 1006–1013

Laanemets, J., Väli, G., Zhurbas, V., Elken, J., Lips, I., and Lips, U. (2011) Simulation of mesoscale structures and nutrient transport during summer upwelling events in the Gulf of Finland in 2006, Boreal Environment Research, 16(A), 15-26

Munk, W., Armi, L., Fischer, K., and Zachariasen, F. (2000) Spirals on the sea, Proc. R. Soc. Lond. A, 456, 1217-1280

Männik, A., and Merilain, M. (2017) Verification of different precipitation forecasts during extended winter-season in Estonia, HIRLAM Newsletter 52, 65–70

Väli, G., Zhurbas, V. M., Laanemets, J., and Lips, U. (2018) Clustering of floating particles due to submesoscale dynamics: a simulation study for the Gulf of Finland, Fundamentalnaya i prikladnaya gidrofizika, 11(2), 21-35

Zhurbas, V., Väli, G., Golenko, M., and Paka, V. (2018) Variability of bottom friction velocity along the inflow water pathway in the Baltic Sea, J. Mar. Syst., 184, 50-58

Zhurbas, V., Väli, G., Kostianoy, A., and Lavrova O. (2019) Hindcast of the mesoscale eddy field in the Southeastern Baltic Sea: Model output vs. satellite imagery, Russian Journal of Earth Sciences, 19.

Topic 2

Land-Sea biogeochemical linkages

Modern trophic state indexes of Baltic waters derived from structural signatures of biofilm colonies covering submerged solid substrata

K. Boniewicz-Szmyt [1], M. Grzegorczyk[2], S.J. Pogorzelski[2], and P. Rochowski[2]

[1] Department of Physics, Gdynia Maritime University, Poland (k.boniewicz@wm.umg.edu.pl)
[2] Institute of Experimental Physics, University of Gdansk, Poland

1. Abstract

A biofouling phenomenon on artificial and biotic solid substrata was studied in several locations in the Baltic Sea brackish water (Gulf of Gdansk) during a three-year period with contact angle wettability, confocal microscopy and photoacoustic spectroscopy techniques. Short generation time, sessile nature and fast responsiveness to environmental conditions make biofilms being water chemistry bioindicators suitable as a sensitive monitoring tool in Baltic Sea eutrophication studies. The apparent surface free energy γ_{SV} and other interfacial interaction parameters: 2D film pressure Π, work of adhesion and spreading (W_A, W_S) were monitored semi-continuously and on-line using the contact angle hysteresis (CAH) approach at different stages of biofilm development from the conditioning film via microfouling and then to macrofouling (Pogorzelski et al. (2013, 2014)). Further structural and morphological biofilm signatures: biofilm biovolume, substratum coverage, area to volume ratio, mean thickness, roughness and fractal dimension were on-line determined from confocal reflection microscopy (COCRM) data (Grzegorczyk et al. (2018)). Recently, photosynthetic properties (photosynthetic energy storage ES, photoacoustic amplitude and phase spectra) of biofilm communities exhibited a seasonal variability, as indicated with a novel closed-cell type photoacoustic spectroscopy PAS system (Pogorzelski et al. (2019)). That allowed mathematical modeling of a marine biofilm under steady state, in particular the specific growth rates and induction times, to be derived from simultaneous multitechnique signals. A multistep approach involving chemical, wettability, photoacoustic and microscopy techniques can be used to assess ecological features of microperiphyton, and as robust indicators for marine bioassessment. A set of the established biofilm structural and physical parameters could be modern water body trophic state indexes.

2. Keywords

Baltic waters, Submerged substrata biofilm, Biofilm growth, Multitechnique biofilm parameters, Eutrophication effect, Water quality monitoring, Environmental stressors

3. Experimental methodology

Several artificial solid substrata (glass, metallic, polymeric) and biotic (wood, macrophytes) of varying surface energy were deployed at a depth of 0.5 m in shallow coastal waters of the Baltic Sea (Gulf of Gdansk) for a certain time. Biofilm accumulation time was ranging from 1 to 24 days; probes were studied every month from May to November, 2016. Biofilm samples (5-10 from the particular location) together with the adjacent water were collected in a plastic bottle, not allowed to dry out, and further processed under laboratory conditions with contact angle captive bubble set-up, confocal microscopy and photoacoustic spectroscopy techniques, as presented in (Grzegorczyk et al. (2018)).

A trophic water body status was determined according to the following parameters: pH, dissolved O_2, phosphate (PO_4^{3-}), nitrite (NO_2^-), nitrate (NO_3^-), ammonium (NH_4^+), and Secchi depth. The seawater chemical parameters, primary production, chl. a, nitrogen, phosphorus concentrations were taken from SatBałtyk System data base (available at http://satbaltyk.iopan.gda.pl).

4. Cross correlations between chemical trophic state indicators and biofilm structure signatures

Relationships between the physicochemical variables and the biofouled solid substrata wettability, geometric - morphological, and photoacoustic spectra parameters were analyzed by Spearman's rank correlation coefficient. Its values for surface wettability energetics parameters versus the chemical ones are collected in Tab. 1.

Table 1. Spearman's rank correlation coefficients between trophic status indicators and wettability parameters of glass substrata submerged in Baltic Sea coastal waters ; [a] $p<0.05$, n=9; [b] $p<0.01$, n=6.

Trophic State Indicators	CAH (deg)	Π (mNm^{-1})	γ_{SV} (mJ m^{-2})	W_A (mJ m^{-2})	W_S (mJ m^{-2})
1. pH	0.631	0.673	0.712	0.551	0.684
2. Dissolved O_2 (mg dm^{-3})	0.845	0.781	0.893	0.613	0.697[b]
3. Secchi depth (m)	-0.621	-0.755	-0.825	-0.654	-0.715
4. Total P (mg dm^{-3})	0.751	0.912[a]	0.789	0.572	0.542[b]
5. Total N (mg dm^{-3})	0.824	0.933[a]	0.726	0.683	0.402[b]

All the parameters are negatively correlated to Secchi depth, although the absolute values indicated a strong correlation effect only for the wettability parameters: CAH, γ_{SV}, Π (with R = 0.68 - 0.96). The remaining ones i.e., W_A are W_S are much less correlated to the trophic status indicators (R = 0.40 - 0.69). The geometric-morphological biofilm parameters derived from a confocal microscopy study, for the particular structure, are shown in Figure 6 of (Grzegorczyk et al. (2018)), are as follows: mean thickness = 14.2 µm, biovolume = 46,700 µm^3, coverage area fraction f = 60.2 %, roughness parameter r = 0.49, fractal dimension = 1.36, Hopkins aggregation index = 2.89. It turned out that, that a certain positive correlation appeared between: biovolume vs biofilm wet matter (BWM) (R = 0.78), biofilm coverage fraction f vs BWM (R = 0.82), biofilm thickness vs Π (R = 0.86), and biofilm thickness vs γ_{SV} (R = - 0.83). Periphyton is a mixture of algae, cyanobacteria, heterotrophic microbes and detritus, stand for a photosynthetic system with a mixture of pigments, being attached to submerged surfaces in most aquatic ecosystems. Biofilm colony photosynthetic apparatus properties (photosynthetic energy storage (ES), PA

amplitude and phase spectra) exhibited a seasonal variability. The photoacoustic parameters (ES and PA signal amplitude) turned out to be unequivocally related to the biofilm structural signatures (thickness, volume, number of cells, surface energy of biofilm, fractal dimension etc.), as learned from confocal scanning microscopy and wettability measurements (Grzegorczyk et al. (2018)). Effectiveness of photosynthetic part of biomass accumulation in a biofilm structure is a substratum-specific quantity. The peak values in PA signal amplitude spectra maximum at ~ 680 nm were found highest for a biotic substratum (wood), lower for filtered planktonic phase, and lowest for metallic abiotic surfaces. *Chl. a* was determined by photoacoustic method, based on the proportionality of the photoacoustic signal to the amount of pigment. Exemplary marine biofilm on glass PA amplitude (blue) and phase (red) spectra obtained in summer (A) and autumn (B) seasons are shown in Fig. 11 of Grzegorczyk et al.(2018). The spectrum exhibits three maxima at wavelengths ca 430, 490 and 690 nm. The first and third of these maxima corresponds to absorption by *Chl. a*, that at 480 - 490 nm to absorption of pigments accessory to *Chl. a*. The lower maximum, for *Chl. a* at 675 nm, for the sample collected on 19 Sept. 2016 in reference to the one on 28 Nov., 2016, can result from a lower *Chl. a* content in this time or very effective process of oxygen production. It should be noticed that the PA amplitude is dependent on the photoacoustically-induced heat production (proportional also to biomass) but the PA signal phase is proportional to oxygen production effectiveness. The phase of the PA signal is more sensitive to the changes of optical and thermal properties of the layered sample than the magnitude of the PA signal.

ES could be an indicator of water pollution; they were lower than or equal to those measured for samples in a pollution-free environment. Nutrient limitation and anthropogenic eutrophication are among the most important factors determining the overall status of water bodies which can be followed by ES efficiency of biofilm cultures. ES values were higher for a season of high primary production, and increased by a factor of 1.5 - 2, for biofilm settled on biotic substrata. Exemplary plots ES versus primary production and N concentration are depicted in Fig. 1 (a) and (b), respectively.

ES turned out to be inversely correlated to biogenic elements concentrations N (R= - 0.76); P (R= - 0.81); O (R= - 0.67), and positively correlated to primary production (R=0.86) and *Chl. a* concentration (R= 0.82) in the Baltic. Photoacoustics can be used to reliably estimate the concentration of photosynthetic pigments in biofilm cultures, the efficiency of ES by periphyton photosynthesis can be determined directly by photoacoustics, the effects of any environmental stressor, such as temperature, nutrient limitation, high/dim light and pollutants on the photosynthetic capacity of biofilm colony can be evaluated.

There are several other factors affecting the marine biofilm adhesion, apart from the surface free energy of substrata like surface electricity, surface architecture, temperature, fluid shear stress or contact time. Finally, short generation time, sessile nature and fast responsiveness to environmental conditions make biofilms being water chemistry bioindicators particularly suitable as a monitoring tool in Baltic Sea eutrophication studies.

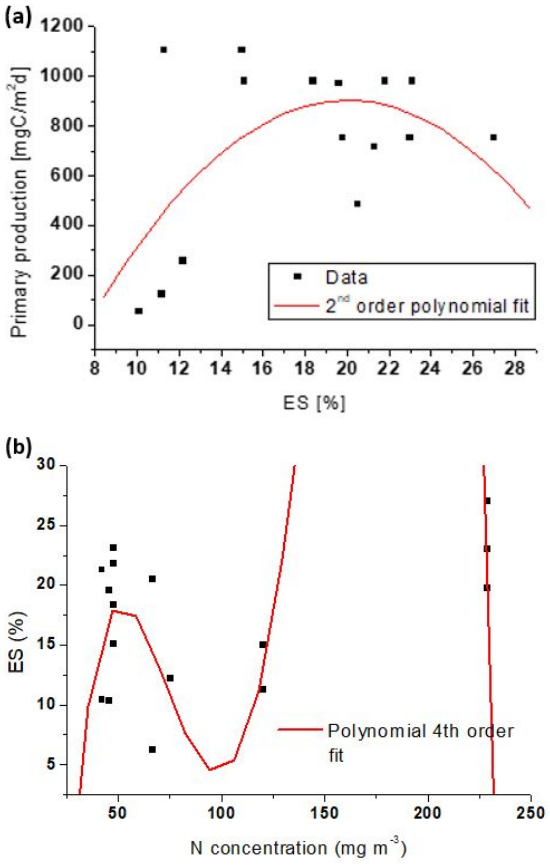


Figure 1. ES versus primary production (a) and N concentration (b), Baltic Sea data from Pogorzelski et al. (2019).

5. Conclusions and future work

A collection of biofilm structural and physical parameters could be modern water body trophic state indexes. More comprehensive data remain to be collected in order to establish functional dependences of practical value in water bioassessment. Original open-type cell photoacoustic spectroscopy systems, and contact angle wettability arrangements designed to *in-situ* and at field work are currently constructed and tested.

References

Pogorzelski, S.J., Mazurek, A.Z., Szczepańska, A. (2013) In-situ surface wettability parameters of submerged in brackish water surfaces derived from captive bubble contact angle studies as indicators of surface condition level, J. Marine Systems, 119-120, pp. 50-60

Pogorzelski, S.J., Szczepańska, A. (2014) On-line and in-situ kinetics studies of biofilm formation on solid marine submerged substrata by contact angle wettability and microscopic techniques, IEEE Conference Publications, Baltic International Symposium (BALTIC), 2014 IEEE/OES, IEEE Xplore, pp. 1-8

Grzegorczyk, M., Pogorzelski, S.J., Pospiech, A., Boniewicz-Szmyt, K. (2018) Monitoring of marine biofilm formation dynamics at submerged solid surfaces with multitechnique sensors, Front. Mar. Sci. 5:363

Pogorzelski, S.J., Rochowski, P., Grzegorczyk, M. (2019) Photosynthetic energy storage efficiency in biofilms determined by photoacoustics, Proc. of SPIE Vol. 11210, 112100C-1-5

Benthic fauna influence on the marine silicon cycle in the coastal zones of the southern Baltic Sea

Zuzanna Borawska, B. Szymczycha, K. Koziorowska-Makuch, M. J. Silberberger, M. Szczepanek, and M. Kędra

Institute of Oceanology, Polish Academy of Sciences, Sopot, Poland (zborawska@iopan.pl)

1. Introduction

Silicon is an important macronutrient in the ocean, required for the skeleton growth of many marine organisms (Tréguer and De La Rocha, 2013). The bioavailable form of silicon in the sea is dissolved silica (DSi), represented by $Si(OH)_4$ and $Si(OH)_3^-$ (Struyf et al., 2010). Since DSi is crucial for growth of diatoms, the key phytoplankton group in the global ocean, its availability can shape organic matter quality, and thus influence pelagic and benthic communities (Conley et al., 2008). Siliceous skeletons are produced by living organisms in form of biogenic silica (Tréguer and De La Rocha, 2013). Biogenic silica is not chemically stable and its dissolution starts immediately in the water column after organism's death and continues to dissolve after deposition in the sediment. This process causes increased DSi concentrations in the pore waters and drives return fluxes of DSi from sediments to the water column (Presti and Michalopoulos, 2008). DSi is mainly released to the marine environment from the chemical weathering of continental rocks and it is discharged via rivers and groundwater (Tréguer and De La Rocha, 2013). However, the release of DSi from marine sediments (return fluxes) can also represent an important source of Si in the sea (Schulz and Zabel, 2006).

Benthic macrofauna has been recognized as an important factor shaping coastal ecosystems. Their presence and activities in marine sediments, such as bioturbation and bioirrigation, influence the rates of solute fluxes through sediment-water interface, including DSi fluxes (Levinton, 1995). Therefore, benthic fauna can have different impacts on DSi fluxes depending on its diversity, abundance, biomass and sediment type (Norkko et al. 2015, Janas et al. 2019).

Coastal ecosystems are highly dynamic due to complex bathymetry, changeable salinity and temperature, variable sediment properties and different benthic fauna distribution (Carstensen et al. 2019). The biogeochemical processes occurring in the coastal zone is not sufficiently recognized due to the significant variability of environmental conditions and still limited measurements.

The aim of this study was to investigate the impact of benthic fauna diversity, and species abundance and biomass on DSi fluxes in the southern Baltic Sea. Our sampling sites differed in terms of environmental conditions, anthropogenic pressure and benthic communities characteristics. Our results bring a new insight on the benthic communities' contribution to the temporal and spatial biogeochemical processes in the coastal zone.

2. Material and methods

This study was conducted in the southern Baltic Sea during winter, spring and autumn 2019 and winter 2020. In order to study benthic fauna influence on DSi benthic fluxes formation, four areas along the Polish coast were chosen: Szczecin Lagoon, open waters near Łeba, Puck Bay and Gulf of Gdańsk (Vistula river estuary; figure 1). These localities differ in terms of riverine input, with highest riverine influence and lowest salinity in Szczecin Lagoon, and lowest riverine influence in the open waters near Łeba. These ecosystems remain under variable anthropogenic pressure, with intensive human impact in Szczecin Lagoon, Gulf of Gdańsk and Puck Bay, and smaller anthropogenic impact in the open waters near Łeba, which is close to the protected area of Słowiński National Park. For this study, stations between 0.5 m and 30 m were chosen, with one additional station at 60 m depth in Gulf of Gdańsk.

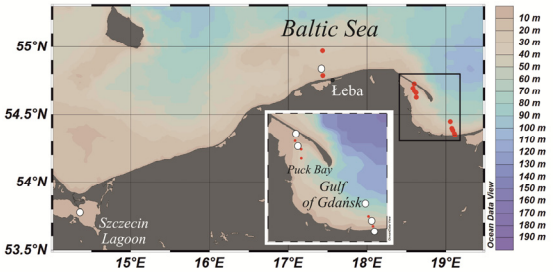


Figure 1. Bathymetry of the Polish Baltic Sea coast. Red points indicate stations where bottom water was collected, while white points indicate stations chosen for DSi fluxes measurements (Ocean Data View).

Sampling was conducted from s/y *Oceania* (IO PAN, Sopot, Poland) and directly from the shore. Bottom water was collected with Niskin bottle in all seasons for DSi concentration analyses. Water temperature and salinity were measured with CTD probe. Additionally, pH and redox conditions were measured with Hach HQ40D Multi Meter. In spring, autumn 2019 and winter 2020 sediment cores (n=4-5) with natural benthic assemblages were collected using box corer for *ex situ* incubations at selected sites (figure 1).

Cores were sealed and incubated in the dark at *in situ* temperatures. A stirring mechanisms in the lids ensured constant mixing of bottom water. Oxygen level was monitored using PreSens oxygen probe, to ensure that decrease doesn't exceed 20% of initial concentration. Samples of bottom water for DSi concentrations were collected at the beginning and at the end of incubation. Fluxes were calculated as a difference between initial and final concentrations. At the same time, bottom water from the station was incubated separately to measure concentration changes caused by water related processes. After incubations, sediment from cores was sieved (0.5 mm mesh size) and fixed in 4% formaldehyde solution buffered with borax. Later, benthic organisms from each core were picked up under

stereomicroscope and identified to the lowest possible taxonomic level.

DSi concentrations were analyzed using standard spectrophotometrical Heteropoly Blue Method (Mullin and Riley, 1955).

3. Results and discussion

Study on DSi concentrations in the bottom water allowed to investigate seasonal changes in DSi availability in coastal ecosystems. High variability in DSi concentrations was observed among studies localities and between winter and spring 2019. DSi concentrations generally increased with depth, however, in some shallower stations high concentrations were observed in areas directly affected by riverine inflow (Vistula in Gulf of Gdańsk and Odra in Szczecin Lagoon). The highest DSi concentration (58 µmol dm^{-3}) was observed in Szczecin Lagoon during winter (January 2019); however, the lowest concentration was measured at the same station during spring (April 2019; 2,6 µmol dm^{-3}) which, most probably, was caused by diatom blooms.

In spring 2019 significant differences in DSi fluxes rates were observed among investigated stations. Fluxes ranged from -0.14 to 4.08 mmol $d^{-1}m^{-2}$. The highest variation among cores was observed in the Puck Bay at 16 m depth (figure 2). The lowest rates of DSi fluxes were measured at shore stations (~0.5 m depth) in the Puck Bay and close to the Vistula river mouth. Negative DSi fluxes (from water column to the sediments) were observed during spring at shore stations, which may be caused by active benthic diatoms producing their frustules (Tallberg et al., 2017). The highest values of DSi flux in spring were measured in the Puck Bay at 16 m depth (4.08 mmol $d^{-1}m^{-2}$).

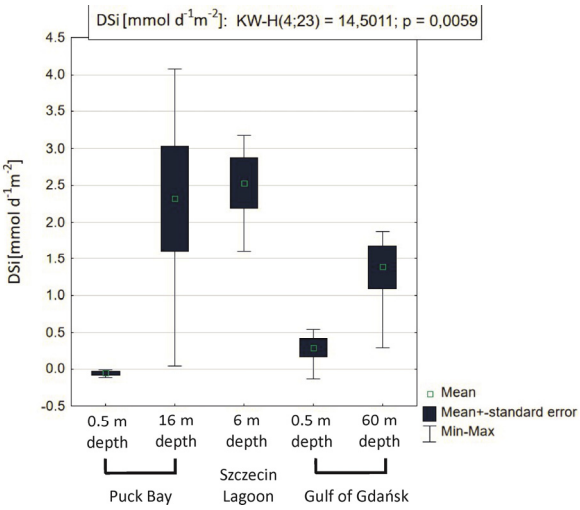


Figure 2. DSi fluxes measured in cores (n=4-5) at 5 stations during spring 2019. Results of Kruskal-Wallis test used to investigate differences among sites are shown.

Benthic communities in the investigated cores varied along studied areas during spring 2019, with the highest species richness observed in the Puck Bay (13 taxa) and lowest in Szczecin Lagoon (4 taxa). However, DSi flux was rather related to benthic abundances, as the highest rates of DSi fluxes were measured in the cores with the highest abundance of macrofauna.

4. Conclusions

Coastal ecosystems are highly differentiated in terms of abiotic and biotic components. This variability has impact on the DSi fluxes.

This study provides insights into relation between benthic fauna characteristics and marine silicon cycle in the coastal zone of the southern Baltic Sea.

5. Acknowledgements

This study was funded by Polish National Science Centre, project no 2017/26/E/NZ8/00496 „Coastal Ecosystem functioning under different anthropogenic pressure - linking Benthic communities And biogeochemical Cycling in the southern Baltic Sea (COmEBACk)".

References

Carstensen, J., Conley, D.J., Almroth-Rosell, E., Asmala, E., Bonsdorff, E., Fleming-Lehtinen, V., Gustafsson, B.G., Gustafsson, C., Heiskanen, A.-S., Janas, U., Norkko, A., Slomp, C., Villnäs, A., Voss, M., Zilius, M., 2019. Factors regulating the coastal nutrient filter in the Baltic Sea. Ambio.

Conley, D.J., Humborg, C., Smedberg, E., Rahm, L., Papush, L., Danielsson, Å., Clarke, A., Pastuszak, M., Aigars, J., Ciuffa, D., Mörth, C.-M., 2008. Past, present and future state of the biogeochemical Si cycle in the Baltic Sea. J. Mar. Syst. 73, 338–346.

Janas, U., Burska, D., Kendzierska, H., Pryputniewicz-Flis, D., Łukawska-Matuszewska, K., 2019. Importance of benthic macrofauna and coastal biotopes for ecosystem functioning – Oxygen and nutrient fluxes in the coastal zone. Estuar. Coast. Shelf Sci. 225, 106238.

Levinton, J., 1995. Bioturbators as Ecosystem Engineers: Control of the Sediment Fabric, Inter-Individual Interactions, and Material Fluxes, in: Jones, C.G., Lawton, J.H. (Eds.), Linking Species & Ecosystems. Springer US, Boston, MA, pp. 29–36.

Mullin, J.B., Riley, J.P., 1955. The colorimetric determination of silicate with special reference to sea and natural waters. Anal. Chim. Acta 12, 162–176.

Norkko, J., Gammal, J., Hewitt, J.E., Josefson, A.B., Carstensen, J., Norkko, A., 2015. Seafloor Ecosystem Function Relationships: In Situ Patterns of Change Across Gradients of Increasing Hypoxic Stress. Ecosystems 18, 1424–1439.

Presti, M., Michalopoulos, P., 2008. Estimating the contribution of the authigenic mineral component to the long-term reactive silica accumulation on the western shelf of the Mississippi River Delta. Cont. Shelf Res. 28, 823–838.

Struyf, E., Smis, A., van Damme, S., Meire, P., Conley, D.J., 2010. The global biogeochemical silicon cycle. Silicon 1, 207–213.

Schulz, H.D., Zabel, M. (Eds.), 2006. Marine Geochemistry, 2nd ed. Springer-Verlag, Berlin Heidelberg.

Tallberg, P., Heiskanen, A.-S., Niemistö, J., Hall, P.O.J., Lehtoranta, J., 2017. Are benthic fluxes important for the availability of Si in the Gulf of Finland? J. Mar. Syst., Towards a healthier Gulf of Finland – results of the International Gulf of Finland Year 2014 171, 89–100.

Tréguer, P.J., De La Rocha, C.L., 2013. The World Ocean Silica Cycle. Annu. Rev. Mar. Sci. 5, 477–501.

Short-term vs. long-term effects of rewetting coastal peatlands - are they fueling eutrophication and climate change with regard to nitrogen?

Anne Breznikar, Joachim W. Dippner and Maren Voss

Leibniz-Institute for Baltic Sea Research, Biological Oceanography, Rostock, Germany (anne.breznikar@io-warnemuende.de)

1. Introduction

Coastal areas are highly dynamic interfaces between terrestrial and marine ecosystems. They are impacted by rising sea levels, higher precipitation in winter and higher temperatures in summer due to climate change (IPCC, 2013), as well as by high riverine nutrient inputs leading to eutrophication and hypoxia (Howarth et al., 2011; Breitburg et al., 2018).

While nutrient inputs via rivers are monitored regularly in the Baltic Sea, not much is known about nitrogen (N) inputs or retention capacities of unconnected catchments along the German coastline (Hannerz & Destouni, 2006; HELCOM, 2018). The land had been used for agricultural purposes and thus been drained for decades. Rising storm surges and coastal protection measures now require novel approaches including the rewetting of coastal peatlands.

Flooding these peatlands may not only contribute to eutrophication by leaching N, but it could also fuel the production of the climate-relevant greenhouse gas nitrous oxide (N_2O) due to enhanced microbial activities (Seitzinger & Kroeze, 1998).

For this study, two peatlands in different rewetting phases are selected, one only recently connected to the Baltic Sea, the other already 25 years ago. By examining the N exchange between the coast and adjacent rewetted peatlands, it is possible to gain information about potential impacts of future sea level rise and its further consequences on fueling eutrophication and climate change.

2. Research questions / Aims of the study

The aim of this study is to compare short-term vs. long-term effects of rewetting coastal peatlands. By now rewetting is mostly seen as positive measure concerning the natural uptake of carbon (C) (Strack, 2008). Very little is known about actual leaching of N into the Baltic Sea, for instance due to the interference with saltwater (Rysgaard et al., 1999; Weston et al., 2010). One hypothesis is that leaching of N decreases over time because N is washed out, so that a longer rewetted peatland may contain less N than a freshly rewetted one (Figure 1).

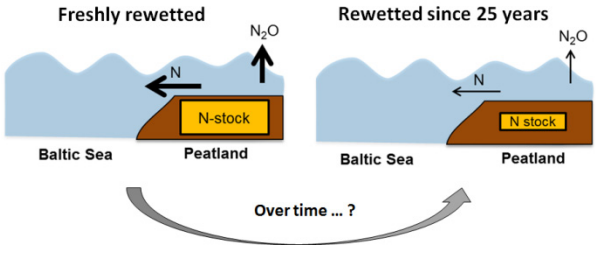


Figure 1: Cartoon to visualize the hypothesis that a freshly rewetted peatland contains and releases more nitrogen to water and air (left) than a longer rewetted one (right).

The study also aims to gain insight into the effect of fluctuating salinities, caused by changing weather conditions, on N-related processes, for instance on the production of N_2O by nitrification and denitrification. Nitrification is the transformation of ammonium to nitrate, denitrification uses nitrate to produce N_2. Since it is already known that coastal areas can be hot spots for the production of N_2O (Bange, 2006), the main goal of this study is to identify rewetted peatlands as potential N_2O sources or sinks and their ability to fuel coastal N_2O production.

Overall the results may indicate the need to establish a permanent monitoring of rewetting measures along the coast.

3. Study sites

Two study sites in different phases are chosen, which are both located in Mecklenburg-Western Pomerania, Germany (Figure 2).

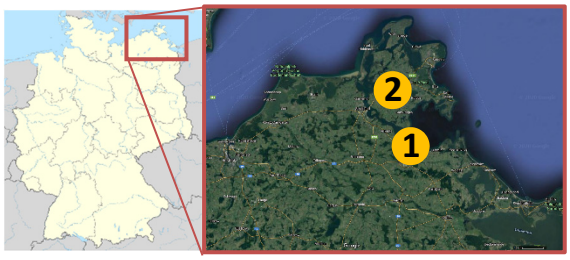


Figure 2: Locations of the two study sites within Germany. One site is located within a nature conservation area near Greifswald (1), the other one further north on the Island of Rügen (2).

Site 1 was drained and used for agriculture over many decades. The rewetting took place roughly 25 years ago. Since then there is an open exchange with the Baltic Sea through a couple of small channels.

Site 2 was also drained for agricultural use over decades, but is now freshly rewetted by removing parts of the dyke in November 2019. A small opening for water exchange with the Baltic Sea was created where the exchange flow can be monitored properly.

4. Material & Methods

Sampling in site 1 is conducted on a monthly basis since April 2019. During each sampling campaign, 5 stations are sampled which are located in front of (coast), within and behind (terrestrial) a small channel. Surface samples for nitrate, nitrite, ammonium, N isotopes, PON, DON, Chlorophyll a, and N_2O are taken. Additionally, the porewater on the land side is sampled and analyzed for nutrients.

Site 2 was sampled in a ditch and at the coast four times before flooding and weekly after flooding since November 2019. Six stations in total are sampled at the

coast and in the flooded area, for the same variables as mentioned above.

Rate measurements for nitrification are conducted at each sampling campaign and all stations by using ^{15}N-tracer incubations. Denitrification rates are measured every three months by using sediment cores to measure the production of N_2 over time.

To finally calculate a budget of N leaching into the Baltic Sea, the water levels, the topography of each study site, and the nutrient concentrations will be used.

5. Preliminary Results and Discussion

Significant differences among the two sites were identified. Higher nutrient concentrations in waters covering the flooded land than at the coastal stations were found in all months at site 1. Also the N_2O saturations in water were higher on the landside than at the coast, suggesting higher microbial activity. First measurements of nitrification rates confirmed this assumption by showing higher rates on the landside.

The freshly rewetted site (site 2) also experienced high nutrient concentrations in the overlying waters, but with higher values compared to site 1. For instance the ammonium concentrations in coastal waters were higher after rewetting which is likely a consequence of nutrient release from the former soils on the landside. This indicates that N seems to leach out from the peatland to the coast.

To quantify the N exchange between land and sea, the changes of the water level and thus volume of water above the soil together with nutrient concentrations will be used. The aim is to show whether freshly rewetted peatlands with N-rich soils are a significant (and understudied) nutrient source at a local scale.

6. Acknowledgements

This study is funded by the German Federal Environmental Foundation (in German “Deutsche Bundesstiftung Umwelt”) and A. Breznikar is associated to the graduate school “Baltic TRANSCOAST” which is funded by the DFG (grant number GRK 2000/1).

References

Bange, H. W. (2006). Nitrous oxide and methane in European coastal waters. Estuarine Coastal and Shelf Science, 70 (3), pp. 361-374.

Breitburg, D., Levin, L. a., Oschlies, A., Grégoire, M., Chavez, F. P., Conley, D. J., … Zhang, J. (2018). Declining oxygen in the global ocean and coastal waters. Science, 359, pp. 1–11.

Hannerz, F., & Destouni, G. (2006). Spatial characterization of the Baltic sea drainage basin and its unmonitored catchments. Ambio, 35(5), pp. 214–219.

Helsinki Commission (HELCOM) (2018). Sources and pathways of nutrients to the Baltic Sea. Baltic Sea Environment Proceedings No. 153.

Howarth, R., Chan, F., Conley, D. J., Garnier, J., Doney, S. C., Marino, R., & Billen, G. (2011). Coupled biogeochemical cycles: Eutrophication and hypoxia in temperate estuaries and coastal marine ecosystems. Frontiers in Ecology and the Environment, 9(1), pp. 18–26.

IPCC (2013). Climate Change 2013: The Physical Science Basis. Contribution of Working Group I to the Fifth Assessment Report of the Intergovernmental Panel on Climate Change [Stocker, T.F., D. Qin, G.-K. Plattner, M. Tignor, S.K. Allen, J. Boschung, A. Nauels, Y. Xia, V. Bex and P.M. Midgley (eds.)]. Cambridge University Press, Cam-bridge, United Kingdom and New York, NY, USA.

Rysgaard, S., Thastum, P., Dalsgaard, T., Christensen, P. B., Sloth, N. P. (1999). Effects of salinity on NH4+ adsorption capacity, nitrification and denitrification in Danish estuarine sediments. Estuaries, 22 (1), pp. 21-30.

Seitzinger, S., Kroeze, C. (1998). Global distribution of nitrous oxide production and N inputs in freshwater and coastal marine ecosystems. Global Biogeochemical Cycles, 12, 1, pp. 93–113.

Strack, M. (2008). Peatlands and Climate Change. International Peat Society.

Weston, N. B., Giblin, A. E., Banta, G. T., Hopkinson, C. S., Tucker, J. (2010). The effects of varying salinity on ammonium exchange in estuarine sediments of the Parker River, Massachusetts. Estuaries and Coasts, 33 (4), pp. 985-1003.

Bioecological evaluation of the quality of the surface runoff from urban territories (case study of the city of Brest)

Ina Bulskaya[1], A. Volchek [2] and A. Kolbas [1]

[1] Brest State University named after A. Pushkin, Brest, Belarus (inabulskaya@gmail.com)
[2] Brest State TechnicalUniversity, Brest, Belarus

1. Aim and scope

The aim of the work was to estimate the pollution of the surface runoff from urban territories (SRUT) in the city of Brest, Belarus and its impact on the receiving river ecosystem (the Mukhavets river, Baltic sea basin).

2. Materials and methods

Standard methods for wastewater analysis – AAS, photometry and titration methods were used for SRUT analysis. Bioassay and the study of the macrophyte communities were conducted to estimate influence on living organisms and ecosystem.

3. Results

SRUT was characterized by seasonal dynamics: the degree of contamination in winter was significantly higher than in summer period, primarily due to the use of sand and salt deicing composites (see Fig. 1.).

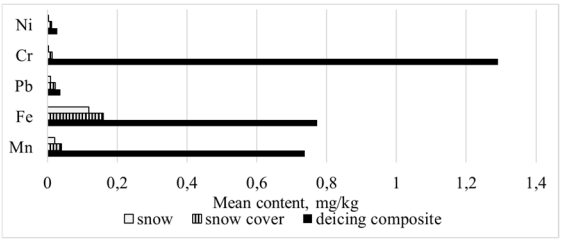


Figure 1. Results of analysis of snow, snow cover and deicing composites in the city of Brest.

Among other identified sources of pollution there were atmospheric precipitation and wash-off from the rooftops and road surfaces. Chloride and phosphate ions, dissolved zinc and copper were recognized as environmentally significant pollutants, because their content had significantly exceeded the regulation levels (maximum permissible concentrations).

The impact of SRUT on water plants was assessed using biotest with duckweed (Lemna minor L.) and the study of the macrophyte communities of the receiving river. Significant impact of SRUT on the biochemical parameters of L. minor was proved (See Fig. 2.). The presence of strong anthropogenic pressure, primarily due to pollution from surface runoff was identified in the study of macrophyte communities. Results showed significant impact of SRUT on the ecosystem of the receiving river.

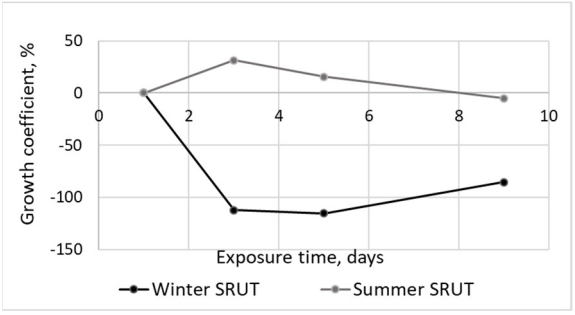


Figure 2. Relative growth of duckweed in samples of winter and summer SRUT.

References

Bulskaya, A. Volchek (2014) Inorganic constituents in surface runoff from urbanised areas in winter: the case study of the city of Brest, Belarus, Oceanologia, № 56 (2), pp. 373–383.

Bulskaya, A. Volchek, Pollution of surface runoff from the territory of Brest, Belarus (2015) Water Science & Technology: Water Supply, № 15.2, pp. 256–262.

Bulskaya, A. P. Kolbas, D. S. Dyliuk, A. V. Kuzmitsky (2016) Implementing biomonitoring for the assessment of urban surface runoff impact on receiving river / Book of abstracts 1st International Scientific Conference WaterLand-2016, Lithuania, 06–12 June, pp. 10–12.

Microbial life and phosphorus cycling along salinity and redox gradients

Simeon Choo, Simon Langer and Heide Schulz-Vogt

Department of Biological Oceanography, Leibniz Institute for Baltic Sea Research Warnemünde, Rostock, Germany (simeon.choo@io-warnemuende.de)

1. Introduction

There exist certain microorganisms which can concentrate the linear organic polymer, polyphosphate (polyP) in large amounts, and have been referred to as polyP-accumulating organisms (PAOs), as described by Tarayre et al. (2016). On this note, Brock & Schulz-Vogt (2011) have previously shown that large filamentous sulfur bacteria have were able to store polyP during favourable growth conditions, and releasing it as phosphate under disadvantageous environmental stimuli such as sulfidic stress. This encourages the possibility that polyP accumulation and utilization in bacteria could possibly be linked to stress response in general. This finding is of interest, in relation to the likelihood that large bacteria have a high capacity for polyP storage and hence have a considerable impact on the local phosphorus cycle, as shown by Schulz & Schulz (2005) with the giant sulfur bacteria *Thiomargarita namibiensis*. In contrast, although other bacteria such as *Sulfurimonas* also accumulate polyP, Schulz-Vogt et al. (2019) postulates that their smaller size significantly limits their polyP storage capacity.

In semi-aquatic habitats such as the northern German coastal peatlands, geochemical and microbiological processes likely have a large influence on the fluctuation of biologically-available phosphorus concentrations along redox and salinity gradients (Worrall et al., 2016). However, the significance of the microbial role in the local phosphorus cycle is not fully understood yet, and furthermore, marine environmental studies in this context are scarce. Since microbial metabolic processes are in turn influenced environmental changes, it would be crucial to investigate the effect of fluctuations in salinity and redox potentials on PAOs, particularly those with large phosphate storage capacities.

2. Hypothesis and Aims

Accordingly, we hypothesize that under unstressed conditions, PAOs would take up significant amounts of phosphate, causing the top layer of sediment to be a major polyP-storage zone in coastal peatlands. Along the Baltic coast, three main stressors are identified: temperature and salinity fluctuations, and drying-rewetting situations. Therefore, we aim to find out how different stressors affect the release of phosphate, and in turn discover if PAOs play a significant role in this release.

3. Ongoing Research and Results

We conducted bimonthly microscopic analyses of samples from two ditch sites in Karrendorfer Wiesen, which revealed the presence of numerous filamentous cyanobacteria. DAPI-staining procedures semi-quantitatively revealed that significantly large amounts of polyP were accumulated by these filaments (Figure 1). Preliminary measurements of collected samples also reflected a notable concentration of about 7 µM polyP in the top layer sediment.

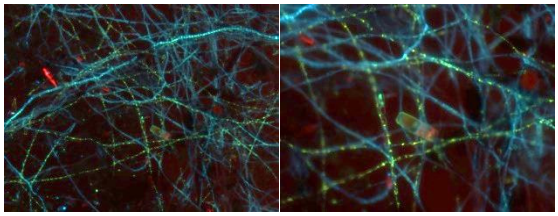


Figure 1. DAPI-stained fluorescent imagery (ZEISS Axioscope) of polyP-filled cyanobacteria filaments at x10 (left) and x20 magnification (right) from sediment samples of Karrendorfer Wiesen, Germany.

Incubation of the Karrendorfer sediment samples (triplicates) has shown increased rates of phosphate release in response to temperature stress conditions (Figure 2). Henceforth, ammonia production in the sediments and bottom water will be measured in order to determine that this release is not derived from decomposition processes, but instead originating from the breakdown of polyP stored in the resident bacteria. The amount of particulate phosphorus will subsequently be measured to understand if the sediments become a P-source or sink during temperature stress.

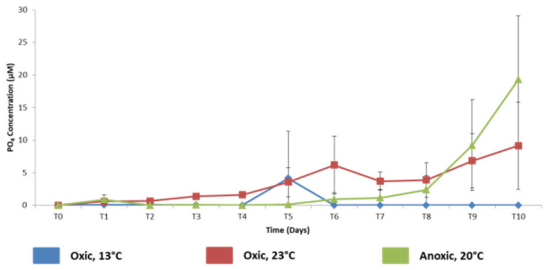


Figure 2. A 10-day temperature stress incubation experiment revealed substantially higher release of phosphate (PO_4^{3-}) at 23°C as compared with normal temperature (13°C) conditions (determined according to the sampling season).

Aside from temperature stress, similar experiments have been planned to assess the response to salinity as well as drying-rewetting stresses.

4. Desired Outcome

Ultimately, we want to understand if polyP metabolism is crucial for bacteria during stressful conditions. Concurrently, the determination of phosphate release from bacteria can offer a possibility that large polyP-accumulating bacteria do indeed influence the phosphorus cycle in Baltic coastal wetlands.

References

Cédric Tarayre, Huu-Thanh Nguyen, Alison Brognaux, Anissa Delepierre, Lies De Clercq, Raphaëlle Charlier, Evi Michels, Erik Meers, and Frank Delvigne (2016). Characterisation of Phosphate Accumulating Organisms and Techniques for Polyphosphate Detection: A Review. Sensors; 16 (6): pp. 797.

Fred Worrall, Catherine S. Moody, Gareth D. Clay, Tim P. Burt, and Rob Rose (2016). The total phosphorus budget of a peat-covered catchment. Journal of Geophysical Research: Biogeosciences; 121: pp. 1814-1828.

Jörg Brock and Heide N. Schulz-Vogt (2011). Sulfide induces phosphate release from polyphosphate in cultures of a marine *Beggiatoa* strain. The ISME Journal; 5 (3): pp. 497-506.

Heide N. Schulz and Horst D. Schulz (2005). Large sulfur bacteria and the formation of phosphorite. Science; 307 (5708): pp. 416-418.

Heide N. Schulz-Vogt, Falk Pollehne, Klaus Jürgens, Helge W. Arz, Sara Beier, Rainer Bahlo, Olaf Dellwig, Jan V. Henkel, Daniel P. R. Herlemann, Siegfried Krüger, Thomas Leipe and Thomas Schott (2019). Effect of large magnetotactic bacteria with polyphosphate inclusions on the phosphate profile of the suboxic zone in the Black Sea. The ISME Journal; 13: pp. 1198-1208.

High-resolution ecosystem model of the Puck Bay (southern Baltic Sea)

Dawid Dybowski[1], Maciej Janecki[1], Artur Nowicki[1], Lidia Dzierzbicka-Głowacka[1] and Jaromir Jakacki[1]

[1] Physical Oceanography Department, Institute of Oceanology, Polish Academy of Sciences, Sopot, Poland (ddybowski@iopan.pl)

1. Introduction

The Puck Bay is part of the Gdańsk Basin (southern Baltic Sea). It is separated from deep-water areas by the Hel Peninsula. Puck Bay consists of the inner part called Puck Lagoon and the outer part of Puck Bay. The boundary between them runs from the Rybitwia Sandbank to the Cypel Rewski and has two straits within which there is an intensive water exchange between the Puck Lagoon and the outer part of the Puck Bay. The commonly accepted eastern border of the Puck Bay is the line connecting the Hel Peninsula with Kamienna Góra.

The Puck Bay is an example of a region that is highly vulnerable to anthropogenic impact. Therefore, it has been included into Natura 2000. As a result, it requires preservation or restoration of "favorable conservation status" of species and habitats by introducing appropriate "protection measures". The strategic actions and the policy of the authority of the Puck District regarding the environmental protection involve not only the respect of the Natura 2000 legislation but also realization of European legislation including Water Framework Directive, Marine Strategy Framework Directive, Habitats Directive, Baltic Sea Action Plan and the strategic program of the environment protection for the Puck District. The main aims of the Puck District policy are improvement of the environment, sustainable development, refrain from climate change and protection of the natural resources such as water.

2. WaterPUCK project

The EcoPuckBay model was developed as part of the WaterPUCK project. The aim of the project is to create an integrated information and predictive service for the Puck District through the development of a computer system providing WaterPUCK service, which will clearly and practically assess the impact of farms and land use structures on surface waters and groundwater in the Puck District, and consequently on the quality of the waters of the Puck Bay. The construction of the service is based on *in situ* research, environmental data (chemical, physicochemical and hydrological) and numerical modelling. WaterPUCK service is an integrated system consisting of computer models interconnected with each other, operating continuously by supplying it with meteorological data and consists of 4 main modules:

- a comprehensive model of surface water runoff based on SWAT code,
- a numerical model of groundwater flow based on MODFLOW code,
- a three-dimensional numerical model of the Puck Bay ecosystem,
- a calculator of farms efficiency in Puck District as an interactive application.

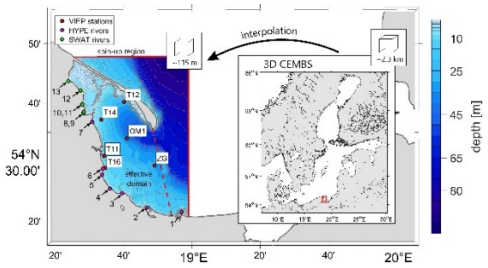


Figure 1. Model effective domain with topography, locations of sampling stations used for evaluation and locations of mouths of watercourses included in domain. Green dots represent rivers that are delivered using SWAT hydrological model.

3. Model configuration

EcoPuckBay origins from Community Earth System Model (CESM) coupled global climate model by NCAR. CESM is a state-of-the-are model system consisting of five separate components with an additional coupler controlling time, exciting forces, domains, grids and information exchange between the models. For the purpose of the WaterPUCK project, CESM was downscaled and adapted for the Puck Bay region.

EcoPuckBay's horizontal resolution is 1/960^o which amounts to a nominal resolution of 115 m (Figure 1). The vertical resolution is 0.4-0.6 m in the upper layers down to 3 m, and then gradually increases to 5 m at depth, with a total of 24 layers. The vertical discretization uses the *z* formulation and the bottom topography is based on Baltic Sea Bathymetric Database (BSBD) from the Baltic Sea Hydrographic Commission. The bathymetric data were interpolated into the model grid using Kriging method. The ocean model time step is 12 s.

4. Summary

To study the complexity of hydro-physical and biological processes in the marine environment, and the links between these processes, modern techniques, i.e. mathematical modelling and computer simulations are required. Although the field work provides the most reliable information on these mechanisms and processes, it requires comprehensive and costly *in situ* observations conducted under a variety of hydrological conditions for long periods of time.

The development of integrated approaches, such as monitoring measures and modelling, became an important tool not only for understanding the processes taking place in both inland and marine ecosystems but also for evaluating the impact of various land-use and climate scenarios on water quantity and quality at the basin scale.

Acknowledgements:
This research was funded by the Polish National Centre for Research and Development within the BIOSTRATEG III program No. BIOSTRATEG3/343927/3/NCBR/2017

Interactive calculators as tools to assist farmers in estimating agricultural holding's balance and nitrogen leaching from field

Dawid Dybowski[1], Lidia Dzierzbicka-Głowacka[1], Stefan Pietrzak[2] and Dominika Juszkowska[2]

[1] Physical Oceanography Department, Institute of Oceanology, Polish Academy of Sciences, Sopot, Poland (ddybowski@iopan.pl)
[2] Department of Water Quality, Institute of Technology and Life Sciences in Falenty, Raszyn, Poland

1. Background

Leaching of nutrients from agricultural areas is the main cause of water pollution and eutrophication of the Baltic Sea. A variety of remedial actions to reduce nitrogen and phosphorus losses from agricultural holdings and cultivated fields have been taken in the past. However, knowledge about the risk of nutrient leaching has not yet reached many farmers operating in the water catchment area of the Baltic Sea.

2. Methods

The nutrient balance method known as “At the farm gate” involves calculating separate balances for nitrogen (N), phosphorus (P) and potassium (K). After estimating all the components of the nutrient balance, the total balance for NPK is calculated and the data obtained is expressed as the ratio of total change (surplus) to the area of arable land on a farm. In addition, the nutrient usage efficiency on a farm is also calculated (Figure 1).

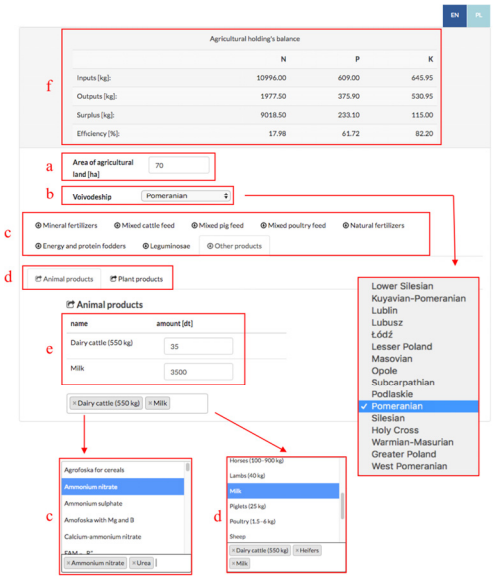


Figure 1. Calculating nutrients balance in farm. Choose parameters for farm: (A) area of agricultural land; (B) Voivodeship; (C) inputs; (D) outputs; (E) amounts of inputs/outputs. The result of the calculations is shown in the table (F).

An opinion poll has been conducted on 31 farms within the Puck Commune, which is approximately 3.6% of all farms located in this commune. Farmers provided data on the manner of fertilizing and cultivating crops on all their farms. For each field individually, on the basis of collected data, an estimated amount of the N leaching from the field has been determined (Figure 2).

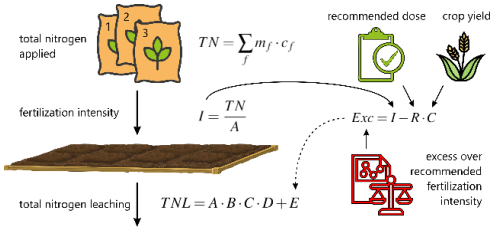


Figure 2. Scheme of total N leaching from the field calculations.

3. Results

The average consumption of mineral fertilizer in the sample population of farms was 114.9 kg N, 9.3 kg P, and 22.9 kg K·ha $^{-1}$ of agricultural land (AL), respectively. N balance in the sample farms being ranged from -23.3 to 254.5 kg N·ha $^{-1}$ AL while nutrient use efficiency ranged from 0.40% to 231.3%. In comparison, P surplus in the sample farms was 5.0 kg P·ha $^{-1}$ AL with the P use efficiency of 0.4–266.5%.

An interactive calculator to assist farmers in determining the quantity of N leaching from the agricultural field has been developed. The influence of factors shaping the amount of N leaching from a single field has been analyzed and it has been determined that autumn ploughing (specifically its absence) and the type of cultivated soil had the greatest average influence on this value in the studied sample.

4. Discussion

Mean N fertilizer consumption in the tested farms was higher than the average usage across Poland and in the Pomeranian Voivodeship. However, mean consumption of potassium fertilizers was lower than mentioned averages. Mean P fertilizer consumption was higher than in the Pomeranian Voivodeship, but lower compared to the entire country. Generally, on the basis of designated research indicators of farm pressures on water quality, concentrations of total nitrogen and total phosphorus were obtained. CalcGosPuck (an integrated agriculture calculator) will help to raise farmers’ awareness about NPK flow on farm scale and to improve nutrient management.

Due to the possible ways of reducing N leaching from agricultural fields, most of the studied fields were fertilized in an appropriate manner. However, in the studied sample there are fields for which the fertilization intensity significantly exceeds the recommended doses. In this context, a tool in the form of an interactive, easy-to-use N leaching calculator should help farmers to select appropriate doses and optimal fertilization practices.

Acknowledgements:
This research was funded by the Polish National Centre for Research and Development within the BIOSTRATEG III program No. BIOSTRATEG3/343927/3/NCBR/2017

Assessing the impact of agriculture on the waters of the Puck Bay within the WaterPUCK project

Dawid Dybowski[1], Lidia Dzierzbicka-Głowacka[1], Beata Szymczycha[2], Ewa Wojciechowska[3], Adam Szymkiewicz[3], Piotr Zima[3], Grażyna Pazikowska-Sapota[4], Stefan Pietrzak[5], Maciej Janecki[1], Artur Nowicki[1] and Tadeusz Puszkarczuk[6]

[1] Physical Oceanography Department, Institute of Oceanology, Polish Academy of Sciences, Sopot, Poland (ddybowski@iopan.pl)
[2] Marine Chemistry and Biochemistry Department, Institute of Oceanology Polish Academy of Sciences, Sopot, Poland
[3] Faculty of Civil and Environmental Engineering, Gdansk University of Technology, Gdańsk, Poland
[4] Department of Environmental Protection, Gdynia Maritime University Maritime Institute, Gdynia, Poland
[5] Department of Water Quality, Institute of Technology and Life Sciences in Falenty, Raszyn, Poland
[6] Municipality of Puck, Puck, Poland

1. Introduction

The Baltic Sea is semi-enclosed sea bordered by intensive agricultural areas of the surrounding developed industrial countries. Its catchment area is fourfold larger than the sea itself. Due to anthropogenic pressure and a positive water balance, the Baltic has become one of the most polluted seas in the world. The main pathways of chemical substance flux to the region are rivers, along with other sources such as atmospheric deposition, diffuse runoff from land, industrial waste, shipping accidents, and wastewater treatment plants. Additionally, submarine groundwater discharge (SGD) has recently been recognized as an important chemical substance source to the sea. Increased loads of nutrients cause different kinds of water deterioration, such as eutrophication, hypoxia, and anoxia. Nutrients discharged to the Baltic Sea originate mainly from anthropogenic activities in the catchment area. Agriculture and managed forestry cause 60% of the waterborne nitrogen and 50% of the waterborne phosphorus inputs to the sea. The Baltic Marine Environment Protection Commission–Helsinki Commission (HELCOM) recommended several actions to reduce nutrient flux to the Baltic that resulted in a regular decrease from the late 1980s, but nutrient concentrations are still relatively high, and eutrophication remains one of the most serious threats to the Baltic. The health of the Baltic ecosystem also suffers from increased concentrations of other pollutants, such as metals and organic compounds.

2. Research area

The Puck District and the Puck Bay are examples of a region where sustainable growth and management is a challenging task due to the region's complex structure. The Puck Bay is an inner basin of the Bay of Gdansk, which covers an area of approximately 40,000 ha. Its inner part is a shallow (average depth of 3 m), sandy seagrass bed, while the outer part's average depth is 20.5 m. The Puck Bay's salinity ranges from 3 to 7 and is known as a nursery ground and breeding area for a number of fish and bird species. The bay contains several types of habitats (from muddy to stony bottom) located at a variety of shore types (i.e., sandy beaches, gravel beds, stony outcrops, clay cliffs, vegetated river mouths, etc.). The Puck Bay is protected as a Natura 2000 site under both the birds and habitats directives. It is also a designated Baltic Sea Protected Area, and its inner waters are part of the Coastal Landscape Park. The area has also been subjected to strong anthropogenic pressure. The main sources of pollution for the Bay of Puck are rivers, SGD, atmospheric deposition, and point sources, while the coastal ecosystem controls the biogeochemical transformations of P and N compounds (e.g., phosphate, nitrate, dissolved organic nitrogen, etc.) through close coupling between water and sediments.

3. Methods

The proposed approach, called WaterPUCK, is an innovative and complex method that enables researchers to identify the sources of nutrient and pesticide pollution, understand the main mechanisms responsible for the transport of these pollutants in surface and groundwater, calculate their flux via rivers and SGD, and directly assess the influence of pesticides and nutrient flux on the Bay of Puck ecosystem, including the creation of scenarios projecting the effects of changes in land use on chemical loads from the Puck District that are transported via surface and groundwater to the Bay of Puck.

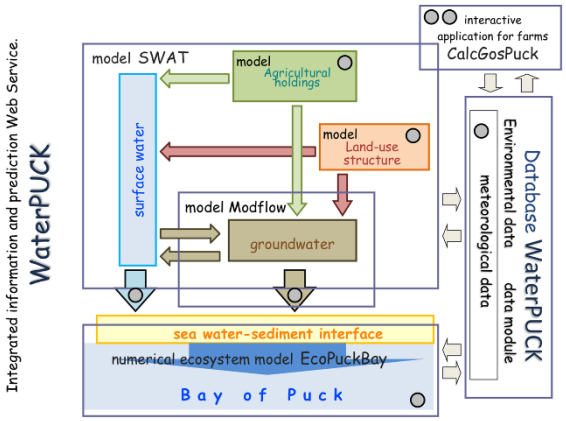


Figure 1. The scheme of the WaterPUCK service. Integrated information and prediction Service WaterPUCK includes surface water model (based on SWAT Soil and Water Assessment Tool), groundwater flow model (based on Modflow code), 3D environmental model of the Bay of Puck Eco- PuckBay (based on the POP code and 3D CEMBS model of the Baltic Sea) and an integrated agriculture calculator called "CalcGosPuck" plus large Database WaterPUCK.

WaterPUCK combines several different components – such as data collection, determining environmental pressure indicators, retrospective analyses of existing monitoring

data sets, in situ measures, and the application of various models – to estimate the main mechanisms and threats responsible for the transport of pollutants from the agricultural holdings and land-use structures to the surface and groundwater. WaterPUCK also has the potential to predict environmental changes in the district and the bay ecosystem. WaterPUCK integrates several models (Fig. 1), such as a surface water model based on SWAT, a groundwater flow model based on MODFLOW, a 3D-ecohydrodynamic model of the Bay of Puck called EcoPuckBay based on the POP code, and an agriculture calculator called CalcGosPuck.

4. Summary

There are several possibilities of using operating systems that assess the impact of pollutants on water quality in order to increase and develop the R&D sector and stimulate the private sector in research activities:

- Providing knowledge about sustainable usage of water resources by modeling the surface water and groundwater percolation (and using it for future predictions) and taking into account climate change (e.g., precipitation change).
- Help in understanding the ecosystem and sustainable management of surface water, groundwater, and land use.
- Environmental protection agencies can also use these tools to address the pollution source that will result in a more efficient monitoring system.
- Developing the numerical methods controlling the environmental status of the surface water, groundwater, and seawater enables for effective environment management and raising of novel and innovative practical solutions in Europe and rest of the World.

WaterPUCK Service allows to:

- Help local governments decide where certain investments should be located or whether the permission or license for the investment should be given.
- Significantly improve the management of natural resources and reduce losses resulting from declining revenues; developed solutions can be applied in other municipalities and coastal regions along the entire coastline of the Baltic Sea.
- Recognize the multiple functions of agroecosystems and many services they provide in order to foster an integrated approach to natural resource management, agricultural production, and food security.
- Help to predict seawater status knowing nutrient inflow to the Bay of Puck (a key Polish tourist region); therefore, tourists could plan their holidays according to the model predictions, knowing when and where harmful blooms will occur.

Acknowledgements:
This research was funded by the Polish National Centre for Research and Development within the BIOSTRATEG III program No. BIOSTRATEG3/343927/3/NCBR/2017

Seasonality of the total alkalinity in the Gulf of Gdansk, southern Baltic Sea

Karol Kuliński, Aleksandra Winogradow, Beata Szymczycha and Marcin Stokowski

Institute of Oceanology of Polish Academy of Sciences, Sopot, Poland; *email: kroll@iopan.pl

The Baltic Sea is one of the largest brackish ecosystems in the world. In accordance with the low salinity (S) the buffer capacity, as reflected by A_T, is also low in almost all regions of the Baltic Sea. Hence, the large scale distribution of the pH is a function of the alkalinity distribution. There are several different A_T vs. S regimes in the Baltic Sea (Fig. 1, Beldowski et al., 2010). They reflect different A_T concentrations in the respective rivers, which can be deduced from extrapolation of regional A_T vs. S relationships to zero salinity. Low alkalinities are observed in rivers draining the northern Scandinavia catchment whereas rivers from continental Europe are rich in alkalinity. These differences are a consequence of different river water alkalinities, which are controlled by the geological conditions and weathering processes in the respective catchment areas. As a result lower alkalinities (low buffer capacity) and lower mean pH are observed in the Gulf of Bothnia and Finland, whereas higher mean alkalinities and thus somewhat higher pH are found in the Gulf of Riga and also in the Gdansk Bay (Kuliński et al., 2017; Beldowski et al., 2010). The central Baltic Sea acts as a mixing chamber for the different water masses, including water originating from the North Sea, resulting in an alkalinity in the surface water of the Baltic Proper (salinity around 7 PSU) of about 1600-1700 µmol the kg^{-1}.

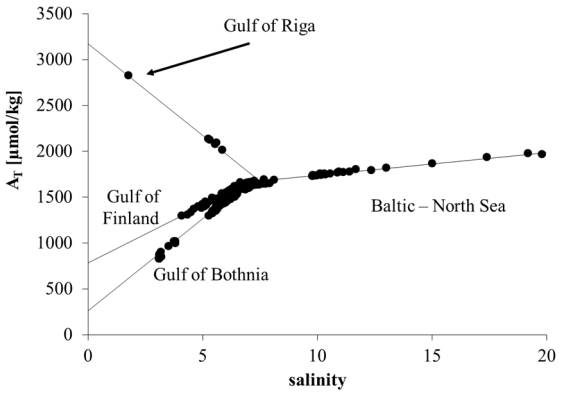


Figure. 1 The total alkalinity (A_T) distribution against salinity in the Baltic Sea (Beldowski et al., 2010).

Due to its low salinity and thus also low total alkalinity (A_T) the Baltic Sea is the basin potentially endangered to the ocean acidification (OA). The recent studies showed, however, that OA in the Baltic Sea is to large extent mitigated by the A_T increase (Müller et al., 2016). The potential source of that increase can be the changes in the riverine A_T loads. In our study we have investigated the A_T, C_T and pH variability biweekly in the Vistula River mouth and weekly at the Sopot Pier in the Gulf of Gdansk over the period 2016-2018. The obtained data provide new parametrization for the riverine A_T and C_T loads to the southern Baltic as well as give new insights on the CO_2 system functioning in this region. The huge variability was found in the Vistula mouth (A_T: 2400 – 3700 µmol kg^{-1}, C_T: 2000 – 4000 µmol kg^{-1}, pH: 7.5 – 8.5) (Fig. 2) compared to the moderate one observed in the seawater (A_T: 1700 – 2000 µmol kg^{-1}, C_T: 1500 – 2000 µmol kg^{-1}, pH: 7.6 – 8.5) (Fig.3). For river water, the maxima for both A_T and C_T concentrations have been found in winter while the lowest in summer. For the seawater, the seasonality was less pronounced and depended more on the salinity distribution.

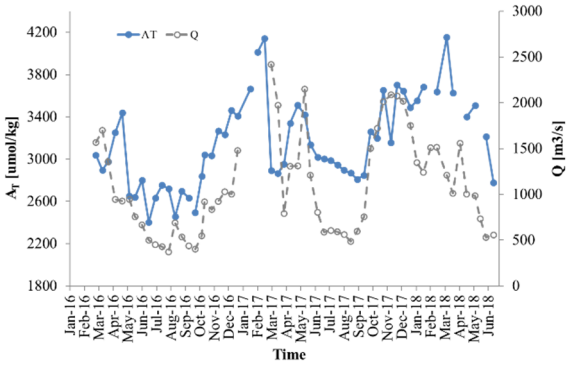


Figure. 2 Seasonality of the total alkalinity (A_T) and water flow (Q) in the mouth of the Vistula River, Kiezmark, Poland.

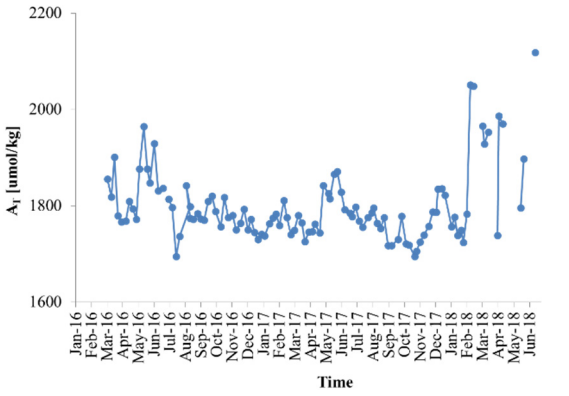


Figure. 3 Seasonality of the total alkalinity (A_T) in the Gulf of Gdańsk, Sopot, Poland.

References

Beldowski, J., Löffler, A., Schneider, B., Joensuu, L., 2010. Distribution and biogeochemical control of total CO_2 and total alkalinity in the Baltic Sea. Journal of Marine Systems 81,252–259.

Kuliński, K., Schneider, B., Szymczycha, B., Stokowski, M., 2017. Structure and functioning of the acid-base system in the Baltic Sea. Earth System Dynamics Discussions 1–28. https://doi.org/10.5194/esd-2017-39.

Müller, J. D., Schneider B., and Rehder G., 2016. Long-term alkalinity trends in the Baltic Sea and their implications for CO_2-induced acidification. Limnol. Oceanogr. 61: 1984–2002. doi:10.1002/lno.10349.

Bioavailability and remineralization of sediment-derived dissolved organic carbon from the Baltic Sea depositional area

Monika Lengier, B. Szymczycha and K. Kuliński

Institute of Oceanology Polish Academy of Sciences, Sopot, Poland (mlengier@iopan.pl)

1. Introduction

The carbon cycle plays a dominant role in the global and regional change. The biological pump is the key mechanism allowing the sequestration of atmospheric CO_2 by the marine environment. Phytoplankton in the course of photosynthesis consumes CO_2 and transforms it into organic matter (OM), which is further transported through the marine food web. Some fraction of OM that escapes remineralization in the water column can be buried in the sediments, in that way, excluding the corresponding amount of carbon from its contemporary cycle (Jiao et al., 2010). A great role in carbon cycling is played by coastal and marginal seas like e.g. the Baltic Sea (Kuliński and Pempkowiak, 2011). This basin is under high anthropogenic influence experiencing enhanced loads of OM and nutrients. This leads to high OM sedimentation rates, especially within the depositional areas. As the Baltic Sea is a shallow sea (average depth of 52 m), the exchange of nutrients and OM between sediments and water column is of great importance within the biogeochemical cycles (Meier et al., 2019). Therefore, quantification of the rates of biogeochemical processes in marine sediments and bottom waters is vital for understanding the carbon cycle (Arndt et al., 2013).

Sediment pore waters in the Baltic Sea are enriched with the dissolved organic carbon (DOC), which results in a diffusive flux of DOC to the water column (Reader et al., 2019). It was found that up to 30% of OM deposited in the sediments returns to the water column (Kuliński and Pempkowiak, 2011) and may alter processes occurring in the water column e.g. increase of oxygen demand in the bottom waters (Reader et al., 2019). Even though there are some data addressing the bioavailability and remineralization of terrestrial DOC (e.g. Lønborg and Søndergaard, 2009; Asmala et al., 2013; Kuliński et al., 2016; Rowe et al., 2018), still little is known about the bioavailability of sediment-derived DOC and its remineralization rates. Thus, the aim of this study was to assess the bioavailability, degradation rate and half-life times of sediment-derived DOC. Although, it is a case study performed in the Gdańsk Deep, it has a universal character with the ability to be conducted for all the depositional areas in the shelf seas, while the obtained data could be of use for the biogeochemical models.

2. Methods

Seawater and sediment samples were collected during r/v Oceania cruise in March 2018. The bottom water samples were collected using Niskin bottles (~2m above the sediments), while surface sediments (0-5 cm) were collected using Gemax gravity corer. The bottom water was collected in pre-cleaned 10l bottle directly after sampling. Seawater samples were passed through pre-cleaned and pre-combusted 0.4 µm MN G5 glass-fiber filters (pre-combusted at 450°C for 8h). In order to obtain pore water, the collected sediments were centrifuged. Then, bottom water was spiked with pore water in a volume ratio of 4:1. To ensure oxic conditions in the experiment, the mixture was bubbled with the ambient air to reach 100% O_2 saturation. Incubation of the prepared samples was conducted in 23±0.1°C for 126 days. At the beginning (t=0) and after 1, 2, 6, 18, 35, 73 and 126 days of the incubation the individual samples were analyzed for total dissolved organic carbon (DOC). Additionally, untreated bottom water was used as a control during the experiment and sampled in three replicates. The concentrations of DOC were analyzed on an automated total organic carbon analyzer TOC-L (Shimadzu).

3. Results

The observed development of the DOC decay had an exponential character. The highest dynamics of DOC remineralization was at the beginning of the experiment and it gradually decreased over time. During the incubation period pore water DOC concentration decreased from 1408 to 850 µmol l^{-1}, which corresponds to almost 40% loss (Fig 1). In the control samples DOC concentration decreased from 304 to 260 µmol l^{-1} i.e. by ~14% (Fig.1).

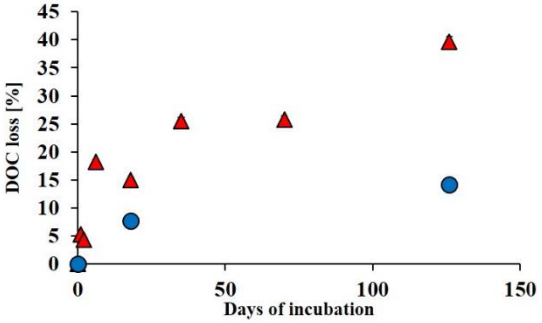


Figure 1. Cumulative DOC losses during incubation presented as percentage of initial concentrations for pore water (triangles) and bottom water (control; circles).

To quantify the DOC remineralization in the incubation experiment the first order kinetics was used (Kuliński et al., 2016). It assumes that the DOC concentration change over time depends on the initial DOC and remineralization rate constant (k_b). Oxic conditions prevailing throughout the whole experiment did not limit the microorganisms' activity. Characterization of remineralization kinetics required establishing apart from remineralization rate constants also the half-life times.

Three different DOC fractions were defined: labile DOC (DOCL), semi-labile DOC (DOCSL) and refractory DOC (DOCR). Each fraction has distinct role in the carbon cycling and is characterized by different bioavailability. DOCL is easily mineralized within hours to days, which provides autochthonous support for the euphotic zone

microbial loop and does not accumulate in the system. In this study, DOCL comprised ~10% of total DOC (147 µmol l^{-1}). Its remineralization rate constant equaled 0.0958 d^{-1}, while half-life time was 7.24 d. DOCSL also supports the microbial loop, but its half-life time is counted in weeks/months. Sediment-derived DOCSL equaled ~44% of initial DOC concentration (623 µmol l^{-1}). DOCSL remineralization rate constant amounted to 0.0082 d-1, while half-life time was 84.53 d. DOCL and DOCSL are considered to be the bioavailable pool of DOC (DOCB). The DOCB derived from the pore water was 770 µmol l^{-1} and exceeded the concentration of refractory DOC (DOCR, 638 µmol l^{-1}), which is believed to be an inactive fraction of DOC on the short and medium time scales. Kuliński et al. (2016) assessed in similar way the remineralization dynamics of terrestrial dissolved organic carbon (tDOC) in the Baltic Sea water. Additionally, incubation experiments were performed with the surface seawater in order to determine the remineralization dynamics of the Baltic Sea DOC (mDOC). The total bioavailable fraction of tDOC and mDOC was 20% and 34%, respectively. In this study, the total bioavailable fraction of pore water DOC amounted to 54%. This shows the potential of pore water DOC as a substrate for microbial heterotrophs is generally much higher than that of terrestrial DOC.

4. Conclusions

The depositional areas of the Baltic Sea are recognized as important source of DOC to the water column. This study, being the first assessment of sediment-derived DOC lability, indicates that about half of this load is bioavailable. This gives a new insight on the Baltic Sea carbon cycle and other shelf regions.

Acknowledgements

The results were obtained within the framework of the following projects: 2015/19/B/ST10/02120 and 2019/33/N/ST10/00161 funded by Polish National Science Center.

References

Arndt, S., Jørgensen, B.B., LaRowe, D.E., Middelburg, J.J., Pancost, R.D., Regnier, P., 2013. Quantifying the degradation of organic matter in marine sediments: A review and synthesis, earth Science-review, 123, 53-86, http://dx.doi.org/10.1016/j.earscirev.2013.02.008.

Jiao, N., Herndl, G.J., Hansell, D.A., Benner, R., Kattner, G., Wilhelm, S.W., Kirchman, D.L., Weinbauer, M.G., Luo, T., Chen, F., Azam, F., 2010. Microbial production of recalcitrant dissolved organic matter: long-term carbon storage in the global ocean, Nat Rev Microbiol, 8, 593-599, https://doi.org/10.1038/nrmicro2386.

Kuliński K., Pempkowiak J., 2011. The carbon budget of the Baltic Sea, biogeosciences, 8, 3219-3230.

Kuliński, K., Hammer, K., Schneider, B., Schulz-Bull, D., 2016. Remineralization of terrestrial dissolved organic carbon in the Baltic Sea, marine Chemistry, 181, 10-17, http://dx.doi.org/10.1016/j.marchem.2016.03.002.

Meier, H.E.M., Edman, M.K., Eilola, K.J., Placke, M., Neumann, T., Andersson, H.C., Brunnabend, S.-E., Dieterich, C., Frauen, C., Friedland, R., Gröger, M., Gustafsson, B.G., Gustafsson, E., Isaev, A., Kniebusch, M., Kuznetsow, I., Müller-Karulis, B., Naumann, M., Omstedt, A., Ryabchenko, V., Saraiva, S., Savchuk, O.P., 2019. Assessment of Uncertainties in Scenario Simulations of Biogeochemical Cycles in the Baltic Sea, Front Mar Sci, 6, 46, https://doi.org/10.3389/fmars.2019.00046.

Reader, H.E., Thoms, F., Voss, M., Stedmon, C.A., 2019. The Influence of Sediment-Derived Dissolved Organic Matter in the Vistula River Estuary/Gulf of Gdańsk, JGR Biogeosciences, 124, 115-126, https://doi.org/10.1029/2018JG004658.

Nitrogen Fixation in a coastal peatland and adjacent sediments

Tina Liesirova[1], Tobias Aarenstrup Launbjerg[2], Lasse Riemann[2], Maren Voss[1]

[1] Institute of Baltic Sea Research, Warnemünde, Germany (tina.liesirova@io-warnemuende.de)
[2] Marine Biological Section, Department of Biology, University of Copenhagen, Helsingør, Denmark

1. Motivation

Nitrogen is essential for living organisms to construct complex bio-molecules like DNA, ATP, and amino acids (Pray 2008). Despite the high abundance of atmospheric dinitrogen, gaseous N cannot be directly metabolized by most organisms and only few groups are capable of the conversion of N_2 into a bioavailable N-compound. This process is called biological nitrogen fixation (BNF) and is a highly energy demanding process. A group of bacteria and archaea, called diazotrophs employ an enzymatic catalyzer (nitrogenase; nifH) to break N_2, which enables the anoxic reduction of dinitrogen to ammonium (Mulholland 2007; Göltenboth 2006; Ferndandez-Mendez et al. 2016; Shiozaki et al. 2018). Photoautotrophic cyanobacteria can be a significant contributor to the reactive nitrogen pool. This applies to the Baltic Sea during summer, leading to the fatal consumption of oxygen in deep waters. In contrast, the importance of non-cyanobacterial diazotrophs (NCD) in marine environments is still largely unknown, yet influential NCDs may operate in benthic environments, such as sulfate reducing bacteria (SRB; Bertics et al. 2011).

On land BNF occurs in nitrogen poor peatlands and mosses often depend on diazotrophic organisms to satisfy their nitrogen demands. But peatlands have also been reclaimed and used as meadows or fields for decades before they were restored. When such ecosystems border the Baltic Sea, they may experience flooding events. Thereby, environmental varianles such as salinity change, and the process of N_2 fixation may get disturbed there.
To determine the extent of diazotrophic activity in a flooded peatland of the southern Baltic Sea, as well as in different types of sediments by NCDs, N_2 fixation rates were studied over several seasons during 2019.

2. Problem

The intensity of Biological Nitrogen Fixation (BNF) in the Baltic during summer blooms was largely focused on the photic layer the water column. NCD have only been studied below the chemocline and in resuspended muddy sediments of the Baltic Sea Straits (Pedersen et al. 2018).

To which extent does dark N_2 fixation at the seafloor contribute to the reactive N-pool throughout the year in the Southern Baltic?

Do SRB execute nitrogen fixation in muddy sediments?
Also, does saline seawater influx in German peatlands diminish diazotrophic activity?

3. Study design

Sampling took place during May (proximity of Rostock, Germany), August (island of Poel, Germany), and September (Gdansk Bay, Poland; Warnemünde beach, Germany). Sediment samples comprised mud, sand, and peat substrate.

To determine N_2 fixation rates, we incubated slurries with a ^{15}N-N_2 tracer under constant rotation (60 rpm), temperature

control (15°C; 20°C) and dark conditions. Peat samples gathered in fall were incubated additionally under light. A separate series of all substrates was treated with sodium molybdate (Na_2MoO_4) to inhibit SRBs. All treatments were conducted in triplicates, but detection limits for N_2 fixation rates lead to the exclusion of rates for several samples. Also, we conducted grain size analysis, and performed DNA/ RNA analysis of subsamples prior to and post incubation.

4. Preliminary Results and Discussion

NCD driven N_2 fixation is linked to the suspension of fine grained sediment particles in water, as microbes may attach to particle surfaces and proliferate there. Thus, they significantly contribute to the reactive N-pool, even in eutrophic environments (Fig. 1; Pedersen et al. 2018). In agreement with this observation, it seems, that increased N_2 fixation rates are found in muddy samples. This implies, that small grained sediments are a favorable environment for microbes and diazotrophs (and microbes in general) potentially perform N_2 fixation there.

Nitrogen fixation rates measured in mud slurries from Gdansk Bay appear to reach the highest N_2 fixation rates from all samples measured and where even higher than mud from Warnemünde, Hütelmoor Beach, and Poel.

This could be plausible, as mud from the Gdansk Deep had the finest grain size compared to the other stations, thus the best/largest microbial habitat. Furthermore, this mud was extracted from 70m depth and present microbes are probable adapted to purely dark conditions, whereas the other mud samples were extracted in photic water zones and microbes potentially suffered a disadvantage from the light-shut incubation.

At present it appears, that sediment samples treated with sodium molybdate –the SRB inhibitor- reached comparably lower N_2 fixing rates, than the untreated ones. As SRBs are known to be abundant in marine environments, their presence in the water was expected, yet the experiment indicates, that they are also active contributors of N_2 fixation of the Southern Baltic coastline, especially in the Gdansk Bay deep mud.

Considering the peat(-water) treatments, dark N2 fixation seems to be a negligible source of N. However, a separated, single run under illuminated conditions in September, provided detectable N_2 fixation. This suggests, that photic diazotrophic communities dominate this environment.

5. Conclusion

So far, dark N_2 fixation seem to be rather low along the Southern Baltic coastline and in a peatland between May and September. Thereby, fine grained sediments, from greater depths seem to have more favorable conditions for diazotrophs operating in dark. SRBs might contribute to benthic N_2 fixation at the sedimentary sampling sites, but not in the peatland, where photic diazotrophic communities appear to be more significant.

To which extend dark N_2 fixation significantly contributes to the N-pool at the Southern Baltic coastline needs to be evaluated.

6. Acknowledgement

This project was supported by the Research Training Group Baltic TRANSCOAST, which received funding from the German Science Foundation (GRK2000/1-2020).

References

Bertics, Victoria, Carolin Löscher, Iines Salonen, R. Schmitz-Streit, Gaute Lavik, M. Kuypers, and Tina Treude. 2011. "Nitrogen Fixation By Sulfate-Reducing Bacteria in Coastal and Deep-Sea Sediments." AGU Fall Meeting Abstracts, December, 08.

Ferndandez-Mendez, M, K Turk-Kubo, P Buttigieg, J Rapp, T Krumpen, J Zehr, and A Boetius. 2016. "Diazotroph Diversity in the Sea Ice, Melt Ponds, and Surface Waters of the Eurasian Basin of the Central Arctic Ocean." 2016. https://www.ncbi.nlm.nih.gov/pmc/articles/PMC5120112/.

Göltenboth, FRIEDHELM. 2006. "Preface." In Ecology of Insular Southeast Asia, edited by Friedhelm Göltenboth, Kris H. Timotius, Paciencia Po Milan, and Josef Margraf, vii–viii. Amsterdam: Elsevier. https://doi.org/10.1016/B978-044452739-4/50000-0.

Mulholland, M. R. 2007. "The Fate of Nitrogen Fixed by Diazotrophs in the Ocean." Biogeosciences 4 (1): 37–51. https://doi.org/10.5194/bg-4-37-2007.

Pedersen, Jeppe N., Deniz Bombar, Ryan W. Paerl, and Lasse Riemann. 2018. "Diazotrophs and N2 Fixation Associated With Particles in Coastal Estuarine Waters." Frontiers in Microbiology 9 (November): 2759. https://doi.org/10.3389/fmicb.2018.02759.

Pray, Leslie. 2008. "Molecular Events of DNA Replication | Learn Science at Scitable." 2008. https://www.nature.com/scitable/topicpage/major-molecular-events-of-dna-replication-413/.

Shiozaki, Takuhei, Amane Fujiwara, Minoru Ijichi, Naomi Harada, Shigeto Nishino, Shinro Nishi, Toshi Nagata, and Koji Hamasaki. 2018. "Diazotroph Community Structure and the Role of Nitrogen Fixation in the Nitrogen Cycle in the Chukchi Sea (Western Arctic Ocean)." Limnology and Oceanography 63 (5): 2191–2205. https://doi.org/10.1002/lno.10933.

Photosynthesis, respiration and growth responses of Baltic Sea benthic diatoms in relation to sea-land exchange processes

Lara R. Prelle, Angelika Graiff, Sigrid Gründling-Pfaff, Veronika Sommer, Kana Kuriyama and Ulf Karsten

Applied Ecology and Phycology, Institute of Biological Sciences, University of Rostock, Rostock, Germany (lara.prelle@uni-rostock.de)

1. Introduction

The coastal region of the Baltic Sea is very sensitive to all types of natural changes, especially due to its enclosure by land. Besides the seasonal and diurnal meteorological impacts on the shallow coastal zones, land-sea transition zones are distinctively affected by terrestrial-marine exchange processes (Jurasinski et al. 2018). These processes, however, do not simply affect the coastal development but also impact the organisms living in this transition zone. Especially phototrophic organisms are strongly affected by the environmental settings in the shallow water zone, such as light limitation due to sediment resuspension which in turn might lead to inhibition of photosynthesis (e.g. Woelfel et al. 2014).

2. Organisms and sampling area

To investigate the effect and ecophysiological response of phototrophic organisms, eight benthic diatom strains were isolated from shallow coastal Baltic Sea sediment samples in front of a coastal fen (Hütelmoor). This sampling area is hypothesized by Baltic TRANSCOAST to facilitate organic matter and nutrient fluxes along the terrestrial-marine gradient.

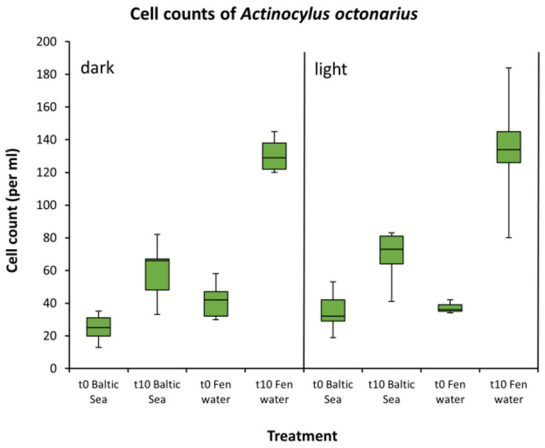


Figure 1. Cell counts of *Actinocyclus octonarius* before (t0) and after cultivation period (t10) in different media and light treatments.

3. Photosynthetic performance of diatoms

Established unialgal diatom taxa were studied for photosynthetic performance at varying photon fluence rates (0 - 1200 µmol photons m^{-2} s^{-1}, recorded at 20°C) and temperatures (5 - 40°C, measured at saturating ~ 270 µmol photons m^{-2} s^{-1}) using oxygen dipping probes. Light saturation was reached at 32 - 151 µmol photons m^{-2} s^{-1} and maximum net primary production rates at 23 - 144 µmol O_2 mg^{-1} Chl *a* h^{-1} with no severe photoinhibition, indicating high photo-physiological plasticity. Photosynthetic performance exhibited eurythermal traits with species-specific optimum temperature for photosynthesis (15 - 30°C) and respiration (25 - 40°C). Photosynthetic efficiency of over 20% at high temperatures was found in half of the taxa.

4. Heterotrophic capabilities in diatoms

Additionally, a growth comparison experiment resulted in growth stimulation for *Actinocyclus octonarius* and *Nitzschia dubiiformis* in light exposed fen water compared to Baltic Sea water. Furthermore, growth of *A. octonarius* was even stimulated in the dark when kept in fen water, pointing to heterotrophic capabilities (Figure 1).

5. Conclusion

In conclusion, shallow water benthic diatoms of the southern Baltic Sea exhibited a high photo-physiological plasticity and a broad temperature tolerance. Under fen water influence mixo- and/or heterotrophic growth of microphytobenthic communities may be supported. These traits are essential in the highly dynamic shallow coastal zones of the Baltic Sea.

References

Jurasinski, G., Janssen, M., Voss, M., Böttcher, M. E., Brede, M., and Burchard, H. (2018). Understanding the coastal ecocline: assessing sea-land-interactions at non-tidal, low-lying coasts through interdisciplinary research. Front. Mar. Sci. 5:342

Woelfel, J., Schoknecht, A., Schaub, I., Enke, N., Schuhmann, R., and Karsten, U. (2014). Growth and photosynthesis characteristics of three benthic diatoms from the brackish southern Baltic Sea in relation to varying environmental conditions. Phycologia Vol. 53, 639–651.

Predicting submarine groundwater discharge from coastal peatlands of northeast Germany using HYDRUS-2D

Erwin Don Racasa, Bernd Lennartz and Manon Janssen

Soil Physics, Faculty of Agricultural and Environmental Sciences, University of Rostock, Rostock, Germany
(erwin.racasa@uni-rostock.de)

1. Submarine Groundwater Discharge from Coastal Peatlands

Submarine groundwater discharge (SGD) is "the flow of water through continental and insular margins from the seabed to the coastal ocean, regardless of fluid composition or driving force" (Taniguchi et al., 2019; Burnett et al., 2003). It is continuously being recognized as an important material pathway from the land to the oceans as evidenced by the exponential increase in scientific articles in recent decades (Ma and Zhang, 2020). Yet, studies on widespread muddy coastlines such as wetlands and saltmarshes are still lacking (Taniguchi et al., 2019).

Coastal peatlands, a type of wetlands, are a common landscape in northeast Germany and throughout the Baltic Sea countries. These wetlands can store vast amounts of carbon, twice as much as the world's forests, highlighting their importance for climate change mitigation (UN Envrionment Programme, 2019). In Mecklenburg-Western Pomerania, these low-lying areas of accumulated organic material (about 40,000 ha) are expected to play a pivotal role in buffering the exchange of water and dissolved and particulate materials (Jurasinski et al., 2018). SGD can still exist in low pressure gradients and be a significant source of nutrients and organic materials, with potential implications on biogeochemical budgets and marine ecosystems.

Since the start of the 18th century, many European peatlands have been extensively modified for agricultural purposes, forestry, and mining for energy generation (Baird and Gaffney, 2000; Schindler et al., 2003). This has led to changes in soil physical and hydraulic properties (Liu and Lennartz, 2018; Schindler et al., 2003) affecting groundwater flow, solute transport, and possibly the eventual submarine groundwater discharge processes. With the current trend on wetland restoration, it is more imperative now to understand how groundwater flows and how materials are transported from coastal peatlands to the Baltic Sea via submarine groundwater discharge.

2. Hypothesis and Objectives

We hypothesize that submarine groundwater discharge occurs even in low-lying coastal peatlands, albeit diffuse and in low fluxes, with controls from a combination of factors.

Our specific objectives are to look at these different factors. By looking at 1) soil physical properties and the state of peat degradation, 2) geological heterogeneity and the extent of the peat layer into the sea, 3) boundary conditions such as sea and groundwater levels and atmospheric input, and 4) topography, we will be able to investigate how various factors influence the occurrence of SGD in peatlands.

3. Numerical Simulation of Groundwater Flow Using HYDRUS-2D

HYDRUS-2D is a widely used modeling package for subsurface water flow and solute transport. The model uses the Richard's equation for saturated-unsaturated water flow and convection-dispersion equations for solute transport in variably-saturated media (Šimůnek et al., 2016; Li et al., 2017). The equations are numerically solved using the method of finite elements with both time and spatial discretization. Despite its widespread use, HYDRUS has not been used for coastal peatlands and submarine groundwater discharge studies to the best of the authors' knowledge.

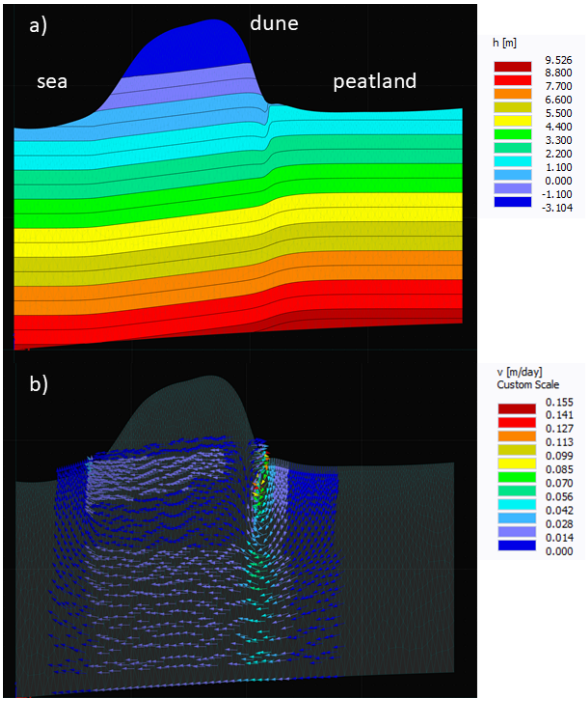


Figure 1. Steady state modeling output for a coastal peatland with a dune barrier showing pressure heads (a) and velocity vectors (b).

4. First Results

HYDRUS is able to simulate the groundwater flow and quantify groundwater fluxes to the sea in coastal peatlands with varying hydraulic gradients/boundary conditions, topography, geology and soil physical properties. Here, we show that a low-lying coastal peatland with a dune barrier may have SGD rates of 0.042 m d^{-1} based on steady state pressure head difference between the Baltic Sea and the peatland of 0.35 m (Figure 1). The results are also based on

average precipitation and evapotranspiration rates. The SGD rates increase with increasing hydraulic gradients.

5. Outlook

Several parameter sets for soil hydraulic properties, geology and topography will be used to determine SGD fluxes under steady state conditions. Magnitude of groundwater discharge will be quantified from coastal peatlands under varying state of peat degradation.

In the future, the resulting SGD fluxes can be integrated with nutrient studies using porewater lances and seepage meters to quantify nutrients and carbon exports from coastal peatlands to the Baltic Sea.

References

A.J. Baird, S.W. Gaffney (2000) Solute movement in drained fen peat: a field tracer study in a Somerset (UK) wetland, Hydrological Process, Vol. 14, pp. 2489-2503

W.C. Burnett, H. Bokuniewicz, M. Huettel, W.S. Moore, M. Taniguchi (2003) Groundwater and pore water inputs to the coastal zone, Biogeochemistry, Vol. 66, pp. 3-33

G. Jurasinski, M. Janssen, M. Voss, M.E. Böttcher, M. Brede, H. Burchard, S. Forster, L. Gosch, U. Gräwe, S. Gründling-Pfaff, F. Haider, M. Ibenthal, N. Karow, U. Karsten, M. Kreuzburg, X. Lange, P. Leinweber, G. Massmann, T. Ptak, F. Rezanezhad, G. Rehder, K. Romoth, H. Schade, H. Schubert, H. Schulz-Vogt, I.M. Sokolova, R. Strehse, V. Unger, J. Westphal, B. Lennartz (2018) Understanding the coastal ecocline: assessing sea-land interactions at non-tidal, low-lying coasts through interdisciplinary research, Frontiers in Marine Science, Vol. 5, No. 342, pp. 1-22

Y. Li, J. Šimůnek, S. Wang, W. Zhang, J. Yuan (2017) Simulating the effects of lake wind waves on water and solute exchange across the lakeshore using HYDRUS-2D, Water, Vol. 9, No. 566, pp. 1-18

H. Liu and B. Lennartz (2018) Hydraulic properties of peat soils along a bulk density gradient – a meta study, Hydrological Processes, Vol. 33, pp. 101-114

Q. Ma, Y. Zhang (2020) Global research trends and hotspots on submarine groundwater discharge (SGD): a bibliometric analysis, International Journal of Environmental Research and Public Health, Vol. 17, No. 830, pp. 1-14

U. Schindler, A. Behrendt, L. Müller (2003) Change of soil hydrological properties of fens as a result of soil development, Journal of Plant Nutrition and Soil Science, Vol. 166, pp. 357-363

M. Schuerch, T. Spencer, S. Temmerman, M.L. Kirwan, C. Wolff, D. Lincke, C.J. McOwen, M.D. Pickering, R. Reef, A.T. Vafeidis, J. Hinkel, R.J. Nicholls, S. Brown (2018) Future response of global coastal wetlands to sea-level rise, Nature, Vol. 561, pp.231-234

J. Šimůnek, M.Th. van Genuchten, M. Šejna (2016) Recent developments and applications of the HYDRUS computer software packages, Vadose Zone Journal, pp.1-25

M. Taniguchi, H. Dulai, K.M. Burnett, I.R. Santos, R. Sugimoto, T. Stieglitz, G. Kim, N. Moosdorf, W. Burnett (2019) Submarine groundwater discharge: updates on its measurement techniques, geophysical drivers, magnitudes, and effects, Frontiers in Environmental Science, Vol. 7, No. 141, pp. 1-26

UN Environment Programme (2019) Peatlands store twice as much as carbon as all the world's forests, https://www.unenvironment.org/news-and-stories/story/peatlands-store-twice-much-carbon-all-worlds-forests

The CO_2 system variability in the vicinity of the Vistula River mouth

Marcin Stokowski, Aleksandra Winogradow, Beata Szymczycha and Karol Kuliński

Institute of Oceanology of Polish Academy of Sciences, Sopot, Poland (stokowski@iopan.pl)

1. Introduction

Ocean Acidification (OA) is believed to be one of the greatest threats for nowadays marine ecosystems. In the Baltic Sea the effect of OA is significantly reduced due to the continuous increase of total alkalinity (TA), which counteracts the acidification effect (Müller et al., 2016). However, it still remains unclear what is the source of that TA increase. It has been found that continental rivers like Daugava, Vistula or Odra, carry huge loads of TA to the Baltic Sea as a consequence of eroding of limestone-rich drainage basin. They supply also the coastal zone with organic matter and nutrients driving both primary production and respiration, which shape the CO_2 system structure and potentially the final loads of the TA to the Baltic Sea.

2. Study Area

The research was conducted in the mouth of the Vistula River, second biggest river entering the Baltic Sea. The mean discharge of 1065 $m^3\ s^{-1}$ and high TA concentrations (>3000 $\mu mol\ kg^{-1}$) make the Vistula likely the largest source of TA to the Baltic Sea.

3. Methods

Three measurable parameters of the CO_2 system were investigated (TA, pCO_2 and pH) in the salinity gradient of the Vistula River Mouth.

TA was analyzed using an automated, open-cell potentiometric titration system developed and provided by Andrew Dickson and his team. The quality of the measurements was provided by using CRMs provided by the Scripps, University of California, San Diego. The measurements precision amounted 3.4 $\mu mol\ kg^{-1}$.

The pCO_2 was measured underway using a bubble-type equilibrator system combined with cavity ring down spectroscopy analyzer by Los Gatos. The response time of the system was about 3 min with the precision and accuracy of ±2 µatm. The analyzer was protected by a device supervising the system against the influence of unwanted moisture (WIPO ST 10/C PL425618, patent pending).

The pH (total scale) was obtained online by the flow-through spectrophotometric pH measurement system using m-cresol purple as indicator dye, characterized by the precision of ±0.001 and an accuracy of ±0.003, by Kongsberg.

4. Results and Discussion

The TA varied from 3474 to 1662 $\mu mol\ kg^{-1}$, while the linear TA-S relations suggest conservative mixing in the vicinity of the Vistula River mouth (Fig. 1). The differences noticed in TA distribution suggest that riverine TA end-member may change seasonally. The pCO_2 showed highest values of ~700 µatm in October 2017 and lowest ~200 atm in May 2018. The negative correlation of pCO_2 with oxygen concentrations suggests that pCO_2 fields are controlled in that region by the biological activity. The pH showed high seasonal variability amounting to 0.72 that was controlled by changes in pCO_2 and TA (Fig. 2).

For the first time we have quantified in this study the Vistula River daily loads of the TA (TA_{Load}) (Fig. 3). They varied between 120 and 492 Mmol day^{-1} and were directly proportional to the water flow (Q) for Q < 1515 $m^3\ s^{-1}$.

5. Conclusions

- The determined riverine TA end-member in the Vistula River varied between 3138 and 3631 $\mu mol\ kg^{-1}$.
- High pH variability in the mouth of the Vistula River was driven by pCO_2 and TA changes.
- The daily TA loads from Vistula River can be largely explained by the changes in the water flow.

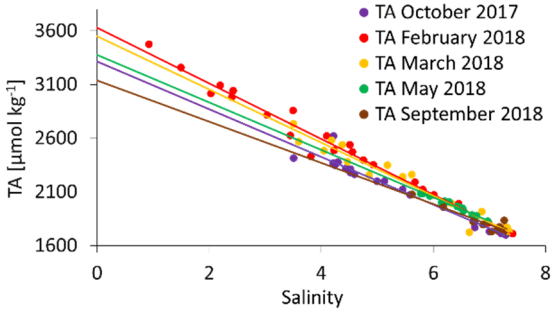


Figure 1. Relationship between total alkalinity (TA) and salinity in the mouth of the Vistula River.

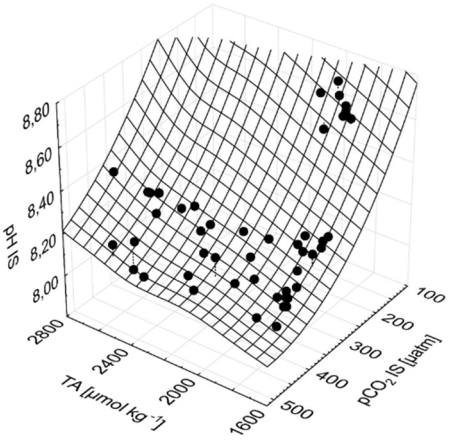


Figure. 2 pH variation as a function of TA and pCO_2 in the Vistula River Mouth.

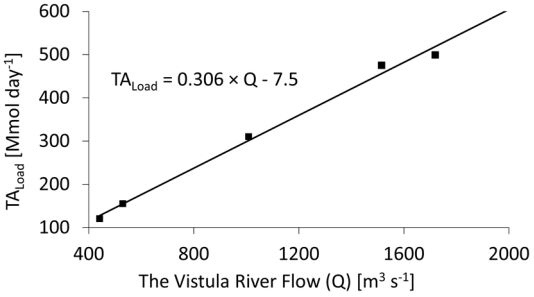


Figure. 3 The daily total alkalinity load to the Baltic Sea (TA_{Load}) as function of the Vistula River Flow (Q).

References

Müller, J. D., Schneider B., and Rehder G., 2016. Long-term alkalinity trends in the Baltic Sea and their implications for CO_2-induced acidification. Limnol. Oceanogr. 61: 1984–2002. doi:10.1002/lno.10349

Submarine groundwater discharge influence on marine CO_2 system

Beata Szymczycha, Aleksandra Winogradow, Karol Kuliński

Institute of Oceanology of Polish Academy of Sciences, Sopot, Poland (beat.sz@iopan.gda.pl

Submarine groundwater discharge (SGD) is defined as all flow of water coming from the seabed to the water column, regardless of the fluid composition or driving force (Burnett et al., 2003). It includes both fresh groundwater discharge derived from terrestrial recharge and recirculated seawater (Burnett et al., 2006).

For many decades, SGD was neglected in the global hydrological cycles. The reason for that is the difficulty to identify and measure SGD. Generally, rivers have been recognized to be a key pathway for terrestrial water to the ocean. Since Moore (1996) showed that chemical mass flux via SGD can exhibit 40% of this coming from the river water the subject has been receiving increased attention.

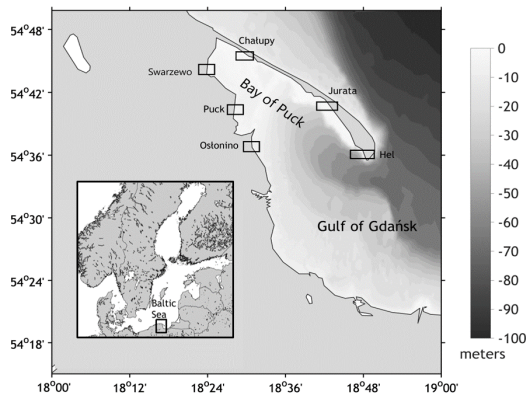


Figure 1. Map showing the Bay of Puck and study sites located on the Hel Peninsula: Hel, Jurata and Chałupy; and on the mainland: Swarzewo, Puck, and Osłonino.

In the Bay of Puck, southern Baltic Sea several studies indicated that SGD is an important component of chemical budgets (e.g. Szymczycha et al., 2014; 2020a; b). Kłostowska et al. (2019) calculated that SGD rates to the entire Bay of Puck ranged from 16.0 m^3 s^{-1} to 127.7 m^3 s^{-1} and were from 2.5 to 25 times more than average discharge of the biggest river entering the Bay of Puck. In addition, Szymczycha et al. (2020a) estimated that seasonal and annual loads of both dissolved inorganic nitrogen (DIN 9303 t yr^{-1}) and PO_4^{3-} (950 t yr^{-1}) via SGD were the most significant source of nutrients to the Bay of Puck and indicate some of the highest rates of sediment-water fluxes reported in the entire Baltic Sea. Yet, SGD influence on CO_2 system is still not completely understood.

The Baltic Sea, being one of the world's largest estuaries, has low buffer capacity due to low salinity (S). However, the recent studies show, that surface water alkalinity (AT) has increased since the early 20th century due to potential changes in precipitation patterns, continental weathering, agricultural liming and internal AT sources (Müller et al., 2016). Furthermore, Gustafsson et al. (2019) indicated that the known AT sources do not explain the AT concentration in seawater. Some of this missing AT input can be attributed to the release form hypoxic and anoxic sediments. Still, some fraction of AT sources remains unknown.

Here, we provide data showing that SGD is a significant source of AT and DIC to the marine environment. The study was conducted in 2018 in the Bay of Puck southern Baltic Sea and included sampling of groundwater (GW), submarine groundwater discharge (SGD), and seawater samples (Figure 1). Additionally, data presenting the surface seawater AT and DIC concentrations from Baltic Proper (BY15, BY20, BY21, BY29; collected in May 2017) were included in this study.

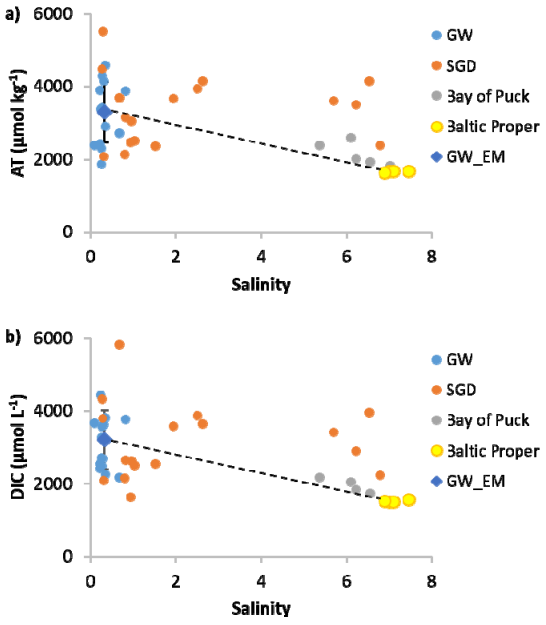


Figure 2. AT (a) and DIC (b) concentrations vs. salinity in several water types: groundwater (GW), submarine groundwater discharge (SGD), seawater: Bay of Puck and Baltic Proper. The dash line indicates the mixing line between groundwater end-member (GW_EM) and surface seawater (Baltic Proper).

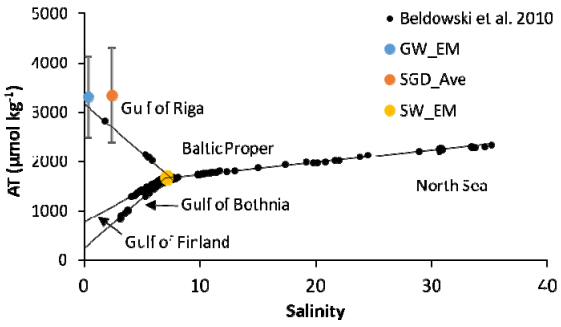


Figure 3. The total alkalinity (A_T) distribution against salinity in the Baltic Sea (modified after Bedowski et al., 2010). The blue, red and yellow dots correspond to groundwater end-member (GW_EM), average SGD (SGD_Ave) and surface seawater end-member (SW_EM), respectively.

The average AT and DIC concentrations in coastal GW equaled to 3302 ± 829 (µmol kg $^{-1}$) and 3210 ± 805 (µmol L^{-1}), respectively while in SGD the average AT and DIC concentrations equaled to 3344 ± 951 (µmol kg $^{-1}$) and 3158 ± 1036 (µmol L^{-1}), respectively. The high range of measured concentrations can be attributed to the seasonal changes of both 1) AT and DIC concentrations and 2) water flow rate intensity. It is worth noticing that AT and DIC in coastal GW and SGD were significantly higher than those obtained in the surface water of the Bay of Puck and the Baltic Proper (Figure 2). In addition, concentrations of AT (Figure 2a) and DIC (Figure 2b) plotted vs. salinity show similar pattern which indicates that carbonate alkalinity is predominant component of AT. Furthermore, the significant influence of SGD on CO_2 system is represented by the increased DIC and AT in surface water of the Bay of Puck in comparison to the Baltic Proper (Figure 2).

In order to show the potential influence of groundwater discharge on the Baltic Sea AT concentrations, the coastal GW and SGD average AT concentrations were incorporated to the A_T vs. S regimes in the Baltic Sea (Figure 3). It turned out that coastal GW and SGD are notably enriched in AT in comparison to the surface seawater.

The obtained results not only can help explaining the presently missing source of AT in the Baltic Sea but also show that SGD can be an important factor shaping the marine CO_2 system.

Acknowledgments

The reported results were obtained within the framework of the statutory activities of the Institute of Oceanology of the Polish Academy of Sciences and the following research projects: WaterPUCK BIOSTRATEG3/343927/3/NCBR/2017 financed by the National Centre for Research and Development (NCBiR) within the BIOSTRATEG III program; and PharmSeepage 2016/21/B/ST10/01213 and SALSA 2015/19/B/ST10/02120 funded by the Polish National Science Centre.

References

Beldowski, J., Löffler, A., Schneider, B., Joensuu, L., 2010. Distribution and biogeochemical control of total CO_2 and total alkalinity in the Baltic Sea. Journal of Marine Systems 81,252–259.

Burnett, W.C., Bokuniewicz, H., Huettel, M., Moore, W.S., Taniguchi, M., 2003. Groundwater and pore water inputs to the coastal zone, Biogeochemistry 66 (1/2), 3–33, https://doi.org/10.1023/B:BIOG.0000006066.21240.5.

Burnett, W.C., Aggarwal, P.K., Aureli, A., Bokuniewicz, H., Cable, J.E., et al., 2006. Quantifying submarine groundwater discharge in the coastal zone via multiple methods, Sci. Total Environ. 367 (2/3), 498–543, https://doi.org/10.1016/j.scitotenv.2006.05.009.

Gustafsson, E., Hagens, M., Sun, X., Humborg, C., Slomp., C.P., Gustaffsson, B.G., Sedimentary alkalinity generation and long-term alkalinity development in the Baltic Sea. Biogeosciences, 16, 437–456, 2019. https://doi.org/10.5194/bg-16-437-2019.

Kłostowska, Ż., Szymczycha, B., Lengier, M., Zarzeczańska, D., Dzierzbicka-Głowacka, L., 2019. Hydrogeochemistry and magnitude of SGD in the Bay of Puck, southern Baltic Sea, Oceanologia 000, 1-11, https://doi.org/10.1016/j.oceano.2019.09.001.

Moore, W.S., 1996. Large groundwater inputs to coastal waters revealed by 226Ra enrichments, Nature 380, 612–614, https://doi.org/10.1038/380612a0.

Müller, J. D., Schneider B., and Rehder G., 2016. Long-term alkalinity trends in the Baltic Sea and their implications for CO_2-induced acidification. Limnol. Oceanogr. 61: 1984–2002. doi:10.1002/lno.10349.

Szymczycha, B., Maciejewska, A., Winogradow, A., Pempkowiak, J., 2014. Could submarine groundwater discharge be a significant carbon source to the southern Baltic Sea? Oceanologia 56 (2), 327–347, https://doi.org/10.5697/oc.56–2.327.

Szymczycha, B., Kłostowska, Ż., Lengier, M., Dzierzbicka Głowacka, L., 2020a. Significance of nutrient fluxes via submarine groundwater discharge in the Bay of Puck, southern Baltic Sea. Oceanologia. https://doi.org/10.1016/j.oceano.2019.12.004.

Szymczycha, B., Borecka, M., Białk-Bielińska, A., Siedlewicz, G., Pazdro, K., 2020b. Submarine groundwater discharge as a source of pharmaceutical and caffeine residues in coastal ecosystem: Bay of Puck, southern Baltic Sea case study. Sci. Total Environ. 713. https://doi.org/10.1016/j.scitotenv.2020.136522.

Estimation of phosphate ion in the waters of the rivers of the Baltic catchment (on the example of the Western Bug River)

Alexander A. Volchak, Maya A. Taratsenkava
Brest State Technical University, Brest, Belarus

1. Introduction

Features of the Baltic Sea: shallow water, low salinity of sea water, difficult water exchange with the North Sea, which lead to low self-cleaning ability with an average time of complete water exchange of about 30-50 years and high sensitivity to anthropogenic effects from developed industrial and agricultural regions located on catchment of the sea, Lass et al (2008). According to HELCOM, today more than 97% of the Baltic Sea region suffers from eutrophication due to past and present excessive amounts of nitrogen and phosphorus, HELCOM et al (2018) [2].

The greatest influence on the transformation of the hydrochemical regime of the Baltic Sea water is provided by countries whose rivers flow into this sea. So 83 800 km2 of Belarus is located within the Baltic Sea basin. As mentioned earlier, the main pollutants are nitrogen and phosphorus-containing substances. The current annual total supply of nutrients to the Baltic Sea is about 826 000 and 30 900 tons of nitrogen and phosphorus, respectively, which mainly form river flows, HELCOM et al (2018).

The Western Bug is a typical transboundary (Belarus, Poland and Ukraine) river on the southern slope of the Baltic Sea. The catchment of the river is 73 470 km^2. In Belarus, the length of the river is 154 km.

2. Initial data and research methods

Hydrochemical analysis of water The Western Bug was based on data from the State Water Cadastre of the Republic of Belarus for the period from 2004 to 2018, for 6 hydrochemical gauges, Water resources et al (2018). To assess the temporal structure of the series of phosphate ions, standard statistical methods were used.

The aim of this work is to identify patterns in the fluctuations in time of the phosphate ion on the example of the Western Bug River.

3. The results obtained and their discussion

Currently, the Western Bug is experiencing a large load in terms of phosphate-ion. In all the observed sections, maximum permissible concentrations (MPC) (0.066 mgP/dm^3) were exceeded. It should be noted that the maximum permissible concentration is observed in the first section on the territory of Belarus (for example, Tomashovka).

Table Statistical parameters of the phosphate-ion in the river Western Bug, mgP/dm^3.

The reason for this is the mass transfer of phosphate-ion from the territory of Ukraine. The location on the river of the regional center - the city of Brest - also affects the increase in the content of phosphate-ion, but to a lesser extent, on average, this increase is 0.027 mgP/dm^3. It should be noted that the situation is stabilizing, as evidenced by the following data. So in 2018, as a result of environmental measures, a decrease in the content of phosphate-ion in river water occurred. The difference between the Tomashovka and Novoselki alignments was 0.033 mgP/dm^3. This is also evidenced by the amount of phosphate-ion discharges into the basin of the Western Bug River (Fig.).

The main statistical parameters of the time series of the phosphate ion for all the sections under consideration are given in the table.

As can be seen from the table, everywhere there is a tendency to a decrease in phosphate-ion. This is especially pronounced in the Tomashovka and Novoselki sections, which indicates the significance of the correlation coefficients of linear trends (Table 1). The coefficient of variation indicates the average degree of dispersion of the considered parameter.

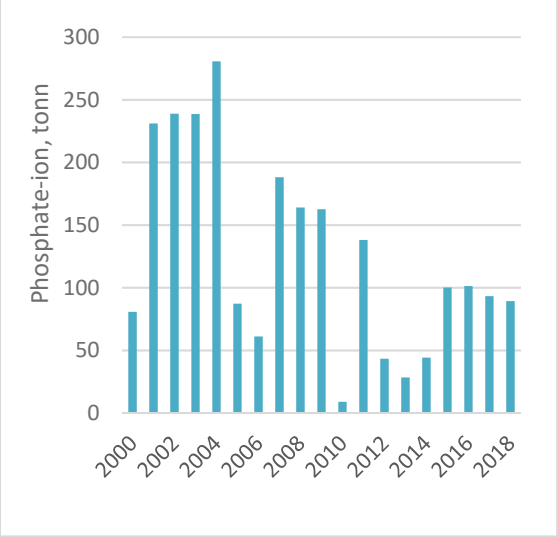


Figure 1. Dynamics of phosphate ion collection into the Western Bug River basin in Belarus

	value			odds			
	average	minimum	maximum	variations	asymmetries	gradient change	correlations
s. Tomashovka	0.155	0.116	0.217	0.22	0.42	-0.044	-0.61
s. Domachevo	0.155	0.120	0.186	0.15	-0.28	-0.009	-0.14
s. Rechitsa	0.182	0.118	0.220	0.18	-0.77	-0.026	-0.40
c. Brest Kozlovichi bridge	0.180	0.150	0.225	0.14	0.64	-0.024	-0.40
0.1 km west of s. Terebun	0.162	0.130	0.190	0.12	-0.52	-0.026	-0.49
s. Novoselki	0.152	0.089	0.180	0.20	-1.26	-0.044	-0.70

A quantitative assessment of the fluctuations of the phosphate ion is estimated as the gradient of change, which is multiplied by 10 years, i.e. α = a10 years

4. Conclusion

The influence of river waters on the formation of the hydrochemical regime of the Baltic Sea is undeniable, and the waters of the Western Bug River are no exception. The river basin is under heavy pressure in terms of phosphate ion. The average annual indicators of this parameter for 2018 exceed the MPC in all observed sections by 1.4 - 1.8 times. It is also worth noting the positive aspects. A decrease in the discharge of phosphate ion into the Western Bug basin affects the trend in the content of this component in river waters. It was noted that the tendency to a decrease in phosphate ion is observed at all sections, however, only two are significant. This indicates a positive direction of measures taken to preserve and protect the environment.

References

Lass H. U., Matthäus W.(2008) General oceanography of the Baltic Sea. In: Feistel R, Nausch G, Wasmund N, editors. State and evolution of the Baltic Sea 1952–2005. Hoboken, N.J.: John Wiley & Sons, pp. 5–44.

HELCOM (2018). Nutrient inputs to the Baltic Sea HELCOM *http://stateofthebalticsea.helcom.fi/pressures-and-their-status/eutrophication (access 09.02.2020)*

Water resources. their use and water quality (for 2004-2018).(2018). TsNIIKIVR, Minsk, (in Russian).

The impact of submarine groundwater discharge on element fluxes into a temperate shallow coastal bay

Catia M. E. von Ahn [1], M. E. Böttcher [1,2,3], P. Feldens[1], A.-K. Jenner [1], I. Schmiedinger [1], J. Scholten[4]

[1] Department Marine Geology, Leibniz Institute for Baltic Sea Research (IOW), Warnemünde, Germany (catia.vonahn@io-warnemuende.de)

[2] Marine Geochemistry, University of Greifswald, Germany

[3] Interdisciplinary Faculty, University of Rostock, Germany

[4] Institute of Geosciences, University of Kiel, Germany

1. Introduction

It becomes more and more recognized that Submarine Groundwater Discharge (SGD) may act as a source of water and dissolved substances for coastal ecosystem. This may include dissolved carbon species, nutrients and metals. The extend and the route of SGD is controlled by the hydrology and lithology in the recharge area and the actual elemental fluxes in the water column may strongly depend on benthic water-solid-microbe interactions close to the sediment-water interface. The development of chemical gradients in relation to transport processes have only recently kept attention and are the focus of this study.

2. Methodology

The present study focused on the distribution of SGD into the Wismar Bay, in the southern Baltic Sea (Figure 1). Offshore seawater samples were collected on board of Littorina research vessel in May 2019. Water column samples were taken for the analysis of radium isotopes, stable isotopes (H, O, C, S), dissolved inorganic carbon (DIC), nutrients and major cations were collected along transects through the Wismar Bay. Sediment cores were retrieved from several stations and pore water samples were extracted.

Water samples for Radium (Ra) isotopes were filtered through a MnO_2 impregnated acrylic fiber (hereafter Mn-fiber) at a flow rate 1 L min^{-1} to quantitatively extract the Ra isotopes. The fibers were washed to remove excess salt, partly dried, and then measured on-board for ^{223}Ra and ^{224}Ra using a RaDeCC (Radium Delayed Coincidence Counting) system (Moore and Arnold, 1996). Water aliquots were immediately filtered for further analyzer by ICP-OES (Thermo iCAP 6300 Duo, Thermo Fisher Scientific) and a QuAAtro nutrient analyzer (SEAL Analytical). Stable C and S isotopes were analyzed with Thermo Finnigan MAT253 mass spectrometer attached to a Gasbench II or and Thermo elemental Flash analyzer. Stable water (H, O) isotope measurements were conducted by means of Picarro CRDS system.

Furthermore, the surface sediments were investigated via geophysical acoustic techniques to identify possible structures associated with submarine ground water discharge.

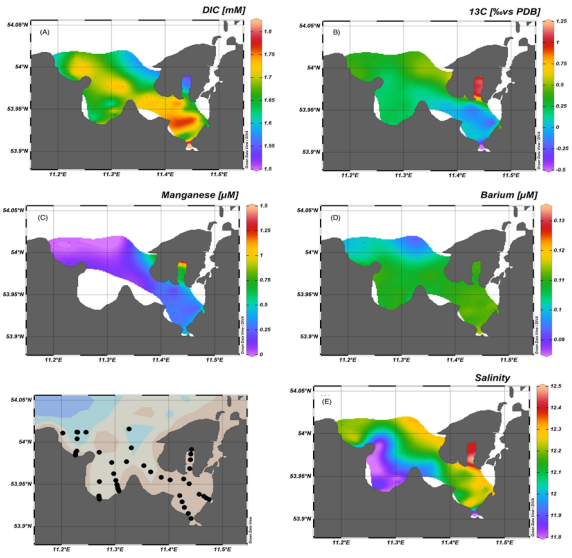


Figure 1. Map of Wismar Bay, southern Baltic Sea, showing the water column stations where samples were taken. Moreover, maps of surface distributions of DIC (A), $^{13}C_{DIC}$ (B), Manganese (C), Barium (D) and salinity (E.

3. Result and discussion

In the present study, Ra isotope and trace metal investigations were used to identify SGD into the Wismar Bay, southern Baltic Sea (Figure 1). Geophysical measurements identified sedimentary structures of areas with potential SGD that seem to be associated with potential methane gas discharge. Pore water investigation, in shallow sediment cores identified chemical gradients that are shaped by intensive early diagenesis with and without the impact of fresh SGD. Mineralization of organic matter using different electron acceptors is the major driver shaping the pore water profiles (e.g. Figure 2). At a site in the central Wismar Bay, freshwater was identified at a sediment depth of about 50 cmbsf with steep physico-chemical gradients developing above. The water isotope composition was close to the regional meteoric water line of Mecklenburg-Western Pomerania and freshwater springs discharging along the coastline into the southern Baltic Sea.

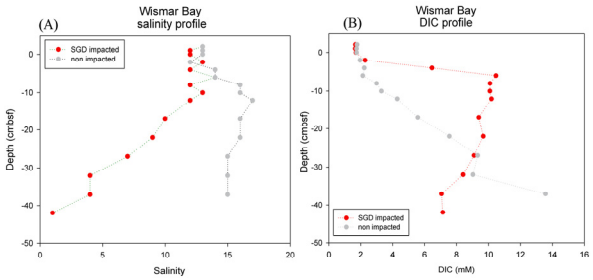


Figure 2. A comparison of vertical pore water profile for salinity (A) and (B) DIC in Wismar Bay at an impacted and not impacted SGD area.

Furthermore, it has an isotopes hydrogeochemical composition only slightly modified from spring and ground waters found in the recharge area (Lipka, et. al., 2018).
The sedimentary pore water gradient at the SGD-impacted sites suggest, that advective upward flow of SGD is increasing the element fluxes across the sediment-bottom water interface, but that the dissolved substances are originating from both: partly from process in the soil zone and aquifer during ground water development, but to a substantial part from the early diagenetic process in the surface sediments. Therefore, the fresh water component is not the major element source, but increases the fluxes into the coastal environmental via enhanced advective vertical water transport.

4. Conclusion

Therefore, the overall contribution of elements to the coastal ecosystem is a function of transport processes which should be investigated in much more detail in order to improve the assessment on the importance of SGD for the coastal ecosystem.

5. Acknowledgments

The investigations are supported by the DFG research training school Baltic TRANSCOAST, DAAD, and Leibniz IOW. We would like to thank the captain and the crew of Littorina research vessel, Sascha Plewe, Maren Staniek, Gerald Nickel for the support in the field and Anne Köhler for technical support.

References

Moore, W.S., Arnold, R. (1996) Measurements of 223Ra and 224Ra in coastal waters using a delayed coincidence counter, J. Geophys., Vol. 101, pp. 1321-1329

Lipka, M., Böttcher, M.E. Wu, Z., Sültenfuß J., Jenner, A. K., Westphal, J., Dellwig, O., Escher, P., Schmiedinger, I., Winde, V., Struck, Y. (2018) Ferrugnous groundwaters as a source for P, DIC and Fe coastal waters in the southern Baltic See: (Isotope) hydrobiogeochemistry and the role of an iron curtain, E3S Web Conf., Vol. 54, pp. 1-5.

The spatiotemporal variation of Sea Surface pCO_2 in the Baltic Sea from 2002 to 2011 using Remote Sensing

Shuping Zhang [1], Anna Rutgersson [1], Petra Philipson [2]

[1] Department of Geosciences, Uppsala University, Uppsala, Sweden (shuping.zhang@geo.uu.se)

[2] Brockmann Geomatics Sweden AB, Kista, Sweden

Oceans uptake a significant share (~25%) of the anthropogenic CO2 emitted to the atmosphere and thus play a fundamental role in the global CO_2 cycle. The Baltic Sea is a marginal sea of high latitude. As a semi-closed brackish sea receiving substantial complex terrestrial input, the Baltic Sea present unique characteristics in global CO_2 air-sea exchange and yet insufficiently investigated or understood. Remote Sensing has shown great potentials in assisting understanding the oceanic processing in a large scale.

In this study we retrieved the sea surface *p*CO2 in the Baltic Sea from remote sensing data for the period from 2002 to 2012 and understand the intra- and inter- annual evolution of pCO_2 in the entire Baltic Sea. Remote sensing products of biological and physical properties of the sea surface including sea surface temperature (SST) and Chlorophyll (Chl-a) serve as input in the pCO_2 retrieval. Robust machine learning approaches (e.g. Random Forest) is adapted and employed to retrieve sea surface pCO_2. The pCO_2 measurements obtained from vessels matching the remote sensing satellite overpasses in the corresponding years are employed as training and validation data. This study presents the spatiotemporal evolution characteristics of sea surface pCO_2 in the Baltic Sea. The output of this study has greatly improved the understanding of the air-sea CO_2 exchange and the oceanic processes in the complex Baltic Sea. This study has paved the road for further analysis of sea surface pCO_2 fluxes in the Baltic Sea with next generation of ocean observation satellites e.g. Sentinel-3.

Topic 3

Natural hazards and extreme events

Long-term statistics of atmospheric conditions over the Baltic Sea and meteorological features related to wind wave extremes in the Gulf of Gdańsk

Witold Cieślikiewicz and Aleksandra Cupiał

Institute of Oceanography, University of Gdańsk, Poland (witold.cieslikiewicz@ug.edu.pl)

1. Introduction

The Gulf of Gdańsk, located in the south-eastern part of the Baltic Sea (see Fig. 1) is a very important sea basin for Poland. There is the Tricity metropolitan area containing three cities of Gdańsk, Gdynia and Sopot located on the south-western coast of the Gulf. The Tricity together with minor towns in its vicinity has a population over one million people. Two of three largest ports in Poland are located in the Gulf of Gdańsk: the Port of Gdańsk and the Port of Gdynia. The Gulf of Gdańsk is semi-enclosed in its northern part by a very characteristic long sandspit, the Hel Peninsula, which defines the Bay of Puck and strongly affects local wind wave generation in the Gulf of Gdańsk and wave propagation into the Gulf from the open Baltic Sea. The Hel Peninsula has a significant impact on wave energy distribution in the western part of the Gulf, in particular in the vicinity of the Tricity's ports. The strategic role of the Gulf of Gdańsk together with significant investments in port's infrastructure and other maritime engineering activities, that are planned, make determining of the long-term statistical characteristic of predominant wind wave conditions crucial. For the same reasons the study and determination of extreme wind wave properties, such as design wave parameters, related to various return periods, are of great importance.

The principal goal of this work is to determine a comprehensive description of wind wave climate and wind wave extremes of the Gulf of Gdańsk and associated meteorological conditions over the Baltic Sea. The objective of the work is reached by computations based on modelled data spanning almost half a century. An important aim of this study is to obtain the most characteristic features of extreme storms that had created extreme risks and hazards in the Gulf of Gdańsk during the investigated period 1958–2001.

2. Data used

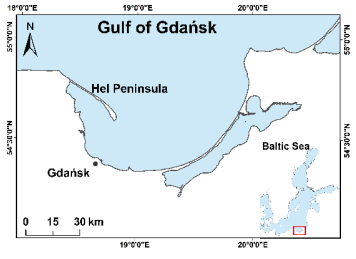


Figure 1. Location of Gulf of Gdańsk in the Baltic Sea.

In this study we analyse two hindcast datasets. The first one is the 44-year long reanalysis of meteorological data produced with the atmospheric model REMO (REgional MOdel; Jacob and Podzun 1997, von Storch et al. 2000 and Feser et al. 2001). The second dataset used in this study is wave data produced with wave model WAM. Both these datasets are the result of an EU-funded project HIPOCAS (Cieślikiewicz et al. 2005, Cieślikiewicz & Paplińska-Swerpel 2008). Its objective was to obtain a multi-decadal hindcast of wind, wave, sea-level, and current parameters for European waters and coastal areas. A high-resolution homogeneous data set was generated in the framework of the project and it covered coastal seas and coastlines of several European countries. A number of statistics essential to almost all marine activities, may be obtained from this data set.

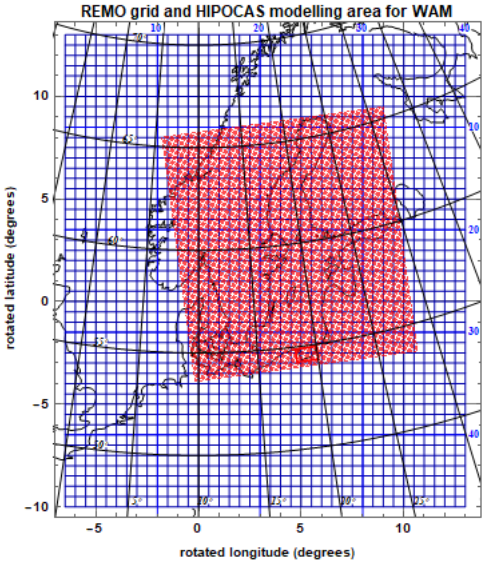


Figure 2. Sub-grid of REMO meteorological data extracted for the wind wave modelling over the Baltic Sea performed within the HIPOCAS project. Computational grid for wind wave modelling with WAM is marked with red. The Gulf of Gdańsk area is shown with the red frame.

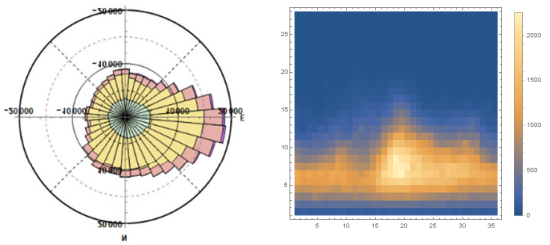
3. Methodology and exemplary results

The meteorological forcing data, used within the HIPOCAS project, were 1-hourly gridded wind velocity fields provided by Forschungszentrum Geesthacht GmbH (GKSS, now Helmoholtz-Zentrum Geesthacht—HZG). The wind velocity hindcast covering the period 1958–2001 was performed in GKSS, with the atmospheric REMO model. The REMO modelling area covers Europe and NE Atlantic with 0.5° × 0.5° resolution. For the modelling of currents and waves over the Baltic Sea, a subset of gridded REMO data were extracted. Fig. 2 presents the area covered by the REMO data extracted for the purpose of Baltic Sea modelling within the HIPOCAS project. Wave data have been produced within HIPOCAS with wave model WAM in a rectangular grid in spherical rotated coordinates with the resolution 5'×5'. The output wave data were validated against observed records presenting a good agreement (Cieślikiewicz and Paplińska-Swerpel, 2008).

The objective of this work is dual. First, we want to estimate long-term stochastic characteristics of some basic meteorological parameters, on one hand, and wind

wave field, on the other hand. Both statistical analyses are applied to hindcast data modelled over the Baltic Sea. In case of meteorological data, the atmospheric pressure at sea level and the wind velocity at 10 m height are analysed.

To characterise long-term statistical features of wind velocity field over the Baltic Sea, the eight locations representing various Baltic Sea basins were selected. For all those locations various statistics has been determined and presented both numerically and graphically. As an example, in Fig. 3a the cumulative distribution of wind speed and direction frequency over the studied period 1958–2001, for the selected point in the Gulf of Gdańsk is shown. It is an elaborated presentation of the 2D frequency histogram over the absolute value and the direction angle of the wind velocity vector domain, which is shown in Fig. 3b. The direction angle is the angle between the East direction axis and the wind velocity vector counted anticlockwise. Thus, the distribution diagram shown in Fig. 3a does not present a conventional wind rose diagram. It shows directions of wind velocity vector, i.e. the directions towards which wind blows rather than the directions from which wind blows. In our study we generally use the cartesian/polar angle convention rather than the nautical convention. The direction bins 1 to 36 marked on horizontal axis of Fig. 3b represent wind velocity vector direction sectors of 10° width counted from – 180° to + 180° with centres at directions from – 170° to + 180°. The convention applied means that the frequency of western winds is shown at the centre of the 2D frequency histogram in Fig. 3b and is represented by the bin No. 18 on the horizontal direction axis—the central direction of this direction sector is 0° and represents the East direction.



(a) (b)

Figure 3. Basic long term characteristics of wind velocity vector over the Gulf of Gdańsk: (a) cumulative distribution of wind speed and direction frequency over years 1958–2001; the numbers labelling radii indicate numbers of data points that fall into the given wind speed-direction angle bin; wind speed ranges marked with different colors are: 0–5, 5–10, 10–15, 15–20 m/s; (b) 2D frequency histogram over the absolute value and the direction angle of the wind velocity vector domain for years 1958–2001.

As far as the wind wave data are concerned, we focus on the significant wave height, mean wave period and the mean direction of wave propagation. Moreover, some "combined"/derivative parameters, e.g. the significant wave steepness will be also statistically analysed.

The second principal goal of the study is to determine the most characteristic features of meteorological conditions causing extreme wind wave states in different areas of the Gulf of Gdańsk. For this purpose, a number of extreme storms, that are critical for five chosen different Gulf of Gdańsk regions, are selected based on significant wave height time series taken from the HIPOCAS database, for the computational grid points located in the chosen regions. For those selected storm periods, the storm depressions' tracks and the overall evolution of atmospheric pressure and wind velocity fields are examined. On top of that, we look for the essential characteristics of the extreme meteorological conditions via results of the Empirical Orthogonal Functions (EOF) method, applied to the wind velocity vector fields. Fig. 4 presents the efficiency of the EOF analysis applied to the wind fields over the whole REMO area, for which the meteorological data were extracted for the HIPOCAS project, for years 1958–2001.

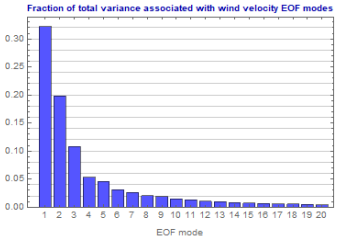


Figure 4. Distribution of total variance over the first 20 EOF modes of wind velocity field over the REMO area used in this study.

Before all the necessary atmospheric data and wind wave data analyses were done, we checked out the quality and reliability of those data based on comparisons with available observations in nature. What is important, not only the time series of modelled and recorded data are compared. In addition, derivative combined parameters and various stochastic characteristics, including probability distributions and some basic results of extreme statistics analysis, estimated from modelled and observed data are compared against each other. This gives a deeper insight into the problem how reliable are the statistics inferred from the modelled hindcast data, e.g. those from the long-term wind wave time series modelled over the Baltic Sea for years 1958–2001.

The planned paper will contain coloured drawings, including maps and various contour plots, as well as numerical results presented in Tables.

4. Acknowledgements

Computations performed within this study were conducted in the TASK Computer Centre, Gdańsk with partial funding from eCUDO.pl project No. POPC.02.03.01-00-0062/18-00 and the University of Gdańsk Project for Young Scientist No. 539-G210-B412-19.

References

Cieślikiewicz, W., Paplińska-Swerpel, B. Guedes Soares, C. (2005). Multi-decadal wind wave modelling over the Baltic Sea. Proc. 29th Intern. Conf. Coastal Engng, ICEE 2004, Lisbon, pp. 778–790.

Cieślikiewicz, W., Paplińska-Swerpel, B. (2008). A 44-year hindcast of wind wave fields over Baltic Sea. Coastal Engineering, 55, pp. 894–905.

Feser, F., Weisse, R., von Storch, H., (2001). Multi-decadal atmospheric modelling for Europe yields multi-purpose data. EoS, Vol. 82, No. 28, July 10, 2001.

Jacob, D., Podzun, R., (1997). Sensitivity studies with the regional climate model REMO. Meteorol. Atmos. Phys., 63, pp. 119–129.

Von Storch, H., Langenberg, H., Feser, F., (2000). A spectral nudging technique for dynamical downscaling purposes. Mon. Weather Rev., 128, pp. 3664–3673.

Convective snow bands over the Baltic Sea in an ensemble of regional climate scenarios

Christian Dieterich[1], Matthias Gröger[2,1], Katharina Klehmet[1], Peter Berg[1], Julia Jeworrek[3], Kirsti Jylhä[4], Erik Kjellström[1], H. E. Markus Meier[2,1], Taru Olsson[4], Lichuan Wu[5] and Anna Rutgersson[5]

[1] Swedish Meteorological and Hydrological Institute, Norrköping, Sweden (christian.dieterich@smhi.se)
[2] Leibniz Institute for Baltic Sea Research Warnemünde, Germany
[3] Department of Earth, Ocean and Atmospheric Sciences, University of British Columbia, Vancouver, Canada
[4] Finnish Meteorological Institute, Helsinki, Finland
[5] Department of Earth Sciences, University Uppsala, Uppsala, Sweden

1. Introduction

Snow bands are a type of precipitation event that occurs in the Baltic Sea in the cold season. Cold air that moves over the warmer open sea can form convection cells triggered by sensible and latent heat fluxes. Interaction of convective processes with the prevalent wind regime can cause strong wind flow parallel snow bands. When these snow bands approach a coast heavy precipitation can occur. Coastal areas in Sweden and Finland are regularly hit by these snowfall events (e.g. Jeworrek et al. 2017, Olsson et al., 2017) that can lead to problems for traffic and infrastructure.

Under projected climate change we expect strong warming in the northern Baltic Sea region, amplified by the ice-snow-albedo feedback. The Bothnian Bay and Bothnian Sea are projected to become ice free more often (Höglund et al., 2017). An ice free Baltic Sea is a requirement for snow bands to develop, so that the atmosphere can take up moisture and heat from the sea and start convection. The hypothesis is that the northern Baltic Sea will be affected more frequently by snow bands under future warmer climate conditions, since the ice free period perisists into winter.

2. Methods

We use a coupled regional atmosphere-ice-ocean model (Wang et al., 2015) to downscale different general circulation models (GCMs) from the Coupled Model Intercomparison Project 5 (CMIP5, Taylor et al., 2012). Using three different representative concentration pathways (RCPs, van Vuuren et al., 2011) of the CMIP5 models allows us to generate a small ensemble of regional climate scenarios for the North Sea and the Baltic Sea region (Table 1).

	RCP8.5	RCP4.5	RCP2.6
MPI-ESM-LR	1961-2099	1961-2099	1961-2099
EC-EARTH	1961-2099	1961-2099	1961-2099
HadGEM2-ES	1961-2099	1961-2099	1961-2099
IPSL-CM5A-MR	1961-2099	1961-2099	
GFDL-ESM2M	1961-2099	1961-2099	1961-2099
CanESM2	1961-2099	1961-2099	
NorESM1-M	1961-2099	1961-2099	1961-2099
MIROC5	1961-2099	1961-2099	1961-2099

Table 1. Ensemble of GCM projections downscaled with RCA4-NEMO.

The analysis of snow band conditions follows Jeworrek et al. (2017). They have shown that the coupled model RCA4-NEMO that we use here shows the effects of snow bands, even though the horizontal resolution of 0.22° (c. 25 km) is rather coarse. RCA4-NEMO tends to underestimate the amount of snowfall and the timing and precise location of the events is not accurately reproduced. The aim of this study is not the analysis of dynamical and thermodynamical processes for snow band formation. We rather focus on how the statistics of snow bands, as they are represented in the regional climate model, change with changing climatic conditions in the northern Baltic Sea.

3. Preliminary Results

Fig. 1 shows the time series of occurrence of moderate conditions (Jeworrek et al., 2017, see Appendix) for snow bands on the Swedish east coast. Contrary to the initial hypothesis that warmer and ice free conditions in the northern Baltic Sea would favor the formation of snow bands, snow band frequency tends to decrease towards the end of the century. For the RCP8.5 scenario the change between the far future (2070 to 2099) and the recent past (1970 to 1999) is significant at the 95% level.

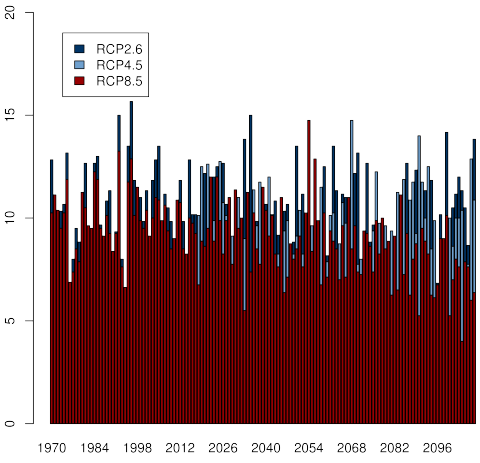


Figure 1. Number of days per year with moderate atmospheric conditions for convective snow bands on the Swedish east coast in the ensemble mean of three different RCP scenarios.

There is a combination of interdependent, changing conditions that lead to an overall decrease of snow band occurrences. The atmospheric boundary layer height increases together with the number of days for heavy precipitation. At the same time, surface temperature

strongly increases and days with a mean temperature of less than 8° C become less frequent. This also leads to a reduction of days where the vertical temperature gradient is sufficiently large for snow bands to occur. Together with increasing temperatures the number of days where precipitation occurs as snow reduces.

As shown by Jeworrek et al. (2017), and reproduced in our analysis, the peak month for snow bands in the recent past on the Swedish east coast is November (Fig. 2). In the course of the century the month with the highest number of snow band conditions shifts to December in the near future (2020 to 2049) and in the far future (2070 to 2099) there are almost as many events in January as in December. This effect is caused primarily by warm surface temperature extending further into the cold season. For conditions in late winter and spring the projections show an increase of the number of days with favorable conditions for snow band formation in line with our hypothesis.

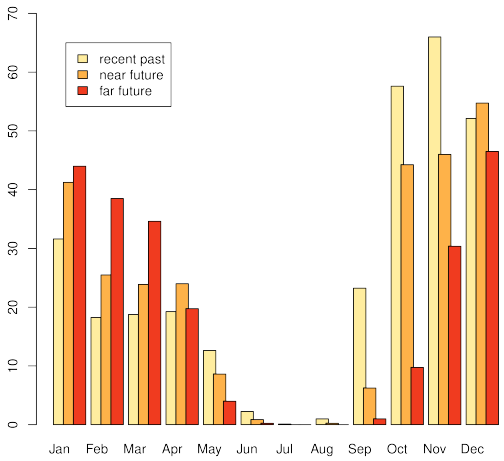


Figure 2. Number of days per month with moderate atmospheric conditions for convective snow bands on the Swedish east coast in the ensemble mean of the RCP8.5 scenarios.

4. Discussion

We have downscaled a number of CMIP5 scenarios with the coupled atmosphere-ice-ocean model RCA4-NEMO to produce regional climate scenarios for the North Sea and Baltic Sea region. These scenarios show strong signals in surface fluxes (Dieterich et al., 2019) and surface conditions (Gröger et al., 2019, Meier et al., 2019) due to climate change. In this study we have analyzed how atmospheric conditions for the formation of snow bands change under projected climate change. Snow bands occur less often during most of the winter season in a warmer climate. The single strongest stressor is the increase in atmospheric surface temperature. During the recent past, 300 days per year would qualify for a daily mean temperature of less than 8° C. In the far future there are on average only 230 days per year that are below 8° C. This also causes the seasonal maximum of snow band occurrence to shift from November towards December and January. The number of snow bands reduces from 10 to 8 per year. Additional analysis is necessary to identify the sensitivity of our conclusions against the criteria of the conditions for convective snow bands. We have applied those that have been developed by Jeworrek et al. (2017), see Appendix.

We plan further analysis to identify whether the changing snow band signal is related to changes in atmospheric circulation patterns.

Appendix

parameter	criteria
max 10m wind speed	> 10 m/s
mean 2m temperature	< 8° C
max temperature difference between surface and 850 hPa	> 13° C
mean wind shear between 700 and 975 hPa	< 60°
mean wind direction at 900 hPa	> 0° and < 90°
max boundary layer height	> 1000 m
max precipiation	> 0.5 mm/h
max snow fall	> 1.5 mm/d

Table 2. Criteria for days with moderate atmospheric conditions for convective snow bands. The precipitation parameters are evaluated along the Swedish east coast. The other parameters are evaluated over the Baltic Sea, north of 56° N. Reproduced from Jeworrek et al. (2017).

References

Dieterich, C.,Wang, S., Schimanke, S., Gröger, M., Klein, B., Hordoir, R., Samuelsson, P., Liu, Y., Axell, L., Höglund, A., Meier, H. E. M. (2019) Surface Heat Budget over the North Sea in Climate Change Simulations, Atmosphere, 10, doi: 10.3390/atmos10050272

Gröger, M., Arneborg, L., Dieterich, C., Höglund, A., Meier, H. E. M. (2019), Summer hydrographic changes in the Baltic Sea, Kattegat and Skagerrak projected in an ensemble of climate scenarios downscaled with a coupled regional ocean-sea ice-atmosphere model, Clim. Dynam., 67, doi:10.1007/s00382-019-04908-91

Höglund, A., Pemberton, P., Hordoir, R., Schimanke, S. (2017) Ice conditions for maritime traffic in the Baltic Sea in future climate, Boreal Environ. Res., 22, 245-265

Jeworrek, J., Wu, L., Dieterich, C., Rutgersson, A. (2017) Characteristics of convective snow bands along the Swedish east coast, Earth Syst. Dynam., 8, 163–175, doi:10.5194/esd-8-163-2017

Meier, H. E. M., Dieterich, C., Eilola, K., Gröger, M., Höglund, A., Radkte, H., Saraiva, S., Wåhlström, I. (2019) Future projections of record-breaking sea surface temperature and cyanobacteria bloom events in the Baltic Sea, AMBIO, 41, doi:10.1007/s13280-019-01235-5

Olsson, T., Perttula, T., Jylhä K., Luomaranta, A. (2017) Intense sea-effect snowfall case on the western coast of Finland, Adv. Sci. Res., 14., 231-239, doi:10.5194/asr-14-231-2017

Taylor, K. E., Stouffer, R. J., Meehl, G. A. (2012) An Overview of CMIP5 and the Experiment Design, B. Am. Meteorol. Soc., 93, 485-498, doi:10.1175/BAMS-D-11-00094.1

van Vuuren, D. P., Edmonds, J., Kainuma, M., Riahi, K., Thomson, A., Hibbard, K., Hurtt, G. C., Kram, T., Krey, V., Lamarque, J.-F., Masui, T., Meinshausen, M., Nakicenovic, N., Smith, S. J., Rose, S. K. (2011) The representative concentration pathways: an overview, Climatic Change, 109, 5-31, doi: 10.1007/s10584-011-0148-z

Wang, S., Dieterich, C., Döscher, R., Höglund, A. , Hordoir, R., Meier, H. E. M., Samuelsson, P., Schimanke, S. (2015) Development and evaluation of a new regional coupled atmosphere-ocean model in the North Sea and Baltic Sea, Tellus A, 67, 24284, doi: 10.3402/tellusa.v67.24284

Estimation of economic effect of the use of hydrometeorological information during exploitation of highways of Belarus

Y. A. Hledko

Belarusian State University, Republic of Belarus, Minsk (gledko74@mail.ru)

In all the countries of the world, including the Republic of Belarus, it notes the rising economic and social losses due to the influence of hydrometeorological environment. The article focuses on the road transport system, the success of which depends on the correct road maitenance, its technical state and, certainly, the effective specialized hydrometeorological providing.

Assessment of the hydrometeorological phenomena impacton the certain type of economic activity allowsto determine the quantitative index of the economic effect. The economic effect, in its turn, is defined as an actually well-kept materiel of the managing party(economic operator)as a result of the use of hydrometeorological informative products (weather forecast orsummarized climatic products) besides the costof the product.

The purpose of the article is to estimate the economic effect of the use of hydrometeorological information during the road maintenance period of the Republic of Belarus.The research is aimedon the studying of thedangerous and unfavorable hydrometeorological phenomenon of cold period of the year, that damage road network of the Republic of Belarus (icing, frost, hoarfrost, powdery snow, ice and snow roll).The research object is the economic effect estimation of the use of hydrometeorological information during the road maintenance period.

As an example could be presented M- 2 (Minsk - the National airport "Minsk") and P- 23 (Minsk - Slutsk) road sections; the assessment of the impact of dangerous hydrometeorological phenomena during the cold period of the year on the state of roadbed is given and a possible economic effect is calculated. The economic effect evaluation was done according to the methodology developed by the employees of the All-russian Research Institute of Hydro meteorological Information and Voronezh State University of Architecture and Construction. As a result, positive assessment of economic effect was calculated, and also a number of shortcomings related to the hydrometeorological information methodology of calculation and data use .

The most difficult weather conditions for road transport are in winter and in transition seasons. All meteorological phenomena during winter period are dangerous because ofslipperiness. Slipperiness is determined by decreasing of the friction coefficient with the roadbed. Winter slipperiness depends on the frequency, intensity and duration of the snowfalls, blizzards and road icing, as well as the same time air temperature. Each type of winter slipperiness is determined by its own criterion and process of formation (Table 1).

Table 1 - Slipperiness types and processes of its formation

Types of winter slipperiness	Aggregate state of precipitation	Formation process
Icing	Liquid	RainFreezing
Frost	Vapour	Ice deposition in fog as a result of water vapor desublimation and freezing of supercooled fog droplets
Hoarfrost	Vapour	Thin layer of ice crystal on the surface of the road formed from the water vapour of the atmosphere
Powdery snow	Solid	During snowfall or blizzard
Snow roll	Solid	Powdery snow consolidation
Ice and snow roll	Solid	Wet snow freezing

Icing phenomena are the most dangerous type of winter slipperiness , so road measuring stations are able to record these phenomena automatically, thereby informing consumers of the current situation in a timely manner through the information board, as well as transmitting data to the information center via communication channels, which will allow to clean theroadbeds soon as possible. The road measuring stations determine ice and frost according to the probable conditions of occurrence, which is attained through practice andthenconfirm by road sensors (Table 2).

Table 2 - Conditions of icing and frost formation on the road surface

Meteorological element	Icing	frost
Temperature, ^{0}C	-2 - -12	1- -7
Relative humidity, %	83-100	86-100
Dew point, ^{0}C	-3 - -14	0- -8
Surface temperature, ^{0}C	-2 - -11	0 - -8

The economic impact was assessed on the example of the winter road maintenance in the Republic of Belarus, as the roads are particularly vulnerable to the weather conditions during the winter period. Winter road maintenance is a set of activities to ensure safe and uninterrupted traffic on the roads in winter, including: roads protection from snow drifts, fight against winter slipperiness, cleaning roads from snow.

The technique is designed for two main types of slipperiness, which most often cause traffic accidents - snow roll and icing. The calculation is carried out for each type separately, for this purpose a matrix of losses in the formation of winter slipperiness is drawn up.

In order to calculate the economic effect, the following initial data is required: the name of the road, the technical category of the road, the intensity of traffic

in the section in question, the adopted level of maintenance, the length of the roadbed section , the cost of anti-icing materials, as well as prognostic and actual hydrometeorological information. Prognostic information comes from the data of the Republican Center of Hydrometeorology, Radioactive Pollution Control and Environmental Monitoring, actual hydrometeorological information is provided by the automated system "Highway."

In the program of economic effect calculation the initial data is included in a number of tables. The Road Base table includes the road name, technical category, level of maintenance and intensity. The table "Initial data" contains the following initial data: duration of the calculated section, type of winter slippery, predicted formation temperature, 1 ton of anti-icing materials cost, as well as the exchange rate of the Belarusian ruble (against the Russian ruble). The Meteorological Data table introduces predictive and actual information.

A feature of entering meteorological data is that the value of "1" means that the meteorological phenomenon was predicted or observed, and the value of "0" means that the prediction is missing or the phenomenon was not observed. This feature is a disadvantage of the technique. By repeated recurrence of the phenomenon, summation of the economic effects for each case of the phenomenon was applied in practice.

In practice, the economic effect of the use of hydrometeorological information was calculated for M-2 road section (Minsk - Minsk National Airport).

During the observed period from February 1 to April 30, 2017, 31 cases of snow fall were forecasted for this section of the road by the Republican Center for Hydrometeorology, Radioactive Pollution Control and Environmental Monitoring, 21 cases were confirmed by road measuring stations, 16 cases of ice formation were forecasted, 9 cases were confirmed, 1 case was registered but not predicted. Above-mentioned data was included in the program of calculation of economic effect from use of hydrometeorological information.

As a result, the economic effect in icing predicting is 55,560 BYN (>23,000€). The road transport system adaptation to the expected weather conditions is one of the most important indicators of the possibility of effective use of hydrometeorological information, therefore it will help saving money for the roads maintenance in proper condition.

From climate variability to heavy precipitation: Learning transfer functions from data

Michał Kałczyński[1,2], Krzysztof Krawiec[2,3] and Zbigniew Kundzewicz[1]

[1] Institute for Agricultural and Forest Environment, Polish Academy of Sciences, Poznan, Poland (kalczynski.michal@gmail.com)

[2] Institute of Computing Science, Poznań University of Technology, Poznan, Poland

[3] Center for Artificial Intelligence and Machine Learning (CAMIL), Poznan, Poland

1. Introduction

Floods have been a major natural disaster that continues to cause significant material damage and fatalities in both industrialized and less developed countries.

Many floods are caused by heavy and/or long-lasting precipitation. Since the warming atmosphere can store more water vapor, there is potential for more intense precipitation that may cause floods. Yet, there is still lack of persuading and ubiquitous upward trend in observed intense precipitation records. A strong natural variability tends to dominate in precipitation records at any spatial scale. Hence, detection and attribution remain challenging research areas.

This contribution deals with intense precipitation at the global scale, with a special focus on the Baltic Sea Basin. Using data-driven modelling, we ask whether the inter-annual and inter-decadal climate variability track plays a dominant role in the interpretation of the variability of heavy precipitation. The study aims at discovering spatially and temporally organized links between indices of four major climate oscillation modes: El Niño-Southern Oscillation (ENSO), North Atlantic Oscillation (NAO), Pacific Decadal Oscillation (PDO), Atlantic Multidecadal Oscillation, and heavy precipitation.

2. Data

The data used in the reported research come from multiple sources of global observations including E-OBS data set derived from the UERRA project (Cornes et al., 2018) and GPCC Full Data Daily (Ziese et al., 2018), as well as the climate variability indices for ENSO, NAO, PDO, and AMO, available from different institutions.

3. Methodology

We induce a range of machine-learning models, primarily recurrent neural networks. The models are thoroughly tested and juxtaposed in hindcasting mode on a separate test set and scrutinized with respect to their statistical characteristics. We expect to identify climate-oscillation drivers for spatial dependence of heavy precipitation.

4. Expected results

This contribution will report on the work in progress aimed at interpretation of observed variability of intense precipitation records. There is vast scientific literature demonstrating the climate variability link between indices of quasi-periodic oscillation in the ocean-atmosphere system and heavy precipitation. A review of the literature on such links, for a range of scales – from global to continental, national and regional, is provided by Kundzewicz et al. (2019). Most existing publications try to establish a local or regional link between time series of precipitation indices and climate variability indices.

This study, by relying on global observation records and state-of-the-art methodological toolbox, aims to analyze big data and to establish spatially variable relationship at the global scale. The present contribution to this conference will focus on the region of the Baltic Sea Basin.

References

Cornes, R. C., van der Schrier, G., van den Besselaar, E. J. M., & Jones, P. D. (2018). An ensemble version of the E-OBS temperature and precipitation data sets. Journal of Geophysical Research: Atmospheres, 123, 9391–9409. https://doi.org/10.1029/2017JD028200

Kundzewicz, Z.W.; Szwed, M.; Pinskwar, I. (2019) Climate variability and floods-A global review. Water 11(7), 1399.

Ziese, M., Rauthe-Schöch, A., Becker, A., Finger, P., Meyer-Christoffer, A., & Schneider, U. (2018). GPCC Full Data Daily Version 2018 at 1.0°: Daily Land-Surface Precipitation from Rain-Gauges built on GTS-based and Historic Data (Version 2018) [Data set]. Global Precipitation Climatology Centre (GPCC) at German Weather Service (Deutscher Wetterdienst). https://doi.org/10.5676/DWD_GPCC/FD_D_V2018_100

Impacts of river discharge and ice phenomena on the extent of storm surges in the Odra River mouth area (the southern Baltic Sea)

Halina Kowalewska-Kalkowska

Institute of Marine and Environmental Sciences, University of Szczecin, Poland (halina.kowalewska@usz.edu.pl)

1. Introduction

Storm surges are main forces of changes in water level in mouth areas of rivers, which are marked by a very low slope of water surface and flow into tideless seas. In contrast, the impact of river discharge on water levels in the river mouth area is of less importance because it affects mainly the mean water level. The Odra River mouth area, located in the southern Baltic Sea, belongs to coastal water bodies that are particularly exposed to storm surges. The resultant water backflow in the lower Odra channels depends on various meteorological and hydrological factors and may penetrate as high up the river as to 160 km south from the sea, sometimes leading to flooding of low-lying areas, polders and areas adjacent to the river (Buchholz, 1991; Kowalewska-Kalkowska and Wiśniewski, 2009; Kowalewska-Kalkowska, 2018).

In the study multivariate exploratory methods of data analysis were applied to assess the impacts of the amount of river discharge and the formation of ice phenomena on the extent of storm surges in the Odra River mouth area.

2. Material and methods

The analyses were carried out based on 10-minute water level readings from 10 gauges located in the Odra River mouth area in the seasons from 2009/10 to 2018/19, designated after Sztobryn et al. (2005) from August to July of the following year.

Prior to the multivariate data analysis, the correlation analysis between water level data series was carried out. Then the cluster analysis was employed to identify natural clustering patterns based on similarities/ dissimilarities between data sets. In the analysis, the Ward's method and the one-minus Pearson correlation coefficient distance were applied. Next the factor analysis was performed to detect and describe structure in the relationships between data series. The factors were extracted using principal component analysis and the varimax rotation method.

3. Results

The cluster and rotated factor analyses employed in this study were found to be useful in offering reliable information on impacts of river discharge and ice phenomena on the extent of storm surges in the Odra River mouth area.

Two storm surges at the coasts of the Pomeranian Bay between 11 and 16 December 2010 were recorded during the increased water supply from the Odra River catchment. In addition, ice phenomena on the lower Odra were observed as well (Ocena…, 2010). As a result, the sea impact was limited to the Szczecin Water Area, that was confirmed by the constructed dendrogram of grouping of water levels within the Odra River mouth area (Fig. 1). The strongest correlations were found between the water levels in the Szczecin Lagoon and within the Szczecin Water Area. They formed a close cluster, which was related to the sea levels in the Pomeranian Bay.

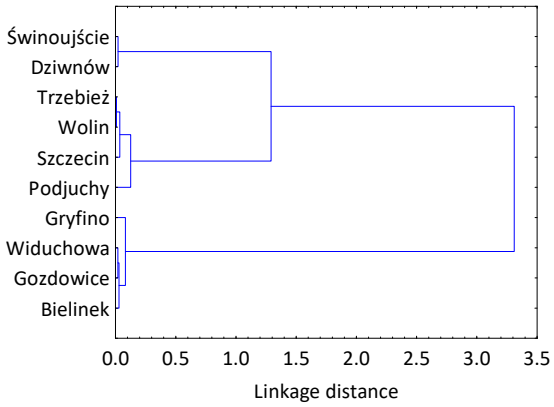


Figure 1. Dendrograms of grouping of water levels in the Odra River mouth area between 11 and 16 December 2010.

The factor analysis resulted in extraction of two hydrologically meaningful factors: the Odra River discharge effect for the rotated factor 1 and the sea level impact for the rotated factor 2 (Fig. 2). The second varifactor was strongly positively loaded only with water levels in the Pomeranian Bay, in the Szczecin Lagoon and within the Szczecin Water Area confirming results of the cluster analysis.

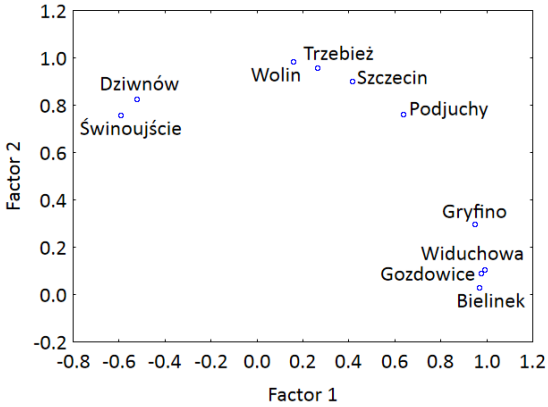


Figure 2. The scatterplots of rotated factor loadings for water levels in the Odra River mouth area between 11 and 16 December 2010.

The most severe high water event in the Odra River mouth area due to the storm surge occurrence was observed in the middle of October 2009 and was recorded during a period of lower than average Odra flows. The analysis of the obtained dendrogram of grouping of water levels in the Odra mouth area between 12 and 18 October 2009 showed a distant influence of sea impact, reaching Bielinek (Fig. 3). The closest affinity between water level readings were those within the Trzebież to Widuchowa

section. They formed a cluster with a very high degree of mutual correlation, which was then closely related to the water levels in Bielinek. Changes in the water level in the section between Trzebież and Bielinek followed those of the sea level, suppressed in the straits between the Szczecin Lagoon and the Pomeranian Bay.

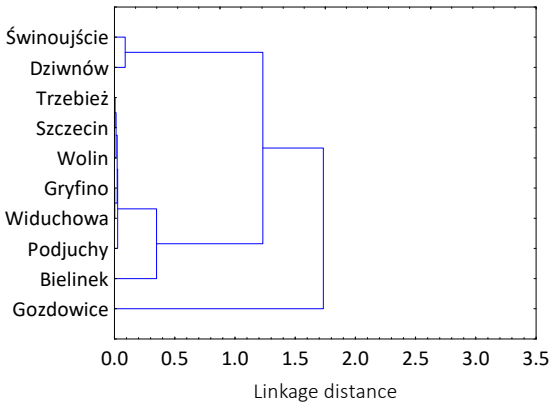


Figure 3. Dendrograms of grouping of water levels in the Odra River mouth area between 12 and 18 October 2009.

The factor analysis resulted in extraction of three rotated factors. The rotated factor 1 was strongly positively loaded with water levels in the Szczecin Lagoon and in the lower Odra channels up to Bielinek (Fig. 4). Lower loadings were found for sea levels in the Pomeranian Bay, which were strongly correlated with the second varifactor. The Odra discharge effect on water levels in the Odra mouth area was noticeable only in Gozdowice, as indicated by the high load of water levels there to the third varifactor.

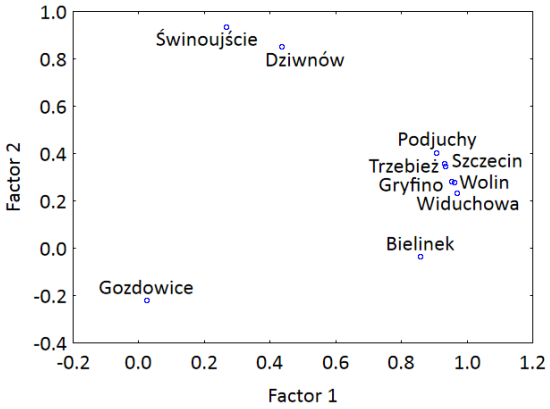


Figure 4. The scatterplots of rotated factor loadings for water levels in the Odra River mouth area between 12 and 18 October 2009.

4. Conclusions

The cluster and rotated factor analyses demonstrated the dependence of the extent of storm surges in the Odra River mouth area on the amount of river discharge and the occurrence of ice phenomena on the lower Odra channels.

In case of the increased water supply from the Odra River catchment and/or the formation of ice phenomena on the lower Odra, the extent of storm surges was limited to the Szczecin Water Area. The spread of surges increased with the decrease of the Odra discharge, and during low water periods it influenced the river level upstream to Bielinek (c. 130 km south from the sea).

5. Acknowledgments

This work was supported through the funds of the Institute of Marine and Environmental Sciences, University of Szczecin, Poland. The calculations were carried out using water level data series drawn from the Institute of Meteorology and Water Management, National Research Institute, Poland via the website https://dane.imgw.pl/.

References

Buchholz W. (ed.) (1991) Monografia dolnej Odry, Hydrologia i hydrodynamika, Prace IBW PAN, 25, Gdańsk [In Polish].

Kowalewska-Kalkowska H. (2018) Frequency and strength of storm surges in the Oder River mouth area, Acta Sci. Pol. Form. Cir., 17 (3), pp. 55-65, doi: 10.15576/ASP.FC/2018.17.3.55.

Kowalewska-Kalkowska H., Wiśniewski B. (2009) Storm surges in the Odra mouth area during the 1997–2006 decade, Boreal Env. Res., 14, pp. 183–192.

Ocena hydrologiczno–nawigacyjna roku 2010 (2010) http://www.informator.szczecin.rzgw.gov.pl/pl/ocena_hydrologiczno_nawigacyjna/pliki/ocena_hydro_nawig_2010.pdf [In Polish].

Sztobryn M., Stigge H.-J., Wielbińska D., Weidig B., Stanisławczyk I., Kańska A., Krzysztofik K., Kowalska B., Letkiewicz B., Mykita M. (2005) Storm surges in the Southern Baltic Sea (western and central parts), Berichte des BSH, 39, BSH, Rostock-Hamburg.

Coastal flooding: Joint probability of extreme water levels and waves along the Baltic Sea coast

Nadia Kudryavtseva[1], Andrus Räämet[1] and Tarmo Soomere[1,2]

[1] Department of Cybernetics, School of Science, Tallinn University of Technology, Tallinn, Estonia (nadia@ioc.ee)
[2] Estonian Academy of Sciences, Tallinn, Estonia

1. Introduction

The Baltic Sea (Figure 2) is a seasonally ice-covered semi-enclosed sea. A few severe storms have hit the area in the last decades. For example, in January 2005, the wind storm Gudrun (Erwin), caused by a combination of multiple factors, such as prolonged winds from a particular wind direction in the North Sea (pushing the water from the North Sea to the Baltic Sea), lack of protecting ice cover and extreme wave heights struck the Baltic Sea countries and caused coastal flooding and widespread damage to infrastructure and forests (*e.g.,* Suursaar et al., 2006). There is increasing evidence that such storms, with extreme wave heights, and sea levels are getting more severe and more frequent over time in the Baltic Sea region and such events can significantly affect the population and economy of the impacted areas.

The *joint* impact of multiple drivers can cause severe extreme events via various cumulative processes. For example, high storm surge in combination with high and long waves may cause significant coastal flooding through the effects of wave set-up and run-up (Masina, Lamberti and Archetti, 2015) or rapid coastal evolution, depending on the approach direction of waves. The risk of catastrophic impacts under such conditions is often much higher than a simple sum of the impacts of the individual components would suggest. It is also critical to assess not only the joint probability of event occurrences but also their spatial distribution and the duration of extreme events.

2. Data and Methods

The analysis of the extreme sea levels is based on simulated sea surface heights using NEMO-Nordic (BaltiX) model (Hordoir et al., 2013), based on the NEMO 3.3.1 ocean engine. A method discussed in Kudryavtseva et al. (2018) was used to extract suitable model cells along the Baltic Sea coastline, which are adjusted to the type of the coastline. Wave heights, periods, and directions over the entire Baltic Sea were extracted for the same locations as the water levels from the simulations using the third-generation wave model WAM ran with adjusted geostrophic wind forcing (Räämet and Soomere, 2010). The simultaneous sea level and wave data have a temporal resolution of one hour and cover the period of 1979–2007.

The water level variability was deconstructed into storm surges and a slowly changing component (a proxy of the water volume of the entire Baltic Sea) using running average with a window of 8.25 days (Soomere and Pindsoo, 2016). The extreme events are identified using a peak-over-threshold approach. A qualitatively fixed threshold, defined as the 97th percentile of storm surge height, was calculated for each location separately. Its quantitative value greatly varies in various regions of the Baltic Sea due to sea-level spatial variability. To create a set of independent extreme water levels, the exceedances were separated into single events, and only the maximal sea-level value per event was taken into consideration. The typical storm duration in the Baltic Sea, interpreted as a declustering timescale, is 10 hours. Subsequent events within less than 10 hours thus cannot be considered as independent ones and represent the same storm. If multiple events appeared within 10 hours between each other, they were considered as one single event with the extreme value calculated as a maximum of all dependent events.

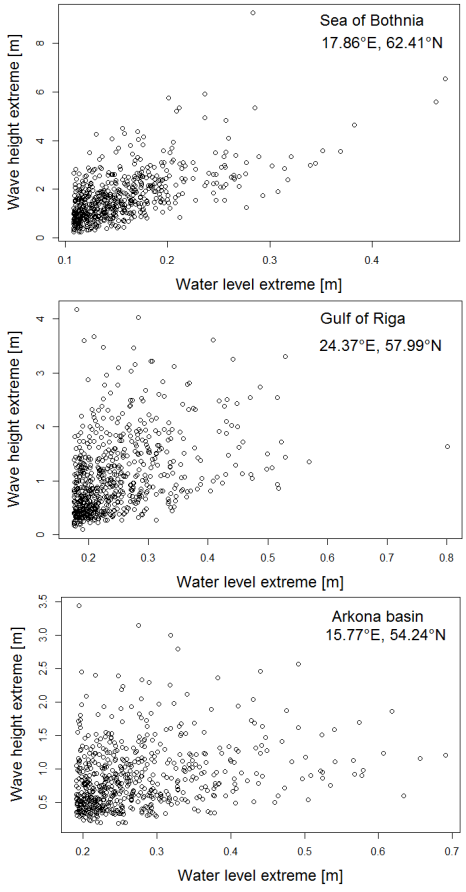


Figure 1. Scatter diagrams between the water level extremes and corresponding wave height extremes for three regions in the Baltic Sea characterised by a strong dependence (Sea of Bothnia, top), intermediate dependence (Gulf of Riga, middle), and low dependence (Arkona basin, bottom).

For each found water level event, the corresponding wave height extremes were identified as the largest wave heights reached during the sea-level event (Masina, Lamberti and Archetti, 2015). Joint probability analysis is performed using the copula approach. It is based on Sklar's theorem stating that for each marginal distributions F_1 and F_2 with a joint distribution H there exist a function copula C that for all real x_1, x_2:

$$H(x_1, x_2) = C(F_1(x_1), F_2(x_2)). \quad (1)$$

Multiple types of copulas were tested using the goodness of fit approach. Based on these tests, Frank copulas (Frank,

1979) (a one-parameter family of the Archimedean class of copulas) were selected for the analysis.

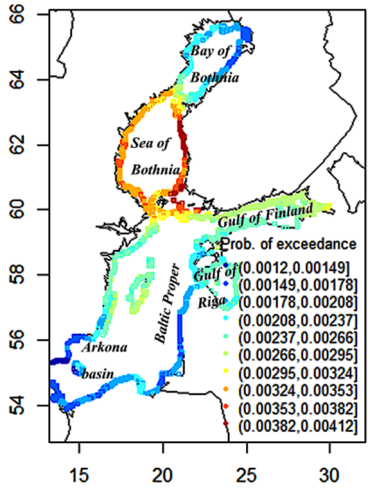


Figure 2. The probability of occurrence of situations when sea-level and wave height extremes both exceed their 97th percentile calculated using the Frank copula. The percentiles are evaluated separately for wave heights and water levels for each location, based on the set of identified extreme events.

3. Results

To find the correlation between the sea level and wave extremes, a set of independent extreme events was created for each cell. Only conditions at the time of each sea-level peak are considered of interest. These sets were tested for dependence using the Pearson, Kendall, and Spearman correlation coefficients. Interestingly, the dependence in terms of these coefficients is significantly different along the Baltic Sea coastline, and four distinctive regions were identified:

1) Most of the Arkona Basin, the southern and eastern part of the Baltic proper have a low number of coinciding strong waves and high water levels, with typical values of the relevant correlation coefficients <0.2.

2) The Gulf of Riga, the Gulf of Finland and north-western part of the Baltic proper exhibit frequent match of high water level and intense wave events, with the relevant correlation coefficients in the range of 0.2–0.5.

3) Strong waves and high water levels are likely to co-occur in the Sea of Bothnia, where the relevant correlation coefficients are in the range of 0.5–0.7.

4) The Bay of Bothnia is characterised by a less frequent match of high water level and wave events, with the relevant correlation coefficients in the range of 0.2–0.4.

Examples of scatter diagrams that characterise the strength of correlation between the sea level extremes and corresponding wave heights are shown in Figure 1 for selected locations of the Sea of Bothnia (strong correlation), the Gulf of Riga (moderate correlation), and the Arkona basin (low correlation). The analysis showed that except for the northern coast of the Arkona basin where the correlation is insignificant (<0.1), all other locations along the Baltic Sea coast exhibit a significant dependence between the sea level and wave height extremes. Therefore, an application of the joint probability analysis is required in those areas.

The results of the application of the Frank copula to the joint water level and wave height extremes (Figure 2) indicate that the probability that both water level and sea level exceed the 97th percentile is highest in the Sea of Bothnia. This probability is lower in the Gulf of Finland, Gulf of Riga, and the west coast of the northern Baltic proper, and reaches the lowest values in the Bay of Bothnia, southern Baltic proper, and the Arkona Basin. The high probability of the joint exceedance corresponds to the higher flood risk. Therefore, the Sea of Bothnia has the largest risk of simultaneously receiving very strong waves (and thus wave set-up) and offshore water level. This risk is lower in the Gulf of Finland, the Gulf of Riga and the northern Baltic proper.

4. Discussion and Conclusions

The Sea of Bothnia has the most severe wave climate compared to the other gulfs of the Baltic Sea. It has a regular shape and is sheltered to waves created in the northern Baltic proper and the Bay of Bothnia. In such water bodies, both storm surge and high waves mainly follow the properties of the local wind and are thus often synchronised. Severe wind and wave conditions in the Sea of Bothnia together with a regular shape can explain a correlated response between the wave height and sea-level extremes. Low correlation between the extreme sea-levels and wave heights in the southern Baltic Sea reflects the asymmetry of wind and wave regime in that region.

A joint probability approach to extreme water levels and wave heights is introduced for the Baltic Sea. The joint probability of occurrence of extreme sea level and wave height greatly varies along the Baltic Sea shores. The risk for the simultaneous appearance of water level and wave height extremes is the highest for the entire Sea of Bothnia, smaller in the Bay of Bothnia, Gulf of Finland, Gulf of Riga and northern Baltic proper, and very small for southern and south-western parts of this sea. The study demonstrates that it is crucial to take into account the combination of both water levels and wave heights in all regions of the Baltic Sea except for its southern areas.

References

Frank, M.J. (1979) On the simultaneous associativity of F(x, y) and x + y – F(x, y), Aequationes Mathematicae, 19 (1), 194–226

Hordoir, R.; Dieterich, C.; Basu, C., et al. (2013) Freshwater outflow of the Baltic Sea and transport in the Norwegian current: A statistical correlation analysis based on a numerical experiment, Continental Shelf Research, 64, 1–9

Kudryavtseva, N.; Pindsoo, K.; Soomere, T. (2018) Non-stationary Modeling of Trends in Extreme Water Level Changes Along the Baltic Sea Coast, Journal of Coastal Research, Special Issue 85, 586–590

Masina, M.; Lamberti, A.; Archetti, R. (2015) Coastal flooding: A copula based approach for estimating the joint probability of water levels and waves, Coastal Engineering, 97, 37–52

Räämet, A.; Soomere, T. (2010) The wave climate and its seasonal variability in the northeastern Baltic Sea, Estonian Journal of Earth Sciences, 59(1), 100–113

Soomere, T.; Pindsoo, K. (2016) Spatial variability in the trends in extreme storm surges and weekly-scale high water levels in the eastern Baltic Sea, Continental Shelf Research, 115, 53–64

Suursaar, Ü.; Kullas, T.; Otsmann, M., et al. (2006) Cyclone Gudrun in January 2005 and modelling its hydrodynamic consequences in the Estonian coastal waters, Boreal Environment Research, 11 (2), 143–159

Agrothermal changes in 1961–2018 in Lithuania

Viktorija Mačiulytė, Gintautas Stankūnavičius

Institute of Geosciences, Vilnius University, Vilnius, Lithuania (viktorija.maciulyte@chgf.vu.lt)

1. Introduction

Temperature is one of the most important factors determining the plant growth conditions. The beginning of the plant vegetation is considered to be at the moment of constant air temperature (mean daily) transition through 5 °C in Lithuania, while active growth period of plants starts – when mean daily temperature constantly transits through 10 °C. The dates of these transitions in spring and autumn seasons vary from year to year.

Early spring and autumn frosts can cause substantial damage in the Lithuanian agricultural sector (Stuogė et al., 2012). Regional climate change is characterized through rising in mean seasonal air temperatures and changing frequency and seasonality of extreme weather events. Despite continuously warming climate over the last 50 years, the frost risk has increased in many regions (Menzel et al., 2020; Crimp et al., 2014).

Warming winters can lead to early onset of vegetation ("false spring") and increase the potential of agricultural frost in Central Europe as well as in Lithuania. Frost has been identified as a medium risk meteorological phenomenon that can lead the plant damage by reducing yields, yield and income (Ma et al., 2019; ASU, 2016).

2. Data and methods

The main task of this study is to estimate the changes of dates of constant air temperature transition through 5 °C and 10 °C in transitional seasons and the changes in spring and autumn frost risk in Lithuania in whole warm season (April–October) from 1961 to 2018. As main variables there were used minimal (t_{min}) and daily mean (t_{mean}) air temperature at standard (1.5 m) height in Dotnuva meteorological station (station 55.4°N and 23.9°E). The soil temperatures have not been used directly in estimations because of their series incompleteness. Dotnuva station is located in the most intensive agricultural region in Lithuania.

The moment (date) of constant air temperature transition through temperature thresholds 5 °C and 10 °C degrees was indicate using constant daily mean air temperature transition.

An agricultural frost is considered when a minimum air temperature drops below +3 °C degrees during active plant growth period.

The detected changes were assessed using Sans-slope trend method and the Mann-Kendall test was used to assess the statistical significance of changes at α=0.05 significance level.

3. Results

Dates of constant air temperature transition through temperature thresholds. The average date of mean daily air temperature transition through 5 °C in 1981–2010 in spring in Dotnuva station occurs on 10th of April, and on 30th of October in autumn. The average date of transitions through 10 °C occurs on 30th of April, and on 2td of October respectively. The total length of the vegetation season (t_{mean}>5 °C) is 203 days and while the mean length of active growth period of vegetation (t_{mean}>10 °C) is 155 days (Table 1).

Table 1. The mean dates of constant air temperature transition temperature thresholds and changes in dates. Statistical significant changes are marked in bold.

Threshold	Parameter	Long term mean 1981–2010	Change in 1961–2018
5 °C	spring	10-april	**-13,4 days**
	autumn	30-october	-3,6 days
	season length	203 days	14 days
10 °C	spring	30-april	**-17,2 days**
	autumn	02-october	**13,1 days**
	season length	155 days	**29 days**

The length of active growth period on average has increased by 29 days during last 58 years. And this change is considered to be statistically significant. The largest changes were found in spring season, when the constant air temperature transition through 10 °C lags by 17 days comparing to the mean date. The smallest changes found in the constant air temperature transition through 5 °C in autumn, which has an opposite trend to the 10 °C date change. Nevertheless, the spring air temperature transition through 5 °C shifted to the early by about 13 days.

It can be concluded that end of vegetation period in autumn appears to be not very variable during analysed historical period. However, the end of the active growth period of vegetation appears to be delayed in autumn season. The period between transitions dates through 10 °C and 5 °C temperature thresholds in autumn became shorter.

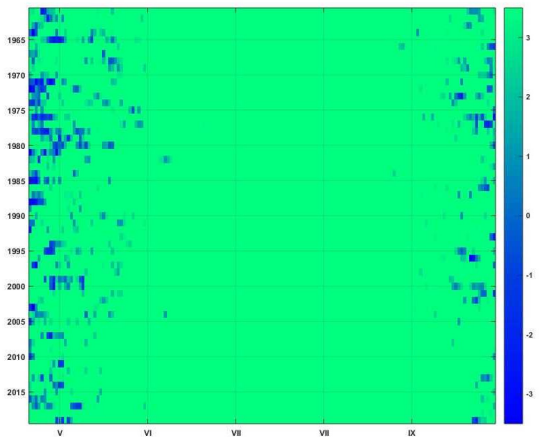


Figure 1. Hovmöller diagram of change of air temperatures (-3 °C – 3 °C) favored for agricultural frost formation in the warm season of the year during 1961–2018.

Frosts. The average number of days with frost (t_{min}<3 °C) in 1981–2010 in Dotnuva station found 4.2 days in

spring and 2.5 days in autumn. During analysed period in 1961-2018, frosts did not occur during the spring (1963, 2003, 2006, 2009, 2018) and autumn (1965, 1967, 1981, 1988, 1992, 2006, 2007, 2011, 2012) of some years.

The number of days with frost during active growth period on average has decreased by 3.2 days in spring and 2.8 days in autumn during last 58 years (Figure 1). These changes are statistically significant.

4. Conclusions

Due to climate change, the length of active growth period of vegetation has increased by almost of one month. Statistical significant changes were found in spring dates of constant air temperature transition through 10 °C - they lag 17 days. The increased length of vegetation season allows growing crops in Lithuania for a longer period.

It was also found that the number of days with frost decreased during the period analyzed. These results suggest that the prolonged active season of vegetation and the decreasing recurrence of frost are detrimental to some crops.

On the other hand, prolonged periods of active vegetation and increasing precipitation volatility and drought frequency can adversely affect crops. This should be analyzed in the future.

References

ASU (2016) Žemės ūkio, maisto ūkio ir žuvininkystės sričių išorės ir vidaus rizikos veiksniai, grėsmės ir krizės bei jų galimas poveikis. 2016 metų baigiamoji ataskaita. Akademija.

Crimp S., Bakar K.S., Kokic P., Jin H., Nicholls N., Howden M. (2014) Bayesian space-time model to analyse frost risk for agriculture in Southeast Australia. Int. J. Climatol. 35, 2092–2108.

Stuogė I., Ribikauskas V., Lazauskas S., Radzevičius G. (2012) Klimato kaitos įtaka Lietuvos žemės ūkiui: iššūkiai, situacijos analizė ir prognozės. *Kaimo raidos kryptys žinių visuomenėje. 2012, 2(4). 43–55. ISSN 2029-8846.*

Menzel A., Yuan Y., Matiu M., Sparks T., Scheifinger H., Gehrig R. and Estrella N. (2020) Climate change fingerprints in recent European plant phenology, *Global Change Biology* DOI: https://doi.org/10.1111/gcb.15000

Ma Q., Huang J. G., Hänninen H., and Berninger F. (2019) Divergent trends in the risk of spring frost damage to trees in Europe with recent warming. Global Change Biology, 25, 351– 360. https://doi.org/10.1111/gcb.14479

Differences in stationary and non-stationary analysis of water level extremes in Latvian waters, Baltic Sea, during 1961-2018

Rain Männikus[1], Nadezhda Kudryavtseva[1] and Tarmo Soomere[1,2]

[1] Wave Engineering Laboratory, Institute of Cybernetics, Tallinn University of Technology, Tallinn, Estonia (rain.mannikus@taltech.ee)
[2] Estonian Academy of Sciences, Kohtu 6, Tallinn, 10130, Estonia

1. Introduction

The core source of information for coastal management are extreme values extracted from observed or measured time-series of water level. However, the length of such records is usually less than 70 years. For reliable design it is necessary to use longer return periods of extreme water levels. Hence, there is a need to calculate reliable values with the help of suitable theoretical statistical distribution of extreme values. This is a complicated issue since data may be too short, inhomogeneous, inaccurate and non-stationary. Moreover, there could be different populations of storms which result in extreme values which do not follow the chosen distribution.

The most challenging is the situation in the easternmost Baltic Sea, where no method of commonly used stationary extreme value estimations seem to be able to cover all observed and hindcast extremes (Eelsalu *et al*. 2014). This is mainly caused by the presence of long-term events of elevated water levels of the entire sea (Lehmann and Post 2015) which may or may not coincide with storm surges depending on the location and openness to the winds of single coastal sections. Also, the spread among different methods can be extensive in areas that experience large wave set-up. Moreover, different drivers of extreme water levels interact in a nonlinear manner so that their joint impact may be larger than the sum of impacts of single drivers (Hieronymos *et al*. 2017). This may result in outliers. This situation calls for other approaches which may solve extreme value estimation in a more reliable way.

In this work, we examine the difference between stationary and non-stationary analysis based on water level extremes in the Gulf of Riga. Here, the extreme water levels are, historically, the third-highest in the entire Baltic Sea after the eastern Gulf of Finland and south-western Baltic Sea (Averkiev and Klevanny 2010). The Gulf of Riga (Figure 1) has approximate dimensions of 130 × 140 km. It has a surface area of 17 913 km², a volume of 406 km³, a maximal depth of 52 m and an average depth of about 23 m. The main connection with the open part of the Baltic Sea is the Irbe Strait, which has a width of 27 km and a sill depth of about 21 m (Suursaar et al., 2002).

2. Data

We use measured water level data from the Latvian Environment, Geology and Meteorology Centre and Estonian Weather Service. We focus on time series starting from 01.01.1961 till 31.12.2018. The quality and properties of these data sets are discussed in (Männikus et al., 2019). We use data from 7 different stations (Liepaja, Kolka, Roja, Daugavgriva, Skulte, Salacgriva and Pärnu) which are most complete in terms of monthly values. However, the data might be influenced by local effects such as wave set-up, river discharge or the presence of extensive shallow regions. In some cases, measurement stations are located in harbours (Roja, Skulte, Salacgriva) or within the city on the shores of a river (Liepaja, Pärnu). The most open stations are Daugavgriva and Kolka.

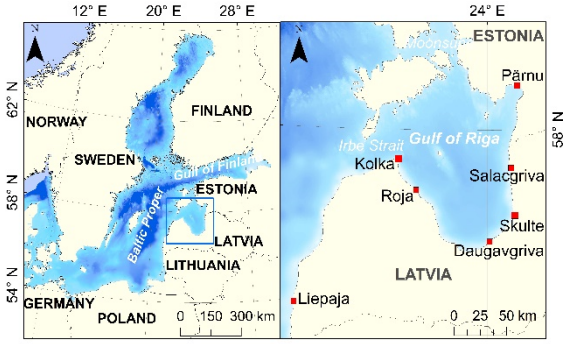


Figure 1. Water level measurement station on the coast of the Gulf of Riga. Red rectangles show stations analysed here.

3. Methods

Projections of extreme water levels and their return period were constructed based on the theoretical extreme value distributions. These are Generalized Extreme Value (GEV) distribution and its particular cases Gumbel, Fréchet and Weibull distributions. The use of these distributions is justified if samples are independent and identically distributed random variables. Hence, block maxima or peak-over-threshold methods are used. The most reliable way to select uncorrelated water level extremes is to use the maxima of the entire relatively windy season starting from July and ending in June next year (called: stormy season; Soomere and Pindsoo, 2016).

The GEV distribution:

$$G(x,\mu,\sigma,\xi) = exp\left\{-\left[1+\xi\frac{(x-\mu)}{\sigma}\right]^{-\frac{1}{\xi}}\right\} \quad (1)$$

is characterized by a location parameter μ∈R, scale parameter σ∈R, and shape parameter ξ∈R. Here x has the meaning of block maxima (e.g., maximum water level for each stormy season). For the shape parameter $\xi \to 0$, the GEV distribution reduces to a Gumbel distribution. If $\xi < 0$, the GEV distribution is equivalent to a three-parameter Weibull distribution, and for $\xi > 0$ to a Fréchet distribution.

In the stationary analysis, the whole available data (also outliers) is used to evaluate the parameters of GEV. Here, different methods (maximum likelihood estimation, biased/unbiased estimation) could be used. As it is not possible to say beforehand which one is the best, the results are usually shown for all of them. If errors are randomly distributed, the average of results could be taken as a reasonable estimate (so-called ensemble approach).

A step further is to check whether the data is stationary (Kudryavtseva *et al.* 2018). A simple approach is to separate the data into, say, 30-year long consecutive sliding windows. In each window, a stationary GEV was fitted to the block maxima x with fixed parameters of location, scale and shape. Annual mean and joint impact of global sea-level rise and local postglacial uplift were removed before the analysis. The resulting variations in the parameters indicate the level of non-stationarity and locations of abrupt changes.

A second step is to assume that the parameters are changing as a function of time. With this hypothesis, a non-stationary GEV distribution was fitted with a distribution with one parameter changing with time (either location, scale or shape parameter). Compared to step one, the whole set of block maxima was used.

4. Results and discussion

An application of the stationary analysis reveals that the extreme water levels with a 100-year return period are the highest at Daugavgriva (ranging from about 180 to 240 cm) and lowest at Liepaja (from 140 to 170 cm). There are 4 outliers at Liepaja which deviate considerably from theoretical projections. These can be caused by local effects in Liepaja (the measurement station is located between a lake and the Baltic Sea) or are measurement errors (Männikus *et al.* 2019).

Further analysis showed that an appropriate length for the sliding window was 30-years. The most dramatic changes in time of >50% of the typical value were observed in the shape parameter. The behaviour of this parameter is different at Liepāja and Kolka (Figure 2) compared to the other locations. Both stations show a relatively smooth change in the shape parameter. This apparently reflects the fact that water level at these stations is most susceptible to the influence of sea-level dynamics in the Baltic proper. The other stations (e.g. Pärnu in Figure 3) experience a drastic abrupt change in the shape parameter.

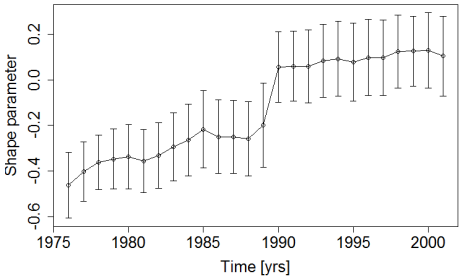


Figure 2. Temporal course of the GEV shape parameter at Kolka. The 30-year sliding window was used and its middle values were used in the x-axis. Even though a relatively abrupt change occurred in 1990, the entire course is approximately linear.

The overall course of the shape parameter of the GEV distribution resembles a step-like manner. The described significant shift in the shape parameter at stations in the interior of the Gulf of Riga signals a dramatic change in the overall appearance of the extreme value distribution from an approximately Gumbel one in most of time to a Weibull-like shape in the 1980s.

In order to describe these abrupt changes and still consider all the data, various functions were fitted with the data of each station. The best fit model for all stations will be described elsewhere.

Our study underlines that the use of the stationary analysis of extreme water levels, albeit it is simple and widely used in other areas, is generally problematic in Latvian waters. The presented analysis shows that considerable variations in the parameters of extreme value distributions have occurred in this region. Therefore, it is necessary to employ more sophisticated non-stationary analysis in order to reach more reliable results. This kind of analysis introduces additional parameters which govern the change of the parameters of extreme value distributions and may alter the projections of extreme water levels and their return periods.

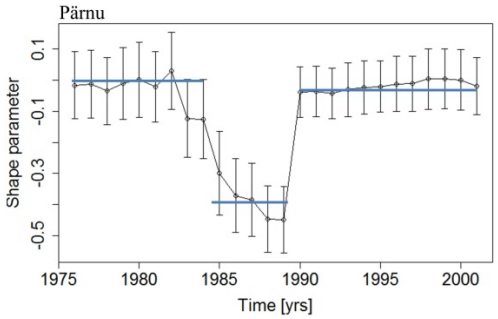


Figure 3. Temporal course of the GEV shape parameter at Pärnu. Also here 30-year sliding window was used. The shape parameter is almost constant, except for the 5 years interval from 1985 to 1990, during which its values were negative.

References

Averkiev, A. S., Klevanny, K. A. (2010) A case study of the impact of cyclonic trajectories on sea-level extremes in the Gulf of Finland. Cont. Shelf Res., 30, 6, pp. 707–714. doi: 10.1016/j.csr.2009.10.010.

Eelsalu, M., Soomere, T., Pindsoo, K., Lagemaa, P. (2014) Ensemble approach for projections of return periods of extreme water levels in Estonian waters. Cont. Shelf Res. 91, pp. 201–210, doi: 10.1016/j.csr.2014.09.012.

Hieronymus, M., Hieronymus, J., Arneborg, L. (2017) Sea level modelling in the Baltic and the North Sea: The respective role of different parts of the forcing. Ocean Model., 118, pp. 59–72, doi: 10.1016/j.ocemod.2017.08.007.

Kudryavtseva, N., Pindsoo, K., Soomere, T. (2018) Non-stationary Modeling of Trends in Extreme Water Level Changes Along the Baltic Sea Coast. Journal of Coastal Research, 85, pp. 586–590, doi: 10.2112/SI85-118.1

Lehmann, A., Post, P. (2015) Variability of atmospheric circulation patterns associated with large volume changes of the Baltic Sea. Adv. Sci. Res., 12, pp. 219–225, doi: 10.5194/asr-12-219-2015.

Männikus, R., Soomere, T., Kudryavtseva, N. (2019) Identification of mechanisms that drive water level extremes from in situ measurements in the Gulf of Riga during 1961–2017. Cont. Shelf Res. 182, pp. 22–36. doi: 10.1016/j.csr.2019.05.014.

Soomere, T., Pindsoo, K. (2016) Spatial variability in the trends in extreme storm surges and weekly-scale high water levels in the eastern Baltic Sea. Cont. Shelf Res., 115, pp. 53–64. doi: 10.1016/j.csr.2015.12.016.

Suursaar, Ü., Kullas, T. Otsmann, M. (2002) A model study of the sea level variations in the Gulf of Riga and the Väinameri Sea Continental Shelf Research, 22, 14, pp. 2001–2019, doi: 10.1016/S0278-4343(02)00046-8.

Study of the influence of zonal and azonal factors on the maximum floods runoff in the Vistula basin (within Ukraine)

Maksym Martyniuk[1], Valeryia Ovcharuk[2]

[1] Department of Land Hydrology, Odessa State Environmental University, Odesa, Ukraine (martyniuk0904@gmail.com)
[2] Hydrometeorological Institute, Odessa State Environmental University, Odesa, Ukraine

1. Introduction

The Vistula River basin is one of the largest in the Baltic Sea basin. The Vistula is also the longest and largest river in Poland. A small part of the Vistula River basin is located in the territory of Ukraine, namely 12892 km^2 from the total area of the Vistula River basin, which covers 198 500 km^2.

In order to reform and improve the water management system of Ukraine and to take into account the experience of other countries on the implementation of the provisions of the Water Framework Directive 2000/60 / EC and the establishment of the River Basin Management Plan (Khilchevsky at all, 2019), a new hydrographic zoning of the territory of Ukraine on the basin principle was conducted (Fig. 1).



Figure 1. Map diagram of the hydrographical zoning of the territory of Ukraine

The Vistula River Basin is divided into two parts by the Dniester River Basin and consists of sub-basins of the Western Bug and San Rivers within Ukraine. The boundary of the Vistula basin runs along the state border with the Republic of Poland, the Republic of Belarus and through settlements along the watershed line. (Fig. 2)

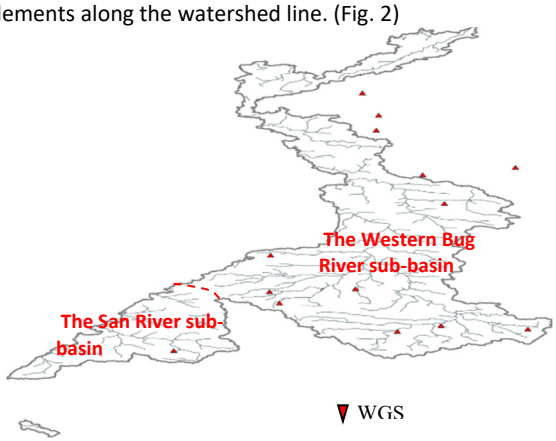


Figure 2. The scheme of Vistula River basin within Ukraine

As noted earlier, the Vistula River basin is divided into two sub-basins - the Western Bug River sub-basin and the San sub-basin. The boundary of the Western Bug sub-basin in turn runs along the state border with the Republic of Poland, the Republic of Belarus and through settlements along the watershed line. The San River sub-basin consists of two parts which separated by the Dniester River basin district, and its boundary runs along the state border with the Republic of Poland and through settlements along the watershed.

An important step in the implementation of the EU Water Directives - EU Water Framework Directive (2000/60 / EC) and the EU Flood Directives (2007/60 / EC) is the identification of the flood risk areas, and therefore the task of researching the maximum runoff of rivers arises, especially the rare probability of excess.

2. Methodology

Significant scientific achievements in the study of maximum runoff in Ukraine belong to the representatives of the Kyiv Scientific Hydrological School (Prof. A.V. Ogievsky, Prof. Y.A. Zheleznyak, Prof. P.F. Vishnevsky, Prof. V.V. Greben, etc.) and the Odessa Scientific Hydrological School (Prof. A.M. Befani, Prof. N.F. Befani, Prof. O.G. Ivanenko, Prof. Ye.D. Gopchenko, Prof. V.A. Ovcharuk, Prof. Z.R. Shakirzanova).

However, one of the main problems for today is insufficient hydrological study of river basins, in particular, this problem exists in the Vistula River basin within Ukraine, where, as shown in Fig. 2, the number of hydrological posts is insufficient and they are unevenly distributed.

In hydrological calculations apply a large number of methods for determining runoff characteristics in the absence of observational data. These methods are based on the spatial generalization of the parameters of the calculation formulas. The limited time and space of available observations on most data series of river runoff in Ukraine creates statistical instability of parameters, which can be effectively compensated by additional information about the spatial patterns of distribution of the considered characteristics of runoff. A background for the spatial generalization of the characteristics of maximum floods runoff is the study of the influence of zonal and azonal factors on the studied characteristics (Gopchenko at all, 2015).

The purpose of this study is to investigate the effect of different factors on flood runoff layers of different origin (spring floods and rain floods) of the rare probability of excess in the Vistula River basin within Ukraine.

3. Data

Rain floods and spring floods are observed in the territory of the Vistula River basin. These high-water phases of the water regime are different in origin, so it is important to research them separately.

To study the characteristics of the maximum runoff of rain floods and spring floods in the territory of the Vistula basin, long-term observation data for 14 water gauging stations (WGS) were selected for the period from the beginning of observations to 2015. Since the number of hydrological posts in the studied area is rather limited, the data used for generalizations also 5 WGS in the Pripyat River basin, which borders on the studied basin.

4. Results

The first stage of the research was to perform statistical processing of series of data of maximum runoff of rain floods and spring floods. As a result, standard statistical parameters of theoretical distribution curves, as well as rain and spring floods depths of runoff and a rare probability of excess - once every 100 years ($Y_{1\%}$, mm) - are calculated.

The second stage of the study was to determine the effect of zonal and azonal factors on the maximum runoff of rain and spring floods. Initially first investigated the dependence of rain floods depths of runoff and spring flood depths of runoff with a rare probability of excess from ehe center of gravity of the catchment area and it was found to be insignificant. Therefore, the maximum runoff of rain floods and spring floods can be affected by local factors.

The influences of local factors such as forestation and swampness, which are known to significantly affect maximum runoff, have been investigated. In both cases, for rain and spring floods, the effect of forestation on the maximum runoff is insignificant, on the another hand, swampness have significant effect for maximum runoff layers of rain and spring flood a rare probability of excess.

After eliminating the effect of swampness on the maximum runoff of rain floods and spring floods, dependence of maximum depths of runoff with a rare probability of excess of rain floods and spring floods from ehe center of gravity of the catchment area has become significant, what is the theoretical basis for mapping the investigated values.

The spatial distribution of maximum depths of runoff of rain flood and spring flood with a rare probability of excess with the exception of the impact of swampness is shown in (Fig.3) and (Fig. 4).

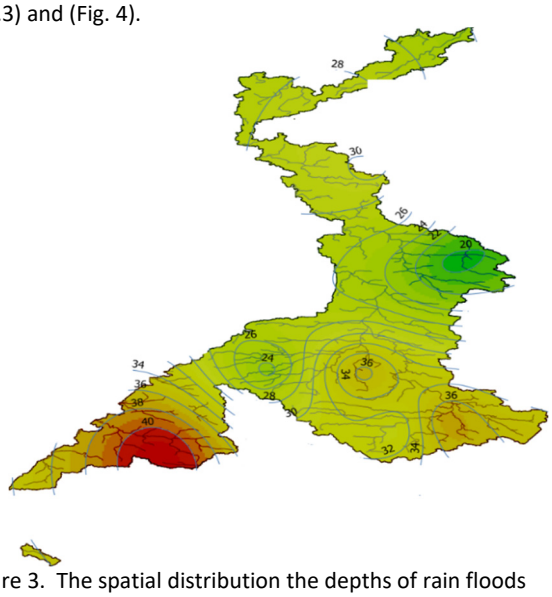


Figure 3. The spatial distribution the depths of rain floods runoff $Y_{1\%}$ (at$f_{swamp} = 0$), mm.

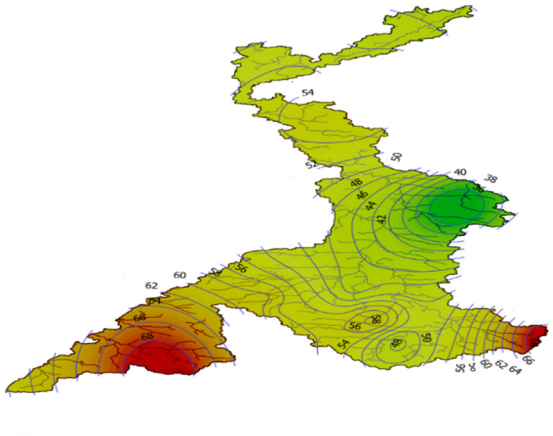


Figure 4. The spatial distribution the depths of spring floods runoff $Y_{1\%}$ (at$f_{swamp} = 0$), mm.

In order to use the maps to determine the maximum depth of runoff of rain and spring floods with the rare probability of excess for any point in the catchment area is to take the values from the map at the desired point using the isolines and then use the formula

$$Y_{1\%} = k_{swamp} Y_{1\%,fswamp=0} \quad (1)$$

Where

For rain floods

$$k_{swamp} = 1 + 0.64\left(lg\left(f_{swamp} + 1\right)\right) \quad (2)$$

For spring floods

$$k_{swamp} = 1 + 1.40\left(lg\left(f_{swamp} + 1\right)\right) \quad (3)$$

f_{swamp} is a relative swampness, %.

5. Conclusions

During performing the study of the influence of zonal and azonal factors on the maximum flood runoff in the Vistula River basin (within Ukraine), the following results were obtained:

- Collection of characteristics of flood runoff in the studied basin;
- Statistical processing of depth runoff of rain floods and spring floods;
- The influence of zonal and azonal factors on the maximum runoff of rain floods and spring floods in the Vistula River basin (within Ukraine) has been determined;
- The spatial distribution maps of runoff depths of rain floods and spring floods with a rare probability of excess, at $\boldsymbol{f_{swamp} = 0}$ was constructed.

References

Gopchenko E.D., Ovcharuk V.A., Romanchuk M.E. A method for calculating characteristics of maximal river runoff in the absence of observational data: Case study of Ukrainian rivers // Water Resources. Pleiades. 2015. Vol. 42. Issue 3. P. 285-291.DOI: 10.1134/S0097807815030057

Khilchevsky V.K., Grebin V.V., Sherstyuk N.P. Modern hydrographic and water management zoning of Ukraine's territory – Implementation of the WFD-2000/60/EC// Electronic book with full papers XXVIII Conference of the Danubian Countries on Hydrological Bases of Water Management. – Kyiv.-2019.- pp.209-223.

Predicting extreme dry spell risk based on probability distribution in coastal region of Tunisia

Majid Mathlouthi[1], Fethi Lebdi [2]

[1]Research Laboratory in Sciences and Technology of Water at INAT, 43 avenue Charles Nicolle, 1082 Tunis; University of Carthage; Tunisia, Majid_Mathlouthi@yahoo.fr
[2]National Agronomic Institute of Tunisia (INAT), 43 avenue Charles Nicolle, 1082 Tunis; University of Carthage; Tunisia, lebdi.fethi@iresa.agrinet.tn

Climate variability and climate change in the longer term consequences of economic, social and environmental. It is likely that climate change increases the frequency and duration of droughts. Event based analysis of dry spell phenomenon, from series of daily rainfall observations was conducted in order to predict extreme dry-spell risk. The case study is a coastal region northern Tunisia of Mediterranean climate. A dry period is defined as a series of days with daily rainfall less than a given threshold. For analysis carried out to provide data for water resources development studies, the rainfall event has been defined even more restrictively by omitting daily rainfall below a certain threshold value. As this limit 3.5 mm j^{-1} has been selected, since this amount of water corresponds approximately to the expected daily evaporation rate, thus marking the lowest physical limit for considering rainfall that may produce utilizable surface water resources. Dry events are considered as a sequence of dry days separated by rainfall events from each other. Thus the rainy season is defined as a series of rainfall and subsequent dry events. Rainfall events are defined as the uninterrupted sequence of rainy days, when at last on one day more than a threshold amount of rainfall has been observed. The evolution of dry events and longest spells in duration and frequency in the region under the influence of a changing climate was studied. The identification of the longest dry and wet events on the history was carried out. For planning purposes, the longest dry spells associated with various statistical recurrence periods are derived on the basis of the fitted GEV type probability distribution functions. Dry spell lengths for return periods of 2, 5, 10, 25 and 50 years indicate the areas where drought phenomena might be more severe, as well as how often they might occur. This analysis is used to calibrate precipitation models with little rainfall records, the study of the effects of climate change on water resources and crops. The results reported here could be applied in estimating climatic drought risks in other geographical areas.

1. Introduction

Dry spell can be defined as a sequence of dry days including days with less than a threshold value of rainfall. A practical procedure to analyze rainfall event time series under semi-arid climatic conditions is the event-based concept. This design of analysis is favored over continuous type data generation method. It is to simulate wet and dry spells separately by fitting their durations to an appropriate probability distribution such as the negative binominal or geometric distribution (Semenov *et al.*, 1998; Mathlouthi & Lebdi, 2008), or empirical distribution (Rajagopalan and Lall, 1999). The characteristics of multi-day wet and dry spells is often important for investigating likely scenarios for agricultural water requirements, reservoir operation for analyses of antecedent moisture conditions (Mathlouthi & Lebdi, 2008), and runoff generation in a watershed. In virtue, this paper is focused on the modelling of rainfall occurrences under climate Mediterranean by wet-dry spell approach for operation dam with basis different from that of observations carried out with regular time's intervals. The event-based concept allow the synthetic rainfall data generation. This used, for example, for reservoir simulation studies, the estimation of irrigation water demand and the study of the effects of a climatologically change. This paper concentrates solely on the characterization of the events of the dry spell in a Dam North of Tunisia.

2. Data and method

The data used in this analysis are the daily precipitation records at coastal region Northern Tunisia. The rainy season starting at September and lasting until the beginning of May. The mean of annual rainfall is 680 mm. Except in occasional wet years, most precipitation is confined to the winter months in this basin. The dry season lasts from May to August. Daily values of precipitation are quite variable.

A rainfall *event* is an uninterrupted sequence of wets periods. The definition of event is associated with a rainfall threshold value which defines *wet*. As this limit 3.5 mm d^{-1} has been selected. This amount of water corresponds to the expected daily evapotranspiration rate, marking the lowest physical limit for considering rainfall that may produce utilizable surface water resources. In this approach, the process of rainfall occurrences is specified by the probability laws of the length of the wet periods (storm duration), and the length of the dry periods (time between storms or inter-event time). The rainfall event *m* in a given rainy season *n* will be characterized by its duration $D_{n,m}$, the temporal position within the rainy season, the dry event or inter-event time $Z_{n,m}$ and by the cumulative rainfall amounts of Hn,m of Dn,m, rainy days in mm:

$$H_{n,m} = \sum_{i=1}^{Dn,m} h_i \qquad (1)$$

Where h_i is positive and represent the daily precipitation totals in mm. Note that for at least one *hi* >3.5 mm.

3. Results and concluding remarks

Independent events are separated by a time period t which follows an exponential distribution (Fogel and Duckstein, 1982):

$$f(t) = b.e^{-bt} \qquad t > 0 \qquad (2)$$

where *b* parameter of the exponential distribution, can be estimated as the reciprocal mean *t* of the sample of times observed:

$$b = \frac{1}{t} \qquad (3)$$

If the waiting time is measured in days, the exponential distribution can be replaced by the equivalent discrete distribution, namely the geometrical distribution:

$$f(n) = p.q^{n-1} \qquad \text{for n = 1, 2, ...} \qquad (4)$$

where the *p* parameter is estimated by the reverse of the expectation of the average duration n of waiting between two successive events.

$$p = \frac{1}{n} \quad ; \qquad \text{and} \quad q=1-p \qquad (5)$$

However, if the series of successive precipitations do not form independent events, the waiting time follows a gamma distribution with two parameters instead of an exponential distribution (Fogel and Duckstein, 1982). Consequently, if the time is discretized in days, the distribution of time separating two events is represented by the negative binomial distribution (Mathlouthi and Lebdi, 2008) which is the equivalent discrete distribution of the gamma distribution:

$$f(n) = \frac{(r + n - 1)}{n!(r - 1)!} . p^r . q^n \qquad (6)$$

where *n* = 0, 1, 2, … , and *r* et *p* are estimated by the variance and mean of the dry event duration.

Approximately 33% of the events last at most one day. The persistence of uninterrupted sequences of rainy days sometimes lasting nearly two weeks (the maximum observed duration is 13 days). However, the frequency of such long-duration events decreases rapidly with increasing duration. An arithmetic mean of 2.79 days and a standard deviation of 1.87 were obtained. The geometric pdf appears most adequate for the fitting.

The regression analysis display that the dry event can be assumed to be independent from the rainfall event and the rainfall depth per event. Thus the distribution of the dry event (interevent time), which can only assume integer values, follows an unconditional probability distribution function. The negative binomial pdf has been found as best fitted to describe the distribution of the dry event (Fig. 1). The shortest interruption (one day) is the most frequent one. Almost a fifth of the observed dry events are only one day long. Dry periods up to 30 or even more days may be recorded (a 56 days maximum is recorded). The arithmetic mean and the standard deviation for the dry event are respectively 7.3 days and 7.9; for the longest dry event there are 30.2 days and 3.6.

Figure 2 shows the best fitting of the beginning of the first rainfall event during rainy season. It was concluded that the first rainfall event occurs in the mid-September, whereas the probability of surpassing this value is 0.52 (a biennial return period). For extreme case, the hydrological year starts about the first decade of October.

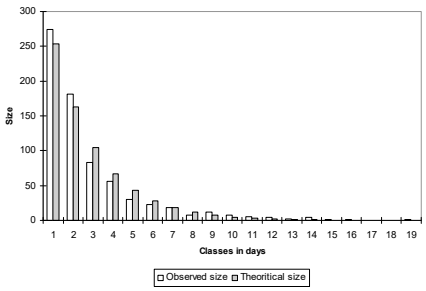


Figure 1. Distribution of the time elapsed between rainfall events (dry events).

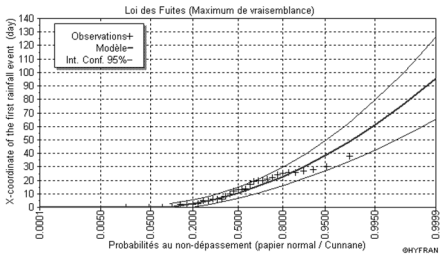


Figure 2. Fitting leaks law for the chronological position of the first rainfall event in rainy season.

The case study confirms the concept of the independence of rainfall and dry event duration. The dry spell phenomenon in this region seems to be particularly well described by fitting a pdf to the length of the interevent time. The negative binomial pdf provides an excellent fit for the prolonged dry periods between subsequent rainfall events. Conceptually, in a true Poisson process, the time "without event" should follow the exponential pdf or, in a discrete case, the geometric pdf (Fogel and Duckstein, 1982). It is relevant to note that this "flaw" could be eliminated by defining the interevent time as the dry event. Consequently, the present role of the interevent time would be taken over by the rainfall events duration. The theoretical requirements of the fitted geometric pdf are satisfied.

Event-based analysis has been used to generate synthetic rainfall event time series. By coupling this with a rainfall-runoff model, one obtains synthetic streamflow series to be used for reservoir simulation studies and design flood estimations. As another application, the study of the effects of a climatologically change.

References

Fogel MM, and Duckstein L, (1982): Stochastic precipitation modelling for evaluating non-point source pollution in statistical analysis of rainfall and runoff. Proceeding of the international symposium on rainfall-runoff modelling, 1981: in Statistical Analysis of rainfall and runoff, Water Resources Publications. Littleton, Colo., USA, pp. 119-136.

Mathlouthi, M. & Lebdi, F. (2008) Event in the case of a single reservoir: the Ghèzala dam in Northern Tunisia. Stochastic Environ. Res. and Risk Assessment 22, 513–528.

Rajagopalan, B. & Lall, U. (1999) A k-nearest-neighbor simulator for daily precipitation and other weather variables. Water Resour. Res. 35, 3089-3101.

Semenov, M. A.; Brooks, R. J., Barrow, E. M. & Richardson, C. W. (1998) Comparison of WGEN and LARS-WG stochastic weather generators for diverse climates. Clim. Res. 10, 95-107.

The assessment of natural hazards as a part of integrated coastal zone management: the case of Haapsalu Bay, Estonia

Valeriya Ovcharuk[1], Maryna Moniushko[1] and Suvendu DaS[2]

[1] Odessa State Environmental University, Ukraine (valeriya.ovcharuk@gmail.com)

[2]Visva Bharati University, Santiniketan, India

1. Introduction

Haapsalu is a seaside resort town located on the west coast of Estonia. It is the administrative centre of Lääne County with area 1,816 km² and density population 11.29 Inhabitants/km². Haapsalu Bay (Fig.1) are situated in the Väinameri area — a low-water region between continental Estonia and its western islands. The surface areas of Haapsalu Bay is only 50 km² and it value are gradually decreasing owing to landlift and riverine sediment discharge Kotta J.at all (2008). The bay is relatively shallow, with a maximum depth of less than 5 m and an average depth of 1.5–2 m (Lutt and Kask 1980).

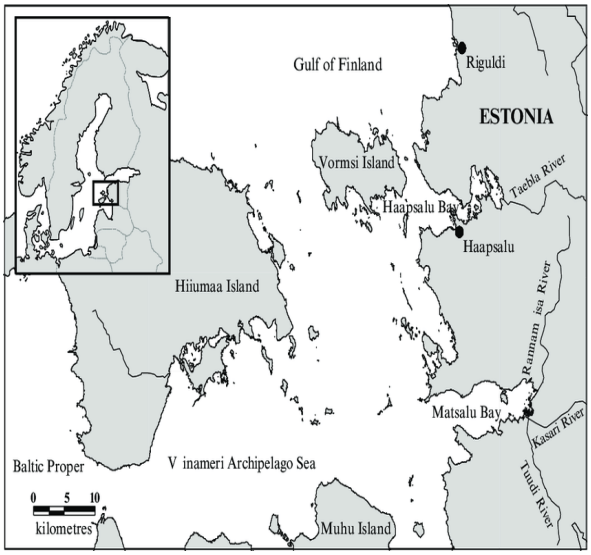


Figure 1. The location map of Haapsalu Bay, Kotta J.at all (2008).

In 1995 World Bank was financed Estonia - Haapsalu and Matsalu Bays Environment Project, which had the aim of implementation over four years an environmental management project for the coastal area of western Estonia. It includes Water and Wastewater Improvement Component (WWIC) and an Environmental Management Component (EMC) The WWIC consists of: a) rehabilitation and expansion of the Haapsalu water and wastewater system, including equipment and works along with engineering services; and b) institutional strengthening and training to assist in establishing an autonomous and financially independent water and wastewater utility in Haapsalu. The EMC consists of: a) technical and financial support through the Ministry of Environment (MOE) for the implementation of selected elements of the Management Plan for Matsalu State Nature Reserve by coordinating and providing funding for identified investments such as access roads, observation towers, and information boards; b) design and implementation of a program of cost-effective activities to reduce point and non-point source pollution of Matsalu Bay from small settlements and agriculture; and c) support for planning and management of eco-tourism. But nowadays, in period of climate change, we need also include estimate influence of natural hazard in the integrated coastal management plan.

2. Problem status

One of the most important principles of integrated coastal zone management is the consideration of the coastal zone as a single natural, economic and social system, thus, the methodology is based on multidisciplinary approach, which considers all processes in their relationship. Therefore, a specialist in the field of coastal management should not only possess sufficient knowledge to understand various processes at the disciplinary level, but also be able to generalize multidisciplinary knowledge within the framework of a single methodology.

On a way to sustainable development of the coastal zone, there is a need to solve a number of problems that can be divided into the scales necessary to solve them (Tabl.1).

Table.1- The significance of the challenges on a way to sustainable development of the coastal zone

Problem scale	
Global	1. The need for rational use or management of coastal resources. Resources are divided into non-renewable and renewable 2. Introduction of alternative energy sources (tides, thermal power plants, wind, waves, etc.), for which the conditions of the coastal zone are most promising for use 3. Global warming problem.
Regional	1. The possibility of conflict between various users during the development of coastal, and in some cases marine activities 2. Erosion of beaches and other types of coasts 3. The necessity to finding a balance between economic development and conservation environmental status, for example, by creating protected areas to conservation biological and landscape diversity
Local	1. The problems of urban development of coastal cities 2. The problem of restoration of territories

The concept of integrated coastal zone management reflects the complexity of modern society and includes scientific, technical, economic, legal and administrative activities, and its task is to: assess coastal resources and the relevant needs of society; determining the technical and economic balance between resources and needs; effective conservation or protection and sustainable development of water and coastal resources; institutional coordination. Modern society is particularly complex, and the need to take into account economic and legal aspects, as well as scientific and technical problems, has led to the concept of integrated use of water and recreational resources of the coastal zone.

Table 2 presents the main areas and activities for integrated coastal zone management.

Table 2. Main directions and activities in the field of integrated coastal zone management

Direction of activity	
Hydrology and coastal resources	1. Monitoring and forecasting the state of coastal and shelf zones; 2. Expert service of planning, designing, building, operation of coastal construction 3. Coastal zone management, including crisis management of anthropogenic and natural nature.
Database management	1. Receiving and distribution data and information: formation of geoinformation system (assessment of operational situation and archival data). Obtaining high-resolution satellite information 2. The use of modern mathematical and physical-statistical modeling software for predicting the development of hydrological processes.
Environmental quality management	1. Assessment of water quality by hydrochemical parameters (operational assessment of the assimilation capacity of the water area) 2. The ecosystem of coastal waters in the conditions of anthropogenic influence
Socio-economic aspects and law	1. National and international maritime law in the field of exploitation of the environment; 2. Management of the use of natural coastal resources with maximum socio-economic benefits.

3. Results

For the Haapsalu Bay coastal zone, a spatial compatibility matrix of different types of marine uses is compiled.

Table 3. Assessment of the spatial compatibility of different types of marine uses

		Offshore wind farms	Marine Protected Areas	Fishing	Sea, as the welfare of the people	Cables	Tourism	shipping	Harbors and ports	Agriculture/effluent	Sand mining	Oil and gas searches	Dumping	Mariculture	Coastal Service Centers	Protection of Nature	Coastal protection	Military use
		1	2	3	4	5	6	7	8	9	10	11	12	13	14	15	16	17
Offshore wind farms	1																	
Marine Protected Areas	2																	
Fishing	3																	
Sea, as the welfare of the people	4																	
Cables	5																	
Tourism	6																	
Shipping	7																	
Harbors and ports	8																	
Agriculture/effluent	9																	
Sand mining	10																	
Dumping	12																	
Mariculture	13																	
Coastal Service Centers	14																	
Protection of Nature	15																	
Coastal protection	16																	
Military use	17																	

non compatible
conditionally compatible
compatible

In some areas, spatial incompatibility is shown, that is, a situation where different types of uses cannot exist in one space. For example, from a safety point of view, wind farms on the open seas are incompatible with shipping lines; designated areas for fish spawning are incompatible with the extraction of sand and gravel. On the other hand, wind farms in the open sea are spatially compatible with some types of mariculture, since such uses do not interfere with each other. The spatial incompatibilities that grow with the Earth-Sea interaction are also shown, since, for example, coastal tourism, should have an unobstructed view of the horizon for aesthetic purposes.

Table 3 shows the standard marine uses in the coastal zone that are taken into account when developing management plans, but natural hazards and disasters can adversely affect all activities and must be taken into account now in time of climate change.

For Haapsalu area coastal zone the most probabilistic natural hazards are:

- Extreme sea level due to strong storm;
- Coastal erosion;
- Rising surface land.

The greatest potential damage to the economy and the population can be caused by extreme sea level rise during storms, as happened in 1967 and 2005 Wolski et al. (2014).

Two other potential risks should also be taken into account, but their possible impact is much smaller and not catastrophic.

Consider, for example, the storm event of 8–9 January 2005. Flooding in 2005 was resulted from the strongest in the last hundred years of wind and storm flooded most of Pärnu and Haapsalu. The storm in England and the Baltic Sea countries gave rise to unusually high temperatures in the Atlantic Ocean. West and north-west wind had reaching in some places 25-32 m/s Post et al. (2014). Rescuers evacuated people from small islands, many trees were felled, thousands of families were left without electricity. 14 people needed medical help, 13 of them suffered from hypothermia. Damage reached hundreds of millions of crowns.

According to Estonian climatologist Andres Tarand, the August storm of 1967, this caused massive destruction, until 2005 was considered the strongest. In 2005, a feature of the storm was a strong rise in water, due to which more coastal zones were flooded. The case was aggravated by the openness of the Pärnu and Haapsalu bays. The most powerful cyclones come in to Baltic region from the southwest. In recent time the number of storms in winter at the study area has increased, the same as Western Europe due to the climate change.

Unlike their Danish, German and Finnish counterparts, Estonian meteorologists did not translate a storm warning in January 2005. If people received more timely information, they could acquire at least sandbags to protect their property. However, according to crisis manager Kalev Timberg, the storm forecast arrived on time at the rescue department, where they immediately began to prepare for the storm. "I have no complaints about weather forecasters, but perhaps more could be reported to the press about this. "

The above example shows that taking into account natural hazards during a period of climate change should become an important part of integrated coastal management.

Conclusion and proposal

The greatest natural risk for Haapsalu territory is the risk of flooding, therefore necessary:

- Creating an efficient public warning system about severe storms.
- This is especially necessary in areas where the population density is very low and people often live far away from each other and from the media.
- All separately living residents must be entered in the register for will be to warn them of an impending storm.

References

Lutt J, Kask J (1980) Matsalu lahe põhjasetted. In: Mägi E (ed) Loodusvaatlusi 1978, vol 1. Valgus, Tallinn, pp 166–178

Kotta J., Jaanus A., Kotta I. (2008) Haapsalu and Matsalu Bays. In: Schiewer U. (eds) Ecology of Baltic Coastal Waters. Ecological Studies (Analysis and Synthesis), vol 197. Springer, Berlin, Heidelberg

Piia Post, Tarmo Kouts. Characteristics of cyclones causing extreme sea levels in the northern Baltic Sea. doi:10.5697/oc.56-2.241 OCEANOLOGIA, 56 (2), 2014. pp. 241–258.

T. Wolski, B. Wiśniewski, A. Giza et al. Extreme sea levels at stations on the Baltic Sea coast. doi:10.5697/oc.56-2.259 OCEANOLOGIA, 56 (2), 2014. pp. 259–290.

Maximal rivers runoff during floods different origin on the coastal zone of Northwestern part of the Black Sea

Valeriya Ovcharuk, Maryna Moniushko, Eugeny Gopchenko, Nataliya Kichuk

Odessa State Environmental University, Ukraine (valeriya.ovcharuk@gmail.com)

1. Introduction

Nowadays, the Black Sea is one of the most studied marine basins of all existing on our planet. At the same time, certain processes require refinement and additional studies, such as the influx of fresh water into it from rivers during climate change. The interest in the Black Sea is caused not only by the special strategic location of the sea itself and the richness of the nature of its basin, but also by its great international economic importance. The economic role of the Black Sea has especially grown in recent years, when, after the collapse of the Soviet Union, six Black Sea states (Bulgaria, Georgia, Russia, Romania, Turkey, and Ukraine) actually re-establish their interests in the sea.

The total number of rivers flowing into the Black Sea is about 1,000 and they are very different from each other in terms of water content and the size of the basins. The most of them are small rivers and only about 500 of them are more than 10 km long. Many temporary waterways also flow into the sea. To the category of large (with a catchment area of more than 10,000 km^2) includes only 10 rivers and 4 of them flow into the sea from the territory of Ukraine.

The Ukrainian or Northwestern part of the Black Sea basin is characterized by an almost ubiquitous articulation of accumulative forms. The abrasion sections of the region make up about 30% of the coastal length, and the accumulative ones - 36%. All rivers and relatively large temporary streams of this huge region (from the Danube to the Southern Crimea) flow into the estuaries, which are formed during the flooding of the lower reaches of the beams and river valleys.

2. Problem status

The rivers of the Black Sea basin are not studied to the same degree. Long-term hydrometric observations are available for most of the rivers of the former socialist camp, but only sporadic data exist on the rivers of the Anatolian coast, and stationary observations on some large rivers have been started only in recent years.

Within Ukraine, four large rivers flow into coastal estuaries: the Dniester, Southern Bug, Ingul and Dnieper. The flow of these rivers is regulated by many reservoirs, and they are under a strong anthropogenic pressure. These rivers annually deliver 55.5 km^3 of water to coastal estuaries. In addition to large rivers, in the northwestern part of the Black Sea several small rivers flow into the coastal salt lakes (Tiligul and others), but their flow volume is so insignificant that they do not affect the sea regime. The flow of small rivers of Crimea is regulated to a large extent, is used for household needs and the total amount of their annual flow is less than 0.3 km^3.

By country and region, the inflow in Black Sea is distributed as follows: from the territory of Russia to the Black Sea influx annually 6.5 km^3 of river water (1.9%), Georgia - 46.0 km^3 (13.2%), Turkey - 38.0 km^3 (10.9%) and Bulgaria 1.8 km^3 (0.52%). The Danube brings 200 km^3 of water into the sea (57.5%). Within Ukraine, large rivers in the sea deliver 55.5 km^3 of water (15.9%) and the rivers of Crimea - 0.3 km^3 (0.08%).

Thus, it is of interest to assess changes in the surface inflow of fresh water into the Black Sea at the present stage and a forecast it for the future, taking into account possible climate changes. The largest runoff on large miss medium rivers of the study area is observed during the spring flood, and for small rivers, separate summer floods are possible when the runoff is even higher than the spring one. A stationary network of hydrological posts does not completely cover the territory, and therefore, techniques are needed to evaluate the flow for ungauged rivers.

3. Results

The author proposed a new modified version of the operator model for determining the maximum runoff of spring flood, which allows taking into account the possible impact of climate change on the estimated values of the maximum modules 1% probability of exceeding. Climate change is taken into account by introducing a separate coefficient, based on a comparison of the main parameters of the method obtained on the basis of current data (maximum snow supply at the beginning of the spring flood, precipitation during the spring flood and runoff coefficients), and similar values obtained from climatic modeling data.

For the plain rivers of Ukraine the author's modified version of the calculating method (Gopchenko ,2015; Ovcharuk,2018) for determining the characteristics of spring flood in climate change conditions has implement. The implementation of the proposed calculation option using different models and scenarios has shown that the results differ significantly, but in practically all cases up to 2050 It is forecasted a significant decrease in the runoff of spring flood (from 10-20% in the north of the studied territory and 40-50% in the south).

On another hand, on regulatory documents forming storm floods associated with maximum values of precipitation per day. Maximum daily rainfall and runoff layers 1% probability of exeedance obtained by applying the method recurrence of extrema and refined through method of collective analysis As a result for the small rivers of the Black Sea basin it is recommended to accept maximum daily rainfall as P1%= 95mm.

References

Gopchenko E.D., Ovcharuk V.A., Romanchuk M.E. A method for calculating characteristics of maximal river runoff in the absence of observational data: Case study of Ukrainian rivers // Water Resources. Pleiades. 2015. Vol. 42. Issue 3. P. 285-291.DOI: 10.1134/S0097807815030057

Ovcharuk, V.A., Hopchenko, Y.D. The modern method of maximum spring flood runoff characteristics valuation for the plain rivers of Ukraine. doi.org/10.15407/ugz2018.02.026 Ukr. geogr. z. 2018, N2:26-33.

Radar-derived convective storms' climatology over Estonia during the warm season

Piia Post[1], Tanel Voormansik[1,2] and Tuule Müürsepp[1]

[1] Institute of Physics, University of Tartu, Tartu, Estonia (piia.post@ut.ee)
[2] Estonian Weather Service, Estonian Environment Agency, Tallinn, Estonia

1. Introduction

Strong convective storms may bring along hazards as hail or wind damage by strong small-scale downbursts or tornadoes, as well as flash floods. Damages by all these dangerous phenomena are actual also in Estonia.

The development of convective storms is forced by various synoptic, regional- and local-scale processes. The local atmospheric preconditions are well-known. Generally, the air-mass is expected to be conditionally unstable with a deep moist layer in the lower atmosphere. Then a source of lift is needed to initiate the convection which is mainly done by mesoscale processes. It may be just solar radiation that brings along nonuniform heating over the surface, but also convergence of air masses by fronts or lifting due to topography. Estonia has no high mountains, but the hilly parts of the country are expected to have higher probability for air uplifts, at least the European climatology of thunderstorm days confirms this hypothesis (Enno et al., 2020). Here the synoptic scale processes set a favorable condition for convection.

The general distribution of thunderstorms in various parts in Europe is known (Wapler 2013; Enno et al., 2020). Several analyses of the occurrence of convective storms dependence on favorable atmospheric parameters or convective indices are carried out (Brooks et al., 2003, Kaltenböck et al, 2009). But the roles of different scale atmospheric conditions are important to predict such events better and to produce nowcasting and forecasting systems. The main aim of the work is to give a better understanding about the spatial and temporal distribution of convective storms over Estonia depending on various scale processes.

2. Data and methods

A seven years long (2010-2016) timeseries of Estonian polarimetric weather radar data gives an opportunity to investigate the spatial distribution and the extent of severe storms. Weather radars give the best spatial and temporal resolution (1 km, 15 min) available in higher mid-latitudes for these purposes. More detailed information about conditions in the atmosphere is obtained from model data. Lightning detection Network data are used for evaluation of storms territorial distributions.

Data from warm season, five months from May to September are used. This the time when more than 99% of convective storms take place (Enno et al., 2014). Limiting the dataset to this period also helps to ensure that radar reflectivities are only from liquid precipitation. Only the data from Estonian Weather Service operated Sürgavere dual-polarization Doppler C-band radar located in central Estonia in Viljandi county were used.

The method bases on identifying convective storms from the lowest radar scan of 0.5 degrees (Kaltenboeck and Steinheimer, 2015). Storm cells were distinguished from the radar data by using a 35 dBZ reflectivity threshold. The 35 dBZ threshold enables the radar-observed lifecycle of entire storm systems to be captured, such as multicellular storms or intense mesoscale convective systems (Voormansik et al., 2017). To find the storm cells from reflectivity data computer vision algorithms from OpenCV freeware were applied.

In order to analyze and classify the storms a number of descriptive parameters were derived for each identified cell: coordinates, area, mean and maximum reflectivity. To eliminate clutter, cells with a smaller area than 5 km^2 were omitted from further analysis.

Territorial distributions of storms were filtered using indices calculated from ERA Interim and ERA5 reanalysis data to evaluate the reliability of them. Several thresholds for Convective Available Potential Energy (CAPE) index and for the wind shear between the 10 m and 500 hPa level were used for that purpose (Kaltenboeck ja Steinheimer, 2015). Circulation types and prevailing air flow directions were calculated from reanalysis to assess the climatological representativity of this 10-year period.

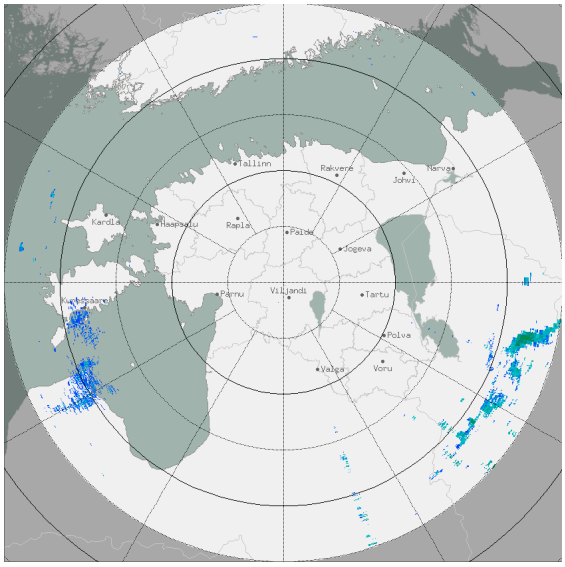


Figure 1. Location of Sürgavere radar (in the middle of the graph) and its 250 km working radius. Circles are with radiuses of 50 km.

The method bases on identifying convective storms from the lowest radar scan of 0.5 degrees (Kaltenboeck and Steinheimer, 2015). Storm cells were distinguished from the radar data by using a 35 dBZ reflectivity threshold. The 35 dBZ threshold enables the radar-observed lifecycle of entire storm systems to be captured, such as multicellular storms or intense mesoscale convective systems (Voormansik et al., 2017). To find the storm cells from reflectivity data computer vision algorithms from OpenCV freeware were applied.

In order to analyze and classify the storms a number of descriptive parameters were derived for each identified

cell: coordinates, area, mean and maximum reflectivity. To eliminate clutter, cells with a smaller area than 5 km^2 were omitted from further analysis.

Territorial distributions of storms were filtered using indices calculated from ERA Interim (Dee et al., 2011) reanalysis data to evaluate the reliability of them. Several thresholds for Convective Available Potential Energy (CAPE) index and for the wind shear between the 10 m and 500 hPa level were used for that purpose (Kaltenboeck ja Steinheimer, 2015). Circulation types and prevailing air flow directions were calculated from reanalysis to assess the climatological representativity of this 10-year period.

3. Results

The overall numbers of storm cells vary from year to year starting with 72299 in 2011 up to 133004 cells in 2013. These numbers differ about two times. The high number of cells is characteristic to the warm summers.

Validation of the method for detecting the convective storm cells is limited as there exist no appropriate observational data of convective storms or phenomena associated with them for this time period. One possibility is to use data from lightning detectors, but it should be kept in mind, that more than half of cloud-to-ground flashes could belong to only one day with a very strong frontal thunder passage. This is valid for 2011, the year with the highest number of flashes, but with smallest number of convective cells by our method. Therefore, we compare the numbers of thunder days and convective storm days during different years in Table 1.

Table 1. Numbers of storm days and thunder days in case of varying Convective Available Potential Energy (CAPE) in J/kg.

year	Number of storm days			Number of thunder days		
	all	CAPE > 100	CAPE > 250	all	CAPE > 100	CAPE > 250
2010	132	49	29	93	45	28
2011	116	39	23	73	26	18
2012	112	36	11	81	31	10
2013	132	38	19	92	37	19
2014	120	44	23	81	35	19
2015	124	27	10	68	23	10
2016	98	22	12	69	28	13
Sum	834	255	127	557	225	117

The numbers of storm days and thunder days correlate well, especially when the days are filtered with CAPE index. The largest number of storm days is in 2010. The 35 dBZ threshold may be too low for strong convection clouds but using even low CAPE values for filtering makes the counts of days comparable.

The prevailing air flow direction in case of our storm days is south and southwest, the higher is the CAPE, the larger percent of flows is from south. The smallest number of storms happen in case of north eastern and north western flows.

Our study is the first attempt to reveal more detailed spatial-temporal distribution of convective storms depending on atmospheric conditions in Estonia and wider Baltic Sea region.

References

Brooks, H. E., Lee, J. W., Jeffrey P Craven, J. P. (2003) The spatial distribution of severe thunderstorm and tornado environments from global reanalysis data, Atmospheric Research, Vol. 67–68, pp. 73-94.

Dee, D.P., et al. (2011) The ERA-Interim reanalysis: configuration and performance of the data assimilation system. Q.J.R. Meteorol. Soc., Vol. 137, pp. 553-597.

Enno, S.-E., Post, P., Briede, A., Stankunaitė, I. (2014) Long-term changes in the frequency of thunder days in the Baltic countries. Boreal Environment Research, Vol. 19, pp. 452–466.

Enno, S.E., Sugier, J., Alber, R. and Seltzer, M. (2020) Lightning flash density in Europe based on 10 years of ATDnet data. Atmospheric Research, Vol. 235, p. 104769.

Kaltenböck, R., Diendorfer, G., & Dotzek, N. (2009) Evaluation of thunderstorm indices from ECMWF analyses, lightning data and severe storm reports. Atmospheric Research, Vol 93, No.1-3, pp. 381-396.

Kaltenboeck, R. and Steinheimer, M. (2015) Radar-based severe storm climatology for Austrian complex orography related to vertical wind shear and atmospheric instability. Atmospheric Research, Vol. 158, pp. 216-230.

Voormansik, T., Rossi, P.J., Moisseev, D., Tanilsoo, T. and Post, P., (2017) Thunderstorm hail and lightning detection parameters based on dual-polarization Doppler weather radar data. Meteorological Applications, Vol. 24, No. 3, pp. 521-530.

Wapler, K. (2013) High-resolution climatology of lightning characteristics within Central Europe. Meteorology and Atmospheric Physics, Vol. 122, No. 3-4, pp.175-184.

Definition of droughts and their recurrence in Lithuania

Egidijus Rimkus, Edvinas Stonevičius, Donatas Valiukas, and Viktorija Mačiulytė

Institute of Geosciences, Vilnius University, Vilnius, Lithuania (egidijus.rimkus@gf.vu.lt)

1. Introduction

Drought is one of the most dangerous natural phenomenon in terms of frequency, extent and magnitude of impact. Droughts has a significant impact on various areas: agriculture (Li et al., 2009), natural vegetation (Vicente-Serrano et al., 2010), water resources (Bond et al., 2008), hydropower (Naumann et al., 2015).), forest fires and etc.

The Intergovernmental Panel on Climate Change stated that there is not enough evidences to prove that the number and intensity of droughts increased statistically significant on a global scale (IPCC, 2014). This is partly due to differences in the definition of drought and criteria for its identification in different countries. However, the number and intensity of droughts has changed in some regions.

It is very likely that the inequality of the distribution of precipitation in Lithuania will increase in the future. Especially in the warm period of year. Although the annual precipitation amount is expected to increase in the 21st century in Lithuania, in the second half of summer and early autumn the precipitation will not change or may even decrease (Keršytė et al., 2015). Meanwhile, the air temperature will increase dramatically. As a result, number and intensity of droughts during the period between July and September may increase in the future.

It should also be noted that as winter temperature will rise in the future, the number of days with snow cover and snow depth will decrease. Such trends have been already observed in the recent decades (Rimkus et al., 2018). In addition, the duration and thickness of the frost layer will also decrease, making it easier for groundwater to transform into river runoff during the winter. Thus, the soil moisture reserves formed by snow-melting water will be lower in spring. Therefore, a much shorter period may be needed for the soil to dry. In conclusion, the risk of drought will increase both in spring and in the second half of summer.

The aim of this study is to propose the most appropriate definition of drought in Lithuania and to evaluate the number of droughts in 1961-2019.

2. Data and methods

Data from 18 Lithuanian meteorological stations were used in this study. The investigation covered period from 1961 till 2019. The following meteorological indicators were used for drought assessment:

- Average, minimum and maximum daily air temperature (° C);
- Daily precipitation amount (mm).

Present study also examined soil water content (mm) in three meteorological stations during the period from 1970 to 1999. Soil water content was measured every 10 days in April - October by gravimetric method (up to 1 meter depth).

3. Definition of agrometeorological droughts in Lithuania

The most accurate way to identify agro-meteorological drought is through direct monitoring of vegetation status but this type of assessment can be done only locally due to the high demand for human resources. Satellite information does not always succeed in associating vegetation anomalies with drought. In addition, although satellite information has a high spatial coverage and a quite good resolution, accurate qualitative evaluation is complicated due to changes in management of agricultural crops.

Another accurate way to evaluate agricultural drought is through direct measurements of soil moisture. However, in this case, the wetting moisture depends on the agricultural crops grown in the field and the same moisture deficit can affect only certain crops. In addition, the ability of the plant root system to absorb water also depends on the type of soil, i.e. the same absolute water content in different soils can lead to unequal effects on agricultural crops. Currently, the possibilities to use soil moisture data for drought identification are very limited in Lithuania.

Selianinov Hydrothermal Coefficient (HTK) is currently used to identify droughts in Lithuania:

$$HTK = \frac{P}{0{,}1\sum t_{10}}$$

where P is the sum of the precipitation (mm) and Σt_{10} is the sum of the average daily temperature over the calculation period (when the daily mean air temperature is above 10 °C). Drought is recorded during the active vegetation period when the HTK is > 0.5 for 30 consecutive days. However, the HTK index has a number of shortcomings. First of all, it cannot determine spring droughts and, in the case of late start of vegetation, the drought can be identified only on the second half of summer. Meanwhile, dry conditions at the beginning of the vegetation period have been increasingly recorded in recent years. In addition, short-term heavy rainfall events may cause a temporary increase of the HTK index value over 0.5, which means that drought will not be recorded nevertheless the drought continues.

In 2009, the World Meteorological Organization recommended that national meteorological services around the world should use the SPI (Standardized Precipitation Index) as a universal meteorological drought indicator (World Meteorological Organization, 2012). Estimation of SPI requires a long homogeneous data series and is suitable only for evaluation of precipitation anomalies. However, it cannot be calculated immediately at the new measuring point and the SPI does not reflect absolute soil water content. While the index is standardized the probability of drought formation will not change even due to changing climate conditions. SPI also can be characterized by a high degree of the index values uncertainty when the theoretical distribution is fitted to empirical data.

Under Lithuanian conditions, smaller soil water content values occurs mostly due to precipitation deficit, but during the spring and early summer (April-June) air temperature (and consequently evaporation) also plays very important role in drought formation (Fig. 1).

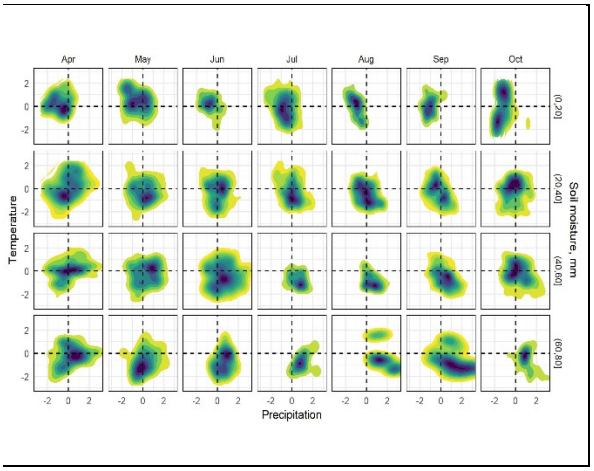


Figure 1. Distribution of standardized 30 days precipitation and air temperature values corresponding to different moisture levels in the top soil layer (0-20 cm). Darker colours represent a greater reoccurrence of meteorological conditions.

Therefore, it is more appropriate to use non-standardized indices for identification of agricultural droughts, which may be related to the amount of soil water. Soil water amount depends on precipitation and air temperature, so it is useful to use an index that combines these meteorological indicators.

We suggested to use the Temperature-Precipitation Index (TPI):

$$TPI = \frac{P}{T} \times 100,$$

where P is the 30-day precipitation amount (mm); T is the sum of the average daily air temperature for the same 30 days period. Drought should be recorded when the TPI index is calculated for the 30-days period with an average air temperature above 5 ° C and a 30 days TPI index average value is lower than 3.0 (or 3.5). Drought is a long-term phenomenon, so drought conditions must persist for some time to make impact. In aridic climates zones droughts can last up to several years, so integration periods of several or even more than ten months are used. Due to the more dynamic changes in drought conditions in Lithuania, it is reasonable to apply a relatively short 30 days integration period.

4. Drought recurrence and trends

According to TPI <3.5, the number of droughts in the territory of Lithuania varied from four to thirteen (Fig. 2A), and according to TPI <3.0 from two to ten (Fig. 2B) in 1961-2019. On average the drought in meteorological station was recorded once per six year according to TPI<3.5 and once per eight years according to TPI<3.0. Analysis of the spatial distribution of droughts during the investigation period shows, that there are considerable territorial differences in Lithuania: droughts are less frequently recorded in southeastern, eastern parts, but more often in western and central parts of the country.

The largest number of droughts was recorded at the last decade of the 20th century and at the first decade of the 21st century (Fig. 3). Only during this period (six times) and in 2019, two-thirds of the country's territory was affected. The droughts of 1994 and 2000 affected almost the entire territory of the Lithuania.

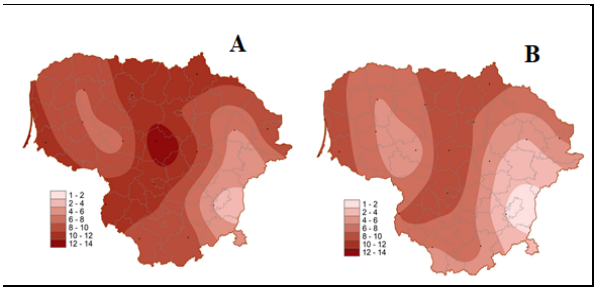


Figure 2. Recurrence of droughts in the territory of Lithuania in 1961-2019: TPI <3.5 (A) and TPI <3.0 (B).

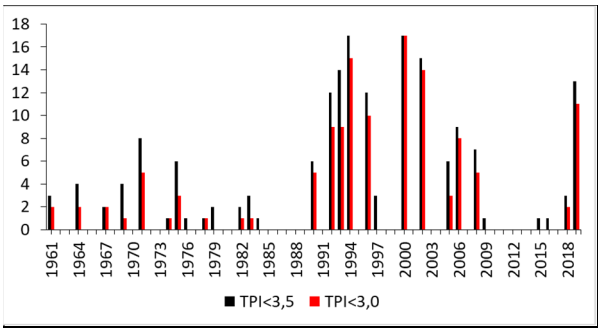


Figure 1. Annual number of meteorological station in Lithuania where droughts were recorded according to TPI <3.5 and TPI <3.0 in 1961-2019.

According to TPI <3.5, droughts at least in one station were recorded in 57% years, and according to TPI <3.0 in 43% years. In both cases there is a positive tendency in reoccurrence of droughts, however according to the Mann-Kendal test the changes are not statistically significant.

References

Bond N. R., Lake P. S., Arthington A. H. (2008). The impacts of drought on freshwater ecosystems: an Australian perspective, Hydrobiologia, Vol. 600, pp. 3-16.

IPCC (2014). Climate Change 2014: Synthesis Report. Contribution of Working Groups I, II and III to the Fifth Assessment Report of the Intergovernmental Panel on Climate Change. Core Writing Team, R.K. Pachauri and L.A. Meyer (eds.). IPCC, Geneva, Switzerland.

Keršytė D., Rimkus E., Kažys, J. 2015. Near-term and long-term climate projections for Lithuania. Geologija. Geografija, Vol. 1, No.1, pp. 22–35 [in Lithuanian].

Li Y., Ye W., Wang M., Yan X. (2009). Climate change and drought: a risk assessment of crop-yield impacts, *Clim. Res.,* Vol. 39, No. 1, pp. 31-46.

Naumann G., Spinoni J., Vogt J.V., Barbosa P. (2015). Assessment of drought damages and their uncertainties in Europe. Environ. Res. Lett., Vol. 10, 124013.

Rimkus E., Briede A., Jaagus J., Stonevicius E., Kilpys J. Viru B. 2018. Snow-cover regime in Lithuania, Latvia and Estonia and its relationship to climatic and geographical factors in 1961–2015. *Boreal Env. Res.* Vol. 23, pp. 193–208.

Vicente-Serrano S. M., Beguería S., López-Moreno J. I. (2010). A multiscalar drought index sensitive to global warming: the standardized precipitation evapotranspiration index. J. Clim., Vol. 23, No.7, pp. 1696-1718.

World Meteorological Organization (2012). *Standardized Precipitation Index User Guide.* (M. Svoboda, M. Hayes and D. Wood). WMO-No. 1090, Geneva.

Projected distribution of the drought in Ukraine until 2050 under RCP4.5 and RCP6.0 climate scenarios

Inna Semenova, Anatoly Polevoy

Odessa State Environmental University, Ukraine (innas.od@gmail.com)

1. Introduction

Drought is a natural phenomenon that occurs in all climates, and is one of the most relevant natural hazards, which propagates through the full hydrological cycle and affects large areas, often with long-term economic and environmental impacts. There is no single definition of drought, and meteorological, agricultural, hydrological, groundwater, and socioeconomic droughts are often distinguished. A prolonged deficit in precipitation over a defined region cause a meteorological drought, while the other types of drought describe secondary effects on specific ecological and economic compartments.

Recent trends in the drought distribution and intensity during 1950-2012 shows that Europe splits into two big areas, in which the southern and western regions have positive trends of drought frequency, duration, and severity, and the northern and eastern regions show a decrease in this parameters (Spinoni et al., 2016). Regarding the long events, territory of Ukraine belongs to the areas in which a prominent decrease in drought frequency, duration and severity are fixed. But positive trends in the drought characteristics are observed on the Black Sea coast, also in the Carpathian region, many droughts occurred in the past three decades. According Caloiero et al. (2018) in the most regions of continental Europe and the Mediterranean basin in the twenty-first century, three main drought events have been detected in 2003, 2011, and 2014.

The spatiotemporal distribution of droughts depends on the temperature and moisture regime of a particular area. Studies of predicted changes in temperature and precipitation across Ukraine have shown (Semenova, 2017) that in the short-term to 2050, **a** temperature increase is expected, which will affect all regions of Ukraine and will especially intense in the north-eastern areas. Within RCP8.5 scenario (IPCC, 2013), by the end of period the temperature anomaly will reach +2.8...+3.1°C. At the same time, precipitation amount is projected to increase during the period, but under rising air temperature it does not rule out droughts' intensification in the future.

A comparative analysis of the spatial distribution and frequency of seasonal droughts, which were determined by the SPI (the Standardized Precipitation Index; Svoboda, Fuchs, 2016) at the scale of 7 months from April to October during 2020-2050 showed (Semenova, 2015) that more drought events are expected under RCP2.6 scenario. Under RCP2.6 scenario the droughts will be most frequently in the northeastern regions and the Carpathian region, but under RCP8.5 scenario the droughts are most often projected in the Azov Sea cost areas, Transcarpathia and the far north of the country. Predominance of moderate and severe seasonal droughts is predicted in the RCP8.5 scenario, and mild droughts are prevailed in the RCP2.6 scenario.

Analysis of the time series of SPI7 for local points in the different regions of Ukraine showed that under the RCP2.6 scenario, there will be no significant fluctuation in the frequency of dry episodes during 2020-2050. Drought periods will change with wet periods of comparable intensity, and most prolonged dry periods from two to three consecutive years are most likely in the 2020s and 2040s. Under RCP8.5 scenario, the intensity and duration of droughts is expected to increase after 2035 in almost all regions except the northeast. Longest and most intense drought is projected in 2042-2045, and in the south it will last until 2050.

This study examines the results of analysis of the spatiotemporal distribution of warm season droughts (April-October) across the administrative areas of Ukraine (Figure 1) in the period 2021-2050 under climate scenarios RCP4.5 and RCP6.0 with them comparing.

2. Data and methods

Drought estimation was performed using the SPEI index (the Standardized Precipitation Evapotranspiration index). The SPEI like the SPI index is based on time series of precipitation, but use an potential evapotranspiration (PET) instead precipitation, which involves the use of air temperature series (Beguería et al., 2014). The inclusion of temperature along with precipitation data allows SPEI to account for the impact of temperature on a drought situation. Like the SPI, the SPEI can be calculated on a range of timescales from 1-48 months. If only limited data are available, as temperature and precipitation, PET can be estimated with the simple Thornthwaite method.

A drought episode for given time scale is defined as a period, in which SPEI is continuously negative and reaches a value of –1.0 or less. Drought intensity is determined by following criteria: mild drought –0.99…0.00; moderate drought –1.49… –1.00; severe drought –1.99…–1.50; extreme drought ≤ –2.00.



Figure 1. Map of Ukraine with administrative areas.

In this study, the gridded fields of monthly air temperature and precipitation intensity from multimodel sets of global CMP5 models are taken for calculations of SPEI. Data access was made through the Climate Explorer

(http://climexp.knmi.nl). All data were averaged over the area of each of 25 administrative regions of Ukraine.

3. Results

Analysis of the time series of the calculated SPEI index for both scenarios showed that in all regions of Ukraine there will be a tendency to transition from moderately wet conditions in 2021-2035 to droughty conditions in 2037-2050. In the first half of the study period drought is expected near 2024, as well as in 2030-2033 almost in all provinces except southern areas. In the second half of the period prolonged seasonal drought is projected in 2044-2047 over all Ukraine and in some areas drought may reach an extreme intensity.

Decade analysis of the SPEI7 time series showed that in both scenarios in all regions of Ukraine, the least number of dry seasons is expected from 2021 to 2030 (Figure 2). The highest number of dry seasons in this period may reach up to 4-5 cases per 10 years in the western regions (Uzhhorod, Lviv, Rivne, Ivano-Frankivsk) under RCP6.0 scenario. The lowest number of dry seasons (1-2 cases per 10 years) is projected under RCP6.0 scenario in different regions except the western areas and in the southern regions (Odessa, Mykolaiv, Kherson, Zaporizhzhia and Crimea) under the RCP4.5 scenario, when the number of drought season is expected ≤ 1 case per decade. In other regions the number of dry warm seasons during this period will be 2-3 cases per 10 years.

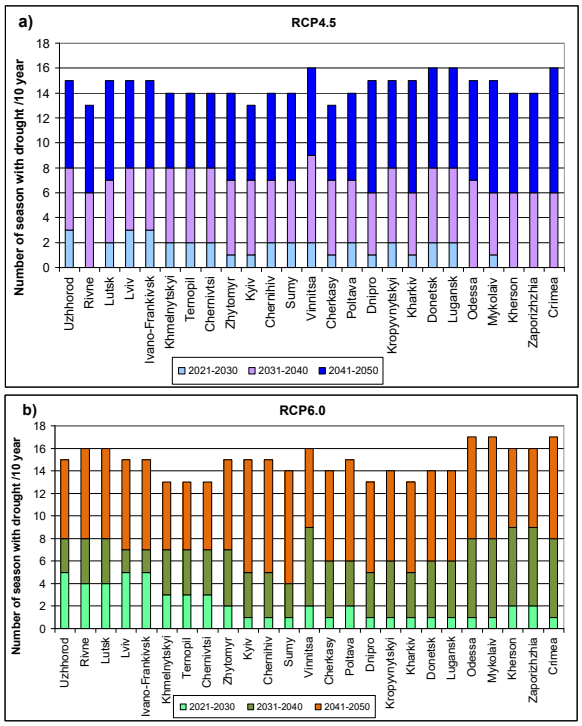


Figure 2. Diagrams for the projected number of seasons with drought per decade during 2021-2050 on the administrative areas of Ukraine under climatic scenarios: a) RCP4.5; b) RCP6.0.

In the period from 2031 to 2040, the number of dry seasons will increase substantially in all regions of Ukraine under RCP4.5 scenario, in which their number will be 5-6 cases per 10 years, and in Vinnytsa region is projected 7 seasons with drought. Under RCP6.0 scenario, an increase in the number of droughts will be observed in all areas except the western regions, where will be from 2 to 4 dry seasons per 10 years. In some regions (Uzhgorod, Ivano-Frankivsk, Lviv), the number of droughts will expect to decrease compared to the previous decade. The greatest increase in the number of dry seasons is projected in the southern regions, as well as in the Vinnytsa region, where they will be 6-7 cases per 10 years.

In the last decade from 2041 to 2050, in both scenarios, the number of dry seasons will increase throughout Ukraine compared to the previous decade. Under RCP6.0 scenario, the greatest increase is projected in the north of the country, in some eastern (Donetsk, Lugansk) and southern (Odessa, Mykolaiv, Crimea) regions, as well as in some western regions, where the maximum number of seasons with droughts will reached up 8-10 cases per 10 years.

4. Conclusions

Comparison of the SPEI7 time series for both scenarios showed that under RCP6.0 scenario the sharper interannual fluctuations of the index are predicted that indicate the increased variability of atmospheric processes, which provide the unstable temperature and moisture regime of the territory. In addition, in this scenario predicts a sharper and faster transition in the mid-2030s from relatively wet conditions to a dry climatic period throughout Ukraine, but the number of extreme droughts is expected to be less than under RCP4.5 scenario. The total number of drought seasons throughout Ukraine will range from 13 to 17 years per 30 years in both scenarios. It is predicted that the frequency of warm seasons with drought will increased by the end of the study period, especially in the north of the country, in some eastern and southern regions, as well as in half of the western regions, where the number of warm seasons with drought may reach 8-10 per 10 years.

References

Beguería, S., Vicente-Serrano, S.M., Reig, F. and Latorre, B. (2014) Standardized precipitation evapotranspiration index (SPEI) revisited: parameter fitting, evapotranspiration models, tools, datasets and drought monitoring, Int. J. Climatol., Vol. 34, pp. 3001-3023. doi: 10.1002/joc.3887.

Caloiero, T., Veltri, S., Caloiero, P., Frustaci, F. (2018) Drought Analysis in Europe and in the Mediterranean Basin Using the Standardized Precipitation Index. Water, Vol. 10, p. 1043; doi:10.3390/w10081043.

IPCC (2013) Climate Change 2013: The Physical Science Basis. Contribution of WG I to the 5th Assessment Report of the IPCC [Stocker, T.F., et al. (eds.)]. Cambridge University Press, Cambridge, UK and New York, NY, USA, 1535 p.

Semenova, I.G. (2015) The spatial and temporal distribution of droughts in Ukraine under the future climate changes. Physical geography and geomorphology, Vol. 1 (77), pp. 144-151 (in Ukrainian).

Semenova, I.G. (2017) Synoptic and climatic conditions for the drought formation in Ukraine. Monograph. Kharkiv, FOP Panov A.V., 236 p. (in Ukrainian).

Spinoni, J., Naumann, G., Vogt, J., Barbosa, P. (2016) Meteorological Droughts in Europe: Events and Impacts – Past Trends and Future Projections. Publications Office of the European Union, Luxembourg, EUR 27748 EN, doi: 10.2788/450449.

Svoboda, M., Fuchs, B.A. (2016) Handbook of Drought Indicators and Indices. Integrated Drought Management Programme (IDMP), Integrated Drought Management Tools and Guidelines Series 2. Geneva, 2016.

Topic 4

Sea level dynamics in the Baltic Sea

Geophysical and geochemical characteristics of four different pockmark sites located in the Gdańsk Basin

Aleksandra Brodecka-Goluch, Jakub Idczak, Natalia Gorska and Jerzy Bolałek

Institute of Oceanography, University of Gdańsk, Poland (aleksandra.brodecka-goluch@ug.edu.pl)

1. Introduction

Pockmarks are seabed structures associated with gas seepage or submarine groundwater discharge, which often occur above dislocation zones. They can be found worldwide, in soft fine-grained sediments on the continental shelves (Hovland and Judd 1988). Their presence can be related to hydrocarbon reservoirs (Hovland et al. 2002). Previous studies (e.g.Pimenov et al. 2010, Jaśniewicz et al. 2019) indicated that such forms may occur at the bottom of the Gdańsk Basin. However, since then they have not been thoroughly mapped nor described in the context of potential impact on the Baltic Sea environment. Based on past publications (e.g. Brodecka et al. 2013), data on shallow gas and the discrepancies in previously collected geochemical data (significantly different concentrations of pore water constituents within some 1 km^2 areas), we selected four potential areas within the Gdańsk Basin and decided to map unusual structures at the bottom.

Our objective was to recognize different pockmark areas located in the Gdańsk Basin with the use of non-invasive geophysical and hydroacoustic techniques and examine bottom sediments of these structures for methane content and possible submarine groundwater discharge.

2. Methods

We collected geophysical (sea bottom) and hydroacoustic (water column) data as well as took sediment cores in the period from 11/2018 to 11/2019 during numerous several-day cruises onboard r/v Oceanograf (a new perfectly equipped ship, designed to conduct complex multidisciplinary scientific studies) in the area of the Gdańsk Basin.

For mapping the sea bottom of four different areas (MET1, MET3, MET4, P1; Fig. 1), we used a multi-beam echosounder (MBES, SeaBat 7125 Reson Teledyne, 400 kHz). Additionally, we set several transects across the pockmarks to investigate potential gaseous forms in shallow sediments with a sub-bottom profiler (SBP, SB-216S Edge Tech, 2-10 kHz). Moreover, we registered gas flares in a water column using a split-beam echosounder (Simrad *EK 80,* Kongsberg, 38, 120 and 333 kHz). Finally, we collected sediment cores with a Rumohr Lot corer (length: 1 m) from different sites inside and outside the pockmark structures and determined CH_4 concentrations (GC-FID) in sediment samples from different depths as well as (not all pockmarks) stable isotope composition ($\delta^{13}C(CH_4)$ and $\delta^{2}H(CH_4)$). Additionally, each time we performed CTD profiles and measured dissolved oxygen (dO_2 probe COG-2 and CX-461 meter, Elmetron). In several sites, where we suspected freshwater seepage, we measured Cl^- concentrations (ion chromatography) in pore waters of sediment cores.

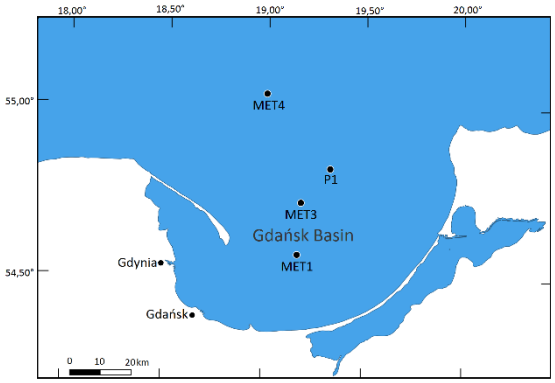


Figure 1. Map of the study area.

3. Results

MET1

We mapped ca. 60 km^2 of the bottom with MBES and found several pockmarks (total area: 0.48 km^2). The biggest pockmark (MET1-MP), located in the central Gulf of Gdańsk was about 500 m wide and 800 m long (Fig. 2). In addition, we found a unique 10 m deep pockmark structure (MET1-BH, max. water depth of 88 m). Above that pockmark we registered large gas flares. It turned out that the intensity of gas emission depended on hydrometeorological conditions (atmospheric pressure and seawater level). Moreover, at MET1-BH we measured 80% lower Cl^- concentrations (decrease from 170 mM to 30 mM) in the near-bottom water (evidence for SGD) than in the water column. Average methane concentrations in sediments of these pockmarks were the highest of all the investigated areas (up to 14 mM).

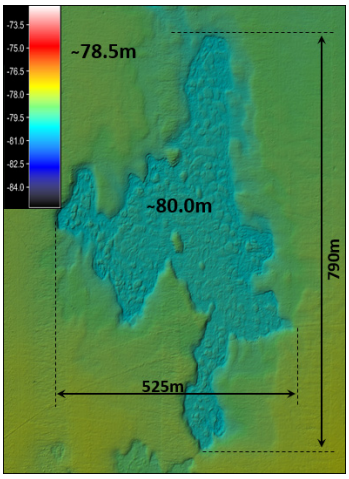


Figure 2. MBES image of the MET1-MP pockmark.

Sub-bottom profiles indicated the presence of numerous very shallow gas chimneys in this area.

MET3

We investigated about 14 km^2 of the MET3 bottom using MBES and discovered one medium-size ca. 2 m deep pockmark structure (Fig. 3). This pockmark is rather inactive and methane concentrations were the lowest of all the investigated structures (1.5 mM at 90 cm bsf).

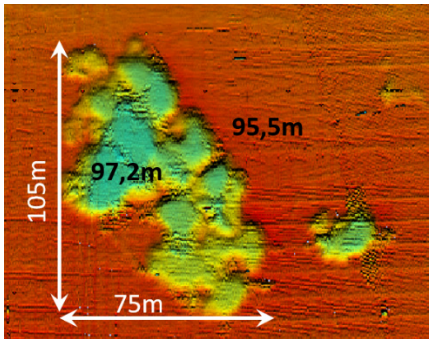


Figure 3. MBES image of the MET3 pockmark.

MET4

Within this area we checked about 27 km^2 and found 0.09 km^2 of the sea bottom covered with pockmarks. There are numerous elongated pockmarks, up to 4.5 m in depth (water depth: ca. 100 m) (Fig. 4). In one of the pockmarks MET4-ID, the shape of methane profile in sediments was surprising as the highest concentrations of about 5-12 mM were determined in the top part of the collected core (5-35 cm bsf), just above the transition between lower grey clayey layer and upper black muddy layer.

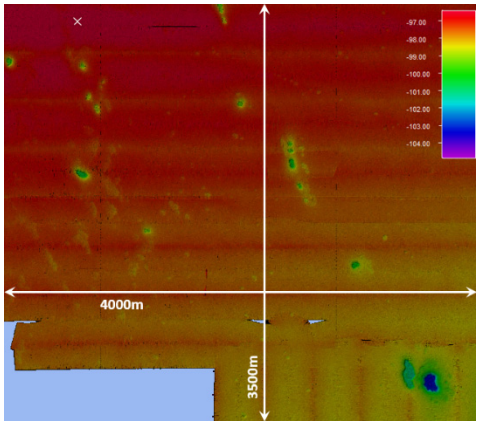


Figure 4. MBES image of the MET4 area.

P1

We examined bottom sediments within a standard monitoring site (P1) in the Gdańsk Deep area. It turned out that it is all covered with small irregular pockmarks (Fig. 5), which constituted about 3% of the total mapped area (7 km^2). Methane concentrations in sediments were rather low in this area. They reached 1-3 mM at sediment depths of 50-100 cm. The bottom in this area is very diversified. The activity of these pockmarks was not investigated. However, previous works indicate that SGD is highly possible in this area (Falkowska and Piekarek-Jankowska, 1999).

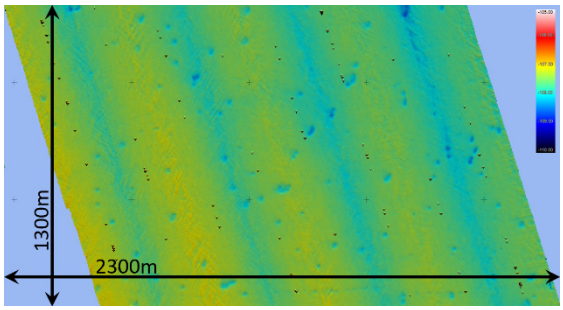


Figure 4. MBES image of the P1 area.

4. Conclusions

There are numerous pockmark structures at the bottom of the Gdańsk Basin. Active pockmarks (e.g. MET1-MP and MET1-BH) with intensive gas and freshwater seepage can be regarded as key areas for future biogeochemical (microbiology of sediments, cycling of different elements), geophysical (deep-sediment structures) and hydroacoustic (gas ebullition and transport in the water column) research. Moreover, the abundance of different (in terms of activity, shape and origin) pockmarks within one basin may help us understand the environmental impact of these structures.

It should also be emphasized that the location of monitoring stations within pockmarked sea bottom (e.g. P1) may significantly influence the obtained biogeochemical results, especially when the measurements are carried out seasonally.

This study was financed by the Polish National Science Centre (UMO-2016/21/B/ST10/02369).

References

Brodecka, A., Majewski, P., Bolałek, J., Klusek, Z. (2013) Geochemical and acoustic evidence for the occurrence of methane in sediments of the Polish sector of the southern Baltic Sea, Oceanologia, 55, 951–978.

Falkowska L., Piekarek-Jankowska H. (1999) The submarine seepage of the fresh groundwater: disturbance in hydrological chemical structure of the water column in the Gdansk Deep, Journal of Marine Science, 56, 153-160

Hovland M., Judd A.G. (1988) Seabed Pockmarks and Seepages. Impact on Geology, Biology and the Marine Environment. Graham & Trotman, London

Hovland M., Gardner J.V., Judd A.G. (2002) The significance of pockmarks to understanding fluid flow processes and geohazards. Geofluids, 2, 127–136.

Jaśniewicz D., Klusek Z., Brodecka-Goluch A., Bolałek J. (2019) Acoustic investigations of shallow gas in the southern Baltic Sea (Polish Exclusive Economic Zone): a review, Geo-Marine Letters, 39(1), 1-17.

Pimenov N.V., Ulyanova M.O., Kanapatsky T.A., Veslopolova E.F., Sigalevich P.A., Sivkov V.V. (2010) Microbially mediated methane and sulfur cycling in pockmark sediments of the Gdansk Basin, Baltic Sea, Geo-Marine Letters, 30, 439–448.

Short-term volumetric changes of the southern Baltic dune coast caused by various hydrodynamic conditions (case study Dziwnow Spit)

Natalia Bugajny, Kazimierz Furmańczyk

Institute of Marine and Environmental Sciences, University of Szczecin, Szczecin, Poland (natalia.bugajny@usz.edu.pl)

1. Introduction

Volumetric changes of the coast can be considered in different timeframes and space (Musielak et al., 2017). The most spectacular changes occur in a short-term as a result of severe single storm or series of such events (Furmańczyk and Dudzińska, 2009). The outcomes are what attracts attention of many scientists. Nonetheless, from forecasting and cognitive perspective, apart from extreme events, these are weak storms that play crucial role in functioning of the coastal system along with changes in a coast they induce and beach recovery process that takes place during storm calming.

In this context, the purpose of this study is to show diversity of magnitude and structure of volumetric changes in the dune coast in the short-term by the example of Dziwnow Spit. The study takes into consideration the area split as natural and protected coast as well as variability of process results along the coast.

2. Data and methods

The studies were carried out on a dune coast of Dziwnow Spit located on the western coast of the southern Baltic. Spit coast is either natural or featured with protected sections armoured with different structures and supplemented with reclamation measures (Dudzińska-Nowak, 2015).

Five types of hydrodynamic conditions: 1 severe storm of 2009, 3 moderate periods of 2012 and storm calming from the break of May and June 2014 were picked for the analysis.

The analysis of the severe storm was based on profile data provided by the Maritime Office in Szczecin (Bugajny et al., 2013), while for other storms, cross-shore profiles were surveyed using GPS RTK (Bugajny and Furmańczyk, 2014). Density of profiles along the coast varied between research periods. For the severe storm, there were 19 profiles considered every 500 m along a 9 km long section. For weak storms, two 2 km long sections were selected: one at natural coats and second at coast protected with groynes. Profile offset was agreed to 100 m. Surveys were taken 14 times between June and December 2012 (Bugajny and Furmańczyk, 2017). The storm calming was analyzed only for the 300 m long section of the natural coast in profiles taken every 20 m twice a day between May 29 and June 1 (Bugajny and Furmańczyk, 2020).

As an addition, hydrodynamic data was collected. Water level data for 2009 was recorded every 4 hours by a tide gauge located in a harbor in Dziwnow and provided as printed sheets by the Harbour Master's Office in Dziwnow. In turn, water level data of 2012 and 2014 were derived from a measurement station of Institute of Meteorology and Water Management – National Research Institute installed in the same harbor. This data is available online at www.pogodynka.pl and updated every hour.

Furthermore, data set on basic wave parameters of WAM model were collected. Studies on verification of WAM model for the Baltic Sea proved good correlation between modelled and measured wave parameters (Paplińska, 1999).

A period of moderate wave conditions was divided into three groups of diverse hydrodynamic structure by means of Ward method (Bugajny and Furmańczyk, 2014). The strongest group is characterized by the significant wave height not exceeding Hs < 2.4 m and maximum changes in water level of 91 cm, moderate group – when Hs < 1.9 m and maximum changes in water level of 82 cm, and the weakest group of Hs < 1.0 m with maximum water level changes of 53 cm.

In each case and for each profile, magnitude of volumetric changes of both natural and protected coast was calculated. Next, average and extreme values from area of study were obtained what is essential during an analysis of volumetric changes variability along the coast.

Moreover, the spread of minimum and maximum changes in beach volume was calculated for each period.

3. Results

The biggest volumetric changes were observed as a result of the significant storm presence which was featured by a significant wave height of ca. Hs = 4 m. On the natural coast volumetric changes were spanning between -14 m^3/m and -22 m^3/m, at an average of -19 m^3/m, whereas on the protected coast, these changes were ranging from -15 m^3/m to -37 m^3/m, at an average of -24 m^3/m. The span of these volume changes for the natural coast was 8 m^3/m and the protected coast 22 m^3/m.

An analysis of volumetric changes caused by moderate hydrodynamic conditions (Hs < 2.5 m), i.e. weak storm (that do not cause dune erosion) proved that for the strongest group (Hs < 2.4 m), the volumetric changes, that took place on the natural coast, were oscillating between -7.97 m^3/m and +7.51) m^3/m, at an average of -0.44 m^3/m, while on the protected coast – they were ranging between -5.70 m^3/m and +11.74 m^3/m, at an average of -1.34 m^3/m. The moderate group (Hs < 1.9 m) was featured by the changes from -4.74 m^3/m to +8,06 m^3/m on the natural coast and from -3.82 m^3/m to +5.78 m^3/m on the protected section. Average values equaled +0.16 m^3/m and +2.10 m^3/m, respectively. Finally, the weakest group (Hs < 1.0 m), that was characterized by average values of volumetric changes at +1.61 m^3/m for the natural coast and +2.88 m^3/m for the protected one, minimal and maximal values were: -0.75 m^3/m and +3.07 m^3/m on the natural coast and -0.45 m^3/m and +3.96 m^3/m on the protected section (Bugajny and Furmańczyk, 2017).

The last considered event, the storm calming, when Hs was decreasing from 1.5 m to 0.5 m and where beachface recovery process took place along the natural coast, the volumetric changes were oscillating between -0.2 m^3/m and +0.8 m^3/m and their average value was +0.35 m^3/m (Bugajny and Furmańczyk, 2020).

4. Conclusions

The magnitude of the volumetric changes along the coast are diversified, as evidenced by their range. Even though, it is about 1 m^3/m over 300 m during the storm calming, it rises up to about 10 m^3/m during longer periods with waves Hs < 1.9 m, and to 15.5 m^3/m on the natural coast and 17.5 m^3/m on the protected coast respectively for Hs < 2.4 m.

At moderate hydrodynamic conditions (Hs < 2.4 m) both erosion and accumulation occur on the both type of the coast: natural and protected.

During the significant storm (which causes dune erosion) coastal erosion occurs along the entire studied area. Its size varies greatly, reaching 8 m^3/m on the natural and 22 m^3/m on the protected coast.

Coastal protection measures favor accumulation at moderate wave conditions Hs < 1.9 m, and increase erosion at Hs < 2.4 m. The range of minimum and maximum volume change is generally greater on the protected coast. However, at Hs > 2.0 m it is just slightly greater, while in the case of a significant storm (Hs = 4m), it is tripled. It seems that coastal protection measures in form of groynes lose their protective nature as the wave height increases, as the magnitude of coastal erosion is about 20% greater on the protected coast during the significant storm.

These observations are in line with the recommendations that followed the EU EUROSION project (www.eurosion.org) regarding leaving undeveloped beach area (both its width and length) for the coastal processes (EU, 2004)

The conducted studies take into consideration an issue of choosing any one profile as a representative for a specific section of the coast. Such profile could be useful for next studies carried out in similar hydrodynamic conditions and geomorphological settings. Unfortunately, the behavior of profiles may be fundamentally different, just a few dozen meters away.

Acknowledgments

This research was conducted and financed within the framework of statutory research at the University of Szczecin and as a part of the SatBałtyk project.

References

Bugajny N., Furmańczyk K., Dudzińska-Nowak J. and Paplińska-Swerpel B. (2013). Modelling morphological changes of beach and dune induced by storm on the Southern Baltic coast using XBeach (case study: Dziwnow Spit). In: Conley D.C., Masselink G., Russell P.E. and O'Hare T.J. (eds.), *Journal of Coastal Research*, SI. 65, pp. 672–677.

Bugajny N. i Furmańczyk K. (2014). Dune coast changes caused by weak storm events in Miedzywodzie, Poland. In: Green A.N. and Cooper, J.A.G. (eds.), Journal of Coastal Research, SI. 70, pp. 211–216.

Bugajny N. i Furmańczyk K. (2017). Comparison of short-term changes caused by storms along natural and protected sections of the Dziwnow Spit, Southern Baltic coast. Journal of Coastal Research, 33, 4, pp. 775–785.

Bugajny, N. and Furmańczyk, K. (2020). Short-term volumetric changes of berm and beachface during storm calming. *In:* Malvárez, G. and Navas, F. (eds.), Journal of Coastal Research, SI 95 (accepted).

Dudzińska Nowak J. (2015). Metody ochrony zachodniego wybrzeża Polski i ich wpływ na zmiany brzegu w latach 1938-2015. Wydawnictwo Naukowe Uniwersytetu Szczecińskiego, Szczecin, 171 p.

European Commision (2004). Living with coastal erosion in Europe: sediment and space for sustainability: Results from the EUROSION study. European Commission, Luxembourg, ISBN 92-894-7496-3, 38 pp.

Furmańczyk K. and Dudzińska-Nowak J. (2009). Effects extreme storms on coastline changes: a southern Baltic example. Journal of Coastal Research, SI 56, pp. 1637–1640.

Musielak S. Furmańczyk K. and Bugajny N. (2017). Factors and processes forming the Polish Southern Baltic Sea coast on various temporal and spatial scales. In: Harff J., Furmańczyk K. and von Storch, H. (eds..), Coastline changes of the Baltic Sea from South to East: past and future projection, Coastal Research Library, vol. 19, pp. 69-86.

Paplińska B., 1999. Wave analysis at Lubiatowo and in the Pomeranian Bay based on measurements from 1997/1998—comparison with modelled data (WAM4 model). *Oceanologia*, 41 (2), s. 241–254.

Land subsidence monitoring due to groundwater changes using InSAR observations - Initial results: the Swedish Islands of Gotland and Öland in the Baltic sea

Mehdi Darvishi[1], Fernando Jaramillo[1,2]

[1] Physical geography department, Stockholm University, Stockholm, Sweden (mehdi.darvishi@natgeo.su.se)
[2] Baltic Sea Centre, Stockholm University, SE–106 91, Stockholm, Sweden

1. Introduction

In the recent years, Sweden has experienced drought conditions in summer times. There is a risk that it will be a difficult summer in 2020, with water shortages in several counties according to the Geological Survey of Sweden, SGU (Bo Thunholm, interview with https://www.krisinformation.se; April 16, 2019). In the years 2018 and 2019, ground water levels have been below normal due to long dry and hot summers and not enough snow in the winter, leading to restrictions of water use in regions such as Gotland and Sala in central. One of the main physical effects of groundwater depletion is land subsidence, a geohazard that potentially damages urban infrastructure, natural resources and generates casualties. It is possible then that land subsidence and uplift may be occurring in Sweden due to the drastic changes in groundwater levels (mainly in the middle and southern regions), besides the observed and expected Postglacial rebound that mainly occurs along the northern Baltic shorelines.

We argue that there is no comprehensive information regarding land subsidence in Sweden and as a result there is a need to provide land subsidence maps of high accuracy and appropriate temporal and spatial resolution, to mitigate the negative effects of land subsidence damages. Furthermore, identification of areas of subsidence can be an indication of groundwater depletion. Figure 1 shows the groundwater level condition in Sweden.

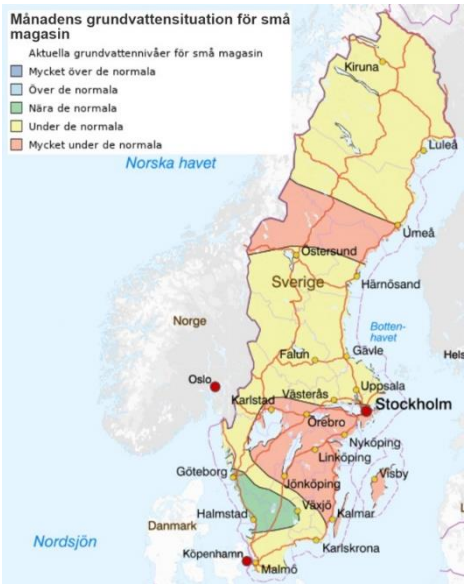


Figure 1. Groundwater level map of Sweden. The map presents the areas where ground water level is below (see the islands of Öland and Gotland in Southern Sweden (map: Geological Survey of Sweden).

Interferometric synthetic aperture radar (InSAR) is powerful tool that has recently been used to detect and monitor land subsidence (Rosen et al., 1999). InSAR technique can map land subsidence with an accuracy of a few millimeters and a spatial resolution of less than 1 meter. Therefore, InSAR technique is an effective hydro-geodesic tool to reveal land subsidence due to de groundwater level changes (Sundell et al., 2019). In this study, we will present the initial results of the InSAR processing of Sentinel-1 (S1) data, covering the time span of 2014-2019, to detect the land deformation of the Gotland and Öland islands in Sweden.

2. Method

We used 147 and 116 S1-A/B data (descending mode) in the region of Gotland and Öland islands and available during the period 2014-2019 (Fig. 2)

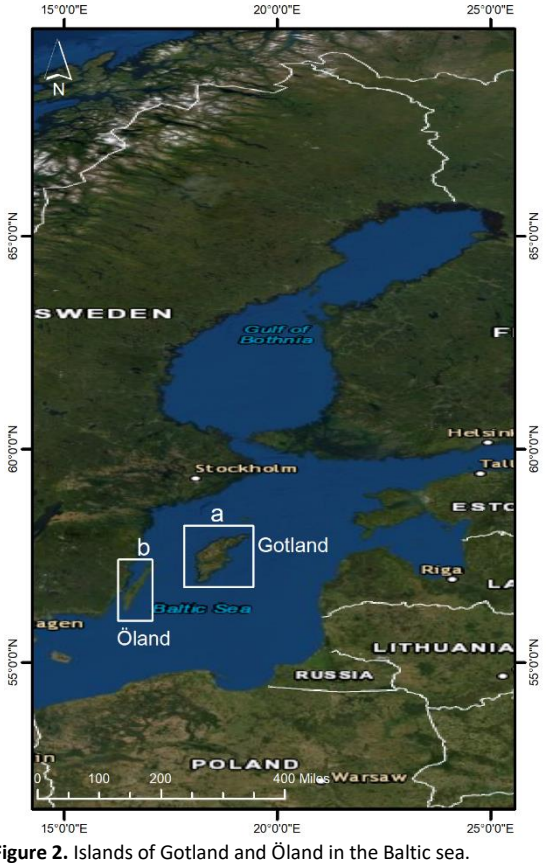


Figure 2. Islands of Gotland and Öland in the Baltic sea.

The small Baseline Subset (SBAS) technique (Berardino et al., 2002) wad used to process the S1 data and produce displacement maps of deformation, in millimeters. The

SBAS relies on the selection of short temporal and spatial baselines and application of space-time filtering to mitigate atmospheric artifacts and determine ground deformation. We processed SBAS in the framework of six main steps: 1) Connection graph generation, 2) interferometric processing, 3) refinement and re-flattening, 4) first inversion, 5) second inversion and 6) geocoding. The final displacement maps were created along the line of sight of the satellite (LOS).

3. Results

Figure 3a and b show the LOS displacement maps of Gotland and Oland as obtained by SBAS processing. Most of the areal surface of Gotland appears stable, however; on the east, west and southern coasts an uplift can be observed. On the other hand, subsidence is evident in the middle of the island. In the LOS displacement map of the Öland (Figure 3b), most part of the island is stable except for the northern part that exhibits an uplift and the south-western part that exhibits a subsidence. It is probable that the subsidence patterns are associated with land subsidence due to ground water depletion, nevertheless, more analysis on groundwater table and water levels from wells and/or permanent GPSs stations measurements with time-series subsidence pattern is necessary.

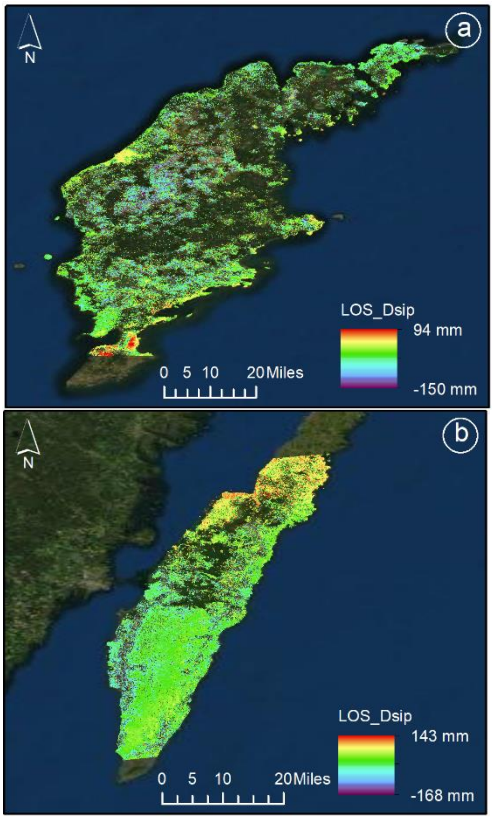


Figure 3. LOS displacement maps. **a)** LOS displacement map of the Gotland and **b)** LOS displacement of the Öland island. Green color indicates almost stable regions with no change in distance along the LOS. The positive values show ground uplift by a decrease in the distance between satellite and ground and the negative values to subsidence, meaning an increase in the distance between the satellite and ground.

Land subsidence due to groundwater extraction is a important global problem that influences many of the world's major aquifers and cities. Monitoring and modeling land subsidence can help us to reduce its destructive effects. InSAR has been widely and recently used to monitor land subsidence that could be considered as an effective monitoring system for groundwater management and prevent ongoing subsidence in the future.

References

Berardino, P., Fornaro, G., Lanari, R., Sansosti, E., 2002. A new algorithm for surface deformation monitoring based on small baseline differential SAR interferograms. IEEE Trans. Geosci. Remote Sens. 40, 2375–2383. https://doi.org/10.1109/TGRS.2002.803792

Rosen, P.A., Hensley, S., Joughin, I.R., Li, F., Madsen, S.N., Rodr, E., Goldstein, R.M., 1999. Synthetic Aperture Radar Interferometry XX, 1–110.

Sundell, J., Haaf, E., Norberg, T., Alén, C., Karlsson, M., Rosén, L., 2019. Risk Mapping of Groundwater-Drawdown-Induced Land Subsidence in Heterogeneous Soils on Large Areas. Risk Anal. 39, 105–124. https://doi.org/10.1111/risa.12890

Morphodynamic of the southern Baltic coast – natural processes & anthropogenic impact

Joanna Dudzińska-Nowak

Institute of Marine and Environmental Sciences, University of Szczecin, Poland (joanna.dudzinska-nowak@usz.edu.pl)

1. Introduction

The southern Baltic Sea coasts, includes dune coast composed of Holocene marine and Aeolian accumulation sediments, mainly sands and also some sections of cliff coast, composed of unconsolidated Pleistocene sediments, mainly glacial till and sands, are very prone to erosion. Morphogenetic processes of this coasts are determined by a complex interplay of the geological setting, eustatic sea-level change, glacio-isostatic adjustment, wind, waves, sediment dynamics, storm surges and eaolian processes, acting on different time scales (Musielak et al. 2017, Harff et al. 2017, Dudzińska-Nowak 2017). Sediment budget is determined by the dominant long-shore sediment transport, along most of the coast areas at the southern Baltic coast (Zhang et al. 2013, Soomere and Viska 2013). The most important erosional coastline changes occur during extreme conditions (Furmanczyk and Dudzińska-Nowak 2009) connected with strong wind, high waves and relative sea-level fluctuations associated with storm surge reinforced by water filling. In terms of presently occurring climate changes, which pose a threat to the coast - an increase of number and intensity of observed storm events and a general deficiency of sediments in the coastal zone - the determination of the accurate spatio-temporal distributions of change occurring on the coast, as well as influence of hydro-engineering protection methods, is of particular importance for broadly defined coastal safety (Dudzińska-Nowak 2017).

2. Materials and methods

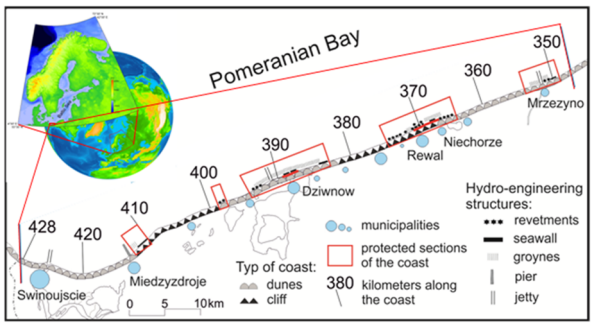


Figure 1. Area of investigation indicating coast type and protected by different type of hydro-technical constructions and protection measures sections.

The analyzes of the dune base/cliff foot line position movement, based mainly on remote sensing datasets photogrammetrically processed, historical and modern aerial photographs and numerical terrain models, allowed to determine the magnitude and rate of long-term coastal changes (1938-2012) of almost 80 km-long coastal section of the Pomeranian Bay (southern Baltic Sea), with a due consideration to factors such as shore orientation, dune base altitude, average beach width within a given period of time, and beach slope (Figure 1). The temporal and spatial variability of the shore, as a dune base/cliff foot line position changes, was subsequently referred to the selected driving forces such as the mean monthly sea level, storm surges, wave action characteristics as well as the antropogenic impact connected to the presence and effects of hydrotechnical constructions and protection measures.

3. Results and analysis

Conducted analyses show unequivocally that any intervention in the coastal zone, in the form of both hydrotechnical construction deployment and shore protection-aimed measures, induces changes in natural hydro-, morpho-, and lithodynamic processes, and ultimately results in enhancing changes in the dune base/cliff foot in the vicinity of the intervention site (Figure 2).

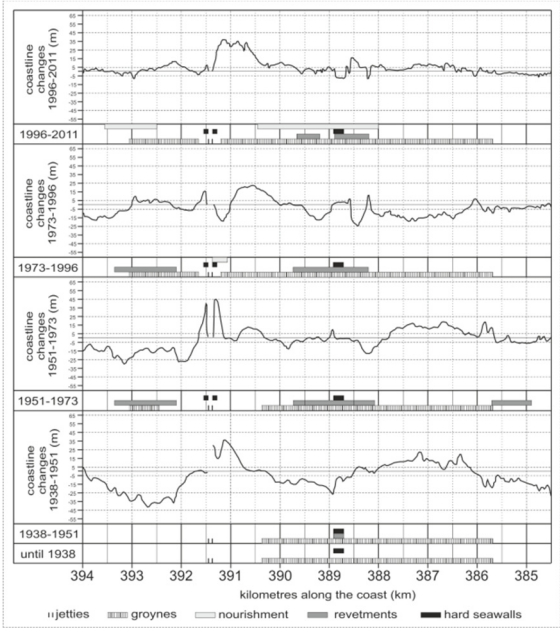


Figure 2. Coastline changes in analyzed time periods for Dziwnow area, in relation to hydro-technical constructions and protection measures existing in a given periods.

The results obtained allow to conclude that hydrotechnical interventions permanently and significantly affect the processes operating in the coastal zone and enhance the shore destruction rate. Particularly noteworthy are the negative effects of heavyweight hydrotechnical constructions and groyne systems, visible as the link side effect observed during the 74 years of records; on the other hand, the positive effects of other, less invasive,

protection measures such as artificial beach nourishment, should be borne in mind. The nature, extent and magnitude of changes produced by both the direct and indirect effects of hydrotechnical constructions deserve further in-depth studies, as knowledge on these processes may aid in effectively counteracting their negative effects in the future. The considerable temporal and spatial variability of the coastal changes taking place in neighbouring, geomorphologically and geologically uniform coastal segments which are similar also in terms of evolutionary trends, is very important in case of future scenarios developing. This result points to the high importance of appropriate selection of representative sites at which to forecast the magnitude of coastal changes. Not less important than the observation site location is also the selection of periods of time for the analyses, as confirmed by the high variability of morphodynamic effects in the periods analysed. An accidental location and a too short period of observations, not accounting for the hydrometeorological variability, may substantially bias the forecast and pose a potential threat for the infrastructure planned to be deployed at such sites. Further interdisciplinary studies based of measured and modelled data of the long-term variations of waves regime, water level changes, storm surges structure and long-shore sediment transport analyses in relation to coastal zone changes as a consequences of such phenomena's are necessary and strongly recommended in order to reveal a mechanism of the coast development.

References

Dudzińska-Nowak J. (2017) Morphodynamic processes of the Swina Gate coastal zone development (southern Baltic Sea). In: J. Harff, K. Furmanczyk, H. von Storch (eds.) Coastline changes of the Baltic Sea from South to East. Past and future projection. Springer Coastal Research Library 19, pp. 219-256

Furmańczyk, K. and Dudzińska-Nowak, J. (2009) Extreme Storm Impact to the coastline changes - South Baltic example. J Coastal Research 56, pp. 1637-1640

Harff, J., J. Deng, J. Dudzinska-Nowak, P. Fröhle, A. Groh, B. Hünicke, T. Soomere, and Zhang, W. (2017) Chapter 2: What determines the change of coastlines in the Baltic Sea? In: Harff J, Furmanczyk K, von Storch H (eds) Coastline changes of the Baltic Sea from south to east – past and future projection. Coastal research library, vol 19. Springer, Cham, Switzerland, pp. 15–36

Musielak S., Furmańczyk K., Bugajny N., (2017) Factors and Processes Forming the Polish Southern Baltic Sea Coasts on Various Temporal and Spatial Scales. In: J. Harff, K. Furmanczyk, H. von Storch (eds.) Coastline changes of the Baltic Sea from South to East. Past and future projection. Springer Coastal Research Library 19, 69-85

Soomere, T. and Viška, M. (2014) Simulated wave-driven sediment transport along the eastern coast of the Baltic Sea. J Marine Systems 129, pp. 1-10

Zhang, W., Deng, J., Harff, J., Schneider, R. and Dudzinska-Nowak, J. (2013) A coupled modeling scheme for longshore sediment transport of wave-dominated coasts - a case study from the southern Baltic Sea. Coast Eng 72, pp. 39-55

A first look to Lagrangian coherent structures in the Gulf of Finland as a mean to identify hotspots of surface particle aggregation.

Andrea Giudici[1], Kabir Adewale Suara[2], Tarmo Soomere[1,3] and Richard Brown[2]

[1] Department of Cybernetics, School of Science, Tallinn University of Technology, Akadeemia tee 21, 12618 Tallinn, Estonia
[2] Environmental Fluid Mechanics Group, Queensland University of Technology (QUT), QLD, 4000, Australia
[3] Estonian Academy of Sciences, Kohtu 6, 10130 Tallinn, Estonia

1. Introduction

The dispersion and aggregation of floating litter in the basin of the Gulf of Finland is governed by the combination of local weather events and the interactions of the flow fields with local morphological features, ranging across a wide temporal scale. The overlap of several processes, operating at several different scales, existing in such system can lead into the chaotic nature of material transport at the sea surface (Suara et al., 2017; Suara et al., 2019).

Material lines admit distinct signatures in almost any diagnostic scalar field or reduced-order model associated with virtually every flow. These signatures, however, do not reveal the root cause of flow coherence. The theory of Lagrangian Coherent Structures (LCS) seeks to isolate this root cause by uncovering special surfaces of fluid trajectories that organize the rest of the flow into ordered patterns (Olascoaga et al., 2006; Haller, 2015). LCS renders lines, occurring in the chaotic two dimensional surface flows, which serve as distinctive barriers that cannot be crossed by tracers (Haller, 2001). They are the local strongest repelling or attracting material lines.

The trajectories of floating particles are generally sensitive to their initial conditions, making the assessment of flow models (as well as observations of single tracer trajectories) quite unreliable (Vandenbulcke et al., 2009). Behind such complex and sensitive tracer patterns in the study area that is frequently affected by energetic upwelling flows that modify even the Ekman transport (Delpeche-Ellmann et al., 2017), however, LCS represent a robust foundation of material surfaces, which play a key role, in shaping those trajectories.

Albeit the description and interpretation of turbulent mixing mechanisms is not an easy task, the identification of such material lines, which act as barriers for repulsion or attraction for clusters of floating particles, can be helpful in the further identification of areas of accumulation of pollutants.

In this work, we apply the finite-time Lyapunov exponent (FTLE) as a diagnostic quantity for LCS, and we make a first attempt at characterizing them, with respect to their appearance pattern and seasonality within the Gulf of Finland. Specifically, the work presented here is aimed at verifying the seasonality in the dynamics of areas prone to patch formation as well as the presence and characteristics of hotspots for upwelling and downwelling events in the Gulf.

2. Data and Methods

The velocity fields used in initial studies on patch generation in the area and this paper are obtained by means of the OAAS (Andrejev and Sokolov, 1989; 1990) hydrodynamic model, as carried out in the framework of BONUS+ BalticWay cooperation (Soomere et al., 2014), with a spatial resolution of 1 nautical mile (NM). In order to have our results compatible with the research into intense patch-formation areas and properties of the emerging patches (Giudici and Soomere, 2013, 2014; Giudici et al., 2018, 2019), we employ the same dataset of surface velocity fields for the Gulf of Finland.

A first-order approximation to the problem of assessing the stability of material surfaces in the domain is to detect those material surfaces, along which infinitesimal deformation is locally maximal or minimal. FTLE fields are computed from the surface velocity data.

The flow map is obtained by advecting tracer particles for a finite time $[t_0, t_1]$ using a Runge-Kutta scheme with an absolute integration tolerance of 10^{-6}. The FTLE field is computed as $FTLE(\vec{x}, t, \tau) = \frac{1}{}\ln\sqrt{\lambda_{max}(\Delta)}$, where is the advection time and is the largest eigenvalue of the Cauchy-Green deformation tensor Δ obtained from the flow map. The computation was performed using scripts modified from BarrierTool [*Katsanoulis & Haller*, 2019]. The LCS can be defined as the ridge line of the FTLE field which is the curve that goes through the local maxima of the FTLE evaluated along the direction of fastest change in the FTLE values [*Haller*, 2001]. This is readily identified from visual examination of the FTLE contour plots. Particles are advected forward ($\tau > 0$) and backward ($\tau < 0$) in time to reveal the repelling/stable and the attracting/unstable material lines, respectively. Repelling (stable) material lines represent lines of maximum spreading, so initially proximal particles separate rapidly. The attracting/unstable material lines represent those with maximum accumulation.

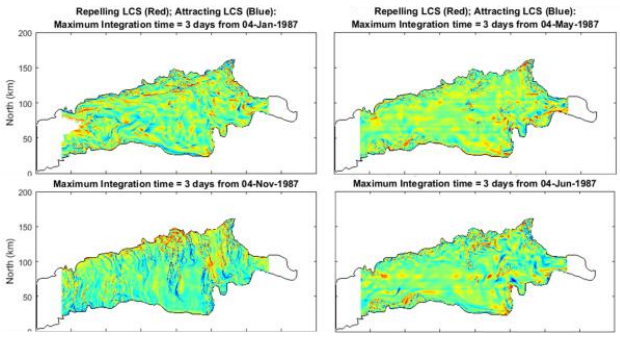


Figure 1. Lagrangian Coherent Structures calculated for the entire Gulf of Finland (integration time is 3 days) during the windy (left column) and calm season (right column) of 1991.

3. Results

We calculated first maps of combined FTLE field = $FTLE^+$ – $FTLE^-$ covering the entire Gulf of Finland, combining the

forward and backward fields following *d'Ovidio et al.* [2004]. These maps (Fig. 1) are a simple and efficient tool to visualize hyperbolic LCS amid a plethora of physical complexities.

Fig. 1 suggests a seasonal dynamics of the gulf which is influenced by the wind.

To further examine this apparent trend, we characterize the overall clustering potential of the Gulf, by employing a spatial average of *forward* FTLE features, as the presence of an attracting (+) LCS indicates the nearby presence of a corresponding repelling (-) LCS.

Following d'Ovidio et al. (2004), the temporal variation of this measure quantifies the overall mixing strength in a system. Fig. 2 shows a plot of such a measure over a time range spanning from 1989 to 1992, which reveals the presence of a trend, where the clustering potential of certain offshore areas of the Gulf of Finland steadily increases, and peaks, during the windy season then decreases, during the calm season.

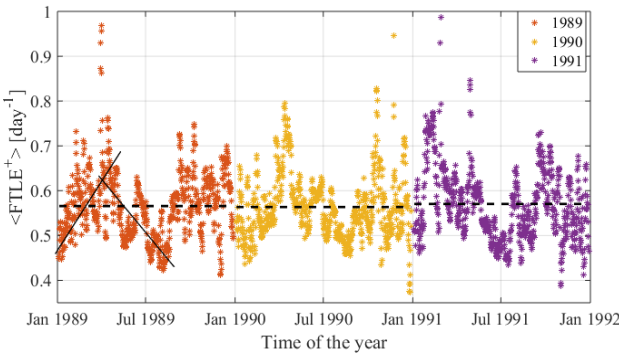


Figure 2. Gulf-wide spatial average of forward (i.e. positive) FTLE features, over the timespan 1989-1992.

This trend is compatible with the notion that surface clustering in the Gulf of Finland is strongly augmented by the combined effect of currents and winds (Giudici et al., 2018).

4. Discussion

LCSs for the Gulf of Finland were calculated for the first time. Snapshots of LCS maps calculated for the entire region are found to be highly dynamic, but a spatial average of the positive (attracting) FTLE features, shows a discernible seasonal trend in the corresponding overall mixing strength. The trend is visible over the considered time span 1989–1992. The trend appears steadily stronger during the windy season and weaker during the calm season.

There exist some limitations to the undertaken approach. Most notably, without some more advanced criteria (as shown for example in Haller, 2002; Haller, 2011; Farazman and Haller, 2012; Tang et al., 2011), the employed FTLE approach to calculate LCS is heuristic, and it ignores the direction of largest stretching, which may be along or close to directions tangent to the initial trajectory. In addition to that, FTLE ridges mark hyperbolic LCS positions which are used to extrapolate information on the mixing strength, but also highlight surfaces of high shear (Haller, 2002).

Although FTLE plots are popular visual diagnostic tools of Lagrangian coherence, more reliable mathematical methods have also been developed for the explicit identification of LCSs, as parameterized material surfaces. Such methods will be taken into consideration as the appearance patterns of LCS in the Gulf of Finland is investigated further.

The next step in investigating LCS in the Gulf will be that of analysing their persistency patterns at 8 locations which were identified as hotspots for particle aggregation in previous stages of the research (Giudici and Soomere, 2013, 2014).

References

Delpeche-Ellmann, N., Mingelaitė, T., Soomere, T. (2017), Examining Lagrangian surface transport during a coastal upwelling in the Gulf of Finland, Baltic Sea, J. Mar. Res. 171, pp.21–30.

Farazmand, M., Haller, G (2012), Computing Lagrangian coherent structures from variational LCS theory. Chaos 22:01328.

Giudici, A., Soomere, T., 2013. Identification of areas of frequent patch formation from velocity fields, Journal of Coastal Research, 65(1), 231–236.

Giudici, A., Soomere, T. (2014), Finite-time compressibility as an agent of frequent spontaneous patch formation in the surface layer: a case study for the Gulf of Finland, the Baltic Sea. Mar. Pollut. Bull., 89(1–2), pp. 239–249.

Giudici, A., Kalda, J., Soomere, T. (2018), Joint impact of currents and winds on the patch formation near the coasts of the Gulf of Finland. J. Coast. Res., Special Issue 85, pp. 1156–1160.

Giudici, A., Kalda, J., Soomere, T. (2019), Generation of large pollution patches via collisions of sticky floating parcels driven by wind and surface currents. Mar. Pol. Bull., 141, pp. 573–585.

Haller, G. (2002), Lagrangian coherent structures from approximate velocity data, Phys. Fluids, 14 (6), pp. 1851–1861.

Haller, G. (2011), A variational theory of hyperbolic Lagrangian coherent structures. Physica D, 240, pp. 574–598.

Haller, G., (2015), Lagrangian coherent structures, Annu. Rev. Fluid Mech., 47, 137–162, doi: 10.1146/annurev-fluid-010313-141322.

Olascoaga, M. J., Rypina, I. I., Brown, M. G., Beron-Vera, F. J., Koçak, H., Brand, L. E., Halliwell, G. R., and Shay, L. K. (2006), Persistent transport barrier on the West Florida Shelf, Geophys. Res. Lett., 33(22), doi:10.1029/2006gl027800.

D'Ovidio, F., et al. (2004), Mixing structures in the Mediterranean Sea from finite-size Lyapunov exponents. Geophys. Res. Lett. 31(17).

Suara, K., H. Chanson, M. Borgas ,& R.J. Brown (2017) Relative dispersion of clustered drifters in a small micro-tidal estuary, Estuarine, Coastal and Shelf Science, 194, pp. 1–15.

Suara, K., Brown, R., and Chanson, H. (2019). Characteristics of flow fluctuations in a tide-dominated estuary: Application of triple decomposition technique, Estuarine, Coastal and Shelf Science, 218, 119-130, doi:10.1016/j.ecss.2018.12.006.

Vandenbulcke, L., Beckers, J.-M., Lenartz, F., Barth, A., Poulain, P.-M., Aidonidis, M., Meyrat, J., Ardhuin, F., Tonani, M., Fratianni, C., Torrisi, L., Pallela, D., Chiggiato, J., Tudor, M., Book, J.W., Martin, P., Peggion, G., Rixen, M., (2009), Super-ensemble techniques: Application to surface drift prediction, Progr. Oceanogr., 82, pp. 149–167.

Katsanoulis, S., and Haller, G. (2019), BarrierTool Manual, Retrieved from https://github.com/LCSETH

Tang, W., Chan, P.W., Haller, G. (2011), Lagrangian coherent structure analysis of terminal winds detected by LIDAR. Part II: structure, evolution and comparison with flight data. J. Appl. Meteorol. Climatol. 50, pp. 325–338.

Sandbar switching as a factor controlling coastal erosion during storm events, Curonian Spit, Lithuania

Rasa Janušaitė, Darius Jarmalavičius, Donatas Pupienis, Gintautas Žilinskas, Viktoras Karaliūnas

Laboratory of Geoenvironmental Research, Nature Research Centre, Vilnius, Lithuania (rasa.janusaite@gamtc.lt)

1. Introduction

Research of sandy coasts has been an issue of scientific interest for years because of its primary importance for recreational and economical purposes. Major storms are one of the main drivers causing the most severe coastal erosion. Rates of coastal erosion under storm conditions are highly variable longshore (Splinter et al., 2018). This variability is determined by many factors including alongshore variations of storm surge level, incident wave height or antecedent beach, dune and nearshore morphology (Cohn et al., 2019; Splinter et al., 2018). Most of the current knowledge about the latter effect on coastal evolution under storm conditions indicates that rip current-related rhythmic patterns of nearshore sandbars induce localized coastal erosion spots (Thornton et al., 2007; Castelle et al., 2015, 2019). Furthermore, Phillips et al. (2017) suggested that nearshore sandbar morphodynamic state determines post-storm shoreline recovery rate. Although considerable amount of research has been devoted to understand connections between the subaerial domain and nearshore dynamics at a range of spatiotemporal scales (e.g., Stive et al., 1997; Aagaard et al., 2004; Umeda et al., 2018; Castelle et al., 2019), their relationship remains poorly understood (Tătui et al., 2013).

At the end of the last century bar switching as a feature of multiple bar system behavior was observed (Wijnberg, Wolf, 1994). It involves bar being discontinuous longshore and on the side of discontinuity joining landward or seaward bar (Shand et al., 2001; Shand, 2003). Bar switches might be either persistent or non-persistent in time, but zones of this bar morphodynamic phenomena are important because they separate nearshore regions with distinct bar system behavior (Walstra et al., 2016). In other words, area of bar switching is a transitional zone between multiple bar systems exhibiting different cross-shore migration rates and morphology properties. It is unknown how these transitional zones of subaqueous domain interact with subaerial domain. The most evident link between those domains might be observed during storm events when rates of coastal evolution are the highest.

In this study sandbar switching is considered as one of the factors determining coastal evolution during storm events. The primary aim of this study is to define relationship between bar switching episodes and aftereffects of high energy events in the subaerial coast. Furthermore, inter-annual persistence of bar switching locations is determined and factors controlling these locations are considered with implications for coastal erosion prediction.

2. Data and methods

Study area is located along the Baltic Sea coast of 98 km long sandy barrier known as the Curonian Spit. Investigation focuses only on northern part of the Curonian Spit (51 km) which is within the territory of Lithuania. Subaerial section of the Curonian Spit coast is characterized by sandy beaches bordered by foredune ridge. Beaches are 30 – 80 m wide and foredune height ranges from 6 to 16 m (Jarmalavičius et al., 2015; Žilinskas et al., 2018). Underwater slope of the Curonian Spit is defined by a multiple bar system. Bar zone is 250 – 750 m wide and consists of 2 – 5 longshore bars. Bar zone slope ranges from 0.009 to 0.014. Characteristics of bar zone morphology vary along the Curonian Spit shoreline. Generally, bar size, bar zone width, slope and depth increase, and number of bars decreases from north to south.

During the last two decades three major storms hit the coast of the Curonian Spit: 'Anatol' in 1999, 'Erwin' in 2005 and 'Felix' in 2015. The most severe damage was done by 'Anatol' with rate of erosion in the beach and foredune reaching 49 m^3/m on average. After 'Felix', average erosion rate was 9 m^3/m, after 'Erwin' – 0 m^3/m. In this study only storms 'Anatol' and 'Felix' is considered.

A fusion of *in-situ* and remotely sensed data was used to determine morphological characteristics of nearshore and subaerial coast before and after the storm event. Beach leveling surveys performed in 19 fixed locations were utilized to assess sand volume changes in the beach and foredune. Nearshore morphology around locations of beach cross-shore profiles was evaluated based on sandbar crest positions derived from Landsat 5 TM and Landsat 8 OLI multispectral imagery. Scenes acquired at dates from half a year before to half a year after the storm with a cloud cover up to 30% were selected for analysis. Additionally, Landsat images and available orthophotographs for the last two decades were examined to determine persistence of bar switches.

3. Results and discussion

Bar switching episodes were observed at 3 out of 19 profiles before the storm 'Anatol' and at 3 locations before the storm 'Felix'. Two of them were at the same locations at the time of both storms. The third one was observed at profiles within 1.2 km distance. During storm 'Felix' profile with realigned outer bar was moderately eroded, meanwhile, the one with continuous outer bar experienced accretion (Figure 1).

Average beach and foredune volume change at profiles with outer bar switches (-13.31 %) was significantly different from profiles without bar switches being a feature of nearshore morphology (-3.13 %) at 95 % confidence (Figure 2), indicating this phenomena as one of the factors affecting coastal evolution under storm conditions.

Further, preferred locations of bar switching episodes and their persistence in time were determined. Boundaries of sandbar realignment transitional zones were assessed. Results of this study could assist in predicting coastal vulnerability during high energy events.

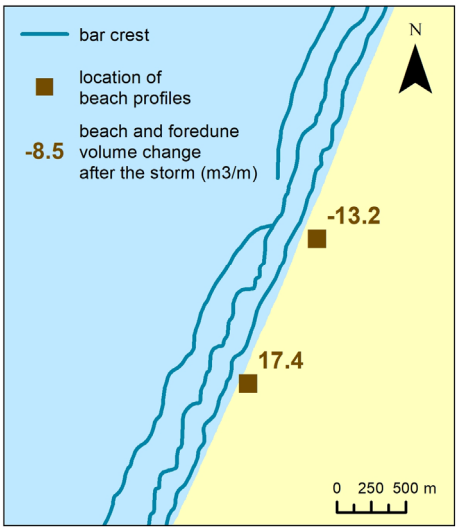


Figure 1. Rates of beach and foredune volume change after the storm Felix in 2015 at two cross-shore profiles (m^3/m) and sandbar crest positions before the storm. In the first profile (further north) where outer sandbar switched before the storm moderate erosion occurred. At the same time, second profile (further south) with continuous nearshore bar system experienced accretion.

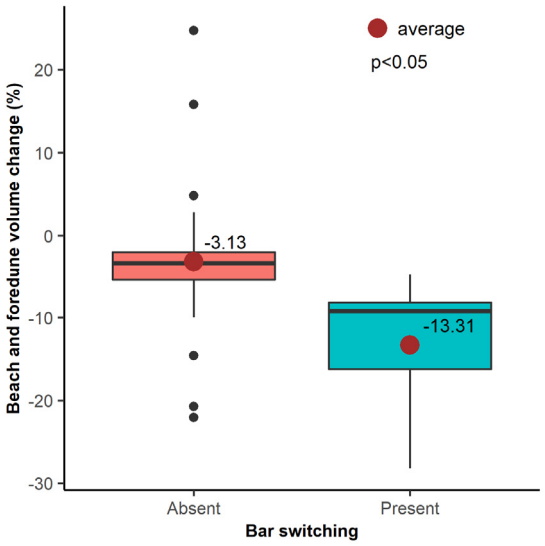


Figure 2. Boxplot comparing volume change (%) in the beach and foredune cross-shore profiles during storm events at locations where sandbar switching was absent or present.

References

Aagaard, T., Davidson-Arnott, R., Greenwood, B., Nielsen, J. (2004) Sediment supply from shoreface to dunes: Linking sediment transport measurements and long-term morphological evolution, Geomorphology, Vol. 60, No. 1–2, pp. 205–224.

Castelle, B., Marieu, V., Bujan, S., Splinter, K. D., Robinet, A., Sénéchal, N., Ferreira, S. (2015) Impact of the winter 2013-2014 series of severe Western Europe storms on a double-barred sandy coast: Beach and dune erosion and megacusp embayments, Geomorphology. Vol. 238, pp. 135–148.

Castelle, B., Marieu, V., Bujan, S. (2019) Alongshore-Variable Beach and Dune Changes on the Timescales from Days (Storms) to Decades Along the Rip-dominated Beaches of the Gironde Coast, SW France, Journal of Coastal Research SI, 88, pp. 157–171.

Cohn, N., Ruggiero, P., Garcia-Medina, G., Anderson, D., Serafin, K. A, Biel, R. (2019) Environmental and morphologic controls on wave-induced dune response, Geomorphology, Vol. 329, pp. 108 - 128.

Jarmalavičius, D., Pupienis, D., Buynevich, I. V., Žilinskas, G., Fedorovič, J. (2015) Aeolian sand differentiation along the Curonian Spit coast, Baltic sea, Lithuania, The Proceedings of the Coastal Sediments, 2015.

Phillips, M. S., Harley, M. D., Turner, I. L., Splinter, K. D., Cox, R. J. (2017) Shoreline recovery on wave-dominated sandy coastlines: the role of sandbar morphodynamics and nearshore wave parameters, Marine Geology, Vol. 385, pp. 146–159.

Shand, R. D. (2003) Relationships between episodes of bar switching, cross-shore bar migration and outer bar degeneration at Wanganui, New Zealand, Journal of Coastal Research, Vol. 19, No. 1, pp. 157–170.

Shand, R. D., Bailey, D. G., Shepherd, M. J. (2001) Longshore realignment of shore-parallel sand-bars at Wanganui, New Zealand, Marine Geology, Vol. 179, No. 3–4, pp. 147–161.

Splinter, K. D., Kearney, E. T., Turner, I. L. (2018) Drivers of alongshore variable dune erosion during a storm event: Observations and modelling, Coastal Engineering, Vol. 131, pp. 31–41.

Stive, M. J. F., Guillen, J., Capobianco, M. (1997) Bar migration and duneface oscillation on decadal scales, Proceedings of the Coastal Engineering Conference, pp. 2884–2896.

Tătui, F., Vespremeanu-Stroe, A., Preoteasa, L. (2013) The correlated behavior of sandbars and foredunes on a nontidal coast (Danube Delta, Romania), Journal of Coastal Research, pp. 1874–1879.

Thornton, E. B., MacMahan, J., Sallenger, A. H. (2007) Rip currents, mega-cusps, and eroding dunes, Marine Geology, Vol. 240, No. 1–4, pp. 151–167.

Umeda, S., Yuhi, M., Karunarathna, H. (2018) Seasonal to Decadal Variability of Shoreline Position on a Multiple Sandbar Beach, Journal of Coastal Research, Vol. 85, pp. 261–265.

Walstra, D.J., Wesselman, D., van der Deijl, E., Ruessink, G. (2016) On the Intersite Variability in Inter-Annual Nearshore Sandbar Cycles, Journal of Marine Science and Engineering, Vol. 4, No. 1, p. 15.

Wijnberg, K.M., Wolf, F.C.J. (1994) Three-dimensional behaviour of a multiple bar system, Proceedings of Coastal Dynamics'94, pp. 59-73.

Žilinskas, G., Jarmalavičius, D., Pupienis, D. (2018) The influence of natural and anthropogenic factors on grain size distribution along the southeastern Baltic spits, Geological Quarterly, Vol. 62, No. 2, pp. 375–384.

Mean sea level changes in the southwestern Baltic Sea over the last 190 years

Jessica Kelln[1], Sönke Dangendorf[2], Ulf Gräwe[3], Holger Steffen[4], Justus Patzke[5] and Jürgen Jensen[1]

[1]Research Institute for Water and Environment, University of Siegen, Siegen, Germany (jessica.kelln@uni-siegen.de)
[2] Center for Coastal Physical Oceanography, Old Dominion University, Norfolk, Virginia, USA
[3] Leibniz Institute for Baltic Sea Research Warnemünde, Warnemünde, Germany
[4] Lantmäteriet, Gävle, Sweden
[5] Technical University of Hamburg-Harburg, Hamburg, Germany

1. Introduction

Over the 20th century a global mean sea level (GMSL) rise of about 1.3 to 2 mm/yr could be observed and it is projected to further accelerate throughout the 21st century (Church and White 2006, Hay et al., 2015; Dangendorf et al., 2017). However, GMSL rise is neither temporally nor spatially uniform. Because of a number of different factors (e.g. mass changes and gravitational effects due to melting ice sheets/glaciers, expanding/contracting volume due to temperature and salinity fluctuations, ocean circulation changes, atmospheric forcing), regional mean sea level (MSL) trends can vary significantly from the global average. In order to develop sustainable coastal protection strategies, local/regional sea level studies are necessary.

In the Baltic Sea the availability of observations with some of the longest tide gauge time series in the world is excellent, but especially in the southwestern Baltic Sea MSL time series have until now only been made available and investigated at a few locations (e.g. PSMSL). This is mainly because so far only handwritten charts have been available for historic measurement periods especially before 1975. Now, after extensive digitization works, the Federal Waterways and Shipping Administration (WSV) have provided electronic high-resolution data (hourly) since about 1950 for a larger number of tide gauge stations at the German Baltic coastline. In the context of the BMBF research project AMSeL_Ostsee these high-resolution data were the first time compiled and assembled with other available data to generate a novel long and high quality monthly MSL dataset (Kelln et al. 2019). In this contribution, we present detailed analysis of MSL changes with a special focus on the southwestern Baltic coastline.

2. Methods and results

We analyze MSL records with a temporal availability of more than 19 years (to take the nodal cycle into account) and (1) calculate relative mean sea level (RMSL) trends, (2) examine interannual variations around the long-term trend, (3) assess potential changes in the rate of rise (i.e. accelerations), and (4) investigate the link to GMSL considering the influencing physical processes.

The analyses in the southwestern Baltic Sea show linear trends of the RMSL over the 20th century (1900 to 2015) from 0.93 mm/yr (Marienleuchte) to 1.67 mm/yr (Travemuende). The differences between the individual tide gauge locations are based on data gaps, local effects (e.g. wind effects, sea level pressure, baroclinic response) (Gräwe et al. 2019) and vertical land movements (VLM). RMSL changes in the Baltic Sea are dominated by VLM due to glacial isostatic adjustment (GIA) and broadly consistent with known patterns of RMSL rates-of-change due to GIA. We corrected our MSL time series for GIA by using the VLM Modell NKG2016LU of the Nordic Geodetic Commission (NKG) (Vestøl et al. 2019). The uncertainties in the estimates of RMSL changes due to GIA are still large, especially for the southwestern Baltic coastline, since it is located in the transition area between land uplift and subsidence due to GIA. Furthermore, monthly MSL changes are characterized by considerable interannual variability with distinct differences to the neighboring stations from the North and Baltic Seas. The long-term GIA corrected mean sea level trend for 1900 to 2015 is estimated to be 1.2 ± 0.1 mm/yr for the southwestern Baltic coastline and lies at the lower limit of current GMSL trend estimators (1.3 to 2 mm/yr) due to regional effects. Mainly responsible are the dominant westerly winds redistributing the water from the southwestern to the northeastern Baltic coast, but at the same time leading to balancing water inflows from the North Sea (see also Gräwe et al. 2019). Furthermore, the investigations show acceleration tendencies in the rates of increase since the end of the 19th century with slight interruptions in the middle of the 20th century.

References

Church, White (2006) A 20th century acceleration in global sea-level rise. In: Geophysical Research Letters, Jg. 33, 1, n/a. doi: 10.1029/2005GL024826.

Dangendorf et al. (2017) Reassessment of 20th century global mean sea level rise. In: Proceedings of the National Academy of Sciences of the United States of America, Jg. 114, 23, 5946-5951. doi: 10.1073/pnas.1616007114.

Gräwe, Klingbeil, Kelln, Dangendorf (2019) Decomposing mean sea level rise in a semi-enclosed basin, the Baltic Sea. In: Journal of Climate, doi: 10.1175/JCLI-D-18-0174.1.

Hay et al. (2015) Probabilistic reanalysis of twentieth-century sea-level rise. In: Nature, Jg. 517, 7535, 481-484. doi: 10.1038/nature14093.

Kelln, Dangendorf, Jensen, Patzke, Fröhle (2019) Monthly sea level from tide gauge stations at the German Baltic coastline (AMSeL_Baltic Sea). PANGAEA, https://doi.pangaea.de/10.1594/PANGAEA.904737

PSMSL (2016) Tide Gauge Data. Retrieved 26 Feb 2016 from. http://www.psmsl.org/data/obtaining/

Vestøl, Ågren, Steffen, Kierulf, Tarasov (2019) NKG2016LU: a new land uplift model for Fennoscandia and the Baltic Region. In: Journal of Geodesy, Jg. 93, 9, 1759-1779, doi: 10.1007/s00190-019-01280-8.

High water level variability in the North Sea and Baltic Sea and objective weather types

Jens Möller and Peter Löwe

Federal Maritime and Hydrographic Agency (BSH), Hamburg, Germany (jens.moeller@bsh.de)

1. Introduction

The German Federal Ministry of Transport and Digital Infrastructure (BMVI) initiated the Network of Experts "Knowledge–Ability–Action" to share expertise between its transport agencies and research institutes to advise on and face common challenges. As a consequence of climate change, atmospheric and oceanographic extremes and their potential impacts on coastal regions are of growing concern to BMVI, responsible for the transportation infrastructure. Highest risks for coastal shipping, coastal protection structures and dewatering low-lying land originate from combined effects of extreme storm surges and heavy rainfall, which sometimes lead to insufficient dewatering of inland waterways. The BMVI therefore has tasked its Network of Experts to investigate the possible increase of joint high water level and high precipitation events. In this study we present results of a comparison of observed sea level variability near the German coast of the North Sea and the Baltic Sea as well as an analysis of their occurrence with certain weather types. We show that extreme water level or precipitation (exceeding the 95 th percentile eventuate together with only two or three weather types most of the time. We also demonstrate the change in frequency of these weather types in the future with the coupled MPI-OM climate model.

2. High water levels and related weather types

The analysis of the dependence of extreme high water levels on weather types was carried out for the southeastern North Sea (German Bight) and the southwestern Baltic Sea. In the German Bight, extreme high water levels presently concur with northwesterly winds (see Fig. 1), while at the German coast of the Baltic Sea they occur conjointly with northeasterly winds. Potential future changes in the strength of these relationships are derived from climate projections from a coupled regional climate model (MPI-OM). While the relationship between extreme water levels and wind directions is not surprising, a less obvious dependence of extreme water levels on the rotational character of near-surface and mid-tropospheric flow will also be discussed.
Finally, results on changes in conjoint events of water level and high precipitation as derived from MPI-OM model-output are presented. While the increase in total frequency of such events would appear small (+5%), the increase in runlength of such events is found to be much larger.

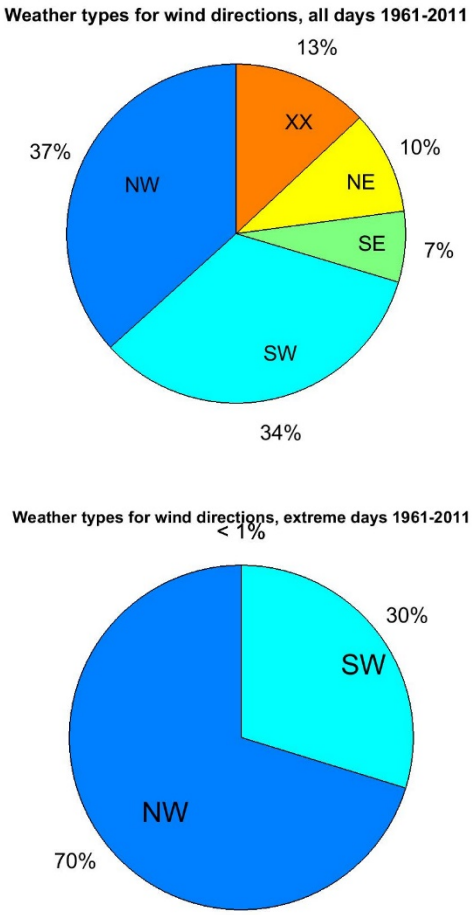


Figure 1. Ratio of different weather types related to wind directions (NW: north-westerly, SW: south-westerly, SE: south-easterly, NE: north-easterly, XX: no prevailing wind direction) in the German Bight for all days between 1961-2011 (top) and days with water levels higher than 95 percentile (bottom).

The impact of dredging works performed during construction of an offshore Wind Farm upon the adjacent areas of the Baltic Sea

Anna Przyborska, Jaromir Jakacki

Institute of Oceanology of the Polish Academy of Sciences, Sopot, Poland, Stockholm, Sweden (aniast@iopan.gda.pl)

1. Introduction

This paper presents the analysis of spreading and sedimentation of material generated while performing construction works on the seabed connected with erection of an Offshore Wind Farm. The analyzed, theoretical investment is located in the central part of the South Baltic Sea, at the foot of the northern slopes of the Słupsk Bank, about 55 km north of Ustka (Figure *1*).

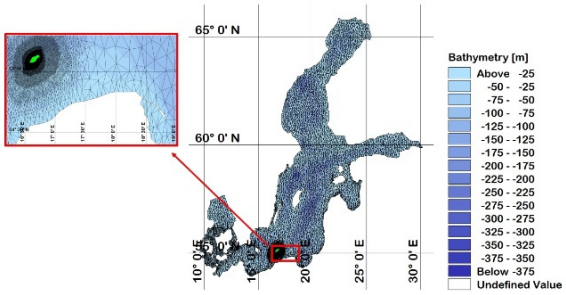


Figure 1 Location of the study area (green polygon), model domain and bathymetry

The Wind Farm area covers approximately 40 km². The offshore wind turbine installation includes dredging work to prepare the seabed for the installation the foundations of wind generators. Any disturbance of anthropogenic nature, even a minor one, more or less disrupts the structure of the water column and sediment(Tyrrell (2011), Newell et al. (1998)). This structure usually returns to normal state after a certain amount of time, which depends on the level of disturbance. The impact of dredging works depends on the method of dredging, the volume of disturbed sediment and type of seabed.

During works, the heavy fraction falls to the bottom immediately, whereas the light fraction creates a suspended matter in the water column. The suspended sediment resulting from dredging works gradually moves and settles. Its range and concentration depend on its initial amount as well as the value and direction of currents and waving.

2. Materials and methods

The assessment of the impact of dredging works upon spreading of the suspended matter has been carried out based on numerical model. The modelling approach of this area that permits to assess the influence of dredging works on the adjacent area requires implementation of quite a complicated system of models (*Figure 2*).

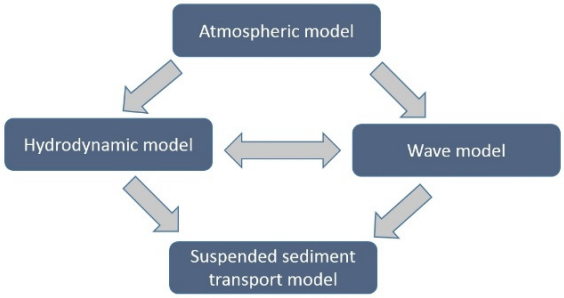


Figure 2 Coupled model diagram

A model has been built based on MIKE by DHI (MIKE Doc. (2010-2014)), a tool provided by the Danish Hydraulic Institute (DHI) and the Weather Research and Forecasting model WRF (Skamarock (2008)) - mesoscale numerical weather prediction system. The atmospheric data, after their verification and validation have been used as an input force in the hydrodynamic and wave model. The results of the models (after validation) have been additionally used as a force in the suspended sediment transport model.

The developed numerical model allowed to analyze the maximum distance which a suspension of sediments generated during seabed works can travel as well as the thickness and extent of the suspension deposited on the seabed.

3. Results

The results show that during installation works performed for one wind farm, the suspended sediment concentration level considered harmful to cod larvae (10 mg/l) will be maintained for no more than 42 hours.

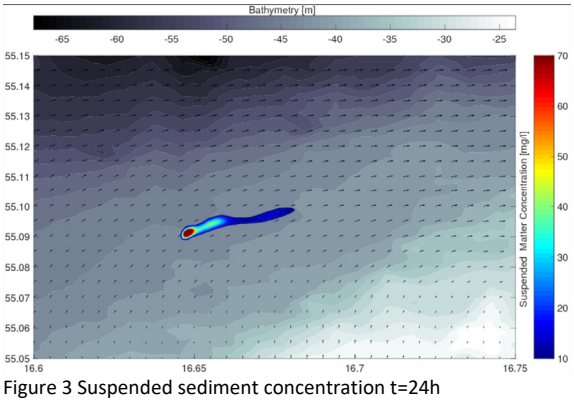


Figure 3 Suspended sediment concentration t=24h

After this time, the concentration of the suspended matter will fall below 10 mg/l. The extent of the impact of the suspended sediment depends mainly on the sea currents. The concentration of suspended sediment largely depends on the location of the measurement points. Maps of the maximum concentrations for the entire area of analysis recorded during a 10-day simulation are shown in figure (Figure *4*).

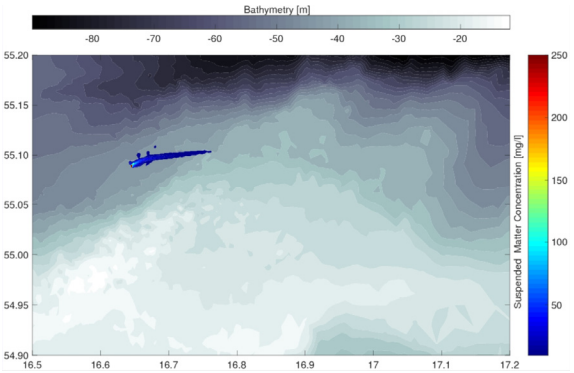


Figure 4 Distribution of the maximum concentration of suspended sediment

The deposition map (Figure *5*) shows that the bottom level changes are minor.

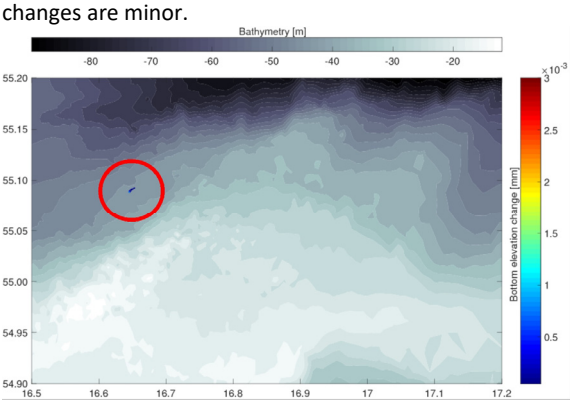


Figure 5 Deposit of sediments during construction work

The deposition reaches a level of the order of a millimeter during and after the dredging operations so the impact may be considered as negligible.

A higher velocity of sea currents will cause a greater degree of deformation and thus a greater energy dissipation, and consequently, although the impact area of the suspended sediment will be greater, its concentration will decrease much faster, which will significantly reduce the area for which the concentration of the suspended matter will be greater than a defined threshold.

4. Final remarks

The analysis shows that the suspended sediment concentration resulting from dredging works related to the construction of the planned wind generators will remain at a level higher than 10 mg/l for maximum 48 hours. The largest range of the spreading suspended matter was observed in the wind farm area. The extent of movement of the suspended matter will not exceed 15 km.

The impact of dredging works performed during construction of an offshore Wind Farm is at a level of 15 km, with a change in the bottom level not exceeding a millimeter for the entire area occupied by the suspended matter. Maximum values will occur at the work sites and will decrease with the distance from the site of the dredging works.
Cumulative effects, when simultaneous actions are taken to prepare the foundations for more than one wind farm at a time, significantly increase the concentration of the suspended sediment. In order to avoid the cumulative effects, simultaneous works should not be carried out at distances shorter than 2 km.

As a result of disturbance of marine sediments during the assembly of wind turbines at sea, water transparency will temporarily decrease and as a result some species of fish and marine mammals can temporarily avoid the area of works but such a situation may cause the emergence of new species in the investment area, attracted by new sources of food.

The scale of influence is regional. The impact is of short duration, generally of local nature, and it is likely that the species that will leave the investment area for the duration of the construction will return to it once the works are complete.

References

Jakacki J., Meler S., (2019) An evaluation and implementation of the regional coupled ice-ocean model of the Baltic Sea, Ocean Dynamics, January 2019, Volume 69, Issue 1, pp 1–19

MIKE and Doc. (2010–2014) MIKE 21 MIKE 3 Flow Model FM. Hydrodynamic Module, Sci. Doc., DHI Water and Enviornment, Hørsholm, Denmark

Newell R. C., Seiderer L. J., Hitchcock D. R., (1998) The impact of dredging works in coastal waters: a review of the sensitivity to disturbance and subsequent recovery of biological resources on the sea bed, Oceanography and Marine Biology: an Annual Review, 36,127-78

Skamarock W., Klemp J., Dudhia J., Gill D., Barker D.M., Duda M.G., Huang X.Y., Wang W., Powers J., (2008) A description of the advanced research WRF. Version 3, NCAR Technical Note, NCAR/TN–475+STR, available at http://www2. mmm.ucar.edu/wrf/users/docs/arw_v3.pdf (data access 23.02.2017)

Tyrrell T. (2011), Anthropogenic modification of the oceans, Philosophical Transacttions of the Royal Society, A369, 887–908

ESA Baltic+ SEAL: Using the Baltic Sea as a test-bed for developing advanced, regionalised sea-level products

Laura Rautiainen[1], Laura Tuomi[1], Jani Särkkä[1], Milla Johansson[1], Felix L. Müller[2], Marcello Passaro[2], Adili Abulaitijiang[3], Ole B. Andersen[3], Denise Dettmering[2], Jacob L. Høyer[4], Julius Oelsmann[2], Ida M. Ringgaard[4], Eero Rinne[1], Rory Scarrott[5], Christian Schwatke[2], Florian Seitz[2], Kristine Skovgaard Madsen[4], Americo Ambrozio[6*], Marco Restano[6**], Jérôme Benveniste[6]

1 Finnish Meteorological Institute (FMI), Finland
2 Deutsches Geodätisches Forschungsinstitut, Technische Universität München (DGFI-TUM), Germany
3 SPACE National Space Institute, Technical University of Denmark, (DTU), Denmark
4 Danish Meteorological Institute (DMI), Denmark
5 MaREI Centre, Department of Geography, Environmental Research Institute, University College Cork (UCC), Ireland
6* DEIMOS, c/o ESA-ESRIN, Italy 6** SERCO, c/o ESA-ESRIN, Italy 6 ESA-ESRIN, Italy

The Baltic Sea opportunity

For sea level studies, coastal adaptation, and planning for future sea level scenarios, regional responses require regionally-tailored sea level information. Global sea level products are now available through the European Space Agency's (ESA) Climate Change Initiative. These are derived using measurements from satellite altimeters. However, these global approaches are not entirely appropriate for supporting regional actions. Complications arise when coastal areas and sea-ice contaminate the altimeter's footprint.
This places the Baltic Sea at the forefront of efforts to understand and circumvent these issues. Its low tidal signal, complex coastlines, thousands of small islands in the coastal archipelagos, and seasonal sea-ice conditions, provides a near-perfect test-bed to explore the coastline and sea-ice issues. Also, regional investment has ensured the availability of high quality, long-term tide gauge data to suppor validating any new sea-level products.

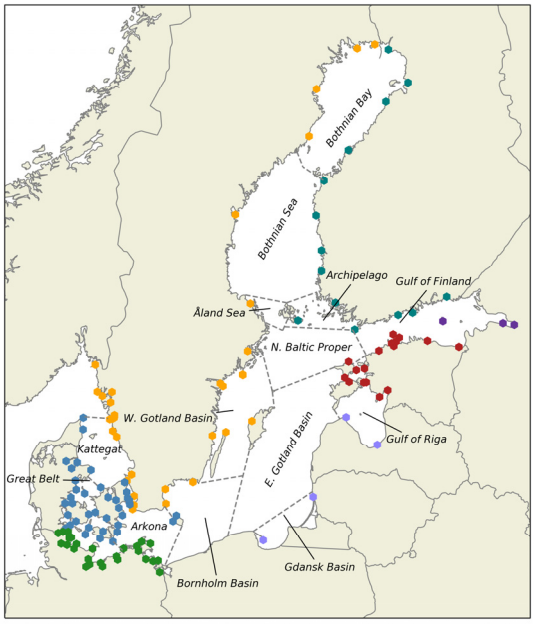


Figure 1. All the tide gauges in the Baltic Sea. Annotations coloured by country: Blue for Denmark, green for Germany, orange for Sweden, purple for Poland, Latvia and Lithuania, dark purple for Russia, red for Estonia and teal for Finland.

Advancing state-of-the-art in sea level altimetry

Developing regional sea-level products fit for coastal purposes requires expertise, and advanced tools for pre-processing the data before use. The ESA-funded Baltic SEAL project is developing such state-of-the-art methodologies to develop and validate a novel multi-mission altimeter sea level product for coastal areas. New technological improvements (e.g. Delay-Doppler / SAR altimetry) enable advanced solutions in pre-processing and post-processing, for which the Baltic Sea as a semi-enclosed area with plenty of long-running observations, provides a laboratory for testing. Such advances include:

- The homogenous retracking strategy applied for open-ocean, coastal and sea-ice conditions (ALES+),
- The unsupervised classification method based on artificial intelligence developed to detect radar echoes reflected by open-water gaps within the sea-ice layer, and
- The multi-mission cross-calibration, which allows the user to exploit along-track data from the full constellation of altimetry missions in combination
- The development of the gridded product based on a triangulated surface mesh, characterised by a spatial resolution higher than 0.25° degree and enhanced utility for coastal areas.

Building on international investment in tide gauge infrastructure

The envisioned products aim to provide a consistent description of the Baltic Sea's sea-level variability in terms of long-term trends, seasonal variations and a mean sea-surface that is available for users from all backgrounds and levels of expertise. Product development benefits from the region's long-running history and expertise in tide gauge measurements, dating back to the 18th century. Currently, quality-flagged data, collected from the national data providers, are readily available from the Copernicus Marine Environment Monitoring Service. There are also national open data services which provide data, such as datasets hosted by the Finnish Meteorological Institute (FMI), Danish Meteorological Institute (DMI), and the Swedish Meteorological and Hydrological Institute (SMHI).
Currently, there are several national height coordinates used for sea level data in the Baltic Sea. These were unified to the EVRF2007 system, and the effect of vertical land motion was

removed by detrending the tide gauge time series. In addition to vertical land motion, sea level in the Baltic Sea varies geographically and on multiple time scales from short to long, due to changes in sea level pressure, wind patterns, presence of sea ice, precipitation and thermosteric effects. Although there are many tide gauges available, the validation of the altimeter data can only be performed with the tide gauges that are located near the altimeter track points. This limits the amount of tide gauges that can be used for validation. This is pronounced in certain areas, for example, in the eastern coast of the Baltic Proper, where the tide gauges are sparse.

Unlocking regional opportunities for sea-level studies and coastal adaptation

The Baltic SEAL project will provide a consistent description of sea level, to support regional sea-level studies, coastal adaptation, and future-proofing coastal communities. A focus on ensuring products capture seasonal and inter-annual variations, at scales fine enough for coastal applications, will aid identifying the forcings associated with the variability. A new, reliable altimetry dataset could also improve the characterisation of circulation in the Baltic Sea. Furthermore, after establishing an advanced processing chain for the Baltic Sea, the strategy can be adapted for other regions. This of particular interest for initiatives such as the Sea Level ESA-CCI programme, which is currently promoting the development of dedicated products for regional sea level analysis.

Acknowledgements

The Baltic SEAL project is an eighteen month project funded by the European Space Agency (ESA), under the remit of the Earth Observation Envelope Programme 5 (EOEP5) Regional Initiative, through contract no. 4000126590/19/I-BG. For more information on the Baltic+ SEAL project, see www.balticseal.eu.

Overview of remote sensing methods for run up tracing after high energy events on sandy beaches, Baltic Sea coast, Lithuania

Kristina Viršilaitė[1], Donatas Pupienis[1,2]

[1]Institute of Geosciences, Vilnius University, Vilnius, Lithuania (kristina.virsilaite@chgf.stud.vu.lt)
[2]Nature Research Center, Vilnius, Lithuania

1. Abstract

The study discusses the methods of wave run up evaluation on the southeastern Baltic Sea coast of Republic of Lithuania, extending 90.66 km from the Latvian border to the border with the Russian Federation. The Lithuanian continental coast (38.5 km) belongs to accumulative-abrasive coastal type, and the Curonian Spit (51.0 km) is the largest accumulative coastal landform in the Baltic Sea region, which was formed on the remnant of a glacial moraine as a result of sand accumulation by alongshore sediment transport (Jarmalavičius et al., 2012; Pupienis et al., 2017; Žilinskas et al., 2018). During storm season beaches are flooded due to elevated wave height and set-up, therefore the margin of the floodwaters can reach the foot of the foredune. The upper limit of the wave run up is an informative indicator of the high energy event as it directly depends on the hydrometeorological conditions. However, the storm-caused impact on the coastal zone can only be assessed by surveying the aftermath. Previously the evaluations were made by estimating the total washed sand volume (Jarmalavičius et al., 2015), however geological sedimentary studies are more informative as upper run up limits can be measured (Jagodziński et al. 2008; Pupienis et al. 2013). Recently run up measurement approaches employing empirical calculations, numerical modelling and remote sensing became more favourited (Paprotny et al., 2014, Gutiérrez et al., 2014; Staneva et al., 2016).

The aim of this study is to overview the available remote sensing resources for the run up detection for the case study area of Baltic Sea Coasts, Lithuania.

2. Introduction

One of the greatest challenges posed by the climate change for the future generations is the rise of the global sea level. According to the IPCC (Intergovernmental Panel on Climate Change) forecast, by the 22nd century the average global ocean level will rise between 0.26 and 0.98 m. With the risen global sea level, the frequency of moderate and extreme storms is expected to increase, causing beaches and nearby settlements being frequently flooded (Goodwin et al., 2017). Due to the increased likelihood of high energy events, there has recently been considerable research on the effects of storms (Swindles et al., 2018). These studies are important to assess the resilience of the coast and to provide insight into future planning of the urban infrastructure. In some countries, data on extreme flood events have begun to be collected and databases have been compiled that include detailed records of recent centuries, information of relic evidence found on geological surveys (Kortekaas et al., 2007; Bateman et al., 2018). On the swash zone of sandy beaches extreme floods, storm magnitude and intensity can be traced back to the highest flow limit, i.e. the seam left by the wave run up, which is formed by waves breaking and periodically flooding the beach. The flow-formed seam can be distinguished by the presence of heavy minerals and phytodetritus samplers or by the boundary of wet sand.

Previously the highest limit of the run up was identified during *in situ* field studies by measuring the characteristics of sand: granulometry, mineralogy or magnetic properties (Linčius, 1991; Jagodzinski et al., 2008; Pupienis et al., 2011) (Fig. 1). However, such surveys would be carried out once or couple times per year which left many extreme storm events unstudied, likewise scarcity of monitoring caused difficulties in interpreting the data. Growing potential of remote sensing technologies would suggest a new approach – a supplement to storm effect studies.

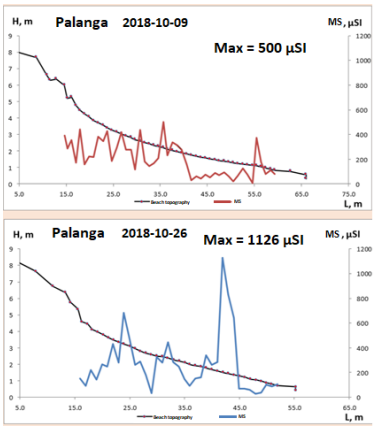


Figure 1. Changes in magnetic susceptibility and beach topography before and after the storm of October 22-25, 2018 (*in situ* data from 2018-10-08 and 2018-10-26).

3. Methods

Due to the need for high resolution, remote sensing resources are relatively limited: high definition satellites are commercial, thus data is not open access. The high-resolution raster satellite image examples used for this study were compiled from *Google Earth* software, all images made by the satellites of *Maxar Technologies*. The best quality and distinctive beach sediment images were selected and regarding the quantity of imagery, characteristic parameters (deposits, run up flow seams) were analyzed.

Visual analysis of data (data availability, resolution, quality and utilization) was performed on ortho-photos and imagery resources *of Google Earth* and unmanned aerial vehicles (UAV). Raster image processing analysis using ArcGIS software was performed to evaluate remote sensing capabilities (color RGB compositions).

Hydrometeorological data (wind speed and direction, wave height, water level) collected from LHMT (Lithuanian Hydrometeorological Service) and EPA (Environmental Protection Agency) Marine Research Department of Klaipeda were also considered when evaluating run up seam evolution in time frame.

4. Results

Raster image analysis using remote sensing methods showed that:

• In the vast majority of profiles, the run up seam is visible in the central part of the beach, but due to coastal morphometry this position may differ between profiles. Similarly, the upper run up limit in the same profile may vary seasonally or due to storm-induced flooding.

• Analysis of satellite data over time has shown that under favourable hydro-meteorological conditions and in the absence of major flood events, the seam of highest run up limit – a relic of previous storm - can be seen for several months, and deposits of aeolian origin – even longer.

The results of *in situ* and remote data verification will be presented during the conference.

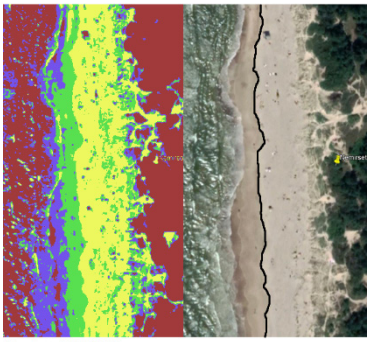


Figure 2. Run up limit detection in terms of dry/wet sand properties. Raster analysis was performed using ArcGIS software.

5. Discussion and Conclusions

Due to the high resolution, analysis of UAV imagery proved to be the most accurate method for upper limit detection, however due to the nature of available imagery database for this study, identification of the highest run up limit was not successful because of the low contrast between wet and dry sand, and barely visible heavy mineral deposits. Nevertheless, authors conclude that if this study was conducted on a beach with characteristic traces of a storm, complemented by *in situ* measurements the study would likely be more effective.

The selected satellite imagery which was of a lower resolution, had visually better contrast between damp and dry sand but large time breaks between images did not allow for a more detailed analysis of the run up seam evolution. As previous studies have shown, detailed analysis requires continuous observation and *in situ* monitoring.

6. Acknowledgments

This study was supported by the Lithuanian Science Council (Grant No. 09.3.3-LMT-K-712-16-0159).

References

Bateman, M.D., Rushby, G., Stein, S., Ashurst, R.A., Stevenson, D., Jones, J.M., Gehrels., W.R. (2018). Can Sand Dunes be used to Study Historic Storm Events? Earth Surface Processes and Landforms, 43(3), 779-790.

Goodwin, P., Haigh, I.D., Rohling, E.J., Slangen, A. (2017). A new approach to projecting 21st century sea-level changes and extremes. Earth's Future, 5, 240–253.

Gutiérrez, O., Aniel-Quiroga, Í., González, M., & Guillou, L. (2014). Tsunami run up in coastal areas: A methodology to calculate run up in large scale areas. Proceedings of the Coastal Engineering Conference, 2014-Janua, 1–5.

Jagodziński, R., Sternal, B., Szczuciński, W., & Lorenc, S. (2009). Heavy minerals in 2004 tsunami deposits on Kho Khao Island, Thailand. Polish Journal of Environmental Studies, 18(1), 103–110.

Jarmalavičius D., Satkūnas J., Žilinskas G., Pupienis D. (2012). Dynamics of beaches of Lithuanian coast (the Baltic Sea) for the period 1993-2008 based on morphometric indicators. Environmental Earth Sciences, 65(6). 1727-1736.

Jarmalavičius, D., Žilinskas, G., & Pupienis, D. (2015). Stipraus štormo „Feliksas“ padariniai Lietuvos jūriniame krante. Geologija. Geografija, 1(1), 10–21.

Kortekaas S., Dawson A.G. (2007). Distinguishing tsunami and storm deposits: an example from Martinhal, SW Portugal. Sedimentary Geology, 200 (3-4), 208-221.

Linčius A. (1991). Baltijos jūros pietrytinės pakrantės sąnašynai kaip ilgalaikių gamtinių procesų padarinys. Geografijos metraštis, 27. 122-127.

Paprotny, D., Andrzejewski, P., Terefenko, P., & Furmańczyk, K. (2014). Application of empirical wave run-up formulas to the polish baltic sea coast. PLoS ONE, 9(8), 1–8.

Pupienis D., Buynevich I. V., Bitinas A. (2011). Distribution and Significance of Heavy-Mineral Concentrations along the Southeast Baltic Sea Coast. Journal of Coastal Research, SI 64, 1984–1988.

Pupienis, D., Buynevich, I. V., Jarmalavičius, D., Žilinskas, G., Fedorovič, J. (2013). Regional distribution of Heavy-mineral concentrations along the Curonian Spit coast of Lithuania. Journal of Coastal Research, 165(65), 1844–1849.

Pupienis, D., Buynevich, I.V., Jarmalavičius, D., Žilinskas, G., Fedorovič, J., Ryabchuk, D., Kovaleva, O., Sergeev, A., & Cichon-Pupienis, A. (2017). Spatial patterns in heavy-mineral concentrations along the Curonian Spit coast, southeastern Baltic Sea. Estuarine, Coastal and Shelf Science, 197(5), 41-50.

Staneva, J., Wahle, K., Koch, W., Behrens, A., Fenoglio-Marc, L., & Stanev, E. V. (2016). Coastal flooding: Impact of waves on storm surge during extremes – A case study for the German Bight. Natural Hazards and Earth System Sciences, 16(11), 2373–2389.

Swindles, G. T., Galloway, J. M., Macumber, A. L., Croudace, I. W., Emery, A. R., Woulds, C., … Barlow, N. L. M. (2018). Sedimentary records of coastal storm surges: Evidence of the 1953 North Sea event. Marine Geology, 403(June), 262–270.

Žilinskas, G., Jarmalavičius, D., Pupienis, D. (2018). The influence of natural and anthropogenic factors on grain size distribution along the southeastern Baltic spits. Geological Quarterly, 62(2), 375–384.

Applicability assessment of multi-date medium resolution satellite remote sensing data for detection and interpretation of coastline fluctuations: case study Russian part of the eastern Gulf of Finland

Eugenia Volynets, Aleksandr Volynetc and Evgeniy Panidi

Department of Cartography and Geoinformatics, Institute of Earth Sciences, Saint Petersburg University, St. Petersburg, Russia, (evgenia59â€007@mail.ru)

1. Introduction

Coastal zone monitoring plays a significant role in environmental protection (Rasuly A., 2010). Detection and monitoring of coastlines should be regarded as a fundamental research economic and social importance as a key element for coastal resource management, coastal environmental protection and sustainable coastal development and planning. In the current study we have taken a close look at the coastal zone of the Russian part of the eastern Gulf of Finland (including the shore of the Neva Bay), which is characterized by a specific regime of morphodynamics caused by fluctuations of the sea level, seasonal ice-forming processes and different intensive anthropogenic activities.

Main goal of the study is an assessment of applicability of medium resolution satellite images for detection and interpretation of coastline and its fluctuations in area located in eastern Gulf of Finland for monitoring and effective strategy planning for coastal protection.

2. Materials and methods

Multi-date satellite images have been used to demarcate shoreline positions - a set of Landsat and Sentinel time-series from year 2000 till the end of 2018 during the ice-free interval between May to October which include Landsat 7, 8 and Sentinel-2 were processed. Landsat archive still the best source of data available as it is very important considering the both long-time data acquisition and relatively high temporal resolution.

Delineation of shoreline boundary could be marked as a challenging task due to several reasons such as coastal movement because of erosion, water turbidity as well as marshy areas along the coast most of which are misclassified as parts of water. Pixels quite often represent the mixture of different spatial classes because of relatively coarse spatial resolution.

In this paper, various semi-automated methods have been accordingly applied: NDWI (satellite-derived index from the Near-Infrared (NIR) and Short Wave Infrared (SWIR) channels; although the NDWI index was created for Landsat Multispectral Scanner (MSS) images, it has been successfully used with other sensor systems including SENTINEL to detect open water) (Gao, 1996), MNDWI (Modified NDWI, where near infrared band replaced by shortwave infrared band) (Seynabou T., 2019), AWEI (Automated Water Extraction Index, improving classification accuracy in areas that include shadow and dark surfaces that other classification methods such as MNDWI often fail to classify correctly) (Sharma R.C., 2015), EWI (Enhanced Water Index, provides discrete mask of the surface water and non-water, but not the continuous measure of the wateriness of the land surface) (Jason Yang, 2017).



Figure 1. Study area.

3. Results and discussion

Results were analyzed with GIS methods - it shows annual and mid-term coastline fluctuations, that were assessed in the context of the applicability of approach for shoreline detection and interpretation. Comparative analysis of the indexes and received extracted coastlines was implemented.

It has been found that the coastal zone of the Eastern Gulf of Finland is actively changed under the influence of complicated natural and anthropogenic factors. The result of the shoreline fluctuations including erosion and swamps formation is possible to observe using remote sensed data. It shouldn't be noted that erosion has devastating effect on coastal areas - according to the results of coastal monitoring undertaken by A.P. Karpinsky Russian Geological Research Institute (VSEGEI) (Sergeev, A, 2018), the remote sensing data show that the average rates of shoreline retreat within the Kurortny District (recreation zone situated in the north-western part of St. Petersburg) are 0.5 m/year, the maximum rates reach 2 m/year and as a consequence there are road, building havoc and, for the most part, decrease of a unique valuable area for recreation of St. Petersburg. The total beach recession in the period of 1990–2005 reached values as high as 25–40 m in the vicinity of Serovo, Ushkovo, and Komarovo villages.

A significant outcome of this study will provide an opportunity to make a reliable prediction of the coastal zone development as well as effective strategy for coastal protection for integrated coastal zone management.

References

Seynabou Toure, Oumar Diop, Kidiyo Kpalma, Amadou Seidou Maiga (2019) Shoreline Detection using Optical Remote Sensing: A Review, International Journal of Geo-Information

Sharma, R.C.; Tateishi, R.; Hara, K.; Nguyen, L.V. (2015) Developing Superfine Water Index (SWI) for Global Water Cover Mapping Using MODIS Data, Remote Sens.

Rasuly, A.; Naghdifarb, R.; Rasoli, M. (2010) Monitoring of Caspian Sea Coastline Changes Using Object-Oriented Techniques, International Society for Environmental Information Sciences 2010 Annual Conference, Procedia Environ. Sci., 416–426

Sergeev, A., Ryabchuk, D., Zhamoida, V., Leont'yev, I., Kolesov, A., Kovaleva, O., Orviku, K., (2018) Coastal dynamics of the eastern Gulf of Finland, the Baltic Sea: toward a quantitative assessment, Baltica, 31 (1), 49–62

Gao, B.-C. (1996) NDWI—A normalized difference water index for remote sensing of vegetation liquid water from space, Remote Sens. Environ, 257–266

Jason Yang & Xianrong Du (2017) An enhanced water index in extracting water bodies from Landsat TM imagery, Annals of GIS, 23:3, 141-148

Characteristics of seasonal changes of the Baltic Sea extreme water levels

Tomasz Wolski[1], Bernard Wiśniewski[2]

[1] Institute of Marine and Environmental Sciences, University of Szczecin, Szczecin, Poland (natal@univ.szczecin.pl)
[2] Institute of Marine Navigation, Maritime University of Szczecin, Szczecin, Poland

1. Introduction

Fluctuations in water levels are an important element of the hydrodynamic processes that occur in the coastal zone. Particularly extreme sea levels, i.e. the highest and lowest levels recorded in many years, in the course of a year or during a given storm event, can stimulate current processes, sea abrasion and accumulation of sedimentary material in different sections of the coastal zone. High sea levels, usually of a stormy nature, often lead to catastrophic situations, such as loss of shore, beach disappearance, as well as destruction of shore infrastructure. Storm storms flood low-lying areas of the coastal zone, which are usually densely populated and heavily exploited economically. On the other hand, low sea levels cause significant disruptions to shipping by diminishing depths on fairways to ports and at the port's seafront.

The aim of this study is to characterize the seasonal changes of extreme water levels along the whole Baltic Sea coast on the basis of hourly observations.

2. Materials and methods

Material research included hourly sea level observation data from 37 gauges stations located along the Baltic Sea coasts from the period 1960-2010 and 8 gauges stations with a shorter observation series. Such period was chosen as the longest possible one that could provide sea level data from national meteorological and hydrological institutes of Baltic countries (Poland, Germany, Denmark Sweden, Finland, Estonia, Latvia, Lithuania). Hourly sea level data were corrected to the single vertical datum which is NAP in the practical realization of the EVRS system called EVRF 2000. Basic calculations were done using the Coordinate Reference Systems in Europe (CRS EU). Details and examples of these calculations have been previously presented in another study by the authors - Wiśniewski et al. (2014) .

In order to present the seasonal variability of sea levels, the spatial distribution of time of occurrence (average monthly number of hours) of high (≥70 cm relative to the zero point of a sea level gauge) and low (≤-70 cm relative to the zero point of a sea level gauge) sea levels in subsequent months of the year has been determined. This research result has been visualised in the form of maps of the Baltic Sea coastline in the ArcGis programme. Kriging was the main ArcGIS module that was a basis of spatial analysis.

The influence of circulation variability on extreme sea levels has been confirmed by the study of the degree of relationship (correlation coefficient) between the analyzed, maximum and minimum (as well as average) water levels of the Baltic Sea and the NAO and AO zonal circulation indices for individual months of the year and seasons in the 1960-2010 period. Data on the value of monthly NAO circulation indicators were taken from the Climatic Research Unit, University of East Anglia. The monthly indexes for AO were taken from the National Oceanic and Atmospheric Administration (NOAA, Climate Prediction Center , National Weather Service) .

3. Results and discussion

The duration of high levels is longest in the year for January and ranges from 10 to more than 50 hours on average per month for most of the Baltic Sea basins with intensity in the north and east coasts. On the other hand, the duration of low levels in the same month is between 10 and 20 hours for the Western Baltic Sea and a smaller number of hours for the other Baltic Sea areas (Fig. 1 a,b).

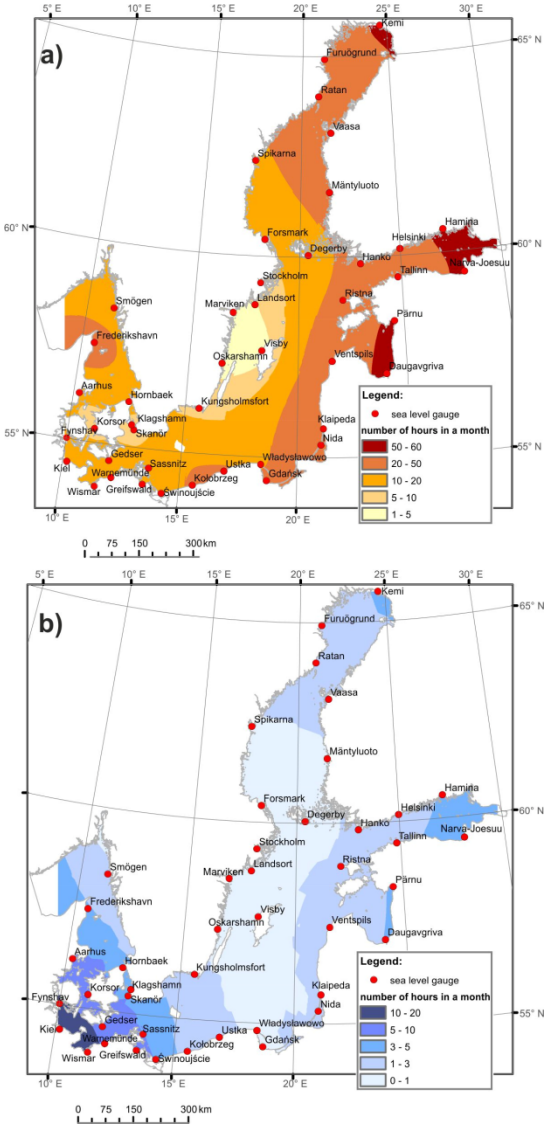


Figure 1. Time of occurrence (number of hours) in January : a) high sea levels ≥ 70 cm b) low sea levels ≤-70 cm

Duration time of extreme sea levels increase from the open sea waters of the Baltic Sea (Baltic Proper) to the innermost parts of its bays (Gulf of Bothnia, Gulf of Finland, Gulf of Riga, Bay of Mecklenburg and Bay of Kiel). The responsibility for this situation is taken by the so-called bay effect, i.e. the impact of geomorphological and bathymetrical configuration of the coastal zone on water dynamics (Wolski et al. 2014; Wolski et al. 2016).

The annual duration of extreme sea levels is well correlated with the number of storm surges, which prevail in the autumn-winter months.

Study of the degree of relationship between the analyzed, maximum and minimum (as well as average) sea levels and the NAO and AO zonal index indicate the strongest relationship in the winter months and later in the autumn. Thus, the influence of circulation variability on extreme sea levels has been confirmed

Another regularity that can be observed in the analyses is the spatial differentiation of correlation and its increase in value on the main axes of the Baltic Sea from west to east and from south to north, especially well visible in the autumn-winter months . Such variation may be due to the fact that with a positive phase of NAO and AO (high values), western air masses distribute water from the Danish Straits to the eastern and northern ends of the Baltic Sea, causing a slope of the Baltic surface from the north-east to the southwest. This reinforces the impact of the NAO index on sea levels in the northeast and weakens the effect in the southwest. This is consistent with the conclusions in the works: Johansson et al. (2003), Jevrejeva et al. (2005), Ekman (2007, 2009), Jaagus and Suursaar (2013).

4. Summary

The annual pattern of storm surges, which result in high and low sea levels, is consistent with the annual variability of atmospheric circulation both locally, regionally and globally. Zonal circulations (NAO, AO) through the increased inflow of air masses from the western directions cause an increase in extreme sea level phenomena on a weekly and monthly basis. Therefore, they are mainly responsible for the slow process of filling the Baltic Sea with the North Sea waters. This effect is an important but not the only component in the formation of extreme sea levels during storm situations.

References

Ekman, M. (2007). A secular change in storm activity over the Baltic Sea detected through analysis of sea level data, Small Publications in Historical Geophysics, 16, pp. 1–13

Ekman, M. (2009). The Changing Level of the Baltic Sea Turing 300 Years: A Clue to Understanding the Earth, Summer Institute for Historical Geophysics, Aland Islands, 155

Jaagus, J., Suursaar, Ü. (2013). Long-term storminess and sea level variations on the Estonian coast of the Baltic Sea in relation to large-scale atmospheric circulation, Estonian Journal of Earth Science, 62, 2, 73–92

Jevrejeva, S., Moore, J.C., Woodworth, P.L., Grinsted, A. (2005). Influence of large-scale atmospheric circulation on European sea level: results based on the wavelet transform method, Tellus, 57A, pp. 183–193

Johansson, M., Kahma, K., Boman, H. (2003). An Improved Estimate for the Long-Term Mean Sea Level on the Finnish Coast, „Geophysica", 39(1-2), pp. 51–73.

NOAA, Climate Prediction Center, National Weather Service, http://www.cpc.ncep.noaa.gov

Suursaar, Ü., Sooäär, J. (2007). Decadal variations in mean and extreme sea level values along the Estonian coast of the Baltic Sea, Tellus, 59A, pp. 249–260

Wiśniewski, B., Wolski, T., Giza, A., (2014). Adjustment of the European Vertical Reference System for the representation of the Baltic Sea water surface topography. Scientific Journals Maritime University of Szczecin 38, pp. 106–117

Wolski, T., Wiśniewski, B., Giza, A. Kowalewska-Kalkowska, H, Boman, H. et al. (2014). Extreme sea levels at selected stations on the Baltic Sea coast. Oceanologia 56(2) pp. 259-290. DOI: 10.5697/oc.56-2.259

Wolski T., Wiśniewski B,. Musielak S., (2016). Baltic Sea datums and their unification as a basis for coastal and seabed studies, Oceanological and Hydrobiological Studies, 2016, 45(2), pp. 239-258, DOI: 10.1515/ohs-2016-0022

Coastal foredunes along the southern Baltic Sea – their current development and future scenarios inferred from numerical modelling

Wenyan Zhang[1] and Joanna Dudzinska-Nowak[2]

[1] Institute of Coastal Research, Helmholtz-Zentrum Geesthacht, Geesthacht, Germany (Wenyan.zhang@hzg.de)
[2] Institute of Marine and Environmental Sciences, University of Szczecin, Szczecin, Poland

1. Introduction

The Glacial Isostatic Adjustment (GIA) and eustatic sea level change impose a first-order control on the long-term coastline change along the Baltic Sea (Harff et al., 2017). In the mildly subsiding southern Baltic Sea coastal region that is composed of sandy dunes and till or sand-till mixed moraine cliffs, water level, surface gravity waves and wind-driven alongshore currents are the major driver for erosion and accretion (Zhang et al., 2015, Dudzińska-Nowak 2017).

Coastal foredunes form a natural barrier for coastal protection along a major part of the southern Baltic coast (Figure 1). Most coastline erosion along the southern Baltic Sea is caused either by storms or human-induced depletion of sediment supply (e.g. side effect of engineering structures). Existing studies reveal a highly nonlinear relationship between storm intensity and the rate of coastline erosion along the southern Baltic Sea coast (Zhang et al., 2015, Dudzińska-Nowak 2017). Thus, to foresee the future development of the Baltic Sea coastline, it is of vital importance to understand the controlling factors that are responsible for formation of the various types of coastal dunes and their interaction with adjoining morphological features such as cliffs, innets and engineering structures.

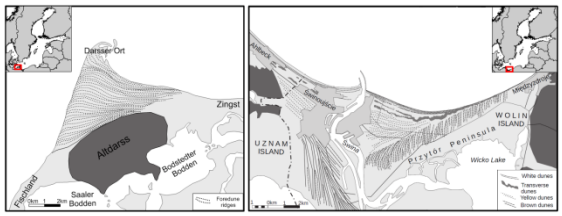


Figure 1. Typical sandy coasts along the southern Baltic Sea characterized by sequence of foredune ridges. Left: Darss-Zingst Peninsula; Right: Swina Gate (modified from Łabuz (2015)).

2. Material and methods

Various datasets, including field measurements and numerical model results, are used in this study to investigate the recent development of coastal foredunes and their future scenarios in response to sea level rise and storm-wave climates (Figure 2). These include high-resolution digital elevation/terrain models, meteorological data of winds and waves, vegetation coverage, model-estimated longshore sediment transport and aeolian transport rates. Morphological change and sediment transport in the subaqueous zone is estimated in a process-based model which calculates the change of coastal bathymetric profile based on the in-situ wave and current parameters. Change of the sediment budget in the subaqueous zone acts as a sediment source or sink for the coastal dunes. Sediment transport and morphological change in the subaerial zone is dominated by an interplay of air flow and vegetation and significantly influenced by a series of environmental factors (e.g. moisture, local beach geometry and fetch length). These subaerial processes and factors are formulated in a probabilistic model based on Cellular Automata (CA) approach (Zhang et al., 2017). The computational time step of the CA model is 1.4 day (~34 h) for normal wind conditions and 0.25 day (6 h) for storms. The maximum wave run-up limit calculated from external input time series of offshore water level defines the land-sea boundary.

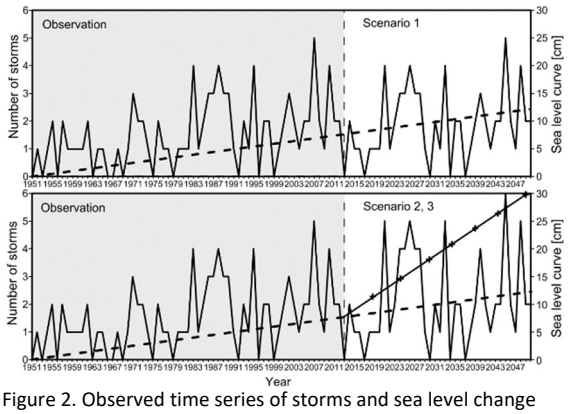


Figure 2. Observed time series of storms and sea level change (relative to the value at 1951, indicated by the dashed line) during the historical period 1951-2012 and setting of these two parameters in three climate change scenarios for future projection till 2050. Scenario 1 replicates the statistics in the period 1975-2012. Scenario 2 and 3 retain a slight increasing trend in the frequency of storms for the period 2013-2050 as observed in 1951-2012. Scenario 1 and 2 adopt the same rate of relative sea level change (1.2 mm/yr) as in the historical period, while an increased rate (7 mm/yr) is used in Scenario 3 (indicated by the solid line marked by crosses). Figure is modified from Zhang et al.(2017).

3. Results and analysis

Simulation results indicate a complex and non-linear relationship among several basic driving mechanisms for morphogenesis and evolution of coastal foredunes. The most important precondition for formation of coastal foredunes is a sufficient sediment supply rate. Prograding coastal foredune sequence develops only when there is a sediment gain in excess of the total amount of loss and that is needed to maintain an equilibrium shape of the cross-shore profile. The minimum amount of the net gain required for formation of an established foredune depends greatly on the local environmental and climate conditions (e.g. grain size, vegetation species, temperature, frequency and impact level of extreme events). An incipient foredune survives and become established only when it grows fast enough in a relatively calm period between two sequential storms to develop a height exceeding the storm impact level. In the southern Baltic Sea most storms have a maximum impact level between 2.5 m and 4 m above the mean sea level

according to recorded data in the 20th century. In beach shoreface characterized by slopes ranging from 0.035 to 0.06, an annual onshore transport rate of 5 $m^3m^{-1}yr^{-1}$ proves to be sufficient to pass the threshold for formation of an established foredune, while a value lower than 3.5 $m^3m^{-1}yr^{-1}$ would result in a foredune degradation according to the simulation results with regard to the environmental and climate conditions in the past few decades (1951-2012). The established foredune ridges developed in the past decades (1951-2012) have a height between 4.5 m and 6 m along the southern Baltic coast (Figure 3). The time span from the formation of a foredune until a final stabilization of its shape varies between 10 to 20 years in this region (Figure 3), depending greatly on the rate of sediment supply and number of storms occurred in the initial stage of 3 to 5 years.

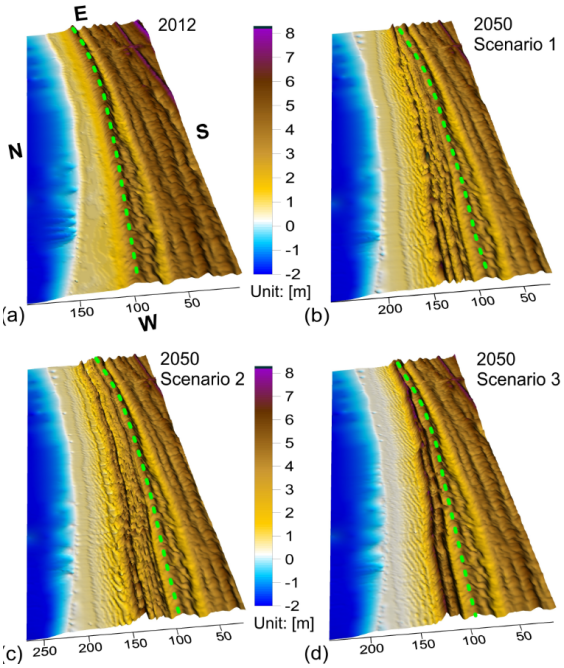


Figure 3. (a) Measured digital elevation model of Swina Gate in 2012; (b),(c),(d): Projected morphology in 2050 based on the climate change scenarios.

In the context of coast progradation, the time needed for the formation of a foredune and its exact location are determined by the specific vegetation species (pioneer grass species) and frequency of storms. A net deposition is required to maintain a growth of the pioneer grass, while a sediment overload, unchanged surface elevation or erosion leads to a decline of the species. An annual sediment deposition thickness of 0.15-1.6 m would favor vegetation growth at the foredunes in the southern Baltic coast, with an optimum level at ~0.5 m according to our results. The spatial expansion of vegetation in front of a pre-existing foredune and the density gradient of vegetation coverage in the cross-shore direction determine the location of a new foredune ridge.

Relative sea level rise in the southern Baltic Sea (~1.2 mm/yr) played a minor role in controlling foredune development during the past decades. In such rate only a small amount of the gained sediment (in prograding coasts) is needed to maintain an equilibrium cross-shore profile in the subaqueous zone, and the rest is transported onshore facilitating a development of foredunes. However, an accelerated sea level rise, which will probably be the case in the 21st century, would become increasingly important to affect coastal morphological change. A rate of e.g. 7 mm/yr in the relative sea level rise would start to dominate the coastal morphological evolution (especially the development of foredunes) by 2030 according to our simulation results (Figure 4). The influence of sea level rise on foredune development (e.g. spatial dimension) does not seem to be steady and linear. A critical threshold, which distinguishes a linear and a non-linear (following a quadratic or a higher power law) relationship between foredune height and rate of relative sea level rise, seems to exist. If a rise by 0.5-0.7 m in the relative sea level will occur by the end of the 21st century, such critical threshold would probably be reached within the first 30 years by 2030 according to our study.

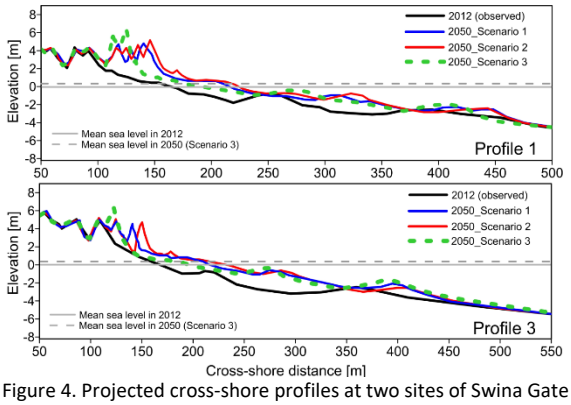


Figure 4. Projected cross-shore profiles at two sites of Swina Gate in 2050 based on the climate change scenarios.

References

Dudzińska-Nowak J. (2017) Morphodynamic processes of the Swina Gate coastal zone development (southern Baltic Sea). In: J. Harff, K. Furmanczyk, H. von Storch (eds.) Coastline changes of the Baltic Sea from South to East. Past and future projection. Springer Coastal Research Library 19, p. 219-256

Harff, J., J. Deng, J. Dudzinska-Nowak, P. Fröhle, A. Groh, B. Hünicke, T. Soomere, and Zhang, W. (2017) Chapter 2: What determines the change of coastlines in the Baltic Sea? In: Harff J, Furmanczyk K, von Storch H (eds) Coastline changes of the Baltic Sea from south to east – past and future projection. Coastal research library, vol 19. Springer, Cham, Switzerland. p. 15–36

Łabuz, T. A. (2015) Environmental impacts – coastal erosion and coastline changes. Chapter 20. In: BACC II Team (eds.), Second assessment of climate change for the Baltic Sea basin. Springer, p. 381–396

Zhang, W., Schneider, R., Kolb, J., Teichmann, T., Dudzinska-Nowak, J., Harff, J., Hanebuth, T. (2015) Land-sea interaction and morphogenesis of coastal foredunes - a modelling case study from the southern Baltic coast. Coastal Engineering, 99, 148-166

Zhang, W., Schneider, R., Harff, J., Hünicke, B., Froehle, P. (2017) Modeling of medium-term (decadal) coastal foredune morphodynamics – historical hindcast and future scenarios of the Swina Gate barrier coast (southern Baltic Sea). In: Harff J, Furmanczyk K, von Storch H (eds) Coastline changes of the Baltic Sea from south to east – past and future projection. Coastal research library, vol 19. Springer, Cham, Switzerland, p.107-126

Topic 5

Regional variability of water and energy exchanges

The peculiarities of the moistening regime in the accordance to the climate change at the eastern part of the Baltic Sea Basin with a focus on Belarus

Irina Danilovich

Institute for Nature management of the National Academy of Sciences, Minsk, Belarus (irina-danilovich@yandex.ru)

1. Introduction

Researches of climate changes over the Baltic Sea Basin and particularly in the territory of Belarus were conducted by various groups of authors. So far, certain knowledge about occurring climate changes in the study region was archived. For instance, the climate warming was marked in the territory of Belarus since 1989. This climate warming period lasts 30 years (1989-2019) and it`s duration is the largest for the last 130 years (Loginov et.al., 2016). The moistening regime changes are expressed in 5% increase in the annual precipitation sums in the north and 7% increase in the central and southern regions of the country during the climate warming period (Melnik et.al., 2018). The largest increase of precipitation observed in the cold season and connected with features of atmospheric circulation in Atlantic-European sector (Partasenok et.al., 2014).

However, despite some growth of precipitation, increase in dryness during the vegetative period was noted in Belarus (Loginov et.al., 2012). The occurring climate changes over the territory of Belarus are synchronized with the changes which are noted over Europe. According to (Bordi et.al., 2009) moistening regime in the Baltic Sea Basin was characterized by precipitation growth in the north of the region within the last 100 years. It is connected with increase in repeatability and intensity of extreme rainfall. At the same time the significant trends in precipitation were not detected in the central and southern regions of the Basin. In the second half of the twentieth century droughty conditions were traced mainly in summer months in the southern regions of the Baltic Sea Basin (Poland, Lithuania and Belarus) (BACC Author Team, 2015).

The aim of the study is an assessment of the changes of different rainfall characteristics, their trends and spatial distribution during the period of climate change over the territory of Belarus which is situated in the eastern part of the Baltic Sea Basin.

2. Methods and Materials

The assessment of moistening regime changes was based on the data from the State Climatic Cadaster of the Republic of Belarus. The data is presented by the following characteristics:

- Monthly, seasonal and annual totals of precipitation;
- Number of days with precipitation of 0,1 and 5 mm and more;
- Maximum precipitation totals (per day);
- Duration of rainfall (hours);
- Duration of the liquid, solid and mixed rainfall (hours).

The generalization of each characteristic was carried out by 40 meteorological stations of the state network of hydrometeorological observations of Belhydromet. The period of generalization covers a time period from the beginning of observations at each station till 2019, but for the comparative analysis the time-series were divided into 2 periods: (1) 1958-1987, that is close to the climatic norm of 1961-1990 which is earlier recommended by World Meteorological Organization and (2) 1989-2019, the modern period of climate warming. The assessment of current changes included the calculations of rainfall characteristic for both periods, their standard deviations, the trends of each characteristic on each meteorological station and their statistical significance.

3. Results

Monthly, seasonal and annual sums of rainfall

The annual sums of precipitation for the considered periods changed insignificantly, the increase within 5-10% was noted over entire territory of the country, with the greatest values in north. In winter the precipitation increased more significantly: in the north of the country up to 20-30% (6-13 mm) in January-March, in the central part of the country up to 25% (8 mm) in February, in the south up to 20% (6 mm) in February-March. During summer season precipitation increased by 10-15% (6-10 mm) in the north. The slight decrease of precipitation was observed in the central and southern parts of the country in June and August. But July is characterized by noticeable growth of precipitation on 15-20% (10-17 mm). In summer months the standard deviation of the monthly sums of rainfall considerably increased that demonstrates the increased extremeness in the moistening regime. In autumn (September and October) precipitation regime is characterized by increase by 10-15%.

Change of *number of days with rainfall more than 0,1 mm and 5 mm* was insignificant and does not exceed 1 day in each months.

Maximum daily amount of precipitation

The maximum totals of rainfall considerably increased during the warm period of year - from May to October over entire territory of the country. The most considerable changes were noticed in the southern and central regions. The maximum totals of rainfall increased on 7-16 mm by month, on 54-58 mm by warm period of the year (May-October). The significant positive trends of the maximum totals were established for the north part of the country of 10-13 mm per decade, for the southern regions of 25-29 mm per decade.

Duration of rainfall

In the majority of months duration of rainfall decreases across entire territory of Belarus. At the same time in the north of the country duration of rainfall practically did not change. The most noticeable reducing is noted in the central regions - for 130 hours per year and south - for 109 hours per year. Seasonal changes are differing: in the winter reducing was more remarkable; duration of rainfall was reduced by 103 hours in the central region and on 85 hours in southern. In summer period rainfall duration reduced by 24-26 hours. The negative trends of 5-7 hours per decade were detected in the central and southern regions of the country.

Duration of the liquid, solid and mixed rainfall

Duration of liquid rainfall increased during a winter season, the greatest change noticed in the north of the country and reaches 101 hour during climate warming period. In the central and southern regions liquid rainfall duration increased by 42-44 hours.

Duration of solid rainfall during the cold period of year was reduced by 11-26 hours by month in the north of the country, for 17-47 hours in the center and for 11-41 hour in the southern regions. The most remarkable changes are observed in January - the negative trend is about 20 hours per decade.

Duration of the mixed rainfall practically did not change during climate warming period.

4. Summary

The study showed that moistening regime over the territory of Belarus changed during climate warming period. Changes are insignificant in the annual sums of rainfall which vary within the climatic norm. Most significant changes are shown in an intra-annual distribution. In winter the monthly sums increased due to the growth of liquid rainfall duration against the decrease in duration of solid rainfall. In summer season the monthly sums of precipitation increased in July. Also the strengthening of precipitation extremeness was noticed in summer which expressed in reduction of rainfall duration and simultaneous growth of the maximum rainfall totals in the central and southern regions of the country.

References

BACC Author Team (2015) Second Assessment of Climate Change for the Baltic Sea Basin, Springer International Publishing, 2015, 501 p.

Bordi I, Fraedrich K, Sutera A (2009) Observed drought and wetness trends in Europe: an update, Hydrol Earth Syst Sci, pp.1519-1530.

Loginov V.F. (ed.) (2016) Assessment of influence of an urbanization and melioration on climatic, water, land and forest resources of Belarus, Research report (final) No. of state registration 20163200, Belhydromet, 103 p.

Loginov, V.F. (2012) Climatic researches in the Institute for Nature Management , Environmental management, Issue 22, pp 123-140.

Melnik V.I., Danilovich I.S., Kuleshova I.Yu (2018) Assessment of agroclimatic resources of the territory of Belarus during 1989-2015, Natural resources, Issue 2, pp. 88-101.

Partasenok I.S., Groisman P.Ya., Chekan G.S., Melnik V.I. (2014) Winter cyclone frequency and following freshet streamflow formation on the rivers in Belarus. Environ. Res. Lett. 9 095005.

Complementing ERA5 and E-OBS20 with high-resolution river discharge over Europe

Stefan Hagemann and Tobias Stacke

Institute of Coastal Research, Helmholtz-Zentrum Geesthacht, Germany (stefan.hagemann@hzg.de)

1. Introduction

The 0.5° resolution of many global observational datasets is not sufficient for the requirements of current state-of-the-art regional climate model (RCM) simulations over Europe. Thus, the ERA5 reanalysis (Copernicus Climate Change Service 2017) of the European Centre for Medium-range Weather Forecasts (ECMWF) and E-OBS data (Cornes et al. 2018) are frequently used as reference datasets when RCM results are evaluated on resolutions higher than 0.5°. In addition, ERA5 data are also commonly used to force regional ocean models. As ERA data do not comprise river discharges, the lateral forcing of freshwater inflow from land is taken from other data sources, such as station data, runoff climatologies, etc. These datasets are not necessarily consistent with the ERA5 forcing over the ocean surface. Moreover, if such data are derived from station data, they are only available for specific rivers and not spatially homogeneously distributed for all coastal areas. In addition, they might not be representative for the river mouth if the respective station location is too far upstream, which is often the case.

In order to mitigate these shortcomings, we extended ERA5 and E-OBS v20.0e with simulated high-resolution river discharge. This also allows a consistent assessment of hydrological changes from these two datasets. The discharge was simulated with the recently developed 5 Min. version of the Hydrological Discharge (HD) model (Hagemann et al. 2020). Note that for the development of this HD model version, no river specific parameter adjustments were required so that the HD model is generally applicable for climate change studies in other regions and over ungauged catchments.

2. Methodology

The HD model separates the lateral water flow into the three flow processes of overland flow, baseflow, and riverflow. Overland flow and baseflow represent the fast and slow lateral flow processes within a grid box, while riverflow represents the lateral flow between grid boxes. The HD model requires gridded fields of surface and subsurface runoff as input for overland flow and baseflow, respectively, with a temporal resolution of one day or higher. To generate these fields from ERA5 and E-OBS v20.0e data, we used the HydroPy global hydrological model, which is the successor of the MPI-HM model (Stacke and Hagemann 2012). The latter has contributed to the WATCH Water Model Intercomparison Project (WaterMIP; Haddeland et al. 2011) and the inter-sectoral impact model intercomparison project (ISIMIP; Warszawski et al. 2014). Note that ERA5 also comprises archived fields of surface and subsurface runoff, but it turned out that its separation of total runoff in these two fluxes is not suitable to generate adequate river discharges with the HD model.

Figure 1 summarizes the main steps of generating simulated discharges with the HD model in stand-alone mode and conducting their evaluation. These steps comprise three parts:

1) Preparation of HD model forcing: Choose an atmospheric forcing dataset (ERA5 and EOBS20) and use a land surface (or hydrology) model (HydroPy) to generate the forcing for the HD model,
2) Simulation with the HD model: Interpolate the forcing data of surface and sub-surface runoff to the HD model grid and simulate daily discharges with the HD model,
3) Evaluation of results: Compare simulated and observed discharges at station location and calculate various evaluation metrics.

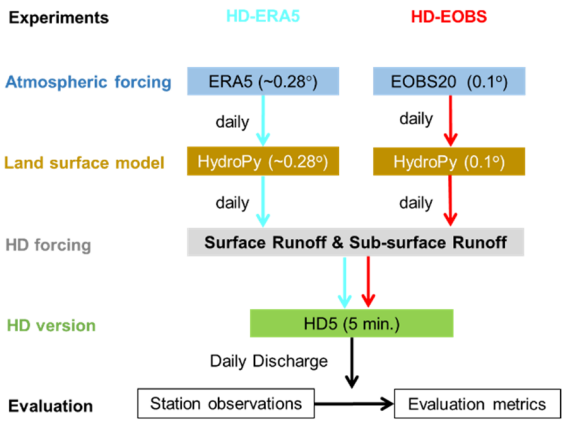


Figure 1. Flowchart showing the main steps of generating simulated discharges with the HD model and conducting their evaluation in the present study.

3. First results

Figure 2 shows the location of several rivers that flow into the Baltic Sea and their respective catchments, for which results from an initial ERA5-based simulation (HD-ERA5) are displayed (Figure 3). Figure 3 show observed and simulated daily discharges for the period 2000-2003. Here, the timing of the main peaks is often captured in the simulated data, especially for the rivers Daugava and Glomma.

As direct anthropogenic impacts, such as discharge regulation or dams, is not regarded in the HD model, those effects can generally not be simulated. Thus, discharges for many heavily regulated rivers in Scandinavia or for the rivers Volga and Don are not well represented by the model. A typical example is given for the Indalsälven (Figure 3 – lower panel). On the one hand, apparent

snowmelt induced discharge peaks in spring are simulated, but only weak indications of such peaks occur in the observed time series. On the other hand, there is only little variation in the observed low flow periods, while there is more variability and generally lower discharge in the simulations. This can be explained by extractions of water during the snowmelt season and supply of the stored water during low flow periods. It can be noted that rainfall induced discharge peaks outside the snowmelt season are rather well captured in the simulation, e.g. in the second halves of the years 2000 and 2001.

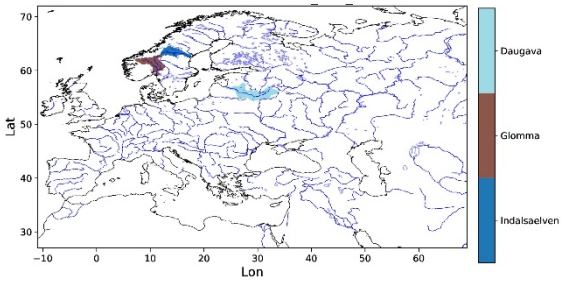


Figure 2: Locations of the Daugava, Glomma and Indalsälven catchments.

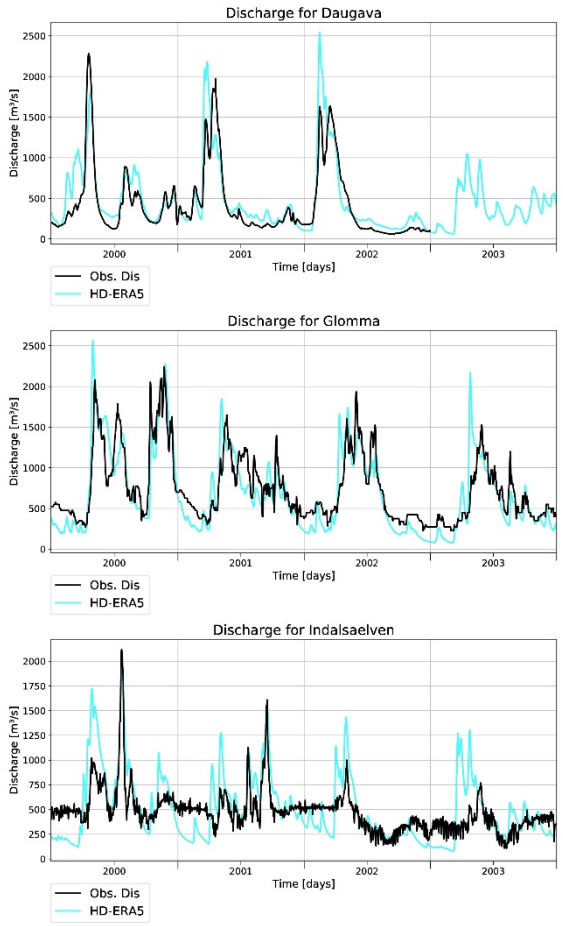


Figure 2 Observed and simulated (HD-ERA5) discharges from 2000-2003 for the rivers Daugava (87900 km²), Glomma (41918 km²) and Indalsälven (26726 km²). The corresponding evaluation metrics for the years 2000-2009 are provided in Table 1.

In our presentation, we evaluate the simulated discharge using various metrics and consider significant discharge trends over Europe. Table 1 summarizes the respective evaluation metrics for the rivers shown in Figure 2 for the period 2000-2009.

TABLE 1: Evaluation metrics (2000–2009) for those rivers shown in Figure 2: Discharge bias, Kling-Gupta Efficiency (KGE), Pearson correlation r_{cor}, normalized RMSE, variability ratio and lag. A negative lag indicates that the simulated discharge is earlier than the observed one.

Metric	Daugava	Glomma	Indalsälven
Bias	8.9%	-5.4%	10.5%
KGE	0.86	0.59	0.13
r_{cor}	0.90	0.83	0.58
RMSE	6.5%	11.4%	14.0%
Var. ratio	95.2%	136.7%	175.2%
Lag	-1 day	-1 day	-1 day

References

Copernicus Climate Change Service (C3S) (2017): ERA5: Fifth generation of ECMWF atmospheric reanalyses of the global climate. Copernicus Climate Change Service Climate Data Store (CDS)

Cornes, R., G. van der Schrier, E.J.M. van den Besselaar, and P.D. Jones (2018) An Ensemble Version of the E-OBS Temperature and Precipitation Datasets, J. Geophys. Res. Atmos., 123, doi:10.1029/2017JD028200.

Haddeland, I., et al. (2011) Multimodel estimate of the global terrestrial water balance: Setup and first results. J. Hydrometeorol., 12, 869–884, doi: 10.1175/2011jhm1324.1.

Hagemann, S., T. Stacke and H.T.M. Ho-Hagemann (2020) High resolution discharge simulations over Europe and the Baltic Sea catchment. Front. Earth Sci., 8:12, doi: 10.3389/feart.2020.00012.

Stacke, T. and S. Hagemann (2012) Development and evaluation of a global dynamical wetlands extent scheme. Hydrol. Earth Syst. Sci., 16, 2915–2933, doi: 10.5194/hess-16-2915-2012

Warszawski, L., et al. (2014) The inter-sectoral impact model intercomparison project (ISIMIP): Project framework. Proc. Natl. Acad. Sci. USA, 111, 3228–3232, doi: 10.1073/pnas.1312330110.

Linking weather types to tense dewatering situations of the Kiel Canal

Corinna Jensen, Jens Möller, Peter Löwe, Nils H. Schade

Federal Maritime Hydrographic Agency, Hamburg, Germany (Corinna.jensen@bsh.de),

1. Motivation

Within the "Network of Experts" of the German Federal Ministry of Transport and Digital Infrastructure (BMVI), the effect of climate change on traffic and traffic infrastructure is investigated. One aspect of this project is the future dewatering situation of the Kiel Canal ("Nord-Ostsee-Kanal" [NOK]). The NOK is one of the world's busiest man-made waterways navigable by seagoing ships. It connects the North Sea to the Baltic Sea and can save the ships hundreds of kilometers of distance. With a total annual sum of transferred cargo of up to 100 million tons it is an economically very important transportation way. In addition to the transportation of cargo and ferry traffic, the canal is also used as drainage of a catchment area of about 1500 km².

The NOK can only be operated in a certain water level range. If its water level exceeds the maximum level, the water must be drained into the tidal areas of the Elbe River during time windows with low tide or the Baltic Sea. If the water level outside the NOK is too high, drainage is not possible and the canal traffic has to be reduced or, in extreme cases, shut down. Due to the expected sea level rise, the potential time windows for dewatering are decreasing in the future (see Ebner von Eschenbach et al, 2020). With a decrease in operational hours substantial economic losses can be expected as well as a shift in traffic routes of the ferries. In order to gain a better understanding of what might cause tense dewatering situations in addition to the expected sea level rise, high water levels in the North Sea are investigated.

2. Method

A linkage between high water levels on the outside of the canal and the general weather situation is made by looking at weather types. Weather types describe large-scale circulation patterns and can therefore give an estimate on tracks of low-pressure systems as well as the prevailing winds, which can explain surges and therefore additional increases in water levels at the coast.

This analysis is conducted for one weather type classification method based solely on sea level pressure fields (see Fig. 1). The Lamb weather types (Lamb, 1950) were chosen because the original main focus area is the North Sea and they also give an additional estimation of gales, which are part of ongoing investigations within the Network of Experts.

3. Data

For this investigation, daily values for water levels and sea level pressure from two regionally coupled climate models, NEMO/RCA4 (Dieterich et al., 2013) and MPI-OM/REMO (Mathis et al., 2017), were used. Water levels near Cuxhaven are used as proxy for the dewatering situation of the Kiel Canal. Daily weather types were derived solely from the sea level pressure field.

4. Results

Distributions of Lamb weather types on days with high mean daily water levels (95. and 99. percentile) were compared to the respective distribution on all days. It was found that especially the percentage of North-West (NW) weather types is dominant in the distribution on days with higher water levels (see fig. 2 top).

The occurrence of NW weather types increases significantly until 2100 whereas weather types that do not contribute to tense dewatering situations (e.g. North-East (NE) and South-East (SE)) decrease significantly (see fig. 2 bottom).

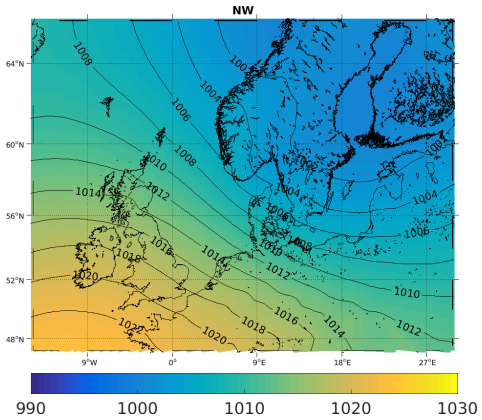


Figure 1. Mean sea level pressure [hPa] during North-West (NW) weather type for the time period 1971 - 2000

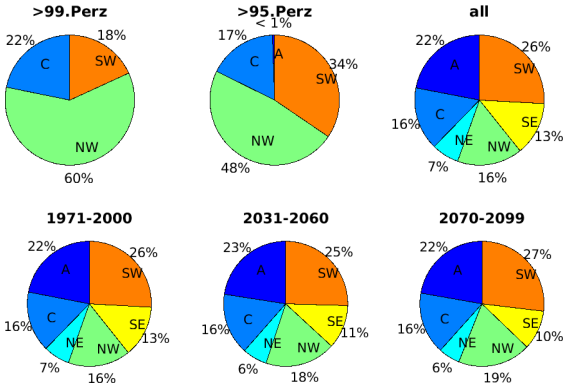


Figure 2. Top: Distribution of weather types (Anticyclonic (A), Cyclonic(C), North-East (NE), North-West (NW), South-East (SE), South-West (SW)) on all days (right), days with water levels over the 95. Percentile (middle) and the 99. Percentile (left) for the time period 1971 – 2000. Bottom: Mean annual frequency in %, for the past (1971-2000), near future (2031-2050) and distant future (2070-2099). Both for MPI-OM/REMO run 3 with RCP 8.5 scenario.

Conclusions

In addition to the rising sea level, an increase in North-West weather types might lead to a higher number of tense dewatering situations at the Kiel Canal. Further investigations within the Network of Experts will include a variety of different weather type classification methods, as well as investigations of gales. An addition of CMIP6 model runs (global, regional) to the model ensemble is also planned.

References

Dieterich, C., et al. (2013): Evaluation of the SMHI coupled atmosphere-ice-ocean model RCA4_NEMO, SMHI.

Ebner von Eschenbach, A.-D., Schade, N.H., Moeller, J., and V. Neemann (2020): Impact of climate change on the water management of the Kiel Canal – A case study, 3rd Baltic Earth Conference, presentation.

Lamb, H.H. (1950): Types and spells of weather around the year in the British Isles: annual trends, seasonal structure of the year, singularities, Quarterly Journal of the Royal Meteorological Society, 76(330), 393-429. https://doi.org/10.1002/qj.49707633005

Mathis, M., Elizalde, A., and U. Mikolajewicz (2018): Which complexity of regional climate system models is essential for downscaling anthropogenic climate change in the Northwest European Shelf? Climate Dynamics, 50(7-8), 2637-2659. DOI: 10.1007/s00382-017-3761-3

Assessment of the impact of the Grodno hydroelectric power station on the hydrological regime of the Neman River (within the borders of Belarus)

Alena Kvach, Maryia Asadchaya and Ludmilla Zhuravovich

State Institution «Center for of hydrometeorology and control of radioactive contamination and environmental monitoring of The Republic of Belarus» (Belhydromet) (gid2@hmc.by)

1. Introduction

The Neman River is one of the main waterways of Belarus, located in the North-Western and Western parts of Belarus. It flows through the territory of Belarus and Lithuania. It flows into the Curonian lagoon of the Baltic sea.

Before reclamation works were carried out in 1985-86, the source of the Neman River, located South-West of the village of Krasnoe in the Uzden district, Minsk region, was taken as the beginning of the Neman river. The change in the location of the source of the Neman River was influenced by land reclamation works carried out within the catchment area, as a result, the length of the Neman River decreased by 24 km.

In may 2008, the construction of the Grodno hydroelectric power station began on the Neman River. According to the project, the capacity of the Grodno hydroelectric power station is 17 megawatts. This is the first hydroelectric power station of this type in Belarus, which was put into operation in September 2012. A characteristic feature of the Grodno hydroelectric power station is that during its operation, the flow rate of the river is almost completely preserved, since the station operates only on household runoff (without regulating the flow of water in the river) with a constant water level in the reservoir. The reservoir of the Grodno hydroelectric power station is a riverbed type with an area of 19.4 km^2 and a total volume of 48.67 million m^3. The peculiarity of the reservoir is its length - 42.0 km. The maximum width is 1.5 km.

2. Methods

The analysis of the influence of the Grodno hydroelectric power station on the hydrological regime of the Neman River was carried out at two nearby hydrological stations: Neman-Grodno – 11.5 km downstream of the existing hydroelectric power station and Neman-Mosty – 66.0 km upstream of the existing hydroelectric power station.

Verification of the hypothesis of homogeneity of series of observations was performed using ten Dixon criteria and two Smirnov-Grubbs criteria. To check the stationarity of the series, the Student and Fisher criteria are calculated. The Student's criterion estimates the stationarity of the time series relative to the average value, and the Fisher's criterion estimates the variance.

To analyze changes in the level and runoff regime, we compared these characteristics before and after the construction of hydroelectric power station at the hydrological station Neman-Mosty and Neman-Grodno. In order to exclude the impact of climate change on the hydrological regime of the Neman River, the period from 1989 to 2018 was selected for analysis. This period was divided into four stages:

1989-2007 – before the start of construction of the Grodno hydroelectric power station;

1989-2011 – up to the commissioning of the Grodno hydroelectric power station;

2008-2018 – after the construction of the Grodno hydroelectric power station;

2012-2018 – after the commissioning of the Grodno hydroelectric power station.

To analyze changes in the ice and thermal regime, we compared these characteristics at the hydrological station Neman-Grodno before and after the construction of the hydroelectric power station. In order to exclude the influence of climate change on the hydrological regime of the Neman River, the period from 1989 to 2018 was selected for analysis. This period was divided into two stages:

1989-2011 – up to the commissioning of Grodno hydroelectric power station;

2012-2018 – after the commissioning of the Grodno hydroelectric power station.

3. Water level

The series of higher annual water levels, lower water levels of winter and lower water levels of the period of open channel at the hydrological stations Neman-Mosty and Neman-Grodno are studied.

For the period from 1989 to 2018, the highest water level was recorded in 1994 at two hydrological stations analyzed.

For the periods of construction and commissioning of the Grodno hydroelectric power station, a decrease in the values of highest annual water levels and lower water levels of winter and lower water levels of the period of open channel on the hydrological station Neman-Grodno. The average value of the highest annual water levels decreased by 30 cm. For the lowest water levels, the most significant changes are observed for the period of open channel and reach a decrease of up to 15 cm. This trend is not typical for the hydrological station Neman-Mosty.

4. Runoff regime

The hydrological stations Neman-Mosty and Neman-Grodno show a smooth distribution of the river's water content during the year. The impact of the construction of the Grodno hydroelectric power station in the context of the studied periods was not noted. When operating the Grodno hydroelectric power station, the flow rate of the Neman River above and below the hydroelectric site is almost completely preserved.

5. Ice and thermal regime

Analysis of the average monthly water temperature and ice phenomena at the hydrological station Neman-Grodno recorded changes in the ice-thermal regime of

the Neman River after the commissioning of the Grodno hydroelectric power station.

As a result of the Grodno hydroelectric power station operation, the water temperature at the hydrological station Neman-Grodno increased by an average of 0.5^0C. The most significant changes in the temperature regime are observed in the winter and autumn period.

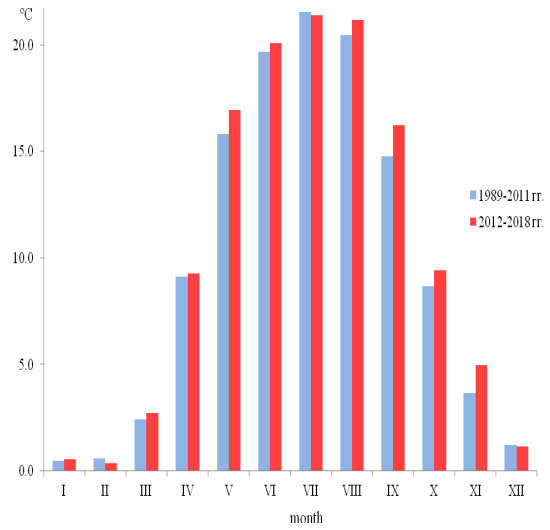


Figure 1. Changes in the average monthly water temperature at the hydrological station Neman-Grodno.

Changes in the temperature regime contribute to the later formation of stable ice phenomena on the Neman River below the hydroelectric dam. At the hydrological station Neman-Grodno, stable ice phenomena began to form on average 20 days later than before the hydroelectric power station was put into operation.

Since the commissioning of the hydroelectric power station, no ice is formed on this section of the river.

6. Conclusions

Based on the research conducted in this paper, we can conclude:

during the operation of the Grodno hydroelectric power station, the flow rate of the Neman River above and below the hydroelectric site is almost completely preserved;

the most significant changes in the water level regime on the hydrological station Neman-Grodno during the work of the Grodno hydroelectric power station recorded lower values of highest annual water levels and low water levels of the period of open channel;

change in the ice and thermal regime on the hydrological station Neman-Grodno was recorded.

References

Reference book «Changes in the hydrographic network of Belarus under the influence of land reclamation works. Part 1. Information about regulated rivers in the main river basins of Belarus» - Minsk, 2008.

Archive database of OGH materials of observations at the posts of the Ministry of natural resources and environmental protection of the Republic of Belarus.

State water cadastre. Annual data on the regime and resources of surface waters for the period 1989-2018 years.

Mid-winter stratification formation in the Gulf of Finland

Taavi Liblik, Germo Väli, Madis-Jaak Lilover, Jaan Laanemets, Villu Kikas, Inga Lips

Tallinn University of Technology, Estonia, Tallinn (taavi.liblik@taltech.ee)

1. Background

Stratification in the Baltic Sea has strong annual cycle. Shallow (10-20 m) upper mixed layer is present from spring to autumn. Thermal convection and wind stirring destroy the thermocline, and water column mixes down to the 40-80 m depth in deeper areas. This annual cycle in stratification reflects in physical, biogeochemical and biological variables.

Temperature usually drops below the maximum density temperature T_{md} in the northern and eastern part of the Baltic Sea (Karlson et al., 2016; Liblik et al., 2013). Onset of the seasonal pycnocline could be related to the advection of lower salinity water instead of thermal stratification (Eilola, 1997; Eilola and Stigebrandt, 1998; Stipa et al., 1999). Temperature values below T_{md} in the cold intermediate layer after establishment of the seasonal pycnocline well prove the important role of haline buoyancy in the onset of stratification (Chubarenko et al., 2017; Eilola, 1997; Liblik and Lips, 2017).

Haline stratification formation under ice has been reported in several locations in the Baltic in winter (Granskog et al., 2005; Kari et al., 2018; Merkouriadi and Leppäranta, 2015). These observations have dealt with the topic in relatively local areas near small rivers.

2. Results

In the present study we aim to study the haline stratification in the larger areas of the Baltic during wintertime. Gulf of Finland receives large amounts of fresh water and could be subject to the process in winter. Hypothesis of the present work is that halocline forms in similar depths as euphotic zone well earlier than temperature rises over T_{md} in the Gulf of Finland.

In order to investigate the hypothesis, we use several data sources: (a) CTD + optical sensors data from the surveys along the gulf in winter 2011/12 and 2013/14; (b) historical CTD data in the Gulf of Finland; (c) Tallinn-Helsinki ferrybox data; (d) GETM model run 2010-2019; (e) satellite derived sea surface temperature data.

Our results include: (a) detailed view on haline stratification formation process in two winters; (b) spatiotemporal information (statistics) about the haline stratification formation process; (c) brief view on the consequences in phytoplankton vertical distributions.

We can conclude that haline stratification in the gulf is common feature already in February (or late January) even if no ice coverage is present. Formation of the haline stratification is not uniform over the gulf. Discrepancies occur both along and across the gulf.

3. Acknowledgements

We would like to thank everybody who has contributed to performing the measurements. This work was supported by the Estonian Research Council grant (PRG602).

References

Chubarenko, I. P., Demchenko, N. Y., Esiukova, E. E., Lobchuk, O. I., Karmanov, K. V., Pilipchuk, V. A., et al. (2017). Spring thermocline formation in the coastal zone of the southeastern Baltic Sea based on field data in 2010–2013. Oceanology 57, 632–638. doi:10.1134/S000143701705006X.

Eilola, K. (1997). Development of a spring thermocline at temperatures below the temperature of maximum density with application to the Baltic Sea. J. Geophys. Res. Ocean. 102, 8657–8662. doi:10.1029/97JC00295.

Eilola, K., and Stigebrandt, A. (1998). Spreading of juvenile freshwater in the Baltic proper. J. Geophys. Res. Ocean. 103, 27795–27807. doi:10.1029/98JC02369.

Granskog, M. A., Ehn, J., and Niemelä, M. (2005). Characteristics and potential impacts of under-ice river plumes in the seasonally ice-covered Bothnian Bay (Baltic Sea). J. Mar. Syst. 53, 187–196. doi:10.1016/j.jmarsys.2004.06.005.

Kari, E., Merkouriadi, I., Walve, J., Leppäranta, M., and Kratzer, S. (2018). Development of under-ice stratification in Himmerfjärden bay, North-Western Baltic proper, and their effect on the phytoplankton spring bloom. J. Mar. Syst. 186, 85–95. doi:10.1016/j.jmarsys.2018.06.004.

Karlson, B., Andersson, L. S., Kaitala, S., Kronsell, J., Mohlin, M., Seppälä, J., et al. (2016). A comparison of FerryBox data vs. monitoring data from research vessels for near surface waters of the Baltic Sea and the Kattegat. J. Mar. Syst. 162, 98–111. doi:10.1016/j.jmarsys.2016.05.002.

Liblik, T., Laanemets, J., Raudsepp, U., Elken, J., and Suhhova, I. (2013). Estuarine circulation reversals and related rapid changes in winter near-bottom oxygen conditions in the Gulf of Finland, Baltic Sea. Ocean Sci. 9, 917–930.

Liblik, T., and Lips, U. (2017). Variability of pycnoclines in a three-layer, large estuary: the Gulf of Finland. Boreal Environ. Res. 22, 27–47.

Merkouriadi, I., and Leppäranta, M. (2015). Influence of sea ice on the seasonal variability of hydrography and heat content in Tvärminne, Gulf of Finland. Ann. Glaciol. 56, 274–284. doi:10.3189/2015AoG69A003.

Stipa, T., Tamminen, T., and Seppälä, J. (1999). On the creation and maintenance of stratification in the Gulf of Riga. J. Mar. Syst. 23, 27–49. doi:10.1016/S0924-7963(99)00049-4.

Intermediate plumes of low oxygen in the southeastern Baltic Sea

Vadim Paka, Maria Golenko, Victor Zhurbas, Andrey Korzh, Alexey Kondrashov

Shirshov Institute of Oceanology, Russian Academy of Sciences, Moscow, Russia (vpaka@mail.ru)

Repeating sections in the Hoburg Cannel (the southern entrance to the Eastern Gotland Basin) reveal signs of a near-bottom inflow current. The salinity and dissolved oxygen concentration (DOC) of the water under the halocline are close to these water parameters in the Słupsk Furrow, and above the halocline a cold intermediate water characterized by maximum DOC is usually observed. The assumed opposite direction of currents in these waters leads to turbulisation of the shear layer and to the enrichment of the inflowing water with oxygen due to entrainment of water from the cold intermediate layer (CIL). This effect clearly plays a positive role, especially during no inflow periods, supporting the ventilation of intermediate layers of the Gotland Deep. However, in August 2019, transects in the eastern flank of the Hoburg Channel showed that the top of the halocline had low DOC, while a deeper water including the bottom layer were moderately oxygenated. Synchronous current profiling with a vessel mounted ADCP showed that the poorly oxygenated layer along with the CIL, located above it, moved to the south, while the underlying, more saline and moderately oxygenated layer reaching the bottom moved to the north (fig. 1). Besides the ADCP measurements, which have a blind zone near the bottom, the near-bottom current was measured by a tilt current meter (TCM) (Paka et al., 2019 a, Paka et al., 2019 b), its position marked with a red dot on the map in fig. 1. The TCM measurements revealed the intermittent bottom current, which, when existed, was directed northward. The nearest area with low DOC in the intermediate depth just below the top of the halocline is the northern Gdańsk Basin, so the layer with low DOC between the brackish CIL with maximum DOC and saline inflow current with moderate DOC supposedly arrived from the east.

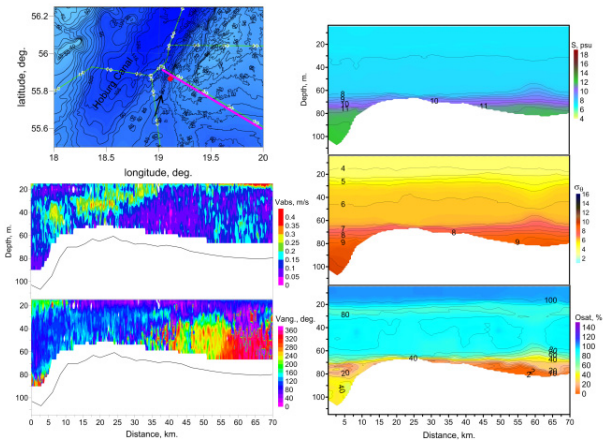


Figure 1. Left - sections of the horizontal current velocity (absolute value and angle, counted clockwise from the north direction) and a map of the area where the section, indicated by the orange line, was carried out; right - sections of salinity, density and oxygen content.

The section was carried out along the border of the EEZ of Russia and Lithuania in August 2019.

In the December 2019 survey, waters with low DOC were observed in the form of intrahaloclinic intrusions in the Słupsk Furrow close to the Slupsk Sill. The structure of the waters adjacent to the Sill indicated a saltwater surge to the Sill from the east (Fig. 2), so we suppose that these intrusions with low DOC arrived from the Gdańsk Basin. The outflow current in the Słupsk Furrow was known, but forming of the hypoxic interface between the inflowing saline and outflowing brackish water, which prevents the oxygen from the CIL to entrain into the inflow current to the Gotland Deep, was observed for the first time.

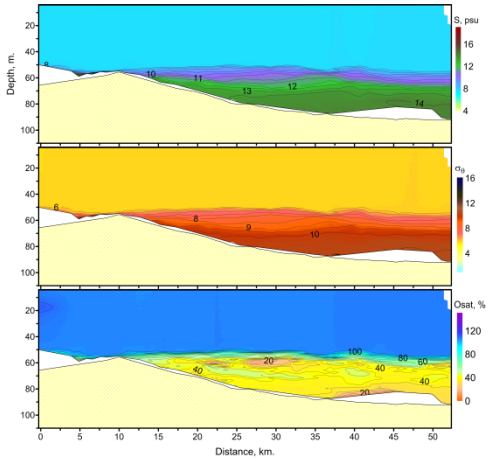


Figure 2. Sections of salinity, density and oxygen content in the Slupsk Furrow, at a distance of 40km from the Slupsk Sill to the east, performed in December 2019.

The reported study was funded by the state assignment of IO RAS, theme N 0149-2019-0013, and RFBR according to the research projects № 18-05-80031 and 19-05-00962.

References

Paka V.T., Zhurbas V.M., Golenko M.N., Korzh A.O., Kondrashov A.A., Shchuka S.A. (2019, a) Innovative Closely Spaced Profiling and Current Velocity Measurements in the Southern Baltic Sea in 2016–2018 With Special Reference to the Bottom Layer, Front. Earth Sci. 7:111. doi: 10.3389/feart.2019.00111

Paka V.T., Nabatov V.N., Kondrashov A.A., Korzh A.O., Podufalov A.P., Obleukhov S.D., Golenko M.N., Shchuka S.A. (2019, b) On the improvement of the tilting bottom current meter, Journal of Oceanological Research, Vol. 47, No. 2, pp.220-229. doi: 10.29006/1564-2291.JOR-2019.47(2).13

Impact of climate change on the water management of the Kiel Canal – A case study

N.H. Schade[1], A.-D. Ebner von Eschenbach[2], J. Möller[1], and V. Neemann[3]

[1] Maritime and Hydrographic Agency, Hamburg, Germany (nils.schade@bsh.de)
[2] Federal Institute of Hydrology, Koblenz, Germany Federal
[3] Directorate General for Waterways and Shipping, Kiel, Germany

1. Background

The Kiel Canal ("Nord-Ostsee-Kanal" [NOK]) is the world´s busiest man-made waterway navigable by seagoing ships. Approximately 100 million tons of cargo are transported on the waterway each year. The canal provides a direct link for the North Sea ports to the Baltic Sea region. The NOK also serves as drainage of a catchment area of about 1,500 km² of Schleswig-Holstein. An important task within the Network of Experts of the Federal Ministry of Transport and Digital Infrastructure (BMVI) is the investigation of the dewatering capacity of the NOK under climate change scenarios.

When balancing the interests of shipping, for example, the requirements of the ferry crossings and hydrological and meteorological conditions, the drainage for the NOK must be controlled such that the water does not exceed or fall below its maximum and minimum levels respectively. A sea level rise (SLR) of approximately 20 cm in the past 100 years has already noticeably reduced the drainage times available. Climate change will result in a further SLR, as well as in changes in the inland hydrology. Since it can be expected that the water levels in the tidal areas of the Elbe River and the Baltic Sea will continue to rise accordingly, the question is whether the frequency of dewatering will change in the future and, if so, how strongly this will affect the NOK and its catchment.

2. Methods

Two different approaches were taken:

(1) On demand of the Federal Waterway and Shipping Agency (WSV), the Federal Institute of Hydrology (BfG) has developed a water balance model to simulate the runoff into the NOK from its catchment, as well as a canal balance model to simulate the NOKs water levels and drainage facilities.

(2) In addition, the Federal Maritime and Hydrographic Agency (BSH) has investigated the NOKs serviceability limit states based solely on oceanographic and atmospheric parameters without running an extensive model setup. This way, both approaches, (1) "model system" and (2) "proxies/ predictors", can be compared. The latter method has been applied to the results of the climate model MPI-OM (Mathis et al., 2017) and possible future changes in long lasting precipitation and high outer water levels have been studied.

3. Results

The drainage potential was calculated using a correlation index from the water level difference between NOK and Elbe. The NOK can only be drained into the Elbe during tidal low waters, when the water level of the Elbe is lower than the NOKs. The drainage of the NOKs catchment area is carried out to 90 % at the southwestern part (Brunsbüttel). This is because the water level difference between NOK and the Elbe allows a more efficient dewatering than at the northeastern part via Kiel-Holtenau into the Baltic Sea.

The climate model MPI-OM provides hourly water levels at the Elbe for the past (the historical run, 1961-2005) and for the future (here the "business as usual"-scenario RCP8.5, 2006-2100). The correlation of the hourly water level difference leads to an amount for the yearly drainage potential. The results are displayed in Figure 2: The impact of SLR on the NOKs drainage potential is crucial; even an expected SLR of 55 cm until 2100 would reduce it around about 40 per cent (Figure 1, blue line). Not included in the climate model's set-up are estimates for future land subsidence in southwestern Schleswig-Holstein (yellow/ orange lines) and for accelerated polar ice melt (purple/green lines) which would reduce the drainage potential even further.

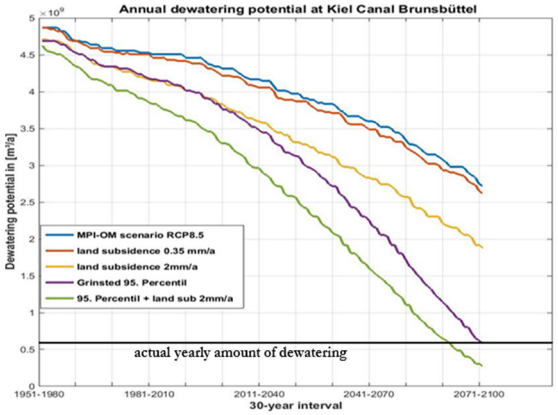


Figure 1. Dewatering potential under RCP8.5 scenario with/ without the effects of land subsidence and an estimation of additional polar ice melting. The black line indicates the actual yearly amount of dewatering needed (600 mill m³/year).

Extremely high tidal low waters reduce or even prevent the possibility of drainage. While it is not difficult to bridge a gap of one tide without dewatering, it is a major challenge in case there are two (or more) consecutive low waters higher than the water level in the NOK (at least 480 cm above gauge normal level). Table 1 displays the events of "no possibility to drainage" per 30-year period for different numbers (1 to 6) of consecutive low waters above the critical water level (480 cm): A rapid increase of consecutive high low waters in the future is apparent and statistically highly significant (at the 99 % level). While on average 10–12 events per year with low water levels higher than the respective water level in the NOK can be observed today (1981-2010), these events will occur much more frequently in the future due to the expected SLR.

These results are supported by the investigations with the canal balance model (BfG-Bericht, 2019): Changes in the dewatering potential are mainly driven by SLR and can

cause severe problems in the future, especially in case the high-end scenario (170 cm SLR) commences.

Table 1. Number of events per 30-year period of low waters (LW) at Brunsbüttel higher than the design water level at Kiel-Canal, for one up to six consecutive low waters.

LW Event	*1951–1980*	*1981–2010*	*2011–2040*	*2041–2070*	*2071–2100*
N=1	347	516	564	965	1 752
N=2	89	136	185	329	702
N=3	31	54	73	165	377
N=4	8	17	24	63	167
N=5	2	4	11	33	90
N=6	1	0	3	15	45

Then, the dewatering potential would be reduced in 300+ days of the year (Figure 2). Furthermore, the almost negligible effects of changes in the hydrology (displayed by the colored bars for the near "nZ" and far "fZ" future in the RCP2.6 and RCP8.5 scenario respectively) are apparent.

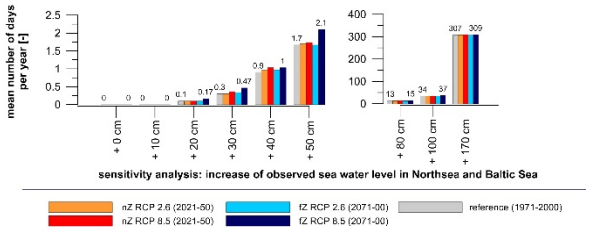


Figure 2. Mean number of days per year with a critical hourly water level W_{NOK} > 5.40 m PNP for different scenarios of changing hydrology in the NOK catchment area (RCP2.6/RCP8.5, nZ = near future, fZ = far future) for different scenarios of SLR (0 - 170 cm).

One possible adaptation could be achieved with the installation of a pumping station (Figure 3), maintaining 2/3 of the present dewatering capacity when used in case the NOKs water level exceeds 5.40 m. In reality, the pumps would already be used at lover water levels.

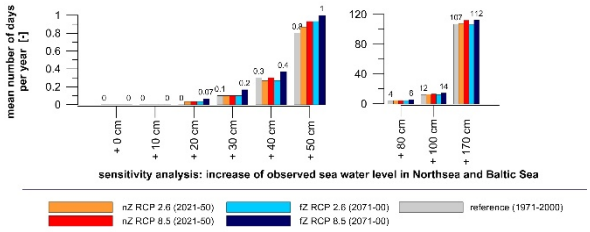


Figure 3. See Figure 2 but for using a pumping station with a capacity of 25 m^3/s in addition to the existing dewatering capacity (sluice gates and dewatering circuits).

4. Applications

With the help of the model system outlined above, serviceability limit states of the NOKs water management have been identified and possible changes in the occurrences thereof due to climate change have been derived. These analyses provide an important contribution to the Federal adaptation strategy on climate change. This task is characterized in the report "Adaptations to the global Climate Change" (Bundesregierung, 2015): One of the activities is focused on a resilient traffic infrastructure for the NOK. Based on the results of the above-described studies, the WSV investigates prospective approaches, e.g., long-term options for action, such as the creation of floodplains or the construction of a new pumping station. The following practical goals can now be achieved:

- The NOKs function as a draining channel can be secured at long term
- Cancellation of the ferry traffic can be reduced/avoided
- The future efficiency of the NOK as a traffic way can be assessed and ensured by goal-oriented measures

The substitution of sluices that ensure the undisturbed shipping traffic, e.g., will be planned according to the new findings about the accelerated sea level rise. The WSV will consider a SLR of about 1.74 m (Grinsted et al., 2015) instead of 0.50 m formerly considered in the "General Plan on Coastal Protection" (MELUR-SH, 2012). In this process, the sluice gates in Kiel-Holtenau will be planned in such a way that it will be possible to adapt the construction along with the actual SLR, which in turn allows optimization of the consumption of resources in line with demands.

The results of this study are part of the latest report of the UNECE Group of Experts on Climate Change Impacts and Adaptation for Transport Networks and Nodes[1].

5. Outlook

The long-term objective is to determine the risks from combined climate impacts (i.e. high outer water levels & heavy precipitation) using an ensemble of climate models, including upcoming CMIP6 model runs (global and regional). Further investigations include linking the general weather situation to tense dewatering situations (see Jensen et al., 2020). In addition, the "proxies/predictor" method will be used to examine possible future changes in the dewatering of other river catchments in coastal areas, where no model setup exists.

References

Bundesregierung (2015) Fortschrittsbericht zur Deutschen Anpassungsstrategie an den Klimawandel, APA II, Stand 2015.

BfG-Bericht (2019) Wassermengenbewirtschaftung des Nord-Ostsee-Kanals unter gegenwärtigen und zukünftigen Verhältnissen, Phase 1 (2014-2019), Authors: Dr.-Ing. A.-D. Ebner von Eschenbach, Dipl.-Hyd. J. Hohenrainer, final draft 23.08.2019, publication in progress.

Grinsted, A., Jevrejeva, S., Riva, R.E.M., and D. Dahl-Jensen (2015) Sea level rise projections for northern Europe under RCP8.5, Climate Research, 64, 15-23. DOI: 10.3354/cr01309

Jensen, C., Moeller, J., Loewe, P., and N.H. Schade (2020): Linking weather types to tense dewatering situations of the Kiel Canal, 3rd Baltic Earth Conference, presentation.

Mathis, M., Elizalde, A., and U. Mikolajewicz (2018): Which complexity of regional climate system models is essential for downscaling anthropogenic climate change in the Northwest European Shelf? Climate Dynamics, 50(7-8), 2637-2659. DOI: 10.1007/s00382-017-3761-3

MELUR-SH (2012) Generalplan Küstenschutz des Landes Schleswig-Holstein - Fortschreibung 2012.

[1] https://www.unece.org/trans/areas-of-work/trends-and-economics/activities/group-of-experts-on-climate-change-impacts-and-adaptation-for-transport-networks-and-nodes-wp5ge3.html

Changes in the Hydrological Seasons of Estonian Rivers During the Period 1928-2017

Mait Sepp

Department of Geography, University of Tartu, Estonia (mait.sepp@ut.ee)

1. Introduction

Recent studies (Jaagus et al., 2017; 2018; Kotta et al., 2018) have shown that the warming of the winter months over the last half century are clearly affecting the runoff rates of Estonian rivers. During the winter months, mainly January and February, the runoff has increased significantly. Increase of drainage rates in March have been particularly drastic, suggesting that spring high water has shifted from April to March. There are no significant changes in the runoff of other months, but it should be noted that in the context of the last half century, a positive trend is observed in June precipitation in Estonia.

Like in other Nordic countries, Estonian rivers typically have four seasons: summer and winter minima and autumn and spring maxima. However, it can be assumed, based on changes in the precipitation and runoff regime of certain months, that certain changes may have occurred also in hydrological seasons.

The aim of this study is to analyze how the changes of runoff are expressed in the hydrological seasons of Estonian rivers over the last 90 years (1928-2017).

2. Data and Methods

The average daily runoff (m^3/s) data gathered from eight hydrological stations (Kasari, Keila, Lüganuse, Oore, Pajupea, Riisa, Tõlliste, Tõrve) are used here. The data are obtained from the Estonian Weather Service. Because the catchment areas characterized by the stations vary in size, the daily average runoff was converted to the specific runoff ($l/s/km^2$). Stations are selected based on quality and length of their data and relative similarity of their hydrographs. For example, the river with the longest observation line in Estonia, the River Emajõgi, has been excluded from this work. The reason is that its water regime is regulated by Lake Võrtsjärv and large swamps, and therefore the annual hydrograph differs from other rivers.

Because hydrographs of stations used here are synchronous, then the daily arithmetic mean of eight rivers was calculated. This can be called the average specific runoff of Estonian rivers, which characterizes the flow of water in the total area of 11128.7 km^2, i.e., about 1/4 of Estonia's territory.

Here we compare three periods of 30 years (1928-1957, 1958-1987, 1988-2017). This means that the average value of specific runoff over a given 30-year period is calculated for each date.

3. Results

The comparison of the 30-year periods shows that the water regime of Estonian rivers has undergone fundamental changes in recent decades (Figure 1). The winter minimum season have virtually disappeared, and the maximum values of spring high water season have decreased significantly. The typical Northern European runoff regime is changing to a regime typical for Western Europe. This means that instead of four hydrological seasons, there are now virtually only two: maximum during the cold half-year (November-April) and minimum during the warm period (May-October).

It is important to note here that this kind of changes in the water regime in Estonia were predicted by model calculations made in the mid-1990s (Kallaste, Kuldna 1998).

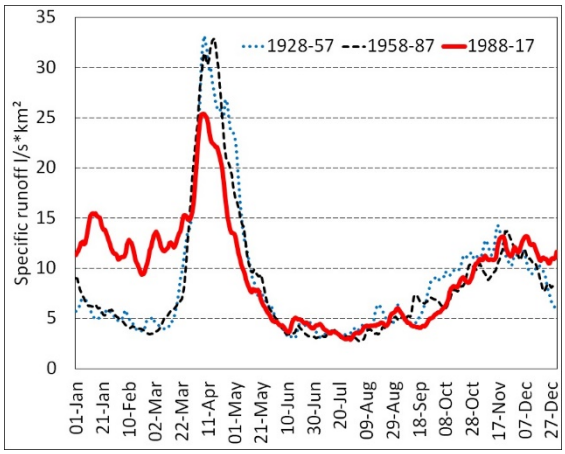


Figure 1. Annual hydrographs of 30-year average specific runoff for Estonian rivers during the years 1928-1957, 1958-1987, and 1988-2017.

References

Jaagus J., Briede A., Rimkus, E., Sepp, M. (2018) Changes in precipitation regime in the Baltic countries in 1966–2015. Theoretical and Applied Climatology, Vol. 131, pp 433–443.

Jaagus J., Sepp M., Tamm T., Järvet A., Mõisja K. (2017) Trends and regime shifts in climatic conditions and river runoff in Estonia during 1951–2015, Earth System Dynamics, Vol. 8, pp. 963–976

Kallaste T., Kuldna P. (eds.) 1998. Climate change studies in Estonia. UNEP/GEF, Estonian Ministry of Environment, SEI-Tallinn, pp. 200

Kotta J., Herkül K., Jaagus J. et al. (2018). Linking atmospheric, terrestrial and aquatic environments in high latitude: Regime shifts in the Estonian regional climate system for the past 50 years. PLOS ONE, Vol. 13, No 12, pp ARTN e0209568–20

Changes in wind parameters in Estonia during the period 1966-2016

Mait Sepp[1], Ain Kull[1] and Piia Post[2]

[1] Department of Geography, University of Tartu, Estonia (mait.sepp@ut.ee)
[2] Institute of Physics, University of Tartu, Estonia

1. Introduction

Several studies (Sepp, Jaagus, 2002; Jaagus, 2006; Hoy et al., 2013; Cahynová, Huth, 2014) have shown that changes in the Baltic Sea region climate are related to the strengthening of the so-called Western circulation. Specifically, the advection of significantly warmer air from the North Atlantic to the Baltic Sea has led to significant warming of winters.

Changes in general atmospheric circulation have also caused shifts in the direction and strength of near-surface winds (Keevallik, Soomere, 2008; 2014; Jaagus, Kull, 2011; Soomere et al., 2015). Generally, wind data from weather stations located on the sea islands was preferred in the cited works. Analyses of this restricted data suggest an increased incidence of strong westerly winds. On the one hand, this preference prevents distortions that may arise from changes in the landscape, such as forests and urbanization. On the other hand, analyzing data from a few "ideal" weather stations do not give a complete picture of wind trends all over Estonia.

The aim of this work is to understand whether there have been any statistically significant changes in some wind direction and speed classes in Estonia over the past half century (1966-2016). Here we are looking at changes in the frequency of certain events: cases of wind blowing from a given direction and given strength.

2. Data and Methods

Wind parameters measured at eight Estonian weather stations (Valga, Võru, Väike-Maarja, Jõhvi, Kunda, Lääne-Nigula, Vilsandi, and Kihnu), obtained from the Estonian Weather Service, were used in this study. The wind speeds (m/s) used here were measured as average speeds of 10-minute periods at 10 meters from the surface. The measurements were made eight times a day (UTC 00:00, 03:00, 06:00, 09:00, 12:00, 15:00, 18:00, 21:00). The wind direction was measured at the same times. Since the introduction of automatic stations (i.e. since 2003), wind data can be obtained every 1 hour. However, for the sake of comparability between periods, the data for the eight measurement periods was selected from the data measured after 2003.

The greatest challenge with wind direction data is that, depending on the weather station, the data is presented in 16 rhumbs (22.5° sectors) until 1981, from then on in 10 degrees, and in 1 degree sectors in case of automatic stations. Thus, defining common direction classes throughout the period was a major problem. Therefore, for some analyses, a shorter period (1980-2016) was used.

The analysis was based on changes in classes of wind speed and direction. The classification of wind speed was based on quartiles. This means that, as a first step, the threshold value for the Quartile I of the wind speed for every station was calculated. It represents lowest wind speeds. In this case, cases of 0 m/s were taken as a separate class and were excluded from the quartile calculation. The following classes were respectively Quartile II (50%) and III (75%) and strong wind events, i.e. values above the 75% limit. Storms, defined for each station as cases when the wind speed exceeds the 95th percentile threshold, were studied separately.

For wind direction classes, attempts were made to find sectors that overlap with all sectors of measurement. This was a difficult task, especially connecting rhumbs and 10-degree sectors. Thus, there are four 90° sectors common to the 1966-2016 wind direction measurements: NE - 0-90; SE-100-180; SW - 190-270, and NW - 280-360 degrees. For these sectors, the trend to be calculated was not dependent on changes in measurement methodology.

In addition, the division of the measured wind directions into 12 sectors (N - 350-10°, NNE - 20-40°, ..., WWN - 290-310°, NNW - 320-340°) for the period 1966-2016 was used. However, the results of this approach must be interpreted with caution, as in this case the data for the 16 rhumbs are not equally distributed across sectors. Therefore, calculations of 12 sectors were made without first period (most of the stations 1966-77, in the case of Jõhvi 1966-1981) data.

Changes were analyzed by linear trend ($p<0.05$). However, as there are concerns about the quality of the data, trend values will not be stated below, but it will be determined whether the trend of statistically significant change is positive or negative. This means whether the number of cases of a given speed class in a given direction sector has increased or decreased during the period under review.

3. Conclusions

The quality of the raw data is generally poor. This is due to changes in the location of some measurement sites, trees and obstructions around some stations, changes in measurement methodologies, and missing data. Changes in measurement methodology, especially the transition of wind direction measurements from the 16 rhumb system to the 10 degree sectors, leave very sharp shifts in the time series.

However, there are clear one-way changes in wind data in Estonia. These cannot be explained solely by inhomogeneity or changes in the landscape. For wind speeds, a general decrease can be observed. While the increase in the cases of weak winds (Quartile I) can be explained by the increase in forest cover in Estonia, the decrease in the number of storms indicates changes in the general atmospheric circulation.

In general, the prevalence of southwest winds has increased and the proportion of wind blowing from the east has decreased. This result is in agreement with several studies confirming the dominance of western circulation in recent decades. At the same time, it cannot be said that in some sectors strong winds have started to blow. Trend analysis suggests that the winds have "calmed down" over the past half century. This includes a decrease in the

number of storms (95th percentile events) and their mean wind speed. However, there is a contradiction – one of the consequences of global warming is usually thought to be an increase in storminess, which has also been observed by Estonian authors (Jaagus, Suursaar, 2013; Suursaar, Jaagus, Tõnisson, 2015). Yet, the ratio of the number of storms to their average wind speed shows that the number of extreme wind storms over the last half century has in fact decreased whereas their average wind speeds have increased.

References

Cahynová, M., Huth, R. (2014) Atmospheric circulation influence on climatic trends in Europe: an analysis of circulation type classifications from the COST733 catalogue. Int. J. Climatol. Vol. 36, pp. 2743-2760

Hoy, A., Sepp, M., Matschullat, J. (2013) Large-scale atmospheric circulation forms and their impact on air temperature in Europe and northern Asia. Theor. Appl. Climatol. Vol. 113, pp. 643-658

Jaagus, J. (2006) Climatic changes in Estonia during the second half of the 20th century in relationship with changes in large-scale atmospheric circulation. Theor. Appl. Climatol. Vol. 83, pp. 77–88

Jaagus, J., Kull, A. (2011) Changes in surface wind directions in Estonia during 1966-2008 and their relationships with large-scale atmospheric circulation. Estonian Journal of Earth Sciences, Vol. 60 (4), pp. 220–231

Jaagus, J., Suursaar, Ü. (2013) Long-term storminess and sea level variations on the Estonian coast of the Baltic Sea in relation to large-scale atmospheric circulation. Estonian Journal of Earth Sciences, Vol. 62(2), pp. 73–92

Keevallik, S., Soomere, T. (2008) Shifts in early spring wind regime in North-East Europe (1955–2007). Climate of the Past, Vol. 4(3), pp. 147–152

Keevallik, S., Soomere, T. (2014) Regime shifts in the surface-level average air flow over the Gulf of Finland during 1981–2010. Proceedings of the Estonian Academy of Sciences, Vol. 63(4), pp. 428–437

Sepp, M., Jaagus, J. (2002) Frequency of circulation patterns and air temperature variations in Europe. Boreal Environment Research. Vol. 7 (3), pp. 273–279

Soomere, T., Bishop, S. R., Viska, M., Räämet, A. (2015) An abrupt change in winds that may radically affect the coasts and deep sections of the Baltic Sea. Climate Research, Vol. 62(2), pp. 163–171

Suursaar, Ü., Jaagus, J., Tõnisson, H. (2015) How to quantify long-term changes in coastal sea storminess? Estuarine Coastal and Shelf Science, Vol. 156, pp. 31–41

Evaluation of changes in the river Viliya annual runoff under the fluctuation climate conditions

Alexander Volchak, Sergey Parfomuk and Sviatlana Sidak

Brest State Technical University, Brest, Belarus (harchik-sveta@mail.ru)

1. Introduction

43% of the territory of Belarus belongs to the Baltic Sea basin (the system of the Neman, the Western Dvina, the Western Bug, the Viliya and the Lovat). The transboundary expending of these river basins works towards to the intense use of water resources for water supply, agriculture, hydropower engineering and navigation. The Viliya is considered to be one of the most loaded rivers. The fact takes place due to the direct water withdrawals for submission into the Vileyka-Minsk water system, and the impact of the current climate fluctuations (Volchak and Parfomuk 2019). They require effective trans-boundary water resources management in the context of such intensive use of water resources and the currently observed climate changes which in turn requires a more detailed assessment of changes in hydro-meteorological criteria.

The aim of the research is to analyze long-term variability of the average annual consumption of water in the basin of the River Viliya (Belarus) in the period 1949 - 2017 in the conditions of the changing climate.

2. Initial data and methods

There are three operating gauging stations on the researching area (Vileyka Town, Steshytsy Village, Mikhalishki Village). The series of annual water consumption during the period 1949 - 2017 are used as the source hydrological data. Missing data in the series of observations was renovated with the help of the applied program "Hydrologist" (Volchak and Parfomuk 2009).

The first step of the research was the analyses of the long-term versatility of the annual average air temperature in three weather stations in the basin of the River Viliya. There were reviewed several periods of observations - the entire observation period (1949 - 2019), as well as broken down into two intervals (1949 - 1978 and 1979 -2019). For the entire research period, the trend of average annual air temperature in the basin of the River Viliya was on average 2.5 °C/100 years. The analysis also showed that during the period 1979 - 2019 there is a trend of increasing average annual air temperatures, the temperature rise is more than 1.8°C over 40 years, whereas during the previous period (1949 - 1978) the temperature remained practically changeless. It is important to note that during the reporting period in the basin of the River Viliya average annual rainfall has increased. This fact should be considered when carrying out hydro-meteorological calculations. Considered climatic changes influence directly on the water regime of the River Viliya.

The next step of this work is to evaluate inter-annual flow variability of the River Viliya. The analysis included valuation of the autocorrelation, trend and statistical homogeneity of the series. There is a graph of a chronological change of annual water consumption at the river stations of the River Viliya in Fig. 1. To evaluate the significance of the linear trend the Student's t-test and the coefficient of correlation are used. The results of the evaluation are shown in table 1.

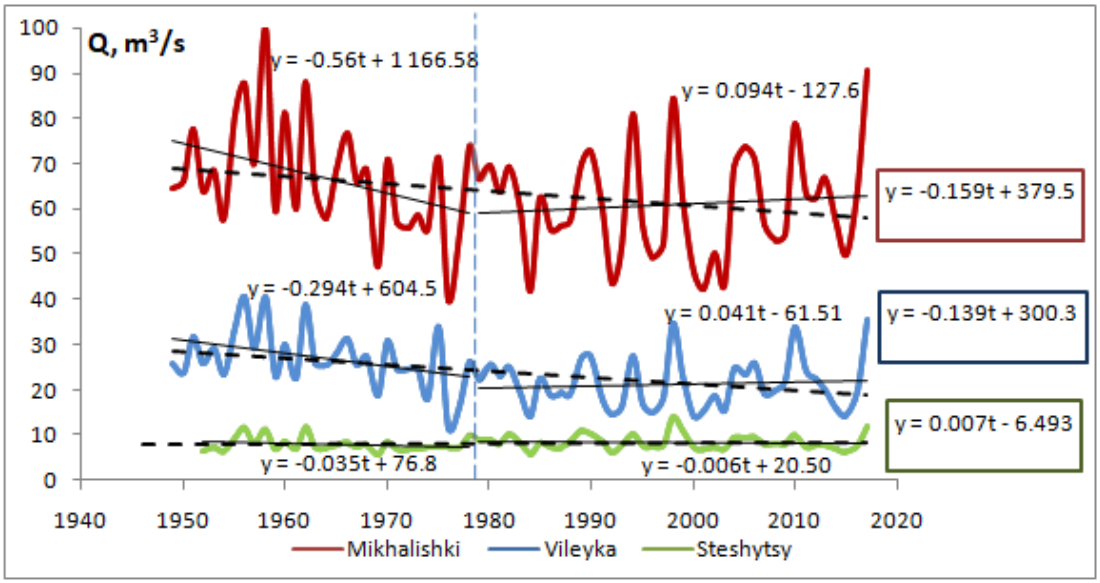


Figure 1. The chronological current of the average annual water consumption at the river stations of the River Viliya during the period 1949 - 2017.

Table 1. An evaluation of the long-term dynamics of annual runoff of the River Viliya for different intervals.

Station	Average annual	Trend equation	Correlation coefficient	Significance of the correlation coefficient	Significance of trend parameters
Averaging period 1949-2017					
Vileyka	23.81	y=-0.139*t+300.3	0.246	significant	significant
Mikhalishki	63.57	y=-0.159*t+379.5	0.144	not significant	significant
Steshytsy	8.17	y=0.007*t-6.493	0.138	not significant	not significant
Averaging period 1949-1978					
Vileyka	27.1	y=-0.294*t+604.5	-0.044	not significant	significant
Mikhalishki	67.0	y=-0.56*t+1166.58	-0.031	not significant	significant
Steshytsy	7.92	y=-0.035*t+76.8	-0.077	not significant	not significant
Averaging period 1979-2017					
Vileyka	21.3	y=0.041*t-61.51	0.174	not significant	not significant
Mikhalishki	60.9	y=0.094*t-127.6	0.161	not significant	not significant
Steshytsy	8.31	y=-0.006*t+20.5	0.286	not significant	not significant

The homogeneity of the series was tested with the involvement of the Student's t-test (for expected value) and the Fisher test (for variance). The ranks were divided into 2 periods: before 1978 and after. As the use of the Student's t-test is possible only to normally distributed random variables, then first the data were checked for the normality of distribution. This was done using the criteria of Kolmogorov-Smirnov and Shapiro-Wilks. The results of the test for uniformity of the series of annual usage are shown in table 2 (the highlighted values are statistically significant).

Table2. The criteria for the statistical tests of homogeneity of the series.

Station	Averaging period	Criterion	
		F	t
Vileyka	1949-1978 – 1979-2017	1.41	**3.94**
Mikhalishki	1949-1978 – 1979-2017	1.16	**2.07**
Steshytsy	1952-1978 – 1979-2017	1.15	1.22

3. Results

The researches have shown that the formation of a water mode of the river River Viliya takes place against the background of statistically significant positive dynamics of average annual air temperature and annual precipitation in recent decades. As shown by the joint analysis of Fig.1, tab. 1 and 2 the average annual runoff at the river river stations station of Steshitsy Village increased during the period 1949 - 2017. There are statistically significant linear negative trends for average annual water consumption at the river stations of the Vileyka Town and Mikhalishki Village during the period 1949 - 2017. For these stations the statistics of the Student's t-test of equality of mathematical expectations exceeded the critical value at a significance level of 5%. Thus the average annual water consumption in the temporal series of the Viliya in the river stations of Vileyka Town and Mikhalishki village the statistical heterogeneity is determined. No statistically significant changes in the current are observed at all stations during the period 1979 - 2017. It is concerned to the run-off regulation due to the Vileyka water storage reservoir.

References

Volchak A, Parfomuk S (2019) Assessment of changes in the Viliya River runoff in the territory of Belarus, Limnological Review, Lol. 18, No. 4, pp. 185–196.

Volchak A, Parfomuk S (2009) The application package for definition of characteristics of the river runoff, Bulletin Of Polessky State University, No. 1, pp. 22–30.

Small-scale Spatial Variability of Hydro-physical Properties of Differently Degraded Peat

Miaorun Wang, Haojie Liu, Bernd Lennart

Faculty of Agricultural and Environmental Sciences, University of Rostock, Rostock, Germany
(miaorun.wang@uni-rostock.de)

1. Introduction

Spatial variability of soil properties is important for hydrological studies. However, little information is available on the spatial variability of hydro-physical properties of peat soils. Liu et al. (2019) reported that peat degradation resulting from drainage and cultivation can significantly alter the soil physical and hydraulic properties, which causes an increase in bulk density but a decrease in saturated hydraulic conductivity and macroporosity. In this study, three study sites in Mecklenburg-Western Pomerania in Germany: natural, degraded and extremely degraded peatland were selected for this study. At each site, 72 undisturbed soil cores were collected from 5m by 5m grid cells in an area of 40m by 45m. The saturated hydraulic conductivity (Ks), soil water retention curves, total porosity, macroporosity, bulk density and soil organic matter (OM) content were determined for all sampling locations. The van Genuchten model parameters (θs, α, n) were optimized using the RETC software package.

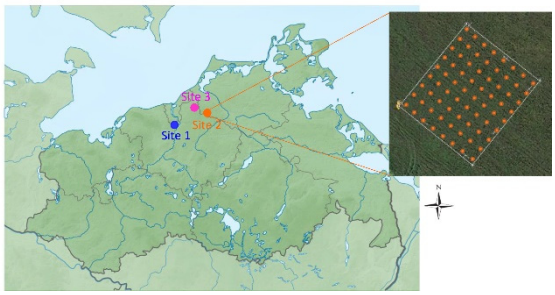


Figure 1. Three sampling sites in Mecklenburg-Western Pomerania in Germany. (right plate: 72 sampling points at each site within 35m×40m plot).

2. Hypothesis and Objectives

We hypothesize that hydro-physical properties could be spatially auto-correlated. Our main objective is to analyze the spatial variability of all peat physical properties and hydraulic properties by using geostatistics.

3. First Results

A strong positive correlation between macroporosity and Ks was observed irrespective of the degradation stage of the peat. However, the relationships between macroporosity and Ks differed for the different sites. The soil physical properties (e.g. OM content and bulk density) exhibited different levels of spatial autocorrelation depending on the soil degradation stage. The cross-semivariograms showed a strong or moderate spatial dependency between soil physical properties and van Genuchten model parameters. The more a peat soil is degraded, the more likely it is that soil physical properties are spatially dependent.

Table 1 Pearson correlation coefficient between different hydro-physical properties of three study sites. (blue: site 1, extremely degraded peatland; orange: site 2, degraded peatland; pink: site 3, natural peatland); n = 72 per site

	1	2	3	4	5	6	7	8
1.SOM	-							
2.BD	-0.861*** -0.792*** -0.121	-						
3. Total Porosity	0.528*** 0.665*** -0.040	-0.821*** -0.788*** -0.004	-					
4. Macroporosity	0.204 -0.171 0.046	-0.336* 0.033 -0.678***	0.218 -0.205 0.045	-				
5. LogKs	0.182 -0.255 0.018	-0.237* 0.244* -0.424**	0.128 -0.477*** -0.073	0.553*** 0.573*** 0.581***	-			
6. θs	0.484*** 0.573*** 0.007	-0.676*** -0.584*** -0.107	0.840*** 0.852*** 0.941***	-0.003 -0.679*** 0.070	0.068 -0.678*** -0.063	-		
7. logα	-0.046 -0.113 -0.123	0.032 -0.021 0.245	-0.168 -0.045 -0.232*	0.575*** 0.715*** 0.208	0.350 0.159 0.182	-0.385 -0.364* -0.469***	-	
8. n	0.152 0.435** 0.098	-0.236* -0.337* -0.745***	0.434** 0.381** 0.078	-0.431** -0.722*** 0.714***	-0.246* -0.327* 0.458***	0.666*** 0.629*** 0.289*	-0.884*** -0.820*** -0.476***	-

4. Conclusion

In conclusion, degradation stage plays an important role and should be considered more often in spatial analysis. The obtained cross-semivariogram may serve as a basis for 2D and 3D hydrological modelling.

References

Liu, H., Lennartz, B. (2019). Hydraulic properties of peat soils along a bulk density gradient – A meta study. Hydrological Processes, 33, 101–114

Features of the formation of hanging dam and ice jam on the rivers of Belarus in a changing climate

Ludmila Zhuravovich, Alena Kvach and Maryia Asadchaya

State Institution «Center for of hydrometeorology and control of radioactive contamination and environmental monitoring of The Republic of Belarus» (Belhydromet) (gid2@hmc.by)

1. Introduction

Among dangerous hydrological phenomena, the most significant damage to the population and economic sectors is caused by floods, which result in flooding of adjacent territories. Floods most often occur as a result of the passage of the spring flood, formed by the influx of meltwater accumulated during the winter season; rain floods, with significant amounts falling over a short period of time. Also, flooding on rivers occurs as a result of backwater associated with ice formation and ice breaking, which is formed annually in many parts of the country's rivers. In recent decades, there has been a marked change in climate conditions, which has led to an increase in the number of cases of retaining phenomena and rising water levels.

2. Methods

The initial data for the analysis were the materials of the State water cadastre, in particular information about the level and ice regimes of rivers. The study analyzed daily water levels and ice phenomena, which determined the presence of congestion and congestion in conjunction with the course of meteorological elements. The period of generalization made 1937-2018 years.

The study examined the following characteristics of hanging dam and ice jam:

the maximum rise of water levels;

the duration of hanging dam or ice jam;

lasting of hanging dam and ice jam. This characteristic varies considerably in time and space. In some places, they are repeated after 2 to 5 years, in others-much less often.

3. Analysis of hanging dam phenomena

An increase in the frequency hanging dam phenomena connected with the shift timing of the freezing of the rivers at a later date and with the process of freezing of the rivers, during which ice formation occurs inside the water mass that leads to increased formation of sludge and increase of water availability and, consequently, the formation of hanging dam.

The average duration of conversations on the Western Dvina River increased by 25%. On Vilia, the duration did not change, and on Neman, it even decreased by 30%.

The maximum reference levels for the period of climate change have changed ambiguously. On the Western Dvina River, the average long-term values of the maximum reference level increased, while on the Vilia and Neman Rivers they remained unchanged.

4. Analysis of ice jam phenomena

The analysis showed that ice jam was observed less frequently on the Neman and Western Dvina Rivers, and their frequency increased on the Vilia River. The decrease in the frequency of ice jam on the rivers under consideration was not high in absolute terms. The decrease is most likely due to unstable weather (returns of cold) during the spring season in recent decades, which contributes to slower destruction of the ice cover and the formation of congestion.

The duration of ice jam decreased on all rivers except the Western Dvina, where it remained unchanged.

A decrease in maximum ice jam levels is observed on the Vilia, Western Dvina and Neman rivers.

The formation of congestion is closely related to the formation of ice cover on rivers. The thickness of the ice during the period of climate change has changed on average by 10-15 cm in the direction of decrease. These changes are most noticeable for the Western Dvina River since 1989, and for the rest - since 1970. On the Vilia and Neman Rivers in some years, the ice is not established or has a discontinuous ice cover.

5. Conclusions

In connection with the noticeable climate change in recent decades, which is most significantly observed in the winter season, there has been a change in the level and ice regime of the rivers of Belarus.

The frequency of hanging dam or ice jam events that cause a significant increase in water levels in rivers has increased.

The increase in the frequency of hanging dam is associated with an increase in the number of thaws that contribute to the formation of loose ice and its accumulation in the riverbed, which is associated with an increase in the duration of hanging dam and maximum levels.

The decrease in the number of ice jam and the increase in ice jam levels are associated with an unstable increase in air temperature during the spring season in recent decades.

References

Hydrological monitoring of the Republic of Belarus. / edited by A. I. Polishchuk, G. S. Chekana-Mn.: Knigazbor, 2009. - 260 p.

Archive database of OGH materials of observations at the posts of the Ministry of natural resources and environmental protection of the Republic of Belarus.

Spontaneous hydrometeorological phenomena on the territory of Belarus: reference book / G. S. Chekan, F. M. Osherov, L. A. Nekrasova, I. S. Danilovich; edited by M. A. Golberg. – Meganewton.: Belnitz Ecology, 2002. - 132 p.

Topic 6

Multiple drivers of regional Earth system changes

Decision support tools for the management of eastern Baltic Sea coasts

Mojtaba Barzehkar[1], Kevin Ellis Parnell[1] and Tarmo Soomere[1,2]

[1] Department of Cybernetics, Tallinn University of Technology, Estonia (mojtaba.barzehkar@taltech.ee)
[2] Estonian Academy of Sciences, 10130 Kohtu 6, Tallinn, Estonia

1. Introduction

Climate change has increasingly become a global environmental challenge in recent years and many coastal ecosystems are threatened by its potentially irreversible effects (Ng *et al.* 2019). The Baltic Sea coasts have a range of natural environments subject to a wide variety of climate change-induced hazards such as sea level rise, storm surges, ice cover changes, and coastal floods (Hünicke *et al.* 2015). Weather events changed or made more severe by climate change could significantly transform the physical characteristics of coastal ecosystems, such as slope, elevation, rate of shoreline change, and the ecological features such as biodiversity in marine protected areas, as well as socioeconomic factors such as human safety, coastal livelihoods and human infrastructure (Bagdanaviciute *et al.* 2015).

Anthropogenic activities such as the provision of new infrastructure (Ning *et al.* 2018) can be contributing factors in intensifying the negative effects of climate change on the coasts of the Baltic Sea (Bagdanaviciute *et al.* 2019). These activities have increased the possibility of coastal erosion and an intense rate of coastline change (Harff *et al.* 2017). Therefore, both the natural changes caused by a changed climate and human developments are perceived among competent experts to potentially have harmful effects on the Baltic Sea coasts (Harff *et al.* 2017).

2. Scientific Background and Research objectives

Many approaches and models have been developed for tackling coastal problems triggered by climate change and human activities. In some locations they have helped mitigate coastal inundation and erosion impacts (Sekovski *et al.* 2019). One of the most efficient strategies is Multi-criteria Evaluation using a Coastal Vulnerability Index (CVI), which provides a quantitative analysis for vulnerability ranking of diverse coastal segments and enables the determination of the most vulnerable coastal areas prone to destructive hazards (Gallego Perez and Selvaraj 2019). The aim of this paper is to advance discussion of the use of Decision Support Tools to promote the sustainability of Baltic Sea coasts and their resilience to the consequences of climate change. The incorporation of local knowledge and perceptions, and experts' knowledge, into scientific decision-support tools to pragmatically understand the root causes of coastal threats is also addressed.

Bagdanaviciute *et al.* (2019) utilized Geographical Information System (GIS) and multicriteria evaluation based on Analytical Hierarchy Process (AHP) methods to quantify and analyze the coastal risks associated with climate change in the Baltic Sea. They found that the combination of GIS and AHP beneficial and applicable to the purpose of environmental planning that needs to evaluate the degree of different risks in low-lying areas. Mullick *et al.* (2019) applied the Fuzzy Logic approach based on geospatial analysis to estimate coastal vulnerability in Bangladesh. They found that this method is an efficient approach to resolve the uncertainty of large-scale vulnerability analysis with the normalization of related factors. Gallego Perez and Selvaraj (2019) used GIS and satellite images extracted from the United States Geological Survey (USGS) website to examine coastal vulnerability in Columbia. They concluded that the integration of GIS and remote sensing can be applied as an effective tool by decision-makers to devise coastal hazards management plans in a more sensible way. Ferreira *et al.* (2019) utilized a Bayesian network to assess coastal vulnerability for the southern coast of Portugal. Their results indicated that the model is able to better investigate and identify coastal management measures that are fundamental in alleviating risks to coastal communities.

For our research, the incorporation of diverse, efficient decision support tools such as GIS, Fuzzy Logic, AHP, Weighted Linear Combination (WLC) accompanied by Google Earth Engine analysis and numerical modelling will be used to progress the identification of vulnerable coastal areas in the Baltic Sea.

3. The contribution of this study

The efficiency and usefulness of coastal management strategies can be improved by decision support tools. GIS has evolved to be a productive decision support tool in its own right, and can produce maps and other information products expressing coastal vulnerability based on different categories of susceptibility (very low, low, average, high and very high) (Ghoussein *et al.* 2018). The application of Google Earth Engine software employing Landsat, Sentinel 2 and TOPEX Satellite images can be used as a decision support tool to efficiently monitor changes of shoreline, sea level rise and land-use over different years (Mullick *et al.* 2019). The use of numerical methods provides an opportunity to test coastal risk mitigation scenarios for the specific conditions of the Baltic Sea coasts.

While all tools provide valuable information, the integration of the outputs of the various robust decision support tools is likely to provide the biggest advance in assisting to tackle Baltic Sea coastal vulnerabilities to climate change effects (Bagdanaviciute *et al.* 2019). One of the methods of this study is to use the combined approaches of Fuzzy Logic, AHP and WLC. Fuzzy Logic can provide flexibility to represent the natural variability of vulnerability on a continuous scale and has the capability to handle the uncertainty of vulnerability analysis processes (Mullick *et al.* 2019). This can help identify coastal vulnerability at small grid scales with wider spectrums, which will be more aligned with the coastal physical, ecological and socioeconomic potentials. Coastal managers will have more options (classified on a scale between 0 and 1) to express the degree of spatial variability of vulnerability (Mullick *et al.* 2019).

Another strong point of this research is using Google Earth Engine with the application of available online satellite images to analyze the rate of shoreline change, land-use changes and so on. Indeed, applying this web platform based on code editor and explorer tools will make it feasible to open access to large numbers of available satellite images. Also, this web-based decision support tool offers access to very high spatial resolution satellite data (Leinonen *et al.* 2018). Figure 1 shows the integration of Decision support tools for assessing the coastal vulnerability of the Baltic Sea.

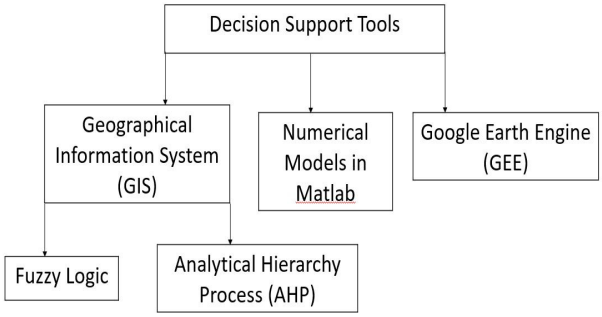


Figure 1. Decision support tools for the management of eastern Baltic Sea coasts

4. Methodology

This research is in its early stage. The methodology will be organized in stages. First, the most important factors for assessing the CVI index for the eastern Baltic Sea coasts will be identified and gathered through a literature review and data collection. Where necessary, the rate of shoreline change and coastal land-use changes will also be extracted using satellite data in Google Earth Engine. Next, the quantification of each parameter to prepare raster layers (with cell size 10×10 m) in ArcGIS will be implemented (Al-Amin Hoque *et al.* 2019).

Normalization of each raster layer using Fuzzy Membership Functions and assigning values (between 0 and 1) to each factor will be undertaken. After this, AHP for the assessment of the relative importance (weight) of different factors (values from 1 to 9) will be applied. Finally, the determination of each sub-index vulnerability by multiplying each factor and its weight and aggregation of all factors will be carried out. As a result, evaluation of the CVI will be performed by combining each sub-index in a raster analysis in ArcGIS (Bagdanaviciute *et al.* 2015; Serafim *et al.* 2019; Mullick *et al.* 2019). ArcGIS is to be used for mapping coastal segments based on the environmental sensitivity concerning coastal physical characteristics and the existing biodiversity and socioeconomic factors (Aps *et al.* 2016).

5. Conclusions

The results are anticipated to show that integration of diverse and efficient decision-making tools including Multi-Criteria Evaluation based on AHP, WLC and Fuzzy Logic based normalization approaches, using GIS and Google Earth Engine, can lead to more flexible and satisfactory coastal management decisions than utilizing only one method to appraise Coastal Vulnerability for micro-tidal low-lying areas of eastern Baltic Sea coasts. Furthermore, GIS models and Google Earth Engine tools for processing available online satellite images will analyze the risk of inundation due to sea level rises and coastline changes efficiently. Additionally, running mitigation scenarios will demonstrate how the most vulnerable areas may be protected from sea level changes.

The outcomes of this research will enable coastal planners to analyze coastal vulnerability at a pixel (cell) level. The integration of pixel-based decision-making tools will make a positive contribution to determine the degree of natural vulnerability particularly based on the environmental conditions of the Baltic Sea and will represent more rationally the spatial distribution of coastal vulnerability.

References

Al-Amin Hoque M, Ahmed N, Pradhan B, Roy S (2019) Assessment of coastal vulnerability to multi-hazardous events using geospatial techniques along the eastern coast of Bangladesh. Ocean and Coastal Management 181(19), 104898.

Aps R, Tõnisson H, Suursaar Ü, Orviku K (2016) Regional Environmental Sensitivity Index (RESI) classification of Estonian shoreline (Baltic Sea). Coastal Research 2(75), 972-976.

Bagdanaviciute I, Kelpsaite-Rimkiene L, Galiniene J, Soomere T (2019) Index based multi-criteria approach to coastal risk assessment. Coastal Conservation 23(4), 785-800.

Bagdanaviciute I, Kelpsaite L, Soomere T (2015) Multi-criteria evaluation approach to coastal vulnerability index development in micro-tidal low-lying areas. Ocean and Coastal Management 104(15), 124-135.

Gallego Perez B.E, Josephraj Selvaraj J (2019) Evaluation of coastal vulnerability for the District of Buenaventura, Colombia: A geospatial approach. Remote Sensing Applications: Society and Environment 16(5), 100263.

Ghoussein Y, Mhawej M, Jaffal A, Fadel A, El Hourany R, Faour G (2018) Vulnerability assessment of the South-Lebanese coast: A GIS-based approach. Ocean and Coastal Management 158(18), 56-63.

Harff J, Furmanczyk K, von Storch H (eds) (2017) Coastline Changes of the Baltic Sea from South to East (Past and Future Projection). Coastal Research Library, Springer, pp.363-388.

Hünicke B, Zorita E, Soomere T, Madsen K.S, Johansson M, Suursaar Ü (2015) Recent change - sea level and wind waves. In: The BACC II Author Team, Second Assessment of Climate Change for the Baltic Sea Basin, Regional Climate Studies, Springer, pp.155-185.

Mullick Md. R.A, Tanim A.H, Samiul Islam S.M (2019) Coastal vulnerability analysis of Bangladesh coast using fuzzy logic based geospatial techniques. Ocean and Coastal Management 174(19), 154-169.

Leinonen U, Koskinen J, Makandi H, Mauya E, Käyhkö N (2018) Open Foris and Google Earth Engine Linking Expert Participation with Natural Resource Mapping and Remote Sensing Training in Tanzania. The International Archives of the Photogrammetry, Remote Sensing and Spatial Information Sciences 4(8), 29-31.

Ng K, Borges P, Robert Phillips M, Medeiros A, Calado H (2019) An integrated coastal vulnerability approach to small islands: The Azores case. Science of the Total Environment 690(19), 1218-1227.

Ning W, Nielsen A.B, Norback Ivarssonc L, Jilbert T, Akesson C.M, Slomp C.P, Andren E, Brostrom A, Filipsson H.L (2018) Anthropogenic and climatic impacts on a coastal environment in the Baltic Sea over the last 1000 years. Anthropocene 21(6), 66-79.

Sekovski I, Del Rio L, Armaroli C (2020) Development of a coastal vulnerability index using analytical hierarchy process and application to Ravenna province (Italy). Ocean and Coastal Management 183(20), 104982.

Serafim M.B, Siegle E, Cristina Corsi A, Bonetti J (2019) Coastal vulnerability to wave impacts using a multi-criteria index: Santa Catarina (Brazil). Environmental Management 230(19), 21-32.

Environmental window of summer blooms in the eastern Baltic Sea

Oscar Beltran-Perez and Joanna J. Waniek

Leibniz Institute for Baltic Sea Research Warnemünde, Rostock, Germany (oscar.beltran@io-warnemuende.de)

1. Introduction

Cyanobacterial blooms of *Nodularia spumigena*, *Aphanizomenon sp*., and *Dolichospermum sp*. occur regularly during summer in the eastern Baltic Sea. Cyanobacterial blooms are trigged by a combination of several parameters (Wasmund, 1997). However, the role of each parameter along the development stages of the bloom as well as its relationship with the other acting parameters are still not well constrained. Furthermore, the response of cyanobacterial blooms to both direct and indirect effects of changing climatic conditions increases the uncertainty related with their occurrence which emphasizes the knowledge gaps.

Occurrence of cyanobacterial blooms may drive substantial changes on the whole ecosystem as basic component of planktonic food web, affecting even the human being through the release of wide-spread toxins in the water (Paerl and Huisman, 2009; Neil et al., 2012). Hence the research interest in these organisms and conditions that trigger their development.

2. Methods

Cyanobacteria biomass and environmental monitoring data were analyzed in order to identified conditions that favor the development of blooms. The analyzed parameters included sea surface temperature, air temperature, net heat flux and its components, wind speed, mixed layer depth, Brunt-Väisälä frequency, salinity, and nutrients.

Data were collected between 1990–2017 in the Baltic Sea by the Leibniz Institute for Baltic Sea Research Warnemünde (IOW), the Swedish Meteorological and Hydrological Institute (SMHI), and the German Weather Service (DWD). ERA-Interim reanalysis data from the European Centre for Medium-Range Weather Forecasts (ECMWF) were also used.

3. Optimum environmental window

The environmental window defines a set of parameters that favor the optimum response of the system while the constraint conditions are minimized (Cury and Roy, 1989). The optimum environmental window was analyzed applying a constrained ordination method in order to define the degree of relation between each parameter and cyanobacteria biomass. The optimum results were compared with data from IOW, DWD, and ECMWF in order to assess the performance of the approach.

4. Results

An optimum environmental window combining several parameters was identified to support the development of cyanobacterial blooms (Fig. 1). As a result, the onset of the bloom was drove by sea surface temperature (13-17°C), air temperature (16-18°C), Brunt-Väisälä frequency (0.024-0.016 s^{-2}), and periods with wind speed below 5.5 m s^{-1} (5-9 days).

On the other hand, the peak of the bloom was related to the air temperature (15-19°C), incoming radiation (187-241 W m^{-2}), net heat flux (99-189 W m^{-2}), and periods with wind speed below 5.5 m s^{-1} (4-10 days). The optimum environmental window during the decline of the bloom comprised sea surface temperature (16-20°C), air temperature (17-19°C), wind speed (4-6 m s^{-1}), and Brunt-Väisälä frequency (0.04-0.02 s^{-2}).

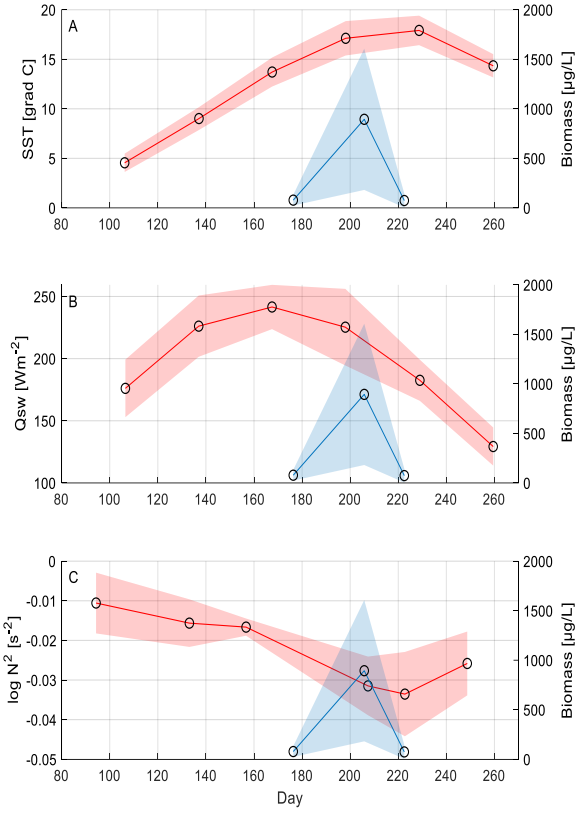


Figure 1. Optimum environmental window. (A) Sea surface temperature, (B) incoming radiation, and (C) Brunt-Väisälä frequency. The red line corresponds to the variable, the blue line to cyanobacteria biomass, and the shaded region to the standard deviation of each variable.

5. Conclusions

In summary, the onset of the bloom was drove by the increments in temperature which in turn make stronger the stratification of the water column (Fig 1). Changes in temperature were favored by wind speed below 5.5 m s^{-1} and the frequency of these wind events. Nutrient stress conditions were also identified as a required condition to start of the cyanobacterial bloom.

The peak of the bloom was drove by the changes in atmospheric conditions. The maximum cyanobacteria biomass was reached when water and air temperatures ceased to rise, a consequence of the reduced incoming radiation and net heat flux involved at this stage of the

bloom. It was also found that changes in air temperature and the number of days with wind speed below 5.5 m s^{-1} played a role more important than water temperature during this stage of the bloom.

On the other hand, changes in temperature, stratification, and wind speed were related to the decline of the bloom. Thus, the combination of these parameters at the different stages of the bloom constrained the occurrence of cyanobacterial bloom events in the eastern Baltic Sea.

Furthermore, the optimum environmental window is a suitable approach to anticipate blooms occurrence based on defined thresholds, enhancing early warning systems and controls in order to mitigate or suppress the development of cyanobacterial blooms.

References

Cury, P., Roy, C., 1989. Optimal Environmental Window and Pelagic Fish Recruitment Success in Upwelling Areas. Can. J. Fish. Aquat. Sci. 46, 670–680. https://doi.org/10.1139/f89-086

Neil, J.M.O., Davis, T.W., Burford, M.A., Gobler, C.J., 2012. The rise of harmful cyanobacteria blooms: The potential roles of eutrophication and climate change. Harmful Algae 14, 313–334. https://doi.org/10.1016/j.hal.2011.10.027

Paerl, H.W., Huisman, J., 2009. Climate change: A catalyst for global expansion of harmful cyanobacterial blooms. Environ. Microbiol. Rep. 1, 27–37. https://doi.org/10.1111/j.1758-2229.2008.00004.x

Wasmund, N., 1997. Occurrence of cyanobacterial blooms in the Baltic Sea in relation to environmental conditions. Int. Rev. der gesamten Hydrobiol. und Hydrogr. 82, 169–184. https://doi.org/10.1002/iroh.19970820205

First results of model sensitivity studies on the influence of global changes to the Baltic Seas

Birte-Marie Ehlers, Frank Janssen and Janna Abalichin

Federal Maritime and Hydrographic Agency, Rostock, Germany (birte-marie.ehlers@bsh.de)

1. Introduction

This contribution is part of the "German Strategy for Adaption to Climate Change" (DAS) which has been established as the political framework to climate change adaption in Germany. One task of the "Adaption Action Plan of the DAS" is the installation of a permanent service for seamless climate prediction. Within DAS the pilot project "Projection Service for Waterways and Shipping" (ProWaS) prepares an operational forecasting and projection service for climate, extreme weather and coastal and inland waterbodies. The target region is the North Sea and Baltic Sea with focus on the German coastal region and its estuaries.

2. Hindcast setup

To set up and validate the ocean component of the regional climate model framework for the operational forecasting and projection service, a 20-year hindcast simulation was carried out. This hindcast simulation used the regional reanalysis of COSMO-REA6 (Bollmeyer et al., 2015) as atmospheric forcing. The modelled region includes the North and Baltic Seas (Figure 1).

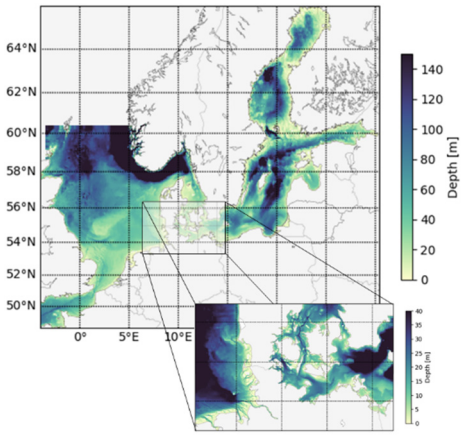


Figure 1. : Bathymetry of model setup used for a 20 year hindcast simulation.

3. Sensitivity studies

Sensitivity studies are performed to evaluate the model response to potential global changes especially in the Baltic Sea. As basis for these sensitivity studies the hindcast simulation is used as reference for different global change scenarios:

- global sea level rise
- changes in global ocean temperature
- changes in global air temperature
- changes in global ocean salinity
- changes of regional river runoffs

Furthermore, the model response is validated for a different atmospheric forcing.

For all change scenarios boundary conditions of the hindcast simulation are adapted to the listed change conditions and sensitivity studies for different periods have been carried out.

4. Study results

With focus on the Baltic Sea we will present first results of the sensitivity studies and draw some conclusions from the changed boundary conditions to the reference hindcast run. As an example figure 2 shows the monthly mean water temperature in the Gotland Basin compared for the hindcast and sensitivity run with an increased air temperature of 2°C.

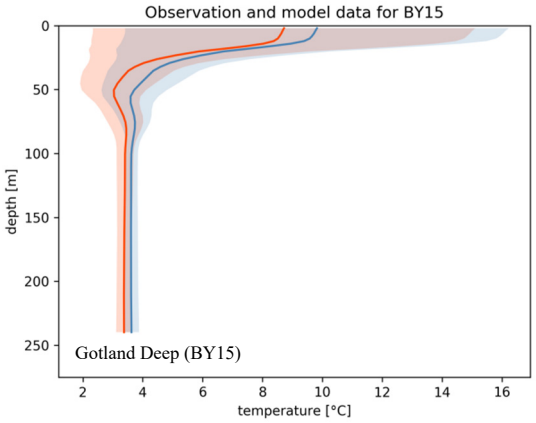


Figure 2. : Model response of water temperature for increased air temperature (2°C) at station Gotland Deep .red: hindcast run, blue: sensitivity run.

5. Outlook

The sensitivity studies help to achieve a proper description of the regional ocean model dynamics and the model response to various global changes. The study results will provide a basis for the calibration process of the ocean model setup for regional climate projections in the North and Baltic Seas.

References

Bollmeyer, C., Keller, J. D., Ohlwein, C., Wahl, S., Crewell, S., Friederichs, P., Hense, A., Ekune, J., Kneifel, s., Pscheidt, I., Redl, S. and Steinke, S. (2015) Towards a high-resolution regional reanalysis for the European CORDEX domain, Quarterly Journal of the Royal Meteorological Society, 141, Pp 1-15.

Assessment of the state of pollution of the Ukrainian part of the Black Sea

Maryna Moniushko, Valeriya Ovcharuk

Odessa State Environmental University, Ukraine (moniuszko@ukr.net)

1. Introduction

Deterioration of the environment of the Black Sea and depletion of its marine resources during last decades entailed the worsening of living standards of population, aesthetic and recreational values of the Black Sea.

The coastal and marine resources of the Azov-Black Sea basin are a national treasure, one of the important material resources of the Ukrainian part of the Black and Azov Seas. Therefore, today, the increasing pollution of sea waters, in particular the Black Sea, by various chemical pollutants, both on the sea surface and in bottom sediments, deserves special attention. Significant pollution by various chemicals causes great harm to the biological resources of the sea, and often completely negates the industrial significance of the marine environment, and leads to the inability to use the sea as recreational resources. Over the past 25 years, out of 23 fishing species in the Black Sea, nine species have remained, one of which is sardelle, which comes from the Sea of Azov. Therefore, an assessment of the quality of sea water is necessary, first of all, with the aim of establishing maximum permissible standards of action that guarantee the environmental safety of the population, ensure the rational use and restoration of natural resources in the context of sustainable development of economic activity.

2. Problem status

The study considers the main environmental problems of the Ukrainian part of the Black Sea, which are very similar to the problems of the Baltic Sea. As well as for the Baltic Sea, among man-made changes, eutrophication is the most negative factor impacting the Black Sea ecosystem and first of all its north-western part. Ecological crisis that broke out in the water of this region in 70th–80th, is at present showing itself as eutrophication, development of large-scale hypoxia, hydrogen sulphide zones and, as the result, degradation of biogeocoenosis (Monyushko, 2015).

3. Results

To assess water quality and compare various water areas by this parameter, the values of the water pollution index (WPI) are calculated, which allow us to classify the waters of the study area as a specific purity class. The analysis of multi-year variability of WPI for the Ukrainian part of the Black Sea is carried out (Fig. 1). The average annual data in the surface water layer for the content of nitrates, nitrites, ammonium nitrogen, petroleum hydrocarbons, synthetic surfactants, phenols and oxygen dissolved in water for the period 2000-2017 were used to calculate the WPI index in the waters of the northwestern Black Sea.

Assessment of water quality in the Ukrainian part of the Black Sea showed that the most polluted area is the port of Odessa, where WPI vary within 1.56-4.67, which corresponds to IV - VI classes of sea water quality and refers to “polluted” and “very dirty” waters, respectively. Also, the Danube River Delta and the mouth of the Southern Bug River are greatly polluted. The WPI values in this part vary between 1.05-2.18 (which corresponds to III - V class water quality) that is, "Moderately polluted" - "Dirty".

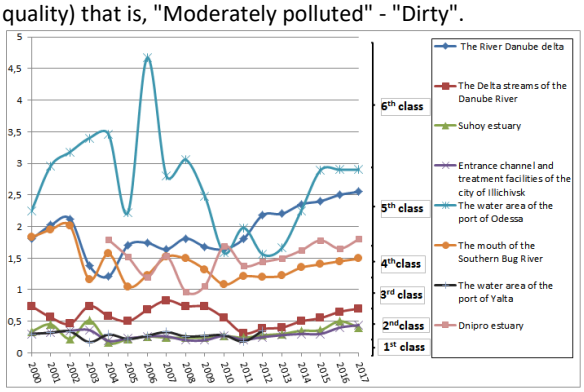


Fig. 1. Multi-year variability of the water pollution index in different parts of the northwestern Black Sea.

The smallest pollution is observed in the Suhoy Estuary, Entrance channel and treatment facilities of the city of Illichivsk, where the WPI values varied within 0.16-0.51, which corresponds to I-II class of water quality, that is, "Very clean" - "Clean." The area of the Danube Delta is also characterized by clean waters (WPI varies within the range of 0.31-0.74) and only in 2007 was III grade water quality observed (WPI=0.83), which is characterized by moderately polluted waters.

Since the port of Odessa is the most polluted area, it was advisable to consider the multi-year variability of the concentrations of priority pollutants that were used to calculate the WPI (Fig. 2).

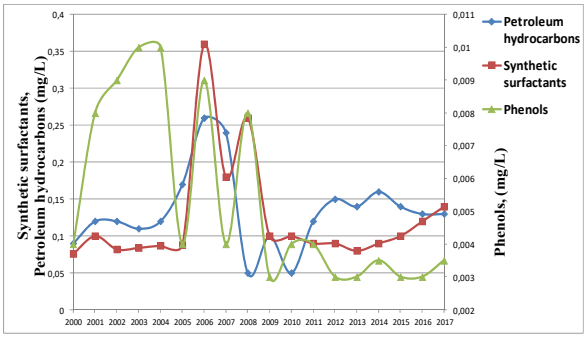


Fig.2. Multi-year variability of concentrations of petroleum hydrocarbons, synthetic surfactants, phenols in the water area of the port of Odessa.

In recent years, the amount of substances used to struggle oil has increased significantly in seawater, for example detergents whose toxicity exceeds the toxicity of the oil itself. Detergents are Synthetic surfactants and of course accumulate at the section boundary between the ocean and the atmosphere.

Considering the multi-year variability of the concentrations of various chemical pollutants in the studied area, the synchronous distribution of petroleum hydrocarbons and synthetic surfactants is quite clearly traced (Fig. 2).

Getting into marine environment synthetic surfactants depletes the stock of dissolved oxygen in the water (spent on the oxidation of detergents) and increase the concentration of petroleum hydrocarbons, due to the emulsification of the latter in surface slicks synthetic surfactants. An analysis of the results of the multi-year variability of the concentration of petroleum hydrocarbons in the water area of the port of Odessa shows that the maximum permissible concentrations (MPC) are exceeded for almost all study period, which is 2-5.2 MPC (except for 2008 and 2010). An analysis of the multi-year variability in the distribution of phenols also showed that their concentrations in the port of Odessa over the entire study period exceed the maximum permissible concentrations.

As the main factor in the eutrophication of marine environments, including the northwestern part of the Black Sea, is the increased entrance of biogenic elements and organic matter, it was interesting to consider first of all the peculiarities of the entrance and distribution of these substances in the studied water area. Of particular interest is the distribution and content of biogenic substances that are indicative of this negative process.

Maps of the spatial distribution of the average long-term (2005-2017) concentrations of biogenic substances for the northwestern Black Sea in the surface layer of seawater, for analyze in accordance with the distribution of temperature, salinity and dissolved oxygen in all seasons of the year had constructed. For example, in the abstracts, maps of the spatial distribution of biogenic substances and dissolved oxygen in the winter season are presented (Fig.3).

The average long-term level of biogenic content in the western part of the shelf is higher than in the eastern part of it. The nitrate content in the western part of the water area is more than an order of magnitude higher than in the eastern part.

The values of nitrate concentrations in the surface layer averaged 4.3 and 0.5 *µmol/l*, respectively, for the western and eastern parts, over the year.

The average annual long-term phosphate level in the surface layer was in both parts of the water area: 0.5 and 0.17 *µmol/l*, respectively.

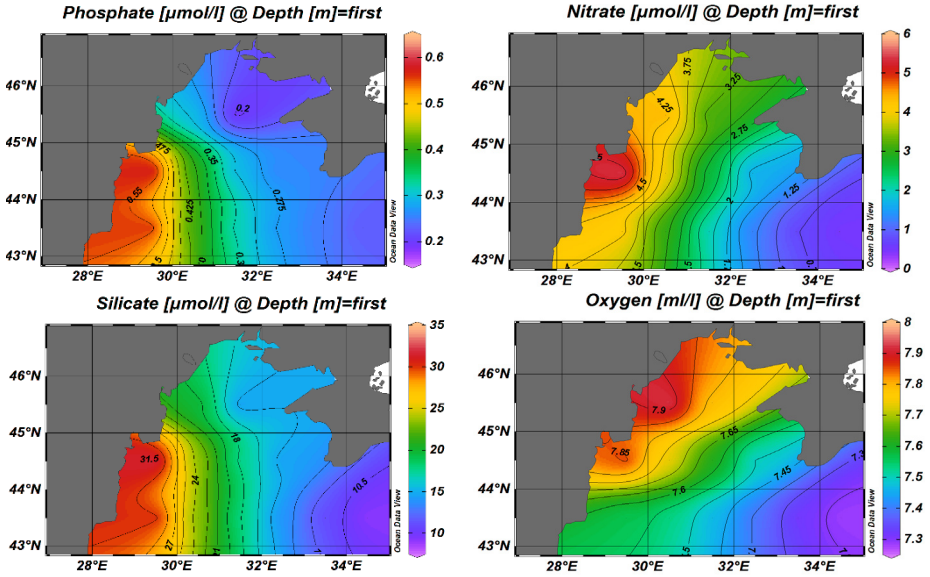


Fig. 3. Spatial distribution of biogenic substances, dissolved oxygen in winter (January-March, 2005-2017)

In the northwestern part of the Black Sea, there are areas where only river runoff is affected (Danube and Dniester), especially the Danube region, where maximum concentrations of all biogenic substances are observed: nitrates (up to 6 *µmol/l*), phosphates (up to 0.6 *µmol /l*), and silicates (35 *µmol/l*).

In the northern part, where the impact of the Dnieper-Bug river runoff is enhanced by industrial water runoff, concentrations of biogenic substances vary within: nitrates (1.1-3.75 *µmol/l*), Phosphates (0.2-0.28 *µmol/l*), silicates (7-17.5 *µmol/l*.)

Conclusions

- The water quality assessment of the Ukrainian part of the Black Sea showed that the most polluted area is the water area of the port of Odessa, where the WPI of water pollution vary within 1.56 - 4.67, which corresponds to IV - VI classes of quality of sea water, and refers to "polluted" and "Very dirty" waters, respectively.
- The main sources of pollution and volumes of discharge of pollutants of the Ukrainian part of the Black Sea are considered.
- The seasonal variability of biogenic substances in the northwestern Black Sea is analyzed. Highlights of areas affected only by river runoff (Danube and Dniester), especially the Danube region, where maximum concentrations of all biogenic substances are observed.

References

Monyushko M. Assessment of water quality by hydrochemical indicators for the waters of the northwest shelf of the Black Sea. // Periodic scientific journal of Kyiv National Taras Shevchenko University "Hydrology, hydrochemistry and hydroecology". –2015. - Volume 3 (38). - pp. 69-77.

Comparison of different data sets for mapping of hypoxic and euxinic regions in the Baltic Sea deep waters

Michael Naumann and Susanne Feistel

Leibniz Institute for Baltic Sea Research Warnemünde, Germany (michael.naumann@io-warnemuende.de)

1. Scientific topic - background

Mapping of hypoxic to euxinic layers in the deep-water from the western to central Baltic Sea allow an evaluation of occasional inflow events, of the progress of oxygen-consuming processes and of the development of hydrogen sulphide distributions over longer periods of time. This is necessary because hypoxia is a major threat of this estuary, limiting habitats for higher organisms. The Baltic Sea is a complex ecosystem characterized by a strongly fluctuating, fragile balance between high freshwater runoff and saline water inflows, a persisting vertical stratification and a bottom topography composed of several interconnected sub-basins. By the sensitivity of this ecosystem "Baltic Sea", climatological fluctuations appear amplified on the decadal time scale. Changes that may be insignificant in the open ocean typically constitute significant indicators in the Baltic Sea. Salt and nutrients remain present in the estuary for 20 and more years before being flushed to the Atlantic along with the freshwater export. This long residence time attenuates short-time fluctuations in environmental conditions, but highlights systematic, even small long-term anomalies. Thus, a main scientific focus is on the evaluation of inflow events, on the progress of oxygen-consuming processes and on the development of hydrogen sulphide distribution over longer periods of time.

2. Summary

Time-series of these lateral property distribution maps are published in 2016 by Feistel et al. of seasonal resolution (Fig. 1) or by Hansen et al. (2019) on annual scale the late summer state since the 1960's. Based on regular seasonal sampling done by intensive environmental monitoring and long-term data programmes of neighbouring countries, a most complete dataset was compiled for a study of spatial analysis of seasonal to decadal changes for the time-span 1969-2016 by Naumann et al. in 2017.

All these products and analysis are homogenously based on water sampling in discrete depths and laboratory analysis for determination of dissolved oxygen by Winkler titration. Sampling of discrete depths is done in 20 m to 40 m intervals and uncertainties are in that vertical range, where the exact threshold value of 2 ml/l in the water column is reached. Spatial interpolation between sampling stations is done from the sampling depth reaching this limit.

In contrast to water sampling, sensor measurements of dissolved oxygen are continuously measured through the water column. The determination of the boundary from oxic to hypoxic conditions would be much more exact, with effects on the spatial interpolation and calculation of hypoxic area between both data sources.

In the beginning of dissolved oxygen measurements via sensor in the 1980's large variations between the sensor types and laboratory data were prominent. Since 2010 oxygen measurements are done with doubled sensors at the CTD and strict data validation, exact sensor calibrations in the long-term data programme conducted by the Leibniz Institute for Baltic Sea Research (IOW). After six further years of intensive systematic water sampling and intensified sensor measurements, the sampling of dissolved oxygen was reduced from 2017 onwards to a minimum needed for validation of sensor measurements. This method break occurred as well on mapping products and this study evaluates the effects induced on the spatial distribution between maps of 2010-2016.

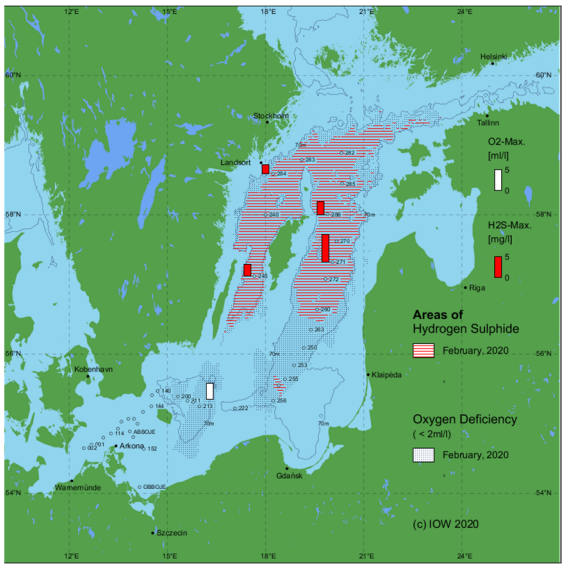


Figure 1. Location of stations and areas of oxygen deficiency and hydrogen sulphide in the near bottom layer of the Baltic Sea. Bars show the maximum oxygen and hydrogen sulphide concentrations of this layer in February 2020; the figure additionally contains the 70 m -depth line

References

Feistel Susanne, Feistel Rainer, Nehring Dietwart, Matthäus Wolfgang, Nausch Günther, Naumann Michael (2016) Hypoxic and anoxic regions in the Baltic Sea, 1969 – 2015, Marine Science Reports, No. 100, 76 pages

Hansson Martin, Viktorsson Lena, Andersson Lars (2019) Oxygen Survey in the Baltic Sea 2019 – Extent of Anoxia and Hypoxia, 1960-2019, Report Oceanography – Swedish Meteorological and Hydrographical Institute, No. 67, 81 pages, Göteborg, Sweden

Michael Naumann, Susanne Feistel, Günther Nausch, Thomas Ruth, Jakob Zabel, Markus Plangg, Martin Hansson, Lars Andersson, Lena Viktorsson, Elzbieta Lysiak-Pastuszak, Rainer Feistel, Dietwart Nehring, Wolfgang Matthäus, H.E. Markus Meier (2017) Hypoxic to euxinic conditions in the Baltic Sea 1969-2016 – a seasonal to decadal spatial analysis, talk, 2nd Baltic Earth Conference, June 2017, Helsingör, Denmark

The application of coastal geomorphic process concepts to eastern Baltic Sea conditions in a changing climate.

Kevin E. Parnell [1] and Tarmo Soomere[1,2]

[1] Department of Cybernetics, Tallinn University of Technology, Estonia (kevin.parnell@taltech.ee)
[2] Estonian Academy of Sciences, 10130 Kohtu 6, Tallinn, Estonia

1. Introduction

It can be difficult to get the attention of politicians, policy makers and business leaders with respect to the effects of climate change. Frequently, attention is given as to whether climate change is caused by humans, but as climate change is clearly occurring, the causes are of lesser importance with respect to the impacts and the actions that must be taken to adapt. The Intergovernmental Panel on Climate Change (IPCC) and other organizations play an important role in informing decision makers, but even their contributions on regional aspects (e.g. IPCC, 2014) are necessarily broad scale (e.g. Europe) with sectoral aspects (e.g. Wong *et al.*, 2014, on coastal systems) being discussed at a global scale.

Coastal erosion is rightly regarded as an important issue, and it is something that politicians, decision makers and communities can see happening and understand. There has been much written on this topic at a regional and country-scale level (Pranzini and Williams, 2013). Coastal erosion, along with permanent or more frequent inundation are going to become more damaging in a changing climate. Relative sea level rise is clearly an important driver. Shorter term changes in sea level associated with storm surge events, which affect the periods over which significant erosion can occur are also important. In this paper we explore some of the lesser discussed coastal processes and process drivers specific to the Baltic Sea, changes to which may cause significant damage or disruption in their own right or which may impact coastal erosion and inundation in unexpected ways. We concentrate on those aspects that can cause changes to sediment transport processes with apparently minor changes to drivers, and we discuss why some variables are particularly significant in the Baltic Sea context.

2. Morphodynamic feedback model

The morphodynamic feedback model (Figure 1) is a useful conceptual framework to consider the sedimentary implications of changes to process drivers. Various coastal drivers (in particular waves) influence the process of sediment transport, which in turn influences the coastal morphology. The changed morphology in turn affects the coastal driver, providing the feedback.

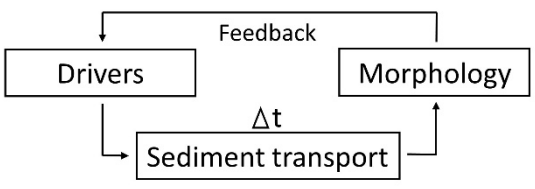


Figure 1. The morphodynamic feedback model. In open coastal situations the most important drivers are the wave parameters: wave period, direction and height.

3. Waves

Much of the classic coastal process theory is derived from observations in areas where long period swell waves dominate most of time, and sediment compartments are large. In such environments, wave refraction causes waves to start to align with the coast a considerable distance off the beach, so that the angle of wave approach (important in determining alongshore sediment transport) is small. On ocean coasts, changes in wave direction cause little change in sediment transport due to the influence of wave refraction.

Where swell waves are minimal or storms are often located relatively close to the shore, as in the case of the Baltic Sea, wave periods (and therefore wave length) are small and waves can approach the shoreline at high angle driving considerable sediment transport, and morpho-logical change. Reversals of transport direction may occur frequently, but even minor long-terms trends in wind and wave direction can have major implications, much more than on more energetic shorelines. Wave direction of approach can also have considerable influence on other variables. Wave setup for example, contributes significantly to water levels at the shoreline during high energy events. Pindsoo and Soomere (2015) have shown that there is high alongshore variation of wave set-up heights dependent on the wave propagation direction and the geometry of the coastline. Rotation of wind directions in storms can lead to certain areas experiencing significantly higher water levels resulting from this single process. While there remains much unknown about changes in wind patterns, it is clear that there are changes occurring (Männikus *et al.*, 2019) including a significant increased frequency of waves from the west (Meier, 2015)

4. Longshore sediment transport

Longshore sediment transport is notoriously difficult to measure, and most often, modelling and semi-empirical approaches are used. One common approach is the so-called CERC method (USACE, 2002), a method that is still widely used despite limitations. It calculates potential, rather than actual, sediment transport, and is valuable for relatively open sandy shorelines where sediment supply is not limited. The results (Figure 2), although an overestimate of the actual transport, show areas that are likely to be hotspots for erosion (and accretion). These results, for example, show divergence at the northern end of the Curonian Spit, and imply consequences should there be even a minor rotation in winds due to climate change, and also the need for careful consideration before potential redevelopment of Klaipėda Port results in the construction of long jetties beyond closure depth and the interruption of longshore sediment transport (Jarmalavičius *et al.*, 2012).

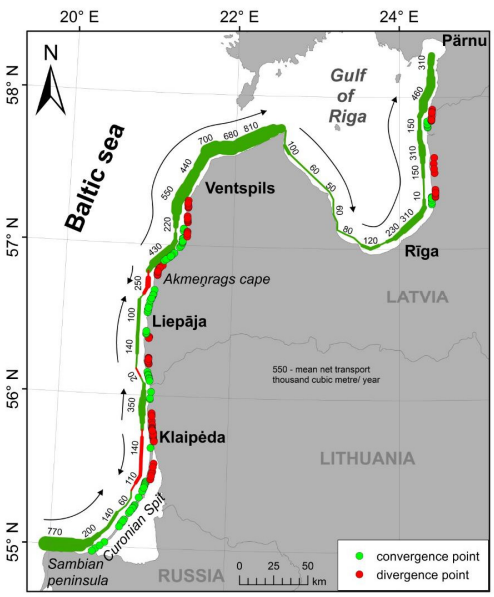


Figure 2. Direction and magnitude (in 1000 m^3) simulated potential net sediment transport using the CERC method (Viška and Soomere ,2013).

Due to the small wave periods typical of the Baltic Sea, alongshore sediment transport is confined to a narrow zone close to the shoreline. Geomorphic work (including longshore sediment transport) is concentrated on a very few stormy days, so therefore, the angle of wave approach on those days is very important. In Estonia, for example, about 60% of the wave generated energy flux arrives within 20 days and as much as ~30% of the energy flux arrives during the 3–4 stormiest days (Soomere and Eelsalu, 2014; Figure 3). It is therefore expected that both rates and volume of sediment transported is highly variable, and dependent on the conditions associated with storm events.

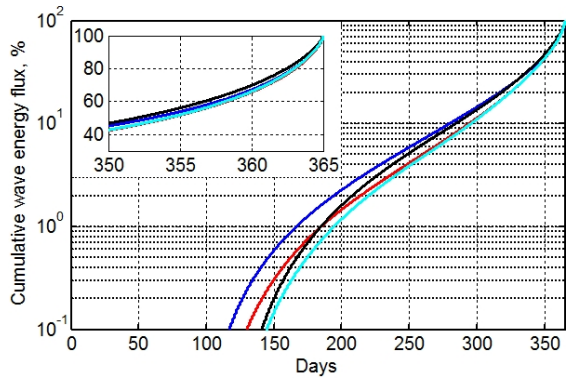


Figure 3. Cumulative wave energy flux on the Estonian coast (Soomere and Eelsalu, 2014).

In areas with highly indented shorelines, such as on the north coast of Estonia, small pocket sand beaches occur, and peninsulas at a range of scales protrude into deep (relative to wave length) water. Sediment compartments are small, with limited sand transport between them, and inputs to the sediment budget are limited to erosion processes within the compartment. The location of beach deposits within compartments (and therefore the areas regarded as eroded or stable/accreted) is therefore highly susceptible to wave parameters, particularly wave direction. For example,

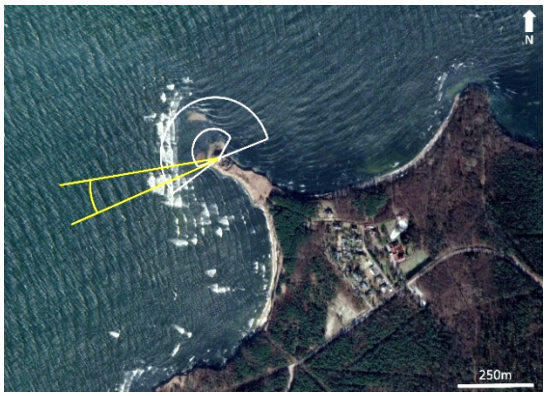


Figure 4. Suurupi Peninsula, near Tallinn, showing a complex wave pattern on 29.03.2019. Wind speed was 6-8 m/s (10 min. averages). The yellow wedge shows the range of wind directions on that day. The white arcs show the fetch lengths, inner arc >20-25km, outer arc 12-20km to the west and 18-25km to the east. Image: © Google Earth, 2020 Maxar Technologies

5. Conclusion

In the eastern Baltic Sea, with limited swell waves, sediment transport is largely influenced by wave angle of approach. Minor rotations in direction can have significant implications for coastal morphology.

References

IPCC (2014) Impacts, adaptation and vulnerability. Part B. Regional Aspects. Working Group II, Fifth Assessment Report of the IPCC. Barros VR *et al.* (eds.) Cambridge University Press, UK and New York, NY, USA, pp 688.

Jarmalavičius D, Žulinskas G and Pupienis D (2012) Impact of Klaipeda port jetties reconstruction on adjacent sea coast dynamics. Journal of Environmental Engineering and Landscape Management 20(2), 240-247.

Männikus, R, Soomere, T, and Kudryavtseva N (2019). Identification of mechanisms that drive water level extremes from in situ measurements in the Gulf of Riga during 1961-2017. Continental Shelf Research, 182, 22-36. 10.1016/j.csr.2019.05.014.

Meier HEM (2015) Projected change – Marine Physics. In: The BACC II Author Team (Ed.). Second Assessment of Climate Change for the Baltic Sea Basin. Springer, 243-252.

Pindsoo K and Soomere T (2015). Contribution of wave set-up into the total water level in the Tallinn area. Proceedings of the Estonian Academy of Sciences, 64, 338–348.

Pranzini E and Williams AT (eds.) (2013) Coastal erosion and protection in Europe. Routledge, Abingdon, UK, pp 825.

USACE (2002). Coastal Engineering Manual. Dept. of the Army. U.S. Army Corps of Engineers. Manual No. 1110-2-1100.

Viška M and Soomere T (2013) Simulated and observed reversals of wave driven alongshore sediment transport at the eastern Baltic Sea coast., Baltica, 26(2), 145-156.

Wong PP, Losada IJ, Gattuso JP et al. (2014) Coastal systems and low-lying areas. In: Climate Change 2014: Impacts, Adaptation, and Vulnerability. Part A: Global and Sectoral Aspects. Working Group II, Fifth Assessment Report of the IPCC. Field CB *et al.* (eds.) Cambridge University Press, United Kingdom and New York, NY, USA, 361-409.

Acknowledgements: Funding sources: Estonian Ministry of Education and Research (Estonian Research Council grant IUT33-3) and European Regional Development Fund program Mobilitas Pluss, 2014-2020.4.01.16-0024 (MOBTT72).

Accuracy assessment of ESA CCI LC over Eastern Europe and the Baltic States from a climate modelling perspective – identification of spatial inaccuracy patterns and misclassification issues using a fuzzy comparison method

V. Reinhart,[1], P. Hoffmann, [1] B. Bechtel,[2], D. Rechid,[1], J. Boehner[3]

[1] Helmholtz Zentrum Geesthacht (HZG), Climate Service Center Germany (GERICS), 20095 Hamburg, Germany (vanessa.reinhart@hzg.de)

[2] Ruhr-University Bochum, Department of Geography, 44801 Germany

[3] Universität Hamburg, Department of Geography, 20146 Germany

1. Introduction

Land use and land cover change (LULCC) are highly relevant drivers of changes in regional climate (Cherubini et al., 2018; Davin et al., 2019; de Noblet-Ducoudré et al., 2012; Feddema et al., 2005; Seneviratne et al., 2010; Swingland et al., 2002). Monitoring these changes for modelling applications is crucial to understand feedback and coupling mechanisms between LULCC and changes in relevant surface parameters. Utilized tools like regional climate models (RCMs) therefore depend on accurate information on LULCC to produce reliable high-quality results regarding impact and attribution studies and regional climate projections. When moving towards finer resolution with RCMs, new flexible LULCC data products need to be implemented in order to represent LULCC dynamics in a reasonable way to investigate feedback and coupling mechanisms (Lorenz et al., 2012; Sertel et al., 2010).

2. Preliminary analyses

Considering current achievements in remote sensing, a wide variety of satellite based global land use and land cover products with varying spatial and temporal resolution are available for use in climate change research (Bartholome & Belward, 2005; Bontemps et al., 2011; Defourny et al., 2017; Justice et al., 2002). A comprehensive assessment of available satellite based LULCC products found that the ESA Climate Change Initiative Land Cover product (ESA CCI LC, Defourny et al., 2017) is suitable for the use in RCM studies with respect to temporal and spatial coverage and resolution. Global availability of the dataset supports the implementation into RCMs for coordinated experiments while annual availability of a global LULC map supports simulations including LULCC. The ESA CCI LC dataset is based on a combination of different specialized satellite sensors including MERIS FR/RR, AVHRR, SPOT-VGT and PROBA-V, which cover overlapping time periods of the annual maps.
The land cover product was originally designed with respect to the needs of the climate modelling (Bontemps et al., 2011; Li et al., 2018). Quality assessment and evaluation of the epoch products against other LC data sets has been carried out globally (Hua et al., 2018). Further, a global database of reference points validated by an expert network is constantly being further developed (Archard et al., 2017). However, a comprehensive quality assessment of the product on a regional scale is still missing.

3. Data and research area

Against this background, the present work includes a comprehensive accuracy assessment of ESA CCI LC over Eastern Europe and the Baltic States. Data from the Coordination of Information on the Environment Land Cover dataset (CORINE) is used as reference data (Heymann, 1994). Countries assessed are Estonia, Hungary, Latvia, Lithuania, Poland, Romania, and Slovakia (Fig. 1).

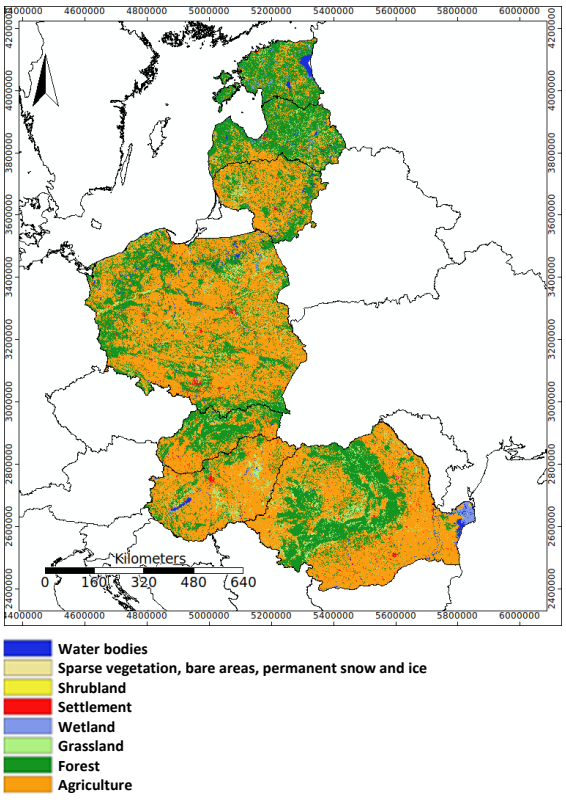


Figure 1. Research area - ESA CCI LC categories from 1992.

4. Methods

Included are investigations on systematic spatial misclassifications and most frequent misclassifications for eight harmonized LULC categories (Vilar et al., 2019). In this analysis the fuzzy interval comparison, an innovative approach to assess accuracy of high resolution LULCC products in a way that breaks open the static grid structure following (Fonte et al., 2019), is applied. Using this fuzzy measure, the quantity of correctly classified cells is divided into a quantity of area that is correctly classified and into a quantity that is independent from the grid structure. The method can be applied to compare gridded datasets with different spatial resolutions and to compare datasets with grid and vector structure. In addition, it can give a spatial pattern of accuracy and point out issues regarding

individual categories in the assessed dataset. In the present work, the method was applied to compare ESA CCI LC to CORINE land cover for all time steps that were available for both datasets (i.e. 1990/1992, 2000, 2006, and 2012). The fuzzy assessment method is considered to be more suitable for comparison of LULC data sets than traditional resampling methods due to its flexible applicability (Fritz & See, 2005).

5. Results and outlook

Overall accuracy of ESA CCI LC for the research area is considered relatively good with ~76%. The results are broadly consistent with the global assessment provided by ESA (Defourny et al., 2017). The two dominant LULC categories, agriculture and forest are overestimated by ~4% for all assessed time steps.

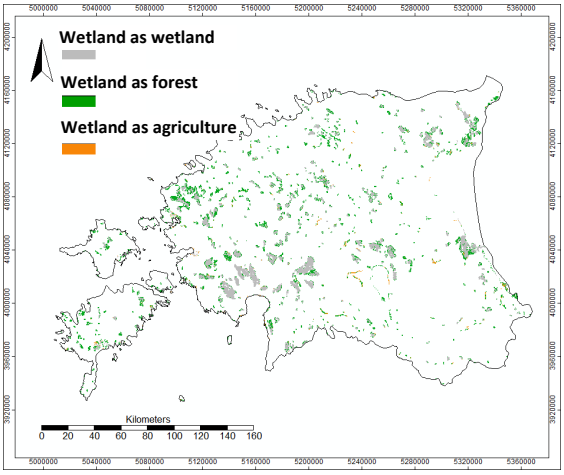


Figure 2. Estonia including the wetland accuracy results for ESA CCI LC 2012.

A spatial pattern of misclassification was found for wetland, grassland, settlements and water bodies. Spatial inaccuracies or inaccuracy patterns, detected for the individual categories are presented in exemplary map sections (example see Fig. 2). Strategies for quantification of the misclassification effects on RCM performance are discussed in the final remarks.

References

Archard, F., Bontemps, S., Lamarche, C., Da Maet, T., Mayaux, P., Van Bogaert, E., Defourny, P., De Maet, T., Mayaux, P., Van Bogaert, E., & Defourny, P. (2017). *QUALITY ASSESSMENT OF THE CCI LAND COVER MAPS*. ftp://geo10.elie.ucl.ac.be/v207/CCILC-UW1_20170831_05_Achard-JRC__Quality-assessment-of-the-CCI-LC-maps.pdf.

Bartholome, E., & Belward, A. S. (2005). GLC2000: A new approach to global land cover mapping from Earth observation data. *International Journal of Remote Sensing*, *26*(9), 1959–1977.

Bontemps, S., Defourny, P., Van Bogaert, E., Arino, O., Kalogirou, V., & Perez, J. R. (2011). GLOBCOVER 2009-Products description and validation report. *URL: http://ionia1.esrin.esa.int/docs/GLOBCOVER2009_Validation_Report_2-2*.

Cherubini, F., Huang, B., Hu, X., Tölle, M. H., & Strømman, A. H. (2018). Quantifying the climate response to extreme land cover changes in Europe with a regional model. *Environmental Research Letters*, *13*(7), 074002.

Davin, E. L., Rechid, D., Breil, M., Cardoso, R. M., Coppola, E., Hoffmann, P., Jach, L. L., Katragkou, E., de Noblet-Ducoudré, N., Radtke, K., Raffa, M., Soares, P. M. M., Sofiadis, G., Strada, S., Strandberg, G., Tölle, M. H., Warrach-Sagi, K., & Wulfmeyer, V. (2019). Biogeophysical impacts of forestation in Europe: First results from the LUCAS Regional Climate Model intercomparison. *Earth System Dynamics Discussions*, *2019*, 1–31.

de Noblet-Ducoudré, N., Boisier, J. P., Pitman, A., Bonan, G. B., Brovkin, V., Cruz, F., Delire, C., Gayler, V., Hurk, B., Lawrence, P., Van der Molen, M., Ller, C., Reick, C. H., Strengers, B., & Voldoire, A. (2012). Determining Robust Impacts of Land-Use-Induced Land Cover Changes onSurface Climate over North America and Eurasia: Results from the First Setof LUCID Experiments. *Journal of Climate*, *25*.

Defourny, P., Boettcher, M., Bontemps, S., Kirches, G., Lamarche, C., Peters, M., Santoro, M., & Schlerf, M. (2017). *Land Cover CCI Product User Guide Version 2.0.* European Space Agency: Louvain la Neuve, Belgium.

Feddema, J. J., Oleson, K. W., Bonan, G. B., Mearns, L. O., Buja, L. E., Meehl, G. A., & Washington, W. M. (2005). The Importance of Land-Cover Change in Simulating Future Climates. *Science*, *310*(5754), 1674–1678.

Fonte, C. C., See, L., Lesiv, M., & Fritz, S. (2019). A preliminary quality analysis of the climate change initiative land cover products for continental Portugal. *International Archives of the Photogrammetry, Remote Sensing and Spatial Information Sciences - ISPRS Archives*, *42*(2/W13), 1213–1220.

Fritz, S., & See, L. (2005). Comparison of land cover maps using fuzzy agreement. *International Journal of Geographical Information Science*, *19*(7), 787–807.

Heymann, Y. (1994). *CORINE land cover: Technical guide*. Office for Official Publ. of the Europ. Communities.

Justice, C., Townshend, J., Vermote, E., Masuoka, E., Wolfe, R., Saleous, N., Roy, D., & Morisette, J. (2002). An overview of MODIS Land data processing and product status. *Remote sensing of Environment*, *83*(1–2), 3–15.

Li, X., Chen, H., Wei, J., Hua, W., Sun, S., Ma, H., Li, X., & Li, J. (2018). Inconsistent Responses of Hot Extremes to Historical Land Use and Cover Change Among the Selected CMIP5 Models. *Journal of Geophysical Research: Atmospheres*, *123*(7), 3497–3512.

Lorenz, R., Davin, E. L., & Seneviratne, S. I. (2012). Modeling land-climate coupling in Europe: Impact of land surface representation on climate variability and extremes. *Journal of Geophysical Research: Atmospheres*, *117*(D20).

Seneviratne, S. I., Corti, T., Davin, E. L., Hirschi, M., Jaeger, E. B., Lehner, I., Orlowsky, B., & Teuling, A. J. (2010). Investigating soil moisture–climate interactions in a changing climate: A review. *Earth-Science Reviews*, *99*(3), 125–161.

Sertel, E., Robock, A., & Ormeci, C. (2010). Impacts of land cover data quality on regional climate simulations. *International Journal of Climatology*, *30*(13), 1942–1953.

Swingland, I. R., Bettelheim, E. C., Grace, J., Prance, G. T., Saunders, L. S., Pielke, R. A., Marland, G., Betts, R. A., Chase, T. N., Eastman, J. L., Niles, J. O., Niyogi, D. dutta S., & Running, S. W. (2002). The influence of land-use change and landscape dynamics on the climate system: Relevance to climate-change policy beyond the radiative effect of greenhouse gases. *Philosophical Transactions of the Royal Society of London. Series A: Mathematical, Physical and Engineering Sciences*, *360*(1797), 1705–1719.

Vilar, L., Garrido, J., Echavarría, P., Martínez-Vega, J., & Martín, M. P. (2019). Comparative analysis of CORINE and climate change initiative land cover maps in Europe: Implications for wildfire occurrence estimation at regional and local scales. *International Journal of Applied Earth Observation and Geoinformation*, *78*(November 2018), 102–117.

Modeling the distribution of microplastics coming with river runoff in the eastern part of the Gulf of Finland

V. A. Ryabchenko [1], S. D. Martyanov [1], A. V. Isaev [1] and G. Martin[2]

[1] Shirshov Institute of Oceanology, Russian Academy of Sciences, Moscow, Russia (vla-ryabchenko@yandex.ru)
[2] Estonian Marine Institute, University of Tartu; Tartu, Estonia

1. Introduction

To study the propagation characteristics of microplastic particles coming with the Neva river waters, in the Neva Bay and in the eastern part of the Gulf of Finland, two three-dimensional hydrodynamic models are used. One of them is based on the Princeton Ocean Model (POM), another one, on the Massachusetts Institute of Technology general circulation model (MITgcm).

2. Runs with POM

The POM is implemented on a uniform quasi-orthogonal horizontal grid with a step of 100 m, in the vertical direction 7 uniformly distributed sigma levels are used. The marine initial conditions and conditions at the western boundary for water level, temperature and salinity were taken from the Baltic Sea operational model HIROMB-BOOS of the Danish Meteorological Institute with discreteness of 1 hour. On the eastern boundary at the mouth of the Neva the average monthly climatic river discharge and temperature of the Neva were set. Atmospheric forcing was taken from the results of the ECMWF ERA-Interim reanalysis with 6-hour temporal resolution and with a spatial resolution of 0.125°×0.125°. Two types of suspension were considered that simulated the propagation of microplastic particles in the water: admixture of neutral buoyancy and a sinking suspension with a sinking velocity of 0.2 m/day. Both types of suspension come from the Neva River with a constant volume concentration of 10^{-6}. To calculate the thickness of the layer of the settling fraction at the bottom the simplified Exner equation is used. The calculations were performed for the period May – August 2018 when the quantity and composition of plastic litter was monitored on the coast of the Neva Bay and the eastern part of the Gulf of Finland.

3. A run with MITgcm

The MITgcm is implemented on a spherical horizontal grid with a step of 0.5 'in latitude and 1' in longitude (≈1 km). The vertical resolution in the upper 20 –meter layer is 2 m, from 20 to 50 m, –3 m, from 50 meters to bottom, –4 m. The studied area covers the Gulf of Finland from the Neva Bay to the meridian of 24.08 E. Marine boundary conditions for temperature, salinity and sea level were set according to the SMHI reanalysis. Atmospheric forcing was prescribed as in case of POM runs. Discharge of rivers flowing into the Gulf of Finland was set according to BED (http://nest.su.se/helcom_plc/). The initial distributions of temperature and salinity were taken from the results of calculations on a larger grid by Vladimirova et al. (2018). Here we consider a neutral buoyancy microplastic, which can be ingested by marine zooplankton and / or adhere to individual organisms, then fall into the bottom layer as part of detritus. Taking into account that the sinking velocity of detritus depends on the temperature T, we set the sinking velocity Wg of microplastics as $Wg = \gamma \times Wg_0 \times \exp(kT)$, if $T \geq 4$ °C and $Wg = 0$, if $T < 4$ °C, where $0 \leq \gamma \leq 1$ is the fraction of microplastics captured by zooplankton and falling into the bottom layer, Wg_0 = 1.2 m/day, k = 0.08 1/°C. This study examines the maximum possible uptake of microplastic by zooplankton and its falling into the bottom layer and, therefore, γ is assumed to be equal to 1. It is assumed that microplastic enters the Gulf of Finland with the river waters and its concentration in the rivers was set equal to 1000 conventional units (cu) / m^3. The run was performed for the period from 2015 to 2018. After the 2-year period (2015 - 2017) of adaption, the quasi-equilibrium solution for 2018 was analyzed.

4. Results from the POM runs

According to model results obtained in Martyanov et al. (2019), the spatial distribution of the sinking particles, in general, repeats the distribution of the admixture of neutral buoyancy, with the only difference being that the farther from the particle source to the west, the lower the concentration of the sinking particles. An essential feature of the distribution is that during most time of the considered period the concentrations of both suspensions in the northern part of the model domain is higher than those found in its southern part.

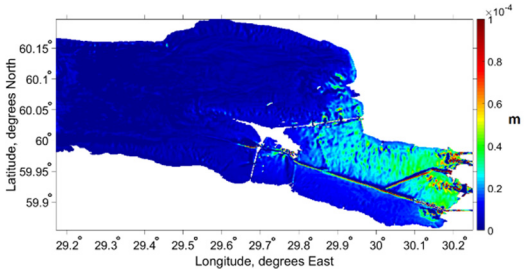


Figure 1. Change of the bottom layer thickness of the settling particles at the end of the model run on August 31, 2018.

The change in the thickness of the bottom layer of the particles of the settling fraction at the end of the period on August 31, 2018, i.e. the accumulation of microplastic particles in bottom sediments for the period under consideration (Fig.1), is characterized by the same feature as the space distribution of the admixture of neutral buoyancy in water: the accumulation of microplastic in bottom sediments in the northern part of the model area outside the Neva Bay was noticeably greater than in the southern part, especially in the coastal zone. The data on monitoring the coastal pollution by plastic litter indirectly confirm the model results: there was practically no plastic litter on the southern coast of the eastern Gulf of Finland outside the Neva Bay between June and August 2018, while it was found on the northern coast in significant quantities.

5. Results from the MITgcm run

Figure 2 shows the mean annual content of microplastics deposited on the bottom. As seen, the main part of the admixture coming with river waters fall into the bottom layer in the Neva Bay and the Zelenogorsk region (regions 1 and 2). Among other regions of the eastern part of the Gulf of Finland, two main areas of microplastics depositions for hydrodynamic conditions of 2018 can be distinguished. The first area of more intense settling is observed along the northern coast of the gulf (region 3). Another area of less intense settling, but at the same time significantly exceeding background values, occurs between the islands of Seskar and Bolshoi Berezovy with the center of the area with coordinates of 60.25 N and 28.25 E (region 4). We also note increased concentrations of microplastic particles in the bottom layer of the coastal zone in the southern part of the gulf near the estuaries of the Luga and Narva rivers.

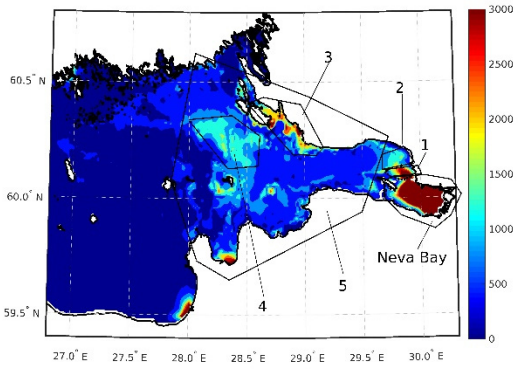


Figure 2. The average annual content of microplastic particles deposited on the bottom (cu/m^2). The numbers indicate individual areas of the eastern part of the Gulf of Finland (see text)

An analysis of the diurnal variability of microplastics settling on the bottom in the different regions described above, as well as for the part of the bay from the dam to the Moshchny Island (region 5), confirmed that most of the neutral buoyant microplastic particles coming from the river Neva settle within the Neva Bay. In the Neva Bay, intense settling begins when water temperature becomes above 4 °C in the spring and ends in the autumn with a decrease in water temperature below 4 °C. In regions 1 and 2 of the gulf adjacent to the Neva Bay (Fig. 2), two pronounced peaks of the admixture settling are observed. The first spring peak is due to the settling of admixture accumulated in the water column in the winter, and the second, autumn peak, is caused by a later temperature drop below 4 °C than in the Neva Bay: when sedimentation ceases in the Neva Bay, the admixture enters the area behind the dam, where the temperature is still above 4 °C, and it falls to the bottom. In the more western regions, there is only one peak of microplastic particles settling, due to heating of water in spring and summer and increasing sinking velocity of microplastic particles with temperature, that leads to the settling of microplastic particles accumulated in the water column earlier, during the winter.

6. Conclusions

A comparison of two figures characterizing the distribution of microplastic particles in the bottom layer indicates that these distributions are qualitatively consistent in the common part of the model domains used in both runs. Thus, the results obtained are fairly reliable and the resulting assessments can be used to justify the selection of areas for future field works focused on the microplastic pollution monitoring of the coastal zone and the coasts of the eastern part of the Gulf of Finland. It should be noted that we considered only one of the possible sources of microplastic in the Gulf of Finland - the river waters. Among the other possible sources that will be investigated in the future we can emphasize urban municipal wastewaters, as well as the transport of microplastic from St. Petersburg' city dumps to the water surface by storm winds

7. Acknowledgement

The work was supported by the Russian Foundation for Basic Research (grant 18-55-76001), project "Litter rim of the Baltic coast: monitoring, impact and remediation" of the Program "ERA.Net Rus Plus".

References

Martyanov S.D., Ryabchenko V.A., Ershova A.A., Eremina T.R., Martin G. (2019) On the assessment of microplastic distribution in the eastern part of the Gulf of Finland. Fundamentalnaya i Prikladnaya Gidrofizika. Vol. 12, No. 4, pp. 32—41.

Vladimirova O. M., Eremina T. R., Isaev A. V., Ryabchenko V. A., Savchuk O. P. (2018) Modelling dissolved organic nutrients in the Gulf of Finland. Fundamentalnaya i Prikladnaya Gidrofizika. Vol. 11, No. 4, pp. 90—101.

Coastal dunes ecosystems change according to normalized difference vegetation index (the case study of Curonian Lagoon)

Rasa Šimanauskienė [1,2], Rita Linkevičienė[1,2], Julius Taminskas[2], Ramūnas Povilanskas[3]

[1] Vilnius university, Ciurlionis str. 21, LT-03101, Vilnius, Lithuania (rasa.simanauskiene@gf.vu.lt)
[2] Nature Research Centre, Akademijos str. 2, LT–08412 Vilnius, Lithuania
[3] Klaipėda university, Herkaus Manto str., LT-92294, Klaipėda, Lithuania

1. Introduction

The Curonian Spit, a narrow sandy barrier situated between the Baltic Sea and the Curonian Lagoon is famous for the unique coastal dunes landscape formed by water, sand, wind, vegetation and anthropogenic activity (Fig. 1).



Figure 1. Location of the Curonian Spit.

The Curonian Lagoon boasts of the distinctive geomorphological feature – Great Dune Ridge (40-60 m a.s.l.) stretching for 33 km along the entire lagoon coast of the Spit (Povilanskas 2009). Being one of the most unique places in Europe, Curonian Spit is included into the UNESCO list of Cultural Heritage Monuments and has National Park (NP) status.

Up to 16th c. the bigger part of Curonian Spit was covered by forests and herbaceous vegetation. During 16-18th c. an intensive human activity (forest cover destruction, fire events and grazing) destroyed the vide natural vegetation areas and open sandy dunes started to prevail – an aeolian activity was extremely high. Consequently, one of the most sensitive problems in 19th c. were buried buildings and roads beneath the sandy dunes. Therefore, starting from the beginning of the 19th c. the main direction of sandy dunes management in Curonian Spit reflected the main tendencies in North-Western Europe and Northern America – open sandy dunes were recognized as a threat and the significant part of the Curonian Spit dunes was artificially forested by plantations of *Mugo* pine. At the same time, the artificial foredune acting as a barrier from the seashore sand drift was formed along the entire length of the marine coast of the Curonian Spit. This was the main factor leading to the prevalence of herbaceous vegetation and forested landscape with some stretches of uncovered natural aeolian massifs. During the 20th c. uncovered aeolian massifs were recognized for their esthetical and ecological values in Western Europe (Urbis et al., 2019). Therefore, nowadays anti-succession management of sandy dunes are supported by EU Habitat directive – shifting (white) dunes and fixed (grey) dunes with herbaceous vegetation are priority habitats in EU (Houston, 2008). Moreover, an artificial recovery of shifting dunes (cutting off *Mugo* pine plantations and grazing) is supported by EU LIFE Program (Litcoast, 2005-2008). Despite this, the implication of anti-succession management becomes complicated for both – climate change, that accelerates natural succession; and the protection status of Curonian Spit (UNESCO area), that restricts visiting this area. Therefore, the existing nature protection and nature management tools applied in coastal dunes should be reconsidered under nowadays climate change.

We hypothesized that evolution of coastal dunes landscape would result in vegetation cover changes (forestation and herbaceous vegetation encroachment) that would be reflected by NDVI values and that changes in NDVI would reflect the synergetic influence of climate change and anthropogenic activities. Therefore, the main objective of the study was to identify succession trends in 3 coastal dunes ecosystem types.

2. Methods

The succession trends were evaluated in three ecosystem types: forest, herbaceous and open sand ecosystems for the period of 2000 – 2018. Territories with homogeneous vegetation cover in spatial (squares of 250x250 m) and temporal (verification was made by orthophotos of 1995, 2005, 2013 and 2017) scale, were selected to represent each ecosystem type: 20 territories for forest, 9 for herbaceous and 6 territories for open sand ecosystems. Each square was also configurated according to MODIS product pixels (250x250 m).

The succession trends were evaluated, according to NDVI index, widely used for the estimation of vegetation's response towards changes in hydroclimatic conditions Usman et al. (2013). The NDVI is calculated on the basis of spectral reflectance from the surface, acquired in the visible red (at 620–670 nm from MODIS) and near-infrared (at 841–876 nm from MODIS) regions of the

electromagnetic spectrum. NDVI varies between −1.0 and + 1.0. Under normal humidity conditions, healthy vegetation has a low reflectance in the visible portion of the electromagnetic spectrum, due to absorption by chlorophyll and other pigments, and has high reflectance in the NIR because of the internal reflectance of the mesophyll spongy tissue of green leaves (Usman et al., 2013). Conversely, due to high reflectance in both the visible and NIR portions of the electromagnetic spectrum, lower NDVI values represent non-vegetated or bare soil surfaces.

Satellite-based NDVI were derived from MODIS, mounted onboard the Terra spacecraft. MODIS product data, called MOD09Q1 (8-day composite product, 250-m resolution) were obtained through NASA's LAADS–DAAC (https://ladsweb.modaps.eosdis.nasa.gov). Cloud-free images from 2000 to 2018 were chosen to estimate the phenological behavior of the raised bog ecosystem in every annual growing season (May–September). This period was selected as it is an active vegetation growing season in Lithuania (when average day temperature is >10°C) as well as considering there were sufficient data sets of cloud free MODIS images during this period.

3. Results

According to Mann-Kendall test significant positive trends of NDVI was detected in all ecosystem types, however with different statistical significance: p<0,05 in forest, p<0,001 in open sand and p< 0,00001 in herbaceous ecosystems. The highest NDVI trend (trend coefficient - 0,006) (Fig. 2) is observed in herbaceous ecosystem indicating the most rapid changes of vegetation cover.

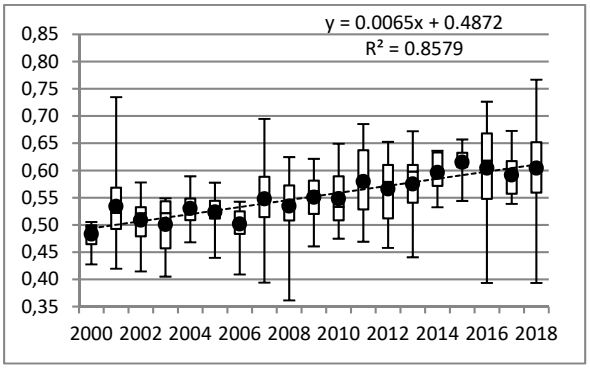


Figure 2. Average annual NDVI box plots during growing seasons in herbaceous ecosystem during 2000-2018. The upper and lower hinges correspond to the first and the third quartiles, upper and lower whiskers correspond to maximum and minimum values.

If we want to maintain this priority habitat of EU, the management tools (ex., grazing) should be taken into consideration. Vegetation encroachment is also observed in open sand ecosystem (Fig. 3). However, NDVI trend in this ecosystem is lower (0,004) to compare it with herbaceous ones. Forest ecosystem is characterized by the lowest positive NDVI trend (0,002) (Fig. 4), indicating that populations of *Mugo* pine have matured and become stable forest ecosystem. Such ecosystem is treated as a potential fire source, that is confirmed by several fire events during the last two decades (2006 and 2014).

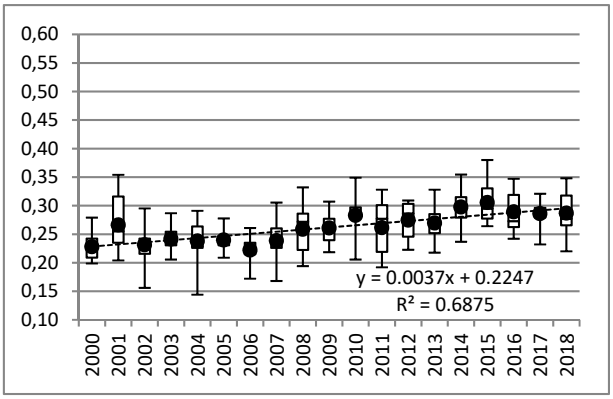


Figure 3. Average annual NDVI box plots during growing seasons in open sand ecosystem during 2000-2018. The upper and lower hinges correspond to the first and the third quartiles, upper and lower whiskers correspond to maximum and minimum values.

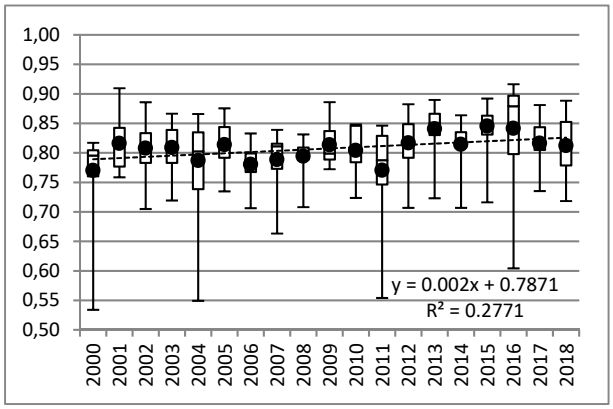


Figure 4. Average annual NDVI box plots during growing seasons in forest ecosystem during 2000-2018. The upper and lower hinges correspond to the first and the third quartiles, upper and lower whiskers correspond to maximum and minimum values.

4. Synthesis

To sum up, the Curonian Spit coastal dunes reflect the synergy of Man and Nature over many years. However, nowadays climate change and its influence upon the succession of different coastal dunes ecosystem types invites to the new discussion about the existing nature protection and nature management tools.

References

Houston J. 2008. Management of Natura 2000 habitats. 2130 *Fixed coastal dunes with herbaceous vegetation ('grey dunes'). European Commission

LITCOAST - Natura 2000 site conservation and management on the Lithuanian coast (2005-2008) LIFE05 NAT/LT/000095

Urbis A., Povilanskas R., Newton A. (2019). Valuation of aesthetic ecosystem services of protected coastal dunes and forests, Ocean and Coastal Management 179, 104832

Usman, U., Yelwa, S. A., Gulumbe, S. U., & Danbaba, A. (2013). Modelling relationship between NDVI and climatic variables using geographically weighted regression. Journal of Mathematical Sciences and Applications, 1, 24–28.

EI-GEO Environmental Impact of Geosynthetics in aquatic systems

Franz-Georg Simon[1], Haitham Barqawi[1], Boris Chubarenko[2], Elena Esiukova [2], Ieva Putna-Nimane[3], Ieva Barda[3], Evita Strode[3] and Ingrida Purina[3]

[1] BAM Bundesanstalt für Materialforschung und -prüfung (franz-georg.simon@bam.de)
[2] Shirshov Institute of Oceanology, Russian Academy of Sciences
[3] Agency of Daugavpils University, Latvian Institute of Aquatic Ecology

1. The ERA.Net-RUS Plus Project EI-GEO

EI-GEO is a multinational research project (Germany, Latvia, Russia) funded under the ERA.Net RUS Plus Call 2017.
Aim of the project is the investigation whether geosynthetics in hydraulic engineering applications could be a source of microplastics (MPs) and other contaminants to the aquatic environment causing negative effects to aquatic organisms. Whereas the behavior of geosynthetics in landfill engineering is well studied and documented since decades, little is known on application in applications such as coastal protection or ballast layers for wind energy plants. However, due to the rapid expansion of offshore wind energy, rising water levels and more extreme weather conditions as a result of climate change more and more hydraulic engineering projects will be realized in the future.
Applied methods are artificial ageing of geosynthetics in environmental simulation chambers, storage of samples under environmental condition for comparison with laboratory simulation, sample characterization by microscopic methods and ecotoxicological testing of water in contact with geosynthetics.
In parallel a case study at the Baltic Sea shore at Kaliningrad Oblast (Russia) will be performed. The aim of study is to estimate the level of pollution of the beaches by geosynthetic debris and identify the possible sources.

2. Project description

Geosynthetics are widely used in hydraulic engineering. Application areas are soil reinforcement, stabilization of ballast layers (e.g. for piles of offshore wind energy plants), waterproofing of dams and canals and scour protection. The application of geosynthetics in hydraulic engineering has huge economic benefits such as savings through substitution or reduction of selected soil materials, through ease of installation and increased speed of construction, life cycle cost savings through improved performance (by increased longevity or reduction of maintenance) and improved sustainability in terms of conserving natural environments as compared to alternative designs (Müller and Saathoff, 2015).
It is commonly accepted that geosynthetics with proper stabilization with antioxidants (e.g. sterically hindered amines) will last in underwater constructions with limited oxygen supply and temperatures at constantly low levels for at least 100 years.
However, after end of service lifetime geosynthetics could be a source of plastic debris in aquatic systems. Further, additives, which are needed as plasticizers or antioxidants, could be emitted with detrimental influence on the environment (Wiewel and Lamoree, 2016). The loss of additives is intimately related to the ageing of the geosynthetic products. Those are the reasons that public authorities are concerned about the approvability of engineering projects using geosynthetics in aquatic systems.
Long term stability of geotextiles is usually investigated related to mechanical stability, which must fulfill certain requirements after ageing. Different methodologies are available (e.g. elevated temperature or pressure) to accelerate ageing in the laboratory. Mechanical properties, tensile strength, investigation on chemical oxidation reaction by infrared spectroscopy and residual content of stabilizers are typical parameters tested with aged samples. Investigation of the possible environmental impact of the application of geosynthetics in aquatic systems is therefore hardly possibly with virgin polymer material. Consequently, the polymers must be artificially aged, best with environmental simulation chambers enabling accelerated ageing. In the case of geosynthetics in hydraulic engineering beside oxidation, mechanical stress (e.g. by tidal fluctuations, wave action, abrasion by sand) and microbiological interactions (formation of biofilms, etc.) play significant roles and must be considered.
Moreover, the chemical composition and small size make MPs effective sorbent of persistent organic pollutants (POPs) which may be transferred to biota, enhancing regularly occurring bioaccumulation. Despite these concerns, the impact of MPs and their role as vectors mediating POP transport and bioaccumulation in aquatic food webs is largely unknown.
It can be expected that geotextiles degradation processes are similar to processes of other plastics reaching the marine environment because they are made from the same types of polymers. Plastic waste exposed to environmental conditions begins to degrade slowly generating a large number of macro-, micro-, and nano-particles. One of the key factors, which determines the fate of microplastics in the environment is the density of polymers. Specific density of microplastic can vary significantly depending of a polymer type, technological processes of its production, additives, weathering and biofouling (Morét-Ferguson et al., 2010, Chubarenko et al., 2016), but with time, most of floating plastics become negatively buoyant as well due to biofouling or adherence of denser particles, and sink to the sea floor (Morét-Ferguson et al., 2010, Lobelle and Cunliffe, 2011). Thus, the seabed becomes the ultimate repository for microplastic particles and fibers (Woodall et al., Barnes et al., 2009). Evaluation of the contamination level is complicated not only because of difficulty of the sampling of bottom sediment, but also due to hardness of the extraction of small plastic particles from marine deposits.
Construction with geosynthetics has various advantages but it has to be ensured that there is no negative environmental impact from the application of

geosynthetics in hydraulic engineering. It is expected that any effect will be visible only on the long-term because the virgin raw material used for the production of geosynthetics has almost no release of particles or substance relevant to the environment (Holmes et al., 2014). Therefore, accelerated ageing is performed to derive requirements for geosynthetics in hydraulic engineering. All testing will be performed with these artificially aged geosynthetics.
Partly from improper material selection and partly from non-professional handling and debris from geosynthetic material can be found on the shore today. Field studies with sampling and monitoring at the shore of the Kaliningrad Oblast (Russia) will help to evaluate the magnitude of this pollution and are therefore a work package of the project.

3. Experimental results

Autoclave tests (Robertson, 2013) were performed in a pure oxygen atmosphere with pressures of 10, 20 and 50 bar at a temperature of 80 °C and durations in the range of 7 to 42 days. The evaluation of the results is ongoing.



Figure 1. Test sample of geosynthetics (Naue Secutex R601). Left. Virgin sample (surface weight 600 g/m^2. Right: after artificial ageing in autoclave (80° C, p(O_2) = 30 bar, 21 days) and checking on tensile testing machine (Zwick).

4. Identification of ecotoxicity tests and preliminary results

Literature analysis of existing studies on plastic leachate toxicity was done in order to identify type of the tests and testorganisms. It was resumed that there are only few marine testorganisms that correspond environmental conditions of the Baltic Sea and more often freshwater organism tests are used in leachate ecotoxicity assessment. For comparability reasons several freshwater organism tests were chosen in order to study ecotoxicity of geosynthetics. Preliminary results of *H. azteca* tests showed that leachates cause negative effect on growth of testorganism.

5. Results of field study

In 2018, the 13 coastal constructions on the shore of the Kaliningrad Oblast (Russia) in which geosynthetic materials are used, were investigated. These structures were built over the past 10 years and protect 7 km of the shore. All of them are potential sources of contamination of the environment with plastic debris.

Monitoring of the beaches of the South-Eastern Baltic by continuous visual scanning showed that fragments of geosynthetic materials from the coastal and engineering structures are unevenly distributed. It was revealed that the greatest visible effect in the pollution of beaches is made by the remnants of woven textiles (big bags / bags), actively breaking up into fibers. These fibers migrate along the coast, settling on the beach and at the bottom. Fragments of nonwoven geotextiles from the coastal protection structures were also found (Esiukova et al., 2018)

6. Acknowledgements

The project EI-GEO “Environmental impact of geosynthetics in aquatic systems” within the Program ERA.Net RUS Plus (No RUS_ST2017-212) is supported via grants of national scientific funding agencies of Latvia (VIAA), Germany (BMBF) and Russia (RFBR, No 18-55-76002), see http://ei-geo.com.

References

Barnes, D. K. A., Galgani, F., Thompson, R. C. and Barlaz, M. (2009). Accumulation and fragmentation of plastic debris in global environments. *Philosophical Transactions of the Royal Society B-Biological Sciences* 364 (1526): 1985-1998.

Chubarenko, I., Bagaev, A., Zobkov, M. and Esiukova, E. (2016). On some physical and dynamical properties of microplastic particles in marine environment. *Marine Pollution Bulletin* 108 (1): 105-112.

Esiukova, E. E., Chubarenko, B. and Simon, F.-G. (2018). Debris of geosynthetic materials on the shore of the South-Eastern Baltic (Kaliningrad Oblast, the Russian Federation), in: Williams, A.J. (ed.), *2018 IEEE/OES Baltic International Symposium (BALTIC)*, pp. 1-6, New York: IEEE Xplore.

Holmes, L. A., Turner, A. and Thompson, R. C. (2014). Interactions between trace metals and plastic production pellets under estuarine conditions. *Marine Chemistry* 167: 25-32.

Lobelle, D. and Cunliffe, M. (2011). Early microbial biofilm formation on marine plastic debris. *Marine Pollution Bulletin* 62 (1): 197-200.

Morét-Ferguson, S., Law, K. L., Proskurowski, G., Murphy, E. K., Peacock, E. E. and Reddy, C. M. (2010). The size, mass, and composition of plastic debris in the western North Atlantic Ocean. *Marine Pollution Bulletin* 60 (10): 1873-1878.

Müller, W. W. and Saathoff, F. (2015). Geosynthetics in geoenvironmental engineering. *Science and Technology of Advanced Materials* 16 (3): 034605 (20pp).

Robertson, D. (2013). The Oxidative Resistance of Polymeric Geosynthetic Barriers (Gbr-P) Used for Road and Railway Tunnels. *Polymer Testing* 32 (8): 1594-1602.

Wiewel, B. V. and Lamoree, M. (2016). Geotextile composition, application and ecotoxicology—A review. *Journal of Hazardous Materials* 317: 640-655.

Woodall, L. C., Sanchez-Vidal, A., Canals, M., Paterson, G. L. J., Coppock, R., Sleight, V., Calafat, A., Rogers, A. D., Narayanaswamy, B. E. and Thompson, R. C. The deep sea is a major sink for microplastic debris. *Royal Society Open Science* 1 (4): 140317.

Atmospheric transport and seasonal variability of trace elements and polycyclic aromatic hydrocarbons in fine-aerosol fraction at the coastal site in Gdynia, Poland

Patrycja Siudek, Ilona Waszak

National Marine Fisheries Research Institute, Gdynia, Poland (psiudek@mir.gdynia.pl)

1. Introduction

The Baltic Sea is one of the most important marine ecosystems in Europe. Due to combined and multi-directional effects of anthropogenic sources on processes in the aquatic environment, the research on air pollutants is crucial and represents a platform for studying chemical composition and transformation of organic and metal-rich particles. Quantifying concentration levels of metals and polycyclic aromatic hydrocarbons (PAHs) in coastal fine atmospheric particles ($PM_{2.5}$) are important due to their toxic and persistent properties as well as the ability to migrate between different environmental and/or biological matrices.

In many coastal environments, the impact of harbour and maritime sectors, i.e. activities related to petroleum, pipelines, maritime transport and ships docked at berths as well as activities generating ship plumes, have been recognized as an important fingerprint of shipping emission. All these maritime activities are regarded as prime chemical drivers for changes in the local air quality (Xiao et al., 2018, Cheng et al., 2019, Wang et al., 2019). The trace elements and PAHs congeners levels in fine coastal aerosol over Baltic Sea region in Poland, have not been regularly monitored, and thus the access to long-term and comprehensive studies is still quite limited.

The aim of this study was to (i) determine multi-component profiles of fine particulate matter in spring, summer, fall and winter season, (ii) identify the most important local and regional anthropogenic sources of trace elements and PAHs congeners, based on long-range transport analysis, (iii) examine the contribution of V and Ni from shipping activities to $PM_{2.5}$.

2. Sampling strategy and methods

Daily measurements of fine aerosol samples ($PM_{2.5}$) were performed from January to December 2019, at the single coastal site in Gdynia, northern Poland (Fig. 1). The sampling site was comprehensively equipped with a temperature-controlled set of automatic sampler (PNS-18T Comde Derenda GmbH) with meteorological sensors to (A) collect $PM_{2.5}$ samples, and (B) register environmental parameters such as air temperature, relative humidity, pressure, wind speed and direction. The quartz microfiber filters (QMA, Whatman, 47 mm in diameter) were used to collect fine fraction ($PM_{2.5}$) of atmospheric particles. Concentrations of trace elements (Ni, V, Pb, As, Cu, Co, Cd, Cr) were quantitatively determined by inductively coupled plasma-optical emission spectrometry (ICP-OES, Varian, Agilent), with argon as a carrier gas, whereas 16 PAHs congeners (naphthalene *Nap*, acenaphthene *Ace*, acenaphthylene *Acy*, phenanthrene *Phe*, fluorine *Flu*, anthracene *Ant*, benz(a)anthracene *BaA*, chrysene *Chr*, pyrene *Pyr*, fluoranthene *Flt*, benzo(b)fluoranthene *BbF*, benzo(k)fluoranthene *BkF*, benzo(a)pyrene *BaP*, indeno(123-cd)pyrene *IPy*, benzo(ghi)perylene *BghiP*, dibenz(ah)anthracene *DahA*) were determined using HPLC system coupled with a fluorescence detector (Shimadzu Prominence).



Fig. 1. Map of the sampling site (SP) in Gdynia, Poland. The colored dots represent major anthropogenic sources: red – coal-fired power plants, blue - port and docks area, green – petrochemical refinery and plants, yellow – municipal solid waste recycling units.

3. Results

The monthly mean $PM_{2.5}$ mass concentration ranged from 13.7 µg m^{-3} to 55.0 µg m^{-3}, and the peak value of 167.2 µg m^{-3} was found in February 2019. Overall, considerable differences in the trace elements (Ni, V, Pb, As, Cu, Co, Cd, Cr) and PAHs congeners concentration were observed. However, their seasonal distribution was not similar.

The Σ_{16} PAHs in coastal $PM_{2.5}$ spanned a wide range of concentrations, from 0.5 to 19.5 ng m^{-3} (winter), 0.14 to 3.85 ng m^{-3} (spring), 0.18 to 2.07 ng m^{-3} (summer), 0.85 to 6.83 ng m^{-3} (fall).

The atmospheric V/Ni ratio has been used as a tracer for maritime transport, refineries and combustion. Both metals from that ratio are present in lubricant additives and residual fuel oil used by ships (Moldanova et al., 2013, Wang et al., 2019). Yuan et al. (2006) have pointed out major contribution of Ni and V to $PM_{2.5}$ in coastal areas, based on the V/Ni ratio used as a factor of heavy oil combustion and shipping emission.

The monthly distribution of the V to Ni ratio for the present study is shown in Fig. 2. The values of the ratio point to the potential input of primary emission from local shipping activities to $PM_{2.5}$ mass concentration. Specifically, the extreme values of the V/Ni ratio were found during experiments in May (2 cases), July (1 case), October (2 cases) and December (2 cases, Fig. 2). On October 1st and July 1st, the V/Ni ratio values were 9.18 and 11.48, respectively and coincided with weak winds from NE to S sectors, representing

the port area and mixed industrial sources. In the case of the May 19th situation, the influence of local petrochemical refinery and a plant located southeast of the sampling station was revealed. These results may indicate that ship and industrial plumes were an important source of contaminated particles.

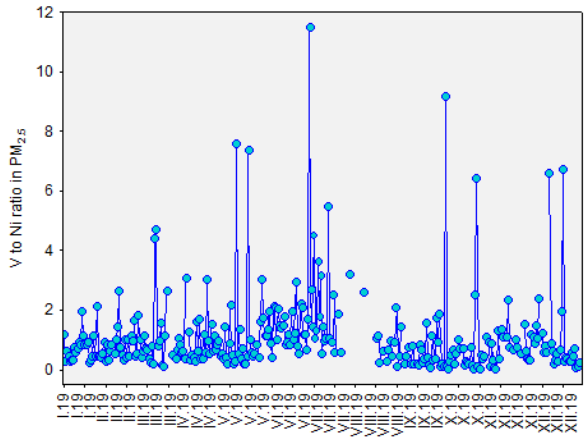


Fig. 2. Time series of V to Ni ratio in coastal $PM_{2.5}$ from measurements at the coastal site in Gdynia, Poland

4. Concluding remarks

In this study, the temporal variability of a large group of anthropogenic metals and 16 PAHs congeners in $PM_{2.5}$ collected at the coastal station in the southern Baltic Sea was investigated. The analysis of 24-h atmospheric samples showed complex and variable profiles of trace elements and PAHs in fine particulate matter. Seasonal differences were directly related to changes in the contribution from local and regional anthropogenic activities, geological sources and impact of meteorological conditions. Based on vanadium-to-nickel ratio, it was found that compounds emitted from the nearby port area and marine traffic significantly contributed to high levels of Ni and V in the coastal atmosphere.

6. Acknowledgments

This study was supported by the National Science Centre, Poland (UMO-2017/27/B/ST10/01200).

References

Cheng, Y., Wang, S., Zhu, J., Guo, Y., Zhang, R., Liu, Y., Zhang, Y., Yu, Q., Ma, W., and Zhou, B. (2019) Surveillance of SO2 and NO2 from ship emissions by MAX-DOAS measurements and the implications regarding fuel sulfur content compliance, Atmospheric Chemistry and Physics, 19, 13611–13626

Moldanova, J., Fridell, E., Winnes, H., Holmin-Fridell, S., Boman, J., Jedynska, A., Tishkova, V., Demirdjian, B., Joulie, S., Bladt, H., Ivleva, N.P., Niessner, R. (2013) Physical and chemical characterization of PM emission from two ships operating in European Emission Control Areas. Atmospheric Measurement Techniques, 6, 3577-3596

Wang, X., Shen, Y., Lin, Y., Pan, J., Zhang, Y., Louie, K.K.P., Li, M., Fu, Q. (2019) Atmospheric pollution from ships and its impact on local air quality at a port site in Shanghai, Atmospheric Chemistry and Physics, 19, 6315-6330

Xiao, Q., Li, M., Liu, H., Fu, M., Deng, F., Lv, Z., Man, H., Jin, X., Liu, S., and He, K. (2018) Characteristics of marine shipping emissions at berth: profiles for particulate matter and volatile organic compounds, Atmospheric Chemistry and Physics, 18, 9527–9545

Yuan, C.S. Lee, C.G. Liu, S.H. Chang, J.C. Yuan, C., Yang, H. Y. (2006) Correlation of atmospheric visibility with chemical composition of Kaohsiung aerosols. Atmospheric Research, 82, 663-679

Polynyas of coastal lagoons of the Baltic sea and other reservoirs of the northern hemisphere

Zhelezova Ekaterina[1, 2]

[1] Laboratory for Coastal Systems Study, Shirshov Institute of Oceanology of Russian Academy of Sciences. Moscow, Russia, (ironkate@inbox.ru)
[2] Immanuel Kant Baltic Federal University, Kaliningrad, Russia

1. Abstract

In the continuation of studying the phenomenon of stationary polynya near the Baltic Strait (Zhelezova et al, 2018), which is a natural indicator of the interaction between the Baltic sea and the ice-covered Vistula/Kaliningrad lagoon, it became necessary to find out how this feature is characteristic for lagoons of the World Ocean. According to the Review of morphometric characteristics of lagoons of the World Ocean (Domnina, Chubarenko, 2012) there are more than 300 of it. The ice regime of the coastal waters depends on the geographical latitude, depth of the reservoir, the system of currents, features of atmospheric circulation and heat exchange with the atmosphere, as well as on the configuration of the coastline. This paper considers lagoons with an area of more than 10 km^2 with one or more straits, the temperate geographical zone of the Northern hemisphere with cold winters and warm summers, located between 40 and 65° C. W. (boreal thermal zone with average annual temperatures -4...+4°C). Lagoons located to the North, in the zone of subarctic and Arctic climate (polar planetary thermal zone with average annual temperatures -23...-15°C), were also included in the analysis.

2. Data

A thorough review of more than 1000 satellite images of 118 lagoons in the period from 2012 to 2019, showed that 56 of them repeatedly recorded the presence of polynya. The search for images is conducted using the programs Google Earth and LandViewer. Sentinel and LandSat images are mostly used. This sample is random, because often free high-quality images, i.e. taken in good weather conditions and with sufficient resolution, are not enough. But there is a hope to confirm the presence of polynya in the several other lagoons as a result of further searches. A total of 15 lagoons situated in the Baltic Sea (Rødsand lagoon (Nysted), Orht Bight, Kamenskie lagoon (Kamminer Bodden), Puck Lagoon, Puck bay, Vistula lagoon, Curonian lagoon, Nevskaya Guba, Odense fjord, Salzhaff, Darss-Zingst Bodden Chain, Western Pomerania Lagoon Area, Strelasund, Achterwasser, Odra Estuary (Schecin lagoon) were examined. They are. In 9 of them (according to satellite images database in LandViewer from 2011 to 2019 years) there are stationary polynyas. Polynyas were observed in 6 lagoons: Vistula Lagoon, Zalew Kamienski, Nevskaya Guba, Darss-Zingst Bodden Chain, Western Pomerania Lagoon Area.

3. Results

Based on the position and configuration of the polynyas, it is proposed to distinguish three types of polynyas. Polynyas formed in the ice cover of the lagoon when it melts as a result of moving ice fields under the influence of wind or currents were not considered. First type is an entrance polynya confined to the strait connecting the lagoon area with the sea area, i.e. to the entrance to the lagoon from the sea. It can be divided into two subtypes - internal or inward (when the polynya is confined to the entrance to the lagoon and is located in the water area of the lagoon) and external or outward (when the polynya is located in the sea area). Second type - the stream-born polynya is formed by the active flow of river waters that are introduced into the lagoon's water area. The third type is quite exotic - "window-polynya", a closed formation in the area of the strait that connects the lagoon with the sea area. The most common type of stationary polynya in coastal lagoons is the entrance internal polynya, and the least common is the "window-polynya".

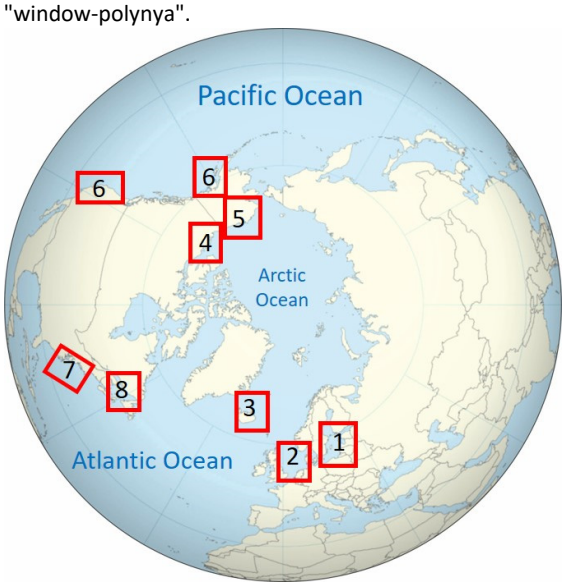


Figure 1. Geographical position of the study lagoons on the map of the Northern hemisphere: 1 – Lagoons of the Baltic Sea, 2 - Lagoons of the North Sea & the Irish Sea, 3 - Lagoons of the Atlantic Ocean, Iceland, 4 - Lagoons of the Beaufort Sea, Canada and, 5 - USA , 6 - Lagoons of the Pacific Ocean, USA, 7 - Lagoons of the Atlantic Ocean, USA, 8 - Lagoons of the Gulf of St. Lawrence, Canada.

4. Acknowledgements

The author is grateful to Chubarenko B. V. for the comments and suggestions. This study was supported by the Russian Foundation for Basic Researches No 19-35-90102 (Zhelezova) and theme 0149-2019-0013 of SIO RAS State Assignment (Chubarenko).

References

A.Yu. Domnina, B.V. Chubarenko. Morphometric characteristics of the lagoons of the world ocean //Izvestiya KGTU. – Kaliningrad: Izdatelstvo KGTU. -2012. - № 24. – p. 133- 140. (in russian)

Zhelezova E., Krek E., Chubarenko B. Characteristics of the polynya in the Vistula Lagoon of the Baltic Sea by remote sensing data. Int. J. Remote Sensing. 2018. 39:24, Pp. 9453-9464, DOI:10.1080/01431161.2018.1524181

Topic 7

Regional climate system modeling

NEMO (Nucleus for European Modeling of the Ocean) regional configuration for the Baltic Sea domain – validation of the water exchange through the Danish Straits.

Jan Andrzejewski[1], Jaromir Jakacki[1]

[1] Institute of Oceanology Polish Academy of Sciences, Sopot, Poland

1. The specifics of the Baltic Sea

The Baltic Sea is inland, shelf sea in northern part of Europe. It is shallow with average depth of 52 meters and deepest point 459 meters located at Landsort Deep. Baltic Sea is connected with North Sea via the Danish Straits (comprising of Great Belt, Little Belt and Øresund). These systems ensure only limited exchange between oceanic waters and seawaters, which affect the low salinity in the Baltic reservoir. Runoff from surrounding lands (approximately 200 rivers) and positive difference of precipitation minus evaporation additionally refreshes water and makes Baltic a brackish sea. The only charge of salt comes from the North Sea with so-called inflows or less frequent occurring Major Baltic Inflows (MBI). This exchange of waters via Danish Straits is the key for properly working numerical simulation.

2. Problem description

In this work the tool, well known as NEMO was used to perform the numerical simulation for the Baltic Sea area. This presentation is focused on the first stage of validation of the model results for the Baltic Sea region where influence of open boundary conditions is noticeable as soon as possible. The main change in the model is the assimilation of sea surface height in Kattegat area. Open boundary conditions are represented by assimilation the sea level in Kattegat from tide-gauge measurements directly from Goteborg (Figure 1). The properly working open boundary conditions affect the water exchange between Baltic Sea and North Sea, thus the MBI and minor saline water inflows are well represented. This is very important part in modeling the Baltic Sea, where narrow Danish Straits limits the water exchange which controls the salt budget, adding the salt with inflows and receiving brackish outflow out to the Ocean.

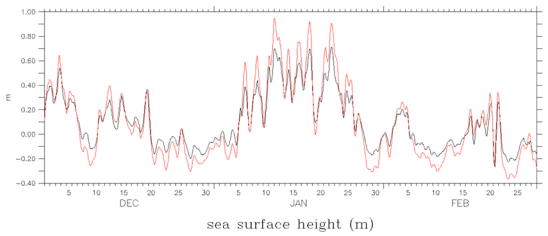


Figure 1 Assimilation of sea level in NEMO model (black) in comparison to sea gauge (red) in Goteborg, Sweden.

3. The way of validation

This work presents comparison between model output with results measured in situ and from another validated model (Huber, et al., 1993) - the compared period represents the Major Baltic Inflow in the beginning of 1993. Figure 1 presents a validation of an open boundary conditions implemented in the model NEMO for presented here Baltic Sea configuration, and this is the starting point of validation of the simulation results. The next step was to compare model outputs with those presented in article (Huber, et al., 1993). The reason to choose the inflow period on the beginning of 1993 was that simulation has started in july 1990 and this period (between model start and beginning of 1993) is enough for checking the spin up process. The area of validation suits very well to issue addressed in this work, because the validation is situated nearby the open boundary conditions (Figure 2).

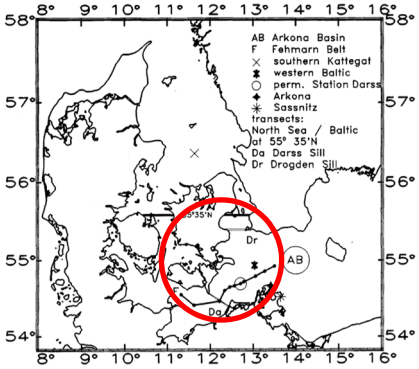


Figure 2 The main core of model validation.

Apart checking the parameters like salinity and sea surface height in the Danish Straits area (Figure 2) above, the mean Baltic volume was taken into account (see Figure 3).

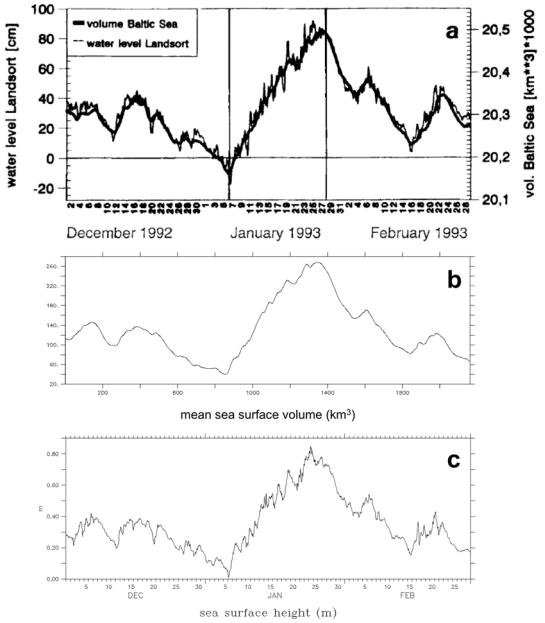


Figure 3 Comparison of sea level in the area of Landsort deep (c), average volume of water in the Baltic Sea (before the straits) with the results from the article (Huber, et al., 1993) (b). Part (a)

presents the results from the work to which the results are referred. The data refer to the period of MBI in 1993.

4. Summary

In this work the preliminary results of model validation are presented. The problem on which this work is focused seems to be narrow and takes into account only a small part of the Baltic Sea area. However, this area is crucial for carrying out correct numerical simulations in the Baltic area, as it is through the straits that the main exchange of the waters of this sea with the waters of the world ocean takes place.

References

Huber K., Kleine E., Lass H.U., Matthäus W., (1994), The major Baltic inflow in January 1993 — Measurements and modelling results, Ocean Dynamics 46, 2, 103-114

Moving climate zones and climate change impact on anomalous weather phenomena in the Euro-Cordex / Baltic Sea region

Matthias Gröger[1], Christian Dieterich [2] and H.E. Markus Meier[1,2]

[1] Leibniz Institute for Baltic Sea Research , Rostock, Germany (matthias.groeger@io-warnemuende.de)
[2] Swedish Meteorological and Hydrological Institute, Norrköping, Sweden

1. Introduction

Anomalous weather phenomena such as prolonged hot and dry periods, tropical nights, as well as winter cold spells have increased the awareness about threats associated with climate change under recent years. One example is the 2003 hot period which presumably has been responsible for more than 35.000 dead people (e.g. https://www.newscientist.com/article/dn4259-the-2003-european-heatwave-caused-35000-deaths/). In this study a regional climate model is used to study the response of dry periods, hot periods, tropical nights and winter cold spells in Europe as forced by climate change at the end of the 21st century.

We consider a suite of different climate scenarios including two high greenhouse gas concentration scenarios (RCP4.5, RCP8.5) as well as one scenario assuming climate mitigation efforts (RCP2.6).

2. Mean response to climate warming

In a first step the effect of climate warming on mean climate is assessed. For this we apply the climate classification scheme developed by Köppen (e.g Köppen, 1923, Kottek et al., 2006, Beck et al., 2018) on both model results, as well as on observation data sets derived from E-OBS data base (Cornes et al., 2018) (Figure 1). The response to climate change shows a characteristic pattern within three latitudinal bands. (1) a northern zone where polar climates (ET,EF) more or less disappear in the high emission scenarios and snow climates (Dfc, Dfb, Dfa) strongly decline especially in continental areas of eastern Europe. In total snow climates are reduce by ~30 % (800.000 km^2). The mid latitudes are characterized by a northward and eastward expansion of the fully humid warm temperated zone (Cf) which in the high emission scenario RCP8.5 even occupies wide areas of southern Finland (Figure 1). The western and southern part of Europe is apparently less effected by climate warming. With respect to major climate classes. This indicates the influence of the vast North Atlantic which in most global earth system models shows less strong warming due to reorganizations in the large scale ocean circulation and reduced oceanic northward heat transport.

The southernmost latitudes are characterized by northward expansion of arid climates (BS, BW) which increase by nearly 50 % in the RCP8.5. A substantial diminishing of winter rain over the Iberian Peninsula causes a dramatic climate change there. At the end of the 21st century in RCP8.5 dry temperated climate (Cs) is replaced by Desert/Steppe climate (BS). This region is already under present climate threatened by summer droughts. Further reduction of winter precipitation by 30 % points to potentially strong impacts on agriculture in RCP8.5

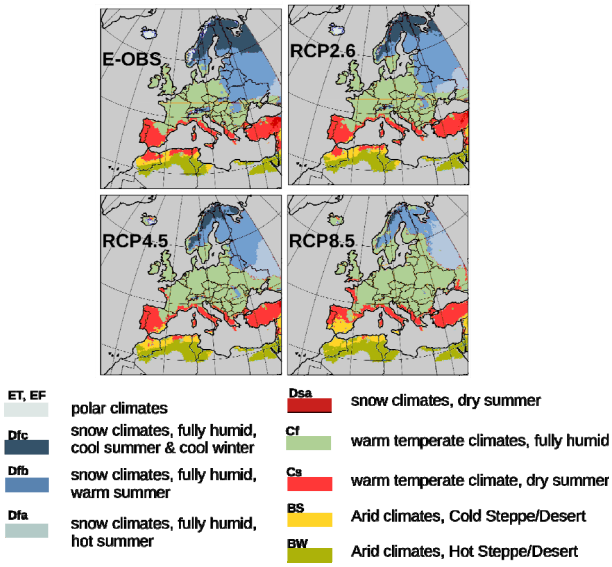


Figure 1. Climate classes according to Köppen (1923). E-OBS =observational gridded data set (Cornes et al., 2018). Shown is the respective ensemble mean over all models for the climate scenarios RCP8.5, RCP4.5, and RCP2.6.

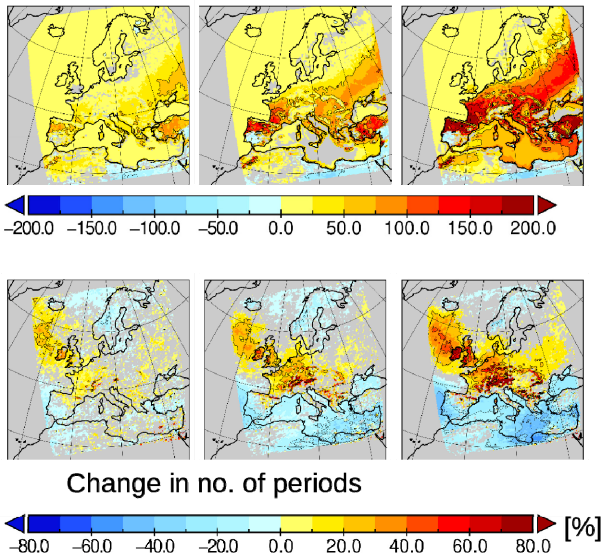
2. Anomalous hot and dry periods

Unlike the described changes in mean climate classes changes in the number of hot periods hot and dry periods have their maximum impact in temperate regions of western mid latitude Europe (Figure 2). A hot spot is the area of Iberia and western France where the frequency of hot periods increases substantially (Fig 2, top). Over the Mediterranean hot periods of at least 5 consecutive days above 30°C only slightly increase or even diminish as the average period duration increases in parallel which limits the total number of possible periods within a 30 year time window. This effect is seen even over southern Iberia.
A similar pattern is simulated for dry periods as defined of at least 5 consecutive dry days (<1 mm). Here the strongest impact is seen in a region comprising the UK, France and Germany as well as over the Alps. Scandinavia and northernmost Russia is less affected by changing dry periods. Noteworthy is however the strong increase in hot periods over Turkey and mid latitude eastern Europe.

3. Implications for mitigation

We have analyzed much more climate indices than shown here. For the overwhelming part we can state that most of climate change impacts on mean climate but on extreme anomalous weather phenomena as well can be avoided or will be much weaker pronounced when climate mitigation

affords are considered in the projected climate scenario RCP2.6 which assumes a stabilization of atm. pCO2 from the mid



century onward.

Figure 2: Top: Change in absolute number of hot periods (2070-2099 minus 1970-1999). From left to right: RCP2.6, RCP4.5, RCP8.5. Bottom: same as a) but showing relative change of dry periods. Shown is the ensemble mean over 9 models (RCP4.5,RCP8.5) or 6 models (RCP2.6)

7. References

Beck, H., Zimmermann, N., McVicar, T. et al. Present and future Köppen-Geiger climate classification maps at 1-km resolution. Sci Data 5, 180214 (2018). https://doi.org/10.1038/sdata.2018.214

Cornes, R., G. van der Schrier, E.J.M. van den Besselaar, and P.D. Jones. 2018: An Ensemble Version of the E-OBS Temperature and Precipitation Datasets, J. Geophys. Res. Atmos., 123. doi:10.1029/2017JD028200

Jacob, D., Petersen, J., Eggert, B. et al. Reg Environ Change (2014) 14: 563. https://doi.org/10.1007/s10113-013-0499-2

Köppen, W., (1923): Die Klimate der Erde, Walter de Gruyter, Berlin.

Kottek, M., J. Grieser, C. Beck, B. Rudolf, and F. Rubel, 2006: World Map of the Köppen-Geiger climate classification updated. Meteorol. Z., 15, 259-263. DOI: 10.1127/0941- 2948/2006/0130. 2948/2006/0130.

Applying the new regional coupled system model GCOAST-AHOI over Europe

Ha T. M. Ho-Hagemann, Stefan Hagemann, Sebastian Grayek, Ronny Petrik, Burkhardt Rockel, Joanna Staneva, Frauke Feser and Corinna Schrum

Institute of Coastal Research, Helmholtz-Zentrum Geesthacht, Geesthacht, Germany (Ha.Hagemann@hzg.de)

1. Introduction

In the present study, we introduce the new regional coupled system model GCOAST-AHOI (Geesthacht Coupled cOAstal model SysTem - Atmosphere, Hydrology, Ocean and sea Ice) and investigate the effect of air-sea coupling on Internal Variability (*IV*) of its atmospheric model compartment COSMO-CLM (CCLM). *IV* is an important source of uncertainty in the results of global climate models and regional climate models. Understanding and potentially reducing these uncertainties is necessary to produce and deliver robust climate information which, e.g., is of paramount importance for climate change impact studies (Giorgi, 2008).

Two six-member ensemble simulations were conducted with GCOAST-AHOI (in short AHOI) and CCLM in a stand-alone mode (CCLM_ctr) for the period 1 September – 31 December 2013 over Europe. *IV* is expressed by spreads within the two sets of ensembles. Analyses focus on specific events during this period, especially on the storm Christian occurring from 27-29 October 2013 in northern Europe.

2. Models

GCOAST-AHOI comprises the Atmospheric model CCLM (Rockel et al., 2008), the Hydrological discharge model HD (Hagemann and Dümenil, 1998), and the Ocean-sea Ice model NEMO-LIM3 (Madec, 2016), which are coupled via the coupler OASIS3-MCT (Valcke et al., 2015).

In this study, we use the CCLM model version 5.0, HD model version 4.0 (Hagemann et al., 2020) and NEMO model version 3.6 and the coupler OASIS3-MCT version 3.0. Variables exchanged amongst the compartment models are shown in Fig. 1.

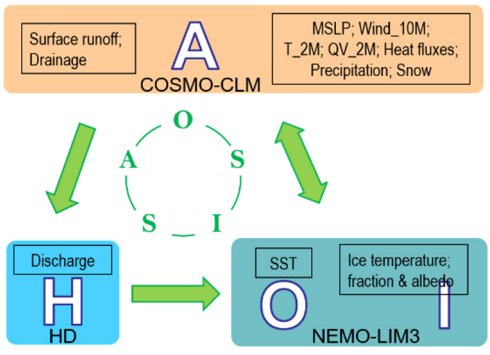


Figure 1. Schematic of GCOAST-AHOI: The Atmospheric model COSMO-CLM (CCLM) vs.5.0, the Hydrological discharge model HD vs.4.0, the Ocean model NEMO vs.3.6 with sea Ice model LIM3 coupled via the coupler OASIS3-MCT vs.3

3. Experimental design

CCLM is set up to simulate the regional climate for the EURO-CORDEX domain (Fig.2) at 0.11° horizontal resolution and 40 vertical levels in the atmosphere. The EURO-CORDEX domain of CCLM is relatively large, therefore, CCLM has a chance to produce its own local weather.

CCLM is driven by the 1 hourly ERA5 reanalysis data (Hersbach & Dee, 2016) at the lateral boundaries. The running time step of CCLM is 75 seconds. HD is set up for the European domain using a grid with the spatial resolution of 1/12° (8-9 km) and a time step of 3600 seconds. NEMO covers the region of the north-west European shelf, the North Sea, the Danish Straits and the Baltic Sea between -19.89°E to 30.16°E and 40.07°N to 65.93°N with a resolution of 2 nautical miles (ca 3.6 km). The vertical grid is the NEMO s-z*-hybrid grid with 50 levels and a tangential stretching below 200 m depth. The running time step of NEMO is 120 seconds. The lateral boundary forcing for tracers (temperature and salinity) is derived from hourly CMEMS FOAM-AMM7 model output (O'Dea et al., 2012). The coupling time step amongst CCLM, NEMO and HD via OASIS is 3600 seconds.

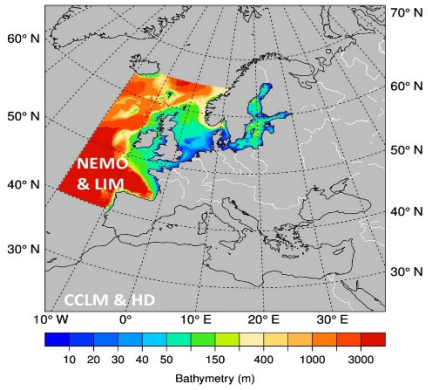


Figure 2. Model domains (CCLM & HD: Grey; NEMO & LIM: color)

To generate an initial condition ensemble for the quantification of *IV*, we started the spin up run CCLM_res at 1.8.2013 and stopped at 1.9.2013, 2.9.2013, …, and 5.9.2013 to obtain the restart conditions for 5 ensemble members: CCLM1-5 for the stand-alone CCLM (hereafter denoted by CCLM_ctr) and CPL1-5 for AHOI. CCLM1-5 and CPL1-5 all restart at 1.9.2013 but with these different restart conditions. The members CCLM0 and CPL0 use a cold start at 1.9.2013. Note that ens.CCLM and ens.CPL are ensemble means of 6 CCLM_ctr and AHOI coupled (CPL) experiments, respectively.

Besides CCLM0-5 and CPL0-5, which are conducted without SN technique, we also set up a CCLM stand-alone run using SN (denoted by CCLM_sn) that is considered as a reference experiment. SN is applied every fourth-time step with a nudging factor of 0.5 for the horizontal wind components (U, V), beginning at a height level of 850 hPa with quadratically increasing strength toward higher layers. Below 850 hPa no SN is applied so that small weather phenomena, which often occur close to the surface, are not affected.

4. Methodology

Hourly and daily model results are validated against the ERA5 reanalysis data and various observations (e.g., FINO1 and FINO3 platform wind data, HOAPS v4 satellite latent heat flux and specific humidity, and REGNIE precipitation data on the 1-km resolution grid).

IV is defined as the inter-member spread which is similar to the standard deviation (SD) of the ensemble

$$SD = \sqrt{\frac{1}{N-1}\sum_{i=1}^{N}(x_i - \bar{x})^2}$$

where $\{x_1, x_2, \ldots, x_N\}$ are the values of each member for a given variable, $\bar{x}$ is the mean value of these members, and N is the number of the members.

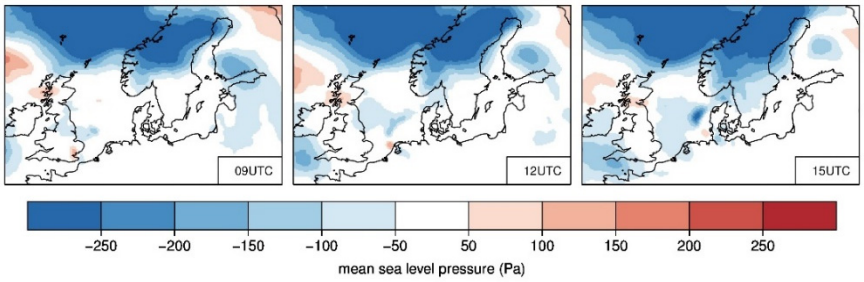


Figure 3. Difference between *IV* of AHOI ensemble and the stand-alone CCLM ensemble for mean sea level pressure MSLP [Pa] at 09 UTC (left), 12 UTC (middle) and 15 UTC (right) on 28 October 2013.

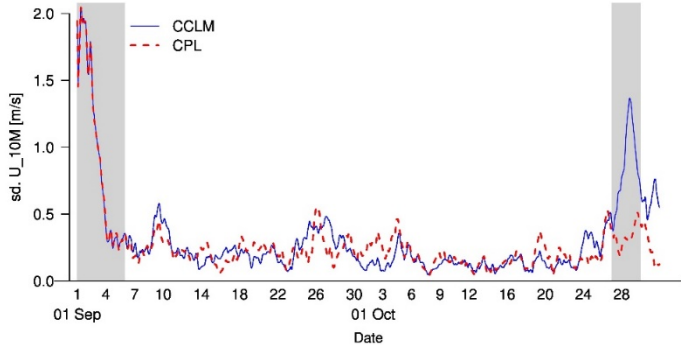


Figure 4. Hourly *IV* of 10-m height u-wind component U_10M [m/s] averaged over the NS_BS area. Time period: 01 September – 31 October 2013. Grey bars mark the two periods 1st - 5th September 2013 and 27th – 29th October 2013.

5. Results

Fig. 3 shows the difference of mean sea level pressure (MSLP) spread between ens.CPL and ens.CCLM for 09-15 UTC on 28 October 2013. Here, the blue colour implies that AHOI reduces the large spread of CCLM_ctr over large parts of the considered area. This stabilization effect of AHOI is found not only over the North Sea where the storm Christian passed by but also, and more pronouncedly, over the Norwegian Sea (NwgSea) and Scandinavia where the low Burkhard (the steering system of Christian) dominates.

IV of U-wind component at 10-m height (U_10M) of CCLM_ctr (CCLM) and AHOI (CPL) are both about 0.5 m/s after the spin-up of about 5 days from 1 to 5 September. However, *IV* of CCLM increases up to 1.4 m/s during the Christian event while a less uncertainty of about 1 m/s is found in the AHOI simulations (Fig. 4). A detailed analysis is provided by Ho-Hagemann et al. (2020).

6. Conclusion

Simulations of CCLM_ctr vary largely amongst ensemble members during the storm. By analyzing two members of CCLM_ctr with opposite behaviors we found that the large uncertainty in CCLM_ctr is caused by a combination of (1) uncertainty in cloud-radiation interaction in the atmosphere, and (2) lack of an active two-way air-sea interaction. When CCLM is two-way coupled with the ocean model, the spread is reduced, not only over the ocean where the coupling is done but also over land due to the land-sea interactions.

References

Giorgi, F. (2008) Regionalization of climate change information for impact assessment and adaptation, WMO Bull., Vol. 57, pp. 86-92

Hagemann, S., Dümenil, L. (1998) A parametrization of the lateral waterflow for the global scale, Clim. Dyn., Vol. 14, pp. 17-31

Hagemann, S., Stacke, T, Ho-Hagemann, H.T.M. (2020) High resolution discharge simulations over Europe and the Baltic Sea catchment. Frontiers in Earth Sci., accepted

Ho-Hagemann, H.T.M. et al. (2020) Internal variability in the regional coupled system model GCOAST-AHOI, Atmos., submitted

Hersbach, H., Dee, D. (2016) ERA5 reanalysis is in production, ECMWF Newsletter, Vol. 147

Madec, G. (2016) NEMO ocean engine, Note du Pole de modélisation 27, Institut Pierre-Simon Laplace (IPSL), France. ISSN-1288-1619.

O'Dea, E.J. et al. (2012) An operational ocean forecast system incorporating NEMO and SST data assimilation for the tidally driven European North-West shelf, Journal of Operational Oceanography, Vol. 5, pp. 3-17

Rockel, B., Will, A., Hense, A. (2008) The regional climate model COSMO-CLM (CCLM), Meteorol. Z., Vol. 17, pp. 347–348

Valcke, S., Craig, T., Coquart, L. (2015) OASIS3-MCT user guide, OASIS3-MCT 3.0. Technical Report TR/CMGC/15/38, CERFACS, Toulouse, France, 2015. CERFACS/CNRS SUC URA No 1875.

Simulated climate in the Baltic Sea region in a standalone atmospheric RCM and in an atmosphere-ocean model: evaluation and future climate change

Erik Kjellström[1,2], Christian Dieterich [1], Grigory Nikulin[1], Minchao Wu[3], Ole B. Christensen[4], Matthias Gröger[5] and H.E. Markus Meier[1,5]

[1] Swedish Meteorological and Hydrological Institute, Norrköping, Sweden (erik.kjellstrom@smhi.se)
[2] Department of Meteorology and the Bolin Centre for climate research, Stockholm University, Sweden
[3] Department of Earth Sciences, University Uppsala, Uppsala, Sweden
[4] Danish Meteorological Institute, Copenhagen, Denmark
[5] Leibniz Institute for Baltic Sea Research Warnemünde, Germany

1. Introduction

Coupled regional climate models (RCMs) involving not just the atmosphere and the land surface, but also ocean and sea ice are successful in representing the climate of the Baltic Sea region (e.g. Döscher et al. 2002, Wang et al. 2015). For some climate features such coupled models have been shown to outperform standalone atmospheric models using prescribed sea sea-surface temperatures (SST). An example relates to the simulations of convective snow bands over the Baltic Sea (Van Pham et al. 2017).

Despite the successful performance of such coupled models most RCM climate change projections for the Baltic Sea region are from standalone atmospheric RCMs. This involves the recent EURO-CORDEX largest ensemble of RCM simulations covering all of Europe at 12.5 km horizontal resolution (e.g. Jacob et al. 2014).

From a regional and local perspective in the Baltic Sea area the lack of a realistic representation of oceanic processes at relevant resolution may have strong influence on the results (e.g. Kjellström and Ruosteenoja, 2007). This representation tends to differ between different global climate models (GCM); thereby making the potential for a coupled regional model more or less pronounced (Meier et al, 2011). In this work we examine results from one RCM used in both coupled and standalone mode to downscale two different GCMs for present day and a future climate change scenario. We aim at quantifying to what degree the results are altered by using a coupled model.

2. Model and experimental setup

The RCA4 regional climate model (Kjellström et al. 2016) has been setup and run for a domain covering Europe (Figure 1) at 25 km horizontal resolution. The model has been run with different boundary conditions in two configurations:

i) The standalone RCA4 atmosphere-land model using prescribed SST and sea-ice conditions from the driving GCM.

ii) The coupled RCA4-NEMO model (Wang et al., 2015) including a physical model interactively calculating sea-ice and ocean conditions in the Baltic Sea and in the North Sea (see Fig. 1). The ocean model has been operated at two nautical miles (c. 3.7 km) resolution.

The models have been run with boundary conditions from the reanalysis ERA-Interim (Dee et al., 2011) and from two different GCMs; EC-Earth (Hazeleger et al. 2010) and the MPI-M-ESM (Popke et al. 2013). The GCM results are taken from CMIP5 (the fifth phase of the Coupled Model Intercomparison Project, Taylor et al. 2012). For the period before 2006 the GCMs have been using historical forcing conditions as prescribed in CMIP5. For the future period 2006-2100 we are focusing on the representative concentration pathway scenario RCP8.5 (Moss et al. 2010). For model evaluation purposes we compare with observations from E-OBS v20.0e (Cornes et al. 2018).

3. Results

The results show that the coupled model performs similarly as the uncoupled model. This implies that differences are small and mostly concentrated to the areas of coupling. An example is given in Figure 1 showing summertime (June-August) seasonal mean temperature in E-OBS and as simulated by the two versions of the model when forced with boundary conditions from the MPI-M-ESM. The large picture reveals that the simulated climate is too cold in northern Europe, a feature shared with the driving GCM. In more detail it can be seen that differences between the two versions are very small and confined to coastal areas around the Baltic Sea where the coupled model tends to be slightly warmer than the uncoupled model.

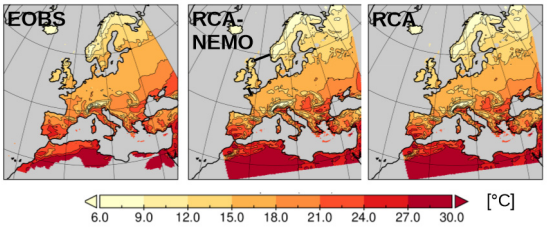


Figure 1. Summer (June-August) seasonal mean temperature according to E-OBS (left), the coupled RCA4-NEMO model (middle) and the atmosphere stand-alone RCA4 model (right). The middle panel also illustrates where the coupling between the NEMO model and the driving global ocean model takes place (black lines).

Also the climate change signal is similar in the two model versions and the impact of the coupling is most

pronounced over the coupled region, i.e. the Baltic Sea and the North Sea. Figure 2 illustrates changes in summer (June-August) seasonal mean temperature in the coupled version of the model driven by the MPI-M-ESM. The typical land-sea warming pattern with more warming over land due to less effective heat capacity compared to the ocean is seen. Also, the impact of the well-known weak warming over the North Atlantic due to changes in large-scale ocean circulation in the Atlantic and reduced oceanic northward heat transport can be seen. Over the northernmost oceanic regions there is instead stronger warming related to reductions in sea-ice cover in the Arctic region. All this applies likewise to the uncoupled RCA version (not shown). The difference in anomaly climatologies (2070-2099 minus 1970-1999) between the coupled minus the uncoupled version indicates the "coupling effect" in summer is most intense directly over the coupled area in the North Sea and the Baltic Sea. The amplitude of the difference reaches locally about half of the climate induced temperature change in both model versions. The shape and length scale of the local anomalies indicate changes in ocean circulation as driver between the coupled and uncoupled RCA versions.

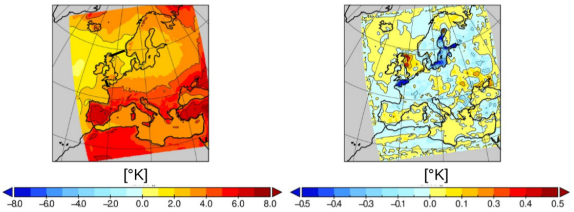


Figure 2. Change in summer (June-August) seasonal mean temperature in the coupled RCA4-NEMO run downscaling the MPI-M-ESM under RCP8.5. The comparison is between 1970-1999 and 2070-2099. The left panel also illustrates where the coupling between the NEMO model and the driving global ocean model takes place (black lines).

4. Conclusions

The presented analysis show that the regional coupled model reproduces features of the observed climate in a good way over the Baltic Sea and North Sea region. Differences between the coupled version and the uncoupled version are relatively small and confined to the coupling region or its proximity. The results also indicate that the coupling may impact climate change in the region. Again, differences are most pronounced over the immediate coupling region. Differences are shown to be significant. The preliminary results showed here points to the fact that such a coupled model is a useful, and possibly necessary, tool for projecting climate change in the Baltic Sea region. In the forthcoming analysis we will make a more in-depth analysis of differences between the coupled and uncoupled model versions with the aim of being able to make a more robust conclusion.

References

Cornes R, van der Schrier G, van den Besselaar EJM, and Jones PD (2018) An Ensemble Version of the E-OBS Temperature and Precipitation Datasets, J. Geophys. Res. Atmos., 123.

Dee DP, Uppala SM, Simmons AJ, Berrisford P, Poli P, Kobayashi S, et al. (2011) The ERA-Interim reanalysis: configuration and performance of the data assimilation system. Q. J. Roy. Meteorol. Soc. 137(656), 553597.

Döscher R, Willén U, Jones C, Rutgersson A, Meier HEM, Hansson U, and Graham LP (2002) The development of the regional coupled ocean-–atmosphere model RCAO. Boreal Environment Research, 7, 183–192.

Hazeleger W, Severijns C, Semmler T, Stefanescu S, Yang S, Wang X, et al. (2010) EC-Earth: a seamless Earth-system prediction approach in action. Bull. Am. Meteorol. Soc. 91, 1357–1363.

Jacob D, Petersen J, Eggert B, Alias A, Christensen OB, Bouwer LM, Braun A, Colette A, Déqué M, Georgievski G, Georgopoulou E, Gobiet A, Menut L, Nikulin G, Haensler A, Hempelmann N, Jones C, Keuler K, Kovats S, Kröner N, Kotlarski S, Kriegsmann A, Martin E, van Meijgaard E, Moseley C, Pfeifer S, Preuschmann S, Radermacher C, Radtke K, Rechid D, Rounsevell M, Samuelsson P, Somot S, Soussana J-F, Teichmann C, Valentini R, Vautard R, Weber B and Yiou P (2014) EURO-CORDEX: new New high-resolution climate change projections for European impact research, Regional Environmental Change, 14, 563–578.

Kjellström E and Ruosteenoja K (2007) Present-day and future precipitation in the Baltic Sea region as simulated in a suite of regional climate models. Climatic Change, 81(Suppl. 1), 281–291.

Kjellström E, Bärring L, Nikulin G, Nilsson C, Persson G and Strandberg G (2016) Production and use of regional climate model projections—A Swedish perspective on building climate services. Climate Services, 2–3, 15–29.

Meier HEM, Höglund A, Döscher R, Andersson H, Löptien U and Kjellström E (2011) Quality assessment of atmospheric surface fields over the Baltic Sea from an ensemble of regional climate model simulations with respect to ocean dynamics. Oceanologica, 53, 193-227.

Moss RH, Edmonds JA, Hibbard KA, Manning MR, Rose SK, van Vuuren DP, CarterTR, Emori S, Kainuma M, Kram T, Meehl GA, Mitchell JFB, Nakicenovic N, Riahi K, Smith SJ, Stouffer RJ, Thomson AM, Weyant JP, Wilbanks TJ (2010) The next generation of scenarios for climate change research and assessment. Nature, 463:747–756.

Popke D, Stevens B, and Voigt A (2013), Climate and climate change in a radiative-convective equilibrium version of ECHAM6, J. Adv. Model. Earth Syst., 5, 1– 14.

Taylor KE, Stouffer RJ, Meehl GA (2012) An Overview of CMIP5 and the Experiment Design, B. Am. Meteorol. Soc., 93, 485-498.

Van Pham T, Brauch J, Früh B and Ahrens B (2017) Simulation of snowbands in the Baltic Sea area with the coupled atmosphere-ocean-ice model COSMO-CLM/NEMO. Meteorol. Z., 21(1), 71–82.

Wang S, Dieterich C, Döscher R, Höglund A, Hordoir R, Meier HEM, Samuelsson P and Schimanke S (2015) Development and evaluation of a new regional coupled atmosphere–ocean model in the North Sea and Baltic Sea, Tellus A, 67, 24284.

Convection permitting regional climate modelling in northern Europe – first results on the summertime precipitation climate from NorCP

Erik Kjellström[1,2], Danijel Belušić[1] , Petter Lind[1], David Lindstedt[1], Erika Toivonen[3], Rasmus A. Pedersen[4], Ole B. Christensen[4], Oskar Landgren[5] and Andreas Dobler[5]

[1] Swedish Meteorological and Hydrological Institute, Norrköping, Sweden (erik.kjellstrom@smhi.se)
[2] Department of Meteorology and the Bolin Centre for climate research, Stockholm University, Sweden
[3] Finnish Meteorological Institute, Helsinki, Finland
[4] Danish Meteorological Institute, Copenhagen, Denmark
[5] Norwegian Meteorological Institute, Oslo, Norway

1. Introduction

High-resolution, convection permitting regional climate models (CPRCMs) operating at scales of a few kilometers that do not rely on convective parameterization schemes have been shown to simulate short-duration high impact intense precipitation events in a realistic way (e.g. Kendon et al. 2012, Lind et al. 2016). Such CPRCMs have also been found to give a stronger intensification of extreme precipitation events in a warmer climate compared to estimations based on conventional RCMs operated at "standard" horizontal resolutions, i.e. 10-50 km, particularly for seasons or regions dominated by convective rainfall (Kendon et al. 2014, Lenderink et al. 2019).

Until recently, long-term climate integrations with CPRCMs have been lacking for many regions. In this paper we describe joint development and application of such a model covering large parts of the Baltic Sea region. The experimental setup is described as well as some results related to model evaluation. Aspects of added value and observational constraints will be presented. Results from the first long climate change scenario simulations covering 20-year time slices at 3 km horizontal resolution will also be presented. The paper focuses on analysis of summertime precipitation on seasonal, daily and sub-daily time scales.

2. Model and experimental setup

The HCLIM regional climate model (Belušić et al., 2020) has been setup for a domain covering most of the Baltic Sea basin (Figure 1). The downscaling is done in two steps; first to 12 km horizontal resolution with the HCLIM-ALADIN model and subsequently to 3 km resolution with HCLIM-AROME.

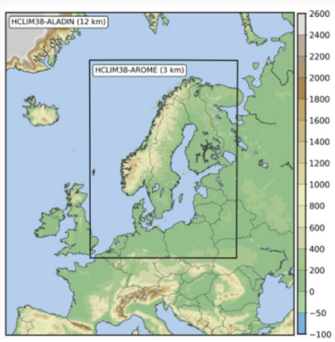


Figure 1. Model domains used for the simulations. The larger domain corresponds to the intermediate runs with HCLIM-ALADIN at 12 km grid spacing and the smaller domain to the high-resolution (3 km) HCLIM-AROME simulations. The color scale indicates the model topography.

The model has been run with different boundary conditions for two experiments:

i) An experiment focusing on model evaluation with boundary conditions from the ERA-Interim reanalysis (Dee et al. 2011) covering 1998-2018.
ii) An experiment for assessing climate change with boundary conditions from EC-Earth (Hazeleger et al. 2010) for a control period (1985-2005) and a future period (2080-2100).

For the future period, EC-Earth was forced with the RCP8.5 scenario representing strongly increased greenhouse gas forcing (Moss et al. 2010). For evaluation we use E-OBS covering Europe at 12 km horizontal resolution (Haylock et al. 2008) and HIPRAD that is a combined radar-gauge product for Sweden at 4 km (Berg et al 2016).

3. Model evaluation

The results show that the HCLIM model represents climate conditions in the region in a good way. This relates both to the large-scale atmospheric circulation and of seasonal mean temperatures and precipitation. However, biases do exist. For precipitation this mostly relates to areas in the Scandinavian mountains with overestimated precipitation compared to E-OBS. The two models, at 12 and 3 km, show similar features at seasonal scales. An exception is summer (June-August) when the 3 km model shows a clear improvement relative to the 12 km model, which overestimates precipitation in a more general sense. This can be related to less frequent low-intensity precipitation in the 3 km model.

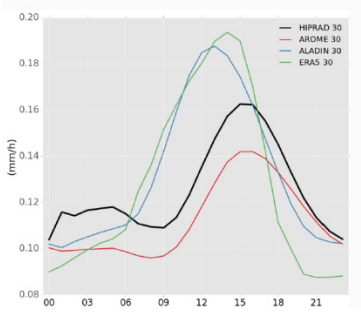


Figure 2. Diurnal cycle of simulated summertime (June-August) precipitation in Sweden. The coarser-scale ERA5 (green) and HCLIM-ALADIN (blue) models precipitates too early while the high-resolution HCLIM-AROME (red) show a considerable improvement compared to the HIPRAD observations (black).

At higher temporal resolution the main advantages with the convective permitting model are clearly seen with considerable improvements in the representation of the diurnal cycle (Figure 2) and intensities of heavy precipitation on hourly time scales (Figure 3).

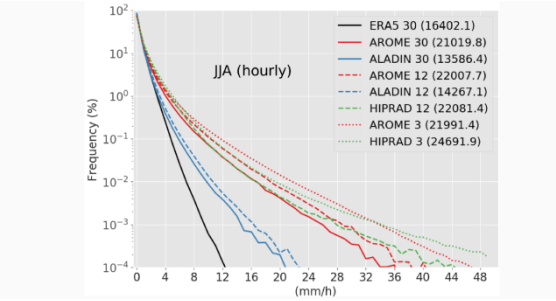


Figure 3. Frequency-intensity diagram for summertime hourly precipitation for Sweden. The coars-scale ERA5 (black) and HCLIM-ALADIN (blue) models show too few intense events while the high-resolution HCLIM-AROME (red) shows a considerable improvement compared to the HIPRAD observations (green). The improvement is clear regardless of which resolution the comparison is made at (e.g. at the ERA5 30 km grid, the HCLIM-ALADIN 12 km grid).

4. Future climate change

Both the EC-Earth model and the downscaled results of HCLIM show generally warmer conditions at the end of the 21st century compared to that in the control climate. Summertime precipitation is increasing in northern Scandinavia and especially along the west coast of Norway while decreases are seen over many areas in the south. Despite decreases in seasonal mean precipitation in relatively large areas heavy precipitation is projected to increase. This is found at both model resolutions and is similar to what has previously been shown (e.g. Christensen and Christensen, 2003).

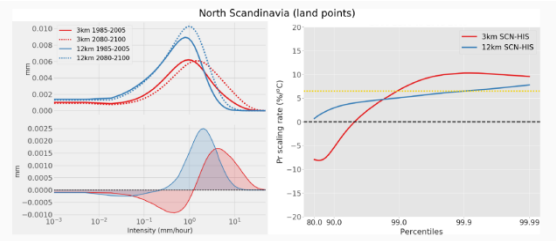


Figure 4. Changes in frequency of hourly precipitation at different intensities. The left upper panel shows control and future climate distributions for the two versions of HCLIM. The lower panel shows the climate change signal. The right panel shows the scaling factor expressed as percent changes per degree of increase in temperature. The yellow line represents the Clausius-Clapeyron relationship (approx. 7 % per degree).

For high-intensity summertime precipitation the high-resolution model shows a stronger increase than the coarser-scale model (Figure 4). The results indicate that there are areas also in northern Europe showing super-Clausius-Clapeyron scaling.

5. Conclusions

Based on the results we conclude that the high-resolution regional climate model HCLIM is suitable for use in the Baltic Sea region. We demonstrate that the model can represent the observed precipitation climatology to a high degree. Notably, the convection permitting model version shows good performance in reproducing the diurnal cycle of precipitation and frequencies of high-intensity precipitation events. In all the results indicate that the CPRCM simulates the precipitation climate with a larger degree of realism compared to coarser-scale climate models. The results show increasing intensities for precipitation extremes in the future under strong global warming. In particular we note that the CPRCM shows a stronger climate change signal for intense precipitation events compared to the coarser-scale models further strengthening the case for CPRCMs.

References

Belušić D, de Vries H, Dobler A, Landgren O, Lind P, Lindstedt D, Pedersen RA, Sánchez-Perrino JC, Toivonen E, van Ulft B, Wang F, Andrae U, Batrak Y, Kjellström E, Lenderink G, Nikulin G, Pietikäinen J-P, Rodríguez-Camino E, Samuelsson P, van Meijgaard E and Wu M (2020) HCLIM38: A flexible regional climate model applicable for different climate zones from coarse to convection permitting scales. Submitted to Geosci. Model Dev.

Berg P, Norin L and Olsson J (2016) Creation of a high resolution precipitation data set by merging gridded gauge data and radar observations for Sweden. J. Hydrol., 541(A), 6-13.

Christensen JH and Christensen OB (2003) Severe summertime flooding in Europe. Nature 421, 805–806.

Dee DP, Uppala SM, Simmons AJ, Berrisford P, Poli P, Kobayashi S, et al. (2011) The ERA-Interim reanalysis: configuration and performance of the data assimilation system. Q. J. Roy. Meteorol. Soc. 137(656), 553597.

Haylock, MR, Hofstra N, Tank AMG, Klok EJ, Jones PD and New M, (2008) A European daily high-resolution gridded data set of surface temperature and precipitation for 1950–2006 J. Geophys. Res. Atmos. 113 D20119.

Hazeleger W, Severijns C, Semmler T, Stefanescu S, Yang S, Wang X, et al. (2010) EC-Earth: a seamless Earth-system prediction approach in action. Bull. Am. Meteorol. Soc. 91, 1357–1363.

Kendon EJ, Roberts NM, Senior CA Roberts MJ (2012) Realism of rainfall in a very high resolution regional climate model, J. Climate, 25, 5791-5806.

Kendon, EJ, Roberts NM, Fowler, HJ, Roberts MJ, Chan SC and Senior CA (2014) Heavier summer downpours with climate change revealed by weather forecast resolution model, Nature Climate Change, 4, 570–576.

Lenderink G, Belušić D, Fowler H, Kjellström E, Lind P, van Meijgaard E, van Ulft B and de Vries H (2019) Systematic increases in the thermodynamic response of hourly precipitation extremes in an idealized warming experiment with a convection-permitting climate model, Environ. Res. Lett., 14, 074012.

Lind P, Lindstedt D, Kjellström E and Jones C (2016) Spatial and Temporal Characteristics of Summer Precipitation over Central Europe in a Suite of High- Resolution Climate Models. J Clim, 29, 3501-3518.

Moss RH, Edmonds JA, Hibbard KA, Manning MR, Rose SK, van Vuuren DP, CarterTR, Emori S, Kainuma M, Kram T, Meehl GA, Mitchell JFB, Nakicenovic N, Riahi K, Smith SJ, Stouffer RJ, Thomson AM, Weyant JP, Wilbanks TJ (2010) The next generation of scenarios for climate change research and assessment. Nature, 463:747–756.

Uncertainties of Baltic Sea future projections under different shared socioeconomic pathways

H. E. Markus Meier[1,2], Christian Dieterich[2], and Matthias Gröger[1]

[1] Leibniz Institute for Baltic Sea Research Warnemünde, Germany (markus.meier@io-warnemuende.de)
[2] Swedish Meteorological and Hydrological Institute, Norrköping, Sweden

1. Introduction

In several BONUS projects, ensembles of scenario simulations for the Baltic Sea ecosystem were carried out. For instance, within the projects ECOSUPPORT and BalticAPP eutrophication abatement scenarios under future climate were assessed (e.g., Meier et al., 2019; Meier and Saraiva, 2020). Questions to be answered were whether the Baltic Sea Action Plan (BSAP) would lead to good ecological status (GES) even in warmer climates, when the targets of GES would be achieved assuming rigorous implementation of the BSAP and when first signals of anthropogenically induced climate change and improved environmental conditions would be detected. In this study, various ensembles of scenario simulations are compared and with regard to the questions listed above uncertainties of the projections are estimated. Uncertainties are caused by shortcomings of global and regional climate models, unknown future greenhouse gas emissions and nutrient loads, and natural variability. In recent studies of historical Baltic Sea climate natural variability were found to be considerable, making the detection of any anthropogenically induced, systematic trends difficult (Kniebusch et al., 2019a; 2019b). We developed a method to estimate uncertainties in future projections with the aim to investigate the potential whether projections of the marine ecosystem might be improved.

2. Methods

First, we compare two ensembles of scenario simulations, ECOSUPPORT and BalticAPP, to illustrate uncertainties (Figures 1 to 3, Tables 1 to 3).

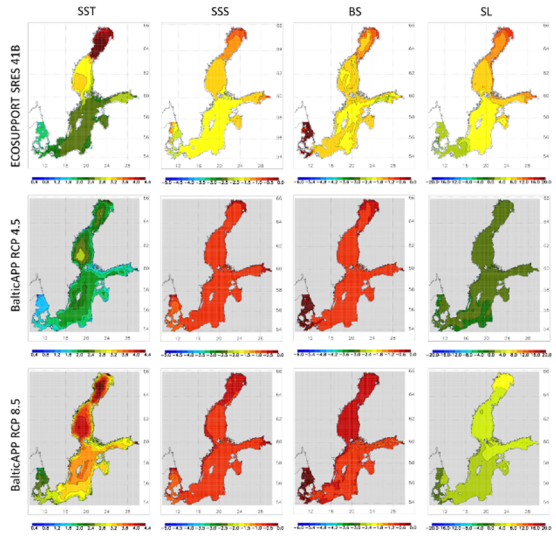


Figure 1. From left to right changes of summer (June – August) mean sea surface temperature (SST) (°C), annual mean sea surface salinity (SSS) (g kg^{-1}), annual mean bottom salinity (BS) (g kg^{-1}), and winter (December – February) mean sea level (SL) (cm) between 1978-2007 and 2069-2098 are shown. From top to bottom results of the ensembles ECOSUPPORT A1B (white background), BalticAPP RCP 4.5 (grey background) and BalticAPP RCP 8.5 (grey background) are depicted. (Source: H. E. Markus Meier, IOW and SMHI)

Second, in a recently developed ensemble of regional scenarios for the Baltic Sea we analyzed the sources of uncertainty in climate indices and environmental quality indicators. The ensemble is based on 32 regionalized scenarios using the regional climate model RCA4-NEMO (Dieterich et al., 2019) and the ecosystem model RCO-SCOBI (Meier et al., 2019), where four different external drivers have been varied. Climate is represented by four different Earth System Models (ESMs). Uncertain future greenhouse gas emissions are represented by two different Representative Concentration Pathways (RCPs), RCP 4.5 and RCP 8.5. Two nutrient load scenarios, REF and BSAP, broadly equivalent to two Shared Socio-economic Pathways (SSPs), describe two distinct evolutions of the regional population development, agricultural practices and food demand and three scenarios for global mean sea level rise (GMSL) measure the impact of the water level on the biogeochemical cycle in the Baltic Sea.

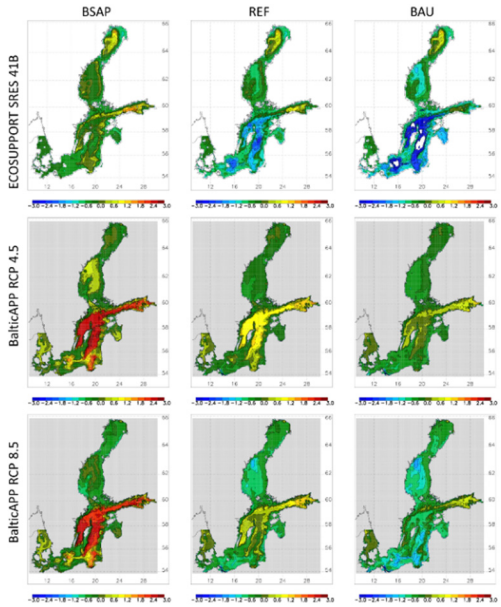


Figure 2. Ensemble mean summer (June – August) bottom dissolved oxygen concentration changes (mL L^{-1}) between 1978-2007 and 2069-2098. From left to right results of the nutrient load scenarios Baltic Sea Action Plan (BSAP), Reference (REF) and Business-As-Usual (BAU) are shown. From top to bottom results of the ensembles ECOSUPPORT A1B (white background), BalticAPP RCP 4.5 (grey background) and BalticAPP RCP 8.5 (grey background) are depicted. (Source: H. E. Markus Meier, IOW and SMHI)

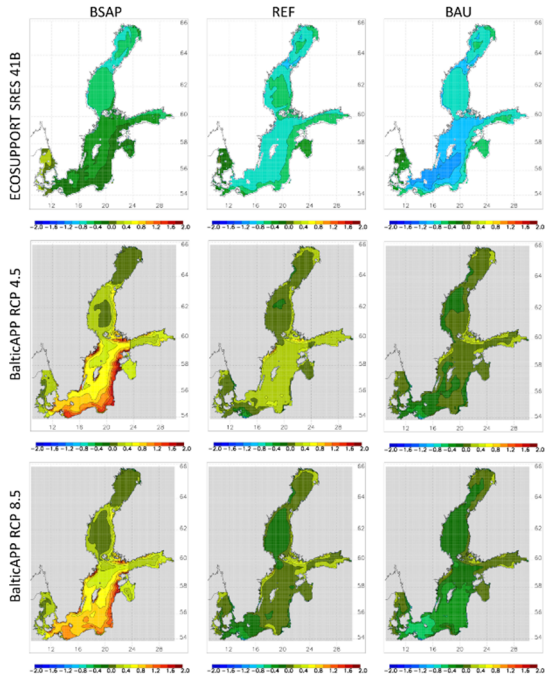


Figure 3. As Fig. 2 but for annual mean Secchi depth changes (m). (Source: H. E. Markus Meier, IOW and SMHI)

3. Results

We found that in the new ensemble the volume averaged temperature increase at the end of the century relative to the reference period 1976-2005 is 1.3 to 2.2 K (RCP 4.5) and 2.9 to 4.2 K (RCP 8.5) depending on the ensemble member (cf. Fig. 1, Tab. 1). Averaged salinity changes by -2.1 and +1.5 g/kg (RCP 4.5) and -3.2 and -2.4 g/kg (RCP 8.5). For temperature, uncertainties before 2080 are dominated by natural variability and ESM biases. After 2080 the largest source of uncertainty is related to the unknown greenhouse gas concentrations. As expected, uncertainties related to either SLR or nutrient loads are negligible. For salinity, the dominating source of uncertainty during the entire 21st century is explained by the biases of the ESMs. However, natural variability and, in particular by the end of the century, uncertainties due to unknown greenhouse gas concentrations and sea level rises are important as well. For hypoxic area, uncertainties before 2040 are dominated by ESM biases. After 2040 the largest source of uncertainty is related to the unknown nutrient loads (SSPs). However, ESM biases, natural variability, unknown greenhouse gas concentrations and unknown sea level rises play an important role as well. Hence, the predictability of hypoxic area on long time scales requires accurate knowledge of various drivers and accurate quality of ESMs.

Table 1. Ensemble mean changes in sea surface temperature (SST) (in °C) in ECOSUPPORT, BalticAPP RCP 4.5 and BalticAPP RCP 8.5 scenario simulations averaged for the Baltic Sea including the Kattegat. (DJF = December, January, February, MAM = March, April, May, JJA = June, July, August, SON = September, October, November) (Source: H. E. Markus Meier, IOW and SMHI)

Δ SST	DJF	MAM	JJA	SON	Annual
ECOSPPORT SRES A1B	2.5	2.8	2.8	2.5	2.6
BalticAPP RCP 4.5	1.7	1.9	2.0	1.8	1.8
BalticAPP RCP 8.5	2.9	3.2	3.3	3.0	3.1

Table 2. Ensemble mean changes in summer mean bottom oxygen concentration (in mL L^{-1}) in ECOSUPPORT, BalticAPP RCP 4.5 and BalticAPP RCP 8.5 scenario simulations averaged for the Baltic Sea including the Kattegat. The project changes depend on the nutrient load scenario Baltic Sea Action Plan (BSAP), Reference (REF) and Business-As-Usual (BAU). (Source: H. E. Markus Meier, IOW and SMHI)

Summer changes	ECOSUPPORT	BalticAPP RCP 4.5	BalticAPP RCP 8.5
BSAP	-0.1	0.6	0.5
REF	-0.6	0.1	-0.2
BAU	-1.1	-0.1	-0.5

Table 3. Ensemble mean changes in annual Secchi depth (in m) in ECOSUPPORT A1B, BalticAPP RCP 4.5 and BalticAPP RCP 8.5 scenario simulations averaged for the Baltic Sea including the Kattegat. The project changes depend on the nutrient load scenario Baltic Sea Action Plan (BSAP), Reference (REF) and Business-As-Usual (BAU). (Source: H. E. Markus Meier, IOW and SMHI)

Annual changes	ECOSUPPORT SRES A1B	BalticAPP RCP 4.5	BalticAPP RCP 8.5
BSAP	-0.3	0.6	0.6
REF	-0.6	0.2	0.1
BAU	-0.8	0.1	-0.1

References

Dieterich, C., Wang, S., Schimanke, S., Gröger, M., Klein, B., Hordoir, R., Samuelsson, P., Liu, Y., Axell, L., Höglund, A., Meier, H. E. M. (2019). Surface Heat Budget over the North Sea in Climate Change Simulations, Atmosphere, 10, doi: 10.3390/atmos10050272

Kniebusch, M., H. E. M. Meier, T. Neumann and F. Börgel (2019a). Temperature variability of the Baltic Sea since 1850 in model simulations and observations and attribution to atmospheric forcing. Journal of Geophysical Research – Oceans, 124, 4168–4187. https://doi.org/10.1029/2018JC013948

Kniebusch, M., H. E. M. Meier, and H. Radtke (2019b). Changing salinity gradients in the Baltic Sea as a consequence of altered freshwater budgets. Geophysical Research Letters, 46, 9739–9747. https://doi.org/10.1029/2019GL083902

Meier, H. E. M., Dieterich, C., Eilola, K., Gröger, M., Höglund, A., Radkte, H., Saraiva, S., Wåhlström, I. (2019). Future projections of record-breaking sea surface temperature and cyanobacteria bloom events in the Baltic Sea, AMBIO, 41, doi:10.1007/s13280-019-01235-5

Meier, H. E. M., and S. Saraiva (2020). Projected Oceanographical Changes in the Baltic Sea until 2100. Oxford Research Encyclopedia of Climate Science, in press.

Objective analysis of climatological fronts in the Atlantic-European sector

Katsiaryna Sumak[1], Inna Semenova[2]

[1] Belhydromet, Minsk, Belarus (katyasbelarus@gmail.com)
[2] Odessa State Environmental University, Ukraine

1. Introduction

The atmospheric front is one of the most complex objects in the atmosphere, which carries an important weather-forming and climatic function. Therefore, the use of methods that allow to simulate the complex structure of the front in order to determine its position in space and time, is an actual and not completely solved problem.

The most common quantitative characteristics of atmospheric fronts are frontal parameters, which functionally link meteorological values and describe their behavior in the frontal zone, which allows to set some limit criteria specific to the fronts. One of the most commonly used is the thermal front parameter (TFP), which is a quantitative characteristic that takes into account the distribution of temperature gradients (Creswick, 1967; Hewson, 1998; Serreze et al, 2001).

The thermal front parameter reflects the basic definition of the atmospheric front, namely, on the cold front, the temperature begins to decrease, and on the warm front, its rise stops. The temperature for calculating the TFP can be taken at any level, or calculated in a certain layer of the atmosphere, which allows taking into account the three-dimensionality of the frontal zones. The equivalent temperature T_e is calculated instead of the usual temperature in order to take into account the moisture content. The position of the front line is determined through the zone with the maximum positive values of TFP.

The aim of this study is to determine the spatial-temporal dynamics of the Polar and Arctic fronts in winter (January) and summer (July) in the Atlantic-European sector in the period of 1995-2015.

2. Materials and methods

The method of objective analysis of the Polar and Arctic fronts was applied using the calculated grid fields of the thermal front parameter in the Atlantic-European sector, bounded by 13° W - 62° E and 35-80° N using the formula:

$$TFP = -\nabla|\nabla T|\frac{\nabla T}{|\nabla T|}, \qquad (1)$$

where $\nabla = \vec{\imath}\frac{\partial}{\partial x} + \vec{\jmath}\frac{\partial}{\partial y}$,

$|\nabla T| = \sqrt{\left(\frac{\partial T}{\partial x}\right)^2 + \left(\frac{\partial T}{\partial y}\right)^2}$ - module of temperature gradient.

The initial data for calculating the TFP were the daily temperature fields T (K) and specific humidity q (kg·kg^{-1}) at the 850 and 700 hPa levels of the Era-Interim reanalysis data with a spatial resolution 1.5×1.5° (https://apps.ecmwf.int/datasets/data/interim-full-daily/levtype=pl/).

The calculated formula (1) includes the field of the average equivalent temperature T_e of the layer 850-700 hPa, determined by the formula:

$$T_{e\,(850-700)} \cong T_{850-700} + 2{,}5q_{850-700}, \qquad (2)$$

where q (specific humidity) is expressed in g·kg^{-1}.

The calculated TFP fields have the order of 10-11^{-2} K·m^{-2}.

3. Results and discussions

For the central months of the cold and warm seasons, the average geographical position of two branches of the Polar front and Arctic front was obtained for the studied period.

It was revealed that the geographical position of climatological fronts changed both in the cold and warm periods of the year compared with climatic data. So, in January both branches of the Polar front shifted north by three degrees of latitude. In July the northern branch of the Polar front descended to the south, but the southern branch took a more northerly position, so the branches of the Polar front came closer through oncoming traffic in summer.

The position of the Arctic front in the cold and warm periods of the year also changed in comparison with the previous climate period - it shifted to the north by four degrees of latitude.

The main areas of polar frontogenesis in the cold period of the year were the sea surface, namely, the southern regions of the Norwegian Sea, central part of the Baltic Sea, the western half of the Mediterranean Sea. In the summer more active atmospheric fronts were over the continent, in the area of the mountain systems – in the south of the Scandinavian mountains, to the North of the Alps and Pyrenees, the Urals and the Lower Volga region.

The Arctic front in all seasons of the year intensified over the Barents and Norwegian seas, in the summer – also over the north of the Greenland Sea.

Inasmuch cyclonic activity is directly related to atmospheric fronts, certain shifts of the Arctic front and branches of the Polar front indicate the changes in regional synoptic processes over the European continent over the past 20 years, which were reflected in the climatic regime of these territories.

References

Creswick W.S. (1967) Experiments in objective frontal contour analysis, J. Appl. Meteor, Vol. 6, pp. 774-781.

Hewson T.D. (1998) Objective fronts, Meteorol. Appl. Vol. 5, pp. 37-65.

Serreze M.C., Lynch A.H., Clark M.P. (2001) The arctic frontal zone as seen in the NCEP-NCAR reanalysis, J. Climate, Vol. 14, pp. 1550-1567.

Does internally generated hydrodynamic noise matter in the Baltic Sea?

Hans von Storch[1], Anders Omstedt[2] and Jüri Elken[3]

[1] Institute of Coastal Research, Helmholtz Zentrum Geesthacht, PO Box, 21502 Geesthacht, Germany
[2] University of Gothenburg. Marine Sciences: Oceanography. Box 460. SE-405 30 Göteborg. Sweden
[3] Tallinn University of Technology, Department of Marine Systems, Akadeemia 15A, EE12618 Tallinn, Estonia

1. Prologue

The findings about unforced variability – here named "hydrodynamic noise" - in models of the dynamics of the South China Sea (Tang et al., 2019, 2020) are reviewed – namely the intensification of the emergence of such noise with increasing spatial resolution, and its dominance (in terms of signal-to-noise ratio) on small scales.

The formation of such noise is significant for the design and evaluation of numerical experimentation with high-resolution models of oceanic dynamics, and for the estimation of the impact related to regional and local manifestations of global change.

We discuss and speculate which physical mechanisms are significant for the generation of noise in the Baltic Sea? Which consequences have these findings for studying the hydrodynamics and impacts in the Baltic Sea.

2. Results for South China Sea

In a series of numerical experiments on the hydrodynamics in the South China Sea (SCS) with the model HYCOM, the issue of intra-ensemble variability has been addressed. The SCS model with a grid resolution of 0.04° is embedded in a West-Pacific model with 0.2° grid resolution – and this, again is, into an almost global model with a 1° grid resolution. The latter model is hardly describing macro turbulent eddy dynamics, but the other two models become better in doing so.

In a first series of experiments (Tang et al., 2019), the ocean models were exposed to atmospheric forcing with a smooth constant annual variation. The intra-seasonal variance of sea surface height in the SCS is rather weak in the 1° grid resolution but substantial in the 0.04° grid resolution grid resolution (Figure 1). This increase is, at least partly, related to the emergence of eddies: A count of eddies finds almost no eddies in the 1°-model, but many in the other two, with a doubling from the 0.2° to the 0.04° grid.

From this result, we conclude that it is not only stationary spatial detail, which is added by increasing resolution, but also the variability. To which level the variability would grow with further increase of resolution, is unknown at this time.

In a second set of simulations an ensemble of 4 simulations, all covering 2008, but with different initial values was constructed. In this case, realistic weather was prescribed. The initial values were 13, 15, 25 and 27 months before January 2008, the beginning of the year which was evaluated (Tang et al., 2020).

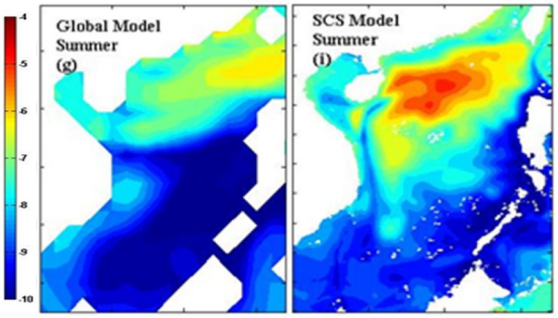


Figure 1. Logarithm of intra seasonal variability of sea surface height in summer in the 1°-grid model (left) and in the 0.04 °-grid model (right) of the SCS. After Tang et al. (2019)

The daily fields of barotropic stream-function (other variables would do as well) were expanded into Empirical Orthogonal Functions (EOFs). The variances represented by the EOFs (thus, their order) is indicative for the spatial scales. Signal-to-noise ratios (S/N) were constructed using the definitions:

Signal = annual intensity of the coherent variations of the four simulations (at the same day)

Noise = annual intensity of daily standard deviation of the four simulations (at the same day)

Three ranges of S/N were found – for the first 10 EOFs scales of on average 220 km and more, for a middle block of 40 EOFs scales of 110 km and for the remaining many EOFs scales of only 30 km. Higher-indexed, thus smaller scale EOFs go with smaller S/N, while low-indexed, thus large-scale EOFs with higher S/N. When recombining the spatial fields with the respective EOFs, we find higher S/N ratios in the coastal ocean, whereas smaller S/N ratios prevail in the deep ocean (Figure 2).

In short – noise dominates in deep water and on small scales – in the South China Sea.

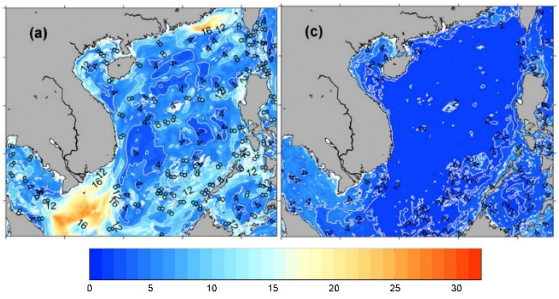


Figure 2. Maps of the S/N ratio for the barotropic stream-function after projection on the large-scale EOFs 1-10 (a) and the small scale EOFs 51-1463 (c) Note that the annual cycle is included in the EOF analysis. From Tang et al. (2020)

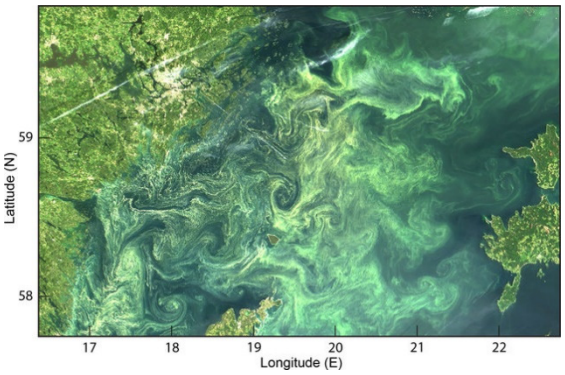


Figure 3. Cyanobacteria (primarily Nodularia spumigena) accumulations in Northern Baltic Proper on 11 July 2005 as shown on MODISTerra quasi true color image at 250 m resolution. Adopted from Kahru and Elmgren (2014)

3. Beddies in the Baltic Sea

The question is how strong such hydrodynamic noise is in the much less deep Baltic Sea, if there are preferred regions etc. We discuss the expectation given by our dynamical understanding of the Baltic Sea.

Most of this dynamical understanding is based on extensive simplifications on the hydrodynamic equations leading to Geophysical Fluid Dynamics (e.g. Cushman-Roisin and Becker, 2011). These simplifications highlight different aspects of the ocean dynamics and hide other aspects. Early studies in numerical modelling of the ocean were based not only on equation simplifications but on coarse model resolution and models with strong numerical viscosity and diffusion. In late 1970ies, when new satellite data became available, the observation of horizontal eddies (similar to Figure 3) challenged a reconsideration of ocean dynamics. In the Baltic Sea these mesoscale eddies (Beddies) have a typical horizontal diameter of 10 -20 km. But also, vertical eddies were found from direct measurements and often organized along the wind direction as Langmuir circulation. Recently, sub-mesoscale variability containing smaller spiral eddies and frontal filaments have gained attention of researchers. Meso- and sub-mesoscale Baltic ocean dynamics is considerably modulating environmental variables on the basin scales. Variability coming from the external forcing as e.g. upwelling, Langmuir circulation or inertial oscillation presents clear deterministic hydrodynamic signals. The question is now: do Beddies constitute part of hydrodynamic noise?

Beddies and sub-mesoscale features have been observed in most regions of the Baltic Sea. Mechanisms of their generation have been theoretically analyzed, suggesting mainly (1) baroclinic-barotropic instability as a random generation processes, and (2) forced vorticity generation when larger scale flow crosses the depth contours (so-called JEBAR effect, joint effect of baroclinicity and relief).

So far, neither in observed nor modelled situations, the mechanisms (1) and (2) have been clearly separated. Using ensemble simulations, as done in the SCS may help to determine signal-to-noise ratios, and thus improve our understanding of predictability of such features. If there are locations and regions, where forced variability dominates (in particular by specific coastlines or topography features), then by improving the models, then chances for skillful forecasts of eddies and filament features may be improved.

4. Outlook

The basic question to be asked is to what extent the dynamics of the Baltic Sea must be considered deterministic or stochastic. From a practical point of view, an answer has been given by forecast practitioners, who have begun to do ensemble forecasting (Büchner and Söderkvist, 2016) – there *is* a significant random component. This is not surprising, both in terms of physical expectation – Hasselmann's (1976) stochastic climate models points in this direction - but also from global modeling efforts such as that of Penduff et al. (2016),

For the longer period basin-scale oceanographic scenarios, it should be important to evaluate whether specific approaches of accounting the random and forced meso- and sub-mesoscale variability will converge when increasing the model resolution, and if there are "bifurcations" of the ocean system (e.g., different future paths for long-term changes in salinity: will be there "oceanization" or "freshening" of the Baltic Sea?).

Apart of these dynamical issues, the derivation of impacts of ocean variability and change need attention – what does a noisy component imply for mixing, what is the effect on sediment dynamics and on ecosystems, which interact with the physical system on smaller scales?

The presence of unprovoked variability has implications for numerical experimentation. It suffices no longer to just compare differences in two simulation, which differ by some specified modification, but null hypotheses need to be formulated and tested, as originally suggested in the 1970s for experiments with global atmospheric models (Chervin e al., 1974)

References

Büchmann, B., and J. Söderkvist (2016) Internal variability of a 3-D ocean model. *Tellus*, 68A, 30417

Chervin, R. M., W.L. Gates, and S.H. Schneider (1974) The effect of time averaging on the noise level of climatological statistics generated by atmospheric general circulation models. *J. Atmos. Sci.* 31, 2216–2219.

Cushman-Roisin, B., and J. Beckers (201). *Introduction to Geophysical Fluid Dynamics: Physical and Numerical Aspects*. Academic Press, 875 pp.

Hasselmann, K. (1976) Stochastic climate models Part I. Theory. *Tellus*, 28, 473–485,

Kahru, M., and R. Elmgren (2014) Multidecadal time series of satellite-detected accumulations of cyanobacteria in the Baltic Sea. *Biogeosciences* 11, 3619.

Penduff, T., and Coauthors (2018) Chaotic variability of ocean heat content: Climate-relevant features and observational implications. *Oceanography*, 31 (2), 63–71

Tang S., H. von Storch, and Chen X, (2020) Atmospherically forced regional ocean simulations of the South China Sea: Scale-dependency of the signal-to-noise ratio. *J. Phys. Oceano.* 50, DOI 10.1175/JPO-D-19-0144.1 133-144

Tang S., H. von Storch, Chen X., and Zhang M. (2019) "Noise" in climatologically driven ocean models with different grid resolution. *Oceanologia* 61, 300-307.

Topic 8

Climate Change and its impacts

Research of climate change in South-Eastern Baltic sea coastal areas

Inga Dailidienė[1,2], Indre Razbadauskaitė – Venskė[1,2] , Remigijus Dailidė[1,2], and Lina Davilienė[3]

[1] Faculty of Marine Technology and Natural Sciences, Klaipeda University, Klaipeda, Lithuania (dailidiene.ku@gmail.com)
[2] Department of Informatics, Lithuania Business University of Applied Sciences, Klaipeda,
[3]Institute of Physics, Savanoriu 231, LT-02300 Vilnius, Lithuania. E-mail: lina@ar.fi.lt

1. Introduction

Recently society in many countries is concerned about the effect of global climate change. In the last decades climate change has caused impacts on natural and human systems on all continents and across the oceans (IPCC 2014). Socio-economic costs, associated with climate change damage and need for adaptation, are expected to escalate (Christel *et al.* 2018). The effect of the global climate change on air and sea temperature changes has drawn widespread interest, as a changing water temperature has ecological, economic and social impact in coastal areas of the European seas, including Baltic Sea.

The study results show that increasing trends of water level, air and water temperature and decreasing ice cover duration are elated to the changes in meso-scale atmospheric circulation, NAO variation, and increasing anthropogenic pressures on natural Earth ecosystems. The investigation of the climate change in different regions is important in both scientific and practical aspects as the global processes take place under a particular agency of local factors.

Not only climate change, but also a great anthropogenic load (increased coastal urbanization, recreation, deepening of port area, construction of hydraulic equipment, river water regulation, intensive navigation and etc.) directly affects the ecological balance of the Baltic Sea, including the lagoons.

The main task of the present work was to investigate the peculiarities of changes in the long-term hydro-climatic conditions along with the processes that could have determined these changes in the Curonian Lagoon that located in the Southeastern (SE) part of the Baltic Sea (Fig. 1). The studies of the trends in climate parameters variations are relevant not only for knowledge of climate change processes but also for development of the strategies of adaptation to the consequences of these processes.

2. Results

The Curonian Lagoon is the biggest shallow lagoon in the Baltic Sea and all European seas. It is located in the SE Baltic and is separated from the open sea by the relatively narrow sandy Curonian Spit (0.5–3km wide) and connected to the sea solely through the Klaipeda Strait at the northern end of the lagoon. The Curonian Lagoon are most vulnerable to direct impacts of climate change.

The study results suggest that rise the sea level (Fig. 2), increase the air and water temperature, decrease the duration of ice phenomena probably due to changes in atmospheric circulation, wind climate. It is in good correlation with increasing trends in local storminess and in higher intensity of westerly wind, and with the winter NAO index that indicates the change of the atmospheric circulation in the North Atlantic region, including European. The rising global temperatures affect the Baltic Sea's region, especially on the rising warm seasons and decreasing periods of wintertime. The increasing rise in air and water temperatures since the late 20th century in the Baltic Sea region (BACC II, 2015) may have contributed to these larger differences. The contrasts of coastal climate and more continental climate illustrate a distinguishable effect of the Baltic Sea on its coastal areas air temperature (Dailide *et al.* 2019).

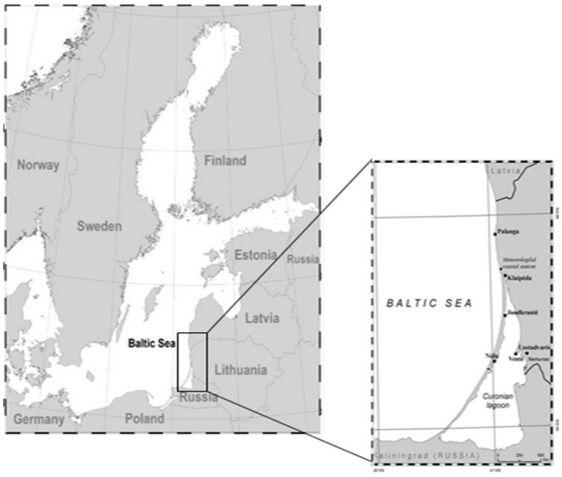


Figure 1. Study site: SE Baltic Sea and Curonian Lagoon.

Future changes in climate system components may stronger effect on the heat and water balances in the Baltic Sea coastal areas, such as lagoons.

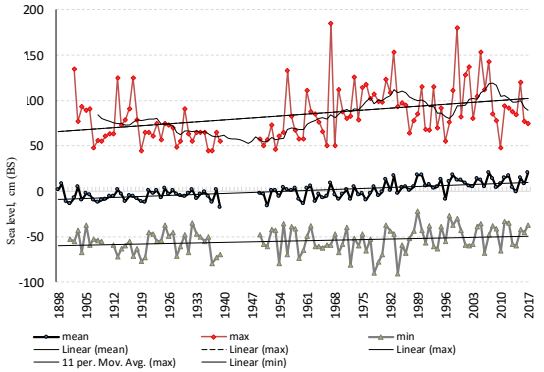


Figure 2. Sea level change, SE Baltic Sea, Klaipeda (1898-2017).

Global climate warming, the rising global sea level as well as anthropogenic activities may affect this transitional water system and, consequently, salinity in the Curonian Lagoon. The problem of the Curonian Lagoon ecosystem stability frequently raised. However, water salinity and its variations in time and space in the Curonian Lagoon during the last decades only fractionally described.

Not only climate change, but also a great anthropogenic load directly affects the coastal areas, including lagoons. Observed significant increase of marine litter (macro) in investigated Baltic Sea areas. Major marine litter type – plastics (Fig. 3).



Figure 3. Major marine litter type – plastics.

Research of geographical sustainable consumption becoming more relevant of consumer behavior on marine litter in different Baltic Sea coastal areas, including the Lithuanian seacoast. As the warmer period grows, the anthropogenic pressure on the coastal zone will be rising according human activities impact, as well as will be longer period of the tourism and recreation response.

3. Conclusions

The long-term changes of hydrological and meteorological parameters observed in the Southeastern part of the Baltic Sea and in the Curonian Lagoon that located in the southeastern part of the Baltic Sea. Specific warming - „jump“ observed in all physical parameters of the SE Baltic Sea and the Curonian Lagoon started in the 8-9th decade of the 20th century. Coastal lagoons of Baltic Sea could be most vulnerable to direct impacts of future climate change.
The knowledge of processes taking place in nature is one of the links that contributes to the successful environmental management and the appropriate evaluation of risk factors followed by the application of preventive measures.

References

BACC II Author Team, 2015. Second Assessment of Climate Change for the Baltic Sea Basin. Springer International Publishing, https://doi.org/10.1007/978-3-319-16006-1

Christel, I., Hemment, D., Bojovica, D., Cucchiettia, F., Calvoa, L., Stefanerd, M., Buontempo, C. 2018. Introducing design in the development of effective climate services. Elsevier. Climate Services. Volume 9, 111-121.

Dailide, R., Povilanskas, R., Pérez, J.A.M., Simanavičiute, G. 2019. A new approach to local climate identification in the Baltic Sea's coastal area. BALTICA, Vol. 32, Nr. 2: 210–218. https://doi.org/10.5200/baltica.2019.2.8

IPCC, 2014. Summary for policy makers. In: Field, C.B., Barros, V.R., Dokken, D.J.,Mach, K.J., Mastrandrea, M.D., Bilir, T.E., Chatterjee, M., Ebi, K.L., Estrada, Y.O.,Genova, R.C., Girma, B., Kissel, E.S., Levy, A.N., MacCracken, S., Mastrandrea, P.R.,White, L.L. (Eds.), Climate Change 2014: Impacts, Adaptation and Vulnerability. Part A: Global and Sectoral Aspects. Contribution of Working Group II to The Fifth Assessment Report of the Intergovernmental Panel on Climate Change. Cambridge University Press, Cambridge, United Kingdom and New York, NY, USA, p. 1132.

Reanalysis based assessment of tropospheric thickness trends in Baltic Sea region

Alina Lerner, Aarne Männik

Department of Marine Systems, Tallinn University of Technology, Tallinn, Estonia (alina.lerner@taltech.ee)

1. Introduction

Several studies have demonstrated the persistent tropospheric warming around the globe (Free et al. 2005, Thorne et al. 2005, Haimberger et al. 2012). An important response to the increase of the temperatures would be the expansion of the troposphere, as the geopotential thickness between any two isobaric surfaces of an atmospheric layer is proportional to the temperature. This should manifest as a rise of geopotential surface or increase of geopotential thickness. Several studies point that atmospheric climate warming in northern regions is faster than global average (Fu et al. 2006, Vinnikov et al. 2006, Perlwitz et al. 2015). Thus, present study investigates the trends of tropospheric geopotential thickness based on reanalysis data to detect changes in troposphere over the Baltic Sea region.

2. Materials and Methods

Present study employs the latest ECMWF reanalysis dataset ERA5 over the 40-year period of 1979 - 2018. The geopotential fields of the 1000 hPa, 500 hPa and 200 hPa pressure levels, specific humidity on the 750 hPa and 350 hPa pressure levels, and sea level pressure (SLP) were used for the calculation of trends and trend maps. The study area is presented in Figure 1. The radiosonde vertical soundings TEMP data, collected by ECMWF, is used to demonstrate the correspondence of reanalysis to observed values.

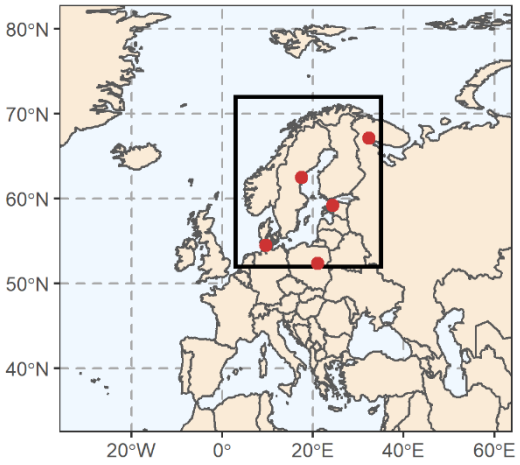


Figure 1. The area represented in the rectangle is examined in the study. The red points refer to the weather stations Tallinn-Harku (Estonia), Kandalaksa (Russia), Legionowo (Poland), Sundsvall-Harnosand (Sweden) and Schleswig (Germany). Vertical soundings performed on these stations are used to assess the correspondence of reanalysis to measured values.

The geopotential thicknesses of the 1000/500 hPa (lower troposphere – LT) and 500/200 hPa (mid- to upper troposphere - MT) layers were calculated. In order to analyze the monthly and annual trends the simple linear regression method is employed and the statistical significance of the trends is estimated by using the *p* value the equivalent temperatures were computed using the hypsometric equation.

3. Results

The statistically significant positive trends of averaged over the region geopotential thicknesses were identified during the July, August, September, November in LT and in the same months plus May in MT. The geopotential thicknesses are experiencing annual average thickening of 0.62±0.14 dam (corresponding 0.31±0.07 °C) per decade in LT and 0.51±0.12 dam (corresponding 0.19±0.04 °C) per decade in MT (Figure 2).

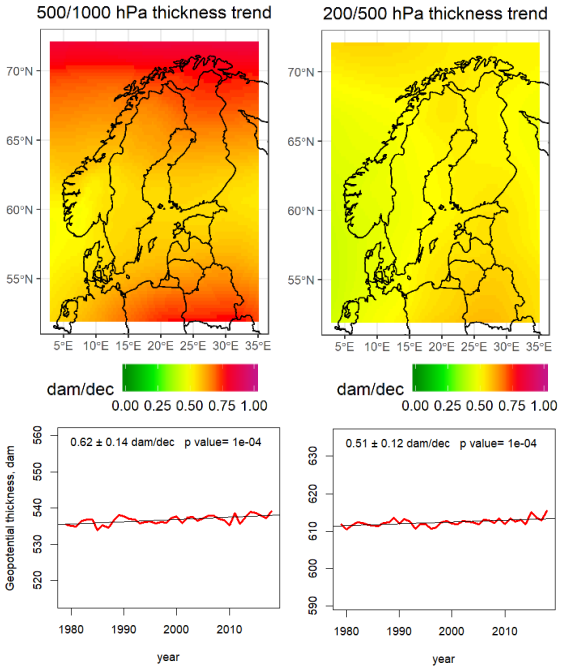


Figure 2. The annual geopotential thickness trend over the Baltic Sea region for the period of 1979-2018. The whole area is experiencing a statistically significant positive trend (p value ≤ 0.05). In both LT and MT layers the expansion trend's slope is higher over the most northern and the southern part on the area. The important difference between the layers is more strongly marked thickening in the 500/1000 hPa field.

Despite the fact that there is no tropospheric expanding detected in January and December on the averaged area, locally there is a trend approaching 2 dam per decade on the north of the region in LT and 1.25 dam per decade in MT. No significant change in SLP is detected, so tropospheric expansion can be reliably linked to the temperature and humidity changes in the layer.

The trends of specific humidity from the middle of LT (750 hPa) and MT (350 hPa) layers also show increase, which is in a more or less temporal agreement with the thickness trends, being significant in July, August and November in the former and the same plus September in the latter. The annual average increase is 29±10 mg/kg per decade on 750

hPa and 3±1 mg/kg per decade on 350 hPa pressure level. Maps of monthly and annual statistically significant trends are created and show regional distribution of positive trends (Figure 2).

4. Conclusion

The present study shows that layer of the troposphere above Baltic Sea region expands, which is linkable to the warming of the air in entire troposphere. The expansion is equivalent to the warming trend of 0.3 degrees per decade in lower troposphere without accounting of moisture effect. This is similar magnitude as temperature trends estimated at surface. Upper troposphere expands due to the warming at slower rate. The significant trend maps for Baltic Sea region are calculated and presented. Lower troposphere trends appear to be higher next to northern and southern edges of the area. In upper troposphere trends are distributed more evenly.

5. Acknowledgements

This work was supported by institutional research funding IUT 19/6 of the Estonian Ministry of Education and Research. The data for the study was generated using Copernicus Climate Change Service Information. TEMP observations were taken from ECMWF observation database.

References

Free M. P., D. Seidel, J. Angell, J. Lanzante, I. Durre, T. Peterson (2005) “Radiosonde Atmospheric Temperature Products for Assessing Climate (RATPAC): A new dataset of large-area anomaly time series”, J. Geophys. Res., Vol. 110, No. D22.

Fu Q., C. M. Johanson, J. M. Wallace, T. Reichler (2006) “Enhanced Mid-Latitude Tropospheric Warming in Satellite Measurements”, Science, Vol. 312, No. 5777, pp. 1179.

Haimberger L., C. Tavolato, S. Sperka (2012) “Homogenization of the Global Radiosonde Temperature Dataset through Combined Comparison with Reanalysis Background Series and Neighboring Stations”, J. Clim., Vol. 25, No. 23, pp. 8108-8131.

Nurmi P. (2003) “Recommendations on the verification of local weather forecasts. ECMWF Technical Memoranda”, ECMWF technical memorandum, No. 430.

Perlwitz J., M. Hoerling, R. Dole (2015) “Arctic Tropospheric Warming: Causes and Linkages to Lower Latitudes”, J. Clim., Vol. 28, pp. 2154-2167.

Thorne P. W., D. E. Parker, S. F. B. Tett, P. D. Jones, M. MacCarthy, H. Coleman, P. Brohan (2005) “Revisiting radiosonde upper air temperatures from 1958 to 2002”, J. Geophys. Res., Vol. 110, No. D18.

Vinnikov K. Y., N. C. Grody, A. Robock, R. J. Stouffer, P. D. Jones, M. D. Goldberg (2006) “Temperature trends at the surface and in the troposphere”, J. Geograph. Res., Vol. 111, No. D3

Changes in haptophyte community structures and the climate in the Arkona Basin (Baltic Sea) over the last 11 kyr recorded by long-chain alkenone distributions and proxies.

Barbara W. Massalska[1,2], Gabriella M. Weiss[1], Rick Hennekam[3], Gert-Jan Reichart[3,4], Jaap S. Sinninghe Damsté[1,4], Stefan Schouten[1,4] and Marcel T. J. van der Meer[1]

[1] Department of Marine Microbiology and Biogeochemistry, NIOZ Royal Netherlands Institute for Sea Research and Utrecht University, Texel, The Netherlands
[2] Department of Regional Geology, Polish Geological Institute – National Research Institute, Warsaw, Poland
[3] Department of Ocean Systems, NIOZ Royal Netherlands Institute for Sea Research and Utrecht University, Texel, The Netherlands
[4] Department of Earth Sciences, Faculty of Geosciences, Utrecht University, Utrecht, The Netherlands

1. Introduction

Long-chain alkenones (LCAs) are a group of polyunsaturated ethyl and methyl ketones with chain lengths between 35 and 43 carbon atoms, and up to 4 degrees of unsaturation. These often well-preserved, haptophyte-derived compounds are identified in a range of aquatic sediments, and are utilized as proxies for reconstructing past climate changes. The U^{K}_{37} index and it's derivatives are well-known LCA-based proxies for reconstructing sea surface temperatures, while the novel $\%C_{37:4}$ and RIK_{37} have been proposed for reconstructing paleosalinity in marine environments. Among haptophyte algae, a common and diverse phytoplankton group, only certain species of the order *Ischrysidales* are known to produce LCA compounds (e.g. 1980; Theroux et al., 2010). Alkenone-producing haptophytes are separated into three distinct Groups based on 18S ribosomal RNA and can be identified based on differences in LCAs distribution patterns (Theroux et al., 2010). Each of the Groups appear to inhabit niches with distinct salinity ranges. Group I haptophytes have been found in freshwater, lacustrine environments in the Northern Hemisphere (e.g. Theroux et al., 2010; Longo et al., 2018). *Isochrysis*, *Ruttenera* and *Tisochrysis* genera are cultured members of Group II haptophytes. Group II haptophytes are found in coastal, estuarine and (saline) lacustrine settings, which makes them accustomed to live in the largest range of salinities among alkenone-producing haptophytes (Theroux et al., 2010; Longo et al., 2016). Exclusively marine haptophyte species, which include *Emiliania huxleyi* and *Gephyrocapsa oceanica*, comprise Group III (Theroux et al., 2010). Mixed contributions between two of the three described Groups have been noted in a number of environments, however, mixing of all three Groups has only been reported from the surface sediments of the Baltic Sea (Kaiser et al., 2019). The presence of all three haptophyte Groups in the Baltic Sea provided the perfect opportunity to determine how alkenone distribution changes can enhance our understanding of shifts in alkenone-producers when environments experienced large fluctuations in salinity, as well as how mixed species contribution affects the utility of LCA-based proxies.

2. Location and climate history

A piston coring technique was used to collect a 12.22 m sediment core (64PE410-S7) from a location (54˚55.208 N, 13˚29.992 E) in the Arkona Basin of the Baltic Sea. The core was recovered with RV Pelagia during the 64PE410 NIOZ Baltic 2016 expedition.

The Arkona Basin is situated at the western edge of the Baltic Sea, next to the narrow connection with the North Sea via the Kattegat and Skagerrak. Therefore, the Arkona Basin is a perfect location for seeking evidence related to major eustatic fluctuations occurring throughout the Baltic Sea history. Over the past 11,000 years, due to Holocene climate fluctuations, the Baltic Sea experienced varying salinities related to the varying capacity of the Kattegat sea passage. The Baltic Sea began as the Baltic Ice Lake at ca. 13 ka B.P. The retreat of the ice seat and the associated sea level rise transitioned the freshwater Baltic Ice Lake into the brackish Yoldia Sea (YS; from 11.6 to 10.6 ka B.P.,). The post-glacial, isostatic continental uplift disconnected the YS from the ocean, giving rise to the freshwater Ancylus Lake (AL; from 10.6 until approximately 7.7 ka B.P.). This freshwater phase came to an end along with a large transgression which brought the North Sea water turning the AL phase into the brackish Littorina Sea phase (LS; from 7.2 to around 3 ka B.P.), which then, as a consequence of continued continental uplift, gradually transitioned into the Modern Baltic (MB; from 3 ka B.P. to recent; Moros et al., 2002).

3. Materials and methods

Prior sampling, the core was scanned with an X-ray fluorescence (XRF) core scanner. Samples collected from the core for geochemical analyses were freeze-dried and extracted using an accelerated solvent extraction (ASE) method. The ketone fraction was separated from the total lipid extracts via column chromatography (detailed description of method is provided in Weiss et al., 2020). Alkenone concentrations were determined by using a gas chromatograph with a flame ionization detector (GC-FID) equipped with an RTX-200 column (Restek, 60 m x 0.32 mm x 0.5 μm). Identification of alkenones was carried out with a gas chromatograph coupled to a mass spectrometer (GC-MS) and equipped with the same 60 m RTX-200 column.

4. Results and discussion

a. Alkenone distributions

Alkenones with chain lengths between 35 and 40 carbon atoms were detected. The recorded LCA distribution patterns show significant variability along the sedimentary profile, which align with Baltic Sea phase boundaries. Samples correlated with the YS phase show alkenone distributions typical for marine Group III by lacking tri-unsaturated isomers, as well as C_{39} and C_{40} alkenones. Tri-unsaturated isomers, both methyl and ethyl C_{39}, and ethyl C_{40} alkenones first appear at the YS/AL boundary. The

distribution patterns of the AL phase are stable and indicate mixing of Group I and II haptophytes. Two samples in the early AL phase show a more marine distribution pattern although still containing isomers indicative of freshwater species. It appears that the short transgressions during the YS phase (Björck, 1995) continued into the early AL phase, overshadowing isostatic rebound by causing some input of saline waters. The species mixing of Group I and II haptophytes was determined using the RIK_{37} and RIK_{38E} indices proposed by Longo et al. (2016), along with a binary mixing model from Longo et al. (2018). Accordingly, Group I was dominant throughout the AL phase (57 to 75%), while significant contributions from Group II (60 to 75%) occurred solely at the beginning and end of the phase. The low-grade transition from the freshwater AL phase to the brackish LS (ca. 0.5 kyr) is characterized by typical Group III alkenone distributions (C_{37} methyl and C_{38} ethyl alkenones), until the latter half of the transition, where $C_{35:2}$ and $C_{36:2}$ alkenones make their first appearance. The LS phase shows distributions with shorter chain-length alkenones and the absence of tri-unsaturated isomers, C_{39} and C_{40} alkenones, indicating Group II haptophytes. The transition between the LS phase and the MB phase is marked by a shift in alkenone distributions showing mixing Group II and III with the presence of the $C_{35:2}$, $C_{36:2}$ and C_{39} ethyl alkenones.

b. Temperature estimates

The U^{K}_{37} index is a widely used alkenone proxy, based on the relationship between sea surface temperatures (SSTs) and the relative degree of unsaturation of C_{37} alkenones (Brassell et al., 1986). Using the U^{K}_{37} calibration for Atlantic surface sediments (Rosell-Melé et al., 1995) resulted in SST estimates ranging between 0.3 and 2.3˚C. With present day Baltic Sea spring mean SST of 8˚C, such low values are likely to result from species contribution from Groups I and II (which produce higher concentrations of $C_{37:4}$), while the Atlantic calibrations are based on Group III alkenone distributions. The modified $U^{K'}_{37}$ index, which excludes the tetra-unsaturated C_{37} alkenone from the equation, was proposed by Prahl and Wakeham (1987). Using the global calibration for the $U^{K'}_{37}$ index (Müller et al., 1998) resulted in SST estimates between 2.2 and 8.5˚C, which is in good agreement with present-day mean spring temperature values. Therefore, the $U^{K'}_{37}$ index seems to be the more reliable of the two indices to reconstruct temperatures for this record. The novel R3b proxy was developed by Longo et al. (2016, 2018) to reconstruct SSTs in freshwater and brackish environments. The R3b index includes tri-unsaturated isomers in the temperature ratios and here it was applied to samples corresponding to the AL phase. Using the R3b calibration form Longo et al. (2018), SST estimates range between 4.0 and 13.5˚C, capturing more variation than estimates from both U^{K}_{37} and $U^{K'}_{37}$ indices.

c. Salinity estimates

Paleosalinity reconstructions were conducted using the $\%C_{37:4}$ for the entire record and the RIK_{37} for the AL phase since it was the only phase containing C_{37} tri-unsaturated isomers (Kaiser et al., 2017, 2019). The obtained values ranged between 4.1 and 8.7 ($\%C_{37:4}$) and between 2.0 and 5.2 (RIK_{37}). Both parameters recorded a rise in salinities at the AL/YS boundary, however, $\%C_{37:4}$ suggests values closest to the modern day spring mean of 8.1. The average salinity recorded for the AL phase using the RIK_{37} calibration was of 3 ± 0.4 and 6 ± 0.5 was obtained from the $\%C_{37:4}$ calibration, which appears more logical for this relatively freshwater Baltic Sea phase. In general, when tri-unsaturated isomers are present, indices accounting for these isomers seem more appropriate for reconstructing temperature and salinity.

5. Conclusions

Improved gas chromatography separation allowed to detect and recognize a wide array of long-chain alkenone isomers in a Holocene sediment record from the Arkona Basin in the Baltic Sea. Changes in alkenone distributions indicate Group II and III mixing during the Yoldia Sea, Littorina Sea and Modern Baltic phases, and Group I and II mixing during the Ancylus Lake phase. For this reason, the traditional alkenone-based temperature and salinity calibrations used for sediments from marine environments must be utilized with extra care, as they may result in anomalous values. More reliable estimates for periods characterized with significant input from Group I and II haptophytes are obtained based on proxies which include alkenone isomers characteristic for these groups. The presented results show that analysis of well-separated alkenone distributions leads to more in-depth understanding of species composition, salinity and hydrological dynamics, and improved application of long-chain alkenone-based proxy.

References

Björck, S. (1995). A review of the history of the Baltic Sea, 13.0-8.0 ka BP. Quaternary International, 27, 19-40.

Brassell, S. C., Eglinton, G., Marlowe, I. T., Pflaumann, U., & Sarnthein, M. (1986). Molecular stratigraphy: a new tool for climatic assessment. Nature, Vol. 320, pp. 129-133.

Kaiser, J., Wang, K. J., Rott, D., Li, G., Zheng, Y., Amaral-Zettler, L., et al. (2019). Changes in long chain alkenone distributions and Isochrysidales groups along the Baltic Sea salinity gradient. Organic Geochemistry, Vol. 127, pp. 92-103.

Longo, W. M., Theroux, S., Giblin, A. E., Zheng, Y., Dillon, J. T., & Huang, Y. (2016). Temperature calibration and phylo-genetically distinct distributions for freshwater alkenones: evidence from northern Alaskan lakes. Geochimica et Cosmochimica Acta, Vol. 180, pp. 177-196.

Longo, W. M., Huang, Y., Yao, Y., Zhao, J., Giblin, A. E., Wang, X., et al. (2018). Widespread occurrence of distinct alkenones from Group I haptophytes in freshwater lakes: Implications for paleotemperature and paleoenvironmental recon-structions. Earth and Planetary Science Letters, Vol. 492, pp. 239-250.

Moros, M., Lemke, W., Kuijpers, A., Endler, R., Jensen, J. B., Bennike, O., & Gingele, F. (2002). Regressions and transgressions of the Baltic basin reflected by a new high-resolution deglacial and postglacial lithostratigraphy for Arkona Basin sediments (western Baltic Sea). Boreas, Vol. 31, pp. 151 – 162.

Prahl, F. G., & Wakeham, S. G. (1987). Calibration of unsaturation patterns in long-chain ketone compositions for palaeotemperature assessment. Nature, Vol. 330, pp, 367.

Rosell-Melé, A., Eglinton, G., Pflaumann, U., & Sarnthein, M. (1995). Atlantic core-top calibration of the UK37 index as a sea-surface palaeotemperature indicator.

Theroux, S., D'Andrea, W. J., Toney, J., Amaral-Zettler, L., & Huang, Y. (2010). Phylogenetic diversity and evolutionary relatedness of alkenone-producing haptophyte algae in lakes: implications for continental paleotemperature reconstructions. Earth and Planetary Science Letters, Vol. 300(3-4), pp. 311-320.

Changes in precipitation in the cold period in Belarus under conditions of modern climate warming

V.I. Melnik, I.V. Buyakov

Institute for Nature Management of the National Academy of Sciences of Belarus, Minsk, Belarus, e-mail: v.melnik2016@mail.ru

1. Introduction

Previous studies of precipitation amount changes in Belarus showed that during the warming period there is a tendency of increasing in almost all the areas in comparison with the climatic norm (1961–1990). Changes in precipitation are expressed in ~5% increase in its annual amounts in northern region of the country, while in the central and southern regions of the country no significant changes are observed (0–3%), with the exception of the Gomel region, where 7% increase is observed. The greatest increase in precipitation is characteristic of winter months, and it is associated with the peculiarities of atmospheric circulation in the Atlantic-European sector (Danilovich et al. 2007). To assess the change in the amount of solid and liquid precipitation, we used the weather station observation data in Belarus with long series of observation for different periods: before warming (1961–1988) and after warming 1989–2018. Due to the lack of data on the amount of liquid, solid and mixed precipitation (in mm), the number of days with solid and liquid precipitation for the cold period of the year (November - March) was used to estimate the change in precipitation.

2. Main research results

During warming period in Belarus there is a tendency for a slight increase in precipitation in almost all regions of the republic comparing to the climatic norm. The greatest increase in precipitation comparing to the climatic norm is observed on certain months (January - March) of the cold period (Melnik et al. 2007). On average, over the past twenty years, precipitation deficit in Belarus was recorded in April, June, and especially in August: monthly precipitation amount was 91%, 93% and 88% of the month norm respectively. In January, February, March, May, July and October observed precipitation amount was slightly greater than the norm. To analyze and evaluate changes in the amount and types of precipitation in the cold period, 18 hydrometeorological stations with long series of observations evenly located throughout the country were selected. The spatial distribution of precipitation over the territory of Belarus in cold period of the year (November - March) for the period before and after warming as a whole confirms the trends in its changes observed in recent studies, namely: an increase in precipitation amount in the north-eastern, eastern and southeastern part of the country and a decrease in its amount in the southwest (Figure 1).

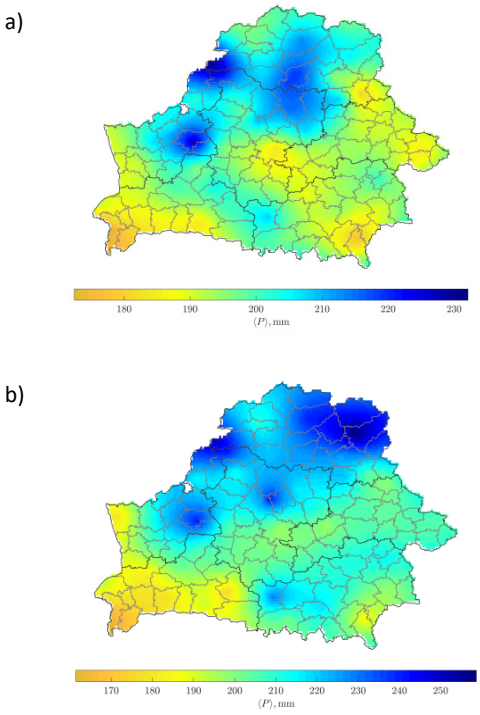


Figure 1. Changes in precipitation amount during the cold period (November – March) in Belarus: a) – the period before warming (1961–1988), b) – the current period of warming (1989–2017)

For a more detailed assessment of changes in solid and liquid precipitation during the cold period, data on the number of days with solid and liquid precipitation for long-row stations for the periods before warming (1961–1988) and after warming 1989–2018 are analyzed. The decrease in the number of days with solid precipitation in Belarus is observed everywhere and averaged over the indicated period 13.2 days or 19%. The greatest decrease in the number of days with solid precipitation occurs in the western and southwestern parts of the republic (maximum 46.8% at Baranovichi station). The smallest change was recorded at Minsk stations - 5.2%, Vitebsk - 5.5% and Gorki - 7.2%. Accordingly, an increase in the number of days with liquid precipitation is observed during this period. On average, in Belarus, the number of days with liquid precipitation during the cold period increased by almost 10 days or 24%. Their greatest increase is observed in the northern part of the country, which is generally consistent with the results on the duration of their deposition described in (Danilovich et al. 2007).

The analysis of changes in the amount of liquid and solid precipitation for the periods before and after the warming in each month of the cold period has been conducted. In the transitional months (November, March), the greatest decrease in the number of days with solid precipitation during the warming period was observed in relation to the period 1961–1988. (22.5 and 23.1% respectively). The greatest increase in the number of days with liquid precipitation during the warming period in the cold period was observed in January and February (68.6 and 70.9% respectively), which is in good accordance with the increase in average monthly air temperatures over these months during the warming period. Figure 2 shows the general trends in changes of the number of days with solid and liquid precipitation during the cold period in Belarus: a) – Verkhnedvinsk station, b) – Minsk station, c) - Brest station. It should be noted that in northern and central regions (Verkhnedvinsk and Minsk stations) the number of days with solid precipitation during the cold period exceeds the number of days with liquid precipitation during the entire analysis period (1961–2018), with the exception of individual years. In the southern regions of the country (Brest station), approximately since 2003 (Figure. 2c) number of days with liquid precipitation tend to exceed the number of days with solid precipitation in the cold period. This example shows that the application of the methodology previously used during the climate handbooks preparation for calculation of the monthly and annual amounts of solid, liquid and mixed precipitation in mm by the ratio of the number of days with solid and liquid and mixed precipitation is currently unacceptable due to changes in this correlation. In all winter months, solid, mixed and liquid precipitation is observed in Belarus.

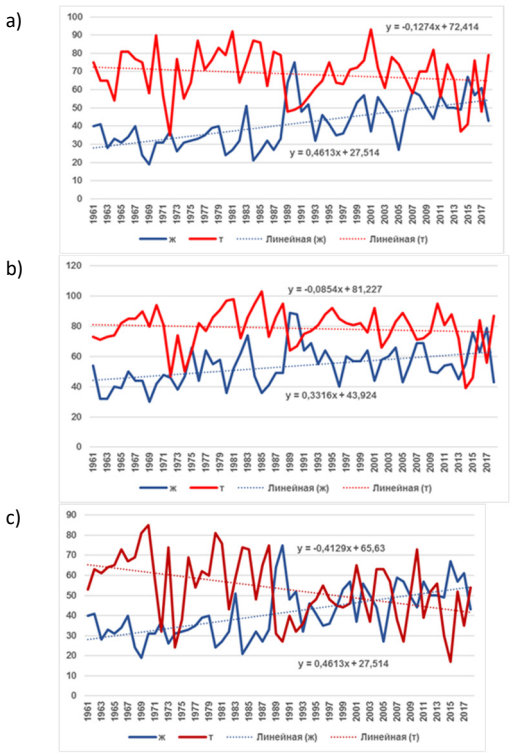


Figure 2. Change in the number of days with liquid and solid precipitation in Belarus over the cold period (XI–III). a) – station Verkhnedvinsk, b) – station Minsk, c) – station Brest

The amount of precipitation of various types serves as an additional characteristic to the total amount of precipitation. This is important when planning construction and other outdoor activities. Therefore, new approaches are needed to obtain calculated data on the amount of liquid, solid and mixed precipitation in mm during the cold season.

3. Conclusion

New data on the change in the amount and type of precipitation in the cold period of the year on the territory of Belarus for the period 1961–2018 were obtained. Increase in the amount of precipitation and the amplitude of its fluctuations in Belarus in the cold season (November-March) during the warming period was highlighted. It is shown that during the period of modern warming (1989–2018) number of days with solid precipitation decreased (on average by 13.2 days or 19%) comparing with the previous period (1961–1988). Number of days with liquid precipitation increased on average by 10 days (24%). The greatest decrease in the number of days with solid precipitation is characteristic to the western and southwestern parts of the country. The greatest increase in the number of days with liquid precipitation is observed in the northern part of the country. The greatest change (decrease) in the number of days with solid precipitation during the warming period was observed in the transition period (November, March). The largest increase in the number of days with liquid precipitation during the cold period was observed in January and February, which is in good accordance with the increase in average monthly temperatures over these months during the warming period.

4. References

Danilovich I.S., Melnik V.I. (2019) Features of the humidification regime of the territory of Belarus in connection with a changing climate / Proceedings of the IVth International Scientific and Practical Conference “Actual Problems of Earth Sciences: Studies of Transboundary Regions”, dedicated to the 1000th anniversary of Brest. Brest, part 1, pp. 208–211.

Melnik V.I., Komarovskaya E.V. (2011) Features of climate change on the territory of the Republic of Belarus for the last decades. Scientific and methodical ensuring of activity on environmental protection: problems and prospects, pp.77-84.

Estimating the wave statistics bias in the partially ice-covered regions of the Baltic Sea

Fatemeh Najafzadeh[1], Nadezhda Kudryavtseva[1], Andrea Giudici[1], Tarmo Soomere[1,2]

[1] Laboratory of Wave Engineering, Department of Cybernetics, School of Science, Tallinn University of Technology, Ehitajate tee 5, 19086 Tallinn, Estonia (fatemeh@ioc.ee)

[2] Estonian Academy of Sciences, Kohtu 6, 10130 Tallinn, Estonia

1. Introduction

The complexity of the wave fields and seasonal existence of ice in the Baltic Sea make this basin a unique water body. The presence of ice has a prominent effect on wave activities, which is the main factor in shaping coastlines (e.g., Tuomi et al. 2011). The ice season duration in the Baltic Sea is characterized by extreme spatial and annual variability (e.g., Jevrejeva et al. 2004). It is predicted that the climate change in this basin will lead to a shorter ice season duration (Haapala & Leppäranta 1997; BACC, 2008) and, therefore, more amount of wave energy will reach the coast. Besides, seasonal changes in the wind and wave properties might deliver a vast amount of energy to the coastline areas. The most disruptive storms happen in late autumn since the ice cover protects the coastal sections during the winter. However, the reduction of the ice season duration together with the changes in the Baltic Sea wave climate can cause rapid erosion in some coastal areas.

Currently, to estimate the risks of coastline erosion, the yearly average wave statistics are calculated, which does not consider the period when the sea is ice-covered. This can introduce a systematic bias in the calculations (e.g., Tuomi et al. 2019). This study systematically analyses the bias introduced by the duration of the ice season to the calculations of the average wave height, average and total wave energy flux.

2. Data and methodology

The analysis relied on significant wave height and peak period time series measured by the Suomenlahti wave buoy, located in the Gulf of Finland with a longitude of 25.24 and latitude of 59.96. The Finnish Meteorological Institute kindly provided the data. The measurements have a variable time resolution, with the highest resolution reaching 0.5 hr. The time-series span the period from 2000 to 2015.

The duration of the ice season at this location was obtained from the satellite-derived ice concentration dataset OSI-450 Global Sea Ice Concentration Climate Data Record (1979–2015 (v2, 2017), Norwegian and Danish Meteorological Institutes, http://osisaf.met.no). For the analysis, only the data obtained simultaneously with the Suomenlahti buoy (in 2000–2015) were considered. In order to remove unreliable ice concentration measurements, only the data with flag 0 were used and measurements thoroughly checked for outliers and possibly erroneous data. The beginning of the ice season was estimated as the time of the first reliable measurement with the ice concentration > ς after 1st of July and the end of the ice season as the time of the last measurement with the ice concentration > ς before 1st of July. The duration of the ice season is very sensitive to the cut-off ς. Using ς ≤ 30% resulted in unrealistic ice season durations of ~6 months and ς > 30% were used in the analysis.

The following parameters were calculated for each year to characterize the wave intensity and its potential impact over the studied period: the average significant wave height (SWH), total wave energy flux (TEF) and normalized total wave energy flux. The most reliable way analyze the wave statistics is to use the values of the entire relatively windy season starting from July and ending in June next year (known as stormy season, Zaitseva-Parnaste & Soomere, 2013).

Since the depth of the studied location is 55 m, the calculation of the wave energy and its flux were carried out using the deep-water approximation. The instantaneous values for the wave energy flux were calculated as

$$P = \frac{\rho g^2}{32\pi} \times H^2 T,$$

where H is the observed wave height, T is the wave period, g is the acceleration due to gravity, and ρ is the density of the water. The values of P were calculated for each Suomenlahti measurement which had both SWH and period records. The total yearly wave energy flux was calculated as a sum of P during the selected year. Since the number of measurements varied for each year, we also used a normalized total wave energy flux $P_n = P/n$, where n is the number of measurements per year. This normalization removes the effect of the different number of measurements per year from the total wave energy flux calculations.

3. Results

The ice season lasted from 0 to 177 days in case of ς = 40% (Figure 1a) and 0 to 120 for ς = 50%. This indicates that the definition of the ice season duration is highly dependent on the level of ice concentration which is used to define the start and end of the ice season.

There is a significant bias between the total wave energy flux calculated for the ice-free season and the whole year. For the 40% ice concentration cutoff, the measured bias reaches 34.5%. This indicates that it is essential to consider the duration of the ice season when using wave height statistics in any coastal or other applications.

The variability of the total wave energy flux is shown in Fig. 1c. However, it highly depends on the number of measurements per year. In recent years with a higher number of measurements, the amount of total wave energy flux is increasing. Therefore, the normalized total energy flux (Fig. 1d) is calculated and used in the further correlation analysis. The normalized total energy flux has a similar variability to the average wave height (Fig. 1b).

In Fig. 2, a linear regression fitted to the normalized bulk energy flux during the ice-free season and the ice season duration is demonstrated. The duration of ice season shows a strong negative correlation of –0.45 with the normalized total energy flux with the significance level of 87% (when using ς = 50% for the definition of the beginning and end of the ice season). A regression line fit resulted in the slope of –0.02±0.01 and intercept 7.4±0.9. Although the fit was performed to the normalized TEF, the conversion to the TEF can be performed by multiplying the values by the average number of n = 8791. Then the slope is –180±110 and intercept is 65000±7600. The ice-free wave energy fluxes calculated using the ice season duration defined with the lower ice concentration cutoff (ς < 50%) have not shown any significant correlations with the ice season duration.

The found negative correlation is similar to the results of Zaitseva-Parnaste & Soomere (2013) where the modelled data at three locations in the Eastern Baltic showed a negative correlation in the range of –0.6 – –0.7. However, only one location at Vilsandi showed a significant correlation of –0.4 in the actual observations. Haapala & Leppäranta (1997) predicted a decrease of the ice season duration by 30 days in 2050 in the Gulf of Finland. Using this prediction and the found dependence between the ice season duration and the total wave energy flux, the energy flux in the Gulf of Finland will increase by ~13 percent by the year 2050.

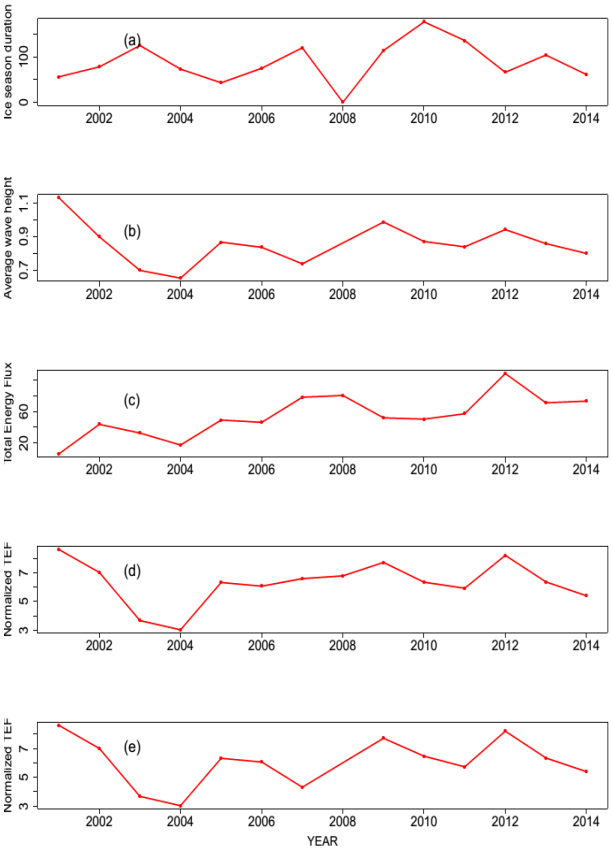


Figure 1. Variability of the ice season duration for 40% ice concentration (a), mean wave height (m) during the ice-free season(day) (b), bulk energy flux (MW/m) for the whole year (c), normalized bulk energy flux (KW/m) for the whole year (d), and normalized bulk energy flux (KW/m) for ice-free season (e) at Suomenlahti location calculated over the period from 2000 to 2015.

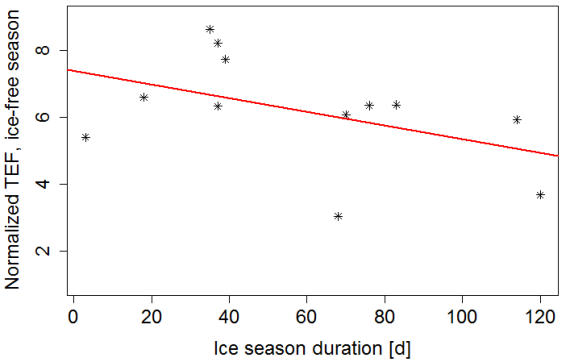


Figure 2. Normalized with the number of observations total wave energy flux (KW/m) during the ice-free season versus the ice season duration (using ς = 50% for the definition of the beginning and end of the ice season). The red solid line shows a fitted regression line.

4. Conclusion

The study of the wave energy flux during the ice-free season and its relation to the ice season duration showed that

- It is crucial to take into account the duration of the ice season at seasonally ice-covered locations. Calculating wave statistics using yearly values can cause a bias up to 35%.
- The normalized total wave energy flux in Suomenlahti during the ice-free season shows a negative correlation of –0.45 with the ice season duration (with a confidence level of 87%).
- The start and end of ice season and, therefore, its duration strongly depend on the level of ice concentration cutoff.

References

J. Haapala, M. Leppäranta (1997) The Baltic Sea ice season in changing climate, Boreal Environment Research, Vol.2, No.1, pp. 93–108

S. Jevrejeva, V.V. Drabkin, J. Kostjukov, et al. (2004) Baltic Sea ice seasons in the twentieth century, Climate Research, Vol.25, No.3, pp. 217–227

BACC Author Team (2008) Assessment of climate change for the Baltic Sea basin, Springer, Berlin

L. Tuomi, K.K. Kahma, H. Pettersson (2011) Wave hindcast statistics in the seasonally ice-covered Baltic Sea, Boreal Environment Research, Vol.16, No.6, pp. 451–472

I. Zaitseva-Pärnaste, T.Soomere (2013) Interannual variations of ice cover and wave energy flux in the northeastern Baltic Sea, Annals of Glaciology, Vol.54, No.62, pp. 175–182

L. Tuomi, H. Kanarik, J. Björkqvist, R. Marjamaa, J. Vainio, R. Hordoir, A. Höglund, K. Kahma (2019) Impact of ice data quality and treatment on wave hindcast statistics in seasonally ice-covered seas, Frontiers in Earth Science, Vol.7, 166

Trend and 7-9-year oscillation of near surface air temperature over Mecklenburg-Vorpommern (Germany) induced by global warming and oceanic processes

Dieter H.W. Peters and Christoph Zülicke

Leibniz-Institute of Atmospheric Physics , University of Rostock, Ostseebad Kühlungsborn, Germany (peters@iap-kborn.de)

1. Series of near surface temperature for Mecklenburg-Vorpommern

A monthly mean near surface temperature series (called MTMV) is derived for Mecklenburg-Vorpommern from observed temperatures of different metrological stations, provided by the Climate Data Center of German Weather Service. The climatological average of the annual mean MTMV series over 99 years (1881-1979) is 8.01°C with a standard deviation of about 0.7 K. No significant trend holds during this centennial period.

2. Annual mean and seasonal trends

This diagnostic part of the study focuses on the 1947-2018 period where up to 15 stations have been in operation with sufficient temporal and spatial cover. Since the beginning of the 1980s a huge increase of 1.72 K is revealed for the annual mean near surface temperature. The difference of 0.81 K between the mean near surface temperature values from 1980 until 2018 and the previous period, 1947-1979, is statistically significant. For the last 4 decades comparable seasonal trends have been determined which are in agreement with the annual mean trend of Europe caused by the global warming process.

3. Regime shift and 7-9-year oscillation after the 1940s

Furthermore, we confirm a finding of a decrease in the summer minus winter difference of near surface temperatures also for Mecklenburg-Vorpommern, with a shift to continental climate regime during the 1940s (e.g., Lauter, 1979). In addition, we determine a pronounced 7-9-year oscillation in MTMV series during the 1947-2018 period. For selected meteorological stations, which cover Europe and Russia, the eastward extension of this near surface temperature oscillation is examined. It is strongest over the North-East Baltic Sea region near St. Petersburg. However, we found a pronounced pattern over Northeastern Europe, between Baltic Sea and Ural Mountains.

4. Structure of linked hemispheric teleconnection patterns

In addition, we found a pattern of positive regression over Northeastern Europe, as well as negative pattern of regression over Labrador Sea and northeastern Canada with anti-correlated counterparts southwards. Furthermore, for winter, the strong anti-correlation between the temperatures over Northeastern Europe and the Siberian Anticyclone was examined, and we confirm that colder (warmer) temperatures over Northeastern Europe are linked to stronger (weaker) Siberian anticyclone as expected. A band-pass filter analysis of the atmospheric indices like AO and NAO confirms an important contribution of the 7-9-year band to the atmospheric multi-year variability in hemispheric teleconnection patterns.

5. Oceanic links

Band-pass filtered selected oceanic sea surface temperature indices like PDO (North Pacific) and AMO (North Atlantic) reveal an increased amplitude of the 7-9 year band for the PDO during last decades. Furthermore, an extended regression analysis based on Kaplan's sea surface temperature field shows positive patterns of correlation for the Baltic Sea and North Sea as expected, but weaker negative correlation patterns in the northwestern North Atlantic, and again positive correlation patterns over southwestern North Atlantic. Surprisingly, a positive weak correlation pattern is revealed in a region near the coast of Peru in the eastern South Pacific. This finding is in agreement with a spectral analysis result of mean sea surface temperatures (SST) for the NINO-1+2- region showing also a significant spectral bin of around 8 years.

6. Cause hypothesis – ECHAM6-AMIP study

Three ensemble runs (called forced runs), each over 30 years (1980-2009), have been performed with AGCM component ECHAM6 of the ESM of MPI-Hamburg under realistic atmospheric conditions (CMIP5) and forced with monthly mean SST and SIC distributions of AMIP phase 2, and are compared with control ensemble runs driven without any inter-annual oceanic variability. We found some reasonable temperature trend in the model for forced runs and indication of a quasi-8-year variability in the difference forced minus control AMIP-2 runs showing the oceanic influence.

7. Summary

The obvious increase of mean near surface temperature over Mecklenburg-Vorpommern since about 1980 of 1.72 degree Celsius is in agreement with the mean trend of Europe caused by the global warming process. In addition, since the 1940s we reveal a dominant 7-9-year oscillation of mean near surface temperature over Mecklenburg-Vorpommern, which belongs to a hemispheric teleconnection patterns of positive regression over Northeastern Europe, as well as negative patterns of regression over Labrador and northeastern Canada with anti-correlated counterparts southwards. Furthermore, we show, that this teleconnection pattern of multi-year variability is mainly induced by oceanic processes.

References

Lauter, E. A. (1979) Long-term temperature variations in middle and west Europe and the influence of solar cycle variations, Z. F. Meteorologie, 29, 331-337

Climate changes in the Baltic sea region as inferred from large RCM ensemble projection

Anastasia Pikaleva, Igor Shkolnik and Sergey Efimov

Voeikov Main Geophysical Observatory, Saint-Petersburg, Russia (pikaleva@main.mgo.rssi.ru)

1. Introduction

Future climate changes and extreme events simulations are accompanied by a wide range of uncertainties associated with differences between the IPCC scenarios, modeling physics, spatial resolution, and multiscale internal climate variability. Large ensemble size along with high model resolution allows one to efficiently minimize the influence of natural climate variability on climatic trends and obtain a more justified estimate of climate changes on regional infrastructure and ecosystems.

In this study, future climate changes are simulated using an ensemble of Voeikov Main Geophysical Observatory (MGO) RCM with spatial resolution 25 km for northern Eurasia (Shkolnik et al. 2018) with focus on Baltic sea region (Figure 1).

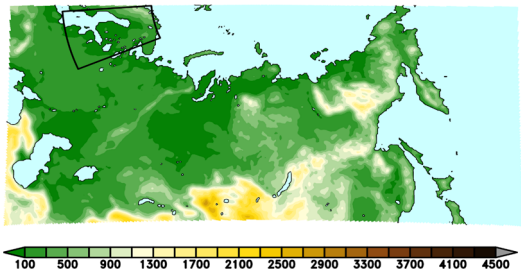


Figure 1. RCM domain and study area

2. Experimental setup

Thirty experiments differing in the atmospheric and land surface initial conditions have been conducted spanning three decadal periods 1990–1999 (baseline), 2050–2059 and 2090–2099 using IPCC RCP8.5 scenario, with each 10-year realization considered equally likely for the same period. Lateral boundary conditions in the atmosphere have been obtained from the MGO AGCM T42L25 ensemble global climate projection. Both models (the MGO RCM and AGCM) use the same prescribed evolution of the sea surface temperature and sea ice concentration derived from the three CMIP5 models' output (ACCESS1–0, CESM1-CAM5 and MPI-ESM-MR) for the same scenario. The changes in the following climate characteristics and specialized indices have been analyzed: seasonal air and surface temperature, mean winter minimum and summer maximum air temperature, seasonal mean precipitation amount, daily maximum 1-hour precipitation rate, first and last freezing date and freeze-free period, first and last snow dates and number of days with snow cover, wind speed.

3. Results

It has been shown that the most pronounced changes in surface air temperature and precipitation are projected across Baltic sea region in winter and fall in the ranges 4-5°C in the eastern part of the area and 20-40% in its north-west, respectively. By the end of the XXI century, the changes in temperature and precipitation are twice as large as compared with that for 2050-2059. The analysis shows that freeze-free season length will increase up to 20 and 40 days in the mid and late XXI century respectively. The number of days with snow cover is projected to decrease more than 30 days in the north by 2050-2059 and will disappear in most of the areas by the end of the century. Simulated changes in wind speed are weak.

To assess the strength of climate change signal in the future climate changes relative to the baseline period, in comparison with natural climate variability (noise), the signal-to-noise ratio is used. The analysis shows that the signal-to-noise ratio larger than 1 is simulated for the changes in temperature and temperature-based characteristics throughout the year and for the cold season precipitation, while the uncertainty of the summer precipitation projection is considerably larger. There expected no significant changes in the wind.

The probabilistic distribution of temperature changes in St. Petersburg has been evaluated at seasonal basis. There is a clear effect of warming that leads to the shift of the distributions towards higher seasonal temperatures, however, there is still a non-zero probability of the occurrence of colder seasons at least until the mid-XXI century, as compared to baseline simulation. The colder seasons can be accompanied by precipitation amounts close to that in the baseline period until the end of the XXI century.

4. References

Shkolnik I., Pavlova T., Efimov S., Juravlev S. (2018) Future changes in peak river flows across northern Eurasia as inferred from an ensemble of regional climate projections under the IPCC RCP8.5 scenario, Clim. Dyn., Vol. 50, pp. 214-230.

The overturning circulation of the Baltic Sea and its sensitivity to long-term atmospheric and hydrological changes

Manja Placke[1], H.E. Markus Meier[1,2] and Thomas Neumann[1]

[1] Department of Physical Oceanography and Instrumentation, Leibniz Institute for Baltic Sea Research Warnemünde, Rostock, Germany (manja.placke@io-warnemuende.de)
[2] Department of Research and Development, Swedish Meteorological and Hydrological Institute, Norrköping, Sweden

1. The overturning circulation

The ocean's overturning circulation is a system of surface and deep currents which flow through and around the ocean basins and transport, amongst others, large amounts of water, heat, and salt. Thus, it connects surface waters with the deep sea and is consequently critically important for the global climate. The overturning circulation is mainly driven by density gradients which arise from changes in temperature and salinity. Another forcing is the wind which can reinforce or weaken the overturning circulation due to the input of horizontal momentum.

In semi-enclosed seas such as the Baltic Sea, density gradients driving the overturning circulation arise predominantly from water exchange with the adjacent sea or ocean and from freshwater input of the surrounding rivers. In the particular case of the Baltic Sea, batch-wise saltwater inflows from the North Sea drive a circulation consisting of a bottom inflow of saline water and a surface outflow of brackish water. Wind that blows in opposite direction to the surface outflow might hamper this circulation because the slowdown of the surface water results in reduced inflow of saline water at the bottom due to mass conservation.

2. Determining the Baltic Sea overturning circulation

The overturning circulation is a basin-wide circulation which is typically determined in the latitude-depth-plane or longitude-depth-plane and is quantified by a meridional or zonal transport stream function, respectively. Maxima of this stream function at any position and depth specify the total amount of water moving meridionally or zonally above and below this depth in opposite directions.

Following Döös et al. (2004) and Hordoir et al. (2018), we determine an overturning stream function in the longitude-depth-plane for the southern Baltic Sea and in the latitude-depth-plane for the central and northern Baltic Sea by using two state-of-the-art ocean circulation models: RCO (Rossby Centre Ocean model) and MOM (Modular Ocean Model). The overturning stream function in the southern Baltic Sea is calculated by meridional integration of zonal volume transport at each longitude and depth and subsequent depth integration from the bottom towards the surface. In the central and northern Baltic Sea, it is calculated by zonal integration of meridional volume transport at each latitude and depth and again subsequent depth integration from the bottom towards the surface.

For illustration purposes, an exemplarily determined overturning stream function from the southern up to the northern Baltic Sea for the model MOM is shown in Figure 1. This annual mean state for the year 1970 reveals strongest water transport in the Bornholm and Gotland Basins. Additionally, the regions for zonal and meridional integration of volume transport for determining the overturning stream function are illustrated.

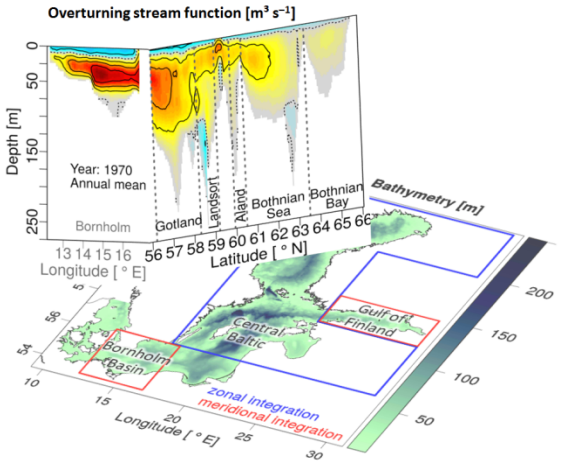


Figure 1. Schematic of the determined overturning circulation of the Baltic Sea from the Bornholm basin in the south up to the Bothnian Bay in the north. The shown overturning stream function is an exemplary annual mean state for the year 1970 of the model MOM. The subjacent chart of the Baltic Sea illustrates the regions for determining the overturning stream function.

3. Strategy

The simulations of the two used models RCO and MOM both start in the year 1850 and last for more than 150 years, such that long-term investigations are possible. The models have slightly different setups leading to a differently pronounced overturning circulation which is compared to each other. Furthermore, different sensitivity experiments are done with the model RCO for simulating the overturning circulation with different atmospheric and hydrological forcing. The experiments are performed for colder or warmer climate, under changed wind conditions, for constant or increased runoff, and for the case of a global mean sea level rise by 1.5 m.

4. Findings

We found that changes in wind or runoff affect the simulated overturning circulation after around 30 years in both models. The overturning circulation decreases basin-wide under wind conditions that hamper saltwater inflows from the North Sea, under warmer future climate or when river runoff increases. However, a global sea level rise by 1.5 m reinforces the overturning circulation. These counteracting responses do not allow a clear projection of the future overturning circulation of the Baltic Sea. Furthermore, we could not find an explicit connection

between the overturning circulation and strong saltwater inflows as not all inflows propagate from the entrance region to the central Baltic Sea. Overall, we found that pronounced variations of the overturning circulation with a period of about 30 years are caused by the wind which blows along the surface currents of this circulation and not by river runoff or large saltwater inflows.

References

Döös, K., Meier, H.E.M., Döscher, R. (2004) The Baltic haline conveyer belt or the overturning circulation and mixing in the Baltic. AMBIO, 33, 261–266. doi: 10.1579/0044-7447-33.4.261

Hordoir, R., Höglund, A., Pemberton, P., Schimanke, S. (2018) Sensitivity of the overturning circulation of the Baltic Sea to climate change, a numerical experiment. Climate Dynamics, 50: 1425–1437. doi: 10.1007/s00382-017-3695-9

Wave scenarios for the Gulf of Bothnia

Jani Särkkä[1], Laura Tuomi[1], Simo Siiriä[1] and Anders Höglund[2]

[1] Finnish Meteorological Institute, Helsinki, Finland (Laura.Tuomi@fmi.fi)
[2] Swedish Meteorological and Hydrological Institute, Norrköping, Sweden

1. Introduction

How will the waves in the Gulf of Bothnia be impacted by future climate change? A changing climate will, in addition to warming, reduce the ice-season, change the sea level, waves and currents. This may in turn have implications for ecosystems, habitats, biodiversity etc., as well as human activities such as fishing, aquaculture, and wind parks. Waves impact coastal erosion and transport of sediments, and add to the extreme sea level hazards. The SmartSea project aims to estimate the climate change impacts in this area. In this study, which is a part of SmartSea, we study the changing wave climate up to 2059.

Wave models are efficient tools in simulating past and future wave conditions. The quality of the Baltic Sea wave models has been shown to be good in open sea areas and even near coastal areas and archipelagos, if measures are taken to account for unresolved islands at the used resolution. Earlier studies have also shown that in the open sea areas, the quality of the wind forcing is the main factor in the accuracy of the wave model results.

2. Methods

For a long time, the resolution and quality of the atmospheric climate scenarios has limited their use in the Baltic Sea. Nowadays, there are downscaled atmospheric products, such as the RCA4 regional climate model by SMHI, that gives us possibility to do wave scenario simulations using wind forcing with adequate horizontal temporal resolution. Furthermore, the seasonal ice conditions, that are important for the wave scenarios, can be calculated with an ice-ocean model using the same atmospheric forcing, thus providing a compatible forcing dataset.

We perform six wave scenario simulations 2006-2059 for the Gulf of Bothnia in 1 nmi resolution using WAM model. We use atmospheric forcing from a matrix of three different global climate models and two different Representative Concentration Pathways (RCP 4.5 and RCP 8.5). These model simulations are downscaled with RCA4 regional model to obtain the surface wind forcing for WAM. Daily ice concentrations for the Gulf of Bothnia are extracted from ice-ocean model simulation utilizing NEMO-SCOBI and LIM3 models, produced within SmartSea. The wave scenarios are used to assess the projected changes in the wave conditions in the Gulf of Bothnia and to calculate the statistics of significant wave heights.

The future of the Gulf of Bothnia: NEMO-SCOBI SmartSea scenarios from the present until 2060

Simo-Matti Siiriä[1], Sam Fredrikson[2], Annu Oikkonen[1], Jenny Hieronymus[2], Anders Höglund[2], Petra Roiha[1], Jani Särkkä[1], Lars Arneborg[2], Laura Tuomi[1]

[1]Finnish Meteorological Institute, Helsinki, Finland (simo.siiria@fmi.fi)
[2] Sveriges meteorologiska och hydrologiska institut, Sweden

1. Introduction

Changes in the physical conditions on the Gulf of Bothnia can have considerable impact on both human activities, as well as the biology on the area. Possibilities for fishing, aquaculture, tourism and wind parks can all change if the ice-season, temperature, salinity or currents change considerably. SmartSea project has simulated the physical and biogeochemical changes on the area up to year 2060 for estimating these changes.

2. Model setup

Simulations were made with NEMO 3.6 model coupled with SCOBI biogeochemical model and LIM3 ice model. Model setup comprises of Gulf of Bothnia area with 1 NM grid. Scenarios used in these studies are forced with 3 different atmospheric models (MPI-ESM-LR, EC-EARTH and HadGEM 2-ES) and with two Representative Concentration Pathways, RCP 4.5 and RCP 8.5.

Historical comparison scenarios for each model span the years 1975 to 2005, and each future scenario continue from 2006 to year 2060.

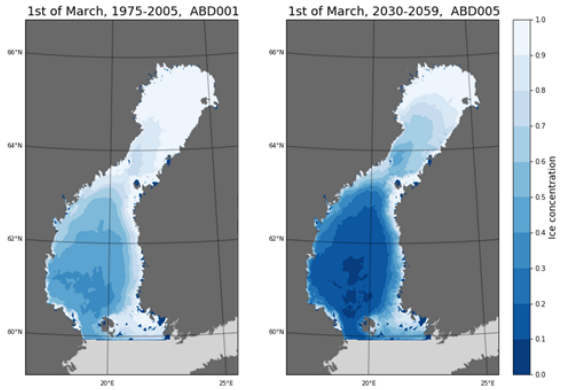


Figure 1: Change of average ice volume, March, during studied period.

3. Change in temperature and Salinity

Increasing temperature is present in all future scenarios studied, varying roughly between 0.15 to 0.3 °C per decade. Changes in salinity are more uncertain, however, in general the models suggest decreasing trend in salinities.

4. Change in ice conditions

Based on these scenarios, the length of ice season keeps shortening with the comparable rate as observed past few decades, roughly 6 days/decade.

Annual maximum ice volume in the Bay of Bothnia will decrease in RCP 4.5 around 50% and in RCP 8.5 around 60%. The timing of the annual ice volume maximum will shift to earlier.

5. Changes in circulation patterns

The changes in circulation patterns have been studied, by comparing the historical runs conditions, to the end periods of the future scenarios on different atmospheric forcing, and RCP's. Our preliminary results show changes in both local maximum flow speed, as in local average speeds.

Trends in total heat content in a very long climate change simulation

Martin Stendel

Dept. for Climate and Arctic, Danish Meteorological Institute, Copenhagen, Denmark (mas@dmi.dk)

1. Introduction

The equivalent potential temperature Θ_e is a versatile measure of the total heat content in the atmosphere, as it is conserved during both dry adiabatic and wet adiabatic processes. It is defined as letting an air parcel expand pseudo-adiabatically until all the water vapour has condensed, release and precipitate all its latent heat and compress it dry-adiabatically to the standard pressure of 1000 hPa.

Changes in surface or air temperature can thus be related to changes in humidity. For example, the relative contributions of temperature and humidity changes in tropical cyclones can be addressed, Arctic amplification due to the fact that saturation mixing ratio follows an exponential curve with temperature can be investigated, and by considering Θe in different vertical levels, an assessment of changes in convective stability can be made.

But also in temperate latitude, the equivalent potential temperature is useful to assess the relative magnitudes of changes in sensible (temperature) and latent heat (humidity).

2. Data

For present-day climate, we consider the ERA5 reanalysis, which is available for the period 1979 to near-present (one- or two-month lag). For future climate, we make use of a very long climate simulation with a global model interactively coupled to a Greenland ice sheet component.

An “extended RCP 8.5” scenario is applied, where emissions of greenhouse gases continue to increase and then eventually level out around 2250. The model is then run for another 1000 years. With such an extreme forcing, all Arctic sea ice has completely disappeared, and a large part of the Greenland Ice Sheet has melted at the end of the simulation.

We examine changes in the total heat content based on observations and model data for past and present as well as for future climate. Daily data, allowing the identification of individual weather systems will be discussed for selected time slices under present-day conditions and with a seasonally and later a totally ice-free Arctic.

Surveying opinions among environmental students on climate science and Baltic Sea issues

Hans von Storch
Institute of Coastal Research, Helmholtz Zentrum Geesthacht, PO Box, 21502 Geesthacht, Germany

1. Prologue

The concern about environmental issues in the Baltic Sea is widespread in the public and in academia. While this concern for a long time was dominated by the issue of eutrophication and overfishing, climate change has become another high profile issue. After having surveyed the opinion among graduate students and mostly young western scholars about climate change and climate policy (e.g., Bray and von Storch, 1999; von Storch et al., 2019; von Storch and Gualdi, 2019), a series of surveys were done among mostly bachelor and master students in Poland, Germany and Sweden. This was done by approaching a few professors, who distributed and later collected the questionnaires. So far, data from 5 surveys have been obtained.

This selection process of locations and teachers was done according to opportunity, and no claim of a representative cover – neither in terms of country, natural science field, age, nor maturity of study – can be made. It is also possible that the teaching of the professors may have had an influence on the students' responses. However, the results allow to derive hypotheses to be tested in additional surveys.

2. The five surveys

The following table lists the locations, and the number of archived responses. Response rates cannot be given in most cases.

	institution	samples
1	Hamburg U, Geology, Germany	22
2	Hamburg U, Oceanography, Germany	9
3	U Gdansk, Geography and Oceanography, Poland	69
4	IOPAN, Sopot, Poland	5
5	U Göteborg, Marine Science, Sweden	26

The questionnaires used mostly the same questions; sometimes some more questions were posed; in one case the question was adapted to the country of the institution. First some demographics were collected, then opinions on climate change and science in general, then an assessment was asked for of the major issues concerning the Baltic Sea.

3. The perceived task of the climate science community

In the earlier studies among European scholars, the responses to one question were standing out, with a large majority favoring the "motivation", whereas the scientific challenges ("define & attribute") got least ticks (see references above; Figure 1). Since this was a bit surprising, this question was a key element in the survey used with the students from the Baltic Sea institutions.

Today, what would you rate as the most important task facing the climate science community?
( ) define the climate problems and attribute cause of climate change
( ) determine solutions to climate change
( ) motivate people to act on climate change
( ) don't know

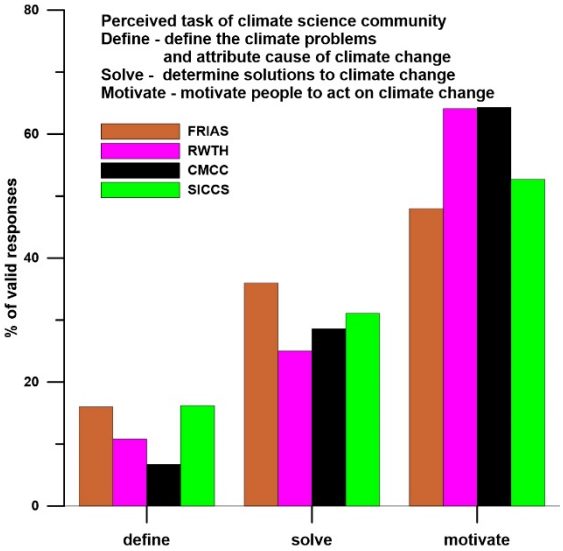


Figure 1: Response rates, in % of valid answers, of the earlier surveys to the question, which task would be rated as the most important task facing the climate science community. Sampled were PhD students and mostly young western scholars at to climate-focused graduate schools (SICCS and CMCC), at one advanced study institute (FRIAS) and an institute of a technical university (RWTH).

Only one choice was accepted as answer. In the following table we provide the numbers and the percentage of valid answers for the five institutions:

	define & attribute		determine solutions		motivate people	
1	3	18%	10	**59%**	4	24%
2	1	11%	7	**77%**	1	11%
3	10	16%	17	27%	37	**58%**
4	1	25%	1	25%	2	**50%**
5	5	24%	8	**38%**	8	**38%**

In all five cases, of which two have very few samples, the scientific issue "define & attribute" was least often clicked at as the "most important task of the climate science community", which is consistent with the surveys among European scholars. However, the students do opt much more often for the determination of solutions as major task and less often for the mobilization than the scholars. Group 3, from Gdansk generated a distribution

similar to that of SICCS. But the others had a considerable smaller skewness towards "motivation" than in the groups of Figure 1. In three out of the five cases, the maximum is with "solve".

4. Serious issues of the Baltic Sea

A second aspect concerns the human pressures on the Baltic Sea. Students were asked if the issues in the table are serious, and need political attention. Multiple clicks were allowed

% of respondents	1	2	3	4	5
climate change	77	78	42	**80**	69
eutrophication	55	22	38	60	85
overfishing	**82**	**89**	65	**80**	**92**
tourism	14	44	19	20	35
waste	27	67	**77**	60	69
constructions	18	55	12	20	23

Note, again, that the surveys 2 and 4 have only very few samples, namely 9 and 5.

The most frequent choice was "overfishing", but "climate change", "eutrophication" and "disposal of waste" received also many clicks. In many, if not most cases, respondents did not identify one issue as the dominant one, but an ensemble of different issues as most pressing. "Tourism" and "construction of pipelines and bridges" received less attention.

As mentioned before, the results can hardly be considered representative of what different groups of students tend to think about the most pressing issues. Noteworthily is that climate change is not the dominant issue, albeit an important one, but comparable with others, such as the "disposal of waste", "eutrophication" or "overfishing".

5. Hypotheses

The results invite for at best some educated hypotheses if not wild speculations:

- In both groups, the students from the Baltic Sea region and the mostly young western scholars in the previous cases, the challenge of better scientific understanding the climate problem is considered less a task of the scientific community; instead the question of how to solve the climate problem and the political need for alarming the public appear as dominant task. The first is a social-science and engineering task, and the latter a political task. For both, climate scientists are not prepared. This observation may imply that science is considered among some scientists mainly as a social actor, supporting the "right" cause, and not an effort to provide society with knowledge for guiding political choices (Pielke's (2007) advocates or stealth advocates).
- The found tendency of grading the task of solving the problem higher, or equal, to the task of political convergence may be a random effect, but if not, it may point to a change of perception among environmental scholars, namely that alarming of the public does not really lead to a solution of the problem, and that instead more realistic options to deal with the climate problem are needed. This would imply that climate science, as it is, is losing importance, while economists and engineers gain importance.
- After the issue of eutrophication in the Baltic Sea has dominated for many years, other issues are also gaining attention, in particular waste and climate change. The dominance of the Baltic Sea eutrophication in the political and public domain has led to certain adverse power-structures within science advisory practice and institutional financing. Therefore, such a change may lead to a change in these power structures.

References

Bray, D. and H. von Storch (1999) Climate Science. An empirical example of postnormal science. *Bull. Amer. Met. Soc.* 80: 439-456

Pielke, Jr., R.A., 2007: *The Honest Broker: Making Sense of Science in Policy and Politics*. Cambridge University Press.

von Storch, H., Chen X, B. Pfau-Effinger, D. Bray and A. Ullmann (2019) Attitudes of young scholars in Qingdao and Hamburg about climate change and climate policy – the role of culture for the explanation of differences. *Advances in Climate Change Research*, online: 10.1016/j.accre.2019.04.001

von Storch, H., and S. Gualdi (2019) What do climate scholars think about climate science and its character in society? A survey at CMCC. *Forsight* https://www.climateforesight.eu/global-policy/what-do-climate-scholars-think-about-climate-science-and-its-role-in-society-a-survey-at-cmcc/

Intraannual and longterm variability of wind in Poland in the period 1966-2018

Joanna Wibig

Department of Meteorology and Climatology, University of Lodz, Poland (joanna.wibig@geo.uni.lodz.pl)

1. Introduction

Wind is one of the basic meteorological and climatological elements determining the conditions in a given area. In addition to air temperature and humidity, it is also one of the parameters determining biometeorological conditions. It affects thermal sensations by increasing discomfort during cold periods or by improving biometeorological conditions during hot periods. It affects the rate of evaporation, thanks to which it significantly affects the local water balance. Despite such a significant importance of wind, there are relatively few items devoted to it in Polish climatological literature.

2. Data

The study uses data from 1951-2018 from 41 meteorological stations in Poland from three observation terms: 6, 12 and 18. Data were taken from the archives of the Institute of Meteorology and Water Management Polish Research Institute (IMWM PRI). These are the values of the average wind speed and its direction. According to the World Meteorological Organization guidelines, the measurements should be provided by anemometer placed 10 m above the ground, and the speed and direction should be 10 minutes average.

There is a lot of potential causes of inhomogeneity in wind data. The most important are station relocations, changes in the environment surrounding station, instrumentation changes, changes in sampling interval and instrumentation malfunction. At synoptic stations of IMWM PRI instruments for wind direction and speed measurements have changed many times. Initially, until the mid-1960s, measurements were made with a Wild's anemometer. Since 1966, Wild's anemometers have been replaced by M47 anemometers (Janiszewski, 1972) at all IMWM PRI stations. The measurements were made manually. Since 1 January 1976, according to the recommendation of the World Meteorological Organization, the sampling interval has changed. The averaging time has been elongated from 2 to 10 minutes.

In the years 1966-1986 measurements of wind speed were made with anemometers of Soviet production, first type M-47, then M-63. From 1986, they were successively replaced by electric anemometers W-863 (Lorenc, 1996). Vaisala cup anemometers WAA151 with wind vanes WAV151 have been used since the turn of the 20th and 21st centuries. In 2014, they were replaced by Vaisala sonic anemometers with WS425 sensors. Both Vaisala anemometers automatically averaged wind speed and direction.

Changes in the instruments often give rise to significant break-points in wind speed series. Unfortunately, changes were usually sudden, without a period of overlapping comparative measurements. The number of papers concerning this issue is very limited. Two the most important changes were transition from measurements using Wild's anemometer to cup anemometers and transition from manual to automatic measurements. In Poland the first one took place in the midsixties, whereas the second one at the turn of the 20th and 21st centuries.

Dziaduszyński et al. (2000) made an attempt of comparison of wind speed measurements by a Wild's anemometer (3 times per day) and by a YOUNG (model 05103-5) automatic weather station anemometer (every 15 minutes). Brazdil et al (2017) compared standard universal anemometers working in the Czech republic till mid 90's with automatic measurements by Vaisala WAA251 sensor (cup anemometer) and WS425 sensor (sonic anemometer). They have shown that the average wind speed measured using both Vaisala automatic sensors are slightly higher than those manualy measured and the differences do not depend on wind direction.

To check whether the replacement of Wild's anemometers by cup anemometers caused a break in the homogeneity of the series, the average wind speed was calculated over two 10-year periods before and after the instrument changeover (1951-1960 and 1971-1980). The transition from Wild's anemometer to cup anemometers resulted in an average change in wind speed of 7%, which means that there was a clear break in the homogeneity of the measurement series. For this reason, it was decided to use only data from the period 1966-2018 for further analysis.

3. Methods

Annual and seasonal average wind speed at three measurement terms is presented. Then the frequencies of calm weather and the wind occurrence in selected speed intervals is discussed. The frequencies of winds blowing from different sectors divided into speed classes is also analysed. 16 sectors are considered. Wind with extreme speeds are discussed. The long-term variability of wind speed and direction is researched at the end.

4. Results

The wind was analyzed on the basis of speed and direction data from three observation terms from 41 meteorological stations in Poland from 1966-2018. Due to the large change in the homogeneity of the series caused by the transition from Wild's anemometers to cup anemometers, the data from 1951-1965 were abandoned. The average annual and seasonal wind speeds were calculated taking into account three observation periods. The incidence of atmospheric calms was investigated. Wind frequencies from different directions were determined, taking into account the 16-sector wind rose. Particular attention was paid to winds exceeding 8 ms^{-1}, the frequency of their occurrence and directions of air masses inflow during strong winds were examined. Seasonal and annual trends of strong winds were counted.

The average wind speed in Poland was 3.6 ms^{-1} and ranged from 1.4 ms^{-1} in Zakopane to 12ms^{-1} on Śnieżka

(Fig.1). In the annual cycle the average wind speed at noon was the highest in spring and lowest in summer. At morning and evening terms the highest wind speed was observed in winter whereas the lowest in summer. In the daily scale the highest wind appeared at noon. There was no significant differences between the average wind speed at the morning and evening observation terms.

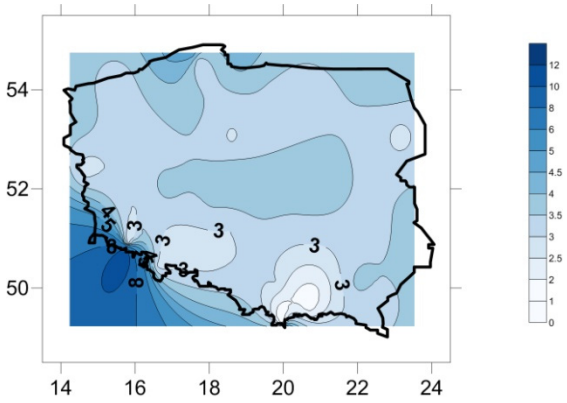


Figure 1. Average wind speed in the period 1966-2018

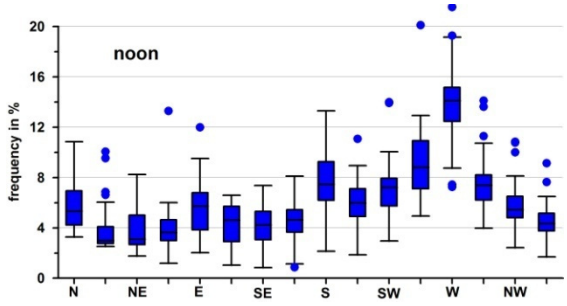


Figure 2. Box and whiskers graphs showing the distribution of frequencies of winds blowing from 16 main directions in the period 1966-2018 at noon.

Windless weather was relatively rare in Poland. It appeared the most often in the morning (12.3% of observations), less often in the evening (8.3%) and least often at noon (3.0%). They were extremely rare at the coast (less than 1% of observations in each term), and appear most often at stations located in mountain valleys: Zakopane, Kłodzko and Nowy Sącz.

During the analyzed period, winds from the western (W) sector were most often observed (Fig.2), next from the west southwestern sector (WSW) and southern (S). The least frequent wind in Poland was from the north north-east (NNE) and north-east (NE).

The long-term average of the highest annual wind speed oscillated between 8.3ms^{-1} in Tarnów to 42.5 ms^{-1} on Śnieżka. On the seasonal scale the lowest maximum wind speeds were recorded in summer and the highest in spring. Strong winds were most often recorded from the west (W), west southwest (WSW) and west northwest (WNW). At several stations in southern Poland it was also the southern (S) direction.

Decreasing trends in annual and seasonal series of wind speed were observed in Poland as well as in other European countries. However many authors wiąże ten trend with the increase of surface roughness. This thesis can be confirmed by the fact that simultaneously, based on NCEP/NCAR data on zonal and meridional wind velocity at the height 10 m above ground level from 35 grids from the period 1951-2005, Central Europe has witnessed increases in wind speed as well as in number of days with strong wind (>8ms^{-1}), both statistically significant (Araźny et al. 2007).

References

Araźny A., Przybylak R., Vizi Z.,Kejna M., Maszewski R., Uscka-Kowalkowska J. (2007) Mean and Extreme wind velocities in Central Europe 1951-2005., *Geographia Polonica*, 80, 2, 69-78.

Brázdil R, Valík A, Zahradníček P, Řezníčková L, Tolasz R, Možný M (2017) Wind-stilling in the light of wind speed measurements: the Czech experience. *Climate Research* 75, 131-143.

Dziaduszyński K, Kozyra J, Doroszewski A (2000) Comparison of wind speed measured by Wild anemometer and automatic weather station anemometer. *Annales Universitatis Mariae Curie-Sklodowska, Sectio B,* 55-56, 127-131.

Janiszewski F. (1972) Anemometer zdalny M-47. *Gaz. Obs. PIHM,* 8, 13-15.

Lorenc H. (1996) *Struktura i zasoby energetyczne wiatru w Polsce*. Mat Bad seria Meteorologia 25, IMGW, Warszawa.

Long-term observations of nitrous oxide and methane at the Boknis Eck Time-Series Station in the Eckernförde Bay (southwestern Baltic Sea)

Xiao Ma [1], Sinikka T. Lennartz [1, 2] and Hermann W. Bange [1]

[1] GEOMAR Helmholtz Centre for Ocean Research Kiel, Germany (mxiao@geomar.de)
[2] now at ICBM, University of Oldenburg, Oldenburg, Germany

1. Boknis Eck Time-Series Station

The Boknis Eck (BE) Time-Series Station (www.bokniseck.de) is located at the entrance of the Eckernförde Bay (54 ° 31 ′ N, 10 ° 02 ′ E) in the southwestern Baltic Sea. Sampling at BE started since 1957 and, therefore, it is one of the oldest continuously operated time-series stations in the world. The water depth of the sampling site is 28 m. There is no significant river runoff to Eckernförde Bay and the saline North Sea water inflow from the Kattegat plays a dominant role for the local hydrographic conditions. Seasonal stratification usually starts to develop in April and lasts until October, during which hypoxia or even anoxia sporadically occurs in bottom water. Significant trends (such as increasing temperature, expanding hypoxia/anoxia, decreasing nutrients, etc.) have been found at BE for the past several decades (Lennartz et al., 2014), but the impact of these changes on greenhouse gases remain unclear.

2. Nitrous oxide

Nitrous oxide (N_2O) is a potent greenhouse gas and it is involved in stratospheric ozone depletion (Ravishankara et al., 2009). Monthly measurements of N_2O started in July 2005. We found a pronounced seasonal pattern with high concentrations (supersaturations) in winter/early spring and low concentrations (undersaturations) in autumn when hypoxic/anoxic conditions prevail (Fig. 1). Unusually low N_2O concentrations were observed during October 2016–April 2017, which was presumably a result of prolonged anoxia and the subsequent nutrient deficiency (Fig. 2). Unusually high N_2O concentrations were found in November 2017 and this event was linked to the occurrence of upwelling which interrupted N_2O consumption via denitrification and potentially promoted ammonium oxidation (nitrification) at the oxic/anoxic interface. Our results indicate a close coupling of N_2O anomalies to O_2 concentration, nutrients and stratification. Given the long-term trends of declining nutrient and oxygen concentrations at BE, a decrease in N_2O concentration, and thus emissions, seems likely due to an increasing number of events with low N_2O concentrations (Ma et al., 2019).

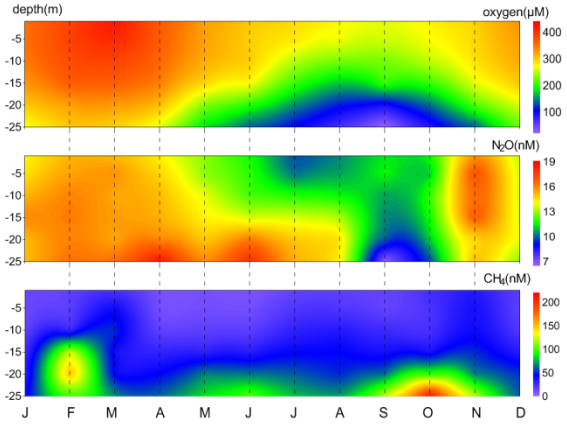


Figure 1. Mean seasonal variations of dissolved O_2, N_2O and CH_4 at the BE time-series station during 2006–2017.

3. Methane

Methane (CH_4) is a strong greenhouse gas and it plays an important role in atmospheric chemistry (WMO, 2018). Monthly measurements of CH_4 started in June 2006. In general CH_4 concentrations increased with depth, indicating a sedimentary release of CH_4. Pronounced enhancement of the CH_4 concentrations in the bottom layer (15–25 m) was found during February, May/June and October (Fig. 1). Unusually high CH_4 concentrations (of up to 696 nM) were sporadically observed in the upper layer (0–10 m) (e.g. in November 2013 and December 2014, Fig. 2) and were coinciding with Major Baltic Inflow (MBI) events. Surface CH_4 concentrations were always supersaturated throughout the monitoring period, indicating that the Eckernförde Bay is an intense but highly variable source of atmospheric CH_4. We did not detect significant temporal trends in CH_4 concentrations or emissions, despite of ongoing environmental changes such as warming and deoxygenation. Overall, the CH_4 variability at BE is driven by a complex interplay of various biological and physical processes.

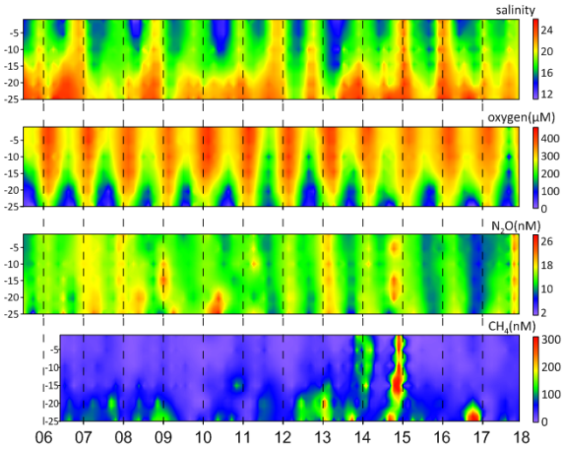


Figure 2. Distributions of salinity, dissolved O_2, N_2O and CH_4 at the BE time-series station during 2006–2017. Please note that the maximum color bar for CH_4 concentration is adjusted to 300 nM for a better visualization.

References

Lennartz, S. T., Lehmann, A., Herrford, J., Malien, F., Hansen, H. P., Biester, H., and Bange, H. W. (2014) Long-term trends at the Boknis Eck time series station (Baltic Sea), 1957–2013: does climate change counteract the decline in eutrophication? Biogeosciences, 11, 6323–6339.

Ma, X., Lennartz, S. T., and Bange, H. W. (2019). A multi-year observation of nitrous oxide at the Boknis Eck Time-Series Station in the Eckernförde Bay (southwestern Baltic Sea). Biogeosciences, 16, 4097–4111.

Ravishankara, A. R., Danielm J., S., and Portmann, R. W. (2009) Nitrous oxide (N_2O) the dominant ozone-depleting substance emitted in the 21st century, Science, 326, 123–125.

WMO: Scientific assessment of ozone depletion: 2018. World Meteorological Organization, Geneva, Switzerland, Global Ozone Research and Monitoring Project–Report No. 58.

Acknowledgments

The time-series at Boknis Eck was supported by DWK Meeresforschung (1957–1975), HELCOM (1979–1995), BMBF (1995–1999), the Institut für Meereskunde (1999–2003), IfM-GEOMAR (2004–2011) and GEOMAR (2012–present). The current measurements at BE are supported by the EU BONUS INTEGRAL project which receives funding from BONUS (Art 185), funded jointly by the EU, the German Federal Ministry of Education and Research, the Swedish Research Council Formas, the Academy of Finland, the Polish National Centre for Research and Development, and the Estonian Research Council. The Boknis Eck Time-Series Station (www.bokniseck.de) is run by the Chemical Oceanography Research Unit of GEOMAR, Helmholtz Centre for Ocean Research Kiel. Data are available from www.bokniseck.de/database-access.

Topic 9

New climate observation systems

Monitoring lake ice extent using optical satellite data

Kirsikka Heinilä[1], Olli-Pekka Mattila[1], Sari Metsämäki[1], Sakari Väkevä[1], Kari Luojus[2], Gabriele Schwaizer[3] and Sampsa Koponen[1]

[1] Finnish Environment Institute, Helsinki, Finland (kirsikka.heinila@environment.fi)
[2]Finnish Meteorological Institute, Helsinki, Finland
[3]ENVEO IT GmbH, Innsbruck, Austria

1. Importance of lake ice coverage

Lake ice affects Earth's energy balance and local weather by reducing the energy exchange between water and atmosphere. Importantly, lake ice extent is a sensitive climate change indicator, with a positive feedback to warming due to the increased absorption of solar radiation into the open water. Gebre et al. (2014) concluded that the enhanced warming, together with changes in other atmospheric variables, will result in a significant decline in lake ice duration and thickness at the end of the 21st century in the Nordic–Baltic region. Changes in duration and even the appearance of full ice cover influences the limnological and biological processes within those lakes. In many areas over Northern latitudes lake ice plays an important role to citizens as a means of transportation (road network, fairways) and recreation (ice fishing, skating).

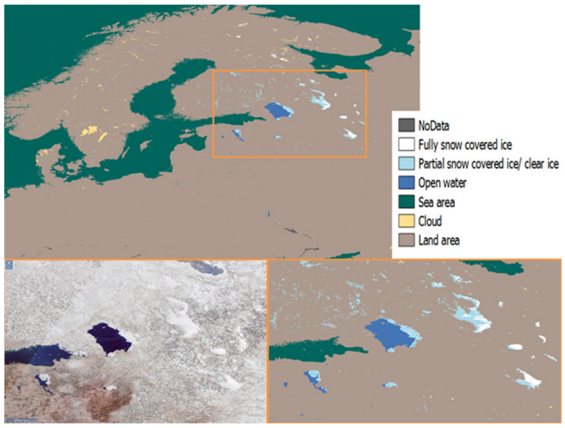


Figure 1. LIE-NE product on 3 April 2019. The service is currently operational in Copernicus Global Land Service and is based on Terra MODIS data.

2. Lake Ice extent mapping under Copernicus Global Land Service

North European Lake Ice Extent (LIE-NE) product was developed at the Finnish Environment Institute (SYKE). LIE-NE is an ice classifier for freshwater bodies (Heinilä et al. 2017) based on 250m Moderate Resolution Imaging Spectroradiometer (MODIS) data and is a member of the Copernicus Global Land Service (CGLS) product family (Fig. 1). The main use of the satellite-based Lake Ice Extent (LIE) data is to define timing of events in the annual cycle of freshwater ice, i.e. the initiation of ice formation, freezing up of lakes (when the lake is completely covered by ice), initiation of melting period, ice-out date (when the lake is completely ice-free). The LIE product can also be used to monitor the extent of ice, and this is usually defined in terms of area (in square kilometers) or percentage of coverage.

A new method has been developed at SYKE to assess Lake Ice Extent using optical and thermal data by Copernicus Program satellite Sentinel-3 Land Surface Temperature Radiometer (SLSTR). The algorithm is based on multidimensional distributions of several reflectance / thermal bands and indices calculated for training data. The classification is provided for each 500m resolution pixel in three categories: i) open water, ii) ice cover and iii) cloud. Also, a statistical probability is assigned to each pixel. Recently, the areal coverage of LIE data has been extended to cover the Northern Hemisphere. Northern Hemisphere Lake Ice Extent product (LIE-NH) will be the new product in CGLS cryosphere products portfolio.

3. Mapping lake ice extent using high resolution data

For the provision LIE in 20m resolution, a new algorithm has been developed at SYKE. The method utilizes Sentinel-2 Multispectral Instrument (MSI) (Fig. 2). the results have been promising even though the instrument lacks the thermal bands needed for cloud detection in general but particularly over snow/ice-covered areas. However, high spatial resolution goes often hand in hand with lower temporal resolution compared to medium resolution satellites. As lake ice extent can be temporally highly dynamic, medium resolution satellites provide a better view on the temporal variation of lake ice extent. Fig. 3 presents the time series from lake Lokka reservoir during spring 2019 for LIE derived using data by both, high resolution MSI and medium resolution SLSTR. The gaps in MSI data are notable even though the Lokka reservoir is located at 68°N where the temporal frequency of S2 MSI images is considerably higher than in mid-latitudes where lakes also go through the freeze-melt events. Fig.3 shows a complete melting of ice several days earlier from SLSTR based time series. However, high resolution images provide a good source of additional ice information, data for validation and ability to monitor small lakes.

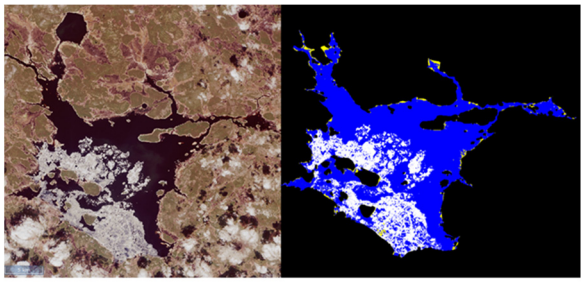


Figure 2: Lake ice cover at Lokka Reservoir in Northern Finland. Left: Sentinel 2 MSI true color image acquired on May 24, 2019. Right: S2 based Lake ice extent product of the same day (white represents ice and blue represents open water).

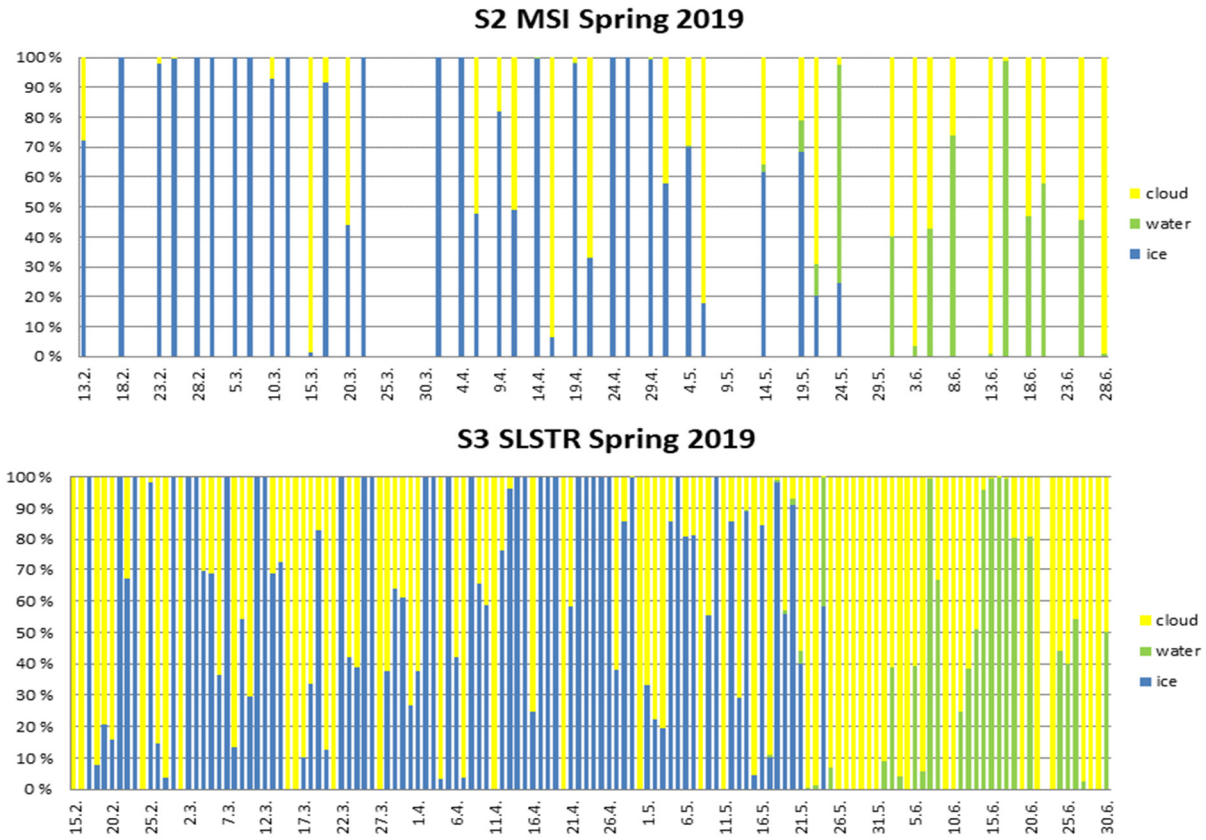


Figure 3: Time series of Lake Ice Extent for Lokka Reservoir calculated using S2 MSI data (Top) and S3 SLSTR data (Bottom)

4. Motivation

The Arctic region is undergoing significant changes due to climate change and other human activities. According to the Arctic Council, the magnitude of warming in the Arctic is twice as large as in the global scale. This has considerable effects on lake ice coverages, which on the other hand affects e.g. the limnological and biological processes of lakes. Information on lake ice is important in many aspects. In situ stations are located sparsely while satellite-based Lake Ice Extent products provide data on lake ice phenology with excellent spatial and temporal coverage. Earth Observation enables thousands of lakes to be monitored all over the world, providing valuable data for climate change studies.

References

Gebre, S., Boissy, T., Alfredsen, K. (2014): Sensitivity of lake ice regimes to climate change in the Nordic region, The Cryosphere, 8, 1589–1605, https://doi.org/10.5194/tc-8-1589-2014

Heinila, K., Metsamaki S., Mattila O.-P. 2017. Product User Manual. Copernicus Global Land Operations – Lot 2, Lake Ice Extent – Collection 250m Baltic Sea Region, Version 1.0.1, Issue 1.02. CGLOPS2_PUM_LIE-250m_V1_I1.02. https://land.copernicus.eu/global/products/lie

Using InSAR observations to understand changes to coastal and inland water resources in the Baltic basin

Fernando Jaramillo[1,2], Saeed Aminjafari[1], Mohammad Nia[3], Mehdi Darvishi[1], Julian García[1]

[1] Department of Physical Geography and Bolin Centre for Climate Research, Stockholm University, SE–106 91, Stockholm, Sweden

[2] Baltic Sea Centre, Stockholm University, SE–106 91, Stockholm, Sweden

[3] Department of Earth Sciences, Institute for Advanced Studies in Basic Sciences (IASBS), Zanjan, Iran

The basins draining into the Baltic Sea provide the desirable fresh water needed for its coastal and Sea ecosystems. However, flow regulation and important agriculture and urban expansions have possibly affected wetland and costal hydrologic connectivity due to water regulations and infrastructure. Global warming is also melting glaciers in the basin and triggering permafrost thaws, with hydrological sampling being difficult where these processes are occurring. Cutting edge hydrogeodetical tools, such as Interferometric Synthetic Aperture Radar (InSAR), can now be used to assess large scale changes to water resources. InSAR is a potent tool to study hydrology and water flow in coastal systems [1] and glaciers [2]. For instance, recent studies in the tropics have used InSAR to generate displacement maps of the water surface employed to detect water movements in wetland coastal systems [3–9]. Even though tropical regions have seen use of this technology, in the Baltic Sea basin it has up to date been mostly overlooked. Here we exploit the cost-effective, climate-independent and easy-to-use InSAR technology to unravel the changes to water resources in the Baltic Sea Basin.

We calculate phase difference between two or more SAR scenes to deliver information on hydrodynamics, hydrological connectivity and sheet flow in coastal wetlands and glacier extent and depth changes in the mountains between Sweden and Norway. We generate a series of interferograms, which are the combination of two or more SAR images, to show changes in the surface water and glacier surfaces in the Polish and Swedish coastal zones, and in the Tarfala station in Northern Sweden, respectively. We find that tidal processes and wetland sheet flow can be identified in these interferograms by coherent patterns of radar phase change called fringes. The fringes are evident even over open water of the Vistula Lagoon in Poland, showing important spatial information on accumulation of sea ice during winter. For the case of the glacier study, InSAR shows the regions were ice has been lost, and regions where it has accumulated. These results will be important for water resource management in the area, aquatic and terrestrial ecosystem restoration, and adaptation and mitigation to future climatic changes inducing pressure on Baltic resources and coastal ecosystems.

References

Wdowinski, S. & Eriksson, S. Geodesy in the 21st Century. *Eos, Transactions American Geophysical Union* **90**, 153– 155 (2009).

Sánchez-Gámez, P. & Navarro, F. J. Glacier Surface Velocity Retrieval Using D-InSAR and Offset Tracking Techniques Applied to Ascending and Descending Passes of Sentinel-1 Data for Southern Ellesmere Ice Caps, Canadian Arctic. *Remote Sensing* **9**, 442 (2017).

Oliver-Cabrera, T. & Wdowinski, S. InSAR-Based Mapping of Tidal Inundation Extent and Amplitude in Louisiana Coastal Wetlands. *Remote Sensing* **8**, 393 (2016).

1. Wdowinski, S., Amelung, F., Miralles-Wilhelm, F., Dixon, T. H. & Carande, R. Space-based measurements of sheet-flow characteristics in the Everglades wetland, Florida. *Geophysical Research Letters* **31**, L15503 (2004).
2. Kim, J.-W. *et al.* Integrated analysis of PALSAR/Radarsat-1 InSAR and ENVISAT altimeter data for mapping of absolute water level changes in Louisiana wetlands. *Remote Sensing of Environment* **113**, 2356–2365 (2009).
3. Lu, Z. *et al.* Helmand River Hydrologic Studies Using ALOS PALSAR InSAR and ENVISAT Altimetry. *Marine Geodesy* **32**, 320–333 (2009).
4. Hong, S. H., Wdowinski, S. & Kim, S. W. Evaluation of TerraSAR-X Observations for Wetland InSAR Application. *IEEE Transactions on Geoscience and Remote Sensing* **48**, 864–873 (2010).
5. Palomino-Ángel, S., Anaya-Acevedo, J. A., Simard, M., Liao, T.-H. & Jaramillo, F. Analysis of Floodplain Dynamics in the Atrato River Colombia Using SAR Interferometry. *Water* **11**, 875 (2019).
6. Jaramillo, F. *et al.* Assessment of hydrologic connectivity in an ungauged wetland with InSAR observations. *Environmental Research Letters* **13**, 024003 (2018).

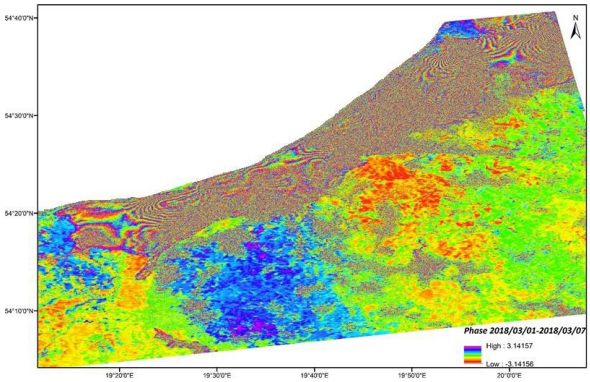


Figure 1. Interferogram of surface water level changes between seven days in March, 2018, with Sentinel observations

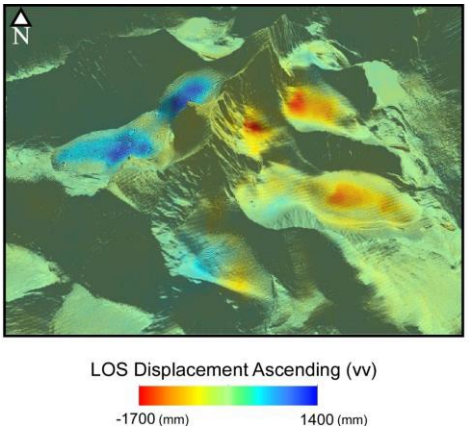


Figure 3. Velocity map of changes in glacier surface in the Tarfala Region, Sweden with Sentinel-1A/B during the period 2017-to date.

The See Baltic Poland: citizen observations of surface water properties

Tomasz Kijewski[1], Artur Palacz[1], Beata Szymczycha[1], Ewa Borkowska[2] and Tymon Zieliński[1]

[1] Institute of Oceanology Polish Academy of Science (tkijewski@iopan.pl)
[2] See Baltic

Measurements of surface water temperature are critical for observations of various phenomena such as upwelling events. While climate and environmental monitoring increasingly relies on information from teledetection systems, in situ measurements are essential for validation of satellite data, especially in coastal and inshore waters.

Citizen observatories enable citizens (and not just scientists and professionals) to collect and share data about the environment. Owing to the fact that scientific output and conclusions regarding the issues of the environment are often disregarded by the public opinion, engaging citizens in collecting scientific data can benefit both science and the society at large.

See Baltic Poland is a citizen science initiative aimed at empowering local citizens living on the polish Baltic coast to fill gaps in surface temperature and other oceanographic data needed to better understand the functioning of marine environment, effects of climate change and ocean health issues in our coastal environment. The initiative is based on a collaborative partnership between a group of ocean enthusiasts from the Polish surfer community, and a group of marine experts from the Institute of Oceanology of the Polish Academy of Science (IO PAN), in collaboration with the International Ocean Carbon Coordination Project (IOCCP) - part of Global Ocean Observing System (GOOS).

See Baltic Poland is powered by Smartfin - a project which develops surfboard fins with sensors that measure several water parameters. The obtained data is accessible to the worldwide scientific community and has the potential to enhance the resolution of oceanographic surveys and validate satellite observations. Besides that, the partnership between marine scientists and the ocean enthusiasts will enhance society's awareness of the science and environmental issues, as well as give the opportunities to take educational and pop-science actions among the local community.

Utilization of Earth Observation to support biogeochemical modeling

Sampsa Koponen[1], Thomas Neumann[2], Dagmar Müller[3], Carsten Brockmann[3], Constant Mazeran[4], Petra Philipson[5], Kari Kallio[1], Jenni Attila[1] and Sakari Väkevä[1].

[1] Finnish Environment Institute, Helsinki, Finland (sampsa.koponen@ymparisto.fi)
[2] Leibniz Institute for Baltic Sea Research Warnemünde (IOW), Rostock, Germany
[3] Brockmann Consult GmbH, Hamburg, Germany
[4] SOLVO, Antibes, France
[5] Brockmann Geomatics Sweden AB, Kista, Sweden

1. Introduction

The Sentinel satellites of the Copernicus programme offer an excellent opportunity for monitoring the state of the Baltic Sea. The current constellation provides daily coverage in moderate resolution (S3 OLCI with 300 m pixels) and twice-weekly coverage in high resolution (S2 MSI with 10-60 m pixels) with spectral characteristics suitable for estimating turbidity, Chlorophyll a and Coloured Dissolved Organic Matter (CDOM). These are related to the land-to-sea fluxes of carbon that occur in coastal zones. The goal of the European Space Agency (ESA) funded project Sea-Land Biogeochemical linkages (SeaLaBio, 2018-2020) is to develop methods for assessing carbon dynamics and eutrophication in the Baltic Sea through integrated use of Earth Observation (EO), models, and ground-based data.

The study logic of the project is the following:

- Improve the accuracy of atmospheric correction and in-water estimation of water quality parameters (especially CDOM) from EO data.
- Utilize CDOM values generated from satellite images as input data for a biogeochemical model.

This abstract presents the results of the second step.

2. Model modifications

In this study we have utilized the Ecological ReGional Ocean Model (ERGOM). It is the biogeochemical part of the 3-dimensional ecosystem model of the Baltic Sea developed by IOW (www.ergom.net). The main inputs for the model are meteorological forcing including river runoff. From these the model simulates the marine nitrogen, phosphorus, and carbon cycles.

During the project ERGOM was modified to have higher spatial resolution (1 n.m. instead of 3 n.m.) and to utilize CDOM values estimated from satellites as input data. The previous version estimated CDOM from salinity. CDOM is used in the model to estimate the light climate controlling primary production.

3. Satellite data

For this study we utilized high resolution images of the Sentinel-2 satellite (S2). The characteristics of this instrument are not optimized for water applications. However, it has provided reasonable results in previous studies and having a high resolution is essential for the estimation of CDOM values in river estuaries (ERGOM input locations).

The processing utilized the C2RCC V2 processor (Brockmann et al., 2016) and post processing steps to remove effects of clouds and shadows. Pixel values were extracted from 80 areas defined to represent the ERGOM input locations (typically a river estuary but sometimes representing a larger area with multiple rivers) and calibrated to absorption by CDOM at 400 nm values (aCDOM(400)) using in situ data from Finnish coastal areas. All data from years 2017 and 2018 were processed and monthly means were derived. Optical satellites cannot observe water in winter time due to lack of light and the presence of ice cover. Thus, we used interpolation to generate data for the missing months. Examples of the values are shown in Figure 1. The behavior of the values is logical: High values in the spring time when melting snow water brings terrestrial matter to coastal areas, low values during summer and again higher values in autumn when the rainfall increases.

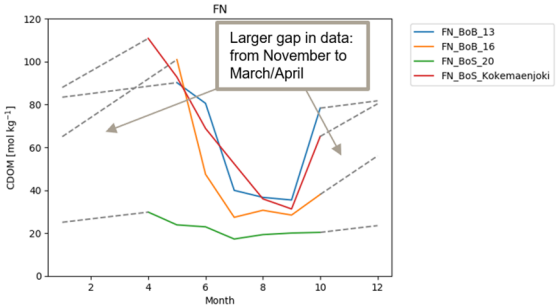


Figure 1. Seasonal behavior of CDOM estimated from satellite data at four ERGOM input locations.

4. Results

The model was then run using the CDOM input data from EO and runoff data obtained from HYPE. The simulation period starts in 1948 and ends in 2018. The simulation period has to be long in order to allow the model result to stabilize. The runoff values change from year to year to correspond with actual conditions. The CDOM data on the other hand was the same for each year. EO data with the required characteristics only exist for the past three years and for the purposes of this study we assumed that the CDOM concentration has remained the same during the study period.

The ERGOM result for one day is shown in Figure 2. In coastal areas the values obtained with the new method correspond with reality better than the earlier model based on salinity. For comparison, Figure 2 also includes mean CDOM values estimated from S2 data acquired during July 1 and September 7, 2017. Clear similarities between the dataset are visible. Both show elevated values in the Bay of Bothnia and in the eastern end of Gulf

of Finland. In the southern areas EO tends to give higher values than the model.

After the first run the model results showed that the values for the Central Baltic are too high when compared to expected values based on in situ data. To mitigate this, we implemented a photobleaching process into the model.

5. Discussion

We have succeeded – to our knowledge for the first time in the Baltic Sea – in utilizing CDOM data generated from satellite images as input data for a biogeochemical model. The model results are now more realistic in coastal areas and comparable to EO values. Thus, the results support the idea of utilizing models and EO data together.

Further development is still needed. For example, the analysis of the input locations showed that additional points are needed in ERGOM in order to better represent the riverine fluxes to the Baltic Sea. Also, the parameterization of the photobleaching process needs to be verified.

On the EO side the required developments include utilization of Sentinel-3 data for the estimation of CDOM in the open sea areas of the Baltic Sea.

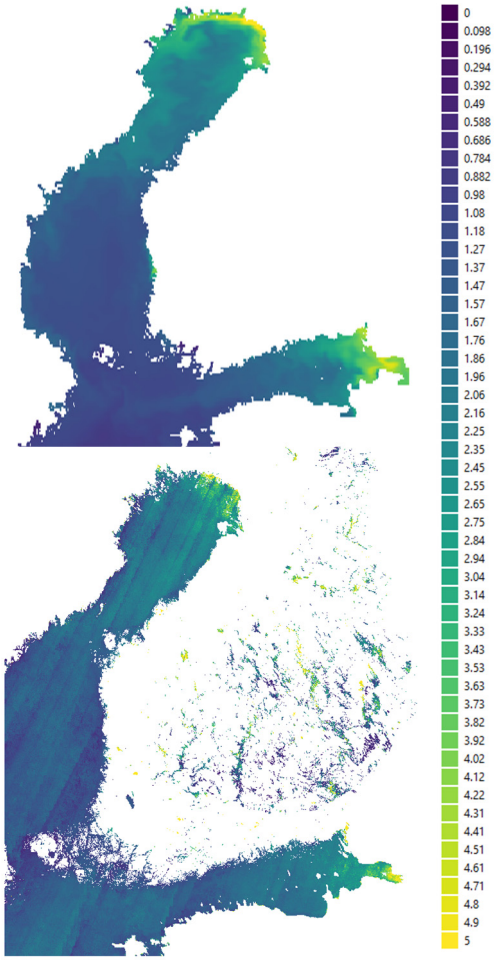


Figure 2. Top: aCDOM(400) values simulated with ERGOM on July 20, 2017. Bottom: Temporal aCDOM(400) composite (Jul and Aug 2017) estimated from S2 satellite data.

References

C. Brockmann, Doerffer, R., Peters, M., Stelzer, K., Embacher, S., Ruescas, A. (2016). Evolution of the C2RCC neural network for Sentinel 2 and 3 for the retrieval of ocean colour products in normal and extreme optically complex waters. European Space Agency, (Special Publication) ESA SP, SP-740

eCUDO.pl - Oceanographic Data and Information System for Polish Baltic data resources

Mirosława Ostrowska[1], Michał Wójcik[2], Urszula Pączek[3], Lena Szymanek[4], Marcin Wichorowski[1]

[1] Institute of Oceanology, Polish Academy of Sciences, Sopot, Poland (ostra@iopan.pl)
[2] Maritime Institute, Maritime University of Gdynia, Poland (Michal.Wojcik@im.umg.edu.pl)
[3] Polish Geological Institute National Research Institute (upac@pgi .gov.pl)
[4] Sea Fishery Institute National Research Institute (lszymanek@mir.gdynia.pl)

1. Introduction

The growth of data volume managed by organizations involved in research in Environmental and Earth Sciences last years is exponential. Data covering domain of one's interest are distributed across variety of infrastructures, data centers, collections, formats making discovery of all available sources of data and their harmonization extremely hard, and rising the assurance of FAIRness of data as the most emerging problem for data managers.

Institute of Oceanology Polish Academy of Sciences (IO PAN), Institute of Meteorology and Water Management National Research Institute (IMGW), Maritime Institute in Gdańsk (IMG), Polish Geological Institute National Research Institute (PIG PIB), National Marine Fisheries Research Institute (MIR PIB) and University of Technology in Gdańsk (PG) - consortium of organizations engaged in research and exploitation of marine resources, established as POLMAR, together with SatBałtyk – the consortium consisting of Gdańsk University (UG), Szczecin University (US) and Pomeranian Academy in Słupsk (APS), with leading role of IO PAS in both consortia, for many years lead actions targeting harmonization, integration and coordinated provisioning of environmental data resources. These are the most of the organizations involved in marine research and continuous acquisition of oceanographic data. This initiative is leading activities towards the deployment of operational state of the system delivering demanded oceanographic data and products to the users and heading to establish Polish Oceanographic Data Committee.

2. Project mission

eOceanographicDataCenter.pl (eCUDO.pl) - Electronic Center for Oceanographic Data Access is in the development phase. Project has started officially at March 1st, 2019. Project is developed within the frame of Digital Agenda Poland.

Deployment of unified system providing access to data resources managed by key scientific organizations in Poland will trigger synergy in data governance and enable an added value for national economy through increase of data availability.

Unified data formats and protocols will boost development of the services based on environmental data. Advanced services provided for clients (including big data processing and analysis services based on deep learning technologies) extend availability of oceanographic data both to Polish and European organizations.

System is open for all stakeholders and ready to aggregate other organizations and data sources. Up to now cooperation has been agreed with Ministry of Environment Protection and Ministry of Maritime Economy and Inland Navigation – System for Spatial Information of Maritime Authorities, and local authorities.

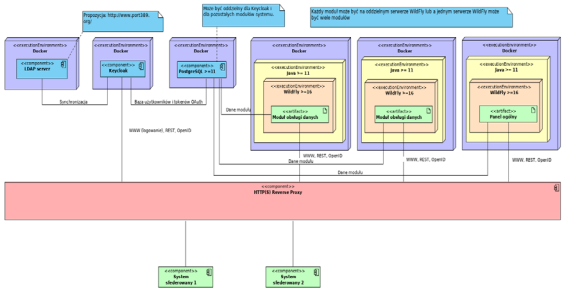


Figure 1. Distributed data management system design for eCUDO.pl

3. System design

The project assumes obtaining data openness at the level of 5 stars according to the "5 Star Open Data" scale, because the project develops a system that gives users not only the ability to access current, open and searched data, but also integrates the resources of other open collections. Data will be described with metadata compliant with the standards applicable to geospatial data. Data will also be marked with unique URIs and in all appropriate places the metadata will contain relevant links to other resources available on the network.

Datacenters run by organizations providing data compose distributed data system (Fig. 1)

4. Summary

The complexity of this distributed system design is forced by geographical topology and technology state of the datacenters infrastructures. This complexity drives the innovation for the efficient management of extensive data infrastructures, to enable users with integrated tools for data analysis and to provide products based on information explored from diverse sources: archives, online data streams, satellite data, numerical models and fleet of autonomous measuring devices.

Unified data formats and protocols will boost development of the services based on environmental data. Advanced services provided for clients (including data analysis services) extend availability of oceanographic data both to Polish and European organizations.

The eCUDO.pl project, when finished will be well integrated with SeaDataCloud and EMODNet systems.

SatBałtyk System - modern tool for tracking changes in the Baltic Sea environment

Mirosława Ostrowska[1], Mirosław Darecki[1], Adam Krężel[2], Dariusz Ficek[3], Kazimierz Furmańczyk[4], Tomasz Zapadka[3], Mrek Kowalewski[1,2], and Marta Konik[1]

[1] Institute of Oceanology Polish Academy of Sciences, Sopot, Poland (ostra@iopan.pl)
[2] University of Gdańsk, Faculty of Oceanography Gdynia, Poland
[3] Pomeranian University in Słupsk, Poland
[4] University of Szczecin, Poland

1. Introduction

SatBałtyk System continually monitors, at the moment, some of 100 different structural and functional properties of the Baltic ecosystem. It was launched in 2015 and founded on the scientific results of optical, bio-optical and other studies (Woźniak 2008, Darecki 2008) of the Baltic environment performed over many years by cooperating teams of scientists from SatBałtyk Scientific Consortium (ie. the Institute of Oceanology PAN in Sopot – the project coordinator, the University of Gdańsk, the Pomeranian Academy in Słupsk and the University of Szczecin). By providing comprehensive easy accessible information about the Baltic it became a modern tool for tracking changes of the marine environment, resulting either from progressive eutrophication or as the effects of climate change.

2. SatBałtyk System descriptions

Scientific research together with remote sensing techniques, allows obtaining generally available, comprehensive information on various processes occurring in the sea. The SatBałtyk Consortium developed and launched the system of Satellite Monitoring of the Baltic Sea Environment - SatBałtyk (Figure 1). It provides qualitative and quantitative information of many state parameters of this environment, the coastal zone as well as certain state parameters and optical properties of the atmosphere. The values and maps of spatial distributions of these parameters are available in near real time to users on the website http://satbaltyk.iopan.gda.pl/. (Woźniak et al. 2011a,b)

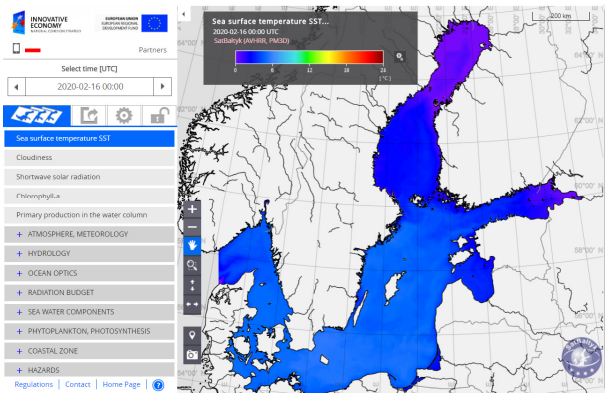


Figure 1. SatBałtyk System starting page, www.SatBaltyk.pl.

Among the others the System monitors the solar radiation influx to the sea's waters in various spectral intervals, short- and long-wave radiation budget at the sea surface and in the upper layers of the atmosphere, sea surface temperature distribution, dynamic states of the water surface, concentrations of chlorophyll a and other phytoplankton pigments in the Baltic water, distributions of algal blooms, the occurrence of upwelling events, and the characteristics of primary organic matter production and photosynthetically released oxygen in the water and many others.

Parameters currently available in the system have been divided into eight groups: 1. Atmosphere, meteorology, 2. Hydrology, 3. Ocean optics, 4. Radiation budget, 5. Sea water components, 6. Phytoplankton, photosynthesis, 7. Coastal zone, 8. Hazards.

To satisfied present-day requirements for the continuous monitoring of the marine environment the SatBałtyk System utilizes data from a number of satellites systematically monitoring the Baltic updated and expanded by use of ecohydrodynamic models. The information is supported by in situ measurements from continuous monitoring systems (buoys, shore stations, drones) and research vessels. Such synergy of data sources enables continuous control of the accuracy of determined parameters.

Using models allow estimation of marine environment parameters not only in the surface layer but also allow the provision of information from various depths. They were also used to deal with the main limitation of remote sensing methods - the cloud cover over the investigated area, when data from visible and infrared domain are unavailable. For this the bioptical and hydrodynamic models used in the SatBałtyk System are divided into two independent but cooperating subsystems: the diagnostic ones named the DESAMBEM, and the prognostic ones referred to as BALTFOS. The environmental parameters determined with the aid of these two systems complement one another: BALTFOS assimilates empirical data obtained from satellite information using the DESAMBEM algorithms, while at the same time filling in gaps in the input DESAMBEM data when the relevant areas were invisible for satellite sensors (Konik 2019).

The SatBałtyk System offers not only current NRT information but also historical data (since 2010) are available at the system together with a short forecast of modelled parameters.

3. Selected results

The system's functionalities not only allow browsing the value distribution map of the selected parameter throughout the entire Baltic Sea area but also reading these values for each pixel with a 1 km side. It is also possible to analyze the variability in time of each of the parameters available in the SatBałtyk System (Figure 2).

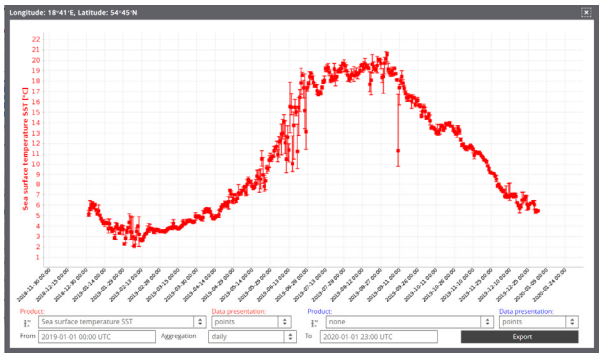


Figure 1. Sea Surface Temperature values observed for 18°41'E, 54°45'N coordinates in 2019. Chart generated using the SatBatyk System

After logging in, you can download the numerical values of the parameters in various formats. It enables their further analysis, for example determining average values in selected areas (see Figure 3).

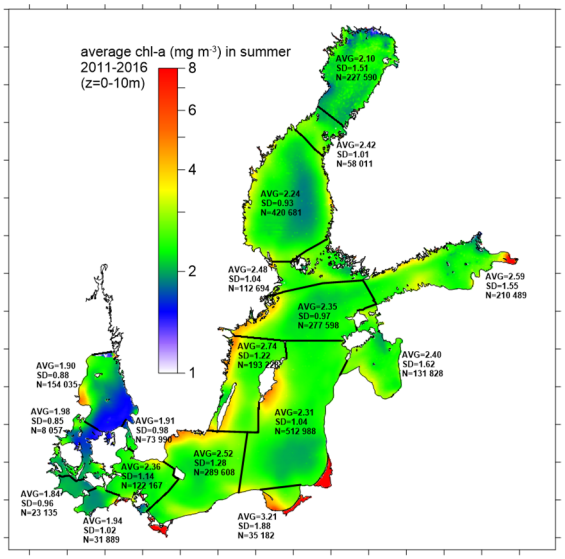


Figure 3. The average chlorophyll a concentration for the summer months in years 2011-2016 for the assessment units of the Baltic defined by HELCOM. Map and values determined on the basis of data from the Satbałtyk System.

4. Summary

This opportunity to efficient global monitoring of the state of the sea and assess the complex processes taking place in the entire water column on the basis of data from satellite sensors has undoubtedly raised the quality of and opened a new chapter in oceanological research.
For the first time it became possible to estimate these magnitudes for the entire Baltic Sea area simultaneously, and not as up to that point in time, only at the location where in situ measurements were being made in the traditional way.

References

B.Woźniak, A. Krężel, M. Darecki, S.B. Woźniak, R. Majchrowski, M. Ostrowska, Ł. Kozłowski, D. Ficek, J. Olszewski, J. Dera, (2008): Algorithm for the remote sensing of the Baltic ecosystem (DESAMBEM). Part 1: Mathematical apparatus, Oceanologia 50(4) 451–508.

M. Darecki, D. Ficek, A. Krężel, M. Ostrowska, R. Majchrowski, S.B. Woźniak, K. Bradtke, J. Dera, B. Woźniak, (2008): Algorithms for the remote sensing of the Baltic ecosystem (DESAMBEM). Part 2: Empirical validation, Oceanologia 50(4) 509-538

B. Woźniak, K. Bradtke, M. Darecki, J. Dera, J. Dudzińska-Nowak, L. Dzierzbicka-Głowacka, D. Ficek, K. Furmańczyk, M. Kowalewski, A. Krężel, R. Majchrowski, M. Ostrowska, M. Paszkuta, J. Stoń-Egiert, M. Stramska, T. Zapadka, (2011a): SatBaltic – a Baltic environmental satellite remote sensing system- an ongoing project in Poland. Part 1: Assumptions, scope and operating range, Oceanologia 53(4) 897–924.

B. Woźniak, K. Bradtke, M. Darecki, J. Dera, J. Dudzińska-Nowak, L. Dzierzbicka-Głowacka, D. Ficek, K. Furmańczyk, M. Kowalewski, A. Krężel, R. Majchrowski, M. Ostrowska, M. Paszkuta, J. Stoń-Egiert, M. Stramska, T. Zapadka, (2011b): SatBaltic – a Baltic environmental satellite remote sensing system- an ongoing project in Poland. Part 2: Practical applicability and preliminary results, Oceanologia 53(4) 925–958.

Konik M., Kowalewski M., Bradtke K., Darecki M., (2019): The operational method of filling information gaps in satellite imagery using numerical models, International Journal of Applied Earth Observation and Geoinformation 75, 68-82

Development of the Argo measurement system for responding challenges in the northern Baltic Sea

Petra Roiha, Simo Siiriä, Laura Tuomi, Pekka Alenius and Tero Purokoski

Finnish Meteorological Institute, Helsinki, Finland (petra.roiha@fmi.fi)

1. Challenges in the northern Baltic Sea

Argo floats are nowadays an essential tool in observing the Baltic Sea (Siiriä et al. 2019, Haavisto et al. 2018). Finnish Meteorological Institute (FMI) has floats in the three basins of the northern Baltic Sea: the Baltic Proper, the Bothnian Sea (Fig. 1) and the Bothnian Bay. The observational network consisting of the traditional monitoring and Argo floats is under development to be able to respond both scientific as well as management challenges with different scales.

The model simulations are suggesting that the sea surface temperatures are rising especially in the central and northern parts of the Baltic Sea (Saraiva et al. 2019). With Argo floats we are able to monitor the trends in the temperatures, temperature variance between years and changes and variances in the stratification in the water column and further improve the predictions.

The oxygen concentration in the Bothnian Sea deep water has been decreasing during the last two decades (Raateoja 2013). The oxygen situation is still fair and there is no evidence for the consistent hypoxia to take place in the near future. However, the oxygen measurements have been sparse and situation has been difficult to assess. In the beginning of year 2020, there were Argo floats equipped with oxygen sensors in three northern Baltic Sea basins: Bothnian Bay, Bothnian Sea and the Baltic Proper measuring a weekly dissolved oxygen profile.

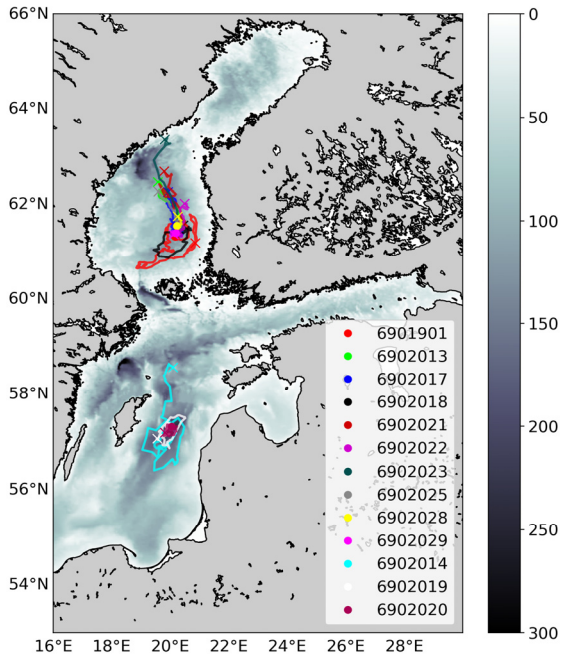


Figure 1. APEX measurements in the Baltic Sea Proper and Bothnian Sea until the end of 2017. (Roiha, 2019)

2. What Argo floats can do?

The first Argo floats in the Baltic Sea were APEX floats, (Haavisto et al. 2018) balanced especially for the certain basin. The other type of floats (e.g. a bottom landing Argo) have been tested and since May 2019 also Arvor-I float has joined the fleet in the Bothnian Sea.

The measurement frequency can be adjusted for different purposes depending the temporal and spatial scale of the phenomenon of interest: the shortest interval is in order of hours while the longest used measurement interval is in order of weeks. The typical frequency used for monitoring is around of seven days.

All of the floats are equipped with pressure, temperature and salinity sensors. There are floats in the Bothnian Sea and the Baltic Sea Proper with turbidity, oxygen and fluorescence sensors. Bothnian Bay floats are equipped with oxygen sensors.

3. Coping with winter conditions

The ice avoidance is common practice in the Argos operating in the cold regions. The Bothnian Sea and the Bothnian Bay have at least partial ice cover in most of the winters. To be able to do year round observations the ice avoidance algorithm has been adjusted for the Baltic Sea conditions. The ice avoidance is activated before expected ice cover in the autumn and the algorithm is active until the estimated end of the ice season. The algorithm does not detect ice itself, but the favorable conditions for ice formatting. In the Bothnian Sea the water temperature between +0,2...+0,4°C in the near surface layer (18...35m) is considered to be a good threshold value for activating the ice avoidance. If the ice avoidance is activated the float measures the profile and then dives without surfacing. When the conditions change so that ice avoidance is not needed anymore, the float reach the surface and sends all the collected data to the ground station.

4. Results and future work

In this work we present the temperature, salinity and oxygen profiles from Argo data in the Baltic Proper, Bothnian Sea and Bothnian Bay from year round measurements. The data was also further analysed statistically and compared with existing monitoring data in these basins. The focus is on profile data and stratification in different basins.

At the moment the floats only measure partial profiles so that the deepest part of the profile is missing. The current floats do not yet have an altimeter so that they could adjust their drifting depth by the bottom topography and start the profile as near of the bottom as possible.

The Argo measurements are not covering the whole basins and the data set is measured in the deepest parts of the basins. The improvement of the usage of new and established monitoring data and optimizing the whole of the observational network is an on-going task.

References

Haavisto, N., Tuomi, L., Roiha, P., Siiriä, S. M., Alenius, P., & Purokoski, T. (2018). Argo floats as a novel part of the monitoring the hydrography of the Bothnian Sea. Frontiers in Marine Science, 5, 324.

Raateoja, M. (2013). Deep-water oxygen conditions in the Bothnian Sea. *Boreal environment research*, *18*.

Roiha, P. (2019). Advancements of operational oceanography in the Baltic Sea. *Doctoral Thesis*

Saraiva, S., Meier, H. M., Andersson, H., Höglund, A., Dieterich, C., Gröger, M., ... & Eilola, K. (2019). Baltic Sea ecosystem response to various nutrient load scenarios in present and future climates. Climate dynamics, 52(5-6), 3369-3387.

Siiriä, S., Roiha, P., Tuomi, L., Purokoski, T., Haavisto, N., & Alenius, P. (2019). Applying area-locked, shallow water Argo floats in BalticSea monitoring. *Journal of Operational Oceanography*, *12*(1), 58-72.

ARGO floats – the modern tool for the Southern Baltic monitoring

Waldemar Walczowski, Małgorzata Merchel, Daniel Rak and Piotr Wieczorek

Institute of Oceanology Polish Academy of Sciences(walczows@iopan.pl)

1. Introduction

It were three revolutions in the world oceanography. The first was developing and introducing of the high-resolution satellite altimetry. Argo floats array has made a second revolution. The third revolution was the development of global operational oceanography, which was strongly linked to previous achievements (Le Traon, 2013).

ARGO program began to be introduced in 1999, the global coverage of the oceans upper 2000 m was achieved in 2006. Nowadays a global network of 4,000 floats covers oceans (Roemmich et. al, 2019). The most popular Argo float type (core Argo) is a small, autonomous underwater platform that measures the temperature and conductivity of seawater versus pressure. Maximal profiling depth is 2000 m. The float height is about 1.80 m, weighs 20 kg and it has neutral buoyancy in the water. Float does not have its own propulsion but drifts freely in the sea. The change of depth is enforced by the change of float buoyancy.

The global Argo array has already grown to be a major component of the ocean observing system. The great advantage of the ARGO system is that it provides data in near-real-time. Quick verification and distribution allow their use in operational oceanographic and meteorological services already 12 hours after the measurement.

Argo floats were designed for open ocean profiling. The typical period of measurements of core Argo float is 10 days, most of the time float drift at 'parking depth' of 1000 m, next descend to the profiling depth (2000 m) and slowly ascend registering water temperature and conductivity versus pressure. At the surface, float sends data to receiving centres via satellite connection and again dive to the parking depth (Fig. 1).

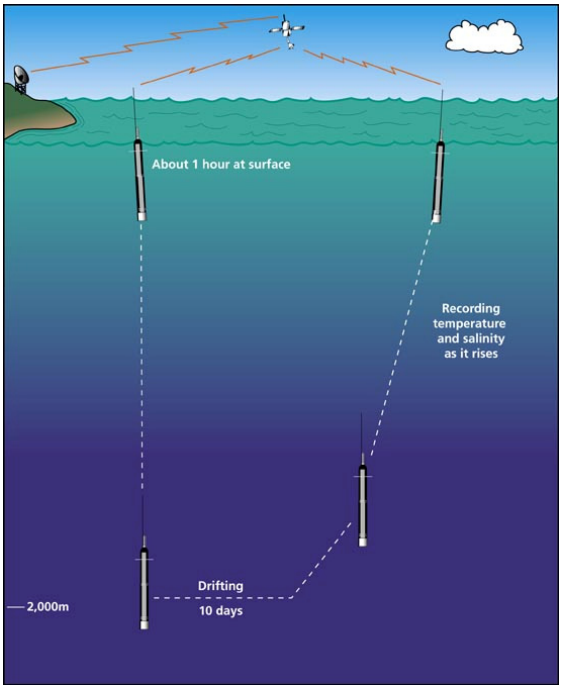


Figure 1. Typical Argo float cycle.

2. First Argo floats at the Baltic Sea

Float operators avoid getting the float closer to the shore and contact with the bottom. Therefore, the conditions of the Baltic Sea are not favorable for launching Argo. Baltic is small, shallow, semi-enclosed water body. The strong pycnocline between surface, brackish waters and deep, more saline waters originated from the North Sea creates additional problems.

Despite these difficulties, Finnish oceanographers launched the first Argo floats in the northern part of the Baltic Sea, Bothnian Sea in 2011 (Purokoski et al., 2013), Haavisto et al., 2018). They used APEX floats and successfully profiled the whole water column. The first Argo in the Southern Baltic was deployed by Institute of Oceanology Polish Academy of Sciences (IOPAN) in 2016. Poland and Finland work in Euro-Argo ERIC (European Research Infrastructure Consortium), whose objective is active coordination and strengthening of the European contribution to the international Argo programme. One of the Euro-Argo aims is to provide enhanced coverage in the European regional seas (Euro-Argo ERIC, 2016).

3. Southern Baltic investigation

The southern Baltic Sea, especially region between Bornholm Basin and Gdansk Deep, connected by Slupsk Furrow is very important for the Baltic Sea environment. The Slupsk Furrow is the only deep channel enabling inflow of well-oxygenated, salty water originating from the North See to the central and northern part of the Baltic Sea. Monitoring the advection processes of this life-giving water is extremely important for knowledge about the state of the Baltic Sea.

Unfortunately, the first attempts with Argo profilers in this region were not fully successful. Due to the strong pycnocline standard, Argo floats had problems reaching the bottom. Only the use of the Arvor float, which is characterized by a large bladder, allowed to overcome these difficulties. They were obtained thanks to the MOCCA program and Euro-Argo provided technical assistance in setting the mission parameters.

By the end of 2019, IOPAN eight times launched Argo floats in the Southern Baltic. Two floats belonged to the MOCCA project, four were purchased from the funds of the Polish Ministry of Science and Higher Education. Two floats were recovered and redeployed. Two Arvor floats were additionally equipped with oxygen sensors. The addition of an oxygen sensor to the standard Argo float greatly increases the value of obtained data, especially in such ecologically sensitive water body as the Baltic Sea.

Argo in the Baltic Sea work in different time schedule than typical oceanic floats. Initially, we introduced one-day cycles, now we mainly use two-days long series. Floats usually drift at 50 m parking depth. Thanks to the high frequency of measurements, until February 2020 Argo floats in the Southern Baltic performed 1600 CTD profiles, including 600 oxygen ones. Measurements covered

Bornholm Basin, Slupsk Furrow, Gdansk and Gotland Deep (Fig. 2).

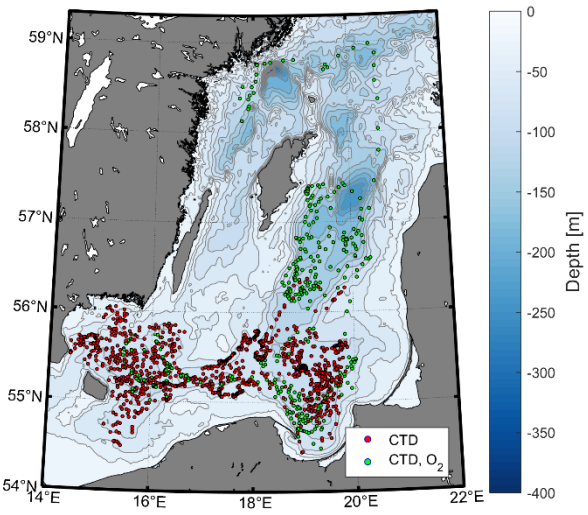


Fig. 2. Positions of Argo floats profiles in the Southern Baltic.

Collected data allow accurate determination of seasonal cycles of temperature, salinity and dissolved oxygen content in seawater. The zones of hypoxia and anoxia have been well recognized. Presence of floats in the Slupsk Furrow and Gdansk Deep have allowed observing the small, baroclinic inflow in summer 2019.

4. Measurements

In the open ocean, the lifetime of modern floats reaches four years. During this time they perform up to 150 profiles reaching a depth of 2000 m. Floats recovering after the battery is depleted is unprofitable. We have no experience yet how long float can work in the Baltic Sea conditions. The longest measurements were performed by Arvor CT float WMO 3901941 (383 dives) and CT/O_2 float WMO 3902101 (349 cycles). Both floats were recovered by IOPAN and after refurbishing will be deployed again.

Float WMO 3902101 except standard CTD measurements gave valuable results of dissolved oxygen content along its drift from the Bornholm Basin through Slupsk Furrow to Gdansk Deep and next to Gotland Deep (Fig 3).

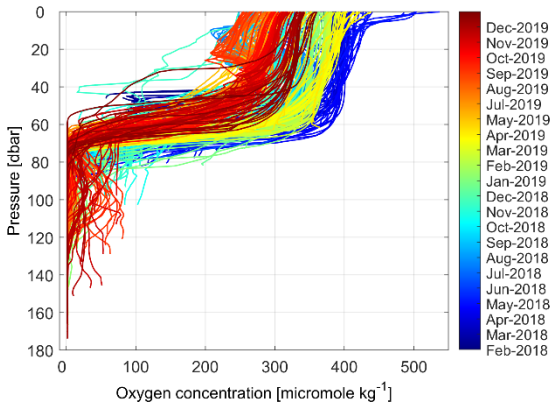


Fig. 3. Float 3902101. Dissolved oxygen concentration profiles.

5. Conclusions

The possibility of using Argo floats as part of a complex South Baltic monitoring system was postulated by Walczowski et al. (2017). Now our three-years' experience with Argo floats in the Baltic Sea allow us to draw conclusions regarding the use of this modern equipment in Baltic Sea practice.

- The importance of autonomous devices in oceanographic measurements is increasing;
- Argo floats are the reliable and cheap sources of oceanographic real-time data;
- Argo array is well organised and maintained;
- Data are freely available in Coriolis Service;
- Practice shows that shallow shelf seas can also be explored using Argo floats;
- Contact with the bottom (grounding), proximity to the shore, collisions with vessel are not as dangerous for the float as it seemed before;
- Small seas as the Baltic Sea gives an opportunity of floats recovery and redeployment;
- Various sources of data as Argo floats, cruises and moorings provide extensive, complementary data set for better monitoring of the Baltic Sea, improvement of numerical models and validation of satellite observation;
- In the near future, in addition to standard CTD floats, the number and importance of BGC floats will increase;
- Even the use of the simplest BGC float-equipped only with an oxygen sensor significantly improves the possibilities of observing important processes and data interpreting.

References

Euro-Argo ERIC (2016): Strategy for evolution of Argo in Europe, v3.2. DOI:10.13155/48526

Haavisto, N., Tuomi, L., Roiha, P., Siiriä, S.-M., Alenius, P., and Purokoski, T. (2018). Argo floats as a novel part of the monitoring the hydrography of the Bothnian Sea. Front. Mar. Sci. 5:324. doi: 10.3389/fmars.2018.00324

Le Traon, P. Y. (2013). From satellite altimetry to Argo and operational oceanography: three revolutions in oceanography. Ocean Sci. 9, 901–915. doi: 10.5194/os-9-901-2013.

Roemmich et. al, 2019, On the future of Argo: A global, full-depth, multi-disciplinary array, Front. Mar. Sci., 02 August 2019 | https://doi.org/10.3389/fmars.2019.00439.

Simo Siiriä, Petra Roiha, Laura Tuomi, Tero Purokoski, Noora Haavisto & Pekka Alenius (2019) Applying area-locked, shallow water Argo floats in Baltic Sea monitoring, Journal of Operational Oceanography, 12:1, 58-72, DOI: 10.1080/1755876X.2018.1544783.

Walczowski W., Wieczorek P., Goszczko I., Merchel M., Rak D., Beszczynska-Möller A., Cisek M., (2017), Monitoring the salt water inflows in the southern Baltic Sea, Proceedings of the Eigth EuroGOOS International Conference 3-5 October 2017, Bergen, Norway, pp 165-169.

Author Index

Aarenstrup Launbjerg T 47
Abalichin J 139
Abulaitijiang A 105
Alenius P 15, 206
Ambrozio A 105
Aminjafari S 199
Andersen OB 105
Andrzejewski J 157
Arias M 15
Arneborg L 188
Asadchaya M 121, 133
Attila J 201
Bange HW 194
Barda I 151
Barqawi H 151
Barzehkar M 135
Bechtel B 145
Bełdowska M 1
Bełdowski J 1
Beltran-Perez O 137
Belušić D 165
Benveniste J 105
Berg P 63
Boehner J 145
Bolałek J 89
Boniewicz-Szmyt K 31
Borawska Z 33
Borkowska E 200
Böttcher ME 58
Brenner M 1
Breznikar A 35
Brockmann C 201
Brodecka-Goluch A 89
Brown R 97
Bugajny N 91
Bulczak A 17, 23, 25
Bulskaya I 37
Buyakov IV 179
Catany R 15
Choo S 38
Christensen OB 163, 165
Chubarenko B 151
Cieślikiewicz W 61
Cupiał A 61
Dailidė R 173
Dailidienė I 173
Dangendorf S 101
Danilovich I 115
Darecki M 204
Darvishi M 93, 199
Das S 80
Davilienė L 173
Destouni G 3
Dettmering D 105
Dieterich C 63, 159, 163, 167
Dippner JW 35
Dobler A 165
Dudzinska-Nowak J 113
Dybowski D 40, 41, 42
Dzierzbicka-Głowacka L ... 40, 41, 42
Ebner von Eschenbach A-D 125
Efimov S 184
Ehlers B-M 139
Elken J 170
Esiukova E 151
Fabisiak J 1
Feistel S 142
Feldens P 58
Fernández D 15
Feser F 161
Ficek D 204
Fredrikson S 188
Furmańczyk K 91, 204
Gabarró C 15
García J 199
Garnaga-Budre G 1
Giudici A 97, 181
Golenko M 27, 124
González-Gambau V 15
González-Haro C 15
Gopchenko E 82
Gorska N 89
Graiff A 49
Gräwe U 101
Grayek S 161
Gregoire M 5
Gröger M 63, 159, 163, 167
Gründling-Pfaff S 49
Grzegorczyk M 31
Hagemann S 117, 161
Heinilä K 197
Hennekam R 177

Hieronymus J 188
Hledko YA 65
Hoffmann P 145
Höglund A 187, 188
Ho-Hagemann HTM 161
Høyer JL 105
Idczak J 89
Isaev AV 147
Jakacki J 17, 40, 103, 157
Janecki M 40, 42
Janssen F 139
Janssen M 50
Janušaitė R 99
Jaramillo F 93, 199
Jarmalavičius D 99
Jenner A-K 58
Jensen C 119
Jensen J 101
Jeworrek J 63
Johansson M 105
Juszkowska D 41
Jylhä K 63
Kalantari Z 3
Kałczyński M 67
Kallio K 201
Karaliūnas V 99
Karsten U 49
Kędra M 33
Kelln J 101
Kichuk N 82
Kijewski T 200
Kikas V 123
Kjellström E 63, 163, 165
Klehmet K 63
Kolbas A 37
Kondrashov A 27, 124
Konik M 204
Koponen S 197, 201
Korzh A 27, 124
Kowalewska-Kalkowska H 68
Kowalewski M 204
Koziorowska-Makuch K 33
Krawiec K 67
Krężel A 204
Kudryavtseva N 70, 74, 181
Kuliński K 44, 45, 52, 54
Kull A 128
Kundzewicz Z 67
Kuriyama K 49
Kuzmina N 28
Kvach A 121, 133
Laanemets J 123
Landgren O 165
Lang T 1
Langer S 38
Lebdi F 78
Lehmann A 19
Lengier M 45
Lennartz B 50, 132
Lennartz ST 194
Lerner A 175
Liblik T 22, 123
Liesirova T 47
Lilover M-J 123
Lind P 165
Lindstedt D 165
Linkevičienė R 149
Lips I 123
Lips U 22
Liu H 132
Löwe P 102, 119
Luojus K 197
Ma Xiao 194
Mačiulytė V 72, 85
Männik A 175
Männikus R 74
Martin G 147
Martínez J 15
Martyanov SD 147
Martyniuk M 76
Massalska BW 177
Mathlouthi M 78
Mattila OP 197
Mazeran C 201
Meier HEM ... 63, 159, 163, 167, 185
Melnik VI 179
Merchel M 208
Metsämäki S 197
Möller J 102, 119
Moniushko M 80, 82, 140
Müller D 201
Müller FL 105
Müürsepp T 83
Myrberg K 19
Najafzadeh F 181
Naumann M 142

Neemann V 125
Neumann T 185, 201
Nia M 199
Nikulin G 163
Nowicki A 40, 42
Oelsmann J 105
Oikkonen A 188
Olmedo E 15
Olsson T 63
Omstedt A 8, 170
Ostrowska M 203, 204
Ovcharuk V 76, 80, 82, 140
Pączek U 203
Paka V 27, 124
Palacz A 200
Panidi E 109
Parfomuk S 130
Parnell K 135, 143
Passaro M 105
Patzke J 101
Pazikowska-Sapota G 42
Pedersen RA 165
Peters DHW 183
Petrik R 161
Philipson P 60, 201
Pietrzak S 41, 42
Pikaleva A 184
Placke M 185
Pogorzelski SJ 31
Polevoy A 87
Popiel S 1
Post P 19, 83, 128
Povilanskas R 149
Prelle L 49
Przyborska A 23, 103
Pupienis D 99, 107
Purina I 151
Purokoski T 206
Puszkarczuk T 42
Putna-Nimane I 151
Räämet A 70
Racasa ED 50
Radtke H 21
Rak D 17, 23, 208
Rautiainen L 105
Razbadauskaitė-Venskė I 173
Rechid D 145
Reichart G-J 177
Reinhart V 145
Restano M 105
Reuter M 1
Riemann L 47
Rimkus E 85
Ringgaard IM 105
Rinne E 105
Rochowski P 31
Rockel B 161
Roiha P 15, 188, 206
Rutgersson A 60, 63
Ryabchenko VA 147
Sabia R 15
Salm K 22
Särkkä J 105, 187, 188
Scarrott R 105
Schade N 119, 125
Schmidt B 25
Schmiedinger I 58
Scholten J 58
Schouten S 177
Schrum C 161
Schulz-Vogt H 38
Schwaizer G 197
Schwatke C 105
Seifollahi-Aghmiuni S 3
Seitz F 105
Semenova I 87, 169
Sepp 127, 128
Shkolnik I 184
Sidak S 130
Siiriä S-M 187, 188, 206
Silberberger MJ 33
Šimanauskienė R 149
Simon F-G 151
Sinninghe Damsté JS 177
Siudek P 153
Skovgaard Madsen K 105
Sommer V 49
Soomere T 10, 70, 74, 97, 135, 143, 181
Stacke T 117
Staneva J 161
Stankūnavičius G 72
Steffen H 101
Stendel M 189
Stokowski M 44, 52
Stonevičius E 85

Strode E 151
Suara KA..... 97
Sumak K 169
Szala M..... 1
Szczepanek M 33
Szymanek L 203
Szymczycha B.....
..... 33, 42, 44, 45, 52, 54, 200
Szymkiewicz A..... 42
Taminskas J 149
Taratsenkava M 56
Tengberg A..... 1
Toivonen E 165
Tuomi L 15, 105, 187, 188, 206
Turiel A..... 15
Undeman E 11
Uścinowicz G..... 12
Väkevä S..... 197, 201
Väli G..... 28, 123
Valiukas D 85
van der Meer MTJ..... 177
Vanninen P..... 1
Vigouroux G 3
Viršilaitė K 107
Volchak A 37, 56, 130
Volynetc A..... 109
Volynets E 109
von Ahn CME 58
von Storch H 170, 190
Voormansik T..... 83
Voss M 35, 47
Walczowski W..... 17, 23, 208
Wang M 132
Waniek J..... 137
Waszak I..... 153
Weiss GM..... 177
Weslawski M..... 13
Wibig J..... 192
Wichorowski M..... 203
Wieczorek P 208
Winogradow A..... 44, 52, 54
Wiśniewski B..... 111
Wojciechowska E..... 42
Wójcik M..... 203
Wolski T 111
Wu L..... 63
Wu M 163
Zapadka T..... 204
Zhang S 60
Zhang W 113
Zhelezova E 155
Zhuravovich L 121, 133
Zhurbas V 27, 28, 124
Zieliński T.....200
Žilinskas G.....99
Zima P.....42
Zülicke C 183

International Baltic Earth Secretariat Publications

ISSN 2198-4247

No. 1 Programme, Abstracts, Participants. Baltic Earth Workshop on ”Natural hazards and extreme events in the Baltic Sea region”. Finnish Meteorological Institute, Dynamicum, Helsinki, 30-31 January 2014. International Baltic Earth Secretariat Publication No. 1, 33 pp, January 2014.

No. 2 Conference Proceedings of the 2nd International Conference on Climate Change - The environmental and socio-economic response in the Southern Baltic region. Szczecin, Poland, 12-15 May 2014. International Baltic Earth Secretariat Publication No. 2, 110 pp, May 2014.

No. 3 Workshop Proceedings of the 3rd International Lund Regional-Scale Climate Modelling Workshop ”21st Century Challenges in Regional Climate Modelling”. Lund, Sweden, 16-19 June 2014. International Baltic Earth Secretariat Publication No. 3, 391 pp, June 2014.

No. 4 Programme, Abstracts, Participants. Baltic Earth - Gulf of Finland Year 2014 Modelling Workshop ”Modelling as a tool to ensure sustainable development of the Gulf of Finland-Baltic Sea ecosystem”. Finnish Environment Institute SYKE, Helsinki, 24-25 November 2014. International Baltic Earth Secretariat Publication No. 4, 27 pp, November 2014.

No. 5 Programme, Abstracts, Participants. A Doctoral Students Conference Challenges for Earth system science in the Baltic Sea region: From measurements to models. University of Tartu and Vilsandi Island, Estonia, 10 - 14 August 2015. International Baltic Earth Secretariat Publication No. 5, 66 pp, August 2015.

No. 6 Programme, Abstracts, Participants. International advanced PhD course on Impact of climate change on the marine environment with special focus on the role of changing extremes. Askö Laboratory, Trosa, Sweden, 24 - 30 August 2015 International Baltic Earth Secretariat Publication No. 6, 61 pp, August 2015.

No. 7 Programme, Abstracts, Participants. HyMex-Baltic Earth Workshop ”Joint regional climate system modelling for the European sea regions”, ENEA, Rome, Italy, 5- 6 November 2015. International advanced PhD course on Impact of climate change on the marine International Baltic Earth Secretariat Publication No. 7, 103 pp, October 2015.

No. 8 Programme, Abstracts, Participants. A PhD seminar in connection with the Gulf of Finland Scientific Forum: "Exchange process between the Gulf of Finland and other Baltic Sea basins". Tallinn, Estonia, 19 November 2015. International Baltic Earth Secretariat Publication No. 8, 27 pp, November 2015

No. 9 Conference Proceedings. 1st Baltic Earth Conference. Multiple drivers for Earth system changes in the Baltic Sea region. Nida, Curonian Spit, Lithuania, 13 - 17 June 2016. International Baltic Earth Secretariat Publication No. 9, 222 pp, June 2016

No. 10 Programme, Abstracts, Participants. Baltic Earth Workshop on ”Coupled atmosphere-ocean modeling for the Baltic Sea and North Sea”, Leibniz Institute for Baltic Sea Research Warnemünde, Germany, 7- 8 February 2017. International Baltic Earth Secretariat Publication No. 10, 24 pp, February 2017

No. 11 Baltic Earth Science Plan 2017. International Baltic Earth Secretariat Publication No. 11, 28 pp, February 2017

No. 12 Programme, Abstracts, Participants. MedCORDEX-Baltic Earth-COST Workshop ”Regional Climate System Modelling for the European Sea Regions”. Universitat de les Illes Baleares, Palma de Mallorca, Spain, 14 - 16 March 2018, International Baltic Earth Secretariat Publication No. 12, 96 pp, March 2018

No. 13 Conference Proceedings. 2nd Baltic Earth Conference. The Baltic Sea in Transition. Helsingør, Denmark, 11 - 15 June 2018. International Baltic Earth Secretariat Publication No. 13, 216 pp, June 2018

No. 14 Programme, Abstracts, Participants. Baltic Earth Workshop "Multiple drivers for Earth system changes in the Baltic Sea region". Tallinn, Estonia, 26-27 November 2018. International Baltic Earth Secretariat Publication No. 14, 58 pp, March 2018

No. 15 Programme, Abstracts, Participants. Baltic Earth Workshop "Hydrology of the Baltic Sea Basin: Observations, Modelling, Forecasting". St. Petersburg, Russia, 8-9 October 2019. International Baltic Earth Secretariat Publication No. 15, 44 pp, October 2019

No. 16 Programme, Abstracts, Participants. Baltic Earth Workshop "Climate projections and uncertainties in the northerb Baltic Sea Region". Helsinki, Finland, 19-20 November 2019, International Baltic Earth Secretariat Publication No. 16, 38 pp, November 2019

No. 17 Anders Omstedt: 45 years of wandering - from processes to systems, through outer and inner seas. An interview by Hans von Storch and Marcus Reckermann with foreword by Jüri Elken, 63 pp. International Baltic Earth Secretariat Publication No. 17, 63 pp, February 2020

No. 18 Conference Proceedings. 3rd Baltic Earth Conference. Earth system changes and Baltic Sea coasts. To be held in Jastarnia, Hel Peninsula, Poland, 1 - 5 June 2020. Held online 2-3 June 2020. International Baltic Earth Secretariat Publication No. 18, 209 pp, June 2020

International Baltic Earth Secretariat Publications
ISSN 2198-4247